



**UNIVERSITY OF
CAMBRIDGE**

Department of Pathology, Faculty of Medicine

Molecular Pathogenesis of MALT Lymphoma

Rifat Akram Hamoudi

Churchill College

Dissertation for the degree of Doctor of Philosophy

University of Cambridge, United Kingdom - September, 2010

| | |
|------------------------|-------|
| Declarations | iii |
| Table of contents..... | iv |
| List of tables..... | xiv |
| List of figures | xv |
| Abbreviations..... | xviii |
| Abstract..... | xxi |
| Publications..... | xxiii |
| Acknowledgements..... | xxv |

Declarations

This dissertation is the result of my own work and includes nothing which is the outcome of work done in collaboration except where specifically indicated in the text.

I also declare that this thesis is not substantially the same as any that I submitted for a degree or diploma or other qualification at any other University, and that no part has already been, or is currently being, submitted for any degree, diploma, or other qualification.

This dissertation comprises a total of 465 pages and a supplemental volume.

Rifat Akram Hamoudi
September 2010

Table of contents

| | |
|--|-----------|
| CHAPTER 1 - General introduction | 1 |
| 1.1 Brief overview of lymphomas | 1 |
| 1.2 Overview of MALT lymphoma..... | 3 |
| 1.2.1 Aetiology of MALT lymphoma..... | 3 |
| 1.2.1.1 Chronic infection..... | 4 |
| 1.2.1.2 Autoimmune disease..... | 6 |
| 1.2.2 Histopathology of MALT lymphoma..... | 7 |
| 1.2.2.1 Mucosa associated lymphoid tissue..... | 7 |
| 1.2.2.2 Extranodal marginal zone B-cell lymphoma of MALT..... | 9 |
| 1.2.3 Immunophenotype..... | 10 |
| 1.2.4 Pathogenesis of MALT lymphoma..... | 12 |
| 1.2.4.1 <i>H. pylori</i> and its role in the development of gastric MALT lymphoma..... | 12 |
| 1.2.4.2 Immunological stimulation..... | 13 |
| 1.2.4.2.1 Direct antigen stimulation..... | 13 |
| 1.2.4.2.2 Indirect antigen stimulation..... | 14 |
| 1.2.4.3 <i>H. pylori</i> virulent and host factors in the development of gastric MALT lymphoma..... | 16 |
| 1.2.4.3.1 Host factors..... | 16 |
| 1.2.4.3.2 Bacterial virulence factors..... | 17 |
| 1.2.4.4 Role of anti-microbial and other therapies in the treatment of MALT lymphoma..... | 19 |
| 1.3 Genetics of MALT lymphoma..... | 21 |
| 1.3.1 Chromosomal translocations..... | 21 |
| 1.3.1.1 <i>t(11;18)(q21;q21)/API2-MALT1</i> | 23 |
| 1.3.1.2 <i>t(1;14)(p22;q32)/BCL10-IGH</i> | 25 |
| 1.3.1.3 <i>t(14;18)(q32;q21)/IGH-MALT1</i> | 26 |
| 1.3.1.4 BCL10 and MALT1 expression patterns in MALT lymphoma with different translocation status..... | 27 |
| 1.3.1.5 <i>t(3;14)(p13;q32)/FoxP1/IGH</i> | 29 |
| 1.3.2 Other chromosome translocations..... | 31 |
| 1.3.3 Genetics of translocation negative MALT lymphoma..... | 31 |

| | | |
|------------|--|-----------|
| 1.4 | NF-κB pathway..... | 33 |
| 1.4.1 | NF- κ B family members..... | 33 |
| 1.4.2 | NF- κ B activation pathways..... | 34 |
| 1.4.2.1 | Canonical pathway..... | 35 |
| 1.4.2.2 | Non-canonical pathway..... | 40 |
| 1.4.3 | NF- κ B negative regulators..... | 44 |
| 1.4.4 | NF- κ B target genes and their biological implications..... | 45 |
| 1.5 | MALT lymphoma associated translocations target common molecular pathways that cause NF-κB activation..... | 48 |
| 1.6 | Summary of current understanding of gastric MALT lymphoma..... | 51 |
| 1.7 | Gene expression microarray..... | 54 |
| 1.7.1 | Advantages of using gene expression microarray..... | 55 |
| 1.7.2 | Limitations of gene expression microarray..... | 55 |
| 1.7.3 | Microarray platforms..... | 57 |
| 1.7.3.1 | The Affymetrix HG-U133 GeneChip..... | 57 |
| 1.7.3.1.1 | Probe versus probe set..... | 58 |
| 1.7.4 | Data analysis..... | 59 |
| 1.7.5 | Advances in lymphoma by gene expression microarray investigations..... | 61 |
| 1.7.6 | Gene expression microarray studies of MALT lymphomas..... | 64 |
| 1.8 | Objectives of the thesis..... | 66 |

CHAPTER 2. Materials and methods 67

| | | |
|------------|--|-----------|
| 2.1 | Materials..... | 67 |
| 2.1.1 | Tissue materials and clinical data..... | 67 |
| 2.1.1.1 | Ethical considerations..... | 67 |
| 2.1.1.2 | Tissue material for expression microarray and phenotypic marker studies..... | 67 |
| 2.1.1.3 | Tissue material for qRT-PCR and immunohistochemistry..... | 69 |
| 2.1.2 | Reagents..... | 69 |
| 2.1.2.1 | Reagents used in gene expression microarray and qRT-PCR..... | 69 |
| 2.1.2.2 | Reagents used in immunohistochemistry..... | 70 |
| 2.1.2.3 | Reagents used in tissue culture..... | 71 |
| 2.1.2.4 | Reagents used in Western blotting and co-immunoprecipitation..... | 71 |
| 2.1.2.5 | Reagents used in cloning and DNA sequencing..... | 72 |
| 2.1.3 | Cell lines..... | 72 |
| 2.2 | Methods..... | 74 |
| 2.2.1 | Overview of the study plan..... | 74 |
| 2.2.2 | Crude microdissection..... | 74 |
| 2.2.3 | RNA preparation..... | 75 |
| 2.2.3.1 | RNA extraction from fresh frozen tissue..... | 75 |
| 2.2.3.2 | RNA extraction from formalin fixed paraffin-embedded tissue..... | 76 |
| 2.2.3.3 | RNA extraction from cell lines..... | 76 |
| 2.2.3.4 | RNA linear amplification..... | 76 |
| 2.2.3.5 | RNA quantification and quality control..... | 77 |
| 2.2.4 | Expression microarray..... | 78 |
| 2.2.4.1 | Affymetrix HG-U133 GeneChips..... | 78 |
| 2.2.4.2 | Preparation of biotinylated cRNA target for Affymetrix GeneChip..... | 78 |
| 2.2.4.2.1 | Double stranded cDNA synthesis..... | 79 |
| 2.2.4.2.2 | cRNA labelling using IVT (In-Vitro Transcription)..... | 79 |
| 2.2.4.2.3 | Fragmentation of cRNA..... | 80 |
| 2.2.4.3 | Hybridisation to HG-U133 Affymetrix GeneChips and data Acquisition..... | 80 |
| 2.2.4.3.1 | Hybridisation mix preparation..... | 80 |
| 2.2.4.3.2 | Hybridisation to HG-U133 GeneChips..... | 80 |
| 2.2.4.3.3 | Hybridisation to Test3 GeneChip..... | 81 |
| 2.2.4.3.4 | Staining of GeneChips..... | 81 |
| 2.2.4.4 | HG-U133 GeneChip data acquisition and quality control..... | 81 |

| | | |
|-----------|---|-----|
| 2.2.5 | Bioinformatics and statistical analysis of gene expression microarray data..... | 83 |
| 2.2.5.1 | Normalisation..... | 83 |
| 2.2.5.2 | Non-specific filtering..... | 84 |
| 2.2.5.3 | Clustering analysis..... | 84 |
| 2.2.5.4 | Gene Set Enrichment Analysis (GSEA)..... | 85 |
| 2.2.5.5 | Analysis of differential gene expression in MALT lymphomas with and without chromosome translocation..... | 86 |
| 2.2.5.6 | Functional annotation using gene ontology (GO)..... | 86 |
| 2.2.5.7 | Phenotypic marker analysis..... | 87 |
| 2.2.5.8 | Statistical analyses..... | 87 |
| 2.2.6 | Quatitative Real-time RT-PCR..... | 88 |
| 2.2.6.1 | Primer design..... | 88 |
| 2.2.6.2 | Complementary DNA (cDNA) synthesis..... | 90 |
| 2.2.6.3 | Quantitative PCR (qPCR)..... | 90 |
| 2.2.7 | Immunohistochemistry..... | 91 |
| 2.2.8 | Expression constructs preparation..... | 92 |
| 2.2.8.1 | Modification of pIRES vectors containing HA and FLAG tag sequences..... | 92 |
| 2.2.8.2 | Generation of tagged <i>BCL10</i> , <i>MALT1</i> and <i>API2-MALT1</i> Expression constructs..... | 95 |
| 2.2.8.2.1 | Preparation of HA-tagged <i>BCL10</i> | 96 |
| 2.2.8.2.2 | Preparation of FLAG-tagged <i>API2-MALT1</i> and FLAG- tagged <i>MALT1</i> | 96 |
| 2.2.8.2.3 | Subcloning of oncogenes into pTRE2..... | 97 |
| 2.2.8.3 | Toll-like receptors constructs..... | 98 |
| 2.2.8.4 | DNA sequencing..... | 98 |
| 2.2.9 | Cell culture..... | 99 |
| 2.2.9.1 | Protocols for freezing cells..... | 99 |
| 2.2.9.2 | Protocols for thawing cells..... | 100 |
| 2.2.9.3 | Cell clot preparation..... | 100 |
| 2.2.9.4 | Transient transfection of cells..... | 100 |
| 2.2.9.5 | Generation of stably inducible MALT lymphoma associated oncogenes cells..... | 101 |

| | | |
|----------|--|-----|
| 2.2.10 | Protein work..... | 102 |
| 2.2.10.1 | Protein extraction from whole cell lysate..... | 102 |
| 2.2.10.2 | Preparation of protein homogenate from frozen tissue..... | 102 |
| 2.2.10.3 | Protein extraction from nuclear and cytoplasmic fractions..... | 103 |
| 2.2.10.4 | Protein quantitation..... | 103 |
| 2.2.10.5 | Antibodies used for functional and cellular work | 103 |
| 2.2.10.6 | Western blot..... | 105 |
| 2.2.10.7 | Stripping of Western blot..... | 106 |
| 2.2.10.8 | Co-immunoprecipitation..... | 106 |
| 2.2.11 | Dual luciferase reporter assays..... | 106 |
| 2.2.11.1 | NF- κ B luciferase reporter assay..... | 106 |
| 2.2.11.2 | AP-1 luciferase reporter assay..... | 107 |

CHAPTER 3 – Characterisation of the gene expression profiles of MALT lymphoma with and without chromosome translocation 108

| | | |
|------------|--|------------|
| 3.1 | Introduction..... | 108 |
| 3.2 | Aims of the study..... | 109 |
| 3.3 | Experimental design..... | 110 |
| 3.3.1 | Case selection..... | 110 |
| 3.3.2 | RNA quality check using Agilent nanochip..... | 110 |
| 3.3.3 | Validation of the in house linear RNA amplification protocol..... | 111 |
| 3.3.4 | Unsupervised clustering analysis..... | 111 |
| 3.3.5 | Characterisation of gene expression features of MALT lymphoma with and without chromosome translocation..... | 111 |
| 3.4 | Results..... | 112 |
| 3.4.1 | RNA quality control..... | 112 |
| 3.4.2 | Comparison of total RNA with amplified RNA..... | 113 |
| 3.4.3 | Validation of microarray data using biological controls..... | 114 |
| 3.4.4 | Unsupervised clustering between MALT, MCL and FL defines MALT lymphoma as a distinct entity..... | 115 |
| 3.4.5 | Unsupervised clustering confirms overlapping features in gene expression profiling between MALT lymphoma with and without chromosome translocation..... | 118 |
| 3.4.6 | Characterisation of gene expression profiles of MALT lymphoma with and without chromosome translocation..... | 122 |
| 3.4.6.1 | NF- κ B target genes are significantly differentially expressed between MALT lymphoma with and without chromosome translocation..... | 125 |
| 3.4.6.2 | Other gene sets differentially enriched between MALT lymphoma with and without chromosome translocation..... | 126 |
| 3.4.6.3 | Gene ontology annotations of genes differentially expressed between MALT lymphoma with and without chromosome translocation confirms findings by GSEA..... | 128 |
| 3.4.7 | Pathway analysis of molecules identified by gene expression microarray and potentially important in MALT lymphoma pathogenesis..... | 131 |
| 3.5 | Discussion..... | 133 |
| 3.5.1 | Molecular mechanism of translocation positive MALT lymphoma..... | 133 |
| 3.5.2 | Molecular mechanism of translocation negative MALT lymphoma..... | 134 |
| 3.5.3 | Nuclear BCL10..... | 135 |
| 3.5.4 | Summary and conclusion..... | 136 |

CHAPTER 4 – Validation of the genes identified by expression microarray of MALT lymphoma with and without chromosome translocation using qRT-PCR and immunohistochemistry 138

| | | |
|------------|--|------------|
| 4.1 | Introduction..... | 138 |
| 4.2 | Aims of the study..... | 138 |
| 4.3 | Experimental design..... | 139 |
| 4.3.1 | Case selection..... | 139 |
| 4.3.2 | Validation of gene expression by qRT-PCR..... | 139 |
| 4.3.3 | BCL2, CD69, MUM1, MALT1, BCL10 and CD86 immunohistochemistry..... | 140 |
| 4.3.4 | Validation of TLR6 using Western blotting..... | 141 |
| 4.4 | Results..... | 142 |
| 4.4.1 | Correlation of mRNA expression of <i>CD69</i> , <i>CCR2A</i> , <i>CCR5</i> , <i>TLR6</i> , <i>BCL2</i> , <i>MUM1</i> , <i>CD86</i> , <i>NR4A3</i> , <i>BCL10</i> and <i>MALT1</i> genes in MALT lymphoma with and without chromosomal translocation..... | 142 |
| 4.4.2 | Comparison of protein expression of CD69, BCL2, CD86, MUM1, BCL10 and MALT1 in MALT lymphoma with and without chromosomal translocation using immunohistochemistry..... | 146 |
| 4.4.3 | Comparison of protein expression of TLR6 in MALT lymphoma with and without chromosome translocation using Western blotting..... | 148 |
| 4.5 | Discussion..... | 150 |

| | |
|---|------------|
| CHAPTER 5 – Cooperation between MALT lymphoma oncogenes and immunological stimulation in activating the NF-κB pathway..... | 155 |
| 5.1 Introduction..... | 155 |
| 5.2 Aims of the study..... | 156 |
| 5.3 Experimental design..... | 157 |
| 5.3.1 Cell lines..... | 157 |
| 5.3.2 Investigation of the cooperation between <i>BCL10</i> , <i>MALT1</i> and <i>API2-MALT1</i> and <i>TLR6</i> on NF- κ B activation with and without LPS stimulation..... | 157 |
| 5.3.3 Investigation of the effect of <i>BCL10</i> , <i>MALT1</i> and <i>API2-MALT1</i> expression and antigen receptor stimulation on NF- κ B activation..... | 158 |
| 5.3.4 Investigation of the effect of MALT lymphoma associated oncogenes expression on canonical NF- κ B pathway activation..... | 158 |
| 5.3.5 Investigation of the effect of BCL10 and MALT1 expression on their sub-cellular localization..... | 159 |
| 5.4 Results..... | 160 |
| 5.4.1 TLR6 (in the presence of TLR2), enhances BCL10 and API2-MALT1 mediated NF- κ B activation in Jurkat T cells..... | 160 |
| 5.4.2 Cooperation of BCL10, MALT1, API2-MALT1 and immune receptor signalling in NF- κ B activation in B-cells..... | 163 |
| 5.4.3 Cooperation between BCL10, MALT1, API2-MALT1 immune receptor signalling on NF- κ B activation in Jurkat T cells..... | 166 |
| 5.4.4 Investigation of the effect of BCL10 and MALT1 expression on their sub-cellular localisation..... | 168 |
| 5.4.5 Effect of BCL10, MALT1 and API2-MALT1 expression on canonical NF- κ B pathway activation | 171 |
| 5.5 Discussion..... | 173 |
| 5.5.1 Cooperation between the expression of MALT lymphoma associated oncogenes and TLR stimulation..... | 173 |
| 5.5.2 Effect of antigen receptor stimulation on MALT lymphomagenesis..... | 174 |
| 5.5.3 BCL10 expression associated with I κ B β degradation..... | 175 |
| 5.5.4 BCL10 sub-cellular localisation and its relationship with MALT1 expression..... | 176 |

| | |
|--|------------|
| CHAPTER 6 - Identification of MALT lymphoma specific phenotypic markers using gene expression microarray..... | 179 |
| 6.1 Introduction..... | 179 |
| 6.2 Aims of the study..... | 180 |
| 6.3 Experimental design..... | 180 |
| 6.3.1 Case selection..... | 180 |
| 6.3.2 Identification of genes highly and specifically expressed in MALT lymphoma by gene expression microarray analysis..... | 181 |
| 6.3.3 Validation of genes highly and specifically expressed in MALT lymphoma by qRT-PCR and immunohistochemistry..... | 181 |
| 6.4 Results..... | 183 |
| 6.4.1 Identification of genes highly and specifically expressed in MALT lymphoma..... | 183 |
| 6.4.2 Validation of <i>Lactoferrin</i> expression in MALT lymphoma..... | 187 |
| 6.5 Discussion..... | 190 |

| | |
|---|------------|
| CHAPTER 7 - General Discussion..... | 193 |
| 7.1 MALT lymphoma is a distinct entity within the lymphomas but with heterogeneity between MALT lymphoma with and without chromosome translocation as indicated by gene expression profiling ... | 193 |
| 7.2 Overview of the molecular mechanisms underlying the pathogenesis of MALT lymphoma..... | 193 |
| 7.2.1 Aberrant molecular mechanisms of translocation positive MALT lymphoma..... | 194 |
| 7.2.2 Aberrant molecular mechanism of translocation negative MALT lymphoma..... | 200 |
| 7.2.3 Molecular mechanisms of BCL10, MALT1 and API2-MALT1 mediated NF- κ B activation..... | 202 |
| 7.3 MALT lymphoma specific phenotypic marker identification..... | 206 |
| 7.4 Conclusions..... | 208 |
| 7.5 Future perspectives..... | 209 |
| 7.5.1 CCR2 involvement in the molecular mechanism of MALT lymphomagenesis..... | 209 |
| 7.5.2 Nuclear BCL10 function..... | 210 |
| 7.5.3 Lactoferrin expression in MALT lymphoma by immunohistochemistry..... | 211 |
| References..... | 212 |
| Appendices..... | 241 |
| Publications..... | 281 |

List of tables

| Table | Title | Page |
|--------------|---|-------------|
| 1.1 | Typical immunophenotyping of MALT lymphoma cells | 11 |
| 2.1 | Summary of clinico-pathological, molecular and immunohistochemical data of MALT lymphoma cases used in gene expression microarray studies | 68 |
| 2.2 | Primers used to investigate candidate genes by qRT-PCR | 89 |
| 2.3 | Immunohistochemistry antibodies and conditions | 92 |
| 2.4 | Primers used in construct preparation | 95 |
| 2.5 | Primary and secondary antibodies used in co-immunoprecipitation and Western blotting | 104 |
| 3.1 | Gene sets differentially over-represented between MALT lymphoma with and without chromosome translocation | 124 |
| 3.2 | Representation of gene ontology terms in over-expressed genes in MALT lymphoma with and without chromosome translocation | 130 |
| 4.1 | Correlation of BCL2, CD69 and CD86 expression in MALT lymphoma with and without chromosome translocation | 147 |
| 6.1 | Descriptive statistical properties of the 5 potential phenotypic marker probes calculated for MALT and other lymphomas separately | 186 |

List of figures

| Figure | Title | Page |
|---------------|--|-------------|
| 1.1 | Morphology of MALT and gastric MALT lymphoma from the gastrointestinal tract | 8 |
| 1.2 | Cytological and histological features of MALT lymphoma | 9 |
| 1.3 | The role of T- and B- cell interaction in the development of MALT lymphoma | 15 |
| 1.4 | Schematic representation of chromosome translocations implicated in MALT lymphoma | 22 |
| 1.5 | Incidence of MALT lymphoma translocations in various sites | 27 |
| 1.6 | BCL10 and MALT1 staining patterns in MALT lymphoma translocations | 28 |
| 1.7 | Canonical (classical) and non-canonical (alternative) NF- κ B pathway | 42 |
| 1.8 | B-cell receptor mediated NF- κ B activation and constitutive NF- κ B activation by MALT lymphoma associated translocations | 43 |
| 1.9 | Role of NF- κ B target genes in immune response, cell proliferation and survival and maintaining cellular homeostasis | 47 |
| 1.10 | Multistep development of gastric MALT lymphoma | 52 |
| 2.1 | Summary of the study plan | 74 |
| 2.2 | Crude microdissection of gastric MALT lymphoma | 75 |
| 2.3 | Strategy for generating hybridisation target from total RNA | 78 |
| 2.4 | pIRESpuro vector | 94 |
| 2.5 | pTRE vector | 97 |
| 3.1 | Typical good quality data of total, complementary and fragment RNA on RNA nanochip | 112 |
| 3.2 | Correlation between total and amplified RNA from the same fresh frozen specimen of t(11;18) positive MALT lymphoma | 113 |

| | | |
|------|---|-----|
| 3.3 | Expression of hallmark genes in MALT lymphoma, FL and MCL | 114 |
| 3.4 | Summary of bioinformatics strategy to combine FL and MCL with MALT microarray GeneChips | 115 |
| 3.5 | MALT lymphoma shows distinct gene expression profiles from follicular lymphoma and mantle cell lymphoma using unsupervised hierarchical clustering | 116 |
| 3.6 | Summary of bioinformatics strategy used to compare MALT lymphoma with and without chromosome translocations | 118 |
| 3.7 | Unsupervised hierarchical clustering of MALT lymphoma with different translocation status | 119 |
| 3.8 | Supervised hierarchical clustering of MALT lymphoma with different translocation status | 121 |
| 3.9 | Summary of bioinformatics strategy used for GSEA on MALT lymphoma with and without chromosome translocation | 122 |
| 3.10 | Gene set enrichment analysis (GSEA) of NF- κ B target genes in MALT lymphomas with and without chromosome translocation | 126 |
| 3.11 | Presence of high proportion of NF- κ B target genes in the leading edge core set of various gene sets related to inflammation and immune responses | 127 |
| 3.12 | Summary of bioinformatics strategy used for Gene Ontology analysis on MALT lymphoma with and without chromosome translocation | 128 |
| 3.13 | analysis of molecules derived from MALT lymphoma microarray analysis | 132 |
| 4.1 | Validation of gene expression in MALT lymphoma with and without chromosome translocation by real-time quantitative RT-PCR | 143 |
| 4.2 | Unsupervised hierarchical clustering of qRT-PCR data on MALT lymphoma cases with various translocation status | 144 |
| 4.3 | Immunohistochemistry of BCL2, CD69, CD86 and MUM1 | 146 |
| 4.4 | TLR6 expression in MALT lymphoma with and without chromosomal translocation using Western blot analysis | 149 |

| | | |
|-----|--|-----|
| 5.1 | TLR6 enhances BCL10 and API2-MALT1 mediated NF- κ B activation, in the presence of TLR2 but not TLR1, in Jurkat T-cells | 161 |
| 5.2 | BCL10, MALT1 and API2-MALT1 mediated NF- κ B activation, with and without LPS stimulation in BaF3 murine B-cells | 163 |
| 5.3 | BCL10, MALT1 and API2-MALT1 mediated NF- κ B activation, with and without 6 hours of LPS, anti-IgM and CD40-L stimulation in WEHI murine B-cells | 165 |
| 5.4 | BCL10, MALT1 and API2-MALT1 mediated NF- κ B activation, with and without 6 hours of CD3/CD28 stimulation in Jurkat T cells | 166 |
| 5.5 | Immunohistochemistry on cell clots expressing various MALT lymphoma associated oncogenes | 168 |
| 5.6 | Co-immunoprecipitation showing that expression of BCL10 leads to increased interaction with MALT1 | 170 |
| 5.7 | Activation of canonical NF- κ B pathway by BCL10, MALT1 and API2-MALT1 and association of I κ B β degradation with BCL10 expression | 171 |
| 6.1 | Summary of bioinformatics strategy to combine MALT lymphoma, FL, MCL, SMZL and CLL microarray data and identify the genes highly and specifically expressed in MALT lymphoma | 183 |
| 6.2 | (A) Supervised hierarchical clustering of MALT lymphoma, FL, MCL, SMZL and CLL (B) Volcano plot of MALT v other lymphomas showing Lactoferrin position near the top | 185 |
| 6.3 | Variation of the raw gene expression microarray data of Lactoferrin across the 5 lymphoma groups | 186 |
| 6.4 | Validation of Lactoferrin expression in MALT, FL and MCL lymphomas by real-time quantitative RT-PCR | 189 |
| 6.5 | Validation of Lactoferrin expression in MALT, FL and MCL lymphomas by immunohistochemistry | 189 |
| 7.1 | Summary and hypothesis on molecular mechanisms of MALT lymphoma with and without chromosomal translocation | 205 |

Abbreviations

Some abbreviations used only once or a few times, particularly with gene names, may not be included in this list, but are explained in the main text. In general gene names and translocations are written in italics.

| | |
|------------------|---|
| AP-1 | Activator protein 1 |
| CCR | Chemotactic cytokines receptor |
| cDNA | complementary DNA |
| CLL | Chronic lymphocytic leukaemia |
| cRNA | complementary RNA |
| DLBCL | Diffuse large B-cell lymphoma |
| DLR | Dual luciferase reporter assay |
| FL | Follicular lymphoma |
| gcRMA | GeneChip RMA |
| GO | Gene ontology |
| GSEA | Gene set enrichment analysis |
| <i>H. pylori</i> | <i>Helicobacter pylori</i> |
| I κ B | Inhibitor of nuclear factor of kappa light polypeptide gene enhancer in B-cells |
| MALT | Mucosa associated lymphoid tissue |
| MAPK | Mitogen-activated protein kinases |
| MAS5 | Affymetrix Microarray Suite 5 |
| MCL | Mantle cell lymphoma |
| NF- κ B | nuclear factor kappa-light-chain-enhancer of activated B cells |
| NHL | Non-Hodgkin lymphoma |
| PBS | Phosphate buffered saline |

| | |
|------------------|---|
| qPCR | Quantitative PCR |
| qRT-PCR | Quantitative real time PCR |
| RMA | Robust Multiarray Averaging |
| RNA | Ribonucleic acid |
| RT-PCR | Reverse transcriptase PCR |
| SDS | Sodium dodecyl sulphate |
| SMZL | Splenic marginal zone lymphoma |
| TBS | Tris-buffered saline |
| TBST | Tris-buffered saline with Tween |
| TLR | Toll-like receptor |
| AP-1 | Activator protein 1 |
| CCR | Chemotactic cytokines receptor |
| cDNA | complementary DNA |
| CLL | Chronic lymphocytic leukaemia |
| cRNA | complementary RNA |
| DLBCL | Diffuse large B-cell lymphoma |
| DLR | Dual luciferase reporter assay |
| FL | Follicular lymphoma |
| gcRMA | GeneChip RMA |
| GO | Gene ontology |
| GSEA | Gene set enrichment analysis |
| <i>H. pylori</i> | Helicobacter pylori |
| I κ B | Inhibitor of nuclear factor of kappa light polypeptide gene enhancer in B-cells |
| MALT | Mucosa associated lymphoid tissue |
| MAPK | Mitogen-activated protein kinases |

| | |
|----------------|--|
| MAS5 | Affymetrix Microarray Suite 5 |
| MCL | Mantle cell lymphoma |
| NF- κ B | nuclear factor kappa-light-chain-enhancer of activated B cells |
| NHL | Non-Hodgkin lymphoma |
| PBS | Phosphate buffered saline |
| qPCR | Quantitative PCR |
| qRT-PCR | Quantitative real time PCR |
| RMA | Robust Multiarray Averaging |

Abstract

Molecular Pathogenesis of MALT Lymphoma

By **Rifat Akram Hamoudi**, Churchill College, University of Cambridge

Mucosa associated lymphoid tissue (MALT) lymphoma is characterized by *t(11;18)(q21;q21)/API2-MALT1*, *t(1;14)(p22;q32)/BCL10-IGH* and *t(14;18)(q32;q21)/IGH-MALT1*, which commonly activate the NF-κB pathway. Gastric MALT lymphomas harbouring such translocation do not respond to *Helicobacter pylori* eradication, while those without translocation can be cured by antibiotics.

To understand the molecular mechanism of MALT lymphoma with and without chromosome translocation, 24 cases (15 translocation-positive and 9 translocation-negative) of MALT lymphomas together with 7 follicular lymphomas and 7 mantle cell lymphomas were analysed by Affymetrix gene expression microarray platform. Unsupervised clustering showed that cases of MALT lymphoma were clustered as a single branch. However, within the MALT lymphoma group, translocation-positive cases were intermingled with translocation-negative cases. Gene set enrichment analysis (GSEA) of the NF-κB target genes and 4394 additional gene sets covering various cellular pathways, biological processes and molecular functions showed that translocation-positive MALT lymphomas were characterized by an enhanced expression of NF-κB target genes, particularly *TLR6*, *CCR2*, *CD69* and *BCL2*, while translocation-negative cases were featured by active inflammatory and immune responses, such as *IL8*, *CD86*, *CD28* and *ICOS*. Separate analyses of the genes differentially expressed between translocation-positive and negative cases and measurement of gene ontology term in these differentially expressed genes by hypergeometric test reinforced the above findings by GSEA. The differential expression of these NF-κB target genes between MALT lymphoma with and without translocation was confirmed by quantitative RT-PCR and immunohistochemistry or Western blot.

Expression of TLR6, in the presence of TLR2, enhanced both API2-MALT1 and BCL10 mediated NF- κ B activation *in vitro*. In addition, there was cooperation between expression of BCL10, MALT1 or API2-MALT1, and stimulation of the antigen receptor or CD40 or TLR in NF- κ B activation as shown by both reporter assay and I κ B α degradation. Interestingly, expression of BCL10 but not API2-MALT1 and MALT1, in the presence of LPS stimulation, also triggered I κ B β degradation, suggesting activation of different NF- κ B dimers between these oncogenic products.

Study by co-immunoprecipitation showed that BCL10 directly interacts with MALT1. Sub-cellular localisation experiments in BJAB B-cells, showed that BCL10 localisation was affected by MALT1. When BCL10 was over-expressed, the protein was predominantly expressed in the nuclei, but when MALT1 was over-expressed, BCL10 was mainly localised in the cytoplasm. When both BCL10 and MALT1 were over-expressed, BCL10 was expressed in the cytoplasm in the early hours when the protein level was low, but in both the cytoplasm and nuclei after 9 hours when the protein level was high. Over-expression of API2-MALT1 did not show any apparent effect on BCL10 sub-cellular localisation *in vitro*.

Finally, comparison of MALT lymphoma expression microarray with other lymphomas showed *lactoferrin* to be highly expressed in MALT lymphoma. This was confirmed by qRT-PCR, showing *lactoferrin* to be significantly over-expressed in MALT lymphoma compared to FL and MCL. Thus *lactoferrin* may be a potential marker for MALT lymphoma.

Publications

- 1) Rosebeck S, Madden L, Jin X, Gu S, Apel IJ, Appert A, **Hamoudi RA**, Noels H, Sagaert X, Van Loo P, Baens M, Du MQ, Lucas PC, McAllister-Lucas LM
Cleavage of NIK by the API2-MALT1 fusion oncoprotein leads to noncanonical NF-kappaB activation.
Science. 2011 Jan 28;331(6016):468-472. Thesis page: 318 - 349

- 2) **Hamoudi RA**, Appert A, Ye H, Ruskone-Fourmestraux A, Streubel B, Chott A, Raderer M, Gong L, Wlodarska I, De Wolf-Peeters C, MacLennan KA, de Leval L, Isaacson PG, Du MQ.
Differential expression of NF-kappaB target genes in MALT lymphoma with and without chromosome translocation: insights into molecular mechanism.
Leukemia. 2010 Aug;24(8):1487-1497. Thesis page: 350 - 387

- 3) Chanudet E, Huang Y, Ichimura K, Dong G, **Hamoudi RA**, Radford J, Wotherspoon AC, Isaacson PG, Ferry J, Du MQ.
A20 is targeted by promoter methylation, deletion and inactivating mutation in MALT lymphoma.
Leukemia. 2010 Feb;24(2):483-487. Thesis page: 388 - 392

- 4) Chanudet E, Ye H, Ferry J, Bacon CM, Adam P, Müller-Hermelink HK, Radford J, Pileri SA, Ichimura K, Collins VP, **Hamoudi RA**, Nicholson AG, Wotherspoon AC, Isaacson PG, Du MQ.
A20 deletion is associated with copy number gain at the TNFA/B/C locus and occurs preferentially in translocation-negative MALT lymphoma of the ocular adnexa and salivary glands.
Journal of Pathology. 2009 Feb;217(3):420-30. Thesis page: 393 - 404

- 5) Chanudet E, Zhou Y, Bacon CM, Wotherspoon AC, Müller-Hermelink HK, Adam P, Dong HY, de Jong D, Li Y, Wei R, Gong X, Wu Q, Ranaldi R, Goteri G, Pileri SA, Ye H, **Hamoudi RA**, Liu H, Radford J, Du MQ.
Chlamydia psittaci is variably associated with ocular adnexal MALT lymphoma in different geographical regions.
Journal of Pathology. 2006 Jul;209(3):344-51. Thesis page: 405 - 412

- 6) Zhou Y, Ye H, Martin-Subero JI, **Hamoudi R**, Lu YJ, Wang R, Siebert R, Shipley J, Isaacson PG, Dogan A, Du MQ.
Distinct comparative genomic hybridisation profiles in gastric mucosa-associated lymphoid tissue lymphomas with and without t(11;18)(q21;q21).
British Journal of Haematology. 2006 Apr;133(1):35-42. Thesis page: 413 - 420
- 7) Ye H, Gong L, Liu H, **Hamoudi RA**, Shirali S, Ho L, Chott A, Streubel B, Siebert R, Gesk S, Martin-Subero JI, Radford JA, Banerjee S, Nicholson AG, Ranaldi R, Remstein ED, Gao Z, Zheng J, Isaacson PG, Dogan A, Du MQ.
MALT lymphoma with t(14;18)(q32;q21)/IGH-MALT1 is characterized by strong cytoplasmic MALT1 and BCL10 expression.
Journal of Pathology. 2005 Feb;205(3):293-301. Thesis page: 421 - 429
- 8) Liu H, **Hamoudi RA**, Ye H, Ruskone-Fourmesttraux A, Dogan A, Isaacson PG, Du MQ.
t(11;18)(q21;q21) of mucosa-associated lymphoid tissue lymphoma results from illegitimate non-homologous end joining following double strand breaks.
British Journal of Haematology. 2004 May;125(3):318-329. Thesis page: 430 - 441
- 9) **Hamoudi, RA**, Johnston, S, Hutchinson, G, D'Errico, J.
High throughput methods for gene identification, cloning and functional genomics using the GeneTAC G3 robotics workstation.
Journal of the Association for Laboratory Automation. 2002 Nov;7(5):53-59.
Thesis page: 442 - 448
- 10) Liu H, Ye H, Ruskone-Fourmesttraux A, De Jong D, Pileri S, Thiede C, Lavergne A, Boot H, Caletti G, Wündisch T, Molina T, Taal BG, Elena S, Thomas T, Zinzani PL, Neubauer A, Stolte M, **Hamoudi RA**, Dogan A, Isaacson PG, Du MQ.
T(11;18) is a marker for all stage gastric MALT lymphomas that will not respond to H. pylori eradication.
Gastroenterology. 2002 May;122(5):1286-1294. Thesis page: 449 - 457
- 11) Liu H, Ye H, Dogan A, Ranaldi R, **Hamoudi RA**, Bearzi I, Isaacson PG, Du MQ.
T(11;18)(q21;q21) is associated with advanced mucosa-associated lymphoid tissue lymphoma that expresses nuclear BCL10.
Blood. 2001 Aug 15;98(4):1182-1187. Thesis page: 458 - 463
- 12) Liu H, Ruskon-Fourmesttraux A, Lavergne-Slove A, Ye H, Molina T, Bouhnik Y, **Hamoudi RA**, Diss TC, Dogan A, Megraud F, Rambaud JC, Du MQ, Isaacson PG.
Resistance of t(11;18) positive gastric mucosa-associated lymphoid tissue lymphoma to Helicobacter pylori eradication therapy.
Lancet. 2001 Jan 6;357(9249):39-40. Thesis page: 464 - 465

Acknowledgements

Many people have provided me with invaluable encouragement and moral support, throughout the course of carrying out work for this thesis which turned out to be a most difficult time, characterised by changing laboratories, war, deaths and illnesses within my family requiring me to put extra effort to focus on the work done for this thesis.

In particular, I would like to thank the following:

Professor Ming Du, who has provided excellent supervision, generous support and constructive criticisms throughout my time in his laboratory, and who has also kept me motivated through periods of personal difficulties and at times slow progress due to lack of samples. Thank you.

Dr Hongtao Ye for assistance with immunohistochemistry.

Dr Alex Appert for assistance with generation of stable inducible cell lines.

Dr. Liping Gong for assistance with microdissection of MALT lymphoma cases and expertise in the pathology of MALT lymphoma

I would like to thank also our many collaborating pathologists who provided samples on which this work was conducted and in particular: Professor PG Isaacson (University College, London, UK) and Professor Laurence de Leval (University Institute of Pathology, Centre Hospitalier Universitaire Vaudois, Lausanne, Switzerland).

I would also like to thank Dr Ian McFarlane at the Institute of Metabolic Science, Addenbrooke's Hospital for allowing me to use his laboratory to carry out Affymetrix gene expression microarray experiments.

Dr Hongxiang Liu and Dr. Jim Watkins for stimulating discussions.

Dr. Connie Parkinson, Dr. Tim Diss, Dr. Estelle Chanudet, my uncle Mr. Mohammad Rifaat and Professor Dennis Wright for help in critically reading the thesis. Dr. Alex Freeman and Mr. Keith Miller for their support throughout the period of the thesis.

I would like to thank my wife Kamile for her patience and endless support for my work and putting up with the loneliness and emptiness in her life whilst I was working on this thesis. Çok teşekkür ederim.

Finally, I would like to dedicate this thesis to my wife and to all those who are about to give up on a difficult problem. This thesis is the proof that if you persevere long enough with a difficult problem, eventually a solution will be found.

CHAPTER 1 – General introduction

1.1 Brief overview of lymphomas

Lymphoma is defined as a neoplastic proliferation of lymphoid cells. 90% of all lymphoid malignancies are of B-cell lineage, whilst a minority are of T-cell (7%) or NK-cell lineage (<2%). In 1832 Thomas Hodgkin first described what became known as Hodgkin lymphoma. Hodgkin lymphoma (HL) accounts for approximately 30% of all lymphomas and comprises 2 distinct disease entities, the more frequent classical Hodgkin lymphoma (cHL) (95%) and the uncommon nodular lymphocyte predominant Hodgkin lymphoma (NLPHL) (5%). In cHL, the neoplastic cells are usually a minority population whose survival appears to be dependent on the majority of reactive or inflammatory cells (Aldinucci *et al*, 2010). In the majority of cases the neoplastic (Reed-Sternberg (Reed, 1902)) cells appear to be of B-cell origin. NLPHL is characterised by lymphocytic and histocytic (L&H) or “popcorn” cells in that are distributed amidst abundant non-neoplastic inflammatory and accessory cells.

Approximately 70% of lymphomas do not have the clinical and pathological features of HL and have therefore been categorised historically as non-Hodgkin lymphomas (NHL). NHL are frequently disseminated and are all considered malignant or potentially malignant. Some are aggressive from the outset, while others are indolent for varying lengths of time, but may transform to more aggressive tumours. According to the World Health Organisation (WHO) 2008 classification (Swerdlow *et al*, 2008), these lymphoid neoplasms which together account for the majority of lymphomas are classified as distinct disease entities under the broader categories of precursor lymphoid neoplasms, mature B-cell neoplasms, mature T and NK-cell neoplasms, immunodeficiency-associated lymphoproliferative disorders and histocytic and dendritic cell neoplasms.

Most NHLs are mature B-cell neoplasms corresponding to a clonal proliferation of B cells at various stages of differentiation. They can be categorised into pre-germinal, germinal and post-germinal centre origin according to their differentiation stage using the germinal centre reaction as a reference. The most common type of NHL is diffuse large B-cell lymphoma (DLBCL) which represents 37% of all NHL and consists of a heterogeneous group of large B-cell tumours (Swerdlow *et al*, 2008), followed by follicular lymphoma (FL) which represents 29% of all NHL and is characterised by clonal expansion of neoplastic follicle centre-type cells. The third most frequent subtype of B-cell NHL is chronic lymphocytic leukaemia/small lymphocytic lymphoma (12%), followed closely by extranodal marginal zone lymphoma of mucosa associated lymphoid tissue (MALT lymphoma) which accounts for 9% of all B-cell lymphomas. Both MALT and follicular lymphomas may transform to a high grade lymphoma, most frequently diffuse large B-cell lymphoma. Nodal marginal zone (MGZ) lymphoma and splenic MGZ lymphomas are separate rare entities that involve lymph nodes (nodal MGZ lymphoma) and spleen usually with bone marrow and blood involvement (splenic MGZ lymphoma) respectively (Swerdlow *et al*, 2008).

MALT lymphoma can occur in a wide range of organs (Swerdlow *et al*, 2008). Amongst the various extranodal sites, gastric MALT lymphoma is the most common and thus the best characterised form of this disease (Du & Isaccson, 2002). Nodal MZL may be seen as an apparently primary disease as a result of either splenic MZL or extranodal MZL.

1.2 Overview of MALT lymphoma

MALT (Mucosa associated lymphoid tissue) lymphoma is an indolent neoplasm where tumours tend to stay localised at their site of origin until the late phase of the disease. It occurs at various extra-nodal sites. The most common site is the gastrointestinal (GI) tract, comprising 50% of all cases, and within the GI tract, the stomach is the most common location accounting for 85% of GI MALT lymphomas. The small intestine is typically involved in patients with immunoproliferative small intestinal disease (IPSID). Other frequent sites include salivary gland, lung, ocular adnexa, skin, thyroid and breast (Swerdlow *et al*, 2008). Apart from the small intestine, these anatomical sites are normally devoid of organised lymphoid tissues, thus MALT lymphoma appears to arise from acquired MALT, commonly due to chronic immunological stimulation, resulting either from pathogen infection or autoimmune disorders (Du, 2007). Patients generally present with MALT lymphoma at stages I or II. The average age of disease onset is 61 and the 5-year survival rate of patients has been as high as 93% in some studies. The median time before progression of the disease is approximately 5 years although it is significantly longer for cases with a gastrointestinal origin compared to those from other sites (Thieblemont *et al*, 1997). 2-20% of patients have bone marrow involvement and up to 10% have lymphoma in multiple extra-nodal sites (Isaacson & Spencer, 1987; Wotherspoon *et al*, 1993), but they generally respond well to therapy and have a good overall prognosis (Fischbach *et al*, 2007).

1.2.1 Aetiology of MALT lymphoma

As mentioned in section 1.2, pathogen infection and autoimmune disorders play a major role in the development of MALT lymphoma. In this section, the aetiological role of pathogens such as *Helicobacter pylori*, *Campylobacter jejuni*, *Borrelia burgdorferi* and *Chlamydia*

psittaci and autoimmune disorders such as Sjögren's syndrome and Hashimoto's thyroiditis will be discussed.

1.2.1.1 Chronic infection

It has been shown that infection with certain microorganisms leads to the acquisition of lymphoid tissue at extra nodal sites that are normally devoid of any organised lymphoid tissues and hence plays a role in MALT lymphoma development (Banks, 2007).

Helicobacter pylori

In 1984 Marshall and Warren isolated a newly recognised bacterium, *Helicobacter pylori*, from patients with chronic gastritis and gastric ulcer (Marshall & Warren, 1984). *H. pylori*, originally called *Campylobacter pylori*, is a unipolar, multiflagellate spiral shaped, microaerophilic, gram negative bacterium that lives in the luminal surface of the stomach and duodenum (Bolin *et al*, 1995). *H. pylori* is widespread and has been implicated in several gastrointestinal diseases, such as chronic gastritis and peptic ulcer, (Howden & Hunt, 1998) gastric adenocarcinoma, (Asaka *et al*, 1997) and MALT lymphoma (Hussell *et al*, 1993b).

In 1987, Smith *et al.* showed monoclonal rearrangements of the Ig-heavy chains in IPSID, including cases that responded to antibiotics (Smith *et al*, 1987), and suggested the possible involvement of bacteria-driven antigen stimulation in the development of the lymphoma. Subsequent studies established that, in the stomach, MALT is acquired as a result of colonisation of the gastric mucosa by *H. pylori* (Stolte *et al*, 2002; Wotherspoon *et al*, 1991). In 1991, Wotherspoon *et al.* demonstrated the presence of *H. pylori* in 101 of 110 (92%) patients with gastric MALT lymphoma (Wotherspoon *et al*, 1991) and suggested for the first time that gastric MALT lymphoma may develop from the MALT acquired in response to *H. pylori* infection.

At least 80-90% of patients with gastric MALT lymphoma are infected with *H. pylori*, which is much higher than the frequency of infection in the rest of the population (Wotherspoon *et al*, 1991). The gastric mucosa is a hostile environment to most organisms due to its acidic environment. However, *H. pylori* secretes urease that raises the local pH so it is able to survive and colonise the gastric mucosa. The incidence of gastric MALT lymphoma was found to be high in North Eastern Italy where *H. pylori* infection is prevalent (Doglioni *et al*, 1992).

Campylobacter jejuni and *Borrelia burgdorferi*

These were shown to be associated with a proportion of primary cutaneous MALT lymphoma and IPSID respectively (Cerroni *et al*, 1997; Lecuit *et al*, 2004).

Chlamydia psittaci

Chlamydia psittaci (*C. psittaci*) infection was recently shown to be associated with the development of ocular adnexal MALT lymphoma. In Italian studies, *Chlamydia psittaci* was detected in 80% of these lymphomas (Ferreri *et al*, 2004). However, the association between *Chlamydia psittaci* and ocular adnexal MALT lymphoma was not reproduced by several other studies from the USA (Vargas *et al*, 2006), Japan (Daibata *et al*, 2006) and the Netherlands (Mulder *et al*, 2006). Subsequently, Chanudet and co-workers confirmed geographical variation in the association between *Chlamydia psittaci* and ocular adnexal MALT lymphoma (Chanudet *et al*, 2006).

Further investigations are needed to confirm or refute the causal association between the organisms described above and extranodal marginal zone lymphoma at various sites.

1.2.1.2 Autoimmune disease

In addition to microbial infections discussed in section 1.2.1.1, autoimmune disease plays a role in MALT lymphomagenesis. For example, thyroid MALT lymphoma is associated with Hashimoto's thyroiditis and salivary gland MALT lymphoma is associated with lymphoepithelial sialadenitis (Kassan *et al*, 1978;Kato *et al*, 1985). Patients with Sjögren's syndrome, and a number of other autoimmune disorders such as rheumatoid arthritis show an increased risk of lymphoma development (Smedby *et al*, 2006). These autoimmune diseases result in chronic immune responses and the formation of acquired MALT. Patients with these diseases are approximately 40 times more likely to develop lymphoma, and 85% of the lymphomas developed are MALT lymphoma (Kassan *et al*, 1978;Talal *et al*, 1967). In both Hashimoto thyroiditis and Sjögren's syndrome, lymphomagenesis is thought to be mediated by sustained T-cell dependent antigenic stimulation, similarly to that in *H. pylori*-driven gastric MALT lymphoma (Yamamoto, 2003).

1.2.2 Histopathology of MALT lymphoma

Since the development of MALT lymphoma relies on the acquisition of organised MALT, it is best to describe MALT followed by MALT lymphoma.

1.2.2.1 Mucosa associated lymphoid tissue

The mucosa-associated lymphoid tissue is situated within mucosal tissues. The main function of MALT is to prevent foreign antigen invasion from the mucosal sites. In response to antigen specific T-cell activation, naïve B cells undergo clonal expansion, differentiation and become effector cells secreting immunoglobulins, thus conveying the mucosal immune response. Native MALT is found in the gastrointestinal tract where it is abundantly present in the Peyer's patches of terminal ileum (Figure 1.1a). Typically, MALT in the Peyer's patches consists of germinal centres where B cells encounter antigens and undergo a series of mutations to enhance their antigen specificity. Germinal centres contain activated B cells, named centroblasts, as well as their differentiated counterpart expressing immunoglobulins called centrocytes, macrophages and follicular dendritic cells essential to germinal centre reactions. The germinal centre is surrounded by a follicular mantle, formed by naïve B cells not yet exposed to antigen. Outer to the mantle zone is a marginal zone, where memory B cells reside. A distinct marginal zone, although a feature of Peyer's patches is not present in human tonsillar tissue, and therefore not universally present in all MALT. However, there is evidence to show that intra-epithelial B-cells in tonsillar tissue could represent the equivalent of marginal zone B cells (Morente *et al*, 1992).

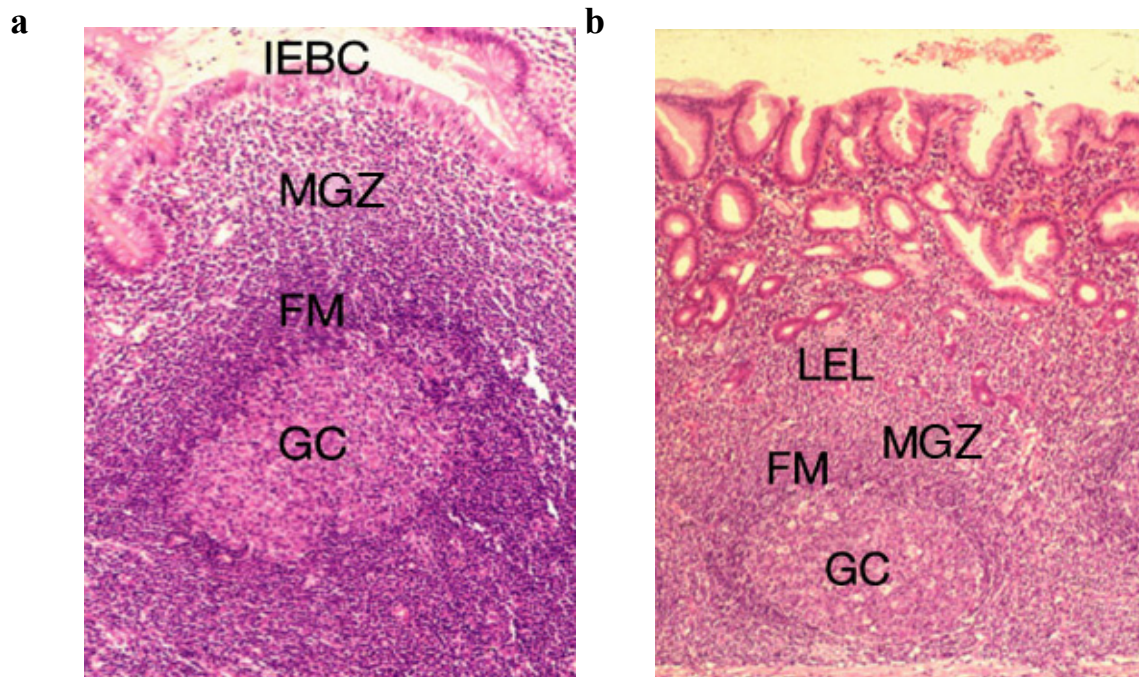


Figure 1.1 - Morphology of MALT and gastric MALT lymphoma from the gastrointestinal tract.

a. The Peyer's patches are characterised histologically by the presence of a germinal centre (GC) surrounded by a follicular mantle (FM) and a marginal-zone (MGZ). Intraepithelial marginal-zone B cells (IEBC) are observed within the epithelium covering the Peyer's patch, forming the lymphoepithelium characteristic of MALT.

b. The morphology of gastric MALT lymphoma. The germinal centre (GC), where B cells proliferate and mature following antigen stimulation, is surrounded by a follicular mantle (FM), which comprises naive B cells. The reactive B-cell follicle is surrounded by neoplastic marginal-zone (MGZ) B cells that infiltrate the neighbouring epithelium forming characteristic lymphoepithelial lesions (LEL).

Figure adapted from Isaacson *et al.* (2004). Nature Review Cancer, 4, 644-653.

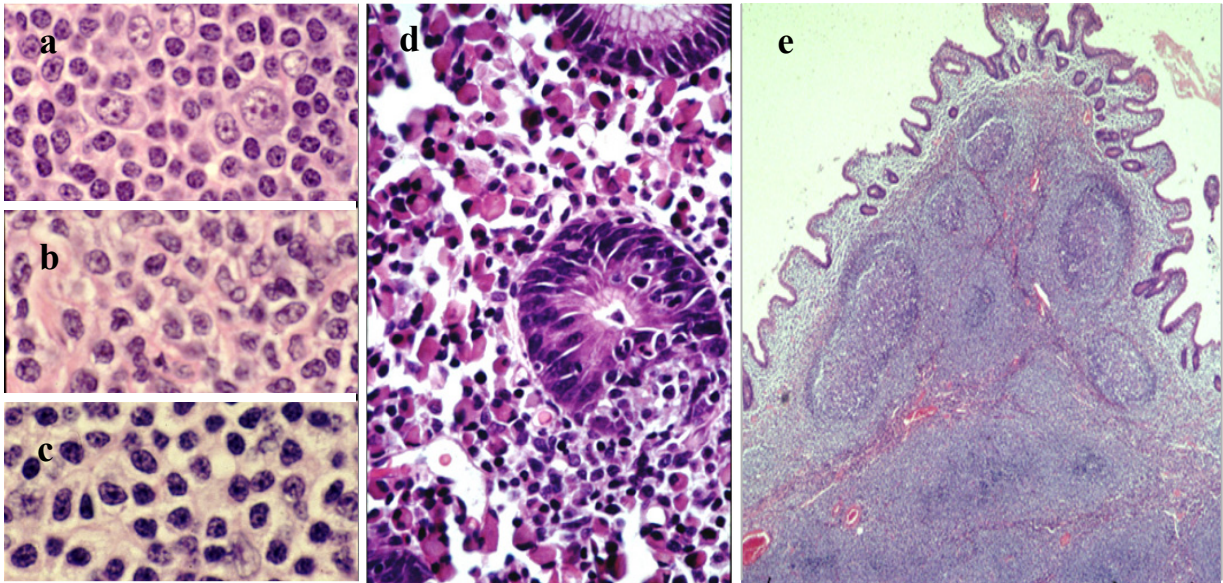


Figure 1.2 - Cytological and histological features of MALT lymphoma.

a-c. Cytology: neoplastic cells can resemble small lymphocytes (a), or have the appearance of centrocytes but with more abundant cytoplasm (b), or rather have the features of monocytoid cells with abundant pale cytoplasm and well-defined borders (c). Scattered transformed centroblasts or immunoblast-like cells can also be observed (a). **d-e.** Histological features: MALT lymphoma can show prominent plasma cell differentiation (d). The neoplastic cells can infiltrate the surrounding epithelium, forming lymphoepithelial lesions (d), or invade B-cell reactive follicles (follicular colonisation) (e).

Figure adapted from Isaacson *et al.* (2005). *Journal of Pathology*, 205, 255-274.

1.2.2.2 Extranodal marginal zone B-cell lymphoma of MALT

Histologically, MALT lymphoma mimics the features of normal MALT (Figure 1.1b). The striking histological resemblance between some low grade B-cell lymphomas of the stomach, IPSID and the morphology of the Peyer's patches which led to the proposition of the MALT lymphoma entity by Isaacson and Wright in 1983 (Isaacson & Wright, 1983). Similar to the structure of Peyer's patches, MALT lymphoma consists of neoplastic B-cell infiltrates that are primarily located in the marginal zone (which lies outer to the mantle zone that surrounds reactive germinal centres) and can extend into the interfollicular region (Figure 1.1b). An important feature of MALT lymphoma is the presence of aggregates of neoplastic cells

infiltrating individual mucosal glands or other epithelial structures. Such aggregates, referred to as lymphoepithelial lesions (Figure 1.1b, Figure 1.2d), resemble lymphoepithelium in Peyer's patches (Figure 1.1b) (Isaacson & Du, 2004).

Cytologically, MALT lymphoma cells are variable in their appearance, resembling centrocyte-like cells, sometimes with round nuclei and pale staining cytoplasm, monocytoid B cells or small lymphocytes (Figure 1.2 a-c). Lymphoma cells may also show prominent plasma cell differentiation particularly in the sub-epithelial lamina propria (Figure 1.2d). In some cases the lymphoma cells may invade B-cell reactive follicles (Figure 1.2e). This so-called follicular colonisation can lead to morphological resemblance to FL.

1.2.3 Immunophenotype

The typical immunophenotype of MALT lymphoma is detailed in Table 1.1. MALT lymphoma cells mostly share the immunophenotype of non-neoplastic MGZ cells (Isaacson & Spencer, 1987). Currently there is no available marker specific to MALT lymphoma, nevertheless immunophenotyping is helpful for the differential diagnosis, notably from other small B-cell lymphomas (Table 1.1).

Table 1.1 - Typical immunophenotyping of MALT lymphoma cells.

| Cellular marker | MALT lymphoma | FL | MCL | SLL | DLBCL |
|-----------------------|---------------|-------|-----|-----|----------|
| CD20 | + | + | + | + | + |
| CD79a | + | + | + | + | + |
| BCL2 | +/- | + | + | + | +/- |
| CD43 | +/- | - | + | + | |
| CD5 | - | - | + | + | +/- |
| CD10 | - | + | - | - | +/- |
| CD23 | - | +/- | - | +/- | |
| Cyclin D1 | - | - | + | - | |
| BCL6 | - | + | - | - | +/- |
| Ig heavy chain | M>>A>G | G>M+D | M+D | M | Variable |
| CD21 and FDC meshwork | + | + | +/- | - | - |

Abbreviations: MALT, mucosa-associated lymphoid tissue; FL, follicular lymphoma; MCL, mantle-cell lymphoma; SLL, small lymphocytic lymphoma; DLBCL, diffuse large B-cell lymphoma; CD, cluster of differentiation; FDC, follicular dendritic cell; + positive; - negative.

The neoplastic cells of MALT lymphoma share the cytological features and immunophenotype (CD20⁺, IgM⁺, IgD⁻) of marginal zone B cells (Spencer *et al*, 1985). MALT lymphoma cells are typically negative for CD10 and BCL6, which are characteristically positive in FL. Unlike mantle cell lymphoma (MCL) and small lymphocytic lymphoma, MALT lymphoma is only infrequently positive for CD5. It is negative for cyclin D1, a feature which helps to distinguish it from MCL (Table 1.1). The most important immunophenotypic feature favouring MALT lymphoma diagnosis is the presence of a diffuse infiltrate of CD20⁺, IgM⁺, IgD⁻ B cells outside the mantle zone of reactive follicles. Once the marginal zone phenotype is established, light chain restriction in this marginal zone population, or if present, within the plasma cells confirms the diagnosis. However, having a marker specific for MALT lymphoma would lead to more accurate MALT lymphoma diagnosis.

1.2.4 Pathogenesis of MALT lymphoma

The development of MALT lymphoma is a multistage process which is best understood in the gastric disease (Isaacson & Norton, 1994; Isaacson & Spencer, 1995; Isaacson, 1995). Both gastric MALT lymphoma and pre-lymphomatous lesions are aetiologically related to *H. pylori* infection. Understanding the role of *H. pylori* has provided insights into the pathogenesis of MALT lymphoma.

1.2.4.1 H. pylori and its role in the development of gastric MALT lymphoma

There is now strong evidence that *H. pylori* is causally linked to gastric MALT lymphoma and this fulfils all criteria of Koch's postulates set in 1884 (Koch, 1884); Firstly, *H. pylori* was found in the majority of gastric MALT lymphomas (Eidt *et al*, 1994). Secondly, *H. pylori* could be isolated from gastric MALT lymphoma, and grown in culture. Thirdly, infecting the stomach of pathogen-free mice with *H. pylori* could induce the development of MALT lymphoma (Enno *et al*, 1995).

Additionally, early functional and clinical studies provided evidence of the crucial role of *H. pylori* in the development of gastric MALT lymphoma. Hussell and colleagues demonstrated that lymphoma cell growth *in vitro* was dependent on *H. pylori* specific T cells (Hussell *et al*, 1996). Furthermore, Wotherspoon and colleagues first showed that *H. pylori* eradication by antibiotic treatment led to lymphoma regression in *H. pylori*-associated gastric MALT lymphomas (Wotherspoon *et al*, 1991). Taken together, these data established that *H. pylori* infection could cause gastric MALT lymphoma.

It is now known that the inflammatory process triggered by *H. pylori* infection is directly responsible not only for the acquisition of MALT in the gastric mucosa, but also for subsequent malignant transformation and the development of gastric MALT lymphoma

(Isaacson & Du, 2004). As in other bacterial diseases, the development of *H. pylori*-associated MALT lymphoma is hypothesised to be associated with the host response and bacterial status. However, the precise role of *H. pylori* in MALT lymphomas is not clear.

1.2.4.2 Immunological stimulation

Several histological features of MALT lymphoma including the presence of plasma-cell differentiation, blasts, follicular colonisation and proliferation, suggest that MALT lymphoma cells preserve B-cell properties and that their growth may be partially driven by antigenic stimulation via antigen receptors (Isaacson & Du, 2004) and T-cell and B-cell interaction. Recent studies indicate that both direct and indirect antigen stimulation mechanisms are involved.

1.2.4.2.1 Direct antigen stimulation

MALT lymphomas invariably express surface immunoglobulin. The anti-idiotypic antibody has been shown to stimulate MALT lymphoma cell proliferation and synergise with mitogen stimulation (Hussell *et al*, 1993b). The data also showed that the tumour-derived immunoglobulin does not recognise *H. pylori*, but recognises various autoantigens (Hussell *et al*, 1993a). Antibodies to gastric epithelial cells are commonly present in serum samples from patients with *H. pylori* gastritis (Negrini *et al*, 1996). An anti-idiotypic antibody to immunoglobulin of a gastric MALT lymphoma cross-reacts specifically with reactive B cells in *H. pylori*-associated gastritis (Greiner *et al*, 1997). These findings suggest that gastric MALT lymphoma cells are transformed from autoreactive B cells, which are induced after *H. pylori* infection.

Sequence analysis of the rearranged *immunoglobulin* of MALT lymphoma also reveals evidence that MALT lymphoma cells respond to direct antigen stimulation, indicating the

tumour clone has undergone antigen selection (Bertoni *et al*, 1997;Du *et al*, 1996b). During the evolution of gastric MALT lymphoma, particularly in the early stage, the rearranged tumour immunoglobulin gene frequently showed further somatic mutations, commonly referred to as ongoing mutations (Bertoni *et al*, 1997;Du *et al*, 1996a). Since somatic mutations occurs in the rearranged immunoglobulin gene only during the germinal centre reaction, and depends on antigen and T cells, the finding of ongoing immunoglobulin mutations in MALT lymphoma suggests that tumour-cell growth is partially driven by direct antigen stimulation.

1.2.4.2.2 Indirect antigen stimulation

The close association of *H. pylori* infection with gastric MALT lymphoma development prompted research into the immunological responses of the tumour cells to *H. pylori*. By co-culturing tumour cells with 13 clinical strains of heat-killed *H. pylori*, Hussell and co-workers demonstrated that *H. pylori* induced tumour cells to proliferate (Hussell *et al*, 1993b). The effect was strain-specific but was T-cell mediated and not due to specificity of lymphoma cells for *H. pylori* antigens. This effect was associated with expression of interleukin-2 (IL-2) receptors and secretion of immunoglobulin by tumour cells. Removal of tumour-infiltrating T cells before the experiment abolished all the effects of *H. pylori* on tumour cells. Furthermore, these authors confirmed that *H. pylori* did not directly stimulate tumour cells but did so via specifically activated tumour infiltrating T cells (Hussell *et al*, 1996). Furthermore, the stimulating effect of *H. pylori* on tumour B cells can be completely blocked by an antibody to CD40L. Thus, *H. pylori* stimulates lymphoma B cells through tumour-infiltrating T cells, involving CD40 and CD40L. It is possible that CD80/CD86 costimulatory molecules promote T-cell-mediated neoplastic B-cell growth.

The active role of tumour-infiltrating T cells in the growth of tumour B cells is further supported by a study of T-cell clones isolated from gastric MALT lymphoma. T-cell clones responding to *H. pylori* stimulation were CD4-positive helper cells rather than CD8-positive cytotoxic cells. These specific T-cell clones activated tumour B cells in a dose dependent manner (D'Elis *et al*, 1997).

Additionally, complete regression of gastric MALT lymphoma following *H. pylori* eradication strongly indicates the role of *H. pylori* stimulation in the survival and growth of gastric MALT lymphoma (Begum *et al*, 2000; Wotherspoon, 1996). Unlike low-grade tumour cells, high-grade tumour cells do not show any growth response to *H. pylori* mediated T-cell stimulation *in vitro* (Hussell *et al*, 1993b). High grade lymphomas tend to be resistant to *H. pylori* eradication therapy (Bayerdorffer *et al*, 1995; Thiede *et al*, 1997), though recently published reports show a complete remission rate of 62.5% with a median follow-up of over 30 months in gastric DLBCLs (Chen *et al*, 2001; Morgner *et al*, 2001).

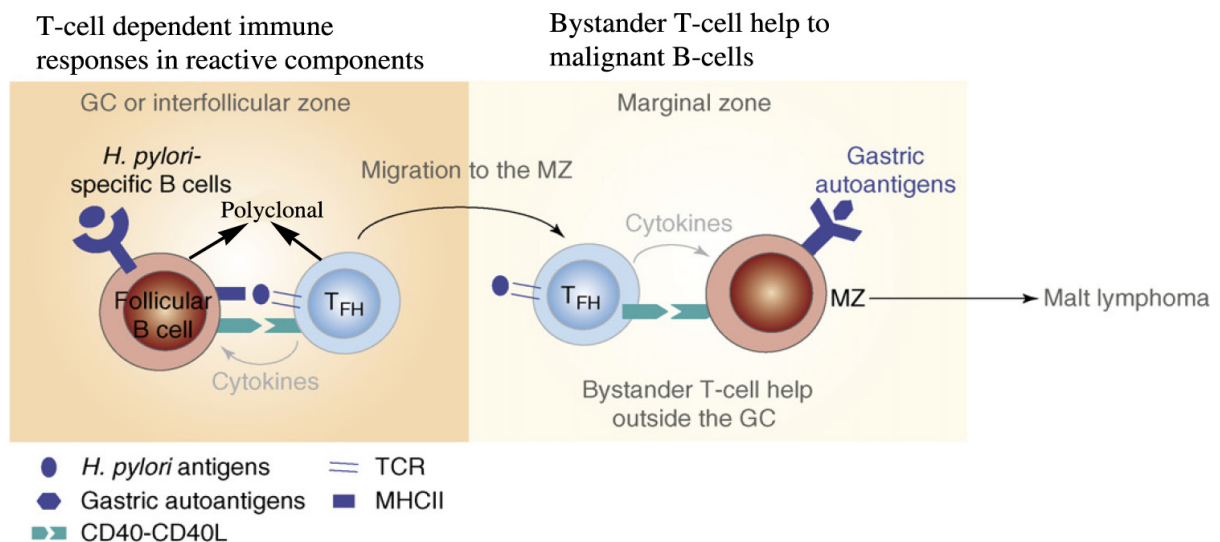


Figure 1.3 - The role of T- and B- cell interaction in the development of MALT lymphoma.

FH: Follicular Helper cells, TCR: T-cell receptor, MZ: marginal zone.

Figure adapted from Roulland *et al*. (2008). Trends in Immunology, 29, 25-33.

Therefore, it can be hypothesised that in MALT lymphomas, cells are autoreactive and can be stimulated at low levels by autoantigens, but additional stimuli are required for their enhanced proliferation and ultimate malignant transformation. In gastric MALT lymphoma, *H. pylori* infection may cause two main events. Firstly, T-cell dependent immune responses in reactive components lead to the generation of a sustained pool of polyclonal *H. pylori*-specific T cells. Secondly, these *H. pylori* specific T cells in the marginal zone containing tumour cells provide non-cognate bystander T-cell help to the autoreactive MALT lymphoma cells (Figure 1.3). This working hypothesis explains how polyclonal *H. pylori* specific T cells can be critical for the growth and survival of monoclonal neoplastic B cells, which recognise autoantigens rather than *H. pylori*.

1.2.4.3 H. pylori virulent factors and host genetics in the development of gastric MALT lymphoma

The fact that the a majority of patients infected with *H. pylori* are asymptomatic and only a small proportion of them develop gastric MALT lymphoma, indicates a role of bacterial virulence factors and host genetic susceptibility. The interaction between the bacterium and the host immune reaction may determine the risk of MALT lymphoma development.

1.2.4.3.1 Host factors

A number of gene polymorphisms are associated with susceptibility to autoimmune disorders (Lettre & Rioux, 2008) and some have been shown to be associated with MALT lymphoma development. Polymorphisms in immune regulators such as cytokines are commonly involved in auto-reactive conditions (Hajeer & Hutchinson, 2000). A recent large case control study on 1172 patients with NHL and 982 population-based controls demonstrated a significantly higher susceptibility to NHL among patients with an autoimmune disorder and

TNFA (tumour necrosis factor A) G308A variant, or *interleukin 10 (IL10)* T3575A variant (Wang *et al*, 2007). *TNFA* G308A polymorphism associates with higher levels of *TNFA* expression which enhances chronic inflammatory responses (Bayley *et al*, 2004). Among NHLs, *TNFA* G308A polymorphism particularly increases the risk of several lymphoma subtypes, including MALT lymphoma and DLBCLs (Morton *et al*, 2008).

A number of other genetic polymorphisms have been investigated, particularly in genes encoding molecules involved in immune or inflammatory responses. For example, gene polymorphisms in *toll-like receptors (TLR)* have been shown to be associated with an increased risk of lymphoma, including MALT lymphoma (Nieters *et al*, 2006). The *TLR4* Asp299Gly variant increases susceptibility to gram-negative bacteria infection, thus potentially representing one of the host factors affecting the risk of lymphoma among *H. pylori* infected individuals (Nieters *et al*, 2006). Likewise, polymorphisms in the T-cell receptor cytotoxic T-lymphocyte antigen 4 (*CTLA4*) gene, encoding a negative regulator of T-cell activation, increase the risk of gastric MALT lymphoma, especially in patients with *H. pylori* infection (Cheng *et al*, 2006).

1.2.4.3.2 Bacterial virulence factors

In addition to host genetic susceptibility, virulence factors associated with infectious agents also play a critical role in the outcome. The risk of developing gastric carcinoma has been shown to depend on the combined effect of pro-inflammatory cytokine gene polymorphisms in the host and virulence-associated genes in *H. pylori* (Figueiredo *et al*, 2002). Several *H. pylori* virulence factors are associated with an increased risk of gastric ulcer and gastric carcinoma (Maeda & Mentis, 2007), especially the cytotoxin-associated antigen (CagA), vacuolating toxin (VacA) and outer membrane adhesion (BabA) virulence factors. CagA

antigens are known to induce a strong inflammatory response. CagA-positive strains contain a long pathogenicity island including over 30 genes (Prinz *et al*, 2003). Such pathogenesis-associated genes are usually absent in *H. pylori* strains isolated from asymptomatic hosts (Baldwin *et al*, 2007). t(11;18)(q21;q21) associated gastric MALT lymphoma cases are significantly associated with infection by CagA strains of *H. pylori* (Ye *et al*, 2003). CagA-positive strains of *H. pylori* are also associated with a strong response mediated by neutrophils. This is thought to increase the release of ROS (reactive oxygen species) within the environment of inflammation, which may not only promote cell growth via activation of kinases (Cerutti & Trump, 1991), but may also contribute to the genomic instability already inherent in B cells. *H. pylori* are strong inducers of interleukin-8, a potent chemokine for neutrophil activation. Activated neutrophils are known to release reactive oxygen species, which can cause a wide range of DNA damage, including double-strand breaks (Wiseman & Halliwell, 1996). *H. pylori* VacA strains can alter intracellular vesicular trafficking, ultimately inducing the formation of large intracellular vacuoles and mediating mucosal damage (Smoot, 1997). BabA strains express the BabA adherence factor that can bind to Lewis blood sugar molecules present on the membrane of gastric epithelial cells. This results in enhanced adhesion and higher colonisation capacity. Nonetheless, no differences in the above *H. pylori* virulent factors have yet been observed between patients with *H. pylori*-associated MALT lymphoma and those with *H. pylori*-induced gastritis (Lehours *et al*, 2004). Virulence factors associated with gastric MALT lymphoma remain largely unknown. Similarly, *C. jejuni* has been shown to produce a toxin that can directly cause DNA damage by inducing double-strand DNA breaks. This may be responsible for the truncated Ig observed in IPSID (Al Saleem & Al Mondhiry, 2005).

1.2.4.4 Role of anti-microbial and other therapies in the treatment of MALT lymphoma

The role of *H. pylori* infection in the development of gastric MALT lymphomas has led to the successful use of antibiotic treatment in the cases localised to the stomach and had a profound implication in the clinical management of MALT lymphoma. Evidence indicates that eradication of *H. pylori* with antibiotics such as metronidazole, tetracycline, clarithromycin and amoxicillin can be effectively employed as the first line therapy of localised gastric MALT lymphoma. *H. pylori* eradication is the primary therapy for stage I gastric MALT lymphoma. Multiple trials carried out in independent reference centres on large cohorts of patients with long follow-up, have demonstrated that complete histological remission can be obtained in roughly 80% of early stage gastric MALT lymphomas following *H. pylori* eradication (Morgner *et al*, 2007). Such a response is durable, as illustrated by the low incidence of lymphoma relapse (3%) at 75 months follow-up after *H. pylori* eradication (Wundisch *et al*, 2005). When they occur, relapses are often due to *H. pylori* re-infection (Fischbach *et al*, 2004;Montalban & Norman, 2006). Presence of histological residual disease or clonal neoplastic cells is seen in gastric biopsies after *H. pylori* eradication. The cells are detected by PCR in a proportion of antibiotic-responsive cases, but are not associated with lymphoma progression, nor with transformation into DLBCL (Fischbach *et al*, 2002;Fischbach *et al*, 2007), supporting a “watch and wait” strategy with regular monitoring instead of a systematic second line treatment.

Overall, about 30% of gastric MALT lymphomas do not respond to *H. pylori* eradication, which suggests the acquisition of an antigen-independent autonomous growth. The majority of the non-responsive cases are at stage II or higher (Ruskone-Fourmestreaux *et al*, 2001), while a high proportion of stage I cases show complete remission following *H. pylori* eradication (Stolte & Eidt, 1989). Resistance to *H. pylori* treatment is mainly accompanied by

the presence of t(11;18)(q21;q21) (Liu *et al*, 2001a;Liu *et al*, 2002b) and infrequently to t(1;14)(p22;q32) (Ye *et al*, 2006). The role of *H. pylori* eradication in the treatment of transformed MALT lymphoma is controversial. Although gastric MALT lymphomas of stage II or higher are less likely to respond to *H. pylori* eradication (Ruskone-Fourmestraux *et al*, 2001;Sackmann *et al*, 1997), antibiotic treatment showed noticeable success in some *H. pylori*-positive cases, particularly those with limited dissemination. If the presence of the bacterium is confirmed, concurrent eradication of *H. pylori* is recommended, along with other treatment approaches, in order to limit the risk of lymphoma relapse (Morgner *et al*, 2007). This strategy also applies to transformed MALT lymphoma. A significant proportion of stage I *H. pylori* positive transformed MALT lymphomas achieve complete lymphoma regression after *H. pylori* eradication (Morgner *et al*, 2007).

MALT lymphoma that is non-responsive to antibiotic therapy can be treated with surgical resection alone or in combination with radiotherapy or chemotherapy. This treatment results in 90-100% 5-year survival for cases at stage I_E and 82% survival at stage II_E (Du & Isaccson, 2002;Schechter & Yahalom, 2000). Unfortunately, partial resection cannot remove all lymphoma cells, as they disseminate widely in the gastric mucosa. To completely remove the lymphoma, a total gastrectomy needs to be carried out which significantly reduces the patient's quality of life (Zucca *et al*, 2000). Low-dose localised radiotherapy can be used alone to treat gastric MALT lymphoma. In a small study, patients with gastric MALT lymphoma with no evidence of *H. pylori* infection or with resistance to antibiotic therapy were treated with radiotherapy alone. 100% event-free survival was achieved by this treatment with a median follow-up time of 27 months (Parveen *et al*, 1993). Other treatments include the use of therapeutic monoclonal antibody drugs such as rituximab. The improvement of some autoimmune conditions following the administration of rituximab leads

to new therapeutic strategies in the treatment of autoimmune-related MALT lymphomas. A phase II clinical trial including patients with salivary gland MALT lymphoma associated with Sjögren's syndrome showed that rituximab could lead to complete remission in 3 out of 7 patients (Pijpe *et al*, 2005). Further investigations are needed, especially as other B-cell targeting therapies are emerging.

The therapeutic model of *H. pylori*-associated gastric MALT lymphoma may be extended to MALT lymphomas of other anatomical locations similarly associated with infectious agents. For example, eradication of *Borrelia burgdorferi* and *Campylobacter jejuni* infections has been shown to result in complete regression of some cases of cutaneous MALT lymphoma and IPSID respectively (Kutting *et al*, 1997; Lecuit *et al*, 2004). Ferreri and colleagues similarly demonstrated lymphoma regression in 13 out of 27 ocular adnexal MALT lymphomas (6 complete and 7 partial regressions) associated with *Chlamydia psittaci* infection, following eradicating antibiotic therapy with doxycycline (Ferreri *et al*, 2006).

1.3 Genetics of MALT lymphoma

1.3.1 Chromosomal translocations

In addition to chronic immune stimulation, which plays an important role in the development of MALT lymphoma particularly at the early stages, the acquisition of genetic abnormalities contributes to both the genesis and the progression of the lymphoma. Four recurrent balanced chromosomal translocations have been described in MALT lymphoma (Du, 2007). Three of the four translocations involve *MALT1* or *BCL10* genes.

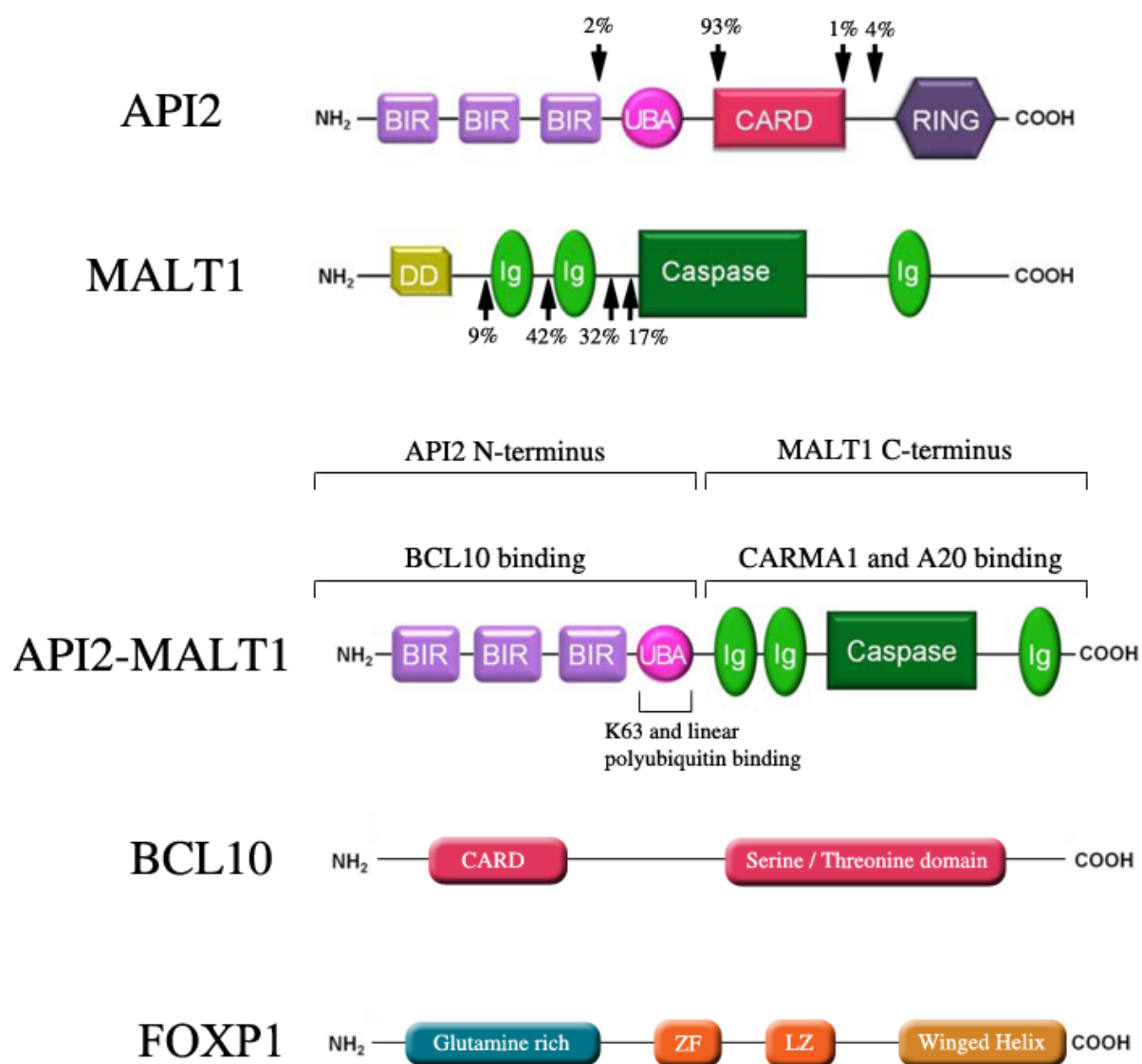


Figure 1.4. Structural domains of the oncogenic products resulting from MALT lymphoma associated chromosomal translocations.

BIR = baculovirus IAP repeats; UBA = ubiquitin associated domain; CARD = caspase associated recruitment domain; RING = really interesting new gene domain; Ig = immunoglobulin-like domain; ZF = zinc finger domain; LZ = leucine zipper domain. Arrows indicate the distribution of sites of fusion between *API2* and *MALT1* in individual MALT lymphomas.

API2 belongs to the inhibitor of apoptosis family and mediates apoptosis suppression by binding caspases via its caspase recruitment domain (CARD). *API2* baculovirus inhibitor of apoptosis protein repeats (BIR) domains can mediate oligomerisation of BIR-domain containing proteins. *MALT1* is a paracaspase. In addition to a caspase-like domain, *MALT1* contains a death domain (DD) and 2 immunoglobulin-like domains (Ig). Although various breakpoints have been reported (Du, 2007), especially within the *MALT1* gene, *API2-MALT1* fusion transcript always contains the 3 intact BIR domains of *API2* and the intact caspase-like domain of *MALT1*, suggesting a role for these domains in oncogenesis. *BCL10* is an intracellular protein with a CARD domain and a serine/threonine-rich domain of unknown function. *FOXP1* is a member of the FOX family of transcription factor containing both DNA-binding domains (zinc finger domains ZF; leucine zipper domain, LZ; winged helix) and protein-protein binding glutamine-rich domains.

1.3.1.1 t(11;18)(q21;q21)/API2-MALT1

t(11;18)(q21;q21) fuses in frame the amino-terminal sequence of the baculovirus inhibitor of apoptosis protein repeats (BIR) containing 3 (*BIRC3*, also known as *API2*) gene (11q21), to the carboxyl-terminal caspase-like domain of the MALT lymphoma translocation gene 1 (*MALT1*) (18q21) (Figure 1.4). *API2* suppresses apoptosis by inhibiting specific caspases via its BIR domains (Roy *et al*, 1997). *MALT1* is an essential component in the antigen-receptor-mediated activation of the master transcription factor nuclear factor κ B (NF- κ B) (Ho *et al*, 2005; Lin & Wang, 2004). t(11;18)(q21;q21) generates a functional fusion protein API2-MALT1 capable of activating NF- κ B (Ho *et al*, 2005; Uren *et al*, 2000). An intact UBA (Ubiquitin Associated Domain) is present in roughly 98% of API2-MALT1 fusions and a functional UBA is required for efficient API2-MALT1 mediated NF- κ B activation, although the precise molecular mechanism has yet to be established (Gyrd-Hansen *et al*, 2008).

Incidence. t(11;18)(q21;q21) is the most common and specific structural chromosomal abnormality in MALT lymphoma. It has not been described in other B-cell lymphoma subtypes, including nodal and splenic MGZ lymphoma, nor in MALT lymphoma associated inflammatory conditions such as *H. pylori* associated gastritis, lymphoepithelial sialadenitis or Hashimoto's thyroiditis (Du, 2007). t(11;18)(q21;q21) occurs frequently in MALT lymphomas of the lung (40%), stomach (25%) and ocular adnexa (~10%), but not in those of the salivary gland and thyroid (Isaacson & Du, 2004; Ye *et al*, 2003) (Figure 1.5).

Clinical impact. In gastric MALT lymphoma, t(11;18)(q21;q21) is associated with advanced stages, but not transformation into DLBCL (Huang *et al*, 2003; Liu *et al*, 2001a). t(11;18)(q21;q21) is associated with gastric MALT lymphomas that do not respond to *H. pylori* eradication, irrespective of the clinical stage of the lymphoma (Liu *et al*, 2001b; Liu *et*

al, 2002a), and that are resistant to oral alkylating agents (Levy *et al*, 2005). The detection of t(11;18)(q21;q21) is thus critical for the clinical management of gastric MALT lymphoma.

Genetic correlations. t(11;18)(q21;q21) is mutually exclusive from other MALT lymphoma-associated chromosomal translocations (Du, 2007;Liu *et al*, 2004a). t(11;18) positive cases rarely show aneuploidies frequently associated with translocation negative MALT lymphoma, such as trisomies 3, 12 and 18 (Remstein *et al*, 2002;Starostik *et al*, 2002).

Function. The biological importance of the API2–MALT1 fusion is indicated by the analysis of breakpoints at both the genomic and transcript levels. Although some genomic breakpoints were found to cause frameshifts, the API2–MALT1 fusion transcripts are always in frame, because of splicing out of the exon that causes the frameshift (Mestecky *et al*, 1999). The API2 gene contains three amino-terminal baculovirus IAP repeats, a central caspase recruitment domain (CARD) and a carboxy-terminal zinc-binding RING finger domain. The MALT1 protein comprises an N-terminal death domain, followed by two Ig-like domains and a caspase-like domain. Within the API2 gene, all breakpoints occur downstream of the third BIR domain, upstream of the C-terminal RING domain, with 91% occurring just before the CARD domain. In the *MALT1* gene, the breakpoints occur in four different introns upstream of the caspase-like domain (Liu *et al*, 2004a). Therefore, the resulting API2–MALT fusion transcripts always comprise the N-terminal region of API2 with three intact BIR domains and the C-terminal MALT1 region containing an intact caspase-like domain. The specific selection of these domains of the API2 and MALT1 gene to form a fusion product strongly indicates that they are required for the oncogenic activities of the fusion product. API2–MALT1 fusion product is capable of activating the NF-κB pathway in the absence of any surface receptor stimulation, although neither API2 nor MALT1 alone are able to activate NF-κB (Hu *et al*, 2006b).

1.3.1.2 *t(1;14)(p22;q32)/BCL10-IGH*

t(1;14)(p22;q32) translocates the entire B-cell leukaemia/lymphoma 10 (*BCL10*) gene on chromosome 1p22 under the control of the immunoglobulin heavy chain locus (*IGH*) gene enhancer on chromosome 14q32 (Willis *et al*, 1999;Zhang *et al*, 1999). This translocation thus results in the over-expression of BCL10 which contains an N-terminal CARD, followed by a serine/threonine rich C-terminal.

The CARD motif of BCL10 can interact with the Ig-Like domains of MALT1 (Figure 1.4). *In vivo* studies showed that BCL10 and MALT1 link antigen receptor signalling and NF- κ B activation pathway (Ruland *et al*, 2001;Xue *et al*, 2003).

Incidence. *t(1;14)(p22;q32)* is specifically associated with MALT lymphoma, though relatively infrequently. It is mostly seen in MALT lymphoma of the lung (7%) and stomach (4%) but not in those of other sites (Figure 1.5).

Clinical impact. Strong BCL10 nuclear localisation, characteristic of *t(1;14)(p22;q32)*-positive MALT lymphoma, correlates with gastric MALT lymphomas of advanced stages and those not responsive to *H. pylori* eradication (Ye *et al*, 2006). Also, nuclear BCL10 expression is associated with advanced MALT lymphoma (Liu *et al*, 2001b), and associated with shorter treatment failure-free survival in ocular adnexal MALT lymphomas (Franco *et al*, 2006).

Genetic correlations. *t(1;14)(p22;q32)* is mutually exclusive from other MALT lymphoma-associated chromosomal translocations. Translocation positive cases commonly harbour trisomies 3, 12 and or 18 (Streubel *et al*, 2006).

Function. BCL10-knockout mice showed that BCL10 is essential for both the development and function of mature B and T cells, linking antigen-receptor signalling to the NF- κ B pathway (Ruland *et al*, 2001;Xue *et al*, 2003). Over-expression of BCL10 activates the I κ B

kinase (IKK) complex through CARD domain-mediated oligomerisation, resulting in NF- κ B activation (Hofmann *et al*, 1997). In line with these findings, a recent *in vitro* study indicated that BCL10 could prevent an immature B-cell line from antigen receptor induced apoptosis (Tian *et al*, 2005b).

1.3.1.3 *t(14;18)(q32;q21)/IGH-MALT1*

t(14;18)(q32;q21) brings the entire *MALT1* gene (18q21) under the regulatory control of *IGH* (14q32), leading to the over-expression of *MALT1* (Figure 1.4) (Streubel *et al*, 2003). The *MALT1* gene is 5Mb away from the B-cell CLL/lymphoma 2 (*BCL2*) gene, targeted by *t(14;18)(q32;q21) IGH/BCL2* characterising follicular lymphoma (Sagaert *et al*, 2007).

Incidence. *t(14;18)(q32;q21)/IGH-MALT1* is a rare translocation, mainly described in MALT lymphomas of the lung (6%) and ocular adnexa (7%) (Remstein *et al*, 2006;Ye *et al*, 2005) (Figure 1.5). It is also seen in some DLBCLs (Du, 2007).

Clinical impact. As *t(14;18)(q32;q21)* occurs exclusively in extra-gastric MALT lymphoma, for which a specific therapy has not yet been established, the potential impact of this translocation in the clinical management of MALT lymphoma remains unknown.

Genetic correlations. *t(14;18)(q32;q21)* is mutually exclusive from other MALT lymphoma-associated chromosomal translocations. Translocation positive cases commonly harbour trisomies 3 and/or 18 (Streubel *et al*, 2003).

Function. Initial studies of *MALT1* demonstrated that the wild-type protein has no independent ability to activate NF- κ B and shows only modest enhancement of *BCL10*-mediated NF- κ B activation, despite direct physical association with BCL10 (Uren *et al*, 2000). *MALT1* over-expression led to increased constitutive NF- κ B activity and enhanced I κ B kinase (IKK) activation induced by CD40 stimulation (Ho *et al*, 2005).

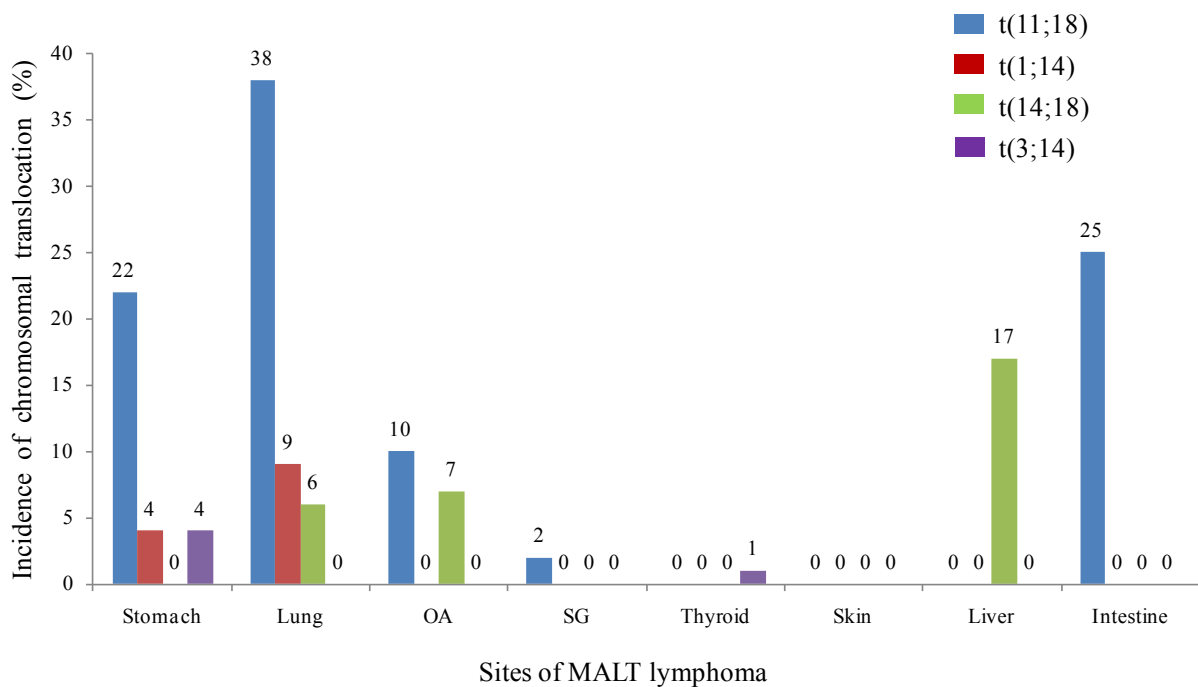


Figure 1.5 - Incidence of MALT lymphoma translocations in various sites

Figure adapted from Ye *et al.* (2005). *Journal of Pathology*, 205, 293-301.

1.3.1.4 BCL10 and MALT1 expression patterns in MALT lymphoma with different translocation status.

MALT1 and BCL10 proteins are essential components of NF-κB activation signalling pathway (Thome, 2004). In normal MGZ B cells, both MALT1 and BCL10 are weakly expressed, predominantly in the cytoplasm (Ye *et al.*, 2005). In MALT lymphoma, tumour cells with different translocations show distinct BCL10 and MALT1 expression patterns (Ye *et al.*, 2005). MALT lymphoma cells with t(11;18)(q21;q21)/API2-MALT1 display moderate BCL10 nuclear expression and weak MALT1 cytoplasmic expression (Figure 1.6). Tumour cells with t(1;14)(p22;q32)/BCL10-IGH show strong BCL10 nuclear expression and weak/negative cytoplasmic expression of MALT1. Tumour cells with t(14;18)(q32;q21)/IGH-MALT1 show strong homogeneous cytoplasmic expression of both BCL10 and MALT1 (Figure 1.6). Around 20% of MALT lymphoma cases without

translocation show BCL10 nuclear expression and around 6% show high BCL10 nuclear expression similar to that seen in t(1;14) positive MALT lymphomas (Liu *et al*, 2001b).

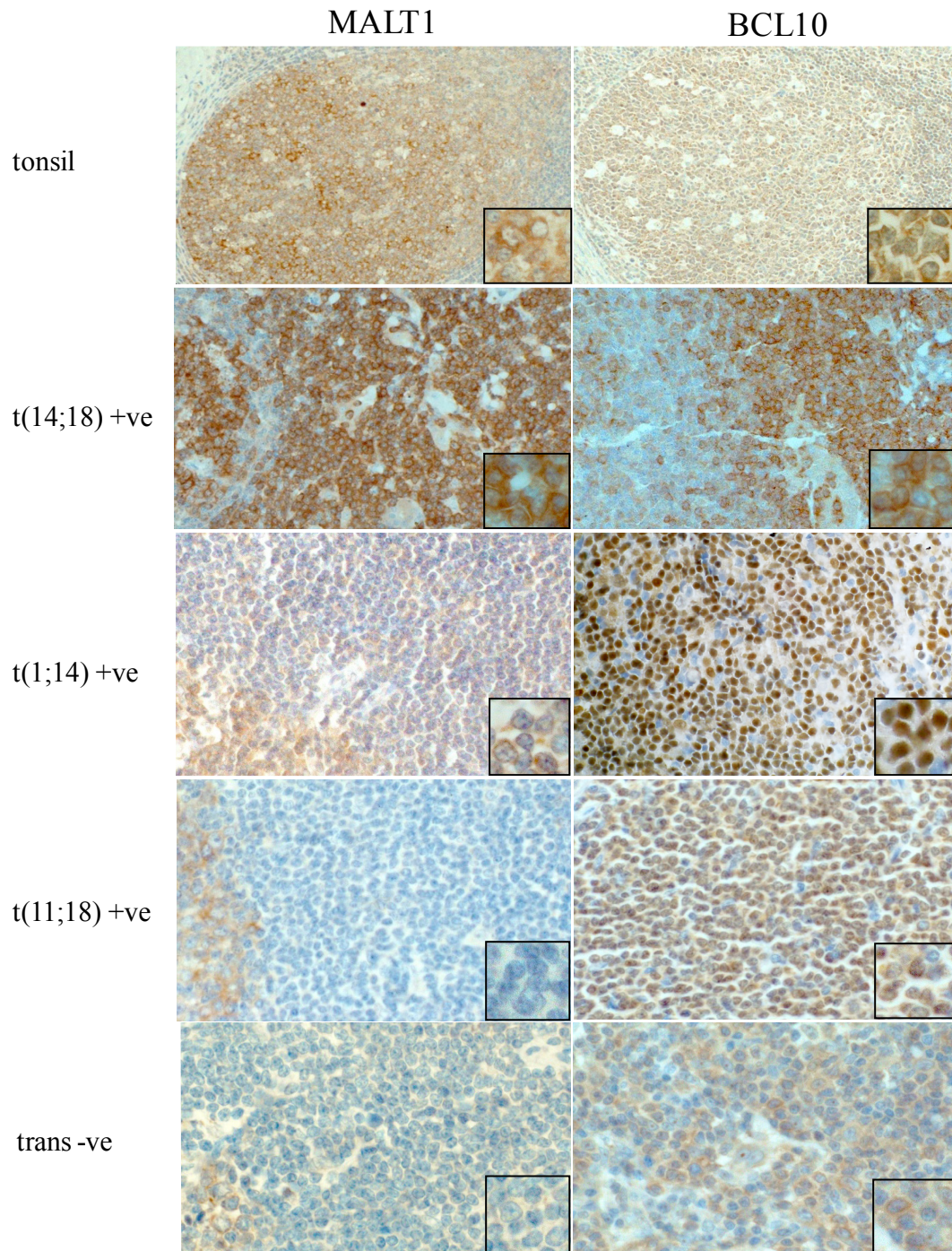


Figure 1.6 - BCL10 and MALT1 staining patterns in MALT lymphoma translocations. BCL10 and MALT1 immunohistochemistry on FFPE translocation positive and negative MALT lymphoma tissue.

Figure adapted from Ye *et al*. (2005). Journal of Pathology, 205, 293-301.

Nakagawa and colleagues demonstrated that MALT1, but not its fusion counterpart API2-MALT1, was involved in BCL10 export from the nucleus to the cytoplasm, providing an explanation for the various BCL10 expression patterns observed in MALT lymphoma with different chromosomal translocations (Nakagawa *et al*, 2005). In cells with $t(11;18)(q21;q21)/API2-MALT1$, MALT1 expression is reduced by half due to the API2-MALT1 fusion, hence an expected reduced efficiency of BCL10 nuclear export. In cells with $t(1;14)(p22;q32)/BCL10-IGH$, MALT1 normal expression may not be sufficient for the export of the over-expressed BCL10, resulting in BCL10 nuclear retention. Finally, in cells with $t(14;18)(q32;q21)/IGH-MALT1$, the over-expression of MALT1 results in an increased export of BCL10 from the nucleus to the cytoplasm, where both proteins are thus strongly expressed in the cytoplasm (Ye *et al*, 2005). The temporal interplay between API2-MALT1, MALT1 and BCL10 in cellular localisation *in vivo* remains to be investigated.

1.3.1.5 t(3;14)(p13;q32)/FOXP1-IGH

$t(3;14)(p13;q32)$ is a newly described MALT lymphoma-associated translocation involving *IGH* (Streubel *et al*, 2005). It deregulates the forkhead box protein P1 (*FOXP1*) gene (3p13), a member of the FOX transcription factor family, which includes numerous proteins involved in a variety of functions such as cellular differentiation and immune regulation. Foxp1 has been recently shown to be an essential regulator of early B-cell development (Hu *et al*, 2006a), but the molecular mechanism underlying its oncogenic activity in lymphoma remains to be investigated.

Incidence. Streubel *et al*. (Streubel *et al*, 2005) initially showed that FOXP1 was involved in $t(3;14)(p13;q32)$ in MALT lymphoma which was present in 10% of MALT lymphomas, in those from the ocular adnexa (20%), thyroid (50%) and skin (10%), but not in those from the

salivary gland, stomach and lung (Streubel *et al*, 2005). However, the translocation was not found in 122 extranodal MALT lymphomas from various sites (9 cutaneous, 13 salivary gland, 50 pulmonary, 36 ocular adnexa, 8 thyroid gland and 6 gastric tumors) (Haralambieva *et al*, 2006b). The t(3;14)(p13;q32) was subsequently found in one case of MALT lymphoma of the stomach (Wlodarska *et al*, 2005), seven cases of diffuse large B-cell lymphoma of the stomach, thyroid and lymph nodes and also in two cases of B-cell non-Hodgkin lymphoma unclassified (Haralambieva *et al*, 2006b;Wlodarska *et al*, 2005). On a larger series of 321 MALT lymphomas, Goatly *et al*. showed that t(3;14)(p13;q32) is rare in MALT lymphoma, and primarily found in gastric cases (4%) (Goatly *et al*, 2008;Haralambieva *et al*, 2006a) (Figure 1.5).

Clinical impact. No correlation has yet been established between the presence of t(3;14)(p13;q32) and response to *H. pylori* eradication in gastric MALT lymphoma. In DLBCL, strong expression of FOXP1 identifies cases with poor prognosis (Barrans *et al*, 2004). Similarly, FOXP1 over-expression is associated with MALT lymphomas with poor clinical outcome (Sagaert *et al*, 2006a). MALT lymphomas with concurrent over-expression of FOXP1 and trisomies 3 and 18 may be at risk of transformation into DLBCL (Sagaert *et al*, 2006a).

Genetic correlations. t(3;14)(p13;q32) is mutually exclusive from other MALT lymphoma-associated chromosomal translocations. Cases with t(3;14)(p13;q32) often harbour additional genetic abnormalities, especially trisomy 3 (Streubel *et al*, 2005).

Function. Activation of the NF- κ B pathway by isoforms of FOXP1 has been investigated (unpublished data in Professor Ming Du's laboratory). The full length FOXP1 protein and 2 short isoforms were able to activate NF- κ B both alone and synergistically with cell surface stimulation of B cells by LPS and T cells by CD3 and CD28. The mechanism of NF- κ B

activation is unknown but there is evidence that it is not through the classical or alternative pathways, in keeping with the nuclear localisation of FOXP1.

1.3.2 Other chromosomal translocations

In addition to the oncogenes mentioned in sections (1.3.1.1 – 1.3.1.4), novel translocations were identified using cytogenetics and long distance inverse PCR. Those include rearrangements of t(6;7)(q25;q11), t(1;14)(p22;q32)/CNN3-IGH, t(5;14)(q34;q32)/ODZ2-IGH and t(9;14)(p24;q32)/JMJD2C-IGH (Vinatzer *et al*, 2008), t(X;14)(p11;q32)/GPR34-IGH (Novak *et al*, 2008;Wlodarska *et al*, 2009) and t(3;13)(q24;p11) (Aamot *et al*, 2005). It has been shown that over-expression of GPR34 activated NF-κB *in vivo* (Novak *et al*, 2008). However no functional characterisation for any of the translocations listed above has been performed. Nonetheless, the translocations above illustrate the heterogeneous nature of genetic alterations in MALT lymphoma.

1.3.3 Genetics of translocation negative MALT lymphoma

Trisomies are frequently associated with MALT lymphoma, particularly those without t(11;18)(q21;q21) (Brynes *et al*, 1996;Streubel *et al*, 2004). Trisomies 3 and 18 are found in about 35% and 25% of cases respectively. However, beyond those numerical aberrations, the molecular genetics of MALT lymphoma, especially those without chromosomal translocation, is poorly understood (Isacson & Du, 2004). The chromosomal gains and losses in translocation negative MALT lymphomas of the stomach and salivary glands were investigated using metaphase comparative genomic hybridisation (CGH) and recurrent chromosomal gains involving the whole or major part of chromosomes 3, 12 and 18, as well as recurrent discrete gains at 9q34 and 11q11-13 were found (Zhou *et al*, 2006;Zhou *et al*, 2007). Array comparative genomic hybridisation (aCGH) showed frequent microdeletions

involving 6p25.3 to be associated with outcome of *H. pylori* eradication in translocation negative gastric MALT lymphoma (Fukuhara *et al*, 2007).

Recently, work in Professor Ming Du's group showed that *A20* deletion was associated with copy number gain at the TNFA/B/C locus and occurred preferentially in translocation negative MALT lymphoma of the ocular adnexa and salivary glands but not in the stomach, lung and skin (Chanudet *et al*, 2009). In addition to the *A20* gene deletions and mutations, promoter methylation was shown to be an alternative mechanism for *A20* inactivation in MALT lymphoma and *A20* complete inactivation was significantly associated with a shorter lymphoma-free survival in ocular adnexal MALT lymphoma (Chanudet *et al*, 2010). The *A20* protein (also known as Tumour Necrosis Factor Alpha-Induced Protein 3 or TNFAIP3) is a key player in the negative feedback regulation of NF- κ B signalling in response to multiple stimuli. For example, A20 regulates tumour necrosis factor (TNF)-induced NF- κ B activation. Recent genetic studies demonstrated a clear association between several single nucleotide polymorphism (SNPs) in the *A20* locus and autoimmune disorders such as Crohn's disease, Rheumatoid arthritis, systemic lupus erythematosus, psoriasis and type 1 diabetes (Vereecke *et al*, 2009) further implicating its link with both autoimmune disease and lymphoma development.

More recently, inactivating mutations predicting truncated A20 products were identified in 6 (19%) of 32 marginal zone lymphomas, including 2 (18%) of 11 extranodal marginal zone lymphomas, 3 (33%) of 9 nodal marginal zone lymphomas, and 1 (8%) of 12 splenic marginal zone lymphomas (Novak *et al*, 2009). Another study identified inactivating mutations in A20 in 21% MALT lymphoma patients (Kato *et al*, 2009). Collectively, *A20* can be completely inactivated by homozygous deletion, hemizygous deletion plus mutation or promoter methylation and bi-allelic mutations. A20 inactivation abolishes the major negative

regulation of the NF- κ B pathway, thus potentially contributing to the constitutive NF- κ B activation in lymphoma subtypes such as DLBCL, particularly the (activated B-cell) ABC subtype, classic Hodgkin lymphoma and Burkitt's lymphoma.

1.4 NF- κ B pathway

As mentioned in section 1.3, MALT lymphoma associated oncogenes target the NF- κ B pathway, thus in this section the NF- κ B pathway will be discussed.

Nuclear Factor- κ B (NF- κ B) (nuclear factor kappa-light-chain-enhancer of activated B cells) is a protein complex that controls the transcription of DNA. NF- κ B was first discovered in the laboratory of Nobel Prize laureate David Baltimore via its interaction with an 11-base pair sequence in the immunoglobulin light-chain enhancer in B cells (Sen & Baltimore, 1986). NF- κ B is a ubiquitous transcription factor found in almost all animal cell types and is involved in cellular responses to diverse stimuli such as stress, cytokines, free radicals, ultraviolet irradiation, oxidized low density lipoproteins, and bacterial or viral antigens (Gilmore, 2006).

1.4.1 NF- κ B family members

NF- κ B is a family of 5 inducible transcription factors, sharing a highly conserved reticulo-endotheliosis viral oncogene homology (REL) domain, REL homolog A (RelA, also known as p65), REL homolog B (RelB), NF- κ B1 (also known as p50) and NF- κ B2 (p52). All have a transactivation domain in their C-termini. 15 transcription factors can be formed from the homo- and heterodimerisation of the five NF- κ B subunits (Gilmore, 2006). The NF- κ B1 and NF- κ B2 proteins are synthesised as large precursors, p105, and p100, which undergo processing to generate the mature NF- κ B subunits, p50 and p52, respectively. The processing

of p105 and p100 is mediated by the ubiquitin/proteasome pathway and involves selective degradation of their C-terminal region containing ankyrin repeats. Whereas the generation of p52 from p100 is a tightly-regulated process, p50 is produced from constitutive processing of p105. The particular dimers present are dependent on the cell type, its stage of differentiation, and environmental signals (Hayden & Ghosh, 2004). As all dimers are able to bind to κ B consensus sites in promoters and enhancers, they can all be termed as “NF- κ B”. The components of each dimer affect its specificity for DNA binding, its interaction with other proteins, and the set of genes that it controls (Hayden & Ghosh, 2004). NF- κ B dimers have the ability to activate or repress transcription of genes (Perkins, 2007). NF- κ B dimers are sequestered in an inactive form in the cytoplasm by inhibitory proteins of the I κ B family (also known as nuclear factor of κ light polypeptide gene enhancer in B-cell inhibitor, NFKBI). Diverse surface receptor signalling can activate the molecular pathways that allow NF- κ B nuclear translocation and activate its target gene expression.

1.4.2 NF- κ B activation pathways

There are two main pathways within a cell that result in NF- κ B activation, namely canonical and non-canonical pathways (Figure 1.7). Recent data indicate the existence of a third NF- κ B activation mechanism, referred to as linear ubiquitin chain assembly complex (LUBAC) pathway (Tokunaga *et al*, 2009) though this needs further experimental validation.

1.4.2.1 Canonical pathway

Receptor signalling

Whilst many different stimuli are able to activate NF- κ B via surface membrane receptor signalling, the major ones can be broadly categorised into the following groups (Hayden & Ghosh, 2008):

- 1) Antigen receptors such as B-cell receptors (BCR) and T-cell receptors (TCR) which lead to NF- κ B activation via antigenic stimulation
- 2) Toll-like receptors (TLRs) which respond to stimulations by bacterial or fungal products such as lipopolysaccharide (LPS), CagA and CpG, leading to NF- κ B activation
- 3) Tumour necrosis factor receptor (TNFR) which lead to NF- κ B activation by stimulation with TNF ligand and (TNF)-related apoptosis-inducing ligand (TRAIL)

Irrespective of the stimulus involved, the key event of canonical NF- κ B activation is the phosphorylation of I κ B α protein by an I κ B kinase complex (IKK). This targets I κ B α for ubiquitination and subsequent degradation, thus releasing NF- κ B. NF- κ B then translocates to the nucleus and binds the promoters of target genes to regulate their transcription (Figure 1.7a).

Signal transduction

As mentioned above, a number of surface receptor signals lead to activation of the canonical pathway in both B and T cells. In the context of this thesis, only the antigen receptor and TLR signalling will be outlined as this is most relevant to MALT lymphoma. Antigen receptor signalling triggers serial proximal signalling that causes the auto-phosphorylation of phosphoinositide-dependent kinase 1 (PDK1). In T cells, phosphorylated PDK1 binds Protein

Kinase C θ (PKC θ), activating this kinase via phosphorylation of Thr538 (Lee *et al*, 2005;Park *et al*, 2009). Similarly, in B cells, antigen receptor signalling triggers phosphorylation and activation of PKC β . Subsequently, PKC β phosphorylates several residues in the “linker” region (also known as PKC receptor) of CARD11 (Matsumoto *et al*, 2005;Sommer *et al*, 2005). This phosphorylation event triggers a conformational change in CARD11 allowing its CARD domain to interact with the CARD of BCL10. Because BCL10 and MALT1 are constitutively associated in the cytoplasm (Su *et al*, 2005), the CARD11-BCL10 interaction also brings MALT1 into the complex, thereby forming the CARD11-BCL10-MALT1 (CBM) complex (Figure 1.8) (Matsumoto *et al*, 2005). CBM is further stabilised by a direct interaction between the coiled coil domain of CARD11 and the C-terminal portion of MALT1 (Che *et al*, 2004) (Figure 1.8).

Coincident with or downstream of formation of the CBM complex, a proportion of cellular BCL10 and MALT1 becomes oligomerised, as demonstrated by biochemical methodology (Sun *et al*, 2004) and FRET microscopy (Rossman *et al*, 2006), and it is these oligomeric species that are active in NF- κ B signal transduction (Sun *et al*, 2004).

The active/oligomeric forms of BCL10 and MALT1 elicit the E3 ubiquitin ligase activity of the TRAF6 RING domain to synthesize a K63-linked polyubiquitin chain on TRAF6 itself (Stilo *et al*, 2004) (Thome, 2004;Thome, 2008) (Rossman *et al*, 2006;Sun *et al*, 2004) (Figure 1.8). Auto-ubiquitination increases the catalytic activity of TRAF6, enabling TRAF6-mediated K63-polyubiquitination of specific protein targets (Lamothe *et al*, 2007). Activated TRAF6 polyubiquitinates MALT1 on multiple C-terminal lysines and BCL10 on Lys31 and Lys63 (Oeckinghaus *et al*, 2007;Wu & Ashwell, 2008).

K63-polyubiquitination of BCL10 is enhanced by the presence of MALT1 (Wu & Ashwell, 2008), suggesting that MALT1-associated TRAF6 may contribute substantially to K63-

polyubiquitin modification of BCL10 in the CBM complex. Wu and colleagues showed that K63-polyubiquitination of BCL10 is essential for CBM association with the IKK complex and for consequent activation of NF- κ B (Wu & Ashwell, 2008), while Duwel and colleagues showed an inability to detect K63-polyubiquitination of CBM-associated BCL10 (Duwel *et al*, 2009). Overall, data are consistent with a model proposing that NEMO is able to bind to K63-polyubiquitin chains on both BCL10 and MALT1, and that blockade of either of these interactions impairs NF- κ B activation, by preventing efficient physical association between the CBM and IKK complexes. However, it is also possible that ubiquitin modification of BCL10 and/or MALT1 affects the function of one or both proteins in other as yet unidentified ways that are crucial for maximal activation of the IKK complex and do not contribute directly to physical association with the CBM.

CBM complex recruits the IKK complex through a recently identified ubiquitin binding domain (UBD) in the NEMO protein. This specialised UBD, called the UBAN (UBD in ABIN proteins and NEMO), facilitates association between the IKK complex and the K63-polyubiquitinated CBM complex (Wagner *et al*, 2008; Wu *et al*, 2006; Wu & Ashwell, 2008). The association of the CBM and IKK complexes then allows TRAF6 (in cooperation with Ubc13/Uev1A) to add K63-polyubiquitin chains to the C-terminal Zn-finger domain of NEMO at Lys399 and possibly additional lysines (Perkins, 2006).

Biochemical studies suggest that K63-polyubiquitination of NEMO enables physical association with the TAK1/TAB2/TAB3 kinase complex, via the UBD of TAB2. This association allows TAK1 to phosphorylate and activate the IKK β catalytic subunit (Perkins, 2006). However, a more recent T-cell study has provided evidence that the phosphorylation of IKK β is independent of CBM-mediated signalling and NEMO ubiquitination, suggesting that the mechanism of TAK1 association with the IKK complex remains to be defined

(Shambharkar *et al*, 2007). Regardless of the details by which the IKK complex is modified, data from both groups strongly suggest that the combination of NEMO ubiquitination and IKK β phosphorylation is required for activation of IKK β kinase activity (Shambharkar *et al*, 2007;Shinohara *et al*, 2005). IKK β then phosphorylates I κ B α , triggering the terminal activation events of the canonical NF- κ B activation cascade, as described above (Figure 1.7a).

Toll-like receptor signalling pathway

TLRs play a crucial role in the innate recognition of various molecular motifs in pathogens, termed pathogen associated molecular patterns (PAMPs) that are conserved in a large group of pathogens, including bacteria, viruses, fungi and parasites. At least 13 TLR family members in vertebrates and 10 TLRs in humans have been reported (Barton & Medzhitov, 2002). All of these TLRs have extracellular leucine-rich repeats and an intracellular Toll/IL-1 receptor homology (TIR) domain (Takeda *et al*, 2003). These receptors transmit signals via several intracellular molecules, including myeloid differentiation factor-88 (MyD88), IL-1 receptor-associated kinases (IRAKs), TNF receptor-associated factor (TRAF) 6 and mitogen activated protein kinases (MAPKs). When associated with TLR, MyD88 recruits members of the IRAK family through (death domain-death domain) homophilic interactions. IRAK1 and IRAK4 are serine-threonine kinases involved in the phosphorylation and activation of TRAF6. After phosphorylation by IRAKs, TRAF6 forms a complex with Ubc13 and Uev1A, and activates a MAPK kinase kinase (MAPKKK) called transforming growth factor β -activated kinase (TAK-1) (Barton & Medzhitov, 2003). Activated TAK-1, in turn, can phosphorylate MKK3 and MKK6, the kinases upstream of p38 MAPKs and JNK which in turn lead to the activation of AP-1 protein (Takeda *et al*, 2003). In addition, TAK-1 can

activate the IKK complex, which phosphorylates I κ B α consequently leading to NF- κ B activation as detailed above (Barton & Medzhitov, 2003).

Different TLRs show variable recognition for microbial lipo-polysaccharides (LPS). For example *Escherichia coli* (*E. coli*) LPS is a ligand for TLR4. *H. pylori* associated LPS is recognized by the receptor complex containing TLR2–TLR1 or TLR2–TLR6 but not that containing TLR4 (Yokota *et al*, 2007).

Chemokine receptor signalling pathway

Chemokines are small peptides that are potent activators and chemoattractants for leukocyte subpopulations and some non-haemopoietic cells. Their actions are mediated by a family of 7-transmembrane G-protein–coupled receptors (Murphy *et al*, 2000). Chemokine receptors are divided into different families, CXC chemokine receptors, CC chemokine receptors, CX3C chemokine receptors and XC chemokine receptors that correspond to the 4 distinct subfamilies of chemokines they bind (Murphy *et al*, 2000). Some chemokine and cytokines activate central cellular pathways. For example, when CXCL8 (IL-8) binds to its specific receptors, CXCR1 or CXCR2, a rise in intracellular calcium activates the enzyme phospholipase D (PLD) that goes on to initiate an intracellular signalling cascade by activating the NF- κ B and MAP kinase pathway. The initiated NF- κ B and MAP kinase pathways activate specific cellular mechanisms involved in chemotaxis, degranulation, release of superoxide anions and changes in the avidity of cell adhesion molecules called integrins (Murdoch & Finn, 2000). In addition, the binding of chemokines to their respective leukocyte receptors initiates a series of cellular events including NF- κ B and MAP kinase activation, all of which aim to eradicate the infiltrating inflammatory agents. These events include changes in cell shape leading to enhanced locomotion, secretion of lysosomal

enzymes, and production of superoxide anions. Once leukocytes reach the source of inflammation, a cytokine-rich milieu is generated that is sustained until the invading antigen is eliminated. In general, immune responses do not produce endothelial injury; however, on occasion acute or chronic inflammation may occur in which the endothelium and surrounding tissues become damaged (for example, by neutrophil generated products).

Several homeostatic chemokines have been shown to play an important role in mucosal immunology via germinal centre formation, homing mechanisms and local retention of activated mucosal B cells and dissemination of B cells to extra-intestinal secretory effector sites. Homing mechanisms play a role in B-cell recruitment to secondary lymphoid tissue. For example, recent mouse studies suggested that although the CCR7 ligand operating together with the CXCR4 ligand (CXCL12) are crucial for endothelial B-cell adhesion in lymph nodes, B-cell entry into Peyer's patches depends on CXCR5 (Okada *et al*, 2002).

1.4.2.2 Non-canonical pathway

Receptor signalling

The non-canonical NF- κ B pathway is activated largely through signalling via the following main receptors:

- 1) CD40 receptor (a TNFR family member) which leads to NF- κ B activation via CD40 ligand stimulation
- 2) B-cell activating factor family (BAFF) receptor (BAFF-R)
- 3) lymphotoxin α and β (LT β also known as TNFC) receptor (LT β -R)

Signal transduction

Receptor signalling activates NF- κ B inducing kinase (NIK), which phosphorylates IKK α . Activated IKK α induces the partial proteolysis of p100 into p52. Subsequently, p52 binds to

RelB, forming an NF- κ B dimer, which migrates to the nucleus and transactivates its target genes (Figure 1.7b) (Jost & Ruland, 2007).

In contrast to the canonical signalling that relies upon NEMO-IKK β mediated degradation of I κ B α , - β , and - ϵ , the non-canonical signalling critically depends on NIK mediated processing of p100 into p52. Given their distinct modes of regulation, these two pathways were thought to be independent of each other. However, recent studies revealed that synthesis of the constituents of the non-canonical pathway, via RelB and p52, is controlled by the canonical IKK β -I κ B-RelA:p50 signalling (Basak *et al*, 2008). Moreover, generation of the canonical and non-canonical dimers, via RelA:p50 and RelB:p52, within the cellular milieu are also mechanistically interlinked (Basak *et al*, 2008). These data suggest that an integrated NF- κ B system network underlies activation of both RelA and RelB containing dimer and that a malfunctioning canonical pathway will lead to an aberrant cellular response also through the non-canonical pathway. As with most cellular pathways, activation needs to be counter-balanced by inhibition or damping.

A variety of recent evidence, however, suggests that the control of the NF- κ B pathway is more complex than simply IKK-mediated regulation of the I κ B-NF- κ B interaction. For example, RelA and p50 are regulated by ubiquitination, acetylation and prolyl isomerisation, and the transactivation activity of RelA and c-Rel can be affected by phosphorylation. In addition, as a consequence of the induction of NF- κ B activity (at least by tumour necrosis factor), IKK α is also induced to enter the nucleus where it becomes associated with κ B site promoters/enhancers to phosphorylate histone H3 which enhances the transcription of κ B site-dependent genes (Chen & Castranova, 2007).

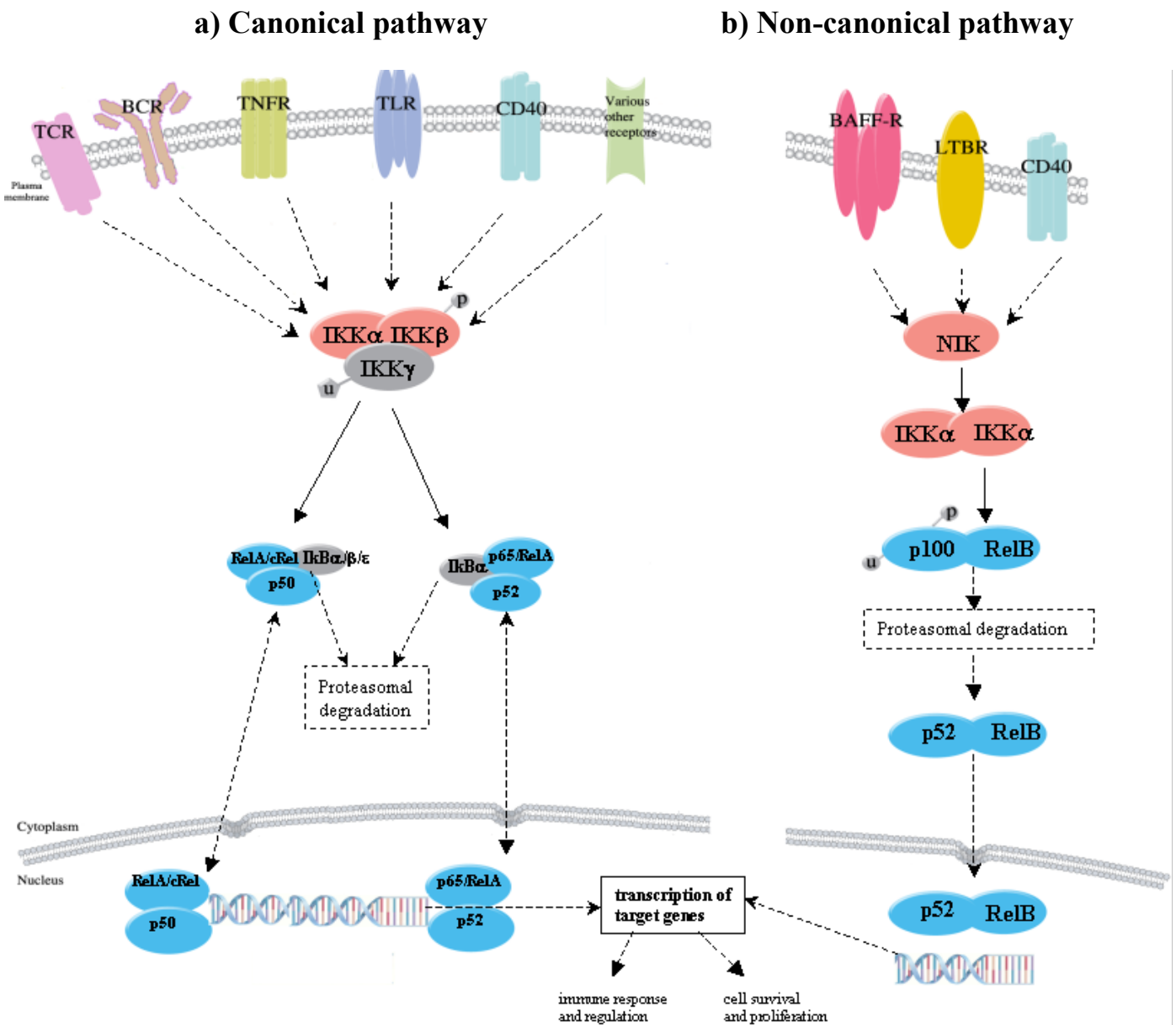


Figure 1.7 - Canonical (classical) and non-canonical (alternative) NF-κB pathway.

Inactive NF-κB dimers are sequestered in the cytoplasm by inhibitory proteins of the IκB family, which includes IκBα, IκBβ, IκBγ, IκBδ, IκBε and BCL3, as well as p100 and p105 respective precursor of p52 and p50. In the canonical pathway, sequestered NF-κB mainly consists of heterodimer p50-RELA. The IKK complex is composed of two kinase subunits (IKKα and IKKβ) and a regulatory subunit, NEMO (also known as NF-κB essential modifier NEMO). The activation of the IKK complex by phosphorylation (P) of IKKβ leads to the phosphorylation of IκB. This targets IκB for ubiquitination (U) and subsequent degradation. In the non-canonical pathway, sequestered NF-κB mainly consists of heterodimer p100-RELB. The IKK complex is a dimer of IKKα. Activated IKKα phosphorylates p100 and triggers its proteolysis, producing p52. This allows the formation of NF-κB active complex p52-RELB. Both the canonical and the non-canonical pathways ultimately lead to the translocation of NF-κB dimers into the nucleus, where they transactivate target genes critical for cellular mechanisms such as proliferation and survival. Some target gene products negatively regulate the NF-κB pathway.

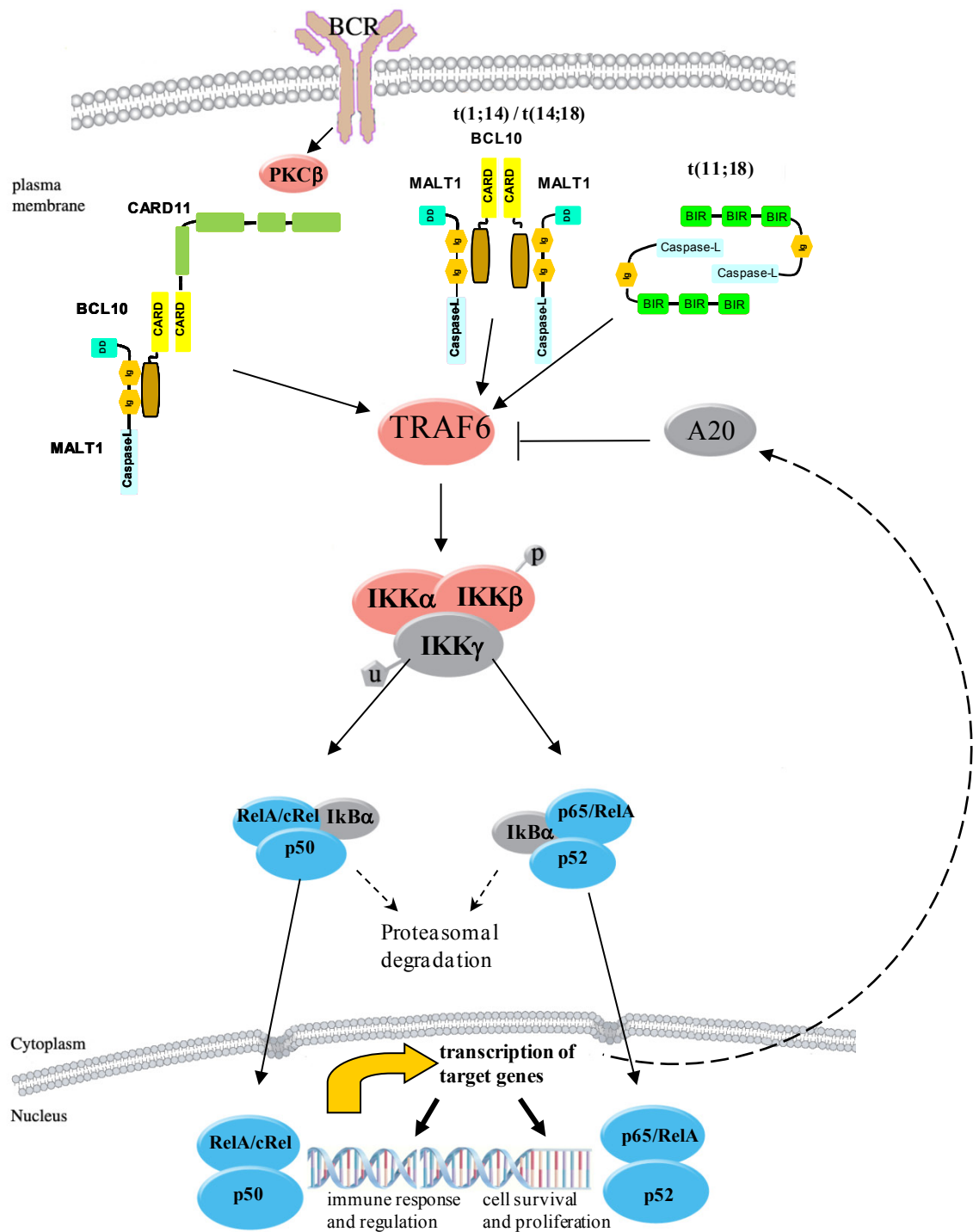


Figure 1.8 - B-cell receptor mediated NF-κB activation and constitutive NF-κB activation by MALT lymphoma associated translocations.

Following antigen recognition via PKCβ, CARD11 recruits BCL10 and MALT1 to the lipid raft at the activated receptor. Subsequently MALT1 binds TRAF6 activating its ubiquitin ligase. This results in TRAF6 and NEMO polyubiquitination and recruitment of kinase complex that phosphorylates IKKβ leading to IκBα phosphorylation and degradation. NF-κB is released and translocated into the nucleus, activating the transcription of target genes. The 3 MALT lymphoma associated translocations are believed to oligomerise and similarly recruit TRAF6 inducing constitutive NF-κB activation.

1.4.3 NF- κ B negative regulators

As mentioned above, in unstimulated cells, the NF- κ B dimers are sequestered in the cytoplasm by a family of inhibitors, called I κ Bs (Inhibitor of κ B).

I κ Bs are related proteins in that they all have an N-terminal regulatory domain, followed by six or more ankyrin repeats and a PEST domain near their C terminus. Although the I κ B family consists of I κ B α , I κ B β , I κ B γ and I κ B ϵ , and BCL3, the best-studied and major I κ B protein is I κ B α . Due to the presence of ankyrin repeats in their C-terminal halves, p105 and p100 also function as I κ B proteins. The multiple copies of ankyrin repeats can mask the nuclear localisation signals (NLS) of NF- κ B proteins sequestering them in an inactive state in the cytoplasm (Jacobs & Harrison, 1998).

Of all the I κ B members, I κ B γ is unique in that it is synthesised from the *NF- κ B1* gene using an internal promoter, thereby resulting in a protein that is identical to the C-terminal half of p105 (Inoue *et al*, 1992). The C-terminal half of p100, that is often referred to as I κ B δ , also functions as an inhibitor (Basak *et al*, 2007). I κ B δ degradation in response to developmental stimuli, such as those transduced through LT β R, potentiate NF- κ B dimer activation in of NIK dependent non-canonical pathway (Basak *et al*, 2007). Unlike other members of the I κ B family, BCL3 was found to function as a transcriptional activator and enhance NF- κ B activity, primarily via forming a complex with the NF- κ B p50 heterodimer to block the latter's mediated suppression of target gene expression (Li & Karin, 2006).

Activation of NF- κ B is initiated by the signal-induced degradation of I κ B proteins via their ubiquitination by the proteasome. With the degradation of the I κ B inhibitor, the NF- κ B complex is then free to enter the nucleus where it can activate the expression of specific genes that have DNA-binding sites for NF- κ B nearby. The activation of these genes by NF- κ B then leads to the given physiological response, for example, an inflammatory or immune

response, a cell survival response, or cellular proliferation. Interestingly, these I κ Bs are part of NF- κ B target genes where the newly synthesised I κ B repressors masks the NLS of NF- κ B sequestering it in the cytoplasm thus, forming a negative feedback loop, which results in tighter control and hence oscillating levels of NF- κ B activity (Nelson *et al*, 2004). This tight control is important as NF- κ B regulates a multitude of target genes that play key roles in cell development and survival. In addition, NF- κ B transactivates several other negative regulators such as A20 (Krikos *et al*, 1992) and its adaptor molecules such as ABIN-1 to 3 (Verstrepen *et al*, 2008).

1.4.4 NF- κ B target genes and their biological implications

NF- κ B activity is essential for development, activation, proliferation and survival of lymphocytes (Hoffmann & Baltimore, 2006). NF- κ B has the ability to regulate the transcription of an extensive variety of genes with a κ B site in their promoter. Promoters that respond to NF- κ B also contain consensus-binding sites for other transcription factors and these may be clustered into enhancers. This indicates that NF- κ B may not act alone in transactivating gene expression (Hoffmann & Baltimore, 2006).

Over 300 genes are regulated by NF- κ B (<http://people.bu.edu/gilmore/nf-kb/index.html>) (Pahl, 1999), including NF- κ B family members such as p50, p52 and RelB (Figure 1.9). A number of these NF- κ B target genes encode NF- κ B positive regulators, while several target genes encode negative regulators. According to their function, these NF- κ B target genes can be categorised into the following groups:

Cytokines, chemokines and their modulators

NF- κ B promotes the transcription of cytokines and chemokines (thus playing a critical role in inflammation) such as BAFF, TNF family members including TNF α , as well as numerous interleukins such as IL8 and IL2 and TRAIL (Apo2-Ligand) (Aggarwal, 2003).

Immunoreceptors

NF- κ B target genes include those encoding immune system modulators such as Toll-like receptors (TLR) (TLR2 and TLR6), chemokine receptors (CCR5 and CCR2), CD40 (Hinz *et al*, 2001), CD86 (Zou & Hu, 2005), CD80 (Fong *et al*, 1996), CD69 (Lopez-Cabrera *et al*, 1995) and IRF4 (Grumont & Gerondakis, 2000). In all cell types studied thus far, the expression of most of the genes induced by inflammatory stimuli are upregulated by NF- κ B (Li & Verma, 2002) and interestingly the over-expression of surface immune receptor genes such as TLRs and CD40 can lead to positive feedback regulation of the NF- κ B pathway.

Apoptosis regulators

NF- κ B regulates genes involved in preventing apoptosis, such as *GADD45 β* (Hoffmann & Baltimore, 2006) and *BCL2* family members (Catz & Johnson, 2001) as well as IAP, FLIP, TRAF1 and TRAF2 (Karin & Lin, 2002)

Cell cycle genes

NF- κ B also regulates genes involved in cell cycle regulation cyclin D1 and MYC (Toualbi-Abed *et al*, 2008) (Hoffmann & Baltimore, 2006).

NF- κ B negative regulators

NF- κ B regulates the expression of its own inhibitors such as I κ B α (Sun *et al*, 1993), and I κ B ϵ (Tian *et al*, 2005a) and NF- κ B negative regulator genes such as *A20* (Krikos *et al*, 1992) and ABIN (*A20* binding and inhibitor of NF- κ B) gene family including ABIN-1 to 3 (Verstrepen *et al*, 2008) playing an important role in negative feedback regulation.

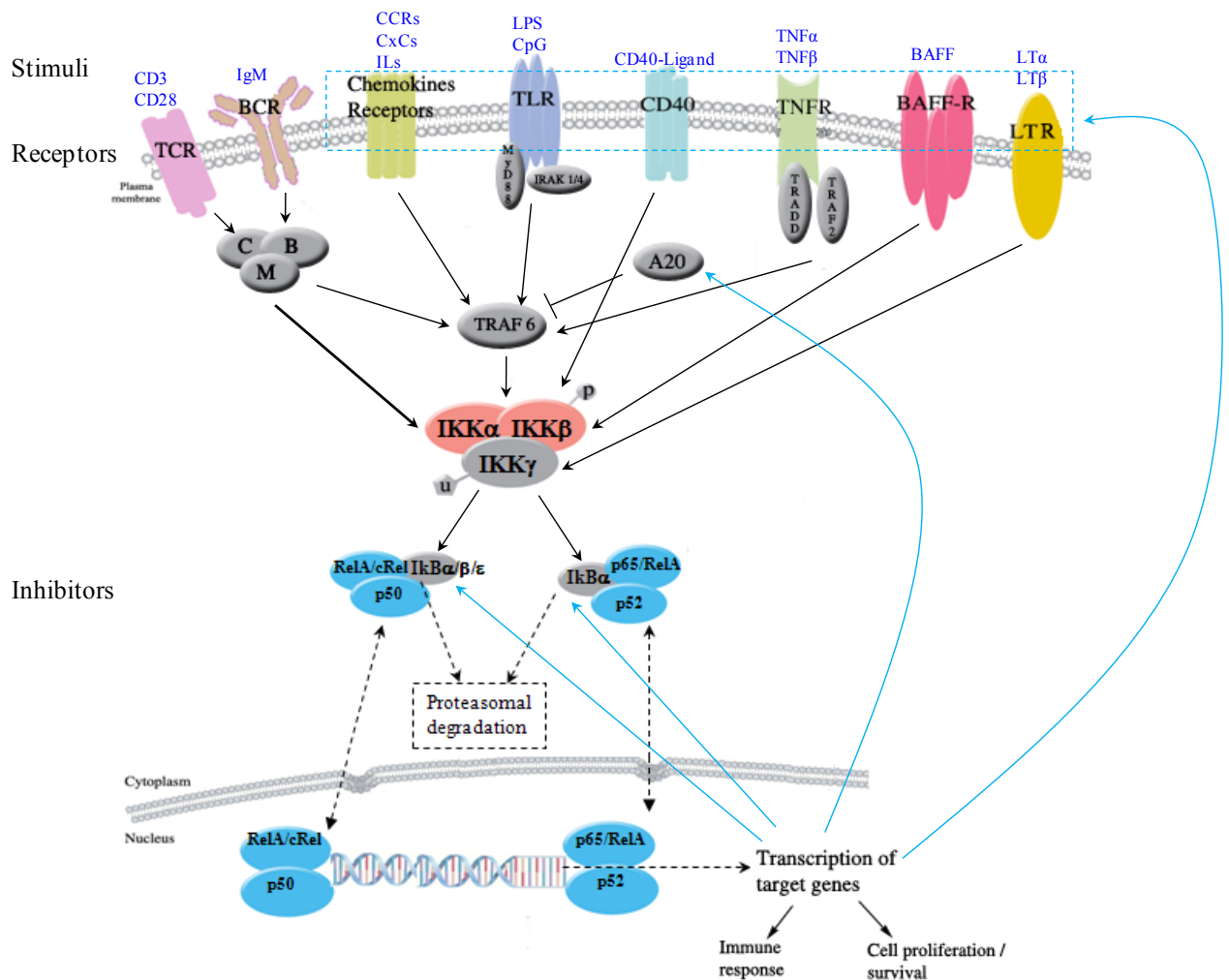


Figure 1.9 - Role of NF-κB target genes in immune response, cell proliferation and survival and maintaining cellular homeostasis.

NF-κB regulates the transcription (shown by the blue arrows) of many target genes involved in cell survival and proliferation as well as immune response and homeostasis. These can be broadly classed as positive and negative regulators of NF-κB. Positive regulators of NF-κB, shown in blue arrows, include immune surface receptors (shown in dotted blue box) that are essential for cell signalling such as chemokine receptors, TLRs, CD40, TNF receptor, BAFF receptor and lymphotoxin receptors. They respond to many pro-inflammatory and environmental stimuli such as LPS, chemokines and cytokines and ligands and lead to positive feedback loop causing constitutive NF-κB activation promoting tumour cell survival. Negative regulators of NF-κB include A20 and IκB family. Interactions between the pro-apoptotic and pro-survival pathways, as well as feedback loops within each pathway contribute to a tightly regulated balance of cell death and survival. B- and T- cell receptors are not target genes but lead to NF-κB activation via CARD11-MALT1-BCL10 (CBM) complex.

1.5 MALT lymphoma associated translocations target common molecular pathways that cause NF- κ B activation

BCL10 and MALT1 are central to the transduction of signals from cell surface immune receptors to the classical NF- κ B activation pathway in both B and T cells (Farinha & Gascoyne, 2005). The three common chromosomal translocations recurrently found in MALT lymphomas that involve the *BCL10* and *MALT1* genes are clearly implicated in the oncogenic process via deregulation of the NF- κ B activation pathway. Mounting evidence indicates that the oncogenic activity of the three MALT-lymphoma associated chromosomal translocations is linked by roles of BCL10 and MALT1 in activating the NF- κ B pathway in lymphocytes (Section 1.4) (Figure 1.8).

The API2-MALT1 fusion protein self oligomerises through a non-homotypic interaction mediated by the API2 region and is capable of activating NF- κ B. However, neither MALT1 nor API2 alone is able to activate NF- κ B *in vitro* (Du, 2007). Among the three BIR domains, only the first, BIR1, is essential for NF- κ B activation by API2-MALT1 (Garrison *et al*, 2009; Zhou *et al*, 2005). BIR1 has been shown to contain an additional TRAF2/TRAF6 binding site, as well as a region that interacts with the C-terminal MALT1 responsible for a heterotypic oligomerisation that is critical for NF- κ B activation (Garrison *et al*, 2009). It is likely that the constituting oligomerisation of the API2-MALT1 fusion protein contributes to its ability to interact with and oligomerise downstream ubiquitin ligase such as TRAF2/TRAF6. TRAF2 and TRAF6 (together with the ubiquitin conjugating enzyme complex, Ubc13/Uev1A) trigger the K63-polyubiquitination of the API2-MALT1 fusion product and the K63-autoubiquitination of the TRAFs, themselves. The polyubiquitinated API2-MALT1 complex then binds to NEMO (Wagner *et al*, 2008; Wu *et al*, 2006). This

molecular association allows the TRAFs associated with API2-MALT1 to K63-ubiquitinate NEMO and causing the terminal events in the canonical NF- κ B activation cascade.

In addition to binding to TRAF2/TRAF6, the API2-MALT1 protein has further activities that can augment signals to NF- κ B (Zhou *et al*, 2004). For example, some data suggest that API2-MALT1 itself possesses ubiquitin ligase activity that is capable of K63-polyubiquitinating NEMO and triggering NF- κ B activation (Zhou *et al*, 2005). Also, recent data indicate that the API2-MALT1 fusion protein binds to K63-polyubiquitinated NEMO via the UBA domain of API2 (Gyrd-Hansen *et al*, 2008). It is possible that this interaction protects the NEMO protein from de-ubiquitination, thereby prolonging activation of the IKK complex. Another possibility is that the UBA-NEMO interaction stabilises the interaction between API2-MALT1 and the IKK complex, increasing the efficiency of NEMO K63-polyubiquitination by API2-MALT1-associated TRAF2 and TRAF6. There is also evidence that API2-MALT1, like MALT1, can mediate proteolytic cleavage of A20, a negative modulator of NF- κ B signalling. This depends on the paracaspase activity of the caspase like domain (Coornaert *et al*, 2008). A point mutation that disrupts this proteolytic activity decreases API2-MALT1 mediated NF- κ B activation by approximately 3-fold (Hu *et al*, 2006b). Thus, the proteolytic activity of API2-MALT1 appears to augment NF- κ B activation by interfering with normal homeostatic mechanisms that serve to limit NF- κ B activation. It remains to be investigated whether A20 is also cleaved when BCL10 or MALT1 is over-expressed.

BCL10 has been reported to interact with the API2-MALT1 fusion protein and synergistically enhance NF- κ B activation in the absence of appropriate stimuli (Hu *et al*, 2006b). In this study, it was shown that BCL10 interacts with a sub-fragment of API2 (1-441), which contains the three BIR domains and the UBA domain (Gyrd-Hansen *et al*, 2008) (Figure 1.4).

For the non-canonical (alternative) pathway, it has been shown that NF- κ B signalling, once activated in a CD40-dependent immune response, is maintained and enhanced through deregulation of MALT1 or formation of an API2-MALT1 fusion (Ho *et al*, 2005).

In contrast to MALT1 and API2-MALT1, BCL10 deregulation was demonstrated to promote survival of antigen-simulated B lymphocytes, by showing that over-expression of BCL10 in primary B cells activated *ex vivo* promoted the survival of these cells after removal of activating stimuli (Tian *et al*, 2005b).

Although BCL10 and API2-MALT1 are potent activators of NF- κ B, over-expression of these oncogenic products alone is not sufficient to induce malignant transformation. Transgenic mice expressing API2-MALT1 or BCL10 alone develop splenic marginal zone hyperplasia but not lymphoma (Baens *et al*, 2006; Macintyre *et al*, 2000; Li *et al*, 2009). However, when transgenic mice expressing the API2-MALT1 fusion protein are immunised with the Freund's complete adjuvant, they develop splenic marginal zone lymphoma-like lymphoid hyperplasia (Sagaert *et al*, 2006a). In line with this, expression of either API2-MALT1 or MALT1 in BJAB B cells enhanced the activation of IKK and NF- κ B by CD40/CD40L stimulation (Ho *et al*, 2005).

FOXP1-involved translocation occurs recurrently in MALT lymphoma and it is hypothesised that it may also confer oncogenesis through activation of NF- κ B. Support for this hypothesis is provided by the observation that FOXP1 is highly expressed in the activated B-cell subtype of DLBCL in which NF- κ B is constitutively active. However, these separate findings may be unrelated and offer no insight into the mechanism by which FOXP1 promotes oncogenesis. The full length and two short isoforms of FOXP1 were able to activate NF- κ B alone and synergistically with cell surface stimulation of B cells by LPS and T cells by CD3 and CD28. The mechanism of NF- κ B activation is unknown but there is no evidence of activation of the

canonical or non-canonical pathways in the cytoplasm, in keeping with the nuclear localisation of FOXP1 (unpublished data in Professor Ming Du's laboratory).

The extent of the oncogenic activities of these translocations is not yet fully understood as indicated by the aberrant pattern of BCL10 expression in some cases of MALT lymphoma. In normal B cells, including those of the marginal zone of B-cell follicles, BCL10 is expressed primarily in the cytoplasm (Ye *et al*, 2000). However, in MALT lymphoma with t(1;14)(p22;q32), BCL10 is strongly expressed in the nuclei (Ye *et al*, 2000). Moderate levels of nuclear BCL10 expression are also seen in up to 50% of t(1;14)(p22;q32)-negative MALT lymphomas, including almost all t(11;18)(q21;q21)-positive cases (Liu *et al*, 2001b; Maes *et al*, 2002; Ye *et al*, 2003). Furthermore, BCL10 was found to be expressed at high levels in the nuclei of splenic marginal-zone B cells in transgenic mice in which BCL10 expression is driven by Ig enhancers (Li *et al*, 2009). These observations indicate that aberrant nuclear BCL10 expression might have a role in MALT lymphoma development. However, the biological activity of nuclear BCL10 remains to be investigated.

1.6 Summary of current understanding of gastric MALT lymphoma

The sequential development of *H. pylori*-associated chronic gastritis, acquisition of MALT, low grade MALT lymphoma and transformation into DLBCL, clearly indicates a multistep process in the development of MALT lymphoma (Figure 1.10), primarily demonstrated by the histological presentation of these pathological conditions (Wotherspoon *et al*, 1993). Recent studies provided further understanding at both the cellular and molecular levels. MALT lymphomagenesis recapitulates many aspects of the normal immune response and lymphocyte development. The patterns of spread of lymphomas reflect the homing patterns

of normal lymphocytes, both microscopically, within lymph nodes, and macroscopically, at a clinical level.

Correlation of the genetic aberrations with clinical outcome will permit improved diagnostic, prognostic and therapeutic sub-classification of MALT lymphomas. Whilst NF-κB deregulation as a consequence of the MALT lymphoma translocations is clearly indicated, further investigation is necessary to clarify the role of these events in oncogenesis. The equivalent events in translocation negative lymphoma also require elucidation.

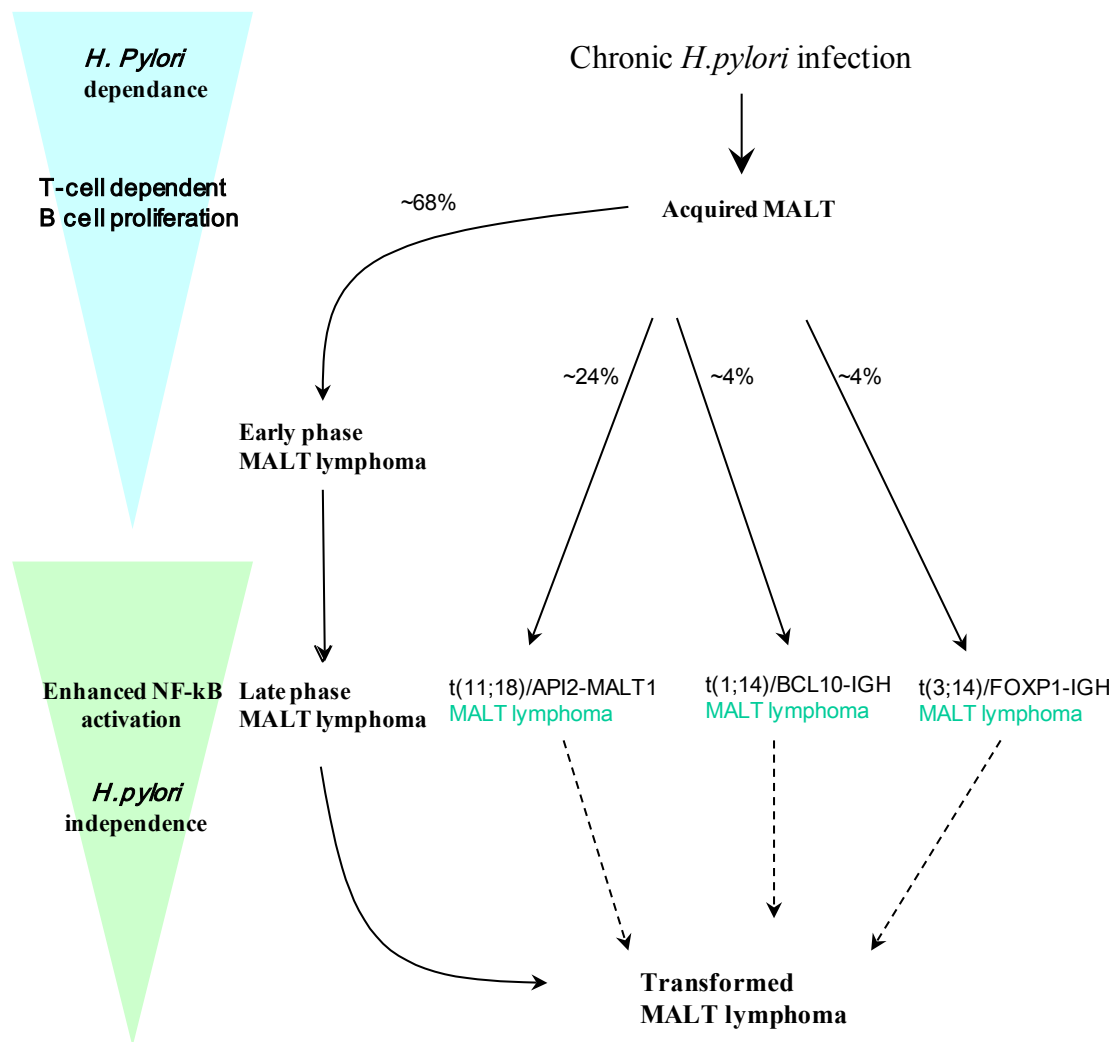


Figure 1.10 - Multistep development of gastric MALT lymphoma.

Figure adapted from Isaacson *et al.* (2004). Nature Review Cancer, 4, 644-653.

Infection by *H. pylori* first induces the formation of acquired mucosa-associated lymphoid tissue (MALT) in the gastric mucosa. The persistence of the bacterial infection results in chronic inflammation. Under sustained immunological stimulation, *H. pylori*-specific tumour-infiltrating T cells stimulate the proliferation of B cells. Genetic abnormalities such as chromosomal translocations (Figure 1.4) might be the result of oxidative stress associated with inflammation (Ye *et al*, 2003). The acquisition of genetic abnormalities leads to malignant transformation. At this early stage, clonal expansion is *H. pylori*-dependent and the resulting MALT lymphoma can be effectively treated by *H. pylori* eradication with antibiotics. However, MALT lymphoma cells can gain autonomous growth ability, presumably through the acquisition of chromosomal translocations such as t(11;18) and t(1;14) or secondary genetic abnormalities such as A20 mutations, and thus, do not respond to *H. pylori* eradication.

The milieu of infection and chronic inflammation provide a common background for the development of MALT lymphomas. It is likely that NF- κ B activation is involved in both translocation positive and negative MALT lymphoma. However despite the overlapping mechanisms there are important differences in the clinical and histological presentations between MALT lymphomas with and without chromosome translocation. Clinically, gastric MALT lymphomas with t(11;18) or t(1;14) are significantly associated with advanced clinical stages and resistance to *H. pylori* eradication (Liu *et al*, 2002b;Ye *et al*, 2006). Histologically, t(11;18) positive MALT lymphomas appear to be more monotonous, lacking apparent transformed blasts (Okabe *et al*, 2003). These clinico-pathological characteristics may indicate the presence of significant differences in molecular mechanisms between MALT lymphomas with and without chromosome translocation. Thus, there are still many unanswered questions regarding MALT lymphomagenesis. Firstly, how chronic antigenic

stimulation in the presence of *H. pylori* or *C. psittaci* infection leads not only to chronic B-cell proliferation, but also to DNA damage which can result in the specific translocations that characterise most MALT lymphomas. Secondly, what are the molecular mechanisms that determine the response to *H. pylori* eradication. Thirdly, what is the molecular basis of NF- κ B activation in MALT lymphoma. Fourthly, what are the molecular profiles and pathways targeted by MALT lymphoma with and without chromosomal translocations that can explain their differences in clinical and histological presentation. In order to answer some of these compelling questions, expression microarray investigations were applied in this thesis to MALT lymphoma cases with and without chromosomal translocation.

1.7 Gene expression microarray

Although all human somatic cells possess the same inherited genomic DNA, each cell transcribes different genes as mRNA according to the cell type. Further variation is provided by biological processes, both normal and abnormal conditions, amongst other parameters. The diversity in gene expression patterns has led to intensive research because of its biological and clinical relevance. Microarray technology allows the simultaneous profiling of the expression of tens of thousands of genes, thus painting a molecular portrait of the tissue or cell lines being studied. The technology, based on the micro-spotting of DNA, protein, tissue or small organic compounds, which can be probed with various labelled binding ligands (Howbrook *et al*, 2003). Different microarray technologies are designed to address distinct biological questions. This thesis focuses on expression microarray technologies, which permit a broad overview of expression patterns.

1.7.1 Advantages of using gene expression microarray

It can be hypothesised within limits that changes in the phenotype of a cell or cell population should be reflected by concomitant transcriptional changes. Large-scale assessment of mRNA transcript abundance should thus provide a molecular signature of the state of gene activity of the biological system in question. Such assessment of gene expression has been considered a useful tool in the study of cellular biology in health and disease.

Currently, expression microarrays are much more reliable, optimised and permit higher throughput than any available proteome-assessing technology. Global and quantitative information on gene expression by measuring mRNA levels far outstrips the available proteomic technologies which are generally more technologically challenging and permit far lower throughput (Clarke *et al*, 2001). Indeed, expression microarray technology has matured impressively in the last 8 years and now has a resolution of approximately one transcript per known gene. Currently available expression microarray platforms can assess gene expression of over 300,000 distinct transcripts in any single experiment. Nonetheless, the complementation of expression with data from high throughput proteomic technologies such as high throughput crystallography and protein-based microarrays is eagerly awaited (Howbrook *et al*, 2003).

1.7.2 Limitations of gene expression microarray

The focus of expression microarray technology is the quantitative assessment of gene expression on a very large scale. Such an approach focusing on transcription is often questioned in relation to its ability to extrapolate findings at the protein level. This is one of the limitations of not only microarray-based, but all transcriptome-assessing technologies in

general. There is no doubt that results from expression technologies would be maximally effective if accompanied by and integrated with studies assessing global protein expression (Clarke *et al*, 2001). However, even this combined approach would not suffice to describe a given cellular biological phenomenon in its entirety as an accurate description but would at least also require extensive study of protein post-translational modification and localisation.

Microarray technology is sensitive to cellular heterogeneity. In this context where RNA sample is obtained from complex tissues, expression results may relate to expression profiles from a number of distinct cell types. Thus it is important to use highly homogenous, carefully selected cell populations (for example lymphoma cells) as this can reduce the possibility of a given expression result being affected by cell types of secondary interest. The use of microdissected tissue may circumvent this problem by including mostly specific cell types in a given expression profiling experiment. Finally, the requirement of often large quantities of RNA (total or messenger) for these technologies may prove limiting especially for studies focusing on rare clinical material. The development of RNA amplification protocols, however, has addressed this issue successfully, significantly lowering the amount of RNA needed per microarray experiment. More recently, the discovery of microRNAs (miRNAs) (which are naturally occurring short non-coding RNA molecules that negative regulate eukaryotic expression through binding to the complementary sequences in the 3'-UTR of target mRNA) adds another limitation as some of the mRNA on the expression array may be negatively regulated by some of those miRNAs. Also studies have shown that some miRNAs such as miR-155, miR-210 and miR-21 are upregulated in the serum from DLBCL patients (Lawrie *et al*, 2008a) whereas miR-150, miR-189, miR-223 and miR-768-3p are downregulated in DLBCL and BL patients suggesting that dysfunctional expression of miRNAs might be a feature in some haematological malignancies (Lawrie *et al*, 2008b).

1.7.3 Microarray platforms

There are several expression microarray platforms, including complementary DNA (cDNA) microarrays (Schena *et al*, 1995), oligonucleotide microarrays (Lockhart *et al*, 1996) and serial analysis of gene expression (SAGE) (Velculescu *et al*, 1995). The first two microarray technologies are the most commonly used platforms. The cDNA microarrays are based on standard microscopic glass slides on which cDNA fragments have been spotted. The oligonucleotide microarrays are constructed with oligonucleotides, 25- or 60-mer in length that are either synthesised *in situ* on a silicon wafer, or robotically spotted or injected on glass slides. The term commonly used to describe the DNA arrayed on a platform is “probe” and the cDNA or cRNA generated from a sample RNA, which represent the gene expression profile of the sample, are referred to as “target”. The types of probes and targets used in each microarray platform differ, but these differences are becoming less significant. The main difference between the two platforms is the method by which the mRNA levels are determined. In cDNA microarrays, the quantitation is made by comparing a selected sample to a ‘control’ sample, while in oligonucleotide microarrays, a well-defined arbitrary unit is produced without the need to compare with a different sample. Generally, it has been shown that oligonucleotide arrays give better results than cDNA microarrays (Woo *et al*, 2004). The most common oligonucleotide platform to study human genome expression is the Affymetrix HG-U133 GeneChip.

1.7.3.1 The Affymetrix HG-U133 GeneChip

The HG-U133 (Human Genome U133) GeneChip microarray set originally consisted of two GeneChips; HG-U133A and HG-U133B. Collectively, the HG-U133 set is capable of assessing a total of around 39,000 transcripts and variants, including more than 33,000 well-

substantiated human genes. The U133A chip alone assess 22,283 transcripts derived mostly from well-characterised genes and U133B can assess 22645 derived mostly from expressed sequence tags (ESTs). Sequences used in the design of the chip were selected from GenBank, dbEST and RefSeq. The sequence clusters were created from the UniGene database (Build 133, April 20, 2001) and then refined by analysis and comparison with a number of other publicly available databases. Subsequently around 2005, Affymetrix commercialised a new GeneChip that includes the whole human genome on one chip, named HG-U133 plus 2.0. This is capable of analysing the expression level of over 47,000 transcripts and variants, including 38,500 well-characterised human genes. It comprises more than 54,000 probe sets and 1,300,000 distinct oligonucleotide features. In addition, there are 9,921 new probe sets representing approximately 6,500 new genes. These gene sequences were also selected from GenBank, dbEST, and RefSeq. Sequence clusters were created from the UniGene database (Build 159, January 25, 2003) from manufacturer's datasheet at

http://www.affymetrix.com/support/technical/datasheets/human_datasheet.pdf.

The unit of expression interrogation of the U133 chip is the probe set. Throughout this thesis, for the purpose of clarity, all genes mentioned will be associated to their probe set(s). The terms gene and probe set may be used interchangeably. It is stressed, however, that all observations refer to probe set signal intensity changes.

1.7.3.1.1 Probe versus Probe set

A major difference between spotted and GeneChip microarray technologies relates to probe design. Spotted microarray technologies employ probes that may either be synthetic oligonucleotides, long PCR products or cloned cDNAs. In all cases however, a single transcript is assessed by a single probe. For Affymetrix GeneChips, transcripts are

interrogated not by a single probe, but by a combination of probes collectively forming a probe set. Each probe in a probe set is designed to be complementary to a distinct region of the transcript queried. For example, the U133A Genechip used in this thesis, employs a total of 11 probes in the interrogation of each transcript assessed. These probes are referred to as perfect match (PM) as they are designed to be perfectly complementary to their respective transcript. In addition, for each probe set, a second set of mismatch probes (MM) with a mutation in the middle of the probe's sequence is employed to control for hybridisation specificity and background.

The generation of probe set values from respective probe values can be addressed in a number of ways. These differ mainly in relation to the use of MM probes and the statistical approaches adopted for obtaining single probe set expression values from individual probe intensities. In the most simplistic scenario, probe set level data can be obtained by initially correcting for background by subtracting each MM probe from its respective PM one and then averaging corrected PM probe intensities.

1.7.4 Data analysis

Regardless of the microarray platform, each experiment produces a data set containing tens to hundreds of thousands of values of gene expression. This overwhelming abundance of data requires the use of powerful statistical and analytical tools. After normalisation and non-specific filtering, there are two basic approaches to analysing gene expression data set. The supervised approach is based on determining genes that fit a predetermined pattern, usually used to correlate between gene expression and clinical data. The two most common supervised techniques are: nearest neighbour analysis (Golub *et al*, 1999) and support vector machines (Brown *et al*, 2000). The unsupervised approach is based on characterising the

components of the data set without the *a priori* input or knowledge of a training signal. This approach is usually used to identify a distinct subgroup of tumours that share similar gene expression profiles. The four most common unsupervised techniques are: principle-component analysis (Raychaudhuri *et al*, 2000), hierarchical clustering (Eisen *et al*, 1998), self organising maps (Tamayo *et al*, 1999) and relevance networks (Butte *et al*, 2000).

The first study utilising microarray technology demonstrated the power of this tool to classify and predict human acute leukaemias. These classifications and predictions were based solely on gene expression monitoring and were independent of previous biological knowledge (Golub *et al*, 1999). Although histopathological evaluation, supplemented by cytogenetics and analysis of a few molecular markers, is still the gold standard in diagnosis and prognosis, gene expression profiling had proved capable of replacing these evaluations providing large numbers of patients are used in extracting the molecular signatures.

The rate-limiting step in functional genomics experiments is neither the handling of the biological samples nor the actual analysis, but instead the post-analytical work in determining what the results actually mean. This is largely restricted by the lack of biological knowledge of the gene studied, reliable bioinformatics methods in mining and interpretation of the massive data generated. Some advances have been achieved, such as the development of ONCOMINE, a cancer microarray database and web-based data-mining platform aimed at facilitating discovery from genome-wide expression analyses. To date, ONCOMINE contains 65 gene expression datasets comprising nearly 48 million gene expression measurements from over 4700 microarray experiments (Rhodes *et al*, 2007) (<http://www.oncomine.org>). Other pathway and data mining software such as Ingenuity Pathway Analysis (<http://www.ingenuity.com>) and GeneGO (<http://www.genego.com>) help in the interpretation of microarray data. However, a precise method to map the genes that are differentially

expressed from the microarray studies to cellular pathways relevant to the cellular and molecular mechanisms of disease is required. Gene set enrichment analysis (GSEA) goes some way to achieve this. GSEA measures whether the individual genes in a signature are differentially expressed in a consistent fashion between two groups of samples (Mootha *et al*, 2003). This method was originally used to demonstrate that genes involved in oxidative phosphorylation are decreased in expression in diabetic muscle (Mootha *et al*, 2003). A recent enhancement of the GSEA method places added emphasis on those genes in a signature that are the most differentially expressed between two groups (Subramanian *et al*, 2005).

1.7.5 Advances in lymphoma by gene expression microarray investigations

Gene expression profiling using microarrays has made huge improvement in disease classification, disease sub-classification, biomarkers identification, and deciphering the molecular pathogenesis in a number of lymphoma subtypes. Highlighted below are examples of such advances:

Disease sub-classification and characterisation

The most prominent examples of gene expression microarray in lymphoma sub-classification are studies of DLBCL. These studies revealed new unexpected subgroups of DLBCL which cannot be classified by conventional histology and immunophenotype. While 40% of patients respond well to chemotherapy, the remaining 60% succumbs to the disease. Using unsupervised analysis of gene expression data, Alizadeh *et al*. (Alizadeh *et al*, 2000) identified two molecularly distinct forms of DLBCL, named germinal center B-cell-like (GCB) GCB-DLBCL and activated B-cell-like ABC-DLBCL. The different gene expression profiles apparently reflected the variation in tumour proliferation rate, host response and

differentiation state of the tumour. Importantly, this stratification proved to be clinically relevant in that activated B-cell (ABC) DLBCL is significantly associated with poor overall and event free survival. Subsequent studies showed that ABC-DLBCL is characterized by constitutive NF- κ B activation and is more frequently associated with *CARD11* and *CD97B* inactivating mutations (Lenz *et al*, 2008; Davis *et al*, 2010).

Disease classification

Identification of molecular profiles that differentiate the lymphoma in question from other B-cell lymphomas can be seen in Burkitt's lymphoma microarray studies. Burkitt's lymphoma is a rare, aggressive B-cell lymphoma that accounts for 30% to 50% of lymphomas in children but only 1% to 2% of lymphomas in adults (NHL Lymphoma Classification Project, 1997; Swerdlow *et al*, 2008). The main diagnostic challenge in Burkitt's lymphoma is to distinguish it from diffuse large B-cell lymphoma. The tumour cells of Burkitt's lymphoma are characteristically medium-sized (smaller than the cells of most diffuse large-B-cell lymphomas) and very high fractions are proliferating. Dave *et al*. (Dave *et al*, 2006) and Hummel *et al*. (Hummel *et al*, 2006), used gene expression microarray technology to improve the accuracy of the diagnosis of Burkitt's lymphoma. The two studies differ in many important ways, but both reach the same conclusion: the gene-expression profiling of cases classified as Burkitt's lymphoma by expert pathologists identifies a characteristic genetic signature that clearly distinguishes this tumour from cases of diffuse large-B-cell lymphoma. Furthermore, the microarray method seems to outperform the expert pathologists: 17% (Dave *et al*, 2006) and 34% (Hummel *et al*, 2006) of cases with the gene-expression signature of Burkitt's lymphoma had been called diffuse large-B-cell lymphoma or unclassifiable high-grade B-cell lymphoma; 0.4% (Dave *et al*, 2006) and 4% (Hummel *et al*, 2006) of cases

without the Burkitt's signature had been called classic or atypical Burkitt's lymphoma; and 3% (Dave *et al*, 2006) and 8% (Hummel *et al*, 2006) of cases diagnosed as diffuse large B-cell lymphoma or unclassifiable high-grade B-cell lymphoma had a Burkitt's signature.

Deciphering the molecular basis of lymphomagenesis

Examples of the use of expression microarrays in understanding the molecular pathogenesis of lymphomas can be seen in mantle cell lymphoma (MCL) and follicular lymphoma (FL). The common cytogenetic alteration in MCL patients, t(11;14), leads to cyclin D1 over-expression. Nevertheless, overexpressing cyclin D1 in transgenic mice was not sufficient to induce lymphomas, and other oncogenic factors, were required (Bodrug *et al*, 1994). Thus, different mechanisms must be required for the development and progression of MCL. The first use of microarrays in studying MCL demonstrated altered apoptosis pathways, in addition to the known over-expression of cyclin D1 (Hofmann *et al*, 2001). A comparison of MCL with normal human B cells revealed a distinct gene expression signature affecting lymphocyte trafficking, differentiation and growth regulation (Ek *et al*, 2002). In follicular lymphoma, gene expression profiling showed that an interaction of tumour cells and the microenvironment determine the clinical behaviour (Glas *et al*, 2007) and that transformation of follicular lymphoma to diffuse large B-cell lymphoma is preceded by distinct oncogenic mechanisms (Davies *et al*, 2007).

Biomarker identification

Blenk *et al*. (Blenk *et al*, 2007) analysed a large data set on DLBCL gene-expression (248 patients, 12196 spots) and identified specific, activated B-cell-like (ABC) and germinal center B-cell-like (GCB) distinguishing genes. These include early (e.g. CDKN3) and late (e.g. CDKN2C) cell cycle genes. Independently from previous classification by marker genes

they confirmed a clear binary class distinction between the ABC and GCB subgroups. The biomarkers set distinguishing marked over-expression in ABC from that in GCB, is built by: ASB13, BCL2, BCL6, BCL7A, CCND2, COL3A1, CTGF, FN1, FOXP1, IGHM, IRF4, LMO2, LRMP, MAPK10, MME, MYBL1, NEIL1 and SH3BP5. It predicts and supports the aggressive behaviour of the ABC subgroup and help to understand target interactions, improve subgroup diagnosis, risk prognosis as well as therapy in the ABC and GCB DLBCL subgroups.

1.7.6 Gene expression microarray studies of MALT lymphomas

There are so far three gene expression microarray studies on MALT lymphomas. O'Rourke *et al.* (O'Rourke, 2008) investigated gastric mucosa of BALB/c mice infected with *H. pylori* and correlated transcriptional profile with histological changes during the progression from chronic inflammatory infiltrate to MALT lymphoma. Huynh *et al.* (Huynh *et al.*, 2008) compared gene expression profiles of 21 gastric MALT lymphomas with corresponding *H. pylori* associated MALT B-cell follicles and aggregates. The study showed that gastric MALT lymphoma has a distinct gene expression profile, characterized by up-regulation of several surface receptor markers of haematopoietic cells such as CD1c, CD40, CD44, CD53, CD83 and CD86 and members of the HLA-D family, indicating antigen-dependent survival of lymphoma cells. Chng *et al.* (Chng *et al.*, 2009) attempted to classify 35 cases of pulmonary MALT lymphoma (10 with t(11;18), 3 with t(14;18) translocations and 22 negative for all known MALT lymphoma translocations) with other B- and T- cell lymphomas. They showed that MALT lymphoma is a distinct entity with a prominent T-cell signature and a marginal zone/memory B-cell profile. Fifty genes were differentially expressed between MALT lymphoma and all the other samples, 13 of which showed over-

expression in MALT lymphoma. Only 4, MMP7, SIGLEC6, WSB1, and PRO1853, were specifically overexpressed in MALT lymphoma, and 2 of these, MMP7 and SIGLEC6 were validated using immunohistochemistry on MALT lymphoma tissue microarrays. Hierarchical clustering of pulmonary MALT lymphoma with and without translocations showed overlapping transcriptional profiles with over-expression of NF- κ B and chemokine signalling pathways in MALT lymphomas with t(11;18). Additionally, spiked expression analysis showed high expression of MALT1 and RARA. Samples with plasmacytic differentiation had high FKBP11 expression, and samples with high RGS13 expression tended to have trisomy 3 and reactive follicles. However, the main criticism of this study is that only 7 out of the 33 cases used had 70% or higher tumour content and including cases that had tumour content as low as 15% (Chng *et al*, 2009). This can lead to false positives and under-powered study. In addition the study only focused on t(11;18) and t(14;18) in pulmonary MALT lymphomas only which can exclude other important genes implicated in MALT lymphoma such as BCL10.

In summary, none of the MALT lymphoma microarray studies thus far, convincingly showed the key molecular events explaining its lymphomagenesis.

1.8 Objectives of the thesis

- 1) To characterise the expression profile of MALT lymphoma with and without translocations with the aim to understand the common and unique molecular mechanisms underlying the disease;
- 2) To investigate the cooperation between the expression of MALT lymphoma oncogenes and immunological stimulation on NF- κ B activation;
- 3) To identify novel phenotypic markers for MALT lymphoma by comparing expression microarray data of MALT lymphoma with other lymphomas such as FL, MCL, CLL and SMZL.

CHAPTER 2 – Materials and methods

2.1 Materials

2.1.1 Tissue materials and clinical data

2.1.1.1 Ethical considerations

The patient materials included in this study were archival fresh frozen and formalin-fixed paraffin-embedded tissues. Tissue material was retrieved from Professor Ming Du's laboratory and his international collaborators. Local ethical guidelines were followed for the use of these archival tissues for research with the approval by the local ethics committees of the relevant institutions.

2.1.1.2 Tissue materials for expression microarray and phenotypic marker studies

A total of 26 well characterised MALT lymphomas, 14 SMZL, 7 nodal FL and 8 nodal MCL were used for the expression microarray study. The MALT lymphoma cases included 9 positive for t(11;18)(q21;q21)/API2-MALT1 (8 gastric and 1 pulmonary), 4 positive for t(1;14)(p22;q32)/BCL10-IGH or t(1;2)(p22;p11)/BCL10-IGk (3 gastric and 1 pulmonary), 2 positive for t(14;18)(q32;q21)/IGH-MALT1 (1 hepatic and 1 ocular adnexal), 1 positive for t(3;14)(p13;q32)/IGH-FOXP1 and 10 gastric cases negative for all known MALT lymphoma associated chromosome translocations (Table 2.1). In all cases, fresh frozen tissue from surgical resection specimens was available. Tumour content was checked based on histological examination of Haematoxylin and Eosin (H&E) slides and where necessary crude microdissection was performed to ensure at least 70% tumour cells were used for molecular investigations. The chromosomal translocation status in these cases was investigated in previous studies using conventional cytogenetics, interphase FISH and RT-PCR where appropriate (Table 2.1). Extensive immunophenotyping including BCL10,

MALT1 and FOXP1 immunohistochemical data was available from previous studies (Goatly *et al*, 2008;Liu *et al*, 2001b;Liu *et al*, 2001a;Liu *et al*, 2004a;Ye *et al*, 2000;Ye *et al*, 2006).

Table 2.1 - Summary of clinico-pathological, molecular and immunohistochemical data of MALT lymphoma cases used in gene expression microarray studies.

| Case No. | Sex | Age | Site | Diagnosis | Translocation status | Stage | Treatment | Follow-up | BCL10 immunohistochemistry |
|----------|-----|-----|---------------|---------------|----------------------|-------|--|-----------------------------|----------------------------|
| 1 | M | 41 | Stomach | MALT lymphoma | t(11;18)(q21;q21) | IIIE | | | Moderate nuclear |
| 2 | F | 72 | Stomach | MALT lymphoma | t(11;18)(q21;q21) | IVE | | | Moderate nuclear |
| 3 | M | NA | Stomach | MALT lymphoma | t(11;18)(q21;q21) | | | | Moderate nuclear |
| 4 | F | 52 | Stomach | MALT lymphoma | t(11;18)(q21;q21) | IIE | | | Moderate nuclear |
| 5 | F | 75 | Lung | MALT lymphoma | t(11;18)(q21;q21) | I | Surgical resection, | | Moderate nuclear |
| 6 | M | 51 | Stomach | MALT lymphoma | t(11;18)(q21;q21) | I | total gastrectomy | CR during 6 year follow up | Cytoplasmic |
| 7 | M | 54 | Stomach | MALT lymphoma | t(11;18)(q21;q21) | I | total gastrectomy | CR during 4 year follow up | Cytoplasmic |
| 8 | M | 48 | Stomach | MALT lymphoma | t(11;18)(q21;q21) | III | total gastrectomy | CR during 10 year follow up | Cytoplasmic |
| 9 | F | 62 | Stomach | MALT lymphoma | t(11;18)(q21;q21) | I | Gastrectomy, no evidence of lymphoma during 3 years follow-up | | Cytoplasmic |
| 10 | M | 71 | Stomach | MALT lymphoma | t(1;14)(p22;q32) | IVE | Gastrectomy | | Strong nuclear |
| 11 | NA | NA | Lung | MALT lymphoma | t(1;14)(p22;q32) | | | | Strong nuclear |
| 12 | F | 55 | Stomach | MALT lymphoma | t(1;14)(p22;q32) | | | | Strong nuclear |
| 13 | M | 67 | Stomach | MALT lymphoma | t(1;2)(p22;q12) | IIIE | Total gastrectomy | | Strong nuclear |
| 14 | F | 62 | Liver | MALT lymphoma | t(14;18)(q32;q21) | I | Surgical resection, no evidence of lymphoma during 6 years follow-up | | Strong cytoplasmic |
| 15 | F | 56 | Ocular adnexa | MALT lymphoma | t(14;18)(q32;q21) | I | Treated by radiotherapy, no evidence of lymphoma during 10 years follow-up | | Strong cytoplasmic |
| 16 | M | NA | Stomach | MALT lymphoma | Negative | | | | Moderate nuclear |
| 17 | M | 62 | Stomach | MALT lymphoma | Negative | | | | Moderate nuclear |
| 18 | NA | NA | Stomach | MALT lymphoma | Negative | | | | Moderate nuclear |
| 19 | M | 64 | Stomach | MALT lymphoma | Negative | | | | Cytoplasmic |
| 20 | M | NA | Stomach | MALT lymphoma | Negative | | | | Weak cytoplasmic |
| 21 | M | 18 | Stomach | MALT lymphoma | Negative | | | | Cytoplasmic |
| 22 | M | 57 | Stomach | MALT lymphoma | Negative | III | Total gastrectomy | CR during 13 year follow up | Cytoplasmic |
| 23 | F | 64 | Stomach | MALT lymphoma | Negative | I | Total gastrectomy | CR during 6 year follow up | Cytoplasmic |
| 24 | M | 50 | Stomach | MALT lymphoma | Negative | I | Total gastrectomy | CR during 2 year follow up | Cytoplasmic |
| 25 | M | 55 | Stomach | MALT lymphoma | Negative | | | | Cytoplasmic |
| 26 | NA | NA | Stomach | MALT lymphoma | t(3;14)(p14;q32) | | | | Cytoplasmic |

CR: complete remission

2.1.1.3 Tissue materials for qRT-PCR and immunohistochemistry

For qRT-PCR and immunohistochemical validation of the microarray study, an additional 73 cases of well-characterised MALT lymphoma were recruited. They included 18 cases positive for t(11;18), 8 cases positive for t(1;14) or variant, 9 cases positive for t(14;18), and 38 cases negative for these translocations.

2.1.2 Reagents

2.1.2.1 Reagents used in gene expression microarray and qRT-PCR

5x First Strand buffer for double stranded cDNA synthesis (Invitrogen)

250mM Tris-HCl (pH 8.3), 375mM KCl, 15mM MgCl₂

5x Second Strand buffer for double stranded cDNA synthesis (Invitrogen)

100mM Tris-HCl (pH 6.9), 450mM KCl, 23mM MgCl₂, 0.75mM β-NAD⁺, 50mM (NH₄)₂SO₄

5x Fragmentation buffer

200mM Tris acetate pH 8.2, 500mM potassium acetate, 150mM magnesium acetate

1x Hybridisation buffer

100mM MES, 1M [Na⁺], 20mM EDTA, 0.01% Tween20

Hybridisation cocktail per chip

3nM Control Oligonucleotide B2, Eukaryotic Hybridisation Controls (*bioB*, *bioC*, *bioD* and *cre*, prepared in concentrations of 1.5, 5, 25 and 100pM respectively), 0.1 mg/ml herring sperm DNA, 0.5 mg/ml acetylated BSA and 1x Hybridisation buffer to a final volume of 275µl with ultrapure deionised water

MES (2-(N-Morpholino) ethanesulfonic acid sodium salt)

To make 12X MES Stock (1.22M MES, 0.89M [Na⁺]) in 1000 ml, add :

70.4g MES free acid monohydrate (Sigma)

193.3g MES Sodium Salt (Sigma)

800ml of Molecular Biology Grade water

Mix and adjust volume to 1000ml with DEPC-treated water

The pH should be between 6.5 and 6.7. Filter through a 0.2 µm filter.

Wash buffer

100mM MES, 0.1M [Na⁺], 0.01% Tween20

Streptavidin-Phycoerythrin (SAPE) solution per chip

10µg/ml SAPE stain, 1x MES stain buffer, 2mg/ml acetylated BSA to a final volume of 600µl with double distilled water

Biotinylated anti-streptavidin per chip

2mg/ml acetylated BSA, 0.1mg/ml normal goat IgG (Sigma), 0.5mg/ml biotinylated antibody (Vector Lab, Burlingame, California, USA), 1x MES stain buffer to a final volume of 600µl with double distilled water

2.1.2.2 Reagents used in immunohistochemistry

PBS-Tween

100µl of Tween 20 (Sigma-Aldrich) was added to 200ml of PBS to give a final concentration of 0.05%

Diaminobezidine tetrahydrochloride (DAB) substrate solution (DAKO)

20µl of Dako REAL DAB Chromogen (Dako Cytomation) was added to 1ml of Dako REAL Substrate Buffer (Dako Cytomation) to make the substrate working solution

Diaminobezidine tetrahydrochloride (DAB) substrate solution (Kem-En-Tec)

This solution was always prepared fresh just before use. One tablet of DAB (Kem-En-Tec, Denmark) was dissolved in 10ml of distilled water. 10µl of 30% hydrogen peroxide solution was added to the solution just before application

Haematoxylin

Mayers haematoxylin was filtered and two drops of Tween 20 (Sigma-Aldrich) were added per 500ml

Citrate Buffer pH 6.0

8.82g of sodium citrate tribasic dehydrate (Sigma-Aldrich) were dissolved in 3 litres of distilled water and the pH was adjusted to 6.0 with 1M HCl

Peroxidase block solution

This solution was prepared fresh before use and was composed of 200µl of 30% hydrogen peroxide (Sigma-Aldrich) in 12ml of methanol

Tris-buffered saline pH 7.6 (TBS)

6.05g of Tris (hydroxymethyl) aminomethane (Sigma-Aldrich) and 80g of NaCl were dissolved in 8 litres of distilled water, the pH was adjusted to 7.6 with 1M HCl and the volume brought up to 10 litres with distilled water

TBS-Tween

Tween 20 (Sigma-Aldrich) was added to TBS to give a final concentration of 0.05%

2.1.2.3 Reagents used in tissue culture

RPMI 1640 10% fetal calf serum (FCS) medium & 10% P/S

50ml of FCS (Invitrogen) were added to 450ml of RPMI 1640 medium (Invitrogen). When culturing BJAB Tet-On and TRex cells, tetracycline (Tet) free FCS was used to prevent inadvertent induction of expression. Add penicillin/streptomycin (P/S) to a final concentration of 100U/ml penicillin and 100µg/ml streptomycin

10x Phosphate buffered saline (PBS)

146.6g sodium chloride, 47.2g hydrogen phosphate and 26.4g sodium dihydrogen phosphate for 2 litres distilled water – pH 7.2

Freezing medium

2ml of DMSO were added to 18ml of FCS

2.1.2.4 Reagents used in Western blotting and co-immunoprecipitation

Triton Lysis Buffer

5ml of 50mM Tris pH 7.4, 30ml of 300mM NaCl, 10ml of 1% Triton X-100 (Sigma-Aldrich), and 400µl of 2mM EDTA were added to 100ml with sterile distilled water and mixed to make a stock solution. One tablet of Protease Inhibitor Cocktail (Roche, Penzberg, Germany) for inhibition of proteases was added to 10 ml of stock solution before use

Protein lysis buffer (2X)

Lysis buffer was composed of 100mM Tris-HCl (pH8.0), 300mM NaCl, 0.04% sodium azide, 0.2% sodium dodecyl sulphate (Sigma-Aldrich), 2% nonidet P-40 (BDH), 1% sodium deoxycholate (BDH), 2mM EDTA, 100mg/ml phenylmethylsulfonyl fluoride (Sigma-Aldrich), and 1mg/ml leupeptin (Sigma-Aldrich)

Sample loading buffer

4µl of β-mercaptoethanol (BDH) was added to 96µl of 4X NuPAGE LDS Sample Loading Buffer (Invitrogen)

Running Buffer

50ml of 20X NuPAGE Running Buffer (Invitrogen) were added to 950ml of deionised water

Transfer Buffer

50ml of 20X NuPAGE Transfer Buffer (Invitrogen) and 100ml of methanol were added to 850ml of deionised water

TBST

40ml of 1M Tris pH 7.4, 18g of NaCl and 2ml of Tween 20 (Sigma-Aldrich) were made up to 2 litres with deionised water and mixed

4% milk/TBST

4g of milk powder (Marvel, Premier Foods, UK) dissolved in 100ml of TBST

Stripping buffer

100ml of 10% SDS (10g in 100ml deionised water) were combined with 31.25ml of 1M Tris-HCl pH 6.8 and made up to 500ml with deionised water

2.1.2.5 Reagents used in cloning and DNA sequencing

LB medium

Autoclaved Luria-Bertani (LB) medium was provided in-house: 1% sodium chloride, 0.5% yeast extract and 1% tryptone (Sigma)

LB agar plates

15g/L bacteriological agar (Sigma) added to LB medium, autoclaved and poured into 100*15mm Petri dishes (Sigma)

1x Blue dextran mix

100mg/ml blue dextran (Sigma), 25mM EDTA

1x Tris-borate-EDTA electrophoresis buffer (TBE)

89mM Tris base (Sigma), 89mM boric acid (BDH), 2mM EDTA

Gel solution

To 900ml of Automatrix 4.5% 29:1 acrylamide:bisacrylamide ready made 6M urea gel solution (National Diagnostics, Hull) add 10ml of 1x TBE

2.1.3 Cell lines

BJAB cells: BJAB is a human Burkitt's lymphoma cell line and is Epstein-Barr virus (EBV) negative (Steinitz & Klein, 1975). BJAB cells were a kind gift from Dr. Rolf Renne (University of Florida Shands Cancer Center, Florida, USA).

BJAB-TetON cells: BJAB-TetON cells were a kind gift from Dr. Rolf Renne (University of Florida Shands Cancer Center, Florida, USA) (An *et al*, 2005). Tetracycline free FCS was used when carrying out experiments involving inducible expression of the oncogene of interest.

T-REx Jurkat cells: Jurkat cells are a human T-cell line derived from a patient with acute lymphoblastic leukemia (Schneider *et al*, 1977). T-REx Jurkat cells (Invitrogen, Paisley, UK) stably express the tetracycline repressor protein. Tetracycline free FCS was used when carrying out experiments involving inducible expression of the oncogene of interest.

BaF-3 cells: An IL-3-independent clone of this murine pro-B cell line was established from the peripheral blood of a BALB/c mouse and was the kind gift of Dr Heike Laman, (University of Cambridge, UK).

WEHI cells: Immature murine pro-B cell line established from the peripheral blood of BALB/c mouse and was the kind gift of Dr Heike Laman, (University of Cambridge, UK).

2.2 Methods

2.2.1 Overview of the study plan

Figure 2.1 outlines the study plan in this thesis integrating the investigations using the primary lymphoma materials and *in vitro* cell lines.

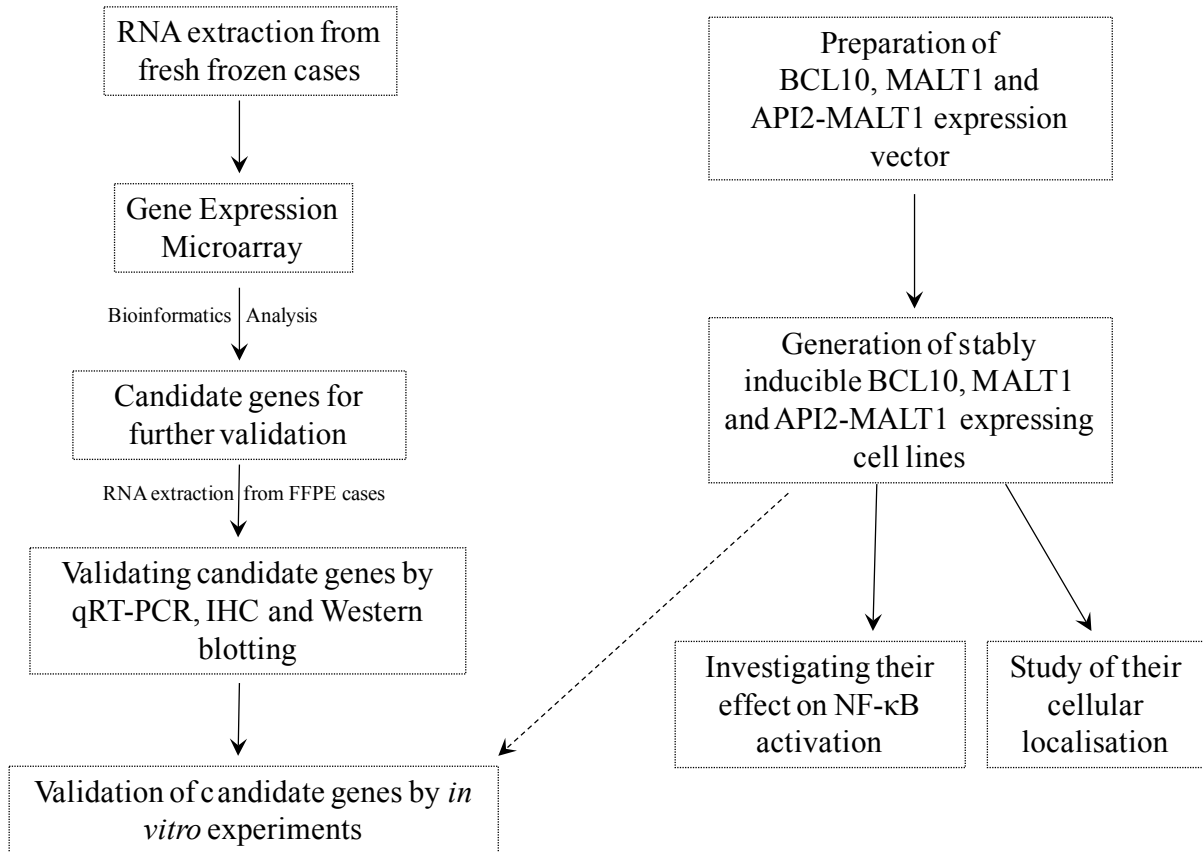


Figure 2.1 - Summary of the study plan.

2.2.2 Crude microdissection

4µm sections of FFPE tissue were cut routinely and mounted on charged glass microscope slides. Sections were dried overnight at 56°C, deparaffinised in xylene and rehydrated using decreasing concentrations of ethanol (100%, 10 minutes; 95%, 5 minutes; 75%, 5 minutes) and immersed in distilled water for 5 minutes, and stained in Haematoxylin for 5 seconds.

The sections were covered in 50% ethanol and the unwanted tissue was scraped away using a needle (Figure 2.2). The selected cell populations were then scraped off the slide into sterile 1.5ml Eppendorf tubes. The microdissected cells were dried and used for RNA extraction.

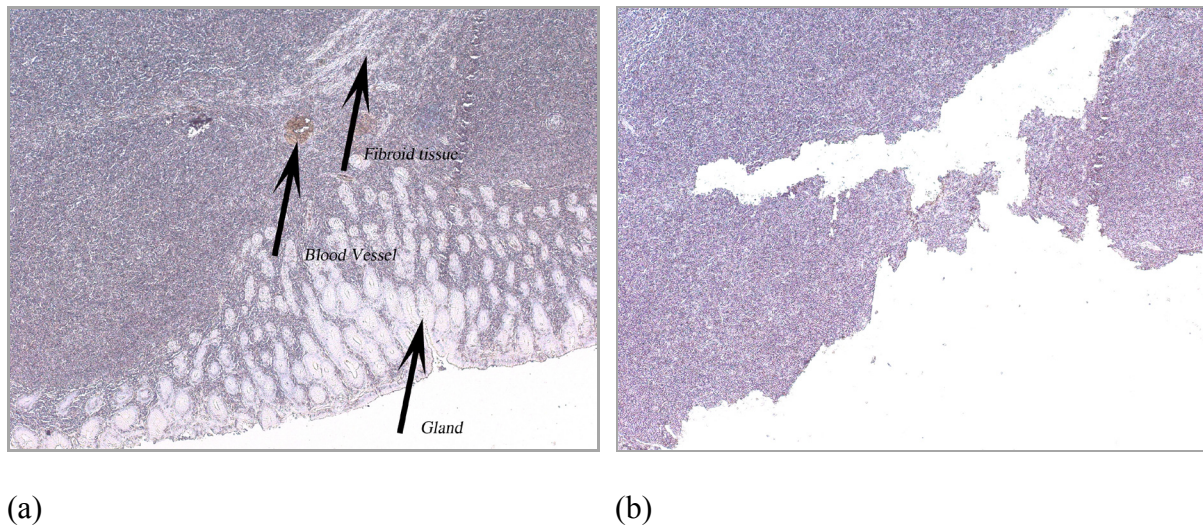


Figure 2.2 - Crude microdissection of gastric MALT lymphoma.

(a) Gastric MALT lymphoma with constitutive normal tissues

(b) Gastric MALT lymphoma after crude microdissection

2.2.3 RNA preparation

2.2.3.1 RNA extraction from fresh frozen tissue

RNA extraction was carried out using RNeasy™ Mini kit (Qiagen, East Sussex, UK) according to the manufacturer's instructions. Briefly, crudely microdissected tumour cells from fresh frozen tissue sections (<5 μm) were lysed in 600 μl of RNeasy lysis buffer (Buffer RLT) containing 1% β -mercaptoethanol. The crude lysate was homogenised by spinning through a QIAshredder column (Qiagen, East Sussex, UK). After addition of absolute ethanol, the samples were applied onto an RNeasy spin column. The column was washed with buffers RW1 and RPE before elution with RNase-free water. To remove all traces of DNA from the samples, they were treated with Turbo DNase (Applied Biosystems,

Warrington, UK) for 30 minutes at 37°C. The DNase was inactivated using the supplied Inactivation Reagent and the RNA yield was quantified.

2.2.3.2 RNA extraction from formalin fixed paraffin-embedded tissue

This was carried out on microdissected tissue using the Ambion RecoverAll Total Nucleic Acid Isolation kit (Applied Biosystems, Warrington, UK) essentially according to the manufacturer's protocol with the exception that the tissue was digested in protease K at 50°C for 3.5 hours.

2.2.3.3 RNA extraction from cell lines

Around 7 million cells were centrifuged at 1200rpm for 5 minutes and the resulting pellet was resuspended in RLT buffer containing 1% β -mercaptoethanol before application to a QIAshredder column. RNA was extracted from cells and the contaminating DNA removed using the protocol described in section 2.2.3.1. The RNA quantity and quality were then measured (Section 2.2.3.5).

2.2.3.4 RNA linear amplification

For gene expression microarray using the HG-U133B GeneChips, there was insufficient RNA to carry out the hybridisation. Therefore a linear RNA amplification method was developed in house and tested with the RNA extracted from fresh frozen tissue. The in house method was based on data showing that reverse transcription using random pentadecamer primers increases yield and quality of resulting cDNA (Stangegaard *et al*, 2006) and the use of T7 and T3 RNA polymerase can be incorporated into the protocol to generate sense and anti-sense RNA (Marko *et al*, 2005; Xiang *et al*, 2003). The goal was to develop a strategy based upon the Eberwine method (Van Gelder *et al*, 1990) but with the ability to produce

sense RNA from small quantities of total or poly-(A)+ RNA extracted from both ideal samples (e.g. cell line RNA) and "real world" samples (e.g. tumours or tissues). This protocol avoids the need for PCR steps and requires two primers only. Additionally, the protocol is cost effective, efficient, and technically simple to perform. Finally, the method gives results consistent with similar amplification techniques when used with subsequent microarray analysis. The in house method used a T7 tagged oligo dT primer to generate a double stranded cDNA from the 3 prime end, followed by T3 tagged pentadecamer to generate a second cycle of double stranded cDNA. This avoided the problems of amplifying degraded RNA and allowed small amounts of RNA to be amplified faithfully for expression microarray studies. 1ng of total RNA was used to generate around 20µg of amplified anti-sense RNA ready to be used for the labelling step before hybridisation to microarray (Section 2.2.4).

2.2.3.5 RNA quantification and quality control

RNA concentration and quality were assessed spectrophotometrically using the GeneQuant Pro (Amersham Pharmacia Biotech, Uppsala, Sweden), and considered to be acceptable for further analysis at a concentration of greater than 500ng/µl RNA with an A_{260}/A_{280} ratio between 1.7 and 2.0. For gene expression microarray studies, the RNA quality was assessed further by running a 100-300ng aliquot on an Agilent 2100 Bioanalyser (Agilent, Berkshire, UK) using Agilent RNA Nano Labchips. RNA extracted from all 26 cases of MALT lymphoma for microarray studies was of good quality varying from 1µg to 5µg total RNA with an A_{260}/A_{280} ratio between 1.7 and 2.0.

2.2.4 Expression microarray

2.2.4.1 Affymetrix HG-U133 GeneChips

Microarray experiments, during the early phase of the study, were carried out on MALT lymphoma cases using the HG-U133A and B, while in the latter phase of the study, FL and MCL cases were analysed using the updated HG-U133plus2 GeneChips.

2.2.4.2 Preparation of biotinylated cRNA target for Affymetrix GeneChips

Total RNA extracted was used to generate double stranded cDNA which acts as a template to generate biotin labelled cRNA that was fragmented using heat and high salt buffer and hybridised to the Affymetrix HG-U133 GeneChip as described below (Figure 2.3).

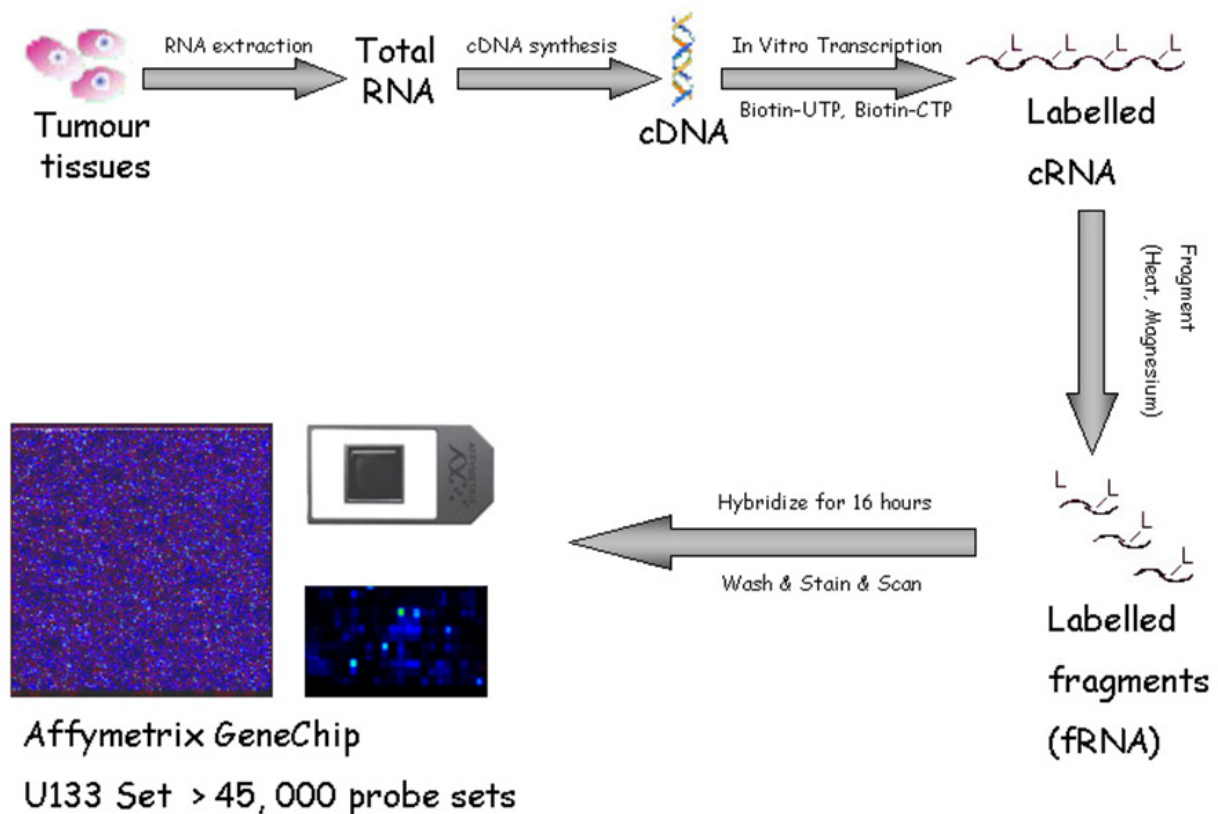


Figure 2.3 - Strategy for generating hybridisation target from total RNA.

2.2.4.2.1 Double stranded cDNA synthesis

First strand cDNA was synthesised from 5µg RNA using 100 pmol HPLC purified oligo(dT) primer conjugated to a T7 promoter (5'-GGC CAG TGA ATT GTA ATA CGA CTC ACT ATA GGG AGG CGG (dT)_{24-3'}) (Thermo Scientific, Surrey, UK), hybridised to the poly-A tail of the mRNA primer. Samples were incubated at 70°C for 10 minutes to denature the secondary RNA structures and placed on ice for the primer to anneal. First strand synthesis was performed in a reaction mix containing; 1× First Strand Buffer, 10mM DTT, 500µM each dNTP (Invitrogen, Paisley, UK) and 100U Superscript II reverse transcriptase (Invitrogen, Paisley, UK) at 42°C for 1 hour. The samples were incubated on ice for 2 minutes followed by brief centrifugation.

The second strand synthesis was carried out in a reaction mixture containing; 1× Second Strand Reaction Buffer, 200µM each dNTP, 10U *E. coli* DNA Ligase, 40U *E. coli* DNA Polymerase I, and 2U *E. coli* RNase H (Invitrogen, Paisley, UK) at 16°C for 2 hrs. T4 DNA Polymerase (Invitrogen, UK) was added at a final concentration of 10U followed by incubation at 16°C for a further 5 minutes. The reaction was terminated by addition of 10µl 0.5M EDTA, pH 8.0 and the double stranded cDNA immediately purified using the cDNA purification columns from the GeneChip sample cleanup module kit (Affymetrix, High Wycombe, UK). The purified cDNA was eluted with 12µl of ultrapure water.

2.2.4.2.2 cRNA labelling using IVT (In-Vitro Transcription)

The generation of cRNA target was carried out using the Enzo Bioarray HighYield RNA Transcript Labelling Kit (Affymetrix, High Wycombe, UK). The reaction was carried out in a 40µl mixture containing: 12µl template cDNA from second strand synthesis reaction, 4µl 10× HY Buffer, 4µl Biotin Labelled Ribonucleotides, 4µl DTT, 4µl RNase Inhibitor Mix,

2µl T7 RNA Polymerase, 10µl water at 37°C for 4.5 hours. The cRNA was purified using the cRNA purification columns from the GeneChip sample cleanup module kit (Affymetrix, High Wycombe, UK). 1µl of each cRNA sample was used to check for sample concentration and purity (Section 2.2.3.5) and the remainder stored at –20°C awaiting array hybridisation.

2.2.4.2.3 Fragmentation of cRNA

20µg biotinylated cRNA was fragmented by incubation in fragmentation buffer and RNase free water at 94°C for 40 minutes followed by 10 minutes incubation on ice. The fragmented cRNA was stored at –20°C until use for hybridisation.

2.2.4.3 Hybridisation to HG-U133 Affymetrix GeneChips and Data Acquisition

2.2.4.3.1 Hybridisation mix preparation

A hybridisation cocktail was prepared in a microfuge tube by adding reagents at the following concentrations; 3nM Control Oligonucleotide B2, Eukaryotic Hybridisation Controls (*bioB*, *bioC*, *bioD* and *cre*, prepared in concentrations of 1.5, 5, 25 and 100pM respectively), 0.1 mg/ml herring sperm DNA, 0.5 mg/ml acetylated BSA and 1x hybridisation buffer to a final volume of 275µl.

2.2.4.3.2 Hybridisation to HG-U133 GeneChips

The cRNA target samples were hybridised to HG-U133 chips. The chips were pre-equilibrated with 200µl 1x hybridisation buffer at 45°C for 10 minutes in a GeneChip 450 Hybridisation Oven (Affymetrix, High Wycombe, UK). The hybridisation cocktail containing the biotinylated cRNA was denatured at 99°C for 5 minutes, and transferred to a 45°C heat block for 5 minutes to pre-equilibrate before being added to the hybridisation chamber and incubated in a 45°C oven for 16 hours with rotation at 60rpm.

2.2.4.3.3 Hybridisation to Test3 GeneChip

A proportion of the biotinylated cRNA target samples was hybridised to Test chips (GeneChip Test3 Array) (Affymetrix, High Wycombe, UK) to ensure successful cRNA biotin labelling using IVT. This was similarly performed as above, with the exception that 80µl 1× hybridisation buffer was used for gene chip pre-equilibration, followed by 80µl hybridisation cocktail.

2.2.4.3.4 Staining of GeneChips

Hybridisation cocktail was removed and replaced with a non-stringent wash buffer (6× SSPE, 0.01% Tween 20). HG-U133A chips were placed in the corresponding slots of the Gene Chip Fluidics Station 450 (Affymetrix, High Wycombe, UK) and subjected to the washing and staining protocol EukGE WASH-WS2V4_450. The GeneChips were washed with a series of non-stringent and stringent wash buffers. Staining was carried out using the following procedure; 40 minutes incubation in Streptavidin-Phycoerythrin (SAPE) solution, then by 20 minutes incubation with biotinylated anti-streptavidin followed by a final 20 minutes incubation in SAPE solution.

2.2.4.4 HG-U133 GeneChip data acquisition and quality control

Chips were scanned at pixel value 2.5µm, wavelength 570 nm using argon laser Affymetrix GeneArray scanner 3000. Data were analysed using Affymetrix MAS and GCOS software. The array was inspected manually for image artefacts such as scratches, overall background, image intensity fluctuations and intensity of hybridisation controls. A grid was automatically placed over the image and correct alignment of grid to image was checked. The Microarray suite (MAS) software (version 5.0) (Affymetrix, High Wycombe, UK) was used to analyse

the scanned image and generate transcript expression data. To allow comparisons between samples, a global scaling technique was used to set the average intensity of each probe set within the array to a target intensity of 100.

The quality control of gene expression microarray varies between different studies and different platforms. Based on Brune *et al.* (Brune *et al.*, 2008) and similar papers involving human tissue, the following quality control parameters for the HG-U133A and HG-U133plus2 GeneChips were used; overall background should be less than 130, scaling factor should be less than 10, the 5'/3' ratio of the housekeeping genes β -actin and glyceraldehyde-3-phosphate dehydrogenase (GAPDH) should be less than 4, hybridisation control *bioB* is called 'present' by the software at least 50% of the time and *bioC*, *bioD* and *cre* called 'present' with increasing signal values representing their relative concentrations and percentage 'present' call of genes should be reproducible between tissues and higher than 20%.

In this study, the HG-U133B GeneChip samples were processed using RNA linear amplification protocol (Section 2.2.3.4) thus the quality control parameters according to (The Tumor Analysis Best Practices Working Group, 2004) and (Brune *et al.*, 2008) were as follows; overall background should be less than 130, scaling factor should be less than 20, the 5'/3' ratio of the housekeeping genes β -actin and glyceraldehyde-3-phosphate dehydrogenase (GAPDH) should be less than 13, hybridisation control *bioB* is called 'present' by the software at least 50% of the time and *bioC*, *bioD* and *cre* called 'present' with increasing signal values representing their relative concentrations and percentage 'present' call of genes should be reproducible between tissues and higher than 10%.

2.2.5 Bioinformatics and statistical analysis of gene expression microarray data

In general, bioinformatics analysis of gene expression microarray starts with normalisation followed by elimination of non-variant probes. The remaining variant probes are the ones that are changing across the samples, and are used for downstream analyses such as unsupervised clustering and differential expression analysis. Full bioinformatics comparison of methods and strategies are presented in Appendix I.

2.2.5.1 Normalisation

After testing many different strategies as outlined in Appendix I.I, the best strategy for generating variant probes that are differentially expressed between the groups was to normalise the array sets using gcRMA and MAS5 and cross reference the probes that passed through non-specific filtering based on coefficient of variation and absolute value thresholding. Raw gene expression data from Affymetrix CEL files were uploaded to bioconductor where MAS5 and gcRMA normalisation were performed separately for each Affymetrix platform. All MAS5 data were scaled to a target intensity of 100. The MAS5 normalised data was imported into Genespring 7.3.1 where they were log-transformed and median centred for further analysis. For comparison between microarray data obtained from HG-U133A&B and HG-U133 plus2 platforms, an additional median polishing normalisation step was applied. MAS5 normalised data were used for unsupervised clustering and fold change calculations; while gcRMA normalised data were used for gene set enrichment analysis (GSEA). Both MAS5 and gcRMA normalised data were subjected to non-specific filtering.

2.2.5.2 Non-specific filtering

To filter out non-variant genes, a combination of noise and variance filtering was applied. To filter out non-expressed genes, only probes with a value of 50 or higher in the MAS5 dataset in 2 or more samples were selected, since the minimum number of cases with a particular translocation, i.e. t(14;18)/IGH-MALT1, was two. To eliminate non-variant genes, only those with a coefficient of variation (CV) value of 10% or higher in the gcRMA dataset across all cases were considered to be variant and thus selected. CV was calculated as the mean / standard deviation of each gene across all cases. Finally, the genes that passed the above two filtering methods were intersected to obtain a common set of variant genes.

For comparison of microarray data between HG-U133A/B and HG-U133 plus2 platform where indicated, the non-specific filtering was similarly performed separately for each of these platforms as outlined above, then intersected to generate a final common set of variant genes. All the above analyses were carried out using scripts written in R programming language (Appendix II.I). The above procedure for analysis of expression microarray data from HG-U133A/B and HG-U133 plus2 platform was validated by a serial empirical testing using the published pulmonary MALT lymphoma expression microarray data from the HG-U133 plus2 platform as a reference (Gene Expression Omnibus: GSE13314) (Chng *et al*, 2009).

2.2.5.3 Clustering analysis

The microarray dataset after the above normalisation and filtering was used for unsupervised clustering and this was carried out using Pearson correlation coefficient and average linkage as the similarity measure and clustering algorithm respectively with Genespring GX 7.3.1.

Separate clustering was performed among all MALT lymphoma, FL and MCL cases and also within the MALT lymphoma cases.

2.2.5.4 Gene Set Enrichment Analysis (GSEA)

GSEA was used to identify gene sets differentially regulated between MALT lymphoma with and without chromosome translocation and this was performed essentially as previously described with minor modification (Subramanian *et al*, 2005). As the original GSEA only identifies the gene set showing either uniformly up or down regulation, for the gene sets displaying both up and down regulated genes, absolute GSEA was additionally performed as previously described (Saxena *et al*, 2006). A total of 4395 gene sets were analysed and they included:

- 1) NF- κ B target genes, which were collated from online data base (<http://www.nf-kb.org>), published works (<http://bioinfo.lifl.fr/NF-KB> and <http://people.bu.edu/gilmore/nf-kb/target/index.html>) and systematic bioinformatics search

- 2) Biological pathways involved in inflammatory and immune response from human immunome database (<http://bioinf.uta.fi/Immunome>) (Ortutay & Vihinen, 2006; Ortutay & Vihinen, 2009), Gene Ontology (<http://wiki.geneontology.org/index.php/Immunology>, <http://www.geneontology.org/GO.immunology.shtml>), and Ingenuity (<http://www.ingenuity.com/>)

- 3) Gene sets from Molecular Signature database (<http://www.broad.mit.edu/gsea/msigdb/index.jsp>). The GSEA results were ranked according to the nominal P value and False Discovery Rate (FDR)

For the gene sets differentially regulated between MALT lymphoma with and without translocation, leading edge analysis was carried out to identify the biologically important gene subset (Subramanian *et al*, 2005). For absolute enrichment, a modification on the original GSEA was made to extract the leading edge set from either end of the list. When generating gene sets, for each sample, only the maximum expression value of the multi-probes for a given gene was used for GSEA as described previously (Subramanian *et al*, 2005), thus avoiding any potential biased representation due to multiple probes for the same gene.

2.2.5.5 Analysis of differential gene expression in MALT lymphomas with and without translocation

Differential gene expression between MALT lymphomas with and without chromosome translocation was investigated using one-way ANOVA with Cross-Gene Error Model in GeneSpring with P value of ≤ 0.05 considered to be significant. The MAS5 normalised and filtered dataset was used for this analysis and the genes differentially expressed between translocation positive and negative MALT lymphomas were obtained. For each of these significantly differentially expressed genes, fold change calculation was carried out and those showing more than 2 fold differences were selected for functional annotation using gene ontology.

2.2.5.6 Functional annotation using gene ontology (GO)

To further assess the biological implications of differential gene expression in MALT lymphomas with and without chromosome translocation, we measured the representation of gene ontology (GO) terms (association of gene products with regard to their associated biological processes, cellular components, and molecular functions) in the above

differentially expressed genes using Genespring and hypergeometric tests provided in the R package GOSTats, version 2.8.0. This allowed us to examine whether any GO term was over or under-represented as compared to chance variations. Independent analyses of GO categories were performed for both over and under-expressed genes in translocation positive MALT lymphoma.

2.2.5.7 Phenotypic marker analysis

The 26 MALT lymphoma cases were compared to 14 SMZL, 7 FL, 8 MCL and 22 CLL. All expression microarrays were performed in house except for CLL which was from a previous study by Calin *et al.* (Calin *et al.*, 2008) and the raw CEL files downloaded from ArrayExpress (<http://www.ebi.ac.uk/microarray-as/ae/>) using the query “E-MEXP-1482“. Normalisation and non-specific filtering was carried out as in sections 2.2.4.1 and 2.2.4.2.

The 26 MALT lymphoma HG-U133A and HG-U133B and FL, MCL and SMZL HG-U133plus2 data were normalised separately using RMA algorithm (Irizarry *et al.*, 2003) and combined using median polish step. Multivariate one-way ANOVA (Welch test) (using GeneSpring 7.3) and Bayesian statistical analysis (using in house R scripts) were carried out independently on all 77 lymphoma cases. The data from both algorithms were intersected to generate a list of common probes to both analyses. The common probes were subjected to SOM and Volcano plot analysis to further filter the gene set. Biological insight, literature search and pathway analysis were used to select the most meaningful phenotypic marker for the study.

2.2.5.8 Statistical analyses

Fisher’s exact test (“stats Package” in R version 2.8.0) is a non-parametric test used to assess the statistical significance of the association between two variables in a 2 by 2 contingency

table. The test is specifically adapted for small sample size, including unequally distributed data among the cells of the table, unlike a Chi-square test. Thus, it was more robust to compare categorical variables from the immunohistochemical staining of each antibody among the various MALT lymphomas with different translocation status.

Student's t-test is a statistical hypothesis test in which the test statistic follows a Student's t distribution if the null hypothesis is supported. It is most commonly applied when the test statistic would follow a normal distribution if the value of a scaling term in the test statistic were known. It was used to calculate the statistics for comparing reporter assay experiments.

Mann–Whitney U is a non-parametric test for assessing whether two independent samples of observations have equally large values. It is one of the best known non-parametric significance tests. It is identical to performing an ordinary parametric two-sample t-test on the data after ranking over the combined samples. Thus it was used to compare the qRT-PCR data of each transcript between the MALT lymphomas with various translocation statuses.

In all the above statistical methods, the null hypothesis corresponded to the independence of the chosen variables. The null hypothesis was rejected if the probability value of the test of association was less than 0.05, meaning the variables were significantly associated.

2.2.6 Quantitative Real-time RT-PCR

2.2.6.1 Primer design

Primers were designed for RT-PCR to validate the expression of candidate genes obtained from expression microarray analysis. All primers were designed using primer3 software (<http://frodo.wi.mit.edu/primer3>) initially and for difficult regions such as GC rich, Oligos software (Institute of Biotechnology, Finland) was used. Where possible, primers were designed to contain a GC clamp at the 3' end. All primers were checked for any possible

primer dimer formation or self-complementarity and primer sequences were checked using BLAST tools (<http://www.ncbi.nlm.nih.gov/BLAST>) from National Centre for Biotechnology Information (NCBI). Details of the primers used for each candidate gene are shown in Table 2.2. Where possible, all gene-specific primer pairs were designed to span exons in order to make them suitable for degraded paraffin-embedded tissue nucleic acid where amplicons of less than 150 base pairs are desired (Liu *et al*, 2002a).

Table 2.2 - Primers used to investigate candidate genes by qRT-PCR.

| Gene name | Exon targets | Primer | Primer sequence | Amplicon size | Accession Number |
|---------------------------|-------------------|------------|--------------------------|---------------|------------------|
| <i>18S_rRNA</i> | N/A | Sense | TGACTCAACACGGGAAACC | 114bp | NR_003286 |
| | N/A | Anti-sense | TCGCTCCACCAACTAAGAAC | | |
| <i>N-MALT1</i> | Exon1 | Sense | CTCCGCCTCAGTTGCCTAGA | 104bp | NM_006785 |
| | Exon2 | Anti-sense | CAACCTTTTTACCCATTAACCTCA | | |
| <i>BCL10</i> | Exon1 | Sense | GAAGTGAAGAAGGACGCCTTAG | 80bp | NM_003921 |
| | Exon2 | Anti-sense | AGATGATCAAAATGTCTCTCAGC | | |
| <i>NR4A3</i> | Exon6 | Sense | TTCCATCAGGTCAAACACTGC | 84bp | NM_173198 |
| | Exon7 | Anti-sense | AATCCACGAAGGCACTGAAG | | |
| <i>CD86</i> | Exon1 | Sense | GGAATGCTGCTGTGCTTATGC | 121bp | NM_006889 |
| | Exon2/3 | Anti-sense | AGCACCAGAGAGCAGGAAGG | | |
| <i>CD69</i> | Exon2 | Sense | CCACCAGTCCCCATTTCTCAA | 125bp | NM_001781 |
| | Exon3 | Anti-sense | TTGGCCCACTGATAAGGCAAT | | |
| <i>TLR6</i> | Only has one exon | Sense | AACAAGTACCACAAGCTGAAG | 100bp | NM_006068 |
| | | Anti-sense | CTCTAATGTTAGCCCAAAAGAG | | |
| <i>CCR5</i> | Exon2 | Sense | ATCCGTTCCCCTACAAGAACTC | 100bp | NM_000579 |
| | Exon3 | Anti-sense | GCAGGGCTCCGATGTATAATAA | | |
| <i>CCR2A</i> | Exon3 | Sense | GCGTTTAATCACATTCGAGTGTTT | 77bp | NM_001123041 |
| | Exon3 | Anti-sense | CCACTGGCAAATTAGGGAACAA | | |
| <i>BCL2</i> | Exon3 | Sense | TTGCTTTACGTGGCCTGTTTC | 94bp | NM_000633 |
| | Exon3 | Anti-sense | GAAGACCCTGAAGGACAGCCAT | | |
| <i>IRF4</i> | Exon7 | Sense | GCCCAACAACTGGAGAGAG | 123bp | NM_002460 |
| | Exon8 | Anti-sense | AAGCATAGAGTCACCTGGAAT | | |
| <i>Lactoferrin</i> | Exon1 | Sense | GCCACAAAATGCTTCCAATGG | 116bp | NM_002343 |
| | Exon2 | Anti-sense | GCCCTGTTTTCCGCAATGG | | |

2.2.6.2 Complementary DNA (cDNA) synthesis

cDNA was generated using the Superscript III Reverse Transcriptase kit (Invitrogen, Paisley, UK) with gene specific primers. Typically, the reaction mixture contained: 1µM of each gene-specific anti-sense primer, 1µl of 10mM dNTP, and 200ng of RNA per reverse primer. After incubation at 65°C for 5 minutes the following were added: 2µl of 10 RT buffer, 4µl of 25mM MgCl₂, 2µl of 0.1M DTT, 1µl of RNase inhibitor and 2U of Superscript III and incubated at 50°C for 50 minutes followed by incubation at 85°C for 15 minutes. RNase H was added and the mixture incubated at 37°C for 20 minutes to remove the original RNA.

2.2.6.3 Quantitative PCR (qRT-PCR)

The expression of each target transcript was normalised against the level of expression of 18S rRNA in each case. Real-time PCR was performed using the iCycler IQ system (BioRad, Hertfordshire, UK) using SYBR Green I Supermix (BioRad, Hertfordshire, UK).

The conditions for real-time PCR were optimised prior to result collection. The specificity of the primers in producing PCR products was confirmed by melt-curve analysis. The efficiency of each primer was designed to be between 95% and 110% by generating standard curves for each candidate gene from serial dilutions of cDNA produced from tonsillar RNA. All qRT-PCR were carried out in triplicate and standard deviation of less than 0.5 was deemed to be acceptable. The average correlation coefficient value (R^2) for each standard curve was above 0.99. The slope of the standard curves was used to determine the exponential amplification and efficiency of the qPCR reaction by the following equation (Tichopad *et al*, 2003):

$$\text{Efficiency} = 10^{(-1/\text{slope})}$$

cDNA was diluted 1/1000 for detection of 18S rRNA as it is highly expressed in most tissues (Ye *et al*, 2005). All samples were amplified by qRT-PCR on 96-well plates in triplicate using the following parameters: initial denaturation at 95°C for 3 minutes, followed by 45

cycles of denaturation at 95°C for 15 seconds and annealing and extension at 60°C for 1 minute. To ensure minimal intra-plate variation, a calibrator sample consisting of high and low C_t values was used in triplicate on each plate and was used to adjust the C_t . Only those samples that showed specific amplification by melt curve analysis were used for data analysis. The ΔC_t value for each sample was calculated by subtracting the C_t value for 18S from that of the target transcripts. The higher the ΔC_t value, the lower the expression of a transcript and *vice versa*. For all qRT-PCR, two negative controls were included; a negative control of water instead of RNA that goes through the cDNA synthesis and qPCR step and a negative control of RNA in the qPCR step to ensure that there is no genomic DNA contamination.

2.2.7 Immunohistochemistry

Paraffin sections (4 μ m) were deparaffinised in xylene (BDH, Leicestershire, UK), rehydrated using decreasing concentrations of ethanol (BDH Leicestershire, UK), and incubated in peroxidase blocking solution for 10 minutes to block the endogenous peroxidase activity. Antigen retrieval was carried out prior to immunostaining. Antigen retrieval conditions and primary antibody dilutions are detailed in Table 2.3. Sections were incubated with primary antibody at an optimal dilution for 1 hour followed by biotinylated secondary antibody (1:200 – 1:300) and peroxidase conjugated ExtroAvidin (1: 200) for 30 minutes, respectively. Finally, the sites of antibody binding were visualised with DAB in H₂O₂ (Kem-En-Tec, North Carolina, USA) and counter-stained with Mayer's haematoxylin. The slides were washed in TBS-Tween, three times for 5 minutes each between all incubation steps and mounted with cover slips for viewing.

Table 2.3 - Immunohistochemistry antibodies and conditions.

| Protein | Primary antibody | Source | Antigen retrieval method | Conditions for immunohistochemistry or Western blot |
|-------------|--|-----------------|--|---|
| BCL10 | Mouse monoclonal antibody to human BCL10 (clone 151) | In house | Microwave in DAKO target retrieval solution pH 6.0 for 25-35 minutes | For immunohistochemistry: primary antibody (1/50), 1 hour at RT; biotinylated rabbit antimouse antibody, 30 mins at RT; peroxidase-conjugated extraAvidin, 30 mins at RT. |
| MALT1 | Mouse monoclonal antibody to human C-MALT1 | In house | Microwave in DAKO target retrieval solution pH 9.9 for 25 minutes | For immunohistochemistry: primary antibody (1/50), 1 hour at RT; biotinylated rabbit antimouse antibody, 30 mins at RT; peroxidase-conjugated extraAvidin, 30 mins at RT. |
| BCL2 | Mouse monoclonal antibody | Novocastra | Pressure cooking with citrate buffer pH 6.0 for 3 minutes | For immunohistochemistry: primary antibody (1/120), 1 hr at RT; biotinylated rabbit antimouse antibody, 30 mins at RT; peroxidase-conjugated extraAvidin, 30 mins at RT. |
| CD69 | Mouse monoclonal antibody | NeoMarkers | Pressure cooking with 1mM EDTA for 3 minutes | For immunohistochemistry: primary antibody (1/20), 1hr at RT; followed by polymer amplification system. |
| CD86 | Sheep CD86 polyclonal antibody | R & D | Pressure cooking with citrate buffer pH 6.0 for 3 minutes | For immunohistochemistry: primary antibody (1/60), 1 hr at RT; biotinylated donkey antisheep antibody, 30 mins at RT; peroxidase-conjugated extraAvidin, 30 mins at RT. |
| IRF4 | Mouse monoclonal antibody | Dako Cytomation | Microwave in DAKO target retrieval solution pH 9.9 for 25 minutes | For immunohistochemistry: primary antibody (1/50), 1 hr at RT; biotinylated rabbit antimouse antibody, 30 mins at RT; peroxidase-conjugated extraAvidin, 30 mins at RT. |
| Lactoferrin | Rabbit polyclonal antibody | Abcam | Pressure cooking with citrate buffer pH 6.0 for 3 minutes | For immunohistochemistry: primary antibody (1/50), 1 hr at RT; biotinylated rabbit antimouse antibody, 30 mins at RT; peroxidase-conjugated extraAvidin, 30 mins at RT. |

2.2.8 Expression constructs preparation

2.2.8.1 Modification of pIRES vectors containing HA and FLAG tag sequences

pIRES contains internal ribosome entry site (IRES) of the encephalomyocarditis virus (ECMV), which permits the translation of two open reading frames from one mRNA thus ensuring that the gene of interest is expressed together with a puromycin antibiotic resistance gene in the vector. This reduces the rate of false positives by ensuring that after selection with puromycin, nearly all surviving colonies will stably express the gene of interest (Jang *et al*, 1988). A forward oligo was designed containing the second half of the *NheI* restriction site, an ATG translation start site and the sequence of the FLAG tag

(5'CTAGCATGGATTACAAGGATGACGACGATAAGG) or HA tag (5'CTAGCATGTACCCATACGATGTTCCAGATTACGCTG). A reverse oligo was designed containing the first half of the *EcoRI* restriction site, ATG translation start site and the sequence of the FLAG tag (5'AATTCCTTATCGTCGTCATCCTTGTAATCCTAG) or HA tag (5'AATTCAGCGTAATCTGGAACATCGTATGGGTACATG). The two oligos for each tag were annealed by mixing 1µg of each oligo with 100mM sodium chloride, 10mM Tris pH7.5 and 1mM EDTA and boiling for 90 seconds, before being allowed to cool at room temperature for 30 minutes. This generated a piece of double stranded sequence containing the *NheI* and *EcoRI* "sticky ends". The pIRESpuro2 vector (Clontech Laboratories, UK) (Figure 2.4) was digested with *NheI* and *EcoRI*. The FLAG or HA tag sequence was ligated into the cut vector with T4 DNA ligase (NEB, UK) to generate FLAG and HA tagged pIRESpuro which were used to generate constructs to make the stable cell lines as described in section 2.2.9.

Table 2.4 - Primers used in construct preparation.

| Construct | Primer Sequence (sense and antisense in 5' to 3') | |
|-------------------|--|---|
| <i>BCL10</i> | Lead <i>EcoRI</i> | BCL10 Exon1 TGAT GAATTC ATGGAGCCCACCGCACCGTCC |
| | Lead <i>NotI</i> | BCL10 Exon3 TGAT GCGGCCGC TCATTGTCGTGAAACAGTACGTG |
| <i>MALT1</i> | Lead <i>BamHI</i> | MALT1 Exon1 TGAT GGATCC ATGTCGCTGTTGGGGGACCCGCTACAG |
| | Lead <i>NotI</i> | MALT1 Exon17 TGAT GCGGCCGC TCATTTTTTCAGAAATTCTGAGCCTGTC |
| <i>API2-MALT1</i> | Lead <i>EcoRI</i> | API2 Exon1 TGAT GAATTC ATGAACATAGTAGAAAACAGCATATTC |
| | Lead <i>NotI</i> | MALT1 Exon17 TGAT GCGGCCGC TCATTTTTTCAGAAATTCTGAGCCTGTC |
| <i>pIRES</i> | | ATCGATATCTGCGGCCTAGC |
| | | CCAGCACACTGGATCAGTTATC |
| <i>pTRE2</i> | | GGATCCTCTAGTCAGCTGACG |
| | | TCTAGAGATATCGTCGACAAGC |

2.2.8.2 Generation of tagged *BCL10*, *MALT1* and *API2-MALT1* expression constructs

A standard 25µl PCR reaction was carried out using 2mM MgCl₂, 0.2mM of each dNTP, 0.2µM of each primer and 1 unit of *Pfu* polymerase (Stratagene, Leicestershire, UK) on a Hybaid Px2 thermal cycler (Thermo Scientific, Surrey, UK). The PCR reaction was heated to 94°C for 2 minutes, followed by 30 cycles of denaturation for 45 seconds at 94°C, primer annealing for 45 seconds starting at 55°C and extension for 90 seconds at 72°C with a final extension time of 10 minutes at 72°C. PCR products were visualised by electrophoresis using 1.5% agarose gels.

2.2.8.2.1 Preparation of HA-tagged BCL10

The full length cDNA sequence of BCL10 was generated by RT-PCR of a t(1;14) MALT lymphoma and sub-cloned into TOPO-TA cloning vector (Invitrogen, Paisley, UK). The full length BCL10 cDNA sequence from the TOPO-TA cloning vector was then amplified by PCR using *Pfu* polymerase with sense primer containing an *EcoRI* site and anti-sense primer containing a *NotI* site. The PCR products were cut with *EcoRI* and *NotI* to produce “sticky ends” and cleaned by gel extraction using the QIAQuick Gel Extraction Kit (Qiagen, East Sussex, UK). The HA-tag containing pIRESpuro2 vector was linearised by *PvuI* restriction followed by *EcoRI* and *NotI* restriction and then ligated with the above BCL10 products. The vector sequences were checked for absence of mutations and to ensure that the gene of interest was in frame by sequencing in both directions.

2.2.8.2.2 Preparation of FLAG-tagged API2-MALT1 and FLAG-tagged MALT1

pcDNA3.1 vectors containing full length MALT1 and full length API2-MALT1 (joining nucleotides 1 to 2048 of API2 to nucleotides 814 to 2475 of MALT1) (Ho *et al*, 2005) were kindly provided by Dr. Liza Ho, Department of Clinical Pathology, Geneva, Switzerland. This API2-MALT1 product represents the most common breakpoint found in 93% of t(11;18) MALT lymphomas. Sense primer was designed with the addition of an *EcoRI* restriction site targeting exon1 of the API2 gene while an anti-sense primer was designed with an addition of a *NotI* site targeting exon 17 of the MALT1 gene. For the MALT1 construct, the sense primer has a *BamHI* restriction site targeting exon1 of MALT1 and the anti-sense primer has a *NotI* restriction site targeting exon 17. Both MALT1 and API2-MALT1 sequences were amplified by a standard PCR reaction using *Pfu* polymerase. The PCR products were cut with *EcoRI* (for API2-MALT1) or *BamHI* (for MALT1) and *NotI* to produce “sticky ends” and cleaned

by gel extraction using the QIAQuick Gel Extraction Kit (Qiagen). The FLAG-tag containing pIRESpuro2 vector was cut with *EcoRI* (API2-MALT1) or *BamHI* (MALT1) and *NotI* and the MALT1 or API2-MALT1 ligated with the above product using T4 DNA ligase. The vector sequences were checked for absence of mutations and to ensure that the gene of interest was in frame by sequencing in both directions.

2.2.8.2.3 Sub-cloning of oncogenes into pTRE2

pTRE2 vector (Clontech, Saint-Germain-en-Laye, France) is a response plasmid that can be used to express a gene of interest in Clontech's Tet-On and Tet-Off cell lines. pTRE2 contains a multiple cloning site (MCS) immediately downstream of the Tet-responsive promoter (Figure 2.5).

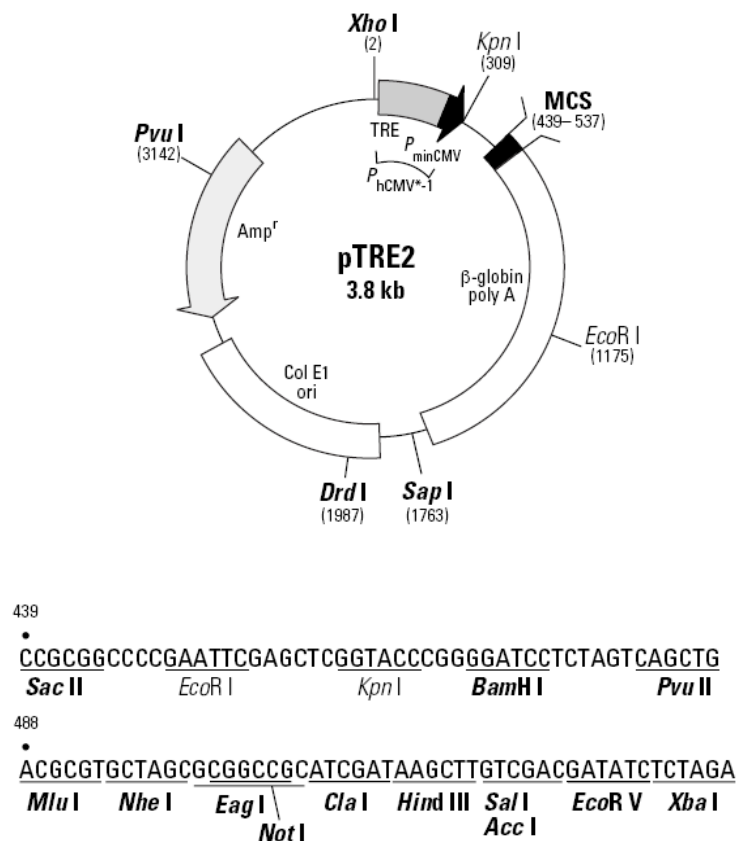


Figure 2.5 - pTRE vector.

cDNA or genes inserted into the MCS will be responsive to the rTA and rtTA regulatory proteins in the Tet-Off and Tet-On systems respectively. $P_{\text{hcmv}-1}$ contains the Tet response element (TRE), which consists of seven copies of the 42-bp tet operator sequence (tetO). The TRE is just upstream of the minimal CMV promoter ($P_{\text{min cmv}}$), which lacks the enhancer that is part of the complete CMV promoter. Consequently, $P_{\text{hcmv}-1}$ is silent in the absence of binding of TetR or rTetR to the TetOs' sequences. pTRE2 puro and pTRE hygro were used to generate inducible BCL10, MALT1 and API2-MALT1 expression cell lines.

In order to generate the cell lines, each oncogene construct and the pTRE vector was cut using *NheI* and *NotI* and the insert containing the oncogene in the correct reading frame was ligated into the pTRE vector with T4 DNA Ligase. Before transfection to the cell lines the vector containing the oncogene of interest was linearised by cutting with *PvuI* restriction enzyme to facilitate its integration into the host genome.

2.2.8.3 Toll-like receptors expression constructs

Toll-like receptor (TLR) 1, 2 and 6 in pFLAG-CMV-1 vector were a kind gift from Dr. Koichi Kuwano (Department of Bacteriology, Kurume University, Japan) (Shimizu *et al*, 2007). pFLAG-CMV-1 expression vector is used for expression and secretion of N-terminal FLAG fusion proteins in mammalian cells, its MCS has preprotrypsin which binds the expressed protein to the plasma membrane. All 3 vectors were verified by sequencing from both ends using pFLAG-CMV-1 vector primers.

2.2.8.4 DNA Sequencing

The sequencing reaction was carried out according to Hamoudi *et al*. (Hamoudi *et al*, 2002) using the dRhodamine Dye Terminator Cycle Sequencing Kit (Applied Biosystems, Warrington, UK). The sequencing reaction was carried out in a 10 μ l reaction mixture

containing 500ng of plasmid DNA, 4µl dRhodamine, 2µl of 5µM primer and 4µl ultrapure water in a thermal cycler (Hybaid Px2 thermal cycler, Thermo Scientific) using the following cycling protocol; 96°C for 30 seconds, 50°C for 15 seconds and 60°C for one minute, for 25 cycles. The products were precipitated with 3 volumes of ethanol and 0.5 volume of 3M sodium acetate at pH 5.2. DNA pellets were resuspended in 1µl of denaturing blue dye and denatured for 2 minutes at 90°C before loading on polyacrylamide gels (29:1 acrylamide:bisacrylamide ready made 6M urea) (National Diagnostics, Hull, UK), and electrophoresis was carried out using an ABI 377 DNA Sequencer (Applied Biosystems). Data was collected via the associated DNA Sequencer Collection software version 2.0 (Applied Biosystems) and the results were analysed using the BioEdit sequence alignment editor version 7 (Ibis Biosciences, California, USA), Sequence Navigator version 1.1 (Applied Biosystems) and online BLAST tools (<http://www.ncbi.nlm.nih.gov/BLAST>).

2.2.9 Cell culture

Cells were cultured in RPMI 1640 with 10% Fetal Calf Serum (FCS) and incubated at 37°C, 5% CO₂ in a humidified, automatically controlled incubator. All cells were checked for the presence of mycoplasma by PCR using VenorGeM kit (Minerva Biolabs, Germany).

2.2.9.1 Protocol for freezing cells

The cells to be frozen were centrifuged at 1200rpm for 10 minutes and the pellet was resuspended in Freezing Medium then transferred to cryotubes (Corning, Dorset, UK). The cell suspension was placed at -80°C overnight and then in liquid nitrogen for storage.

2.2.9.2 Protocol for thawing cells

The frozen cells were thawed at 37°C for 5 minutes with gentle shaking, briefly washed with 8ml of warm culture medium and transferred to a sterile tissue culture flask with appropriate culture medium and antibiotics.

2.2.9.3 Cell clot preparation

Around 5×10^5 cells were centrifuged at 1200rpm for 5 minutes and immediately placed on ice. Five drops of plasma were added to the cell pellet followed by gentle vortexing for 10 seconds. Three drops of thrombin (Diagnostic Reagents Ltd, Oxford, UK) were added and mixed using a plastic pipette in order to clot the cells. The clotted cells were transferred to Speci-wrap paper, which was folded and placed inside a formalin cassette. The cassette was placed inside a formalin jar and left for 4 hours. The samples were processed using a Shandon Excelsior machine to generate formalin fixed paraffin embedded blocks.

2.2.9.4 Transient transfection of cells

Baf-3 and WEHI cell lines were transiently transfected. The required number of cells were centrifuged to form a pellet and washed in PBS (Invitrogen, Paisley, UK). The clean cell pellet was resuspended in 100µl of appropriate Amaxa Cell Line Nucleofector Solution (Lonza, Berkshire, UK). The vector DNA was added at a ratio of around 1µg of DNA to 1 million cells and the cells were transfected using the appropriate programme on a Nucleofector I machine (Lonza, Berkshire, UK). The transfected cells were then routinely cultured. Nucleofector Solution T with programme T16 was used to transfect BJAB, Jurkat T-Rex and Baf-3 cells whereas solution V with programme T30 was used to transfect WEHI cells. These conditions were optimized by transfection of pmaxGFP and subsequent analysis

of the transfected cells by Flow cytometry using FACSCalibur flow cytometer (Beckton Dickson, Oxford, UK).

2.2.9.5 Generation of stably inducible MALT lymphoma associated oncogenes cells

pTRE-BCL10, pTRE-MALT1, pTRE-API2-MALT1 and pTRE wild type were used to generate stable inducible cell lines, whilst pIRESpuro-BCL10 and pIRESpuro wild type were used to generate stable cell lines. 20µg of each different construct were linearised by digestion with *PvuI*, purified by phenol/chloroform extraction and resuspended in 20µl of sterile water to a final concentration of 1µg/µl. For each transfection, 2×10^7 of BJAB, BJAB-TetON or Jurkat TetON (T-REx) cells were washed with PBS, resuspended in 700µl of PBS, mixed with 20µl of the linearised construct and transferred to a 4mm Gene Pulser cuvette. After 5-10 minutes on ice, electroporation was carried out using the Gene Pulser Apparatus (BioRad) at 250 volts and 950µFD (a time between 15 and 20 milliseconds indicates successful electroporation). The samples were incubated on ice for 10 minutes and transferred to a Falcon tube containing 20ml of RPMI 1640 medium with 10% FCS, 30% conditioned medium containing 1mM sodium pyruvate, 50µM α -thioglycerol and 20nM bathocuproindisulfonic acid disodium salt (reagents needed for cell growth and survival) (Brielmeier *et al*, 1998). Various concentrations of transfected cells (1.5×10^5 , 3.75×10^3 and 1.25×10^3 cells) were seeded in 96-well plates for 24 hours in medium containing 4µg/ml puromycin. Clones were checked after 10 to 14 days, and transferred to a 24-well culture plate, then to a small 10ml flask. The cloned cells were subjected to Western blot analysis to check their oncogene expression. Induction of the oncogene expression was carried out by adding 1µg/ml of doxycycline.

A total of 14 cell lines expressing MALT lymphoma associated oncogenes were generated and they included :

Inducible expression cell lines

- 1) BJAB Tet-ON pTREpuro wild type (control)
- 2) BJAB Tet-ON pTREpuro FLAG-MALT1
- 3) BJAB Tet-ON pTREpuro FLAG-API2-MALT1
- 4) BJAB Tet-ON pTREhygro HA-BCL10
- 5) BJAB Tet-ON pTREhygro HA-BCL10 and pTREpuro FLAG-MALT1
- 6) BJAB Tet-ON pTREhygro HA-BCL10 and pTREpuro FLAG-API2-MALT1
- 7) Jurkat Tet-ON (T-REx) pTREpuro wild type (control)
- 8) Jurkat Tet-ON (T-REx) pTREpuro FLAG-MALT1
- 9) Jurkat Tet-ON (T-REx) pTREpuro FLAG-API2-MALT1
- 10) Jurkat Tet-ON (T-REx) pTREhygro HA-BCL10
- 11) Jurkat Tet-ON (T-REx) pTREhygro HA-BCL10 and pTREpuro FLAG-MALT1
- 12) Jurkat Tet-ON (T-REx) pTREhygro HA-BCL10 and pTREpuro FLAG-API2-MALT1

Stable expression cell lines

- 13) pIRESpuro wild type (control)
- 14) pIRESpuro HA-BCL10

2.2.10 Protein analysis

2.2.10.1 Protein extraction from whole cell lysate

Cells were harvested by centrifugation and cell pellets were washed twice in 1×PBS then lysed in Triton Lysis Buffer, on ice for 30 minutes. The cell lysate was centrifuged at 7300rpm for 20 minutes at 4°C, and the supernatant was transferred to a new tube and quantified (2.2.10.4). Samples were stored at -80°C until required.

2.2.10.2 Preparation of protein homogenate from frozen tissue

Frozen tissue sections were homogenised in Triton lysis buffer by gentle pipetting at 4°C for 30 minutes. The lysate was centrifuged at 7300rpm for 20 minutes at 4°C and the supernatant

was transferred to a new tube and quantified as described in 2.2.10.4. Samples were stored at -80°C until required.

2.2.10.3 Protein extraction from nuclear and cytoplasmic fractions

Preparation of nuclear and cytoplasmic protein extracts from cells was carried using CellLytic NuCLEAR Extraction kit (Sigma, Dorset, UK) according to the manufacturer's instructions. The procedure for nuclear protein extraction is to allow cells to swell with hypotonic buffer. The cells are then disrupted and cytoplasmic fraction is removed, and the nuclear proteins are released from the nuclei by a high salt buffer.

2.2.10.4 Protein quantitation

The concentrations of extracted proteins were measured using the Quant-iT Protein Assay kit (Invitrogen, Paisley, UK) according to the manufacturer's instructions with the Victor 3 illuminometer (Perkin Elmer, Warrington, UK).

2.2.10.5 Antibodies used for functional and cellular work

Monoclonal and polyclonal antibodies used in the functional studies described in this thesis are shown in Table 2.5.

Table 2.5 - Primary and secondary antibodies used in co-immunoprecipitation and Western blotting.

| Antibody | Source (Part No.) | Dilution | Application | Type | Host species and (primary/secondary) |
|---|------------------------------------|-----------------|----------------------------|----------------|---|
| C-MALT | In-house | 1:500 | Co-IP and Western blotting | Monoclonal | Mouse - primary |
| BCL10 | In-house | 1:10,000 | Co-IP and Western blotting | Monoclonal | Mouse - primary |
| HA | Sigma-Aldrich (H9658) | 1:10,000 | Western blotting | Monoclonal | Mouse - primary |
| FLAG | Sigma-Aldrich (F3165) | 1:10,000 | Western blotting | Monoclonal | Mouse - primary |
| β-actin | Sigma-Aldrich (A5441) | 1:1,000,000 | Western blotting | Monoclonal | Mouse - primary |
| TLR6 | Abcam (ab62569) | 1:10,000 | Western blotting | Polyclonal | Rabbit - primary |
| IκBβ | Cell Signaling Technology (9248) | 1:20,000 | Western blotting | Polyclonal | Rabbit - primary |
| IκBα | Santa Cruz Biotechnology (sc-203) | 1:10,000 | Western blotting | Polyclonal | Rabbit - primary |
| IκBϵ | Cell Signaling Technology (9249) | 1:10,000 | Western blotting | Polyclonal | Rabbit - primary |
| p65 | Santa Cruz Biotechnology (sc-7151) | 1:10,000 | Western blotting | Polyclonal | Rabbit - primary |
| p50/p105 | Santa Cruz Biotechnology (sc-7178) | 1:10,000 | Western blotting | Polyclonal | Rabbit - primary |
| p100/p52 | Cell Signaling Technology (3017) | 1:10,000 | Western blotting | Monoclonal | Rabbit - primary |
| c-Rel | Cell Signaling Technology (4727) | 1:10,000 | Western blotting | Polyclonal | Rabbit - primary |
| RelB | Cell Signaling Technology (4954) | 1:10,000 | Western blotting | Polyclonal | Rabbit - primary |
| CD3 | eBioscience (16-0037) | 1:10,000 | Western blotting | Monoclonal | Mouse - primary |
| CD28 | Sigma-Aldrich (C7831) | 1:10,000 | Western blotting | Monoclonal | Mouse - primary |
| Donkey anti-rabbit HRP-conjugated | GE Healthcare (NA934) | 1:20,000 | Western blotting | Not applicable | Donkey - secondary |
| Sheep anti-mouse HRP-conjugated | GE Healthcare (NA931) | 1:20,000 | Western blotting | Not applicable | Sheep - secondary |

2.2.10.6 Western blot

Protein lysates were mixed with 4X NuPAGE (Invitrogen, Paisley, UK) loading buffer containing 4% β -mercaptoethanol (BDH, Leicestershire, UK), heated to 99°C for 5 minutes and left on ice for 2 minutes then separated on NuPAGE gels (Invitrogen, Paisley, UK) by electrophoresis at 120V for 90 minutes using SeeBlue size standard (Invitrogen, Paisley, UK).

The proteins were transferred to an Immobilon-P Transfer Membrane (Millipore Corporation, Bedford, USA) using XCell II Blot Module (Invitrogen, Paisley, UK) running at 30V for 90 minutes.

The membrane was first placed in TBST for 10 minutes followed by 4% milk/TBST for 1 hour whilst shaking to block non-specific binding then probed with primary antibody in 4% milk/TBST with 10% FCS overnight at 4°C. After washing in TBST, the membrane was incubated with an anti-species specific (according to Table 2.5) Horseradish Peroxidase (HRP)-conjugated secondary antibody in 4% milk/TBST for a minimum of 1 hour at room temperature. Finally, the protein was detected by the addition of an Immobilon HRP Substrate Peroxide Solution (Millipore Corporation, Watford, UK) and Immobilon HRP Substrate Luminol Reagent (Millipore Corporation, Watford, UK) for 5 minutes. The HRP chemiluminescent reaction resulted in the catalysed oxidation of luminol by peroxide. Oxidised luminol emits light as it decays. The chemiluminescence was detected by exposing an X-ray film to the membrane.

2.2.10.7 Stripping of Western blot

Bound antibody was removed from membranes by immersion in Stripping Buffer at 62°C for 2 hours, washed in TBST and placed in 4% milk/TBST for 1 hour, then probed and detected with the appropriate antibodies (Table 2.5) as described in section 2.2.10.6. The loading control antibody, β -actin was used on stripped blots. Also in section 5.4.5, I κ B α were stripped and re-probed with I κ B β which was stripped and re-probed with β -actin.

2.2.10.8 Co-immunoprecipitation

Co-immunoprecipitation was carried out using the Anti-HA immunoprecipitation kit (Sigma, Dorset, UK) according to the manufacturer's instructions. Some of the immunoprecipitated protein was then subjected to silver staining using the ProteoSilver Stain kit (Sigma, Dorset, UK) and dried for long term storage using the DryEase kit (Invitrogen, Paisley, UK) according to the manufacturer's instructions.

2.2.11 Dual luciferase reporter assays

2.2.11.1 NF- κ B luciferase reporter assay

NF- κ B activity was measured in tissue culture cells using the Dual Luciferase Reporter Assay System (Promega, Southampton, UK). Cells were resuspended in Nucleofector Solution (Lonza, Berkshire, UK) and transfected with the pRL-TK (Promega, Southampton, UK) and pNF- κ B-luc (Stratagene, Leicestershire, UK) reporter vectors, in combination with a pIRES vector containing the oncogene of interest or the pIRES control vector by electroporation or using an inducible stable cell using the Amaxa Nucleofector I machine (Lonza, Berkshire, UK). Luciferase is expressed from pNF- κ B-luc after binding of NF- κ B subunits to the vector. pRL-TK contains a cDNA encoding Renilla luciferase which was used as a control for

normalisation of the data. These cells were incubated at 37°C and 5% CO₂ overnight and then stimulated as follows :

- 1) BaF3 cells with 10µg/ml LPS (Sigma, Dorset, UK) for 6 hours
- 2) Jurkat cells with 1µg/ml anti-CD3 (Sigma, Dorset, UK) and 1µg/ml anti-CD28 (Sigma, Dorset, UK) for 6 hours. For TLRs experiments, cells were stimulated with 10µg/ml LPS (Sigma, Dorset, UK) for 6 hours
- 3) WEHI cells with 10µg/ml LPS (Sigma, Dorset, UK) for 6 hours or 0.1µg/ml CD40 ligand (with 1µg/ml CD40 enhancer) or 10µg/ml anti-IgM

The cells were centrifuged to form a pellet and washed in 1X PBS before resuspension in 1X Passive Lysis Buffer (Promega, Southampton, UK). The cell suspension was rotated for 30 minutes to allow the cells to lyse completely. 15µl of whole cell extract was added to 45µl of Luciferase Assay Reagent 2 (LAR) (Promega, Southampton, UK) and the level of fluorescence produced by the firefly luciferase was detected with the Victor 3 luminometer (Perkin Elmer, Warrington, UK). The reaction was stopped with the addition of 45µl of Stop and Glo (Promega, Southampton, UK) and the fluorescence level produced by the Renilla luciferase was measured by the luminometer. The reading for firefly luciferase divided by the reading for Renilla luciferase gave the NF-κB activity.

2.2.11.2 AP-1 luciferase reporter assay

AP-1 activity was measured in transiently transfected BJAB cells using the Dual Luciferase Reporter Assay System (Promega) similar to that described for NF-κB luciferase reporter assay in section 2.2.11.1. The AP-1 vector used was the AP-1 cis-Reporting system (Stratagene, Leicestershire, UK). pRL-TK was used as the normalisation vector.

CHAPTER 3 – Characterisation of the gene expression profiles of MALT lymphoma with and without chromosome translocation

3.1 Introduction

As detailed in chapter 1, $t(11;18)(q21;q21)/API2-MALT1$, $t(1;14)(p22;q32)/IGH-BCL10$ and $t(14;18)(q32;q21)/IGH-MALT1$ are specifically associated with MALT lymphoma, occurring at variable frequencies in different anatomic sites. Although these translocations involve different oncogenes, their resultant oncogenic products commonly target the canonical NF- κ B activation pathway. Expression of API2-MALT1, BCL10 and MALT1 (in the presence of BCL10) induces the activation of the NF- κ B transcriptional factor, which transactivates a number of genes important for cellular proliferation and survival. The capacity of these oncogenic products to activate NF- κ B is believed to be the crucial molecular mechanism underlying their oncogenic activity. Nonetheless, over-expression of these oncogenic products alone is insufficient for malignant transformation as both $E\mu-API2-MALT1$ and $E\mu-BCL10$ transgenic mice developed splenic marginal zone hyperplasia, but not lymphoma (Morris, 2001; Sagaert *et al*, 2006b; Li *et al*, 2009). *In vitro* assay showed that expression of both API2-MALT1 and MALT1 enhanced by the CD40 induced NF- κ B activation in B cells (Ho *et al*, 2005). It is possible that such immunological stimulation is operational in MALT lymphoma. The extent and the nature of potential cooperation between MALT lymphoma associated oncogenic products and immune surface receptor signalling remain to be investigated.

There are important differences in the clinical and histological presentations between MALT lymphomas with and without chromosome translocation. Clinically, gastric MALT

lymphomas with t(11;18) or t(1;14) are significantly associated with advanced clinical stages (Liu *et al*, 2001b;Ye *et al*, 2006) and resistance to *H. pylori* eradication (Isaacson & Du, 2004;Liu *et al*, 2001a;Liu *et al*, 2002b;Ye *et al*, 2006). Histologically, t(11;18) positive MALT lymphomas appear to be more monotonous, lacking apparent transformed blasts (Okabe *et al*, 2003). These distinct clinico-pathological characteristics indicate the presence of significant differences in molecular mechanisms between MALT lymphomas with and without chromosome translocation. In order to investigate this and understand further the molecular mechanism of MALT lymphomagenesis, the transcriptional profiles of a well characterised series of MALT lymphomas with different chromosome translocation status were determined.

3.2 Aims of the study

- 1) To characterise gene expression profiling of MALT lymphoma with and without chromosome translocation
- 2) To identify the molecular mechanisms involved in translocation positive MALT lymphoma
- 3) To identify the molecular mechanisms involved in translocation negative MALT lymphoma

3.3 Experimental design

3.3.1 Case selection

Fresh frozen tissues from 24 well-characterised MALT lymphomas (case numbers 1 to 24 in Table 2.1), 7 nodal follicular lymphomas (FL) and 8 nodal mantle cell lymphomas (MCL) were used for this part of the gene expression microarray analysis. The MALT lymphoma cases included 9 positive for $t(11;18)(q21;q21)/API2-MALT1$ (8 from stomach and 1 from lung), 4 positive for $t(1;14)(p22;q32)/BCL10-IGH$ or $t(1;2)(p22;p11)/BCL10-IG\kappa$ (3 from stomach and 1 from lung), 2 positive for $t(14;18)(q32;q21)/IGH-MALT1$ (1 from liver and 1 from ocular adnexa) and 9 cases negative for all known MALT lymphoma associated chromosome translocations (all from stomach with two having nuclear BCL10 staining). MALT lymphomas case number 25 was excluded from the analysis due to the fact that it was a mixture of MALT and diffuse large B-cell lymphoma and case number 26 was excluded due to the fact that it is the only fresh frozen case of $t(3;14)(p14;q32)/IGH-FOXP1$ and a minimum of two cases are needed to obtain useful mechanistic information. However both cases were included in the phenotypic marker analysis carried out as described in chapter 6. The percentage of tumour cells are estimated on haematoxylin & eosin stained sections and where necessary, crude microdissection was carried out to enrich tumour cells and ensure that a sample containing at least 70% tumour cells was used for expression microarray analysis.

3.3.2 RNA quality check using Agilent nanochip

Total RNA, complementary RNA and fragmented RNA were subjected to quality control assessment using the Agilent nanochip. The criteria for passing the quality control were as follows: for total RNA both the 18S and 28S bands should be around 2000 and 4000bp

respectively, for cRNA the mean of the size distribution should be around 1000bp and for fragmented RNA, the mean of the size distribution should be around 60 to 100bp.

3.3.3 Validation of the in house linear RNA amplification protocol

To validate the fidelity of the linear amplification protocol developed in house, RNA from a fresh frozen tissue specimen of a t(11;18) positive MALT lymphoma was amplified, then labelled and hybridised to HG-U133A chip according to the method described in section 2.2.5. Pearson correlation comparing the values of all 22283 probes from the amplified RNA and total RNA of HG-U133A GeneChip from the same case was carried out.

3.3.4 Unsupervised clustering analysis

After normalisation and non-specific filtering, the 24 MALT lymphoma cases derived from HG-U133A and HG-U133B, 7 FL and 8 MCL on the HG-U133plus2 platform were subjected to unsupervised clustering using Pearson correlation coefficient and average linkage as the similarity measure and clustering algorithm respectively within Genespring GX 7.3.1. Unsupervised clustering was also carried out within the MALT lymphoma group to investigate whether there are distinct subsets.

3.3.5 Characterisation of gene expression features of MALT lymphoma with and without chromosome translocation

Normalisation followed by non-specific filtering was used to derive set of variant probes which were collapsed and used in interrogating 4395 pathways using GSEA (Section 2.2.5.4). The same set of probes was subjected to one-way ANOVA multivariate analysis to derive a set of differentially expressed genes between MALT lymphoma with and without chromosomal translocation (Section 2.2.5.5). The differentially expressed genes were subjected to Gene Ontology (GO) analysis using hypergeometric testing (Section 2.2.5.6).

Results from both GSEA and GO analysis were compared to characterise the features of MALT lymphoma with and without translocation.

3.4 Results

Details of the bioinformatics analysis including choice of algorithms and software are given in Appendix I. In this section, results of the analysis of gene expression microarray of MALT lymphoma are presented.

3.4.1 RNA quality control

In each case the total RNA, complimentary RNA and fragmented RNA were of good quality as shown by electrophoresis on RNA nanochip (Figure 3.1).

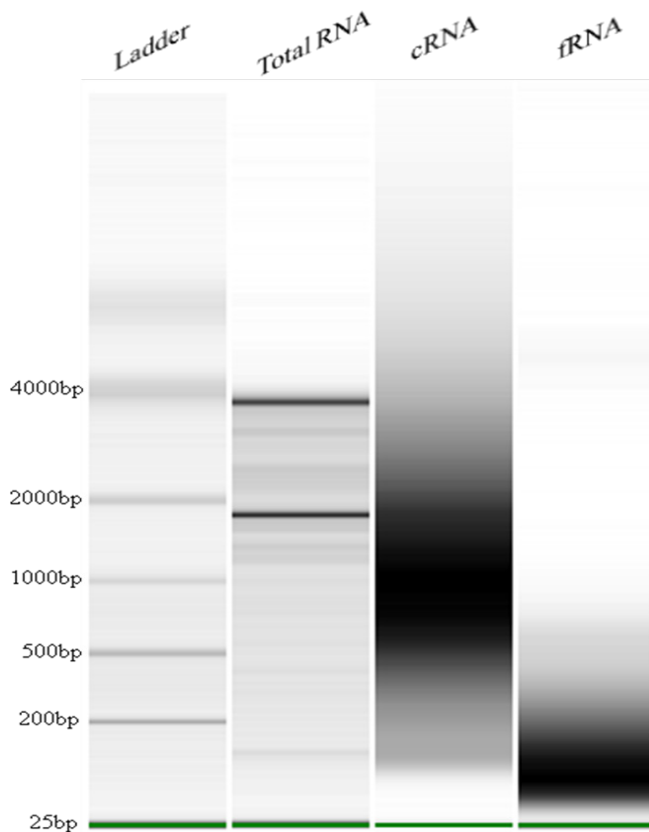


Figure 3.1 - Typical good quality data of total, complementary and fragment RNA on RNA nanochip.

3.4.2 Comparison of total RNA with amplified RNA

Total RNA and linearly amplified RNA from the same t(11;18) positive MALT lymphoma fresh frozen specimen were hybridised on a HG-U133A GeneChip. The Pearson correlation coefficient (R^2) between the two RNA preparations was 97.2% with $p < 0.001$ (Figure 3.2), indicating that linearly amplified RNA faithfully amplifies the same distribution of the starting total RNA.

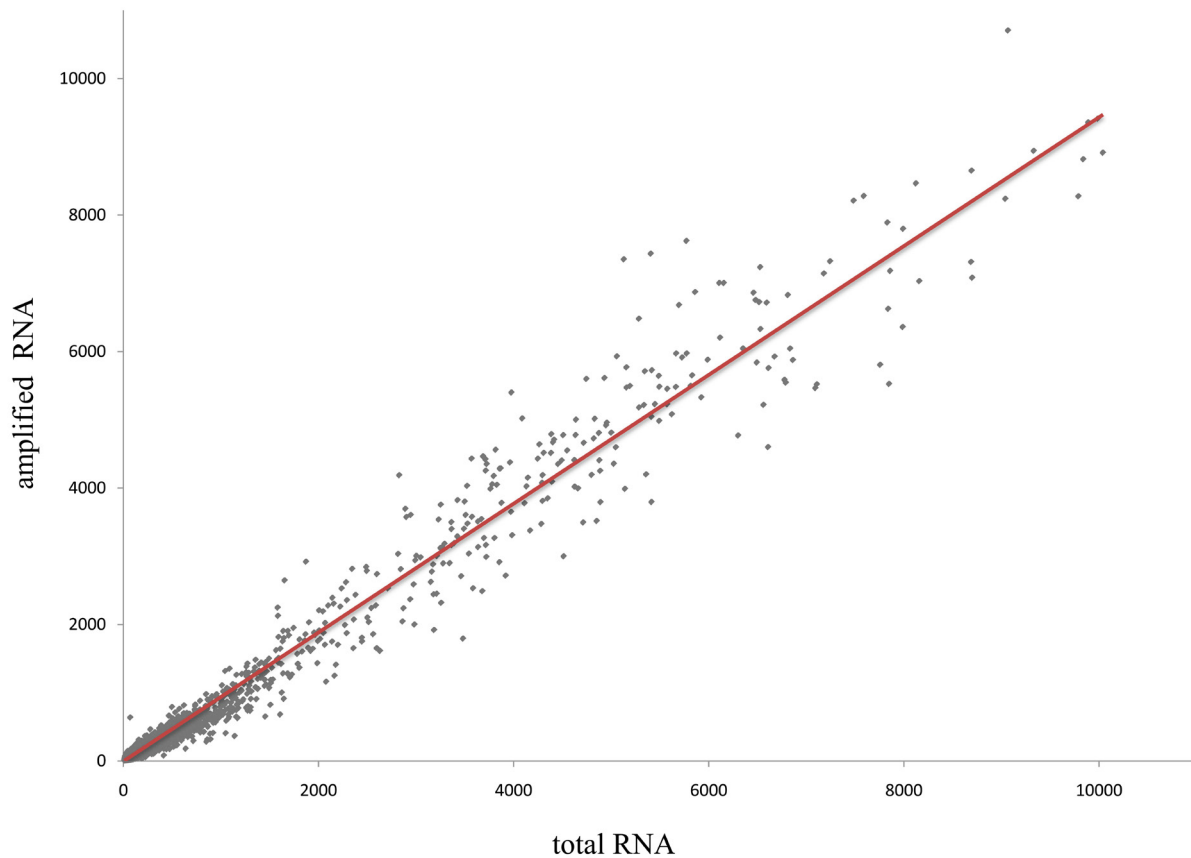


Figure 3.2 - Correlation between total and amplified RNA from the same fresh frozen specimen of t(11;18) positive MALT lymphoma.

Red line is the line of best fit through the points with a correlation coefficient of 97.2%.

3.4.3 Validation of microarray data using biological controls

As expected, the hybridisation signal of the N-terminal MALT1 probe was the highest in the two cases of t(14;18) positive MALT lymphoma, whereas the signals of two C-terminal MALT1 probes were much higher in the cases with t(11;18) than those with t(1;14) or without translocation (Figure 3.3). Cyclin D1 was highly expressed in MCL, while CD10 and BCL6 showed the highest expression in FL. The CD10 expression in MALT lymphoma was low, suggesting the presence of minimal reactive B cells components in the fresh frozen materials used for expression microarray. Despite the fact that *BCL2* t(14;18)(q32;q21)/*IgH-BCL2* translocation is the genetic hallmark of follicular lymphoma, it was not in the hallmark genes probably because *BCL2* was shown to be highly expressed in translocation positive MALT lymphomas (Section 3.4.6.1). Overall, the expected results from the biological controls indicated that the labelling, hybridisation and basic bioinformatics analysis were successfully carried out.

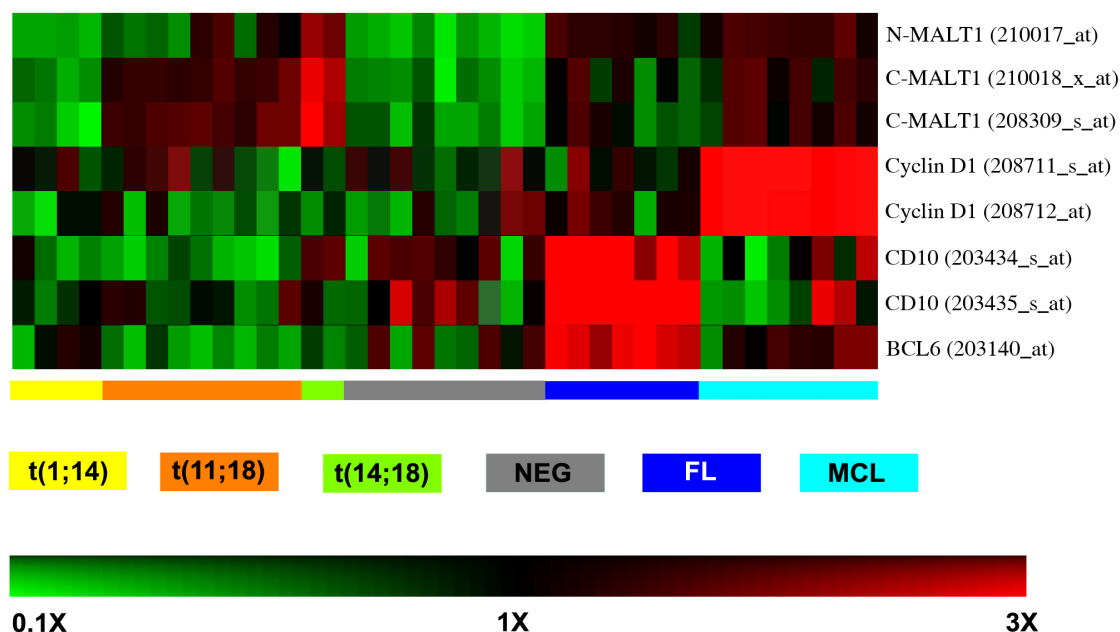


Figure 3.3 - Expression of hallmark genes in MALT lymphoma, FL and MCL.

Correlation of known expression levels of genes with different lymphoma types. N-MALT1 probe (210017_at) detects only wild type MALT1 transcripts, while C-MALT (210018_x_at & 208309_s_at) probes detect both MALT1 and API2-MALT1 transcripts. The chromosome translocation status of MALT lymphoma is indicated by colour. On the heatmap, red represents up-regulated genes and green down-regulated genes, with the scale showed at the bottom of the figure.

3.4.4 Unsupervised clustering between MALT, MCL and FL defines MALT lymphoma as a distinct entity

The methodology used to combine MALT lymphoma HG-U133A with FL and MCL HG-U133plus2 is summarised (Figure 3.4).

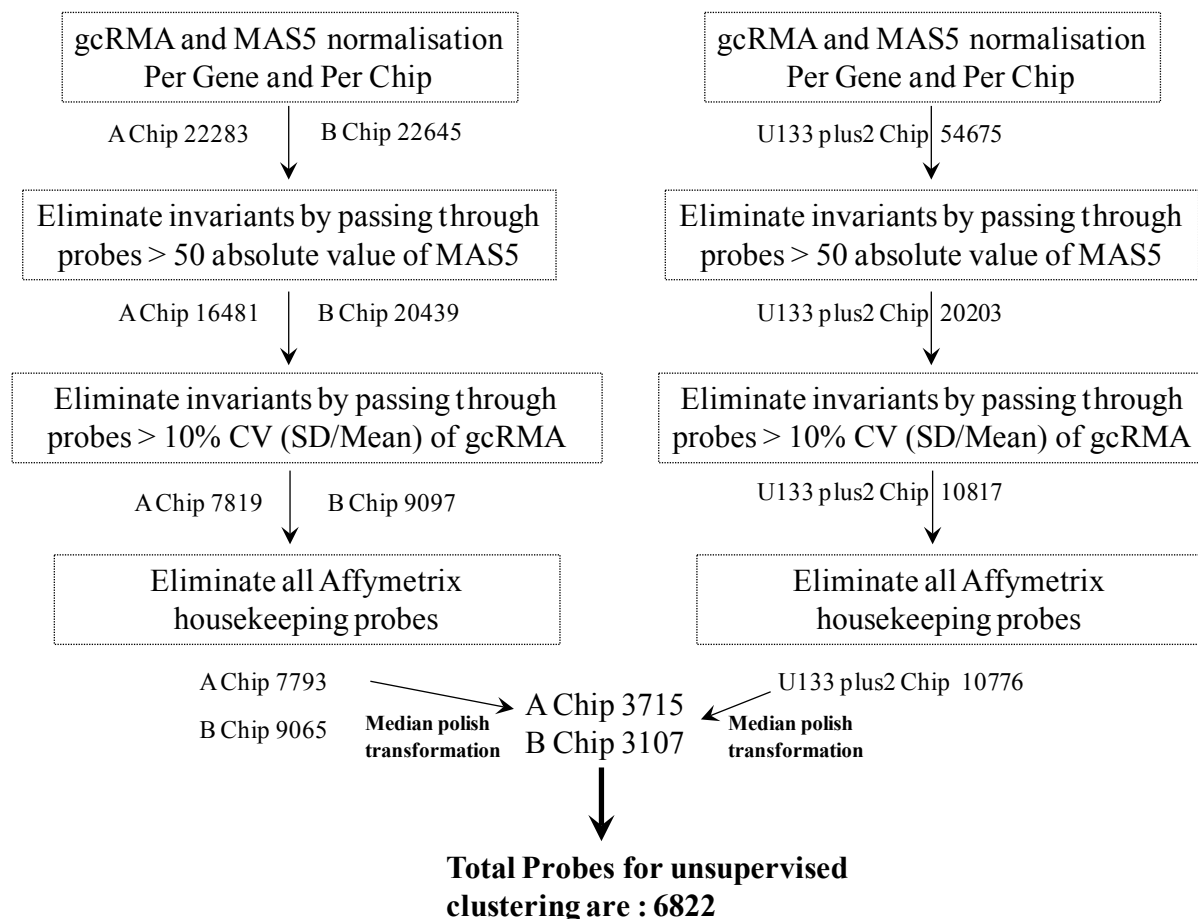


Figure 3.4 - Summary of bioinformatics strategy to combine FL and MCL with MALT microarray GeneChips.

Normalisation is followed by non-specific filtering and exclusion of housekeeping probes for both U133AB and U133plus2. The probes from the two platforms are combined using median polish transformation and the probes used for unsupervised clustering.

Analysis of HG-U133A and B and plus2 were done separately then a median polish step was used to normalise the data from the two different platforms giving rise to 6822 probes. These were used for unsupervised clustering of the 24 MALT lymphomas, 7 follicular lymphoma (FL) and 8 mantle cell lymphoma (MCL).

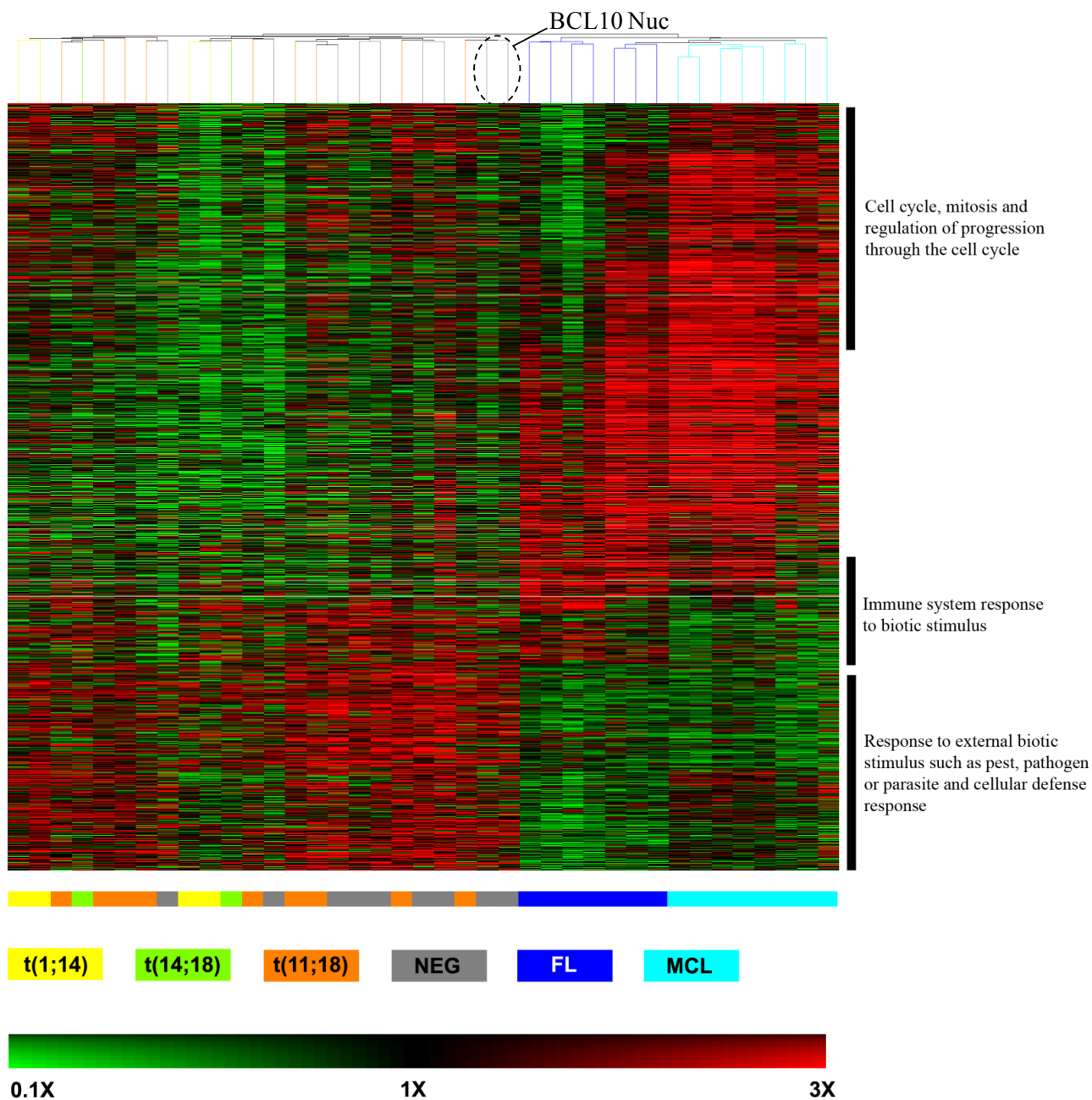


Figure 3.5 - MALT lymphoma shows distinct gene expression profiles from follicular lymphoma and mantle cell lymphoma using unsupervised hierarchical clustering.

After normalisation and filtering across both U133A&B and U133plus2 sets, a set of 6822 probes were obtained and used for unsupervised hierarchical clustering analysis. FL: follicular lymphoma; MCL: mantle cell lymphoma; NEG: translocation negative MALT lymphoma. The chromosome translocation status of MALT lymphoma, FL and MCL are indicated by colour. On the heatmap, red represents up-regulated genes and green down-regulated genes, with the scale shown at the bottom of the figure.

MALT lymphomas were clustered as a single branch, irrespective of their origin from different anatomic sites or chromosome translocation. Within the MALT lymphoma group, the chromosome translocation status appeared to have little impact on the hierarchical clustering as translocation positive MALT lymphomas were intermingled with translocation negative cases (Figure 3.5). The two translocation negative cases with BCL10 nuclear staining clustered together (Figure 3.5).

In order to derive the functional groups in Figure 3.5, the gene tree was ordered according to biological processes defined by gene ontology, and the gene clusters enriched for a particular biological process in a lymphoma subtype as shown by hypergeometric testing as indicated. The gene sets for cell cycle (GO:7049) and regulation of progression through cell cycle (GO:74) were highly enriched in MCL, while those for immune response (GO:6955) and immune response to biotic stimulus (GO:9607) were enriched in FL. The gene sets for immune response to external biotic stimulus such as pest, pathogen or parasite (GO:9613) and cellular defence response (GO:6968) were highly enriched in MALT lymphoma.

3.4.5 Unsupervised clustering confirms overlapping features in gene expression profiling between MALT lymphoma with and without chromosome translocation

The strategy used to compare MALT lymphoma with and without translocation is summarised in Figure 3.6.

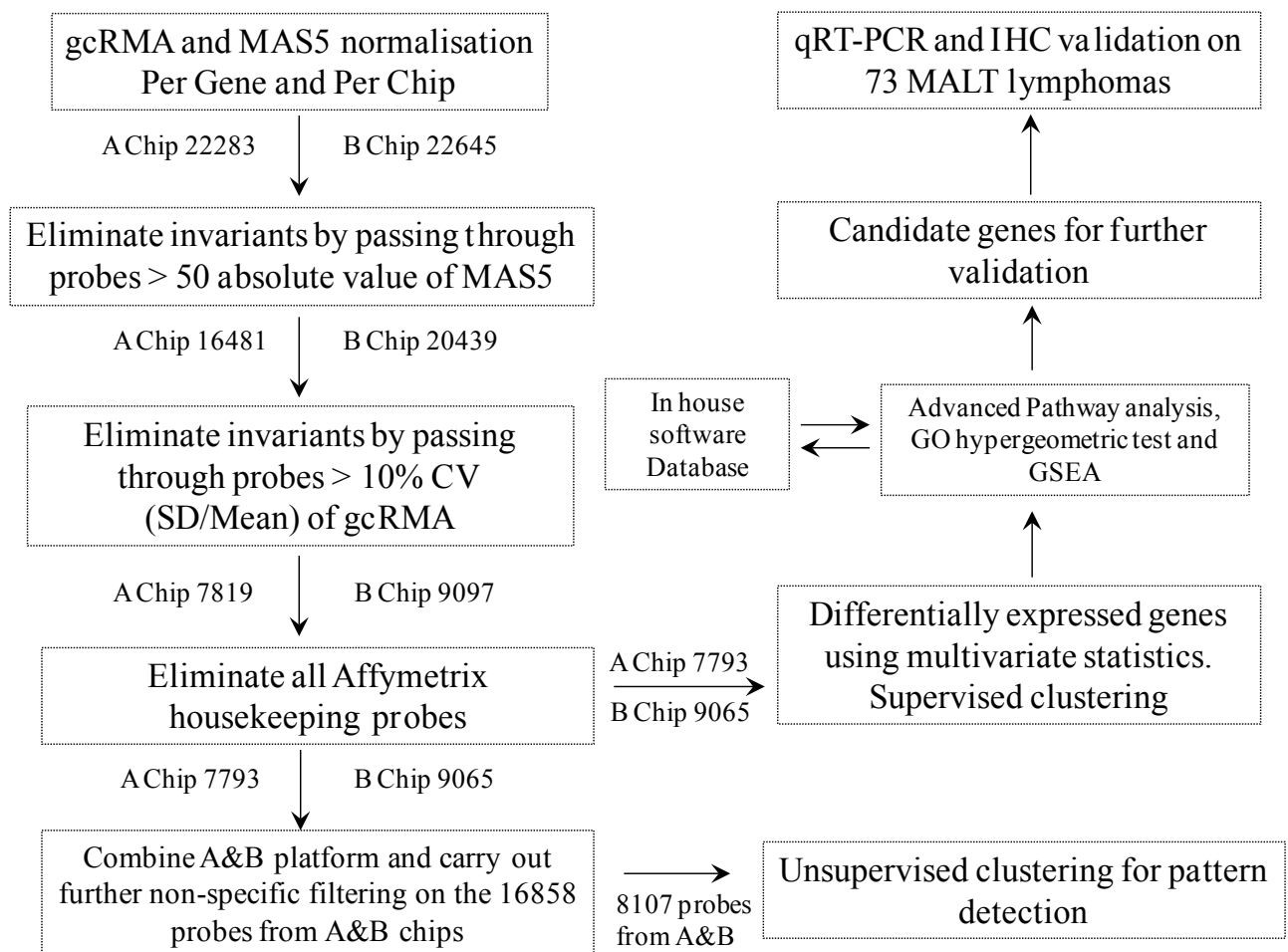


Figure 3.6 - Summary of bioinformatics strategy used to compare MALT lymphoma with and without chromosome translocations.

Normalisation is followed by non-specific filtering and exclusion of housekeeping probes. The probe sets were used to determine differentially expressed genes using multivariate analysis, this is followed by pathway analysis using GSEa and GO and in house datamining. Candidates from this analysis were validated further by qRT-PCR and immunohistochemistry (IHC).

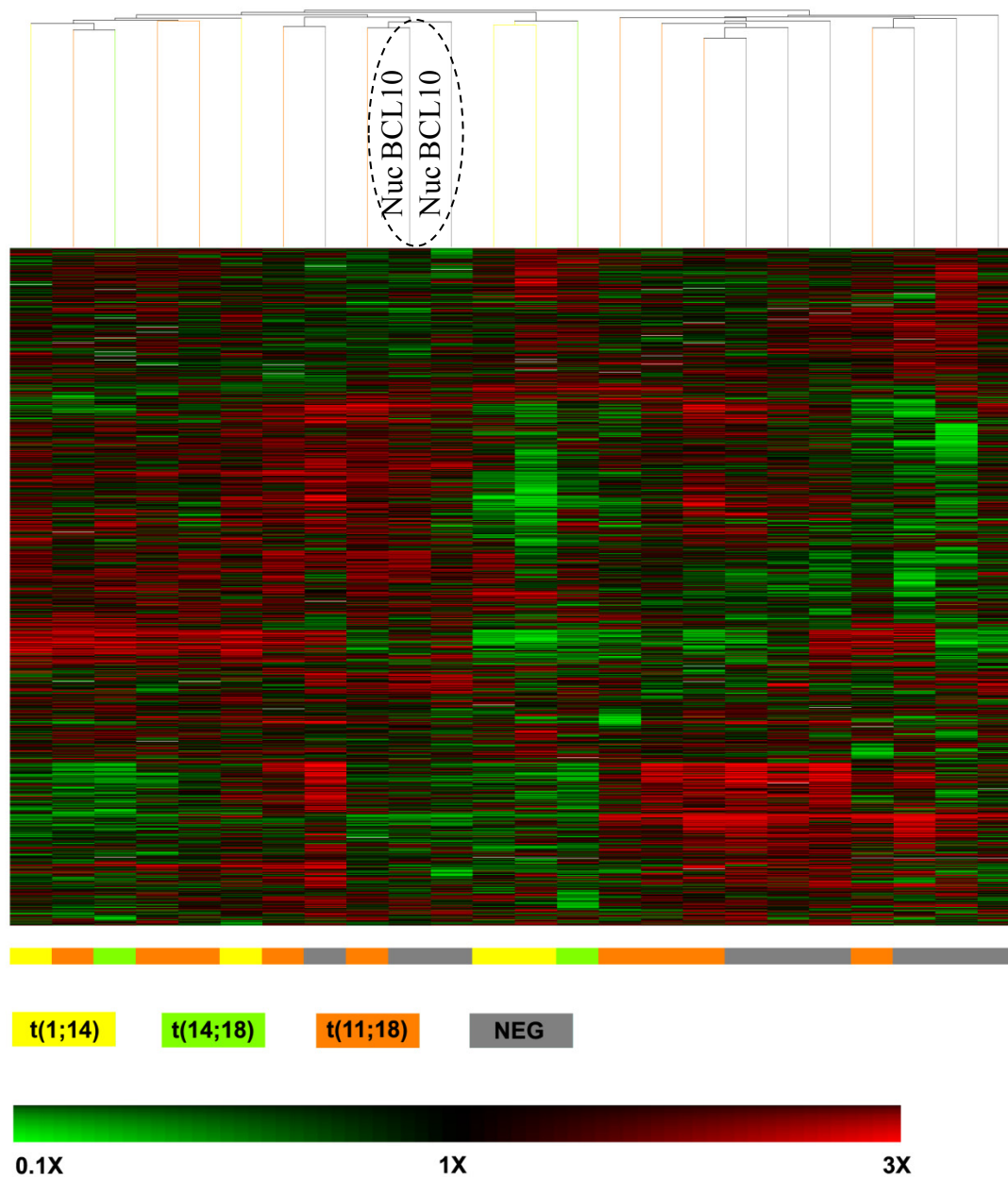


Figure 3.7 - Unsupervised hierarchical clustering of MALT lymphoma with different translocation status.

After normalisation and filtering, a set of 8107 probes were obtained and used for unsupervised hierarchical clustering analysis. MALT lymphomas with and without chromosome translocation are intermingled together. The chromosome translocation status of MALT lymphoma is indicated by different colour scheme. On the heatmap, red represents up-regulated genes and green down-regulated genes, with the scale shown at the bottom of the figure.

The result of unsupervised clustering of MALT lymphoma cases again showed that the chromosome translocation status had little impact on the hierarchical clustering as translocation positive MALT lymphoma cases were intermingled with translocation negative cases (Figure 3.7). The results suggest an overlap in gene expression profile and hence molecular mechanisms between MALT lymphoma with and without chromosome translocation. The clustering showed that the two translocation negative cases with BCL10 nuclear staining clustered together with a group consisting of predominantly translocation positive MALT lymphomas (Figure 3.7). In order to investigate this further, supervised clustering with 733 probes was carried out on the four t(1;14) and nine translocation negative cases including two with nuclear BCL10 staining. The 733 probes were derived by applying one-way ANOVA multivariate analysis across MALT lymphoma with and without translocation groups to the 8107 probes obtained after normalisation and non-specific filtering. The two translocation negative MALT lymphomas with nuclear BCL10 expression still clustered with the four cases with t(1;14) (Figure 3.8).

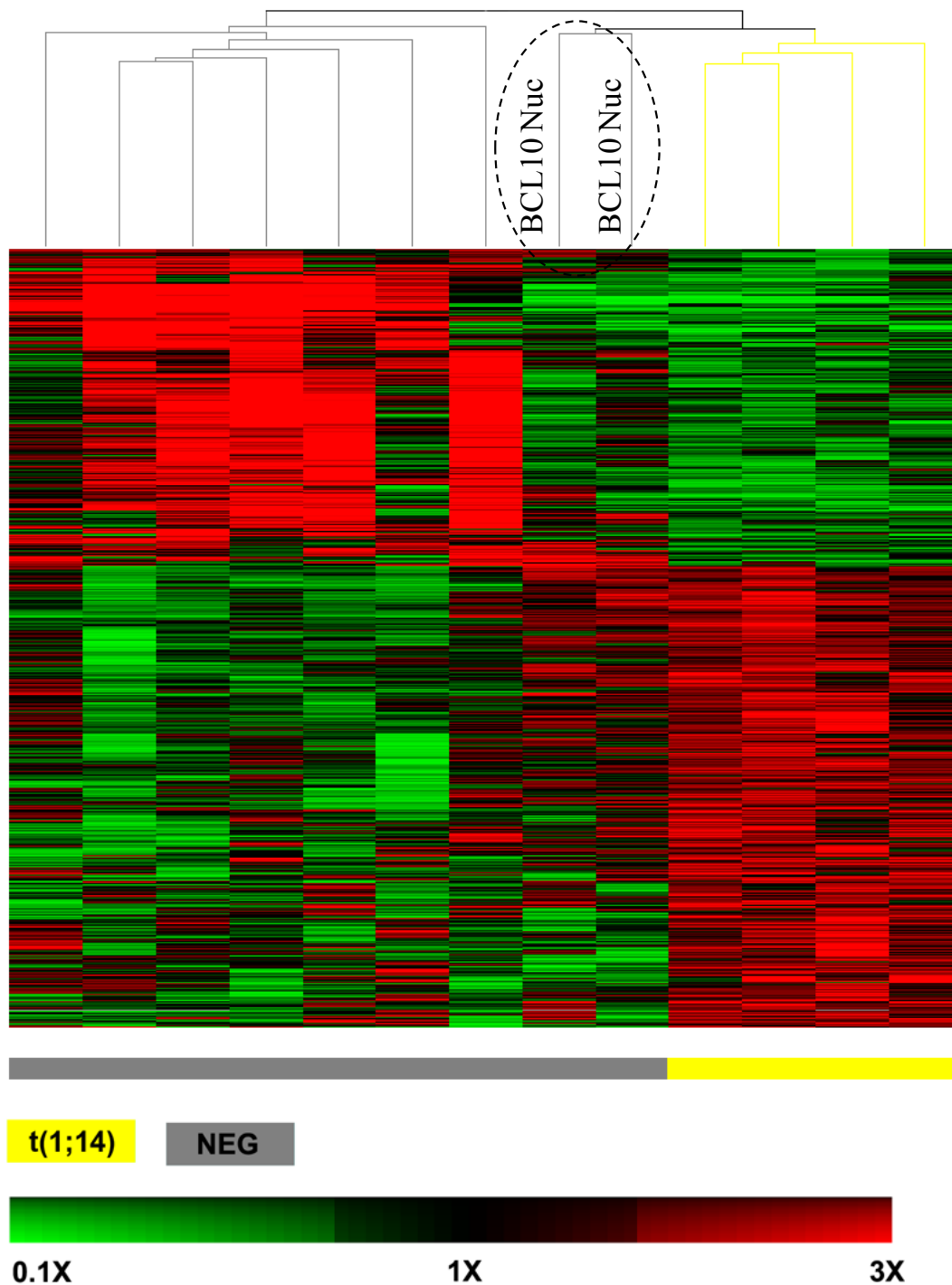


Figure 3.8. Supervised hierarchical clustering of MALT lymphoma with different translocation status.

After normalisation and filtering, a set of 733 probes were obtained and used for supervised hierarchical clustering analysis. MALT lymphoma cases without chromosome translocation but with nuclear BCL10 staining are clustering with t(1;14) positive cases. The chromosome translocation status of MALT lymphoma is indicated by different colour scheme. On the heatmap, red represents up-regulated genes and green down-regulated genes, with the scale shown at the bottom of the figure.

3.4.6 Characterisation of the gene expression profiles of MALT lymphoma with and without chromosome translocation

To gain further insights into the potential difference in molecular mechanisms between MALT lymphomas with and without chromosome translocation, GSEA and absolute GSEA were performed on 4395 gene sets covering various cellular pathways, biological processes or molecular functions derived from in house analysis and molecular signature database (Subramanian *et al*, 2005) as described in Appendix I.III. Results of GSEA was cross validated using GO hypergeometric testing as described in section 2.2.5.6. Summary of the methodology used for GSEA (Figure 3.9).

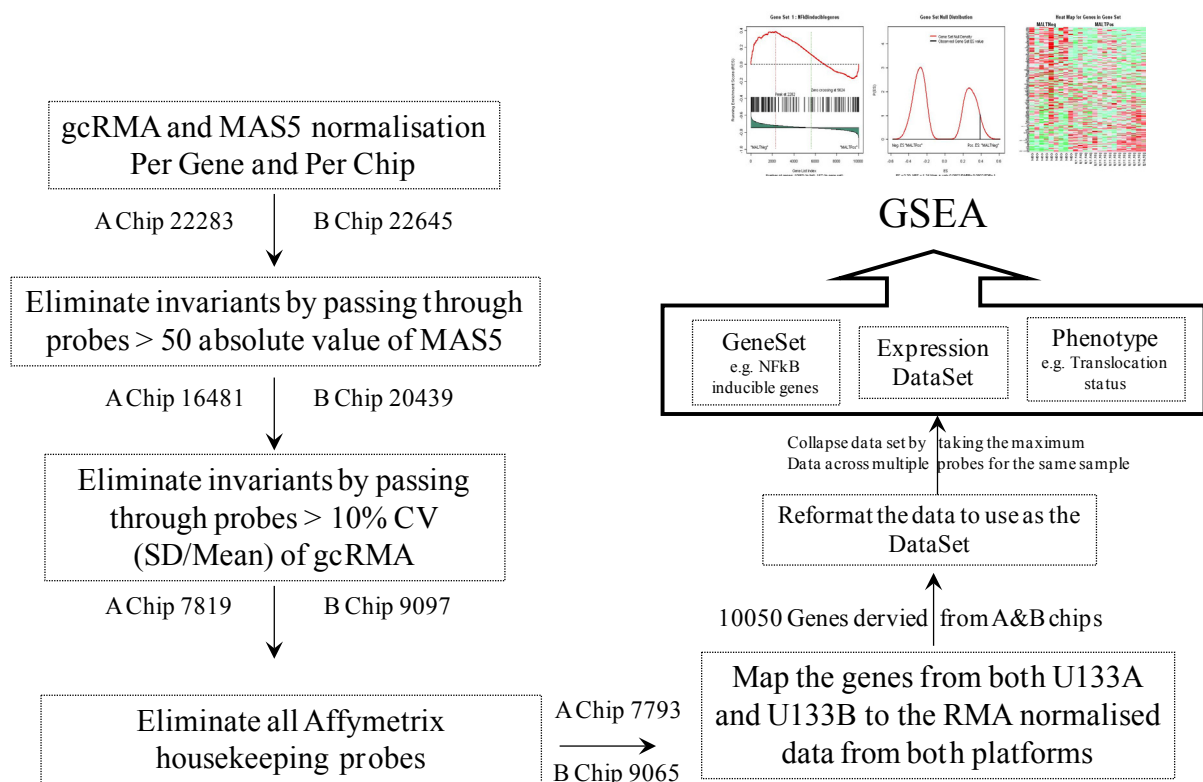


Figure 3.9 - Summary of bioinformatics strategy used for GSEA on MALT lymphoma with and without chromosome translocation.

Normalisation is followed by non-specific filtering and exclusion of housekeeping probes. The probes were then combined and mapped to the RMA normalised data. The probes are collapsed and used as an expression dataset in GSEA together with the relevant geneset and phenotype.

GSEA identified a total of 51 gene sets (not including those with very general terms) with a statistical significance ($P < 0.05$ and $FDR < 0.05$) and were thus differentially over-represented between MALT lymphomas with and without translocation. Remarkably, the NF- κ B target gene signature was the most differentially enriched gene set ($p < 0.0001$ and $FDR < 0.0001$) (Table 3.1).

Table 3.1 - Gene sets differentially over-represented between MALT lymphoma with and without chromosome translocation.

| Gene Set | Size | Source | ES | Norm ES | Nominal P value | FDR q value | FWER P value | Tag % | Gene % |
|--|------|----------------------------|-------|---------|-----------------|-------------|--------------|-------|--------|
| NF-κB related | | | | | | | | | |
| NF-κB target genes | 167 | Appendix III.I for details | 0.531 | 1.826 | 0.0001 | 0.0001 | 0.0000 | 0.455 | 0.249 |
| positive regulation of IKK and NF-κB cascade | 62 | GO:0043123 | 0.466 | 1.541 | 0.0088 | 0.0446 | 0.1235 | 0.274 | 0.157 |
| Inflammation and immune responses | | | | | | | | | |
| Inflammation | 73 | Immunome database | 0.590 | 1.865 | 0.0000 | 0.0065 | 0.0076 | 0.548 | 0.257 |
| Cellular cation homeostasis | 56 | GO:0030003 | 0.519 | 1.842 | 0.0000 | 0.0116 | 0.0710 | 0.429 | 0.264 |
| Inflammatory response | 166 | GO:0006954 | 0.530 | 1.775 | 0.0022 | 0.0116 | 0.0128 | 0.482 | 0.267 |
| Response to other organism | 47 | GO:0051707 | 0.575 | 1.829 | 0.0000 | 0.0124 | 0.0840 | 0.404 | 0.183 |
| Locomotor behaviour | 54 | GO:0007626 | 0.601 | 1.800 | 0.0000 | 0.0153 | 0.1210 | 0.556 | 0.257 |
| Chemokine | 128 | Immunome database | 0.510 | 1.725 | 0.0022 | 0.0163 | 0.0293 | 0.367 | 0.175 |
| Immune responses | 119 | GO:0006955 | 0.517 | 1.648 | 0.0067 | 0.0185 | 0.0266 | 0.429 | 0.259 |
| Defence response | 135 | GO:0006952 | 0.511 | 1.757 | 0.0000 | 0.0210 | 0.1870 | 0.467 | 0.274 |
| B-cell activation | 26 | GO:0042113 | 0.623 | 1.779 | 0.0000 | 0.0222 | 0.0117 | 0.423 | 0.152 |
| Innate immune response | 52 | GO:0045087 | 0.506 | 1.595 | 0.0065 | 0.0311 | 0.0724 | 0.519 | 0.301 |
| Cell adhesion molecules | 86 | HSA04514 | 0.456 | 1.812 | 0.0000 | 0.0321 | 0.0480 | 0.326 | 0.209 |
| Lymphocyte activation | 77 | GO:0046649 | 0.525 | 1.647 | 0.0292 | 0.0322 | 0.0501 | 0.338 | 0.152 |
| Response to biotic stimulus | 71 | GO:0009607 | 0.507 | 1.687 | 0.0000 | 0.0378 | 0.3500 | 0.423 | 0.262 |
| Cellular homeostasis | 74 | GO:0019725 | 0.448 | 1.692 | 0.0000 | 0.0380 | 0.3310 | 0.351 | 0.264 |
| Humoral immunity | 65 | Immunome database | 0.545 | 1.526 | 0.0550 | 0.0395 | 0.1312 | 0.477 | 0.257 |
| Inflammatory response | 66 | GO:0006954 | 0.534 | 1.662 | 0.0065 | 0.0420 | 0.4020 | 0.455 | 0.274 |
| TLR signalling pathway from GeneGo | 33 | GeneGO database | 0.520 | 1.616 | 0.0088 | 0.0421 | 0.0674 | 0.606 | 0.366 |
| Cellular immunity | 47 | Immunome database | 0.542 | 1.537 | 0.0214 | 0.0456 | 0.1269 | 0.489 | 0.262 |
| Chemokine | 29 | GO:0042379 | 0.638 | 1.519 | 0.0338 | 0.0463 | 0.1438 | 0.655 | 0.257 |
| Cell adhesion | 50 | GO:0016337 | 0.483 | 1.634 | 0.0058 | 0.0482 | 0.4860 | 0.42 | 0.259 |
| MAPK pathway related | | | | | | | | | |
| Receptor signalling protein activity | 54 | GO:0005057 | 0.529 | 2.061 | 0.0000 | 0.0015 | 0.0010 | 0.574 | 0.355 |
| Regulation of MAP kinase activity | 41 | GO:0043405 | 0.493 | 1.979 | 0.0000 | 0.0026 | 0.0140 | 0.537 | 0.292 |
| Regulation of protein kinase activity | 95 | GO:0045859 | 0.455 | 1.894 | 0.0000 | 0.0066 | 0.0340 | 0.453 | 0.316 |
| Regulation of kinase activity | 96 | GO:0043549 | 0.450 | 1.875 | 0.0000 | 0.0079 | 0.0420 | 0.448 | 0.316 |
| Activation of MAPK activity | 22 | GO:0000187 | 0.549 | 1.845 | 0.0020 | 0.0118 | 0.0690 | 0.591 | 0.287 |
| MAPKKK cascade | 61 | GO:0000165 | 0.443 | 1.847 | 0.0000 | 0.0121 | 0.0660 | 0.623 | 0.44 |
| Transmembrane receptor protein tyrosine kinase signalling pathway | 48 | GO:0007169 | 0.465 | 1.832 | 0.0000 | 0.0125 | 0.0820 | 0.354 | 0.213 |
| JNK cascade | 28 | GO:0007254 | 0.444 | 1.727 | 0.0000 | 0.0282 | 0.2550 | 0.5 | 0.343 |
| MAPK signalling pathway | 152 | HSA04010 | 0.442 | 1.826 | 0.0000 | 0.0383 | 0.0380 | 0.467 | 0.343 |
| G protein coupled receptor protein signalling pathway | 125 | GO:0007186 | 0.424 | 1.670 | 0.0061 | 0.0412 | 0.3870 | 0.32 | 0.256 |
| Protein kinase cascade | 184 | GO:0007243 | 0.421 | 1.672 | 0.0021 | 0.0414 | 0.3830 | 0.413 | 0.317 |
| JAK STAT cascade | 20 | GO:0007259 | 0.559 | 1.661 | 0.0151 | 0.0419 | 0.4070 | 0.55 | 0.3 |
| Peptide GPCRS | 25 | C2 genmapp | 0.609 | 1.829 | 0.0020 | 0.0457 | 0.0200 | 0.32 | 0.107 |
| G protein signalling coupled to cyclic nucleotide second messenger | 36 | GO:0007187 | 0.502 | 1.644 | 0.0083 | 0.0475 | 0.4560 | 0.278 | 0.154 |
| Cell cycle related | | | | | | | | | |
| Regulation of cell growth | 29 | GO:0001558 | 0.632 | 2.014 | 0.0000 | 0.0013 | 0.0060 | 0.448 | 0.205 |
| Negative regulation of growth | 24 | GO:0045926 | 0.681 | 2.019 | 0.0000 | 0.0016 | 0.0060 | 0.458 | 0.183 |
| Positive regulation of cell proliferation | 87 | GO:0008284 | 0.500 | 1.958 | 0.0000 | 0.0027 | 0.0140 | 0.483 | 0.308 |
| Regulation of cell proliferation | 179 | GO:0042127 | 0.465 | 1.813 | 0.0000 | 0.0136 | 0.1030 | 0.43 | 0.308 |
| Negative regulation of cell cycle | 49 | GO:0045786 | 0.548 | 1.690 | 0.0000 | 0.0370 | 0.3380 | 0.51 | 0.282 |
| Cell cycle arrest | 36 | GO:0007050 | 0.564 | 1.640 | 0.0022 | 0.0480 | 0.4680 | 0.472 | 0.223 |
| Others | | | | | | | | | |
| Cation homeostasis | 57 | GO:0055080 | 0.509 | 1.820 | 0.0000 | 0.0131 | 0.0970 | 0.421 | 0.264 |
| Reproductive process | 59 | GO:0022414 | 0.516 | 1.803 | 0.0000 | 0.0150 | 0.1150 | 0.424 | 0.257 |
| Ion homeostasis | 63 | GO:0050801 | 0.481 | 1.748 | 0.0021 | 0.0218 | 0.2010 | 0.54 | 0.377 |
| mitochondrion organization and biogenesis | 30 | GO:0007005 | 0.551 | 1.690 | 0.0000 | 0.0376 | 0.3360 | 0.4 | 0.23 |
| Positive regulation of transcription | 80 | GO:0045941 | 0.414 | 1.681 | 0.0000 | 0.0379 | 0.3620 | 0.325 | 0.282 |
| Angiogenesis | 22 | GO:0001525 | 0.563 | 1.648 | 0.0206 | 0.0474 | 0.4400 | 0.364 | 0.137 |
| Cyclic nucleotide mediated signalling | 36 | GO:0019935 | 0.502 | 1.644 | 0.0083 | 0.0475 | 0.4560 | 0.278 | 0.154 |
| Protein processing | 26 | GO:0016485 | 0.511 | 1.642 | 0.0019 | 0.0475 | 0.4600 | 0.385 | 0.26 |
| Carbohydrate biosynthetic process | 20 | GO:0016051 | 0.542 | 1.636 | 0.0200 | 0.0484 | 0.4810 | 0.45 | 0.294 |

ES: Enrichment score; Norm ES: Normalised ES; FDR: False discovery rate; FWER: Family wise-error rate; Tag%: the percentage of gene tags before (for positive ES) or after (for negative ES) the peak in the running enrichment score; Gene %: the percentage of genes in the gene list before (for positive ES) or after (for negative ES) the peak in the running enrichment score.

3.4.6.1 *NF-κB* target genes are significantly differentially expressed between MALT lymphoma with and without chromosome translocation

GSEA showed that the expression of the NF-κB target genes was enhanced in both translocation positive and negative cases but with a different signature for each group. A subset of the NF-κB target genes was over-represented in translocation positive MALT lymphomas, while another subset was enriched in translocation negative MALT lymphomas. Leading edge analysis showed that 20 core genes accounted for the significant enrichment in translocation positive MALT lymphomas including *CCR2A*, *BCL2*, *TFEC*, *CD69*, *BCL10*, *TLR6*, *REL*, *LTB*, *IRF4*, *CCR7*, *CCR5* and *MAP4K1* (Figure 3.10A). Similarly, 70 core genes underscored the significant enrichment in translocation negative MALT lymphomas and *CXCL5*, *PTGIS2*, *NR4A3*, *CCL11*, *PTGIS*, *IL8*, *MMP3*, *CXCL2*, *CXCL1* and *CD86* were the top 10 of this biologically significant gene subset (Figure 3.10A). The differential expression of these genes was clearly seen in the heatmap illustration of Figure 3.10A.

In addition, when GSEA was applied to 9 cases with t(11;18) versus 8 without chromosome translocation using non-canonical NF-κB target gene set, the results showed that many non-canonical genes such as *CXCR4* were more highly expressed in the t(11;18) positive tumors confirming the fact that cleavage of NIK by the API2-MALT1 fusion oncoprotein leads to noncanonical NF-κB activation (Rosebeck *et al*, 2011).

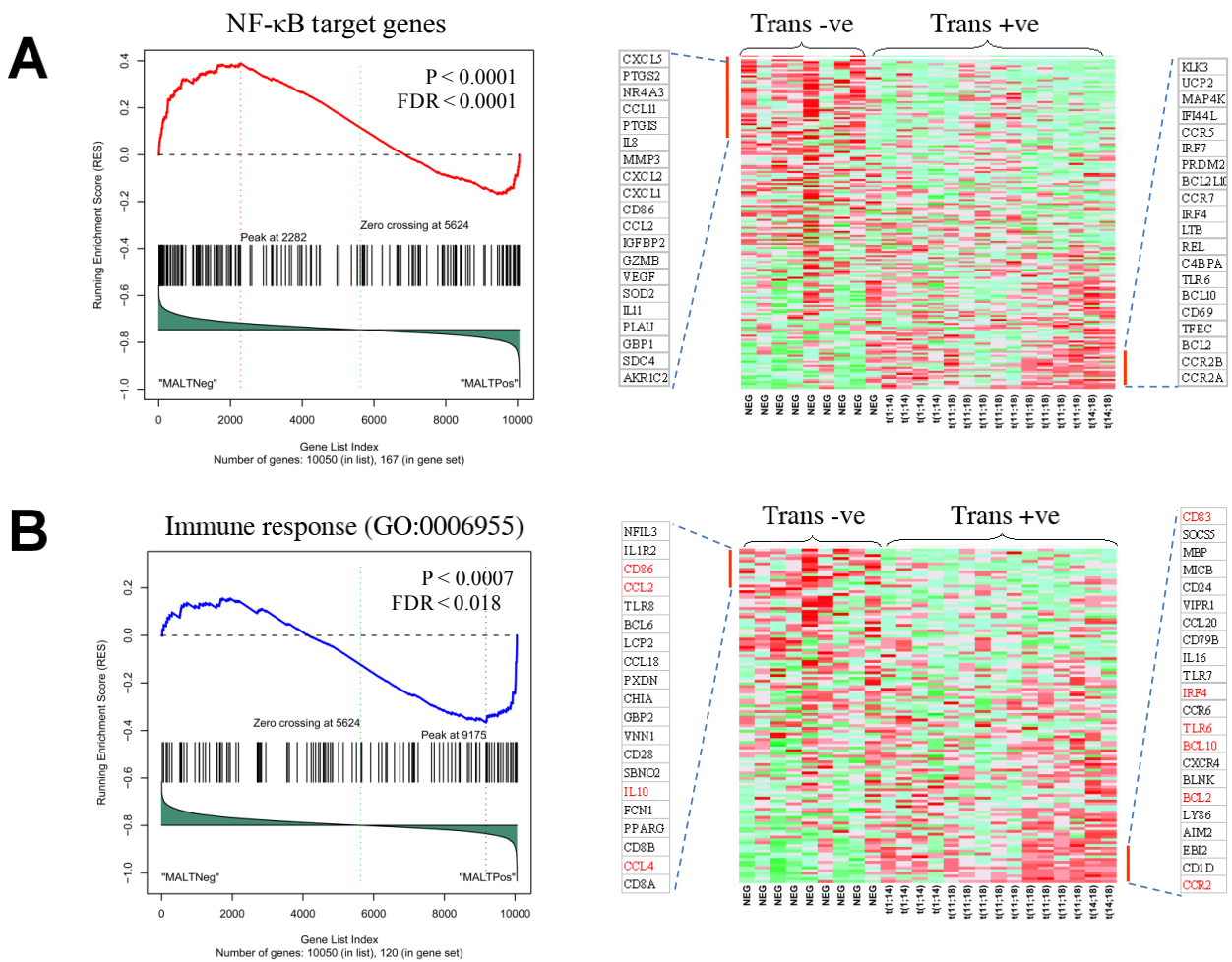


Figure 3.10 - Gene set enrichment analysis (GSEA) of NF-κB target genes in MALT lymphomas with and without chromosome translocation.

(A) NF-κB target genes and (B) Immune response set.

Left panel shows the distribution of NF-κB target genes according to their rank position. Right panel shows heatmap illustration of their expression between MALT lymphoma with and without chromosome translocation. The top 20 leading edge core genes are shown. trans -ve: translocation negative MALT lymphoma; trans +ve: translocation positive MALT lymphoma.

3.4.6.2 Other gene sets differentially enriched between MALT lymphoma with and without chromosome translocation

As there was considerable overlap among some of the gene sets that were associated with the related cellular pathways, biological processes or molecular functions, they were grouped according to their involvement in the NF-κB activation pathway, inflammation/immune responses, MAPK pathways, cell cycle and others as shown in Table 3.1. Leading edge analysis was carried out to identify the core subset genes that underscored the significant

enrichment and were thus most likely to be biologically important. The NF- κ B target genes were frequently represented in each of these core subset genes, often on top end of the list particularly in the gene sets related to inflammation/immune responses (Figure 3.11).

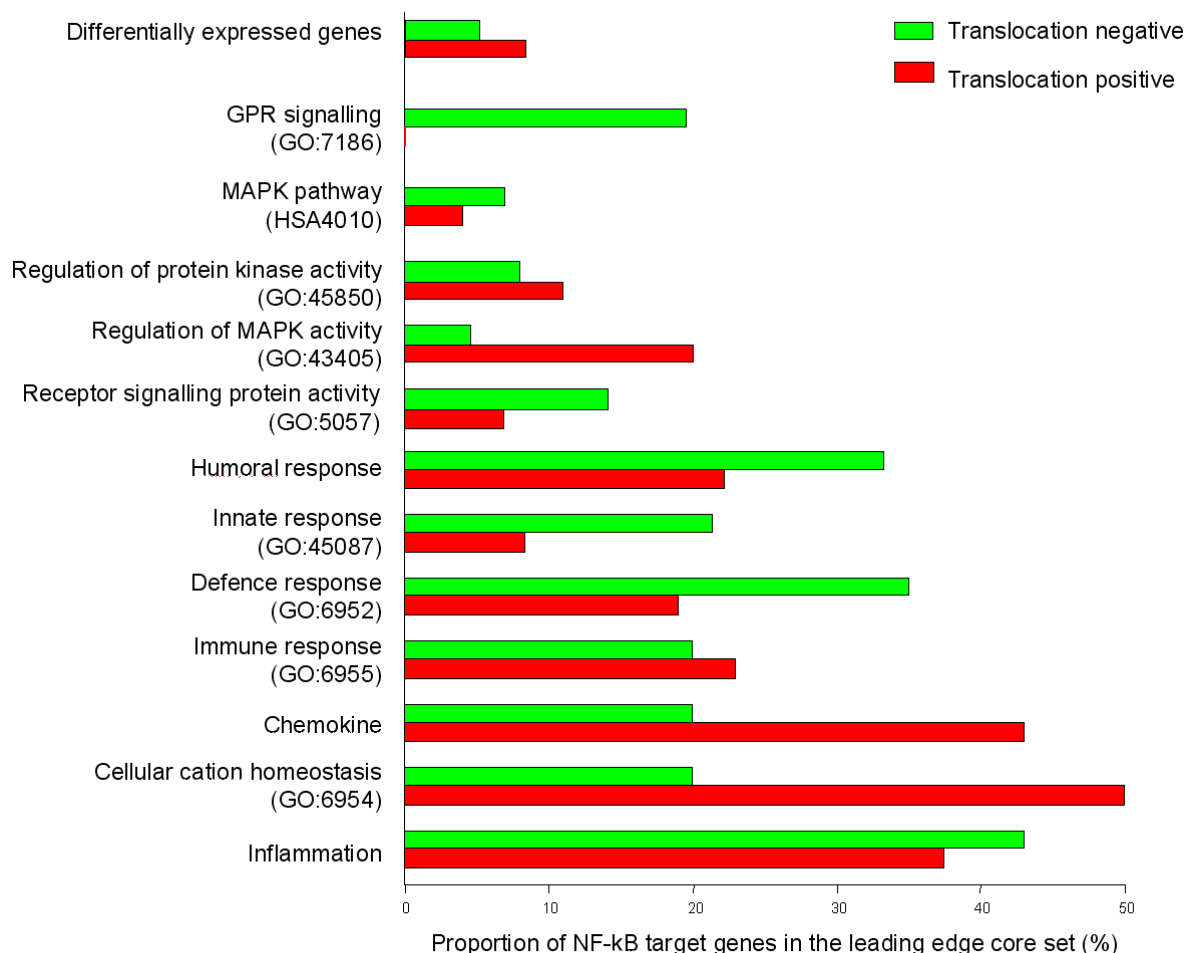


Figure 3.11 - Presence of high proportion of NF- κ B target genes in the leading edge core set of various gene sets related to inflammation and immune responses.

Leading edge analysis of the positive regulation NF- κ B cascade group (GO:43123) shows CD40 as one of the leading edge genes enriched in translocation positive MALT lymphoma and leading edge analysis of immune response genes (GO:6955) (Figure 3.10B) shows CD1D enriched in the translocation positive MALT lymphoma group.

3.4.6.3 Gene Ontology annotations of genes differentially expressed between MALT lymphoma with and without chromosome translocation confirms findings by GSEA

The strategy for analysis of differentially expressed genes between MALT lymphoma with and without chromosome translocation by Gene Ontology (GO) annotation is shown in Figure 3.12.

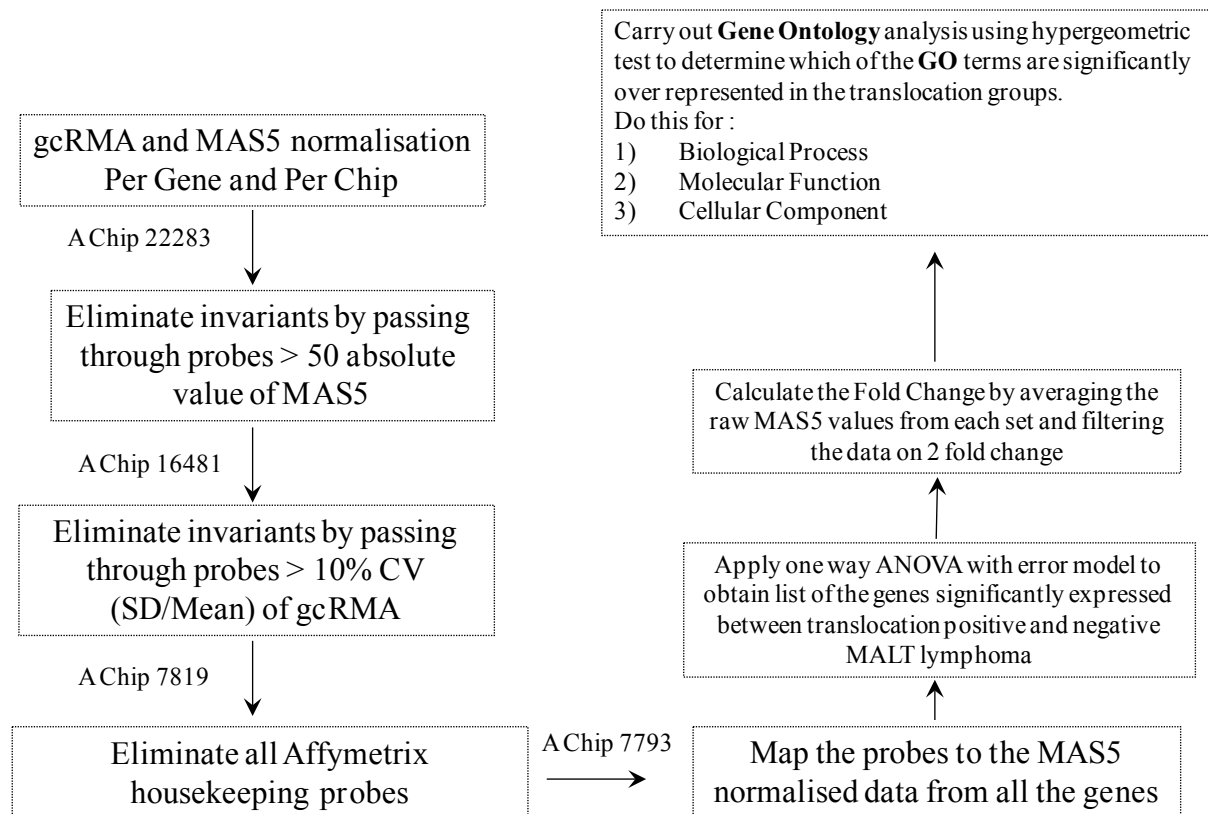


Figure 3.12 - Summary of bioinformatics strategy used for Gene Ontology analysis on MALT lymphoma with and without chromosome translocation.

After normalisation and non-specific filtering, the data is mapped to MAS5 normalised values and a one-way ANOVA was applied to it and reduced further by calculated fold change. The final probes are entered into GO to obtain any relevant pathways.

To gain further insights into the molecular pathways affected by the oncogenic products of MALT lymphoma associated chromosome translocations, genes that were significantly over or under-expressed in translocation positive MALT lymphoma in comparison with translocation negative cases were identified using the one-way ANOVA test. These

differentially expressed genes were further filtered using 2-fold change as a threshold. Ninety six genes were over-expressed in translocation positive MALT lymphoma, while 174 genes were under-expressed in these cases, i.e. over-expressed in translocation negative cases. *TLR6*, *CCR2*, *BCL2*, *CD1D* and *CD69* identified by GSEA were most highly expressed in translocation positive MALT lymphoma, and conversely *IL8*, *NR4A3* and *CXCL5* were on the most highly expressed in translocation negative MALT lymphoma as shown in Table (Appendix III.II).

To further assess the biological implications of the differential gene expression in MALT lymphoma with and without chromosome translocation, the representation of gene ontology (GO) terms in the above gene sets that were over or under-represented in translocation positive MALT lymphoma were measured using hypergeometric tests (Falcon & Gentleman, 2007). Among the genes over-expressed in translocation positive MALT lymphoma, the GO terms relating to NF- κ B pathway activation, defense/immune responses and CCR signalling were significantly over-represented (Table 3.2). While among the genes under-expressed in translocation positive MALT lymphoma, i.e. over-expressed in translocation negative cases, the GO terms relating to chemotaxis, inflammatory response and CCR signalling were significantly over-represented (Table 3.2). These findings from the analysis of differentially expressed genes between MALT lymphomas with and without chromosome translocation reinforce the GSEA results described in sections 3.2.6.1 and 3.2.6.2.

Table 3.2 - Representation of gene ontology terms in over-expressed genes in MALT lymphoma with and without chromosome translocation.

| Gene ontology term | GO category | Genes in Category | % of Genes in Category | Genes in List in Category | % of Genes in List in Category | P value |
|--|--------------------|-------------------|------------------------|---------------------------|--------------------------------|----------|
| Gene ontology term over-represented in translocation positive MALT lymphoma | | | | | | |
| GO:6952: defense response | Biological process | 1306 | 8.029 | 17 | 23.61 | 4.18E-05 |
| GO:9607: response to biotic stimulus | Biological process | 1361 | 8.367 | 17 | 23.61 | 7.02E-05 |
| GO:7243: protein kinase cascade | Biological process | 474 | 2.914 | 8 | 11.11 | 0.00114 |
| GO:7249: I-kappaB kinase/NF-kappaB cascade | Biological process | 181 | 1.113 | 5 | 6.944 | 0.00124 |
| GO:48522: positive regulation of cellular process | Biological process | 881 | 5.416 | 11 | 15.28 | 0.00161 |
| GO:48518: positive regulation of biological process | Biological process | 1028 | 6.32 | 12 | 16.67 | 0.00173 |
| GO:6955: immune response | Biological process | 1187 | 7.297 | 13 | 18.06 | 0.00193 |
| GO:42981: regulation of apoptosis | Biological process | 525 | 3.227 | 8 | 11.11 | 0.00218 |
| GO:43067: regulation of programmed cell death | Biological process | 531 | 3.264 | 8 | 11.11 | 0.00234 |
| GO:7250: activation of NF-kappaB-inducing kinase | Biological process | 17 | 0.105 | 2 | 2.778 | 0.00252 |
| GO:43123: positive regulation of I-kappaB kinase/NF-kappaB cascade | Biological process | 133 | 0.818 | 4 | 5.556 | 0.00286 |
| GO:43122: regulation of I-kappaB kinase/NF-kappaB cascade | Biological process | 141 | 0.867 | 4 | 5.556 | 0.00353 |
| GO:16493: C-C chemokine receptor activity | Molecular function | 22 | 0.128 | 2 | 2.857 | 3.58E-03 |
| GO:19957: C-C chemokine binding | Molecular function | 22 | 0.128 | 2 | 2.857 | 3.58E-03 |
| GO:4197: cysteine-type endopeptidase activity | Molecular function | 155 | 0.901 | 4 | 5.714 | 3.67E-03 |
| Gene ontology term over-represented in translocation negative MALT lymphoma | | | | | | |
| GO:46870: cadmium ion binding | Molecular function | 10 | 0.0582 | 5 | 3.378 | 1.07E-08 |
| GO:1664: G-protein-coupled receptor binding | Molecular function | 67 | 0.39 | 7 | 4.73 | 1.71E-06 |
| GO:5507: copper ion binding | Molecular function | 79 | 0.459 | 7 | 4.73 | 5.24E-06 |
| GO:42379: chemokine receptor binding | Molecular function | 58 | 0.337 | 6 | 4.054 | 1.03E-05 |
| GO:8009: chemokine activity | Molecular function | 58 | 0.337 | 6 | 4.054 | 1.03E-05 |
| GO:5102: receptor binding | Molecular function | 902 | 5.246 | 21 | 14.19 | 3.05E-05 |
| GO:42330: taxis | Biological process | 160 | 0.984 | 8 | 5.882 | 5.96E-05 |
| GO:6935: chemotaxis | Biological process | 160 | 0.984 | 8 | 5.882 | 5.96E-05 |
| GO:7155: cell adhesion | Biological process | 978 | 6.012 | 21 | 15.44 | 6.11E-05 |
| GO:6954: inflammatory response | Biological process | 263 | 1.617 | 10 | 7.353 | 7.33E-05 |
| GO:6817: phosphate transport | Biological process | 124 | 0.762 | 7 | 5.147 | 8.17E-05 |
| GO:9611: response to wounding | Biological process | 568 | 3.492 | 15 | 11.03 | 8.17E-05 |
| GO:7610: behaviour | Biological process | 465 | 2.859 | 13 | 9.559 | 1.43E-04 |
| GO:4295: trypsin activity | Molecular function | 14 | 0.0814 | 3 | 2.027 | 2.12E-04 |
| GO:5125: cytokine activity | Molecular function | 295 | 1.716 | 10 | 6.757 | 2.41E-04 |

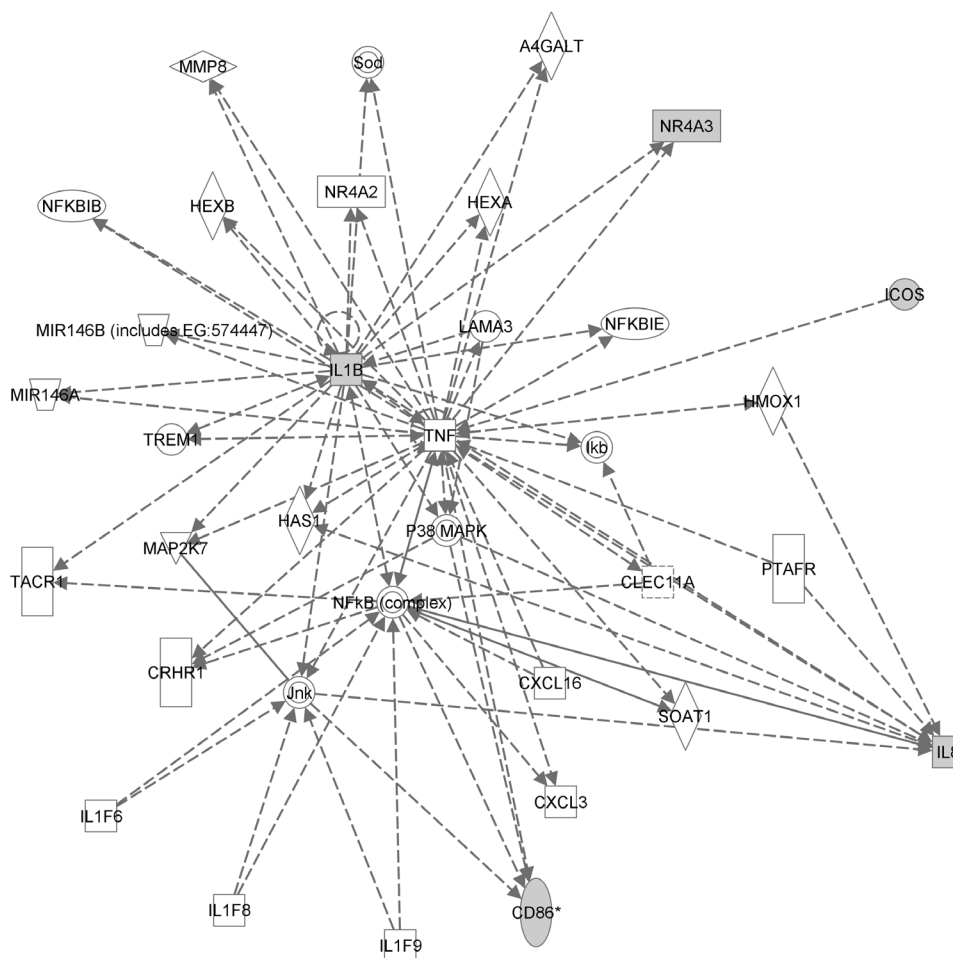
Category: the name of the category within the ontology; Genes in Category: the total number of genes in the genome that have been assigned to the category; % of Genes in Category: the percentage of genes in this category assigned to this GO term; Genes in List in Category: the total number of genes that are present both in the selected gene list and in the category; % of Genes in List in Category: the percentage of genes of this category in the selected gene list that are assigned to this GO term; P-value (hypergeometric p-value) : this is a measure of the statistical significance of the overlap. i.e. the likelihood that it is a coincidence that this many genes were in both the gene list and the category. Only the top 15 are shown.

3.4.7 Pathway analysis of molecules identified by gene expression microarray and potentially important in MALT lymphoma pathogenesis

Basic pathway analysis was carried out to investigate the pathways linked to the molecules derived from the microarray analysis.

For translocation positive MALT lymphoma, immune receptor molecules were TLR6, CD69 and CD1D, chemokine receptors were CCR2, CXCR4, CCR5, CCR6 and CCR7 and the apoptosis inhibitor BCL2. For translocation negative MALT lymphoma, pro-inflammatory cytokines were IL8 and IL1B and co-stimulatory molecules were CD86, CD28 and ICOS. MALT lymphoma with and without translocation were analysed separately using Ingenuity Pathway Analysis.

A



3.5 Discussion

By investigating the transcriptional profile, the present study demonstrated that MALT lymphoma is characterised by a distinct expression profile in comparison with FL and MCL, in line with the recent study by Chng *et al.* (Chng *et al.*, 2009). Although there was considerable overlap in the gene expression profiles between MALT lymphomas with and without chromosome translocation as demonstrated by unsupervised clustering analyses, there were important differences in the expression of NF- κ B target genes between these subgroups. Systematic GSEA of various molecular pathways and biological processes, showed that the NF- κ B target genes are the most differentially over-represented gene set between MALT lymphomas with and without chromosome translocation, followed by those related to inflammation, cellular homeostasis and immune responses. Importantly, several of these molecular pathways or biological processes also lead to NF- κ B activation. These findings were confirmed by independent analyses of differentially expressed genes between MALT lymphomas with and without chromosome translocation using hypergeometric tests of Gene Ontology groups. Our observations provide several novel insights into the molecular mechanisms of both translocation positive and negative MALT lymphomas that potentially explain their different clinical and histological presentations.

3.5.1 Molecular mechanism of translocation positive MALT lymphoma

In comparison with translocation negative MALT lymphoma, GSEA and leading edge analysis revealed a common core subset genes that were enriched and over-expressed in translocation positive MALT lymphoma and a high proportion of these genes are NF- κ B target genes involving multiple related biological processes or molecular pathways. The most

significant ones included immune receptors such as TLR6, TLR7, CD40, CD83, CD1D and CD69, chemokine receptors such as CCR2, CXCR4, CCR6 and CCR7, the apoptosis inhibitor BCL2, positive regulators of the NF- κ B pathway such as REL (a component of NF- κ B transcription factor), LT β (a powerful proinflammatory cytokine) and molecules involved in MAPK pathways (Figure 3.10). All these molecules are involved in promoting tumour cell survival and proliferation either directly or indirectly. Among these, the over-expression of the above immune surface receptors is particularly interesting as this enhances the interaction between tumour cells and their microenvironment, which is known to be critical for MALT lymphoma development.

For example, TLRs are innate immune receptors critical for recognising the conserved microbial structures known as pathogen associated molecular patterns (PAMP), and are capable of activating the NF- κ B pathway (Shimizu *et al*, 2007). CD40, CD83 and CD69 are activation markers and co-stimulating molecules which are also likely to play a role in NF- κ B activation. BCL2 is a classic apoptosis inhibitor, and may account for the prolonged survival of tumour cells.

The expression of these molecules was thus further investigated in independent cohorts of MALT lymphomas and discussed in the next chapter.

3.5.2 Molecular mechanism of translocation negative MALT lymphoma

In contrast to translocation positive MALT lymphoma, translocation negative cases were characterised by expression of a strong inflammatory gene signature. GSEA and leading edge analysis also revealed common core subset genes involving several related biological processes or molecular pathways, which were enriched and over-expressed in translocation negative MALT lymphoma. These included pro-inflammatory cytokines such IL8, IL1 β and

LTA, molecules involved in B- and T- cell interaction such as CD86, CD28 and ICOS, several chemokine and chemokine receptors, TLR2 and NR4A3 (also known as MINOR, or NOR1) (Figure 3.10).

IL8, IL1 β and LTA are the hallmark of a pro-inflammatory cytokine profile in response to *H. pylori* infection. IL8 is critical for neutrophil infiltration and activation, while IL1 β and LTA induce gastrin release, inhibit acid secretion and promotes apoptosis of epithelial cells, thus affecting *H. pylori* colonisation (McNamara & El Omar, 2008). The finding of up-regulation of these pro-inflammatory cytokines in translocation negative MALT lymphomas, all from the stomach, indicates the presence of active *H. pylori* infection. In line with this, the expression of a number of chemokines and chemokine receptors was enriched in translocation negative gastric MALT lymphoma. This may reflect the trafficking and retention of various immune cells in response to an active *H. pylori* infection. In keeping with this, translocation negative gastric MALT lymphomas show more frequently an increased number of blast cells than translocation positive cases (Okabe *et al*, 2003).

Most importantly, GSEA showed that the expression of the surface molecules involved in B- and T- cell interaction, namely CD86, CD28 and ICOS was enriched in translocation negative gastric MALT lymphoma, and this was accompanied by unregulated *IL10* expression, a well known outcome of ICOS stimulation (van Berkel & Oosterwegel, 2006).

3.5.3 Nuclear BCL10

Both supervised and unsupervised clustering analysis showed that translocation negative MALT lymphoma cases with nuclear BCL10 staining clustered together with cases harbouring t(1;14)/BCL10-IGH (Figure 3.8). It was recently demonstrated that nuclear expression of BCL10 is significantly associated with resistance to gastric MALT lymphoma

to *H. pylori* eradication (Kuo *et al*, 2004). In ocular adnexal MALT lymphoma, nuclear BCL10 seemed to correlate with a shorter treatment failure-free survival (Franco *et al*, 2006), although this could not be confirmed by other groups (Vejabhuti *et al*, 2005). Gallardo *et al*. (Gallardo *et al*, 2006) found a significant association between nuclear BCL10 expression and a higher risk of extra-cutaneous involvement in primary cutaneous marginal zone B-cell lymphoma, whereas Li *et al*. (Li *et al*, 2003) reported that nuclear BCL10 was associated with the development of a locally aggressive course. Based on these observations, a role for nuclear BCL10 in lymphomagenesis is suggested, although the precise pathological significance remains unclear. Based on its interaction with transcription factor IIB and its ability to activate transcription as a fusion protein linked to the Gal4-DNA-binding domain in HeLa cells, Liu *et al*. (Liu *et al*, 2004d) suggested a role for BCL10 as a transcriptional activator, whereas Yeh *et al*. (Yeh *et al*, 2006) found nuclear BCL10 to be involved in the transcriptional activity of NF- κ B following TNF- α signalling in MCF7 cells. The current microarray analysis further enforces a role for nuclear BCL10 in the development of MALT lymphoma. However, further functional studies on the role of BCL10 in the nucleus are needed to determine which pathways and interacting molecules are involved.

3.5.4 Summary and conclusion

In summary, gene expression microarray studies showed that MALT lymphoma is a distinct entity, but with overlapping gene expression signatures between MALT lymphoma with and without chromosomal translocation. In both supervised and unsupervised clustering analysis, translocation negative MALT lymphoma with nuclear BCL10 expression clustered with translocation positive MALT lymphoma cases suggesting a role of nuclear BCL10 in MALT lymphomagenesis. Gene set enrichment analysis and Gene Ontology hypergeometric

analysis, showed differences in the molecular pathways involved in MALT lymphoma with and without chromosome translocation. Many of these differences were attributed to different involvement of the of NF- κ B target genes. Leading edge analysis identified a number of important molecules that are potentially important for the pathogenesis of MALT lymphoma with or without chromosome translocation which will be investigated and discussed in the next chapter.

CHAPTER 4 – Validation of the genes identified by expression microarray of MALT lymphoma with and without chromosome translocation using qRT-PCR and immunohistochemistry

4.1 Introduction

Gene expression microarray study of MALT lymphoma with and without chromosome translocation identified a number of genes preferentially over-expressed in either subset (Chapter 3). Translocation positive MALT lymphomas were highly enriched in the expression of *CD69*, *CCR2A*, *CCR5*, *TLR6*, *BCL2* and *IRF4* (also known as *MUM1*) in addition to the already characterised genes *BCL10*, specific to t(1;14), and *MALT1* specific to t(11;18) and t(14;18). In contrast, translocation negative MALT lymphomas were highly enriched in the expression of *CD86* and *NR4A3*. The differential expression of these molecules was thought to play an important role in the pathogenesis of the respective MALT lymphoma subgroups. Thus, it was necessary to validate further their differential expression in MALT lymphomas with and without chromosome translocation in independent cohorts by qRT-PCR and immunohistochemistry and Western blotting.

4.2 Aims of the study

To validate the molecules derived from gene expression microarray studies in a large cohort of MALT lymphoma specimens using qRT-PCR and immunohistochemistry or Western blotting and to correlate the transcript and protein expression with the chromosomal translocation status.

4.3 Experimental design

4.3.1 Case selection

A total of 73 cases of MALT lymphoma with known translocation status were investigated. These included 8 cases with t(1;14), 18 cases with t(11;18), 9 cases with t(14;18), 38 cases without MALT lymphoma associated chromosomal translocations including 10 with nuclear and 28 with cytoplasmic BCL10 expression. These MALT lymphomas originated from the stomach (48), liver (2), ocular adnexa (4), small intestine (4) and lung (15).

4.3.2 Validation of gene expression by qRT-PCR

The mRNA expression level of the genes differentially expressed between MALT lymphomas with and without chromosome translocation (*CD69*, *CCR2A*, *CCR5*, *TLR6*, *BCL2*, *IRF4*, *CD86*, *NR4A3*, *BCL10* and N-terminal part of *MALT1*) was investigated by qRT-PCR. RNA was extracted from microdissected tumour cells of FFPE MALT lymphoma specimens and treated with Turbo DNase to remove genomic DNA (Section 2.2.3.1). Where possible, primer pairs were designed to span exons to prevent amplification of any residual genomic DNA and to target up to 150bp (Table 2.2) (Section 2.2.6.1), and were thus suitable for FFPE tissues. This was the case for all genes except TLR6 which had only one coding exon and CCR2A which shared the sequence with CCR2B except for a small region. For those two primer pairs within exons, the negative control of the RNA that has undergone Turbo DNAase was checked to confirm the amplification was that of the cDNA rather than genomic DNA. All primers were checked on tonsillar RNA to ensure that they gave specific PCR products and ran on gels to ensure they amplified the expected size. The results are presented as ΔCT values calculated as ($\Delta CT = T_{\text{Reference Gene}} - T_{\text{Test Gene}}$), so the higher the value, the lower the transcript expression and *vice versa*. Unsupervised clustering on subset

of the genes across all samples using Ward similarity measure and average linkage was carried out to determine the discriminatory power of those genes on the MALT lymphoma cases. Both BCL2 and IRF4 were excluded from clustering as their qRT-PCR was carried out on a smaller cohort of MALT lymphomas (25 and 24 cases respectively) due to lack of sufficient tissue in the remaining MALT lymphomas.

The results of the qRT-PCR were correlated with the known chromosomal translocation established by conventional cytogenetics, interphase FISH and RT-PCR, as described in Chapter 3. The Mann-Whitney U Test determined whether there were statistically significant differences in the expression of particular transcripts between groups of cases with different chromosome translocation status.

4.3.3 BCL2, CD69, IRF4, MALT1, BCL10 and CD86 immunohistochemistry

Data on BCL10 and MALT1 expression from same cases of MALT lymphoma subgroups was obtained from a previous immunohistochemistry based study (Ye *et al*, 2005) (Figure 1.6). The immunohistochemical conditions, including antigen retrieval, antibody dilution and incubation times, were systematically optimised as described in Chapter 2 (Table 2.3). The immunostaining was evaluated independently by two assessors (Professor Ming Du and Dr. Hongtao Ye) and scored according to the percentage of positive cells in a section (<30%, 30-70%, >70%) and the intensity of staining (weak, moderate, strong). Mr. Rifat Hamoudi helped in section cutting, slide preparation, scoring of immunohistochemistry, collation of the immunohistochemical data and analysis. Cases were considered positive if 30% or more tumour cells were stained. Cases with scoring discrepancies between the assessors were reviewed. The results of the immunostaining were then correlated with the known chromosome translocation status as determined by qRT-PCR and interphase FISH (detailed

in Chapter 3). Differences in the proportion of cases staining positive for each of the six proteins across the different chromosome translocation groups were assessed by the Fisher's exact test.

4.3.4 Validation of TLR6 using Western blotting

Imunohistochemistry of TLR6 antibody did not yield satisfactory results thus, western blotting was carried out using the TLR6 antibody on 5 fresh frozen t(11;18) positive and 9 translocation negative MALT lymphoma cases with one FL case and one Jurkat cell line used as control. Protein extraction and Western blotting were carried out as detailed in Chapter 2. The filter was stripped and re-probed with β -actin used as a loading control, followed by stripping and re-probing with MALT1 (97 kD) as an integrity control to ensure all archival samples used were adequate for investigation using TLR6 (92 kD). TLR6 and β -actin bands were quantified using AIDA (Advanced Image Data Analyzer, version 4.18) (Raytest, Straubenhardt, Germany), and normalised TLR6 expression was calculated as the ratio of TLR6 / β -actin. Differences in the cases with different TLR6 expression across the various chromosomal translocation groups were assessed by Fisher's exact test.

4.4 Results

4.4.1 Correlation of mRNA expression of *CD69*, *CCR2A*, *CCR5*, *TLR6*, *BCL2*, *IRF4*, *CD86*, *NR4A3*, *BCL10* and *MALT1* genes in MALT lymphoma with and without chromosomal translocation

BCL10 transcript expression was highest in the t(1;14) group (p = 0.001) whereas 5' end of *MALT1* (encoding the N-terminus of MALT1) was highest in the t(14;18) group (p = 0.02) reflecting the pattern seen in the gene expression microarray data and confirming the validity of the qRT-PCR methodology (Figure 4.1). In keeping with the results of the gene expression microarray study, *CCR5* was highly expressed in t(1;14) and *TLR6*, *CCR2A*, *BCL2*, *CD69* and *IRF4* were significantly highly expressed in t(1;14) and t(11;18) positive cases in comparison with translocation negative cases (Figure 4.1), whereas *CD86* and *NR4A3* were significantly highly expressed in translocation negative cases in comparison with translocation positive cases (Figure 4.1).

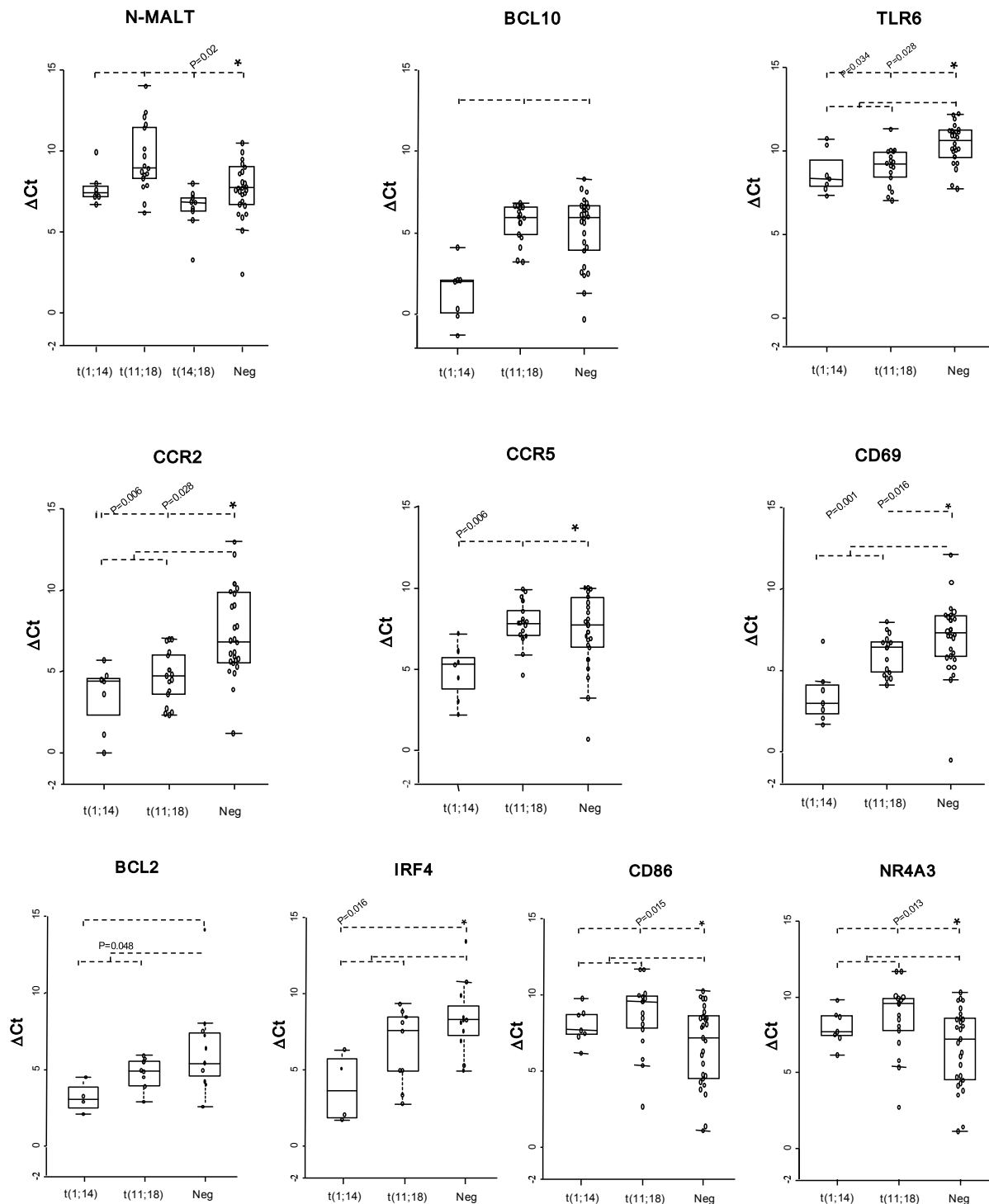


Figure 4.1 - Validation of gene expression in MALT lymphoma with and without chromosome translocation by real-time quantitative RT-PCR.

This was performed in triplicate using RNA samples extracted from tumour cells microdissected from paraffin-embedded tissue sections. Asterisk indicates statistically significant differences between various translocation positive groups and translocation negative group by Mann-Whitney non-parametric statistical test. The medians are indicated by horizontal bars in the rectangular boxes. Error bars show the standard deviation of the results in each group. Neg: translocation negative MALT lymphoma. High ΔCt values reflect low transcript expression and vice versa.

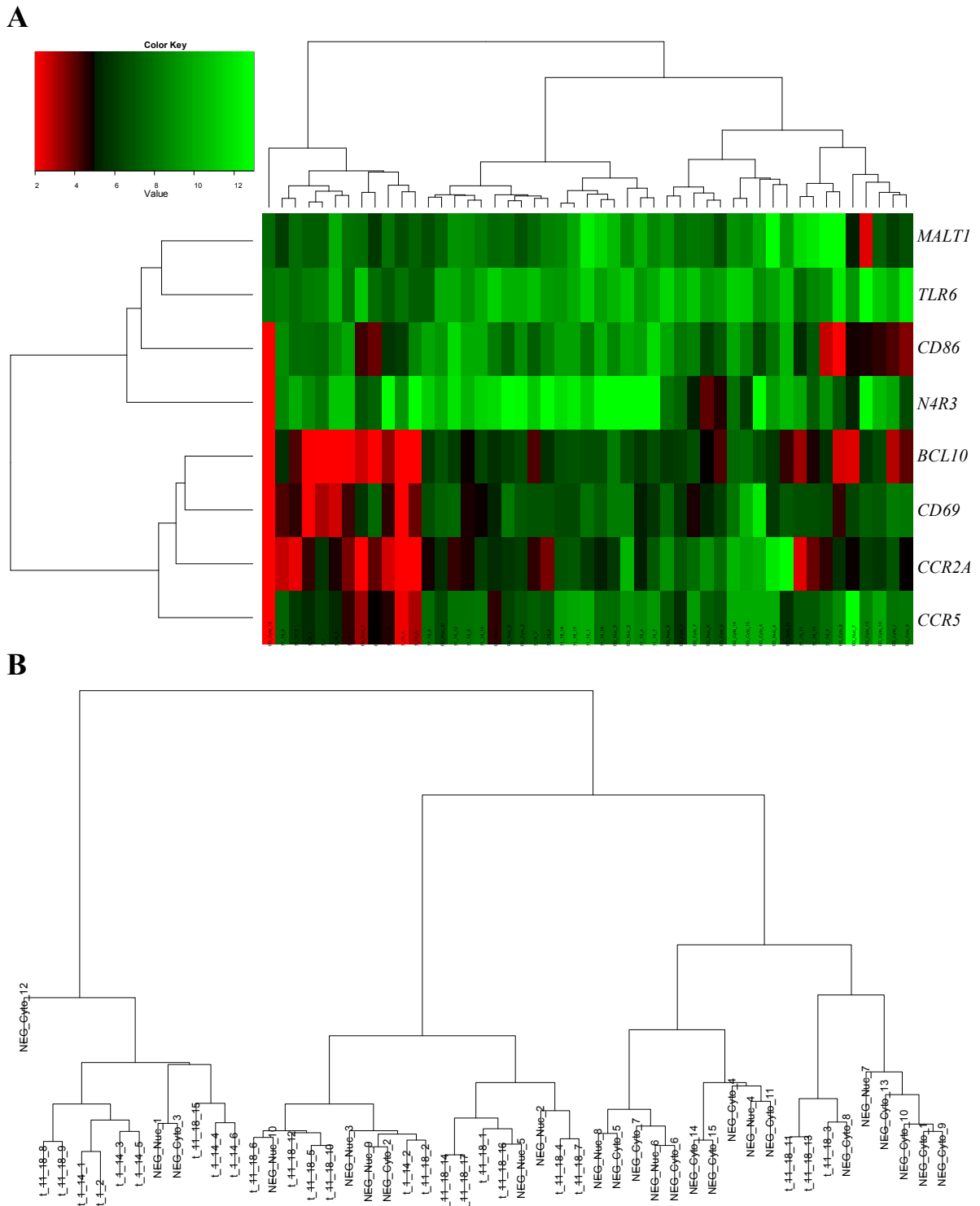


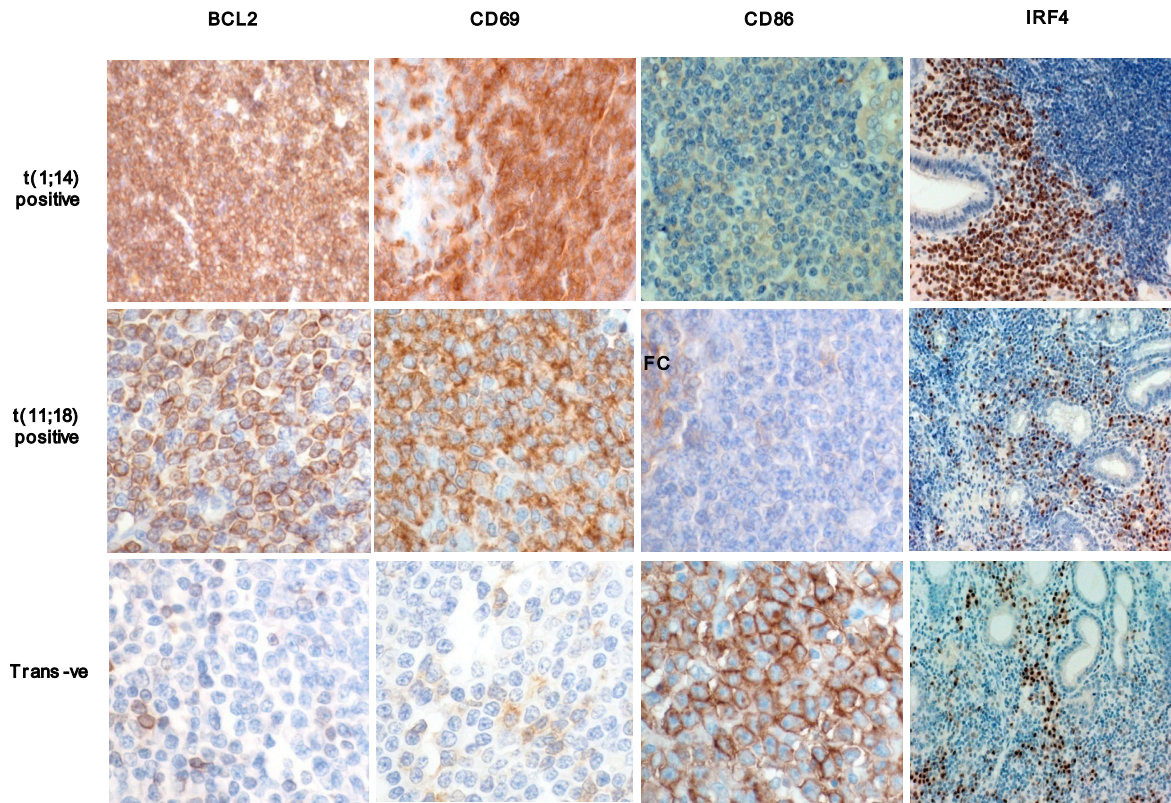
Figure 4.2 - Unsupervised hierarchical clustering of qRT-PCR data on MALT lymphoma cases with various translocation status.

(A) Unsupervised clustering heatmap of the qRT-PCR genes that are differentially expressed between translocation positive and negative MALT lymphoma. Red colour indicates high expression and green low expression. (B) dendrogram of the MALT lymphoma cases shown in the heatmap of part A.

The unsupervised clustering analysis did not show clear segregation between MALT lymphoma with and without translocation. Nevertheless, the dendrogram (Figure 4.2 B) showed 3 main groups; the far right had mainly translocation negative MALT lymphomas (16 negative and 3 t(11;18) positive), the middle group contained a mixture of translocation positive and negative MALT lymphomas but with nuclear BCL10 expression (12 positive, 5 negative with nuclear and 1 cytoplasmic BCL10 expression), and the far left contained mainly translocation positive MALT lymphomas (9 positive and 2 negative one with nuclear and the other with cytoplasmic BCL10 expression) (Figure 4.2B). Both the heatmap and dendrogram, revealed on the left, one MALT lymphoma negative case with cytoplasmic BCL10 expression labelled “NEG_Cyto_12” had high expression for all 8 genes but low expression for TLR6 (Figure 4.2 A and B).

4.4.2 Comparison of protein expression of CD69, BCL2, CD86 and IRF4, MALT1 and BCL10 in MALT lymphoma with and without chromosomal translocation using immunohistochemistry

A



B

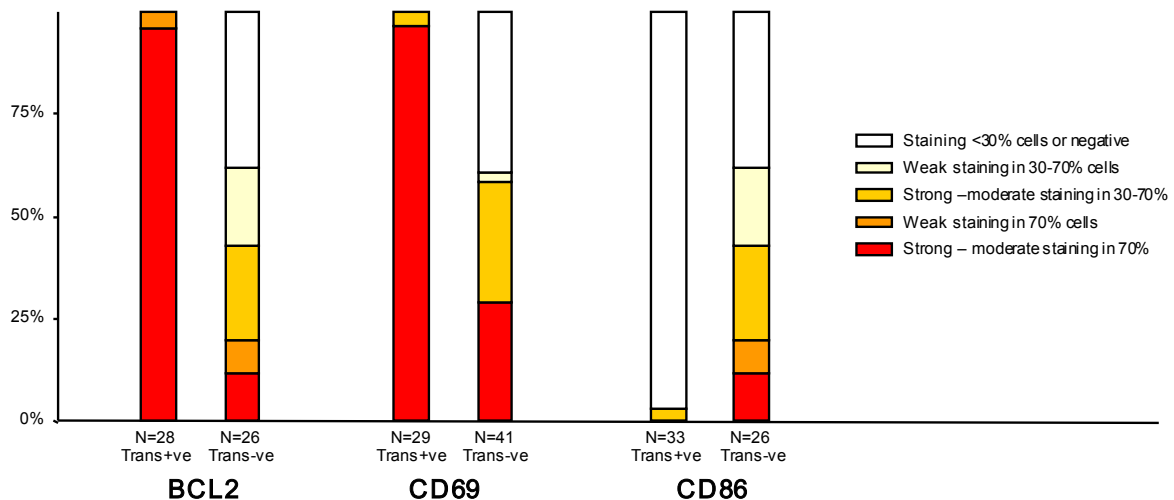


Figure 4.3 - Immunohistochemistry of BCL2, CD69, CD86 and IRF4.

(A) BCL2, CD69 and CD86 immunohistochemistry in MALT lymphomas with and without chromosome translocation.

(B) Summaries of immunohistochemistry showing that BCL2 and CD69 are more strongly and homogeneously expressed in translocation positive than translocation negative MALT lymphoma ($p < 6.9 \times 10^{-5}$, $p < 2.2 \times 10^{-4}$ respectively by Fisher's exact test), while CD86 is more strongly expressed in translocation negative than translocation positive MALT lymphoma ($p < 6.4 \times 10^{-7}$ by Fisher's exact test). IRF4 is typically expressed in activated B cells and cells showing plasma cell differentiation.

FC: follicle centre; Trans-ve: translocation negative.

Table 4.1 - Correlation of BCL2, CD69 and CD86 expression in MALT lymphoma with and without chromosome translocation.

| Marker | MALT lymphoma translocation | No. of cases | Expression in >70% cells | | Expression in 30-70% cells | | Negative or expression in <30% |
|--------|-----------------------------|--------------|-----------------------------|---------------|-----------------------------|---------------|--------------------------------|
| | | | Strong or moderate staining | Weak staining | Strong or moderate staining | Weak staining | |
| BCL2 | Positive | 28 | 27 (96%) | 1 (4%) | - | - | - |
| | Negative | 26 | 3 (12%) | 2 (8%) | 6 (23%) | 5 (19%) | 10 (38%) |
| CD69 | Positive | 29 | 28 (97%) | - | 1 (3%) | - | - |
| | Negative | 41 | 12 (29%) | - | 12 (29%) | 1 (2%) | 16 (39%) |
| CD86 | Positive | 33 | - | - | 1 (3%) | - | 32 (97%) |
| | Negative | 26 | 3 (12%) | 2 (8%) | 6 (23%) | 5 (19%) | 10 (38%) |

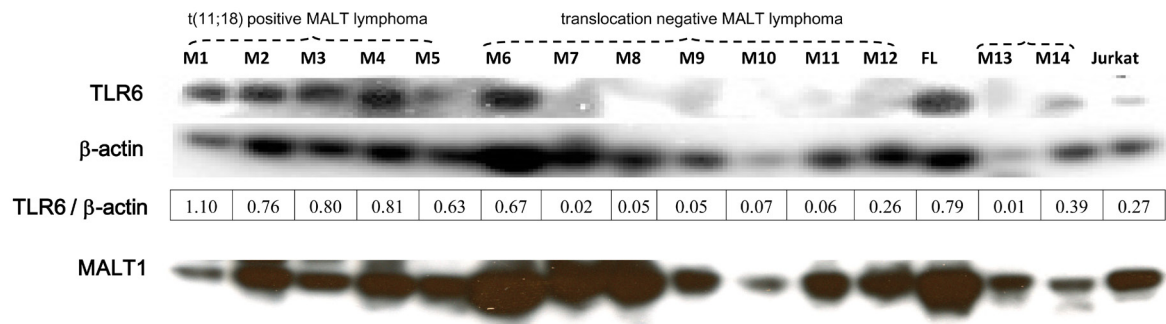
BCL10 and MALT1 staining were carried out as part of the study by Ye *et al.* (Ye *et al.*, 2005) and discussed in section 1.3.1.4. CD69, BCL2, CD86 and IRF4 protein expressions were further investigated by immunohistochemistry in MALT lymphomas (Table 4.1). IRF4, known to be expressed in activated B cells and plasma cells, was highly expressed in the neoplastic plasma cells (confirmed by immunoglobulin light chain staining) of t(1;14) positive MALT lymphoma, which were prominent in the lamina propria. Since BCL10, MALT1 and IRF4 gave staining patterns similar to that reported in the literature, Both BCL2 and CD69 showed homogeneous and strong expression in 97% (28/29) of both t(11;18) and t(1;14) translocation positive MALT lymphoma cases, whereas their expression was heterogeneous and much weaker expression in 29% (12/41) of translocation negative cases (Figure 4.3 and Table 4.1). For example, BCL2 was strongly expressed in at least 70% tumour cells in 96% (27/28) of translocation positive cases but only in 12% (3/26) translocation negative cases. In contrast, CD86 showed heterogeneous and strong expression in translocation negative MALT lymphomas (Figure 4.2) but weak or negative staining in

most (97% or 32/33) translocation positive MALT lymphomas. Statistical analysis using the Fisher's exact test showed that BCL2, CD69 and CD86 were significantly different between translocation positive and negative MALT lymphoma.

4.4.3 Comparison of protein expression of TLR6 in MALT lymphoma with and without chromosome translocation using Western blotting

All MALT lymphoma cases expressed a MALT1 protein of the expected molecular weight (approximately 90 kDa) indicating that the archival protein extracts are adequate for Western blot analysis (Figure 4.4A). TLR6 was highly expressed in translocation positive MALT lymphoma, but at low levels in translocation negative cases (Figure 4.4). Interestingly, case M6 which is a translocation negative MALT lymphoma with nuclear BCL10 showed relatively high expression of TLR6 (ratio of TLR6/actin = 0.67) comparable to t(11;18) positive cases (Figure 4.4B).

A



B

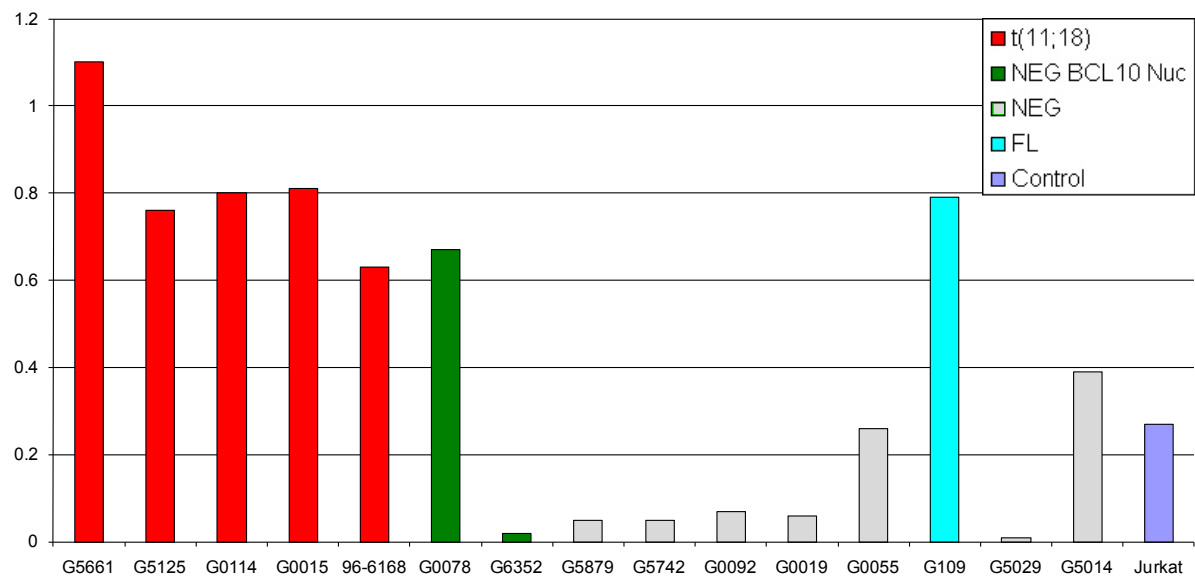


Figure 4.4 - TLR6 expression in MALT lymphoma with and without chromosomal translocation using Western blot analysis.

(A) Western blot showing that TLR6 is highly expressed in translocation positive MALT lymphoma, but at low levels in translocation negative cases. M: MALT lymphoma; M6 and M7 are translocation negative MALT lymphoma with nuclear BCL10 staining; FL: follicular lymphoma. Jurkat cell line used as control.

(B) Graphical representation of the ratio of TLR6 expression across MALT lymphoma cases with and without chromosomal translocation.

4.5 Discussion

MALT1 was highly expressed in cases with t(11;18) and t(14;18) translocation. *TLR6*, *CCR2A*, *CD69*, *BCL2* and *IRF4* were highly expressed in cases with t(11;18) translocation. *BCL10* and *CCR5* were highly expressed in cases with t(1;14) translocation. *CD86* and *NR4A3* were highly expressed in translocation negative MALT lymphomas. This was the case for 20 MALT lymphoma cases that were subjected to microarray analysis, qRT-PCR and immunohistochemistry for *MALT1*, *BCL10*, *BCL2*, *CD69* and *CD86*. Thus this shows that mRNA correlates with protein expression for the above proteins and validates both methodologies as well as providing further evidence of the reliability of the gene expression microarray results in this thesis.

Translocation negative MALT lymphomas were characterised by high expression of *CD86* and *N4RA3*. *CD86* is a surface molecule involved in B- and T- cell interaction and thus might play a role in response to *H. pylori* eradication. In line with this finding, a previous study showed significantly higher *CD86* expression in gastric MALT lymphomas that responded to *H. pylori* eradication when compared with those resistant to the therapy (66% VS 10%) (de Jong *et al*, 2001). Though the chromosome translocation status in these cases is not available, it is most likely that the cases that responded to *H. pylori* were translocation-negative (Liu *et al*, 2002b). Although residual reactive follicles may be present and contribute to the high *CD86* expression in translocation negative cases, the over-expression of *CD86* in tumour cells was clearly demonstrated by microdissection, qRT-PCR and immunohistochemistry. Taken together, these findings suggest that there is an active immune response to *H. pylori* infection in translocation-negative gastric MALT lymphoma, and this most likely underscores the tumour cell survival and expansion and thus determines their response to *H. pylori* eradication.

NR4A3 is another molecule significantly enriched and over-expressed in translocation negative MALT lymphoma. NR4A3 is a member of the nerve growth factor-1B (NGF1B, or NR4A1 or Nur77) subfamily of nuclear orphan receptors. In T cells, NGF1B and NR4A3 are involved in TCR mediated cell death and thymocyte negative selection (He, 2002). These nuclear orphan receptors are also involved in the apoptotic process of other cell types in response to external signals (Hashida *et al*, 2007). The function of NR4A3 in B cells is currently unclear. Nonetheless, NR4A3 is one of the top over-expressed genes in curable, as opposed to fatal/refractory, DLBCL (Shipp *et al*, 2002). It is possible that over-expression of NR4A3 in lymphoma cells might sensitise their response to pro-apoptotic signals following *H. pylori* eradication and elimination of the microbial mediated immune stimulations.

The over-expression of IRF4, BCL2, CD69, CCR2A, CCR5 and TLR6 in translocation positive cases was further confirmed in a separate cohort of MALT lymphomas by qRT-PCR and immunohistochemistry or Western blot analysis.

IRF4 encodes a transcriptional factor and is expressed in activated B cells and cells showing plasma cell differentiation (Pernis, 2002). In line with its known expression pattern, IRF4 is highly expressed in the plasma cell component of MALT lymphoma. Among different subgroups of MALT lymphoma, plasma cell differentiation of neoplastic B cells is most prominent in those with t(1;14) translocation. IRF4 is transcriptionally activated by t(6;14)(p25;q32) in multiple myeloma and strong IRF4 expression has also been found in several lymphoma subtypes including lymphoplasmacytic lymphoma and 75% of diffuse large B-cell lymphoma and primary effusion lymphoma, which are not associated with t(6;14) (Falini & Mason, 2002). IRF4 was one of the molecules found in the activated DLBCL signature profile using cDNA microarrays (Alizadeh *et al*, 2000). The oncogenic activity of IRF4 is thought to be related to its transcriptional repression of interferon (IFN)

inducible genes and thus suppression of the anti-proliferative effects of IFN (Hrdlickova *et al*, 2001; Pernis, 2002). Interestingly, NF- κ B transactivates IFN and a simultaneous up-regulation of IRF4 may block the effect of NF- κ B on IFN activation.

BCL2 is an apoptosis inhibitor protein; its over-expression in lymphocytes alone was shown to be insufficient for malignant transformation, but simultaneous over-expression of BCL2 and the proto-oncogene MYC may produce aggressive B-cell malignancies (Otake *et al*, 2007). Hence in MALT lymphomas, over-expression of BCL2 may lead to oncogenesis by reducing cell death. Currently, the exact anti-apoptotic pathways through which BCL2 exerts its role are only partially understood, involving decreased mitochondrial release of cytochrome C, which in turn is required for the activation of procaspase-9 and the subsequent initiation of the apoptotic cascade (Adams & Cory, 1998).

CD69, a type II transmembrane glycoprotein with an extracellular C-type lectin binding domain, is another potential co-stimulatory receptor and may also have an immunoregulatory role (Sancho *et al*, 2005). Although the precise function of CD69 in B cells is largely unknown, it is a well described activation marker in a number of cell types. CD69 is frequently expressed in low grade B-cell non-Hodgkin lymphomas and in follicular lymphoma, its expression on tumour cells is associated with poor treatment outcome (de Jong *et al*, 2009; Erlanson *et al*, 1998). The finding of enriched expression of CD69 in translocation positive MALT lymphoma in the present study further implicates its role in lymphoma pathogenesis.

Other types of molecule enriched in translocation positive MALT lymphomas are chemokine receptors such as CCR2 and CCR5. These are G protein coupled receptors (GPR) whose major function is to regulate leukocyte trafficking and mediate immune cell migration and their retention in inflammatory sites (Murphy *et al*, 2000). Other functions include angiogenic

activity, apoptosis, T-cell differentiation and phagocyte activation. Following interaction with their specific chemokine ligands, chemokine receptors trigger a flux of intracellular calcium (Ca^{2+}) ions (calcium signalling). This causes cellular responses, including the onset of a process known as chemotaxis that triggers cells to migrate to specific anatomical sites. Several homeostatic chemokines have been shown to play an important role in mucosal immunology including germinal centre formation, homing mechanisms, migration and retention of lymphocytes to the sites of inflammation. Recently a study showed that CCR2 is expressed in several haematopoietic cell lineages and is critical for migration of haematopoietic stem and progenitor cells to sites of inflammation (Si *et al*, 2010). Although the specific role of CCR2 in B-cell trafficking and homing is unclear, it forms a heterodimer with CXCR4 that is critical for B-cell homing to the Peyer's patches and splenic marginal zone (Springael *et al*, 2005), thus potentially playing a role in mature B-cell homing processes. CCR5 is a receptor for a number of inflammatory CC-chemokines including MIP-1-alpha, MIP-1-beta and RANTES, which may prove to be important in translocation positive MALT lymphoma.

Another interesting molecule highly expressed in translocation positive MALT lymphoma is Toll-like receptor 6 (TLR6). Toll-like receptors play a role in innate immunity by recognising conserved microbial structures known as pathogen associated molecular patterns (PAMPs). TLR6 is activated by bacterial lipopolysaccharide (LPS) and signals through MyD88 to activate NF κ B; the signalling pathway of TLR6 is similar to that of the IL-1 receptor upon activation by the cytokine IL-1. In a mouse model, it has been shown that TLR signalling promotes marginal zone B-cell activation and migration (Rubtsov *et al*, 2008). TLR6 typically forms heterodimers with TLR2 on the cell surface to recognize bacterial antigens (Gomariz *et al*, 2007). TLR2/TLR6 signalling activates not only IKK complex that leads to

activation of the NF- κ B transcriptional factor, but also the MAP kinase p38 and Jun amino-terminal kinase (JNK) that leads to activation of the AP-1 transcriptional factor (Akira & Takeda, 2004). Hence, over-expression of TLR6 in translocation-positive MALT lymphoma could potentially augment the NF- κ B activity mediated by MALT lymphoma associated oncogenic products and also activate the MAP kinase pathways. In order to test the former hypothesis, functional studies involving the expression of TLR6, in the presence of TLR2, were carried out to investigate whether they could enhance both BCL10 and API2-MALT1 mediated NF- κ B activation *in vitro* and whether this effect was particularly significant upon LPS stimulation.

In summary, all of the key NF- κ B target genes, found to be over-expressed by expression microarrays, were confirmed by qRT-PCR and immunohistochemistry. Those genes are involved in promoting tumour cell survival and proliferation either directly or indirectly and their over-expression may enhance the interaction between tumour cells and their microenvironment, which is known to be critical for MALT lymphoma development. Thus further investigation of the role of some of those genes in MALT lymphogenesis is warranted and the effect of some of the identified genes (such as TLR6) on NF- κ B activation, will be investigated using *in vitro* model as described in the next chapter.

CHAPTER 5 – Cooperation between MALT lymphoma oncogenes and immunological stimulation in activating the NF-κB pathway

5.1 Introduction

MALT lymphoma commonly occurs in sites that are normally devoid of organised lymphoid tissues where the lymphoma is preceded by the accumulation of reactive lymphoid tissue, suggesting that the tumours arise during a chronic immune response. Several previous studies suggest that surface receptor stimulation may play an important role in MALT lymphoma pathogenesis. MALT lymphomas invariably express surface Ig. Stimulation by the anti-idiotypic antibody has been shown to enhance MALT lymphoma cell proliferation and this synergises with mitogenic stimulation *in vitro* (Hussell *et al*, 1993b). In line with this, expression of either *API2-MALT1* or *MALT1* in BJAB B-cells enhances the activation of IKK and NF-κB by CD40/CD40L stimulation (Ho *et al*, 2005). Both *API2-MALT1* and *BCL10* transgenic mice acquired expansion of the white pulp of the spleen but not lymphoma (Baens *et al*, 2006). However, treatment of these mice with the Freund's complete adjuvant led to the development of marginal zone hyperplasia reminiscent of human MALT lymphoma (Baens *et al*, 2006).

Thus antigen stimulation may play a critical role in the clonal expansion and survival of MALT lymphoma cells. However, the surface receptors involved and the molecular mechanisms underlying the proliferation and survival of MALT lymphoma cells remain to be investigated. Also, TLR signalling activates the IKK complex that leads to activation of the NF-κB transcriptional factor, thus the effect of TLR6/2 on MALT lymphoma associated oncogenes mediated NF-κB activation was investigated. In addition, the potential cooperation

between MALT lymphoma associated oncogenes and immune receptor signalling such as those from TLR, B- and T-cell antigen receptors and CD40 was investigated. The possible molecular mechanisms underlying such cooperation were explored.

In view of the finding of enriched *TLR6* expression in translocation positive MALT lymphoma as described in chapter 4, cooperation between *TLR6* and MALT lymphoma associated oncogenes in NF- κ B activation *in vivo* was first investigated.

5.2 Aims of the study

- 1) To test the hypothesis that there is cooperation between BCL10, MALT1 and API2-MALT1 and TLR6 on NF- κ B activation;
- 2) To investigate whether there is a synergistic effect between expression of *MALT1*, *BCL10* and *API2-MALT1* and antigen receptor stimulation on NF- κ B activation;
- 3) To explore the effect of expression of *MALT1*, *BCL10* and *API2-MALT1* on key regulators of canonical NF- κ B activation pathway in B- and T- cell lines;
- 4) To determine BCL10 and MALT1 sub-cellular localisation and the effect of MALT1 on BCL10 sub-cellular localisation.

5.3 Experimental design

5.3.1 Cell lines

Murine BaF3 and WEHI cell lines were selected to investigate the effect of expression of *BCL10*, *MALT1* and *API2-MALT1* on NF- κ B with and without stimulation by LPS, anti-IgM and CD40L, as they are responsive to such stimulation. The BaF3 clone used was IL-3 independent. Jurkat human T-cell line was selected to investigate the effect of expression of *BCL10*, *MALT1* and *API2-MALT1* on NF- κ B with and without stimulation using anti-CD3 and anti-CD28. BJAB human B-cell line was used to investigate the effect of expression of *BCL10*, *MALT1* and *API2-MALT1* on their sub-cellular localisation. It was not possible to use the BJAB B-cell line for NF- κ B luciferase reporter assays as no increased activity has been observed in response to known NF- κ B activators such as LPS, anti-IgM and CD40L.

5.3.2 Investigation of the cooperation between *BCL10*, *MALT1* and *API2-MALT1* and *TLR6* on NF- κ B activation with and without LPS stimulation

BCL10, *MALT1* and *API2-MALT1* together with *TLR2* and *TLR6* or *TLR1* and *TLR6* expression constructs along with a control vector *pIRES* were transiently transfected into human Jurkat T cells, which are known to be non-responsive to LPS stimulation and thus are a good model to investigate LPS mediated NF- κ B activation. The transfected cells were seeded in multi-well plates, cultured for 18 hours and then treated with LPS or vehicle alone for 6 hours. Twenty four hours after transfection, the cells were harvested and measured for NF- κ B activity using a luciferase assay (Section 2.2.11.1). NF- κ B activities were measured in triplicate experiments and recorded as fold increase of the vector control.

5.3.3 Investigation of the effect of *BCL10*, *MALT1* and *API2-MALT1* expression and antigen receptor stimulation on NF- κ B activation

Murine B-cell lines BaF3, WEHI and Jurkat human T cells were transfected with *BCL10*, *MALT1* and *API2-MALT1* vectors and a control vector independently (Section 2.2.11.1). The transfected cells were seeded in multi-well plates, cultured for 18 hours. Prior to harvest for NF- κ B luciferase assay, BaF3 cells were stimulated for 6 hours with LPS, WEHI cells were stimulated for 6 hours with LPS, anti-IgM or CD40L and Jurkat cells were stimulated for 6 hours with anti-CD3 and anti-CD28. Each of these experiments was performed three times independently. NF- κ B activities were measured in triplicate experiments and recorded as fold increase of the vector control.

5.3.4 Investigation of the effect of MALT lymphoma associated oncogenes expression on canonical NF- κ B pathway activation

This was carried out using *BCL10*, *MALT1*, *API2-MALT1* and *BCL10/MALT1* double inducible BJAB cells and *BCL10* stably expressed BJAB cells. BJAB cells transfected with *pIRES vector* were used as control (Section 2.2.9.5).

The following proteins were investigated by Western blotting 3 NF- κ B negative regulators, I κ B α , I κ B β and I κ B ϵ ; 3 central molecules, IKK α , IKK β and NEMO; and 5 NF- κ B subunits including c-Rel, RelB, p65, p50/p105 and p52/p100. I κ B α and I κ B β are phosphorylated and degraded during activation of the classical NF- κ B pathway. p105 is cleaved into p50 and p100 is cleaved into p52 during activation of the canonical and non-canonical NF- κ B pathway respectively. β -actin was used as loading control. Western blotting results were quantified (Section 4.3.4) and ratio of each molecule over β -actin was calculated.

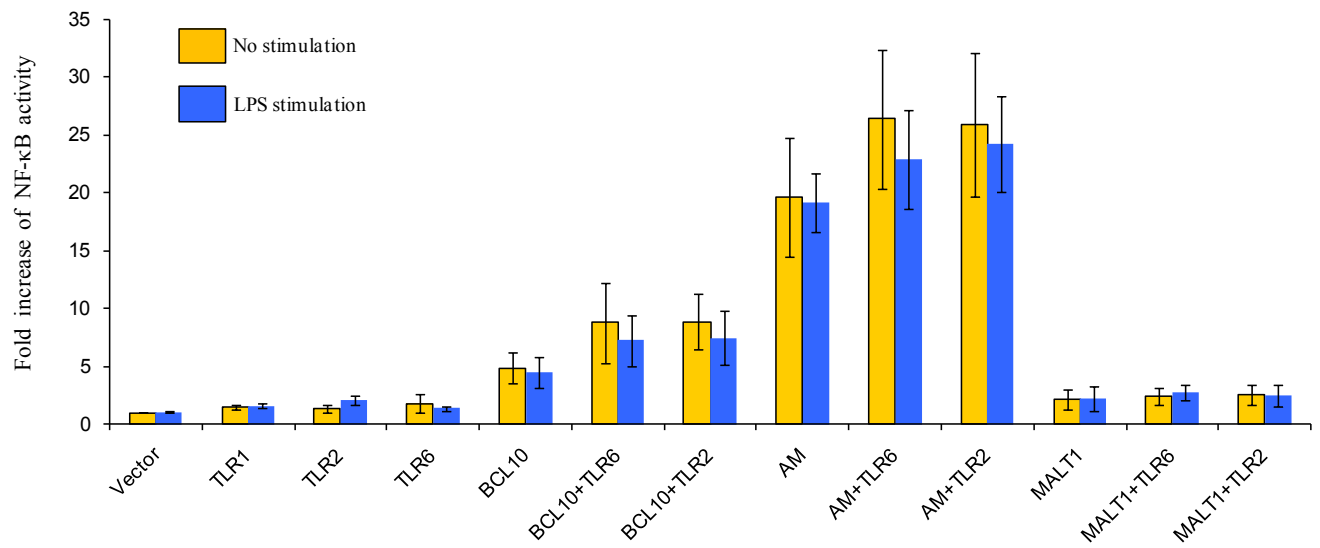
5.3.5 Investigation of the effect of BCL10 and MALT1 expression on their sub-cellular localisation

This was carried out using *BCL10*, *MALT1*, *API2-MALT1* and *BCL10/MALT1* double inducible BJAB cells and *BCL10* stably expressed BJAB cells. BJAB cells transfected with *pIRES vector* were used as control. The expression of each of the oncogenes mentioned above in the BJAB cells was investigated at 9, 16 and 24 hours following induction by the addition of doxycycline to the culture medium. Cell clots were prepared (section 2.2.9.3) and the expression of these oncogenes was investigated by immunocytochemistry using the BCL10 and C-MALT1 antibodies. In addition, co-immunoprecipitation was carried out on BCL10 and MALT1-expressing BJAB cells (section 2.2.10.8). Western blots were probed with BCL10 and MALT1 antibodies.

5.4 Results

5.4.1 TLR6 (in the presence of TLR2), enhances BCL10 and API2-MALT1 mediated NF- κ B activation in Jurkat T cells

A



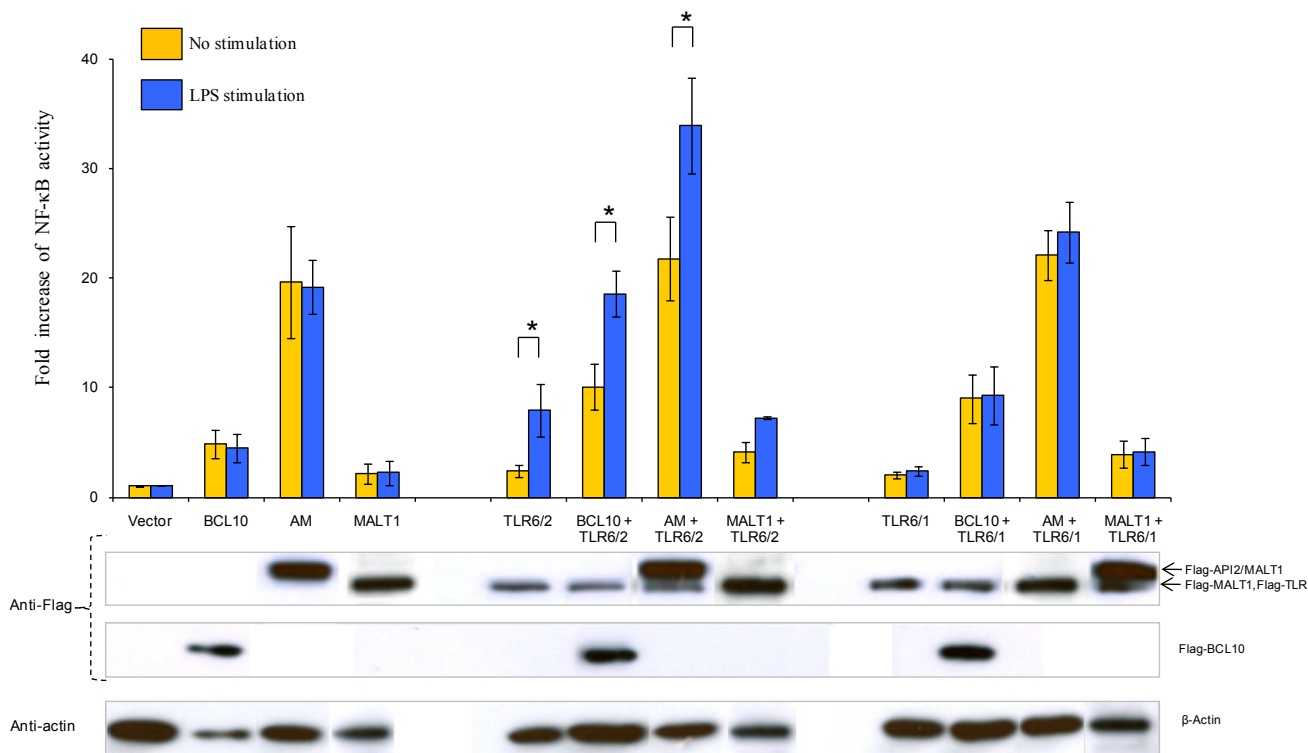
B

Figure 5.1 - TLR6 enhances BCL10 and API2-MALT1 mediated NF-κB activation, in the presence of TLR2 but not TLR1, in Jurkat T cells.

Jurkat T cells were co-transfected with vector (pIRESpuro2) or plasmids containing FLAG-tagged *BCL10*, *API2-MALT1* (AM), *MALT1*, *TLR6*, *TLR2* and *TLR1* as indicated, together with NF-κB luciferase reporter gene. (A) NF-κB luciferase reporter assay data for each oncogene alone and in combination with TLR6 or TLR2 with and without LPS stimulation.

(B) NF-κB luciferase reporter assay data for each NF oncogene alone and in combination with either TLR6/2 or TLR6/1 with and without LPS stimulation.

The transfected cells were seeded in multi-well plate, cultured for 18 hours and then treated with 10μg/ml LPS or vehicle alone for 6 hours. NF-κB activities were measured in triplicate experiments and recorded as fold increase of the vector control. Western blots in (B) show the appropriate expression of the various constructs. *P<0.01 by Student's t-test. Arrows show that *API2-MALT1*, *MALT1* and *TLRs* expression were detected using the anti-FLAG antibody with *MALT1* and *TLRs* having approximately 90 kDa (which is the expected molecular weight) and *API2-MALT1* have slightly higher molecular weight of approximately 125 kDa (which is the expected molecular weight).

Expression of *TLR1*, *TLR2*, *TLR6* alone was insufficient to induce NF-κB reporter activity (Figure 5.1 A). TLR6 alone and TLR2 alone, both failed to enhance BCL10 and API2-MALT1 mediated NF-κB activation in Jurkat cells even in the presence of LPS stimulation (Figure 5.1 A). However, the expression of both *TLR6* and *TLR2* significantly enhanced BCL10 (4.9 fold increase) and API2-MALT1 (19.6 fold increase), but not *MALT1*, mediated

NF- κ B activation, and this effect was much potent in the presence of LPS stimulation. Co-expression of *TLR6/2* and *BCL10* or *API2-MALT1* appeared to be synergistic in NF- κ B activation as shown by the reporter assay (Figure 5.1 B), with *API2-MALT1* showing the highest synergistic effect (Figure 5.1 B). In contrast, there was no co-operation between co-expression of *TLR6/1* and MALT lymphoma associated oncogenes. These results are consistent with the previous finding that TLR6 typically forms a heterodimer with TLR2 in response to stimulation by bacterial antigens (Shimizu *et al*, 2007; Takeuchi *et al*, 2001).

5.4.2 Cooperation of BCL10, MALT1, API2-MALT1 and immune receptor signalling in NF- κ B activation in B-cells

To further understand the potential co-operation between MALT lymphoma associated oncogenes and immunological stimulation in NF- κ B activation, NF- κ B reporter assays in B- and T- cell lines were performed in the presence of stimulation to TLR, antigen receptors and CD40.

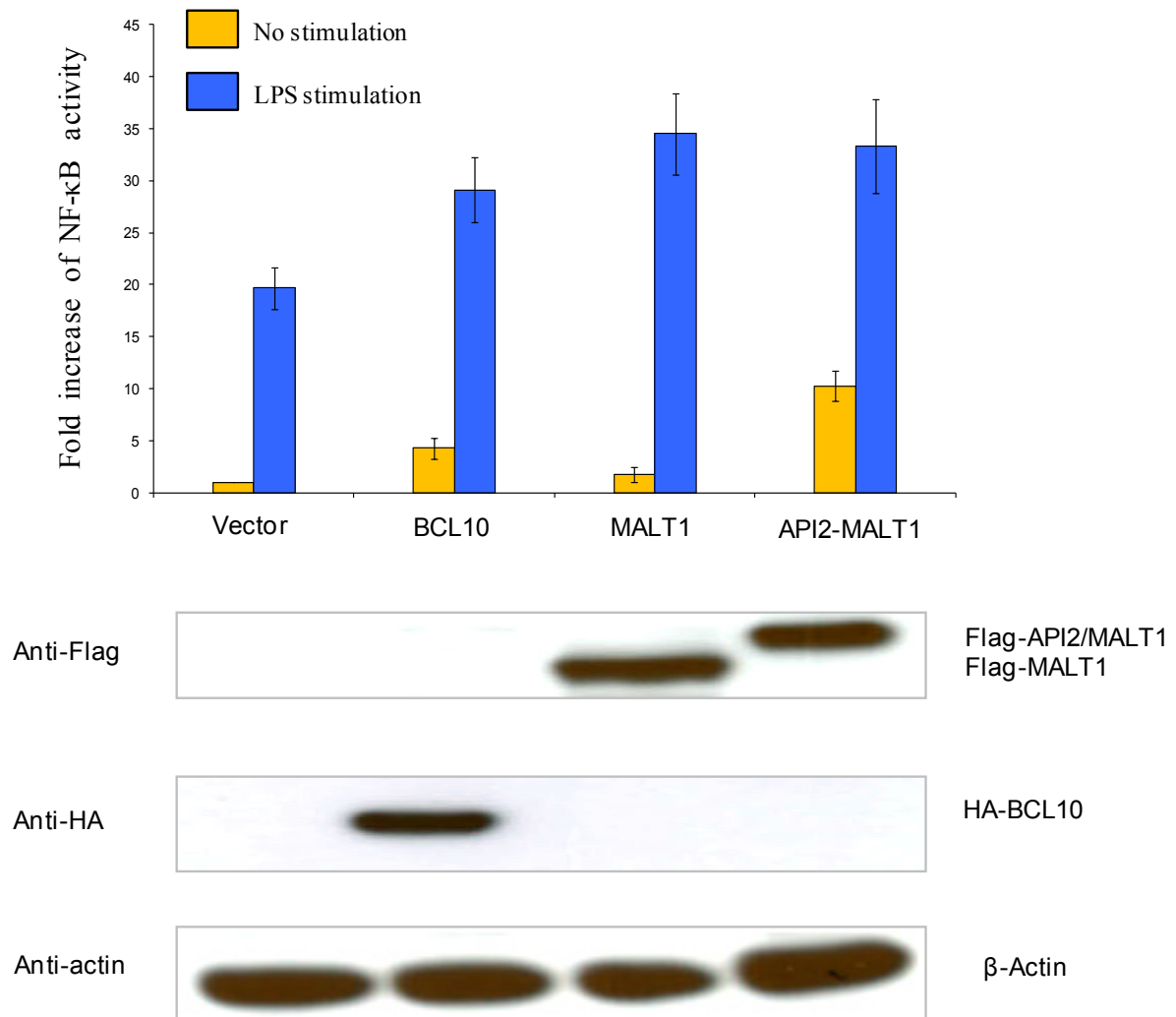


Figure 5.2. BCL10, MALT1 and API2-MALT1 mediated NF- κ B activation, with and without LPS stimulation in BaF3 murine B-cells.

BaF3 B-cells were co-transfected with vector (pIRESpuro2) or plasmids containing HA-tagged *BCL10*, FLAG-tagged *MALT1* and *API2-MALT1* (AM) as indicated, together with NF- κ B luciferase reporter gene. The transfected cells were seeded in multi-well plate, cultured for 18 hours and then treated with 10 μ g/ml LPS or vehicle alone for 6 hours. NF- κ B activities were measured in triplicate experiments and recorded as fold increase of the vector control. Western blot in the lower panel shows appropriate expression of the various constructs.

In BaF3 B-cells, expression of each of the three MALT lymphoma associated oncogenes yielded moderate increase of NF- κ B activity with API2-MALT1 showing the greatest NF- κ B activity in comparison with vector control (Figure 5.2). LPS stimulation of BaF3 B-cells transfected with the *pIRES* control vector produced a mean of 19.7s fold increase of NF- κ B activity over un-stimulated cells (Figure 5.2). The expression of the three oncogenes in BaF3 cells was comparable as shown in the Western blots (Figure 5.2). Thus, it can be concluded that the expression of each of the three oncogenes enhanced the LPS mediated activation of NF- κ B in BaF3 B-cells in a synergistic manner with fold increase of 29.1, 34.5, and 33.3 for BCL10, MALT1 and API2-MALT1 respectively (Figure 5.2). Similar results were also seen in WEHI cells (Figure 5.3).

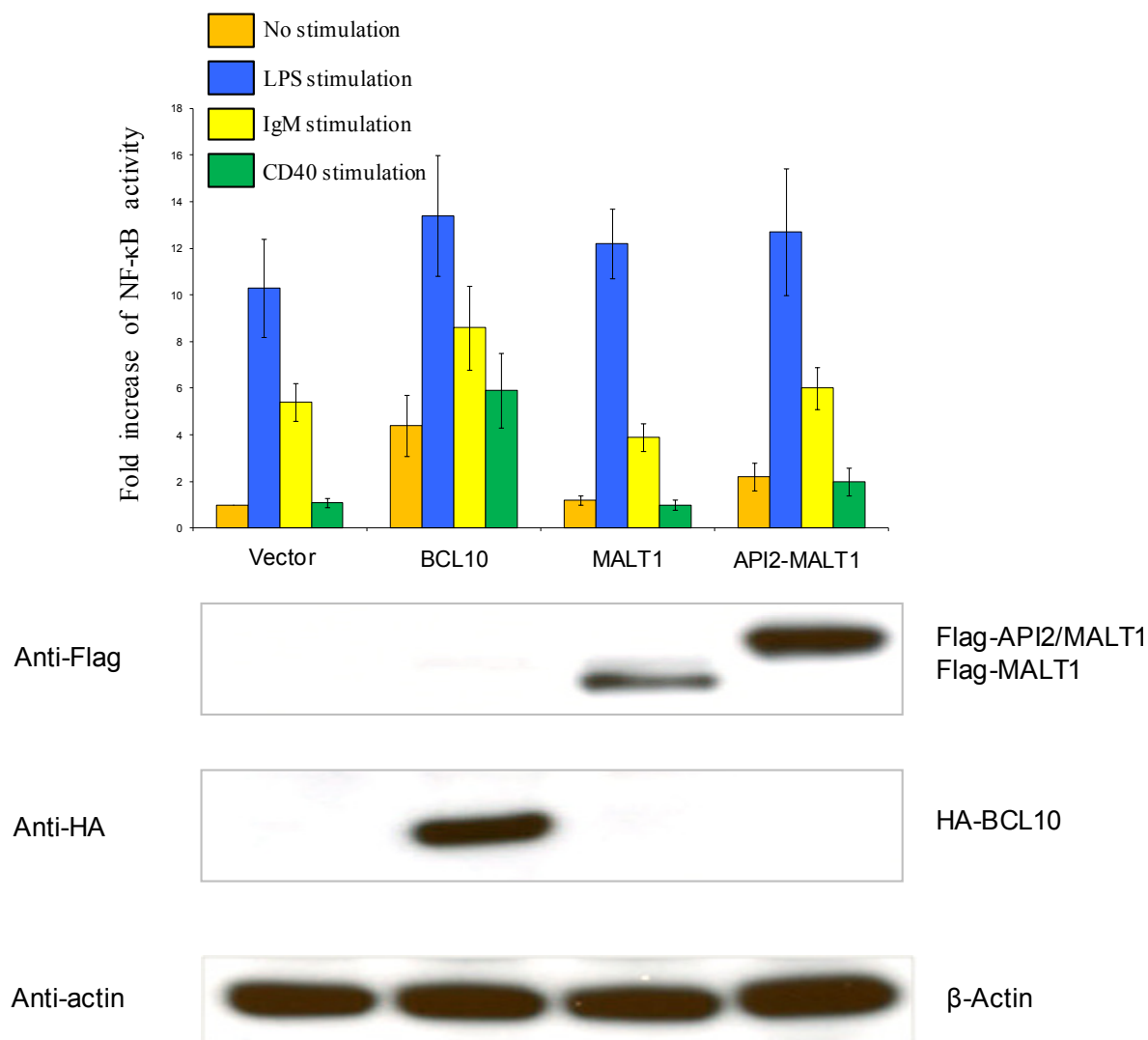


Figure 5.3 - BCL10, MALT1 and API2-MALT1 mediated NF-κB activation, with and without 6 hours of LPS, anti-IgM and CD40-L stimulation in WEHI murine B-cells.

WEHI B-cells were co-transfected with vector (pIRESpuro2) or plasmids containing HA-tagged *BCL10*, FLAG-tagged *MALT1* and *API2-MALT1* (AM) as indicated, together with NF-κB luciferase reporter gene. The transfected cells were seeded in multi-well plates, cultured for 18 hours and then treated with 10μg/ml LPS, 0.1μg/ml CD40 ligand (with 1μg/ml CD40 enhancer), 10μg/ml anti-IgM or vehicle alone for 6 hours where indicated. NF-κB activities were measured in triplicate experiments and recorded as fold increase of the vector control. Western blot in the lower panel shows appropriate expression of the various constructs.

The expression of the three oncogenes in WEHI cells was comparable as shown in the Western blots (Figure 5.3). However, unlike LPS stimulation, antigen receptor stimulation by anti-IgM showed variable co-operation with the expression of MALT lymphoma associated oncogenes in NF-κB activation in WEHI cells (Figure 5.3). *BCL10* expression slightly enhanced anti-IgM mediated NF-κB activation in an additive manner (Figure 5.3). However

both *MALT1* and *API2-MALT1* expression failed to enhance anti-IgM mediated NF- κ B activation. Similarly, stimulation using CD40L enhanced NF- κ B activation mediated by the expression of *BCL10* (but not *MALT1* or *API2-MALT1*) in an additive manner (Figure 5.3).

5.4.3 Cooperation between *BCL10*, *MALT1*, *API2-MALT1* immune receptor signalling on NF- κ B activation in Jurkat T cells

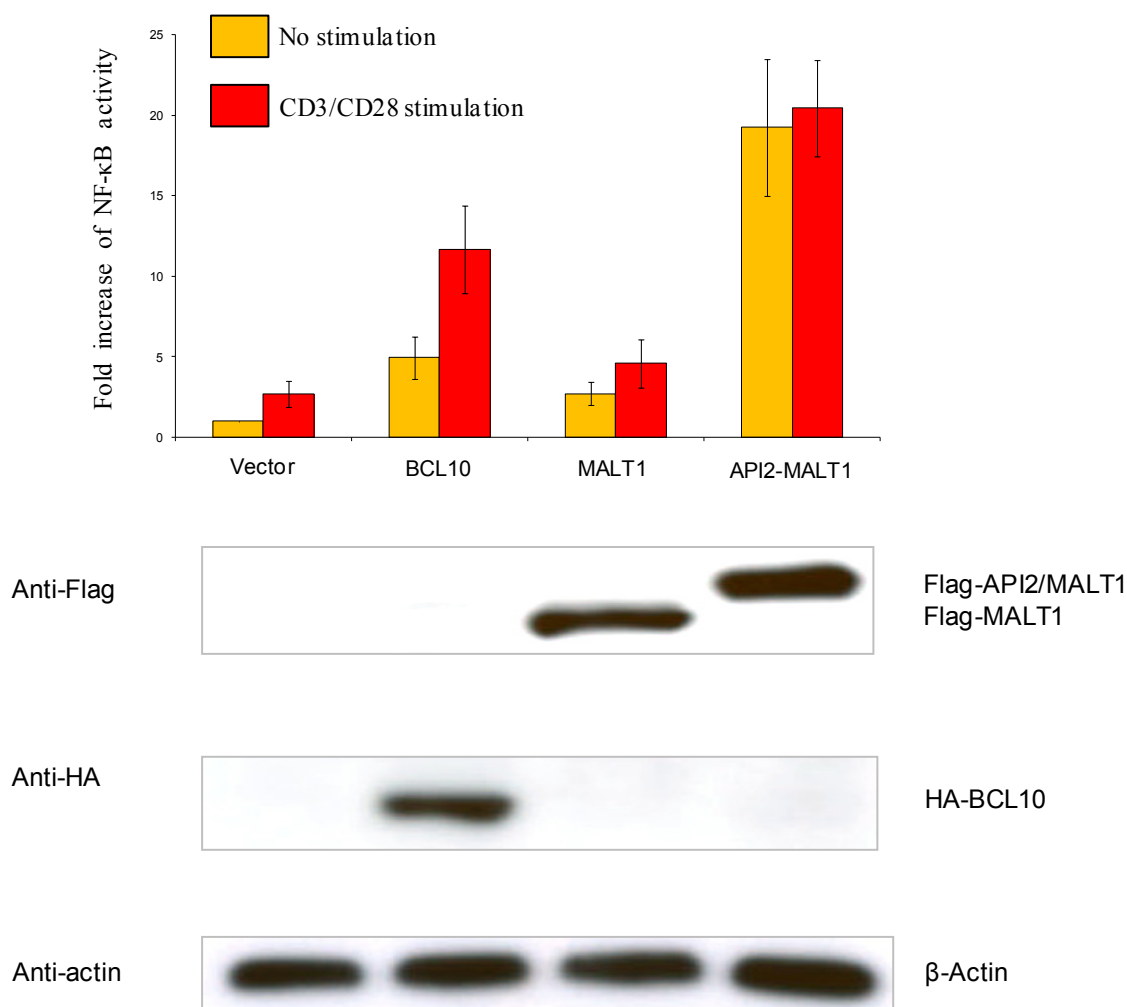


Figure 5.4 - *BCL10*, *MALT1* and *API2-MALT1* mediated NF- κ B activation, with and without 6 hours of CD3/CD28 stimulation in Jurkat T cells.

Jurkat T cells were co-transfected with vector (pIRESpuro2) or plasmids containing HA-tagged *BCL10*, FLAG-tagged *MALT1* and *API2-MALT1* (AM) as indicated, together with NF- κ B luciferase reporter gene. The transfected cells were seeded in multi-well plates, cultured for 18 hours and then treated with 1 μ g/ml anti-CD3 and 1 μ g/ml anti-CD28 or vehicle alone for 6 hours where indicated. NF- κ B activities were measured in triplicate experiments and recorded as fold increase of the vector control. Western blot in the lower panel shows appropriate expression of the various constructs.

The expression of the three oncogenes in Jurkat T cells was comparable as shown in the Western blots (Figure 5.4). Thus it can be concluded that the expression of *BCL10*, *MALT1* and *API2-MALT1* alone showed 5.0, 2.7 and 19.2 fold increase of NF- κ B activity respectively in Jurkat T cells (Figure 5.4). Co-stimulation of CD3 and CD28 produced a mean of 2.7 fold increase of NF- κ B activity over un-stimulated cells (Figure 5.4). In comparison with the control, CD3/CD28 co-stimulation clearly enhanced BCL10 but not MALT1 or API2-MALT1 mediated NF- κ B activation (Figure 5.4).

5.4.4 Investigation of the effect of BCL10 and MALT1 expression on their sub-cellular localisation

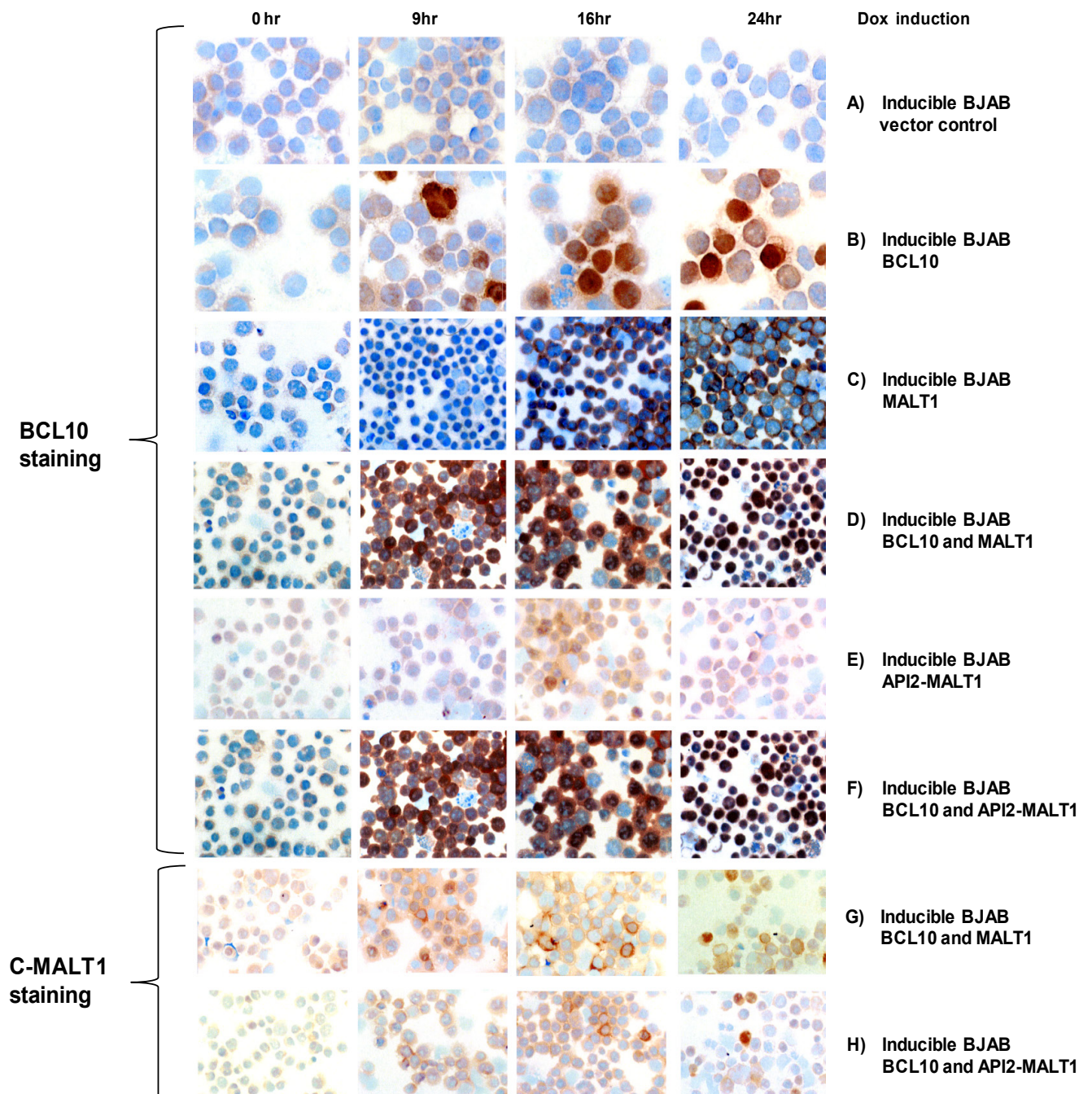


Figure 5.5 - Immunohistochemistry on cell clots expressing various MALT lymphoma associated oncogenes.

BJAB B-cell lines that express various inducible MALT lymphoma associated oncogenes were generated and used for investigation of their subcellular localisation. The expression of MALT lymphoma associated oncogenes were induced by doxycycline (Dox) and cells were harvested at 9, 16 and 24 hours followed by preparation of cell clots and immunocytochemistry with antibodies against BCL10 or C-terminal MALT1 where indicated. For each cell line, a control of cells without doxycycline treatment was used as reference.

BJAB cells transfected with vector only showed weak cytoplasmic BCL10 and MALT1 expression (Figure 5.5 A). In contrast, BJAB cells transfected with inducible BCL10 expression construct showed both strong nuclear and cytoplasmic expression in a proportion (10 - 15%) of cells after 9 hours induction by doxycycline, which increased to around 60% of cells at 24 hours induction (Figure 5.5 B). Interestingly, in BJAB with inducible MALT1 expression, immunostaining showed strong BCL10 in the cytoplasm, suggesting that MALT1 resulted in BCL10 accumulation and retainment in the cytoplasm (Figure 5.5 C). In BJAB cells with both BCL10 and MALT1 inducible expression, BCL10 was largely in the cytoplasm at 9 and 16 hours, but was predominantly in the nuclei at 24 hours after doxycycline induction (Figure 5.5 G and D). In contrast, co-expression of API2-MALT1 did not have any apparent effect on BCL10 sub-cellular localisation (Figure 5.5 E, F and H). Based on the co-localisation of BCL10 and MALT1 upon doxycycline induction, it can be hypothesised that these two molecules may interact. To investigate this further, co-immunoprecipitation investigating the interaction of BCL10 with MALT1 was carried out next.

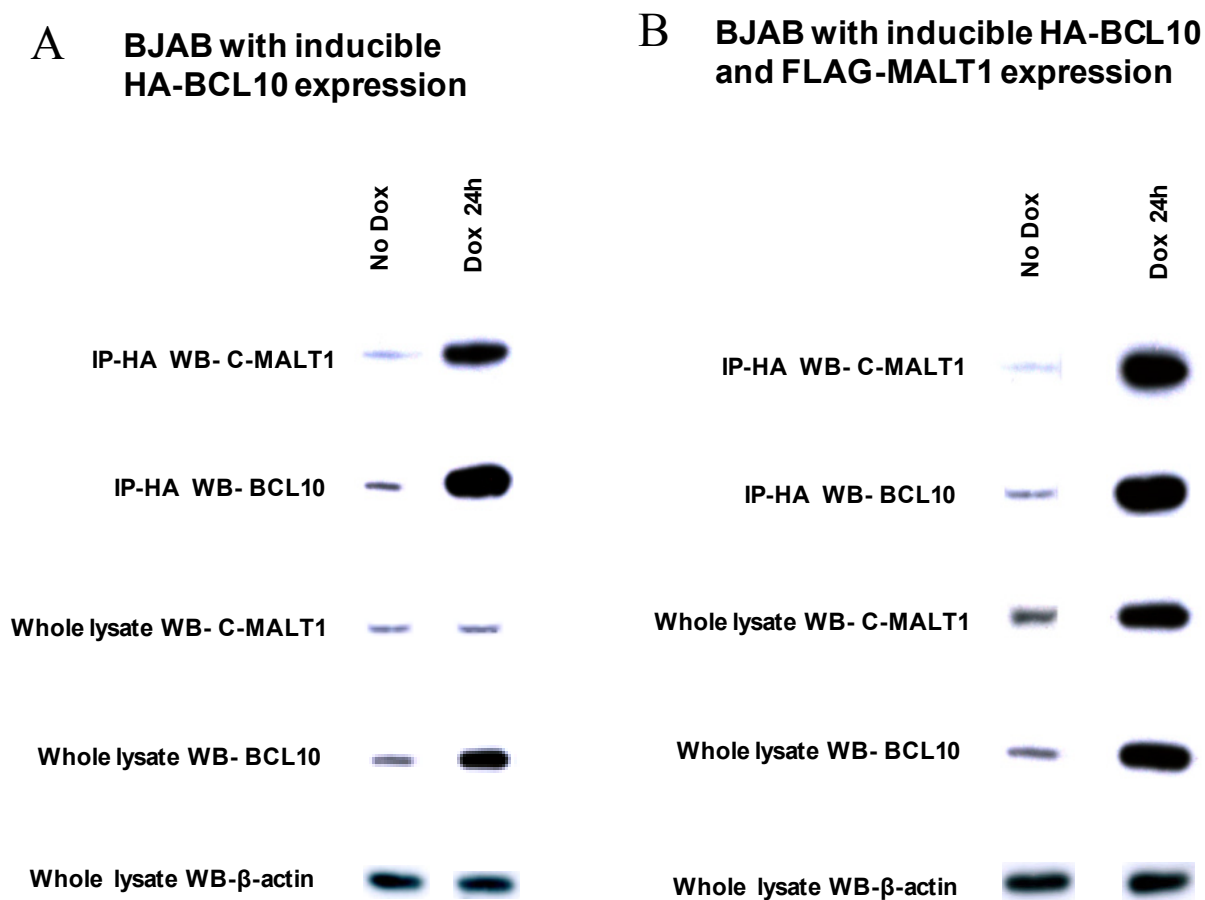


Figure 5.6 - Co-immunoprecipitation showing that expression of BCL10 leads to increased interaction with MALT1.

BJAB B-cells expressing inducible HA-tagged BCL10 or both HA-tagged BCL10 and FLAG-tagged MALT1 were treated with doxycycline (dox) for 24 hours. The protein extracts were subjected to co-immunoprecipitation with HA antibody. Both co-immunoprecipitated products and whole cell lysates were analysed by Western blotting with antibodies against BCL10 or C-MALT1 and β -actin where indicated.

It is known that BCL10 interacts with MALT1 and mediates MALT1 oligomerisation in response to upstream signalling. In line with this, co-immunoprecipitation experiments showed that BCL10 was capable of interacting with both endogenous and exogenous MALT1 (Figure 5.6 A and B). It is most likely that through such direct interaction, MALT1 affects the subcellular localization of BCL10 especially in the cytoplasm where over-expression of BCL10 leads to strong nuclear and cytoplasmic accumulation of BCL10 initially (Figure 5.5 B). In addition, subcellular localization data (Figure 5.5 D) and co-IP data (Figure 5.6 B)

showed more BCL10 in the presence of MALT1 indicating the possibility that increased MALT1-BCL10 interaction might lead to more BCL10 expression.

5.4.5 Effect of *BCL10*, *MALT1* and *API2-MALT1* expression on canonical NF- κ B pathway activation

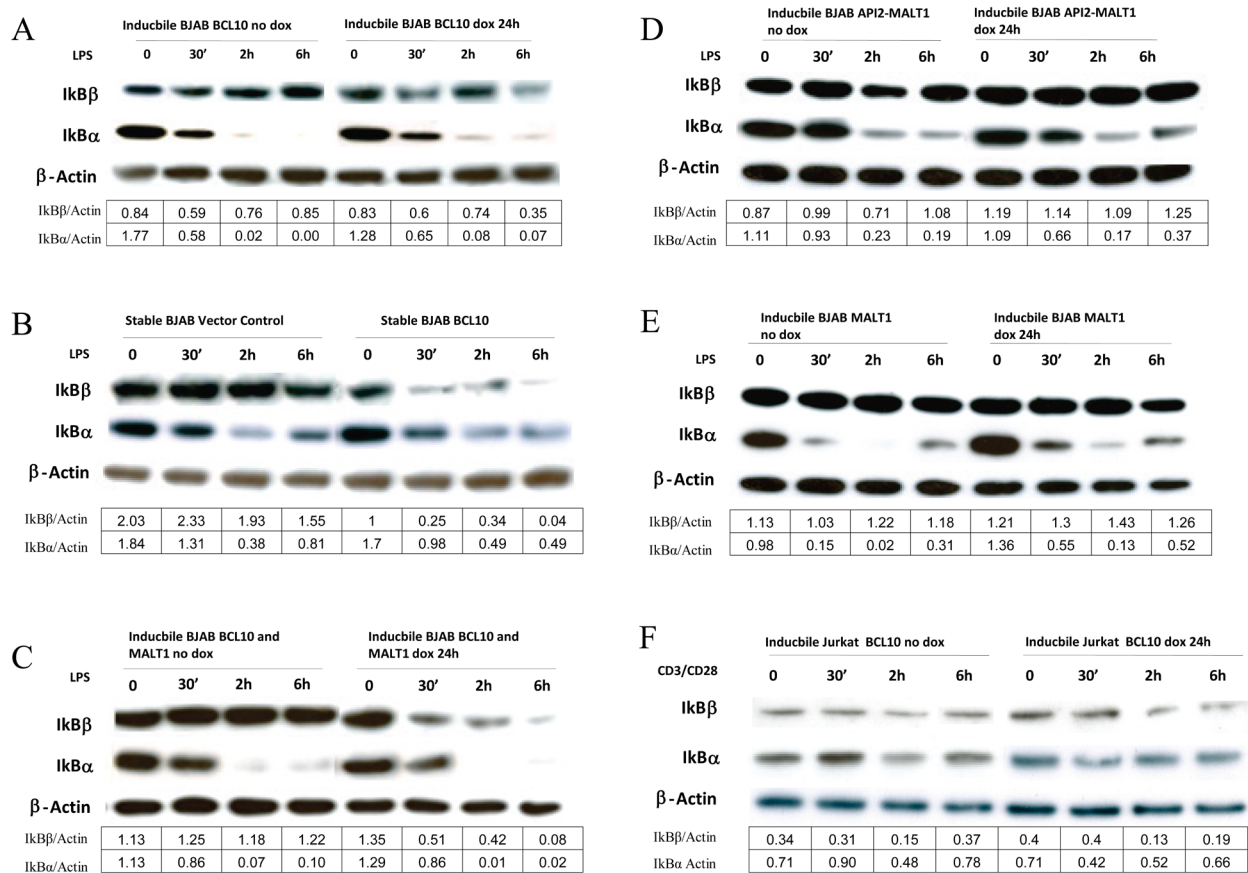


Figure 5.7 - Activation of canonical NF- κ B pathway by BCL10, MALT1 and API2-MALT1 and association of IκBβ degradation with BCL10 expression.

Various BJAB B-cells and Jurkat T cells expressing inducible BCL10, MALT1, API2-MALT1 were subjected to doxycycline (dox) treatment for 18 hours, followed by stimulation with 10 μ g/ml LPS for BJAB and 1 μ g/ml anti-CD3/anti-CD28 for Jurkat for 30 minutes, 2, 6 hours where indicated. Protein extracts from each experiment were subjected to Western blotting with IκB α and IκB β and β -actin as the loading control. The bands were quantified and the ratio of each over β -actin is calculated in the tables accompanying each figure.

The effect of over-expression of *BCL10*, *MALT1* and *API2-MALT1* on canonical NF- κ B pathway was investigated using various BJAB B-cells and Jurkat T-cell lines that inducibly

or stably expressed these proteins. As expected, LPS stimulation, induced prominent $\text{I}\kappa\text{B}\alpha$ degradation in both B- and T- cells (Figure 5.7 A-E). Very interestingly, expression of *BCL10* together with LPS stimulation, also caused $\text{I}\kappa\text{B}\beta$ degradation in BJAB B-cells (Figure 5.7 A-C). $\text{I}\kappa\text{B}\beta$ degradation was strongest with stable BJAB *BCL10* cell lines (Figure 5.7 B), possibly due to the fact that the inducible cell lines have the Tet element which may slightly affect the expression of the transgene.

However, neither LPS stimulation alone nor its combination with *MALT1* or *API2-MALT1* expression induced $\text{I}\kappa\text{B}\beta$ degradation (Figure 5.7 D and E). In Jurkat T cells, expression of *BCL10*, together with CD3/CD28 stimulation, also induced $\text{I}\kappa\text{B}\beta$ degradation (Figure 5.7 F). All other regulators of the canonical NF- κ B pathway including the NF- κ B negative regulators, $\text{I}\kappa\text{B}\epsilon$; 3 central molecules, $\text{IKK}\alpha$, $\text{IKK}\beta$ and NEMO; and 5 NF- κ B subunits including c-Rel, RelB, p65, p50/p105 and p52/p100 did not show any significant difference among the three MALT lymphoma associated oncogenes when they were over-expressed (data not shown).

Similar experiments were carried out with anti-IgM stimulation in BJAB cells but no $\text{I}\kappa\text{B}\beta$ degradation was seen in presence or absence of expression of the above MALT lymphoma associated oncogenes (data not shown).

Taken together, these results suggest that under these conditions, expression of *BCL10* may trigger the release of NF- κ B dimer inactivated by $\text{I}\kappa\text{B}\beta$. In this context, *BCL10* may play a more significant role than *MALT1* or *API2-MALT1*.

5.5 Discussion

In this chapter, the potential cooperation between MALT lymphoma associated oncogenes and immune receptors stimulation in NF- κ B activation was investigated and the common and distinct features of MALT lymphoma associated oncogenes in the activation of the canonical NF- κ B pathway were explored.

5.5.1 Cooperation between the expression of MALT lymphoma associated oncogenes and TLR stimulation

Reporter assay results in Jurkat T cells showed a synergy between MALT lymphoma associated oncogenes, in particular BCL10 and API2-MALT1, and TLR6/2 expression on NF- κ B activation upon LPS stimulation. Similarly, in BaF3 and WEHI B-cells, co-expression of TLR6/2 enhanced BCL10 and API2-MALT1 mediated NF- κ B activation in the presence of LPS stimulation.

Based on the results of *in vitro* assays and expression microarray data, it is pertinent to speculate that TLR signalling may play a role in the pathogenesis of translocation positive MALT lymphoma. This is further supported by the following observations: 1) *H. pylori* activates NF- κ B via both the classical and alternative pathway in B lymphocytes and this effect is dependent on LPS but not the Cag pathogenicity island (Ohmae *et al*, 2005); and 2) *H. pylori* associated LPS induced NF- κ B activation requires TLR2/TLR6 or TLR2/TLR1 complex but not those containing TLR4 (Yokota *et al*, 2007), which typically recognises LPS from other Gram-negative bacteria (Akira & Takeda, 2004).

5.5.2 Effect of antigen receptor stimulation on MALT lymphomagenesis

The three recurrent translocations identified in MALT lymphoma all induce lymphomagenesis through constitutive activation of the NF- κ B pathway (Zhou *et al*, 2005). Functional analysis presented here showed that expression of BCL10, MALT1 and API2-MALT1 alone was capable of activating NF- κ B in both B- and T- cells which are in line with the literature findings. In addition, the *in vitro* experiments showed that the expression of BCL10 enhanced the antigen receptor CD40 mediated NF- κ B activation in B-cells. This finding is important in the context of MALT lymphoma as the lymphoma cells express functional BCRs and remain responsive to antigen, at least in the earlier stages of the disease (Hussell *et al*, 1993b). For example, in an early study by Hussell *et al.*, gastric MALT lymphoma cells are stimulated to proliferate through CD40-CD40L interactions with T cells that recognise *H. pylori* antigens (Hussell *et al*, 1993b). If these gastric MALT lymphoma cells already over-express BCL10, API2-MALT1 or MALT1, then the activation of NF- κ B by CD40 stimulation will be most likely enhanced. In addition, the only case that responded to anti-idiotypic antibody stimulation and showed enhanced MALT lymphoma cell proliferation was a t(1;14) positive case (Hussell *et al*, 1993b) suggesting that a combination of high BCL10 protein expression and surface immune receptor stimulation may play an important role in MALT lymphoma development.

Recent study showed that CD40 signalling can enhance both API2-MALT1 and MALT1 mediated NF- κ B activation in B-cells *in vitro* (Ho *et al*, 2005), however the results in this thesis showed that out of the three MALT lymphoma oncogenes, only BCL10 over-expression moderately enhanced CD40 mediated NF- κ B activation. This discrepancy might be due to the fact that the study by Ho *et al.* used a different strain of the BJAB cell line to

the one used in this thesis which had high constitutive NF- κ B activity. Another possible explanation might be that the NF- κ B activation was assessed indirectly by measuring the degradation of I κ B α (which is transiently degraded) (Ho *et al*, 2005) rather than by measuring the level of NF- κ B transcriptional activity as done in the present study.

Taken together, it is tempting to speculate that the microbe mediated immune responses including help from T cells may also play a role in the pathogenesis of translocation positive MALT lymphoma. The potential involvement of TLR, CD40 and IgM signalling in translocation positive MALT lymphoma may explain the finding that rare cases of translocation positive gastric MALT lymphoma responded to *H. pylori* eradication (Liu *et al*, 2002b; Wundisch *et al*, 2005). The finding that API2-MALT1 and BCL10 mediated the strongest NF- κ B activity is interesting considering the fact that both are highly expressed in translocation positive MALT lymphoma cases. Thus, the constitutive NF- κ B activation seen in translocation positive MALT lymphoma may be, at least in part, due to preferential expression of the API2-MALT1 or BCL10 oncogenic products.

5.5.3 BCL10 expression associated with I κ B β degradation

All cell lines showed an intact I κ B α mechanism, however unlike *MALT1* and *API2-MALT1*, the expression of *BCL10* also induced I κ B β degradation in the presence of CD3/CD28 and LPS stimulation in both Jurkat T- and BJAB B-cells respectively. I κ B α and I κ B β interact with various NF- κ B/Rel dimers with similar affinity, but recent studies demonstrated that they have slightly different mechanisms and operate through distinct properties. I κ B α can shuttle NF- κ B/Rel complexes in and out of the nucleus, whereas I κ B β is more efficient at sequestering NF- κ B/Rel complexes in the cytoplasm. I κ B β causes cytoplasmic retention of NF- κ B due to the masking of two NLSs on the NF- κ B dimers. Interaction between the NF-

κ B/I κ B β complex and the small guanosine triphosphatases κ B-Ras-1, -2 also contributes to the NF- κ B activation. When binding to κ B-Ras, I κ B β cannot be phosphorylated by IKK, thus blocking the NF- κ B activation signal from IKK (Fenwick *et al*, 2000). The differential control between I κ B α and I κ B β may lead to biphasic activation of NF- κ B. I κ B α is promptly upregulated upon NF- κ B activation and thus controls the fast transient activation of NF- κ B, whereas I κ B β controls the persistent activation of NF- κ B (Ladner *et al*, 2003). It can be speculated that BCL10 may affect the regulation of this biphasic activation of NF- κ B, and thus lead to further NF- κ B activation and perhaps the expression of a different set of NF- κ B target genes.

5.5.4 BCL10 sub-cellular localisation and its relationship with MALT1 expression

The temporal interplay between API2-MALT1, MALT1 and BCL10 in cellular localisation *in vivo* showed that over-expression of BCL10 leads to the movement of excess BCL10 to the nucleus. This confirms the observation that tumour cells with t(1;14)(p22;q32)/*BCL10-IGH* show strong BCL10 nuclear expression (Liu *et al*, 2001b), but interestingly the results also showed that over-expression of *BCL10* led to the presence of BCL10 in both the cytoplasmic and nuclear compartments. Over-expression of *MALT1* resulted in strong homogeneous cytoplasmic localisation of both *BCL10* and *MALT1*. But over-expression of API2-MALT1 had no effect on BCL10 localisation probably because *MALT1* expression is reduced by half due to the API2-MALT1 fusion, hence the expected reduced efficiency of the nuclear export of BCL10. In cells with t(1;14)(p22;q32)/*BCL10-IGH*, *MALT1* endogenous expression may not be sufficient for the export of over-expressed *BCL10*, resulting in BCL10 nuclear retention. Finally, in cells with t(14;18)(q32;q21)/*IGH-MALT1*, the over expression of *MALT1* results in an increased retention of BCL10 in the cytoplasm, mimicking the

phenomenon seen in t(14;18) MALT lymphomas, where both proteins are thus strongly expressed in the cytoplasm (Ye *et al*, 2005). In addition, subcellular localization and co-IP data showed more BCL10 in the presence of MALT1 reflecting the possibility that increased MALT1-BCL10 interaction might lead to increase in BCL10 expression.

The phenomenon of nuclear BCL10 warrants further investigation, as it may have an unidentified role in the deregulation of NF- κ B or other cellular pathways that may be linked to MALT lymphomagenesis. Also, BCL10 does not contain NLS, so the mechanism by which it moves to the nucleus remains to be investigated. Co-immunoprecipitation results showed that over-expression of BCL10 protein was able to interact with both endogenous and exogenous MALT1.

Taken together, it can be suggested that MALT1 and BCL10 may play an important role in the generation of the CBM complex, facilitating the initial surface receptors' signal transduction to NF- κ B. Following stimulation of surface receptors such as LPS, IgM or CD40 in B- cells or CD3/CD28 in T- cells, over-expression of BCL10 also leads to the degradation of I κ B β , facilitating the activation of NF- κ B pathway. Thus, BCL10 probably plays a dual role in the NF- κ B pathway by transducing the signals from B- and T- cells to the NF- κ B subunits as well as facilitating NF- κ B activation partly via I κ B β degradation.

In addition to the mechanistic details of how MALT lymphoma associated oncogenes affects NF- κ B activation, the data also showed the heterogeneity of MALT lymphoma in that translocation positive MALT lymphoma has four recurrent translocations, each having different mechanisms of NF- κ B activation. Also, other translocation positive MALT lymphoma rearrangements were recently found such as t(1;14)(p22;q32)/CNN3-IGH, t(5;14)(q34;q32)/ODZ2-IGH and t(9;14)(p24;q32)/JMJD2C-IGH (Vinatzer *et al*, 2008) which so far do not seem to be directly affecting the NF- κ B pathway. Some of the

translocation negative MALT lymphomas have recently been shown to be associated with negative regulators of NF- κ B such as A20 deletion (Chanudet *et al*, 2010;Kato *et al*, 2009). Taken together, it can be concluded that at the molecular level, different molecules and pathways play a role in the pathogenesis of MALT lymphoma. Thus it would be useful to use the expression microarray data to identify putative phenotypic markers that are specifically highly expressed in both translocation positive and negative MALT lymphoma. This will aid in the diagnosis and prognosis of MALT lymphoma and may provide further insights into the molecular pathogenesis of MALT lymphoma.

CHAPTER 6 – Identification of MALT lymphoma specific phenotypic markers using gene expression microarray

6.1 Introduction

Currently, there is no MALT lymphoma specific phenotypic marker. The differential diagnosis of MALT lymphoma includes the reactive inflammatory processes that typically precede the lymphoma including *H. pylori* gastritis, lymphoepithelial sialadenitis, Hashimoto thyroiditis and other small B-cell lymphomas such as follicular lymphoma, mantle cell lymphoma and small lymphocytic lymphoma. Distinction from reactive processes is based mainly on the presence of destructive infiltrates of extra-follicular B cells, typically with the morphology of marginal zone cells (Wotherspoon *et al*, 1993). Immunophenotyping and molecular genetics analysis is used in borderline cases to assess B-cell clonality to help establish or exclude a diagnosis of MALT lymphoma, however molecular analysis may also demonstrate clonal B cells in some non-neoplastic MALT proliferations or persistent clonal population in gastric MALT lymphomas even after histologic complete remissions (Wundisch *et al*, 2003). Distinction from other small B-cell lymphomas is based on a combination of the characteristic morphologic and immunophenotypic features such as the presence of a diffuse infiltrate of CD20⁺, IgM⁺, IgD⁻ B cells beyond the reactive follicles outside the mantle zone. Once the marginal zone phenotype is established, light chain restriction in this marginal zone population or if present, within the plasma cells, would define the diagnosis. Thus, MALT lymphoma diagnosis is rather difficult as well as prone to errors (Pongpruttipan *et al*, 2007) and having a marker specific for MALT lymphoma would

lead to more accurate MALT lymphoma diagnosis and would help both haemtopathologists and non-haemtopathologists to make a correct diagnosis.

6.2 Aims of the study

- 1) To identify genes highly and specifically expressed in MALT lymphoma by comparing the gene expression microarray data of MALT lymphoma with those of FL, MCL, SMZL and CLL;
- 2) To validate the putative phenotypic markers identified by the gene expression microarray study in a large cohort of FFPE MALT lymphomas, FL, MCL and SMZL specimens using qRT-PCR and immunohistochemistry.

6.3 Experimental design

6.3.1 Case selection

A total of 77 cases from five different lymphoma subtypes with expression microarray data were included in this study. These were composed of 26 cases of MALT lymphomas (21 from stomach, 3 from lung, 1 from ocular adnexa and 1 from liver) with Affymetrix HG-U133A/B GeneChips; 7 cases of nodal FL; 8 cases of nodal MCL; 14 cases of SMZL and 22 cases of CLL with Affymetrix HG-U133plus2 GeneChip. The CLL expression microarrays were from a previous study carried out by Calin *et al.* (Calin *et al.*, 2008), while all the other expression microarray data were obtained as part of this study.

6.3.2 Identification of genes highly and specifically expressed in MALT lymphoma by gene expression microarray analysis

After normalisation using RMA, the MALT lymphoma, SMZL, CLL, FL and MCL gene expression microarrays were subjected to the following two different analyses: Firstly, One-way ANOVA with Bonferroni multiple testing correction using Genespring GX 7.3.1 and secondly, Bayesian statistics using in house programs written in R (version 2.8.0). Genes that had $p < 0.05$ were considered significant. Probes that were common in the two analyses were further filtered using SOM and Volcano plot and finally narrowed down using fold change calculation on the raw expression data as well as literature search of the genes preliminarily identified. Supervised clustering was carried out using Pearson correlation and average linkage as the similarity measure and clustering algorithm respectively within Genespring GX 7.3.1 (Figure 6.1).

6.3.3 Validation of genes highly expressed in MALT lymphoma by qRT-PCR and immunohistochemistry

The genes that were found to be specifically expressed in MALT lymphoma were validated by qRT-PCR and immunohistochemistry. mRNA expression was measured using qRT-PCR on a total of 79 cases of lymphoma including 44 MALT lymphomas (38 from stomach, 4 from lung, 1 from ocular adnexa and 1 from liver); 13 nodal FL; 11 nodal MCL and 11 SMZL. No CLL samples were available thus no CLL cases were included in the downstream validation. 18s rRNA was used as the housekeeping gene. RNA was extracted from microdissected tumour cells of FFPE tissue specimens of MALT lymphoma cases and qRT-PCR was carried out as described in Chapter 2. Where possible, primer pairs were designed to span exons to prevent any amplification of genomic DNA and to target up to 150bp (Table 3 in section 2.2.6), and were thus suitable for FFPE tissues. The results were presented as ΔC_t

values, so the higher the value, the lower the transcript expression, and *vice versa*. The Mann-Whitney U Test was used to determine whether there were statistically significant differences in the expression of a particular transcript between the various lymphoma groups. Immunohistochemistry using Lactoferrin antibody was carried on 5 gastric MALT lymphoma, 2 FL and 2 MCL specimens using 1:200 dilution of rabbit polyclonal antibody (product no. ab15811, Abcam) as based on the information given, seemed suited for immunohistochemistry on FFPE tissue.

6.4 Results

6.4.1 Identification of genes highly and specifically expressed in MALT lymphoma

The strategy used to combine HG-U133A&B microarray data of MALT lymphoma with HG-U133plus2 microarray data of FL, MCL, SMZL and CLL is summarised in Figure 6.1.

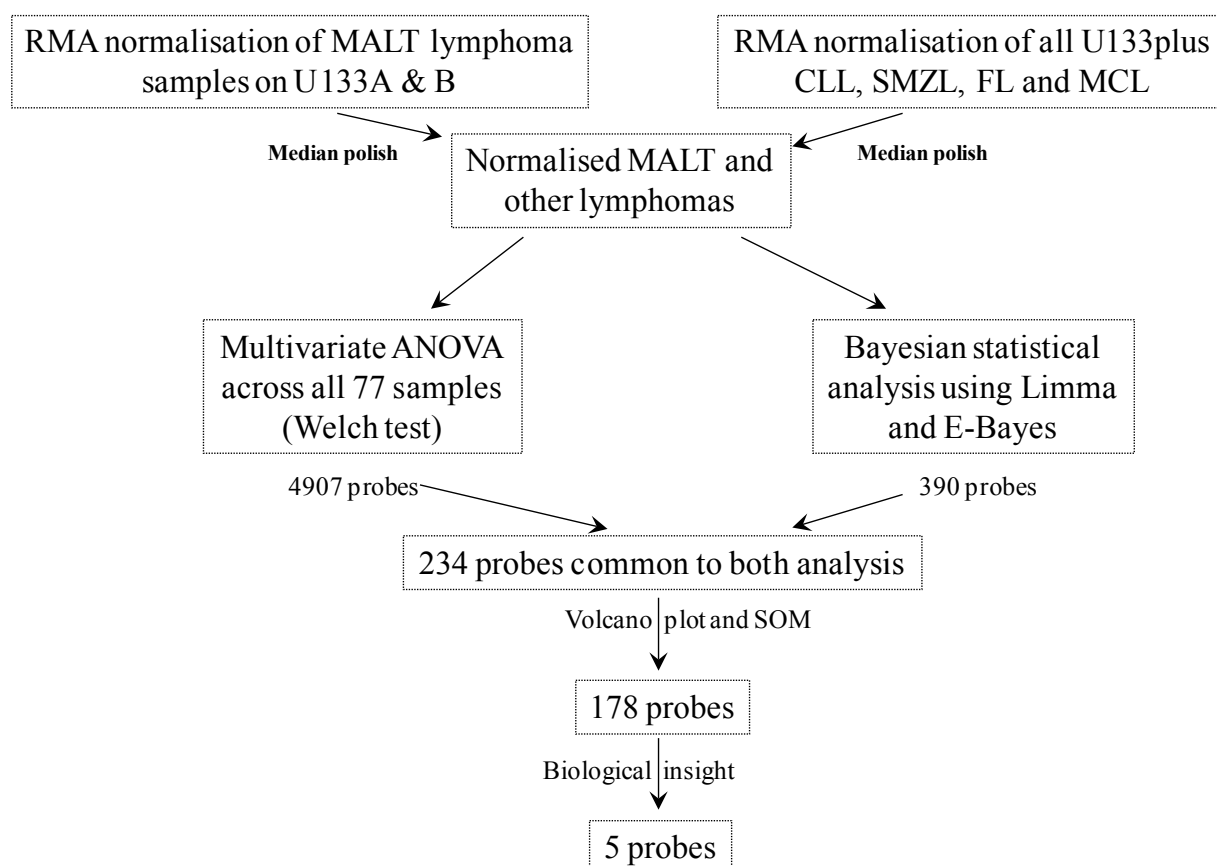


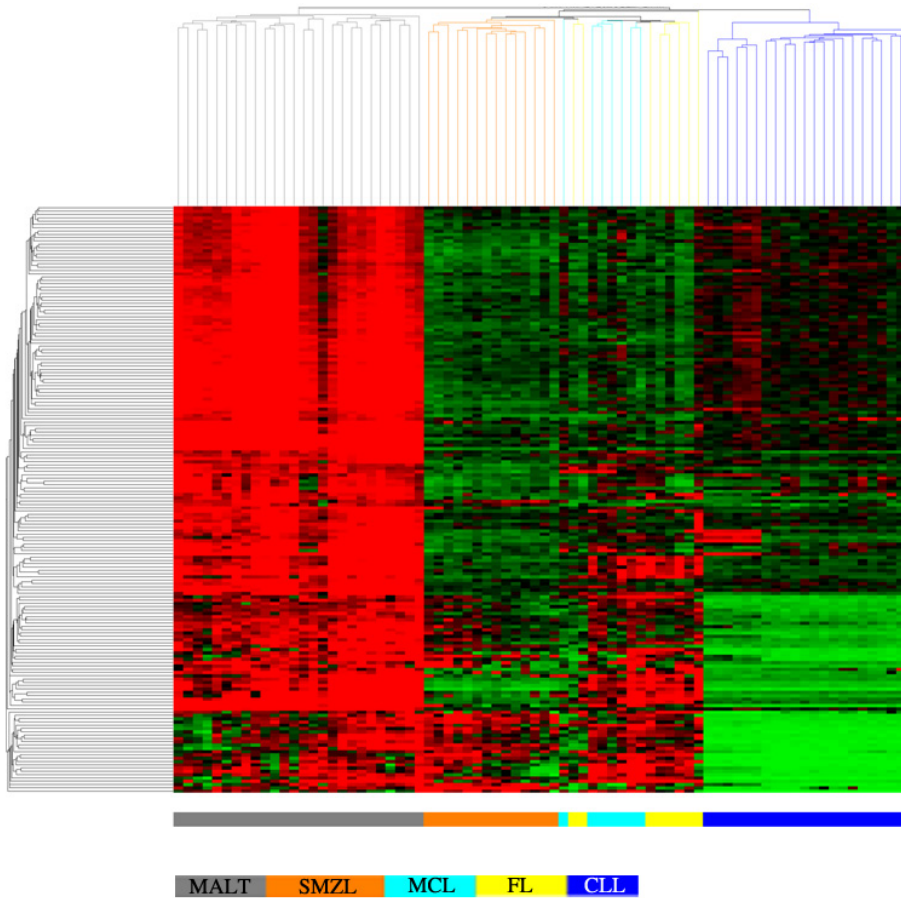
Figure 6.1 - Summary of bioinformatics strategy to combine MALT lymphoma, FL, MCL, SMZL and CLL microarray data and identify the genes highly and specifically expressed in MALT lymphoma.

Both the U133AB and U133plus2 sets were normalised using RMA and combined using median polish. The normalised set was then subjected to multivariate ANOVA and Bayesian statistics (using eBayes) analysis. Common probes from both analyses were reduced by subjecting them to self organising maps (SOM) and volcano plot analyses. The remaining probes were further reduced using biological knowledge and studies from the literature.

Multivariate ANOVA with Bonferroni's stringent multiple testing criterion yielded 4907 probes whereas Bayesian statistical analysis (which tends to shrink the data and eliminate non-variant probes using model fitting) gave rise to 390 probes. The common set between the two analyses was 234 probes. SOM and Volcano plot analysis further filtered the set to 178 probes. The 178 probes were ranked according to their fold change between MALT lymphoma and the other lymphomas. The top 20 probes were selected and known genes that are expressed in non-neoplastic cells were excluded.

Using this approach, 5 probes were selected; 2 probes mapped to *Dermatopontin*, one to *Decorin*, one to *Tetraspanin 8* and one to *Lactoferrin*. Fold change, minimum and maximum raw expression signals and coefficient of variation were calculated for the 5 probes across the 26 MALT lymphoma and the 51 other lymphoma cases separately (Table 6.1). The descriptive statistics showed that *Lactoferrin* had the lowest CV (67%) and the highest average (1027.05) in the MALT lymphoma group indicating that *Lactoferrin* is expressed uniformly at higher level in the MALT lymphoma group (Table 6.1). Plot of the raw expression microarray *Lactoferrin* data confirmed that it is most highly expressed in MALT lymphoma group compared to the other 3 genes (Figure 6.1). This in addition to the fact that a literature search showed Lactoferrin to inhibit the immunostimulatory effect on human B cells (Britigan *et al*, 2001) and might play a role in lymphocyte migration in lymphoid malignancy (de Sousa *et al*, 1978) making it the most likely phenotypic marker and was used for downstream validation.

A



B

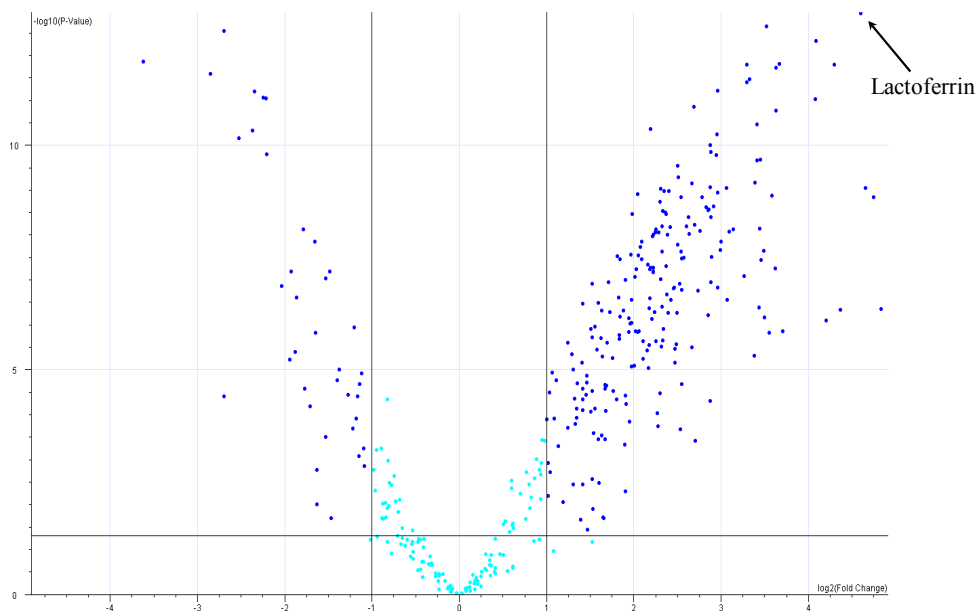


Figure 6.2 - (A) Supervised hierarchical clustering of MALT lymphoma, FL, MCL, SMZL and CLL (B) Volcano plot of MALT v other lymphomas with an arrow showing *Lactoferrin* position near the top.

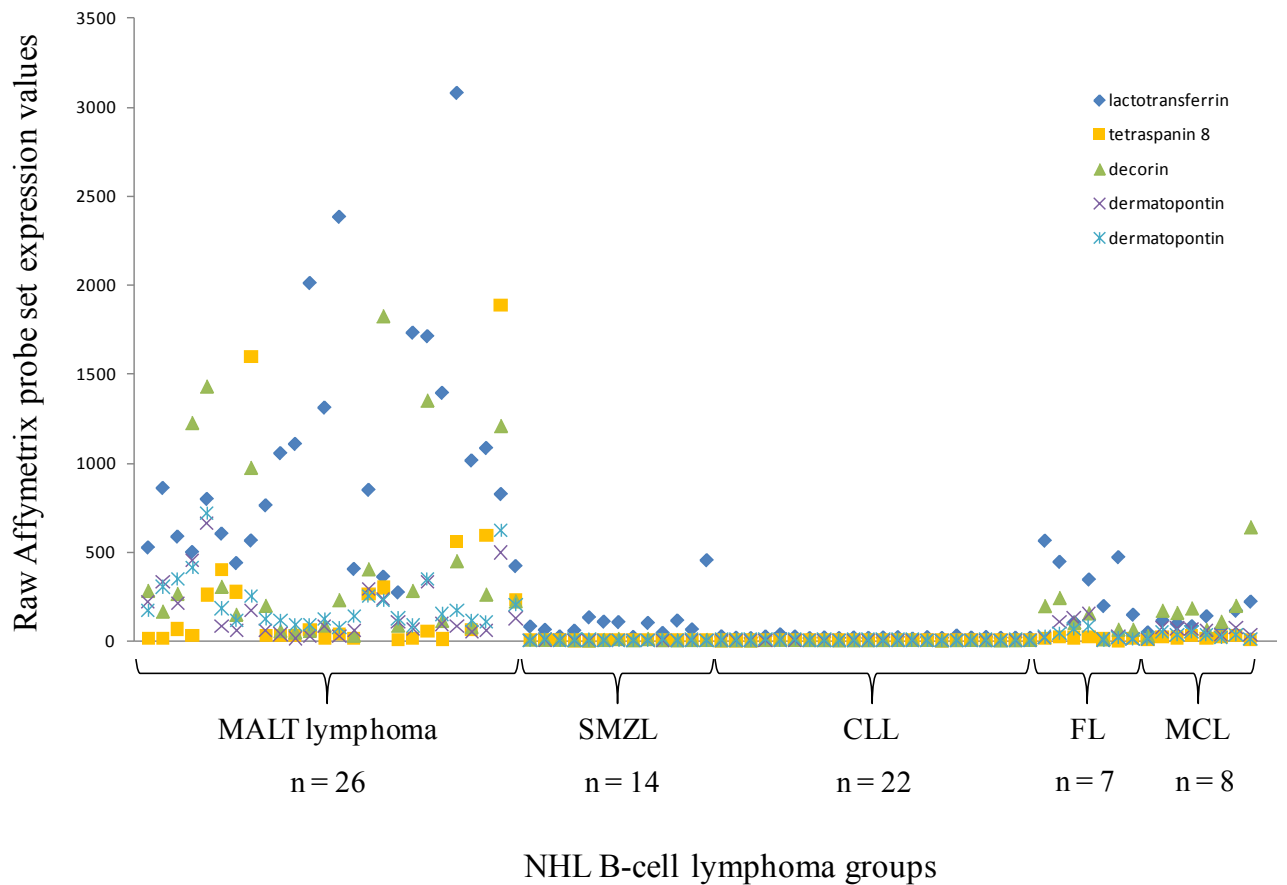


Figure 6.3 - Variation of the raw gene expression microarray data of *Lactoferrin* across the 5 lymphoma groups.

Five probes came in the final analysis two of them localised to the Dermatopontin gene. The groups used are; 26 MALT lymphomas, 14 SMZLs, 22 CLLs, 7 FLs and 8 MCLs.

Table 6.1 - Descriptive statistical properties of the 5 potential phenotypic marker probes calculated for MALT and other lymphomas separately.

| Probe Name | Gene Name | Fold Change | MALT Average | MALT SD | MALT CV | MALT Max | MALT Min | mphomas Avera | Lymphomas SD | Lymphomas CV |
|-------------|---------------|-------------|--------------|---------|---------|----------|----------|---------------|--------------|--------------|
| 202018_s_at | Lactoferrin | 9.61 | 1027.05 | 683.09 | 0.67 | 3081.00 | 274.80 | 106.92 | 133.93 | 1.25 |
| 203824_at | Tetraspanin 8 | 23.59 | 266.72 | 468.33 | 1.76 | 1887.00 | 10.85 | 11.30 | 7.02 | 0.62 |
| 211896_s_at | Decorin | 8.29 | 457.07 | 519.97 | 1.14 | 1829.00 | 34.28 | 55.13 | 105.75 | 1.92 |
| 213068_at | Dermatopontin | 7.66 | 173.85 | 167.19 | 0.96 | 666.10 | 17.90 | 22.70 | 34.23 | 1.51 |
| 213071_at | Dermatopontin | 13.00 | 220.28 | 161.25 | 0.73 | 718.10 | 77.23 | 16.94 | 17.33 | 1.02 |

6.4.2 Validation of *Lactoferrin* expression in MALT lymphoma

The expression of *Lactoferrin* in MALT lymphoma and other lymphoma subtypes was first compared using qRT-PCR on microdissected tumour cells from FFPE tissues. All the expression values of *Lactoferrin* in SMZL were negative, most likely due to tissue degradation and thus the SMZL data were not used in the analysis. *Lactoferrin* mRNA expression was the highest in the 44 MALT lymphomas group as compared to 11 MCL and 13 FL.

Although the range of *Lactoferrin* expression in MALT lymphoma was rather large, there was only small overlap between MALT lymphoma and FL or MCL. Not surprisingly, the Mann-Whitney U test showed a significant difference in the gene expression between MALT lymphoma and FL or MCL (Figure 6.4). Thus *Lactoferrin* could be a potential marker for MALT lymphoma.

To further validate this, immunohistochemistry was performed with Lactoferrin antibody (ab15811) on 5 gastric MALT lymphoma, 2 FL and 2 MCL. The preliminary immunohistochemical results showed high and scattered staining in MALT lymphoma compared to tonsils (Figure 6.5). The intensity and distribution of staining was similar between five cases of MALT lymphoma, FL and MCL (data not shown), probably because this anti-Lactoferrin antibody seem to detect inflammatory infiltrating tissue which can occur as a result of the lymphoma so it was a poor choice to use for this study. Thus, immunohistochemistry need to be repeated with perhaps a different anti-Lactoferrin antibody such as the polyclonal rabbit anti-human (product no. A0061, DakoCytomation, Cambridge, UK) or the monoclonal mouse anti-human (Clone 1A1, product no. H86024M, Meridian Life Science, Maine, USA) where both were successfully used on clear cell carcinomas FFPE tissue (Giuffre *et al*, 2007). Another antibody is the polyclonal rabbit anti-human anti-

Lactoferrin (product no. 07-685, Upstate (Millipore), Massachusetts, USA) which was successfully used on nasopharyngeal carcinoma tissue microarray (Zhou *et al*, 2008). However, it has also been shown that Lactoferrin binding in B-lymphocytes may increase during certain stages of cell maturation (Butler *et al*, 1990) and Lactoferrin is expressed in cells from the upper gastrointestinal tract (possibly related to mucosal defence mechanisms) but has low background staining (Mason & Taylor, 1978), thus immunostaining with either of the two antibodies mentioned above need to be interpreted with caution.

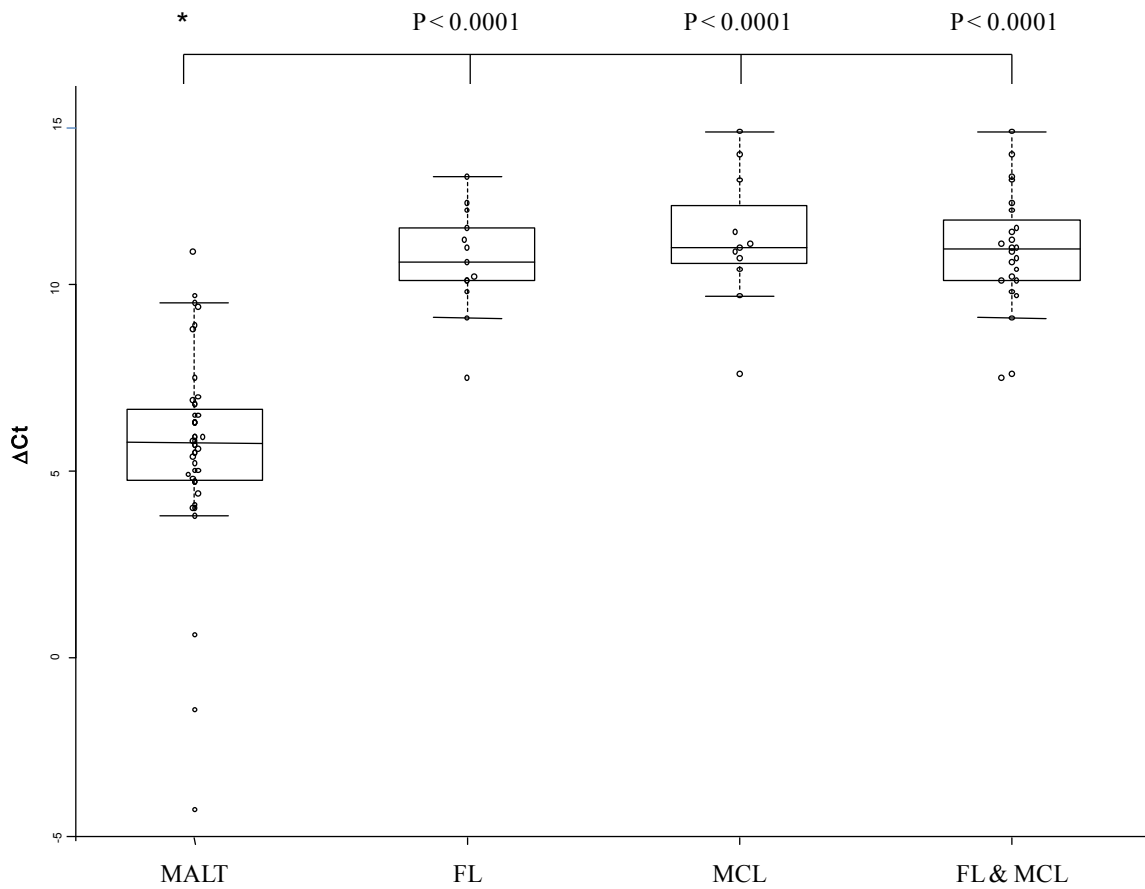


Figure 6.4 - Validation of *Lactoferrin* expression in 44 MALT, 13 FL and 11 MCL lymphomas by real-time quantitative RT-PCR.

This was performed in triplicate using RNA samples extracted from tumour cells microdissected from paraffin-embedded tissue sections. Asterisk indicates statistical significant differences between FL, MCL and combined FL with MCL and MALT lymphoma group by Mann-Whitney non-parametric statistical test. The medians are indicated by horizontal bars in the rectangular boxes. Error bars show the standard deviation of the results in each group. High values reflect low transcript expression and vice versa.

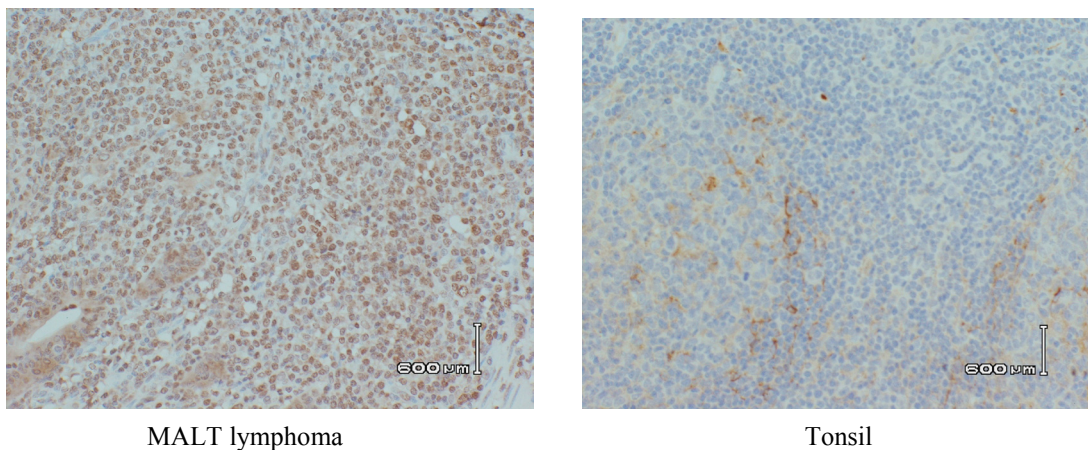


Figure 6.5 - Validation of *Lactoferrin* expression in MALT lymphomas by immunohistochemistry.

Summary of *Lactoferrin* immunohistochemistry showing high and scattered staining in MALT lymphoma compared to tonsils. The pattern of staining between MALT lymphoma, FL and MCL was similar.

6.5 Discussion

By analysis of gene expression profiles of MALT lymphoma, FL, MCL, SMZL and CLL, several genes including *Lactoferrin* were found to be highly expressed in MALT lymphoma whereas the other genes were not found to be highly expressed in MALT lymphoma (Figure 6.3). High expression of *Lactoferrin* in MALT lymphoma was also confirmed by qRT-PCR and awaiting further validation by immunohistochemistry.

Lactoferrin belongs to a family of iron-binding proteins that modulate iron metabolism, haematopoiesis and immunologic reactions. Lactoferrin is an iron binding glycoprotein with approximate weight of 78 kDa. It is present in secretory fluids of mammals and contained in secondary granules of neutrophils (Boxer *et al*, 1982) that defends against microbial pathogens in innate immunity. It has been shown to be bacteriostatic and bactericidal against various infectious agents including *H. pylori* (Ellison, III, 1994). The specific receptor for Lactoferrin has been reported on several cell types including mitogen-stimulated human peripheral blood lymphocytes (Maneva *et al*, 1983), macrophages (Maneva *et al*, 1983), platelets and epithelial cells of human mammary gland (Bennett *et al*, 1983). It is thought that receptor binding is the first step in cell functions related to Lactoferrin. For instance, interaction of Lactoferrin with cells of the immune system induces the release of cytokines (Van Snick & Masson, 1976) and can protect mice against a lethal dose of *E. coli* in experimental infection (Van Snick & Masson, 1976). Lactoferrin is also capable of promoting the proliferation of phytohaemagglutinin-stimulated human peripheral blood lymphocytes (Maneva *et al*, 1983), as well as both human B- and T- cell lines (Dagg & Levitt, 1981).

Unmethylated CpG dinucleotide motifs in bacterial DNA, as well as oligodeoxynucleotide (ODN) containing these motifs, are potent stimuli for many host immunological responses. Lactoferrin has been shown to inhibit CpG (ODN) stimulation of CD86 expression in the

human Ramos B-cell line leading to a decrease in the cellular uptake of ODN, a process required for CpG bioactivity (Britigan *et al*, 2001). Lactoferrin binding of CpG-containing ODN may serve to modulate and terminate host response to immunostimulatory molecules such as Heparin and LPS at mucosal surfaces and sites of bacterial infection (Britigan *et al*, 2001).

Lactoferrin has also been shown to play a role in the control of lymphoid cell migration (de Sousa *et al*, 1978) perhaps via the control of chemokines and cytokine release. Thus, Lactoferrin plays an important role in B-cell physiology.

Mounting evidence from the literature suggest that there is a link between increase in Lactoferrin expression and *H. pylori* infection and gastric inflammation. Microarray analysis of antral biopsies from patients with and without *H. pylori* infection showed *Lactoferrin* expression to be 4.2 folds higher in patients with *H. pylori* infection versus normal controls (Mannick *et al*, 2004). Microarray and qRT-PCR analysis showed *Lactoferrin* expression was upregulated in gastric biopsies with *H. pylori* infection with 19.4 fold change in *H. pylori* positive compared to negative biopsies by qRT-PCR (Wen *et al*, 2004). In a similar study, *Lactoferrin* expression had 14.6 and 16.8 fold induction in *H. pylori* positive compared to negative biopsies using microarray and qRT-PCR respectively (Wen *et al*, 2007). Molecular analysis of *H. pylori* associated gastric inflammation in chronically infected and immune mice, showed Lactoferrin to be expressed 38 fold higher in *H. pylori* infected mice compared to naïve animals (Rahn, 2003). In addition, a study by Zou et al showed that supplementation with Lactoferrin could be effective in increasing eradication rates of anti-*H. pylori* therapy, and could be helpful for patients with *H. pylori* eradication failure (Zou *et al*, 2009) and Hirata et al. showed that faecal Lactoferrin levels were elevated and this was found to be useful in the detection of colorectal diseases including MALT lymphoma (Hirata *et al*, 2007).

Analyses of B-cell malignancies comprising cells representing different maturational stages showed variable Lactoferrin expression (Butler *et al*, 1990). Acute lymphoblastic leukaemia (ALL) derived from progenitor B cells, and hairy cell leukaemia (HCL) derived from late activated memory B cells do not express surface Lactoferrin. In addition, EBV-transformed B-cell lines, representing activated B cells, were virtually negative for Lactoferrin. The same study showed that CLL had the highest percentage of surface Lactoferrin positivity (Butler *et al*, 1990). Microarray analysis in this thesis showed that mRNA expression of Lactoferrin in CLL is minimal. However the CLL microarray data were obtained from a study by Calin *et al*. (Calin *et al*, 2008) in public domain and no CLL tissue was available, thus it was not possible to confirm this finding by qRT-PCR as was the case with FL and MCL. If the qRT-PCR results confirm the microarray data, it can be hypothesised that perhaps the binding (but not the expression) of Lactoferrin to B lymphocytes might increase during certain stages of cell maturation. This might slightly reduce the use of Lactoferrin as a potential phenotypic marker for MALT lymphoma, however the diagnosis of MALT lymphoma is not usually confused with CLL/SLL, as the latter typically is CD5⁺ and CD23⁺. Furthermore, the disease usually manifests as CLL (rather than SLL) with an associated with lymphocytosis at presentation, a feature not associated with MALT lymphoma. Attempts of Lactoferrin immunohistochemistry with commercial antibody failed to yield any conclusive results and validation of Lactoferrin expression in MALT lymphoma remains to be investigated.

CHAPTER 7 – GENERAL DISCUSSION

7.1 MALT lymphoma is a distinct entity within the lymphomas but with heterogeneity between MALT lymphoma with and without chromosome translocation as indicated by gene expression profiling

Gene expression microarray results showed that MALT lymphoma is an entity distinct from other lymphoma subtypes, FL (thought to originate from germinal centre B cells) and MCL (thought to originate from the mantle zone B cells) (Kuppers, 2005). Significantly, MALT lymphomas expressed at high levels, many of the genes related to response to external biotic stimulus. On the other hand, in FL, immune response related genes were highly expressed, and in MCL, cell cycle related genes were highly expressed.

Unsupervised clustering between translocation positive and negative MALT lymphomas showed no clear separation between these cases indicating overlap in the molecular mechanism between the two groups. In all unsupervised clustering analyses, translocation negative MALT lymphomas with BCL10 nuclear staining tended to cluster with translocation positive cases suggesting that such cases at the molecular level resemble more to those with chromosome translocation.

7.2 Overview of the molecular mechanisms underlying the pathogenesis of MALT lymphoma

Although unsupervised clustering analyses showed considerable overlap in the gene expression profiles between MALT lymphomas with and without chromosome translocation, there was a significant difference in the expression of NF- κ B target genes between the two subgroups. Exhaustive and systematic GSEA of various molecular pathways and biological processes, showed that gene sets related to inflammation, immune responses, chemokine and

GPR signalling, were differentially over-represented between these different subgroups. Importantly, several of these molecular pathways or biological processes also lead to NF- κ B activation. These findings were also reinforced by independent analyses of differentially expressed genes between MALT lymphomas with and without translocation using hypergeometric tests. These observations provide several novel insights into the molecular mechanisms of both translocation-positive and negative MALT lymphomas which potentially explain their different clinical and histological presentations.

7.2.1 Aberrant molecular mechanisms of translocation positive MALT lymphoma

GSEA and leading edge analyses revealed a common core subset of genes that were overexpressed in translocation positive cases and a high proportion of them were NF- κ B target genes involving multiple related biological processes or molecular pathways.

Potentially critical immune receptors highly expressed in translocation positive MALT lymphoma were TLR6, CD40, CD83, CD1D and CD69 as shown by GSEA of gene expression microarray study in this thesis.

TLR6 typically forms heterodimers with TLR2 on the cell surface to recognize bacterial antigens (Gomariz *et al*, 2007). TLR2/TLR6 signalling activates not only the IKK complex that leads to activation of the NF- κ B transcriptional factor, but also the MAP kinase p38 and Jun amino-terminal kinase (JNK) that lead to activation of the AP-1 transcriptional factor (Akira & Takeda, 2004). Hence, over-expression of TLR6 in translocation-positive MALT lymphoma could potentially augment the NF- κ B activity mediated by MALT lymphoma associated oncogenic products and also activate the MAP kinase pathways. Data from this thesis in Baf3 B cells and Jurkat T cells showed that expression of TLR6, in the presence of

TLR2, enhanced both BCL10 and API2-MALT1 mediated NF- κ B activation. This effect was particularly significant upon LPS stimulation suggesting a potential biological cooperation between MALT lymphoma associated translocations and TLR signalling in lymphomagenesis. In addition, data from this thesis demonstrated that TLR6 with TLR2 enhanced API2-MALT1, BCL10 and MALT1 mediated AP-1 activation in BJAB B cells regardless of LPS stimulation.

The growth of gastric MALT lymphoma cells is critically dependent on their cognate interaction with *H. pylori* specific tumour infiltrating T cells, involving co-stimulatory molecules such as CD40/CD40L (D'Elis *et al*, 2003;Hussell *et al*, 1996). A recent study showed that CD40 signalling could enhance both API2-MALT1 and MALT1 mediated NF- κ B activation in B cells (Ho *et al*, 2005). In addition, previous studies have also indicated a role of B-cell receptor signalling in *H. pylori* induced MALT lymphomagenesis (Craig *et al*, 2010). In this thesis, the potential cooperation between expression of MALT lymphoma associated oncogenes and BCR and CD40 signalling were investigated. As expected, functional studies in WEHI B cells showed additive effect between CD40L stimulation and BCL10 in NF- κ B activation. GSEA of the expression microarray data demonstrated that the expression of co-stimulating molecules CD40 and CD83 was enriched in translocation positive MALT lymphoma, further supporting their role in lymphomagenesis. In line with this hypothesis, the GSEA also revealed up-regulation of CD1D in translocation positive MALT lymphoma, which is involved in the presentation of microbial lipid and lipopeptide antigens to T cells (Brigl & Brenner, 2004). Thus, it is tempting to speculate that the microbe mediated immune responses including T cells may also play a role in the pathogenesis of translocation positive MALT lymphoma. The potential involvement of TLR, CD40 and CD83 signalling in translocation positive MALT lymphoma may explain the finding that rare

cases of translocation positive gastric MALT lymphoma respond to *H. pylori* eradication (Liu *et al*, 2002b; Wundisch *et al*, 2005).

CD69 is an early cell activation antigen expressed on the surface of activated immune cells by small subset of T and B cells in peripheral lymphoid organs (Hara *et al*, 1986). Although the precise function of CD69 in B cells is largely unknown, it is a well-described activation marker in several cell types, and its expression is up-regulated in marginal zone B cells upon TLR stimulation (Rubtsov *et al*, 2008). CD69 is frequently expressed in low-grade B-cell lymphomas, and in FL, its expression is associated with poor treatment outcome (de Jong *et al*, 2009; Erlanson *et al*, 1998). Also, it has been shown that CD69 functions downstream of IFN α and IFN β , and possibly other activating stimuli, to promote lymphocyte retention in lymphoid organs (Shiow *et al*, 2006). The finding here of enriched expression of CD69 in translocation-positive MALT lymphoma further implicates its role in lymphomagenesis.

Among the genes up-regulated in translocation positive cases, IRF4 showed a significant increase in cases with t(1;14) chromosomal translocation. IRF4 encodes a transcriptional factor and is expressed in activated B cells and cells showing plasma cell differentiation (Pernis, 2002). It is required during an immune response for lymphocyte activation and the generation of immunoglobulin-secreting plasma cells. In line with its known expression pattern, IRF4 is highly expressed in the plasma cell component of MALT lymphoma. Furthermore, plasma cell differentiation of neoplastic B cells is most prominent in MALT lymphoma with t(1;14) translocation. IRF4 is transcriptionally activated by t(6;14)(p25;q32) in multiple myeloma where gene expression profiling and genome wide chromatin immunoprecipitation analysis uncovered an extensive network of IRF4 target genes and showed that although IRF4 is not genetically altered in most myelomas, they are nonetheless

addicted to an aberrant IRF4 regulatory network that fuses the gene expression programmes of normal plasma cells and activated B cells (Shaffer *et al*, 2008). Strong IRF4 expression has also been found in several lymphoma subtypes including lymphoplasmacytic lymphoma, 75% of diffuse large B-cell lymphoma and primary effusion lymphoma, which are not associated with t(6;14) (Falini & Mason, 2002). IRF4 is one of the molecules found in the ABC-DLBCL signature (Alizadeh *et al*, 2000). The oncogenic activity of IRF4 is thought to be related to its transcriptional repression of IFN-inducible genes, and thus the suppression of the anti-proliferative effects of IFN (Hrdlickova *et al*, 2001; Pernis, 2002). NF κ B transactivates IFN, and IFN α and IFN β were moderately up-regulated in t(11;18) or t(1;14) positive MALT lymphoma. A simultaneous up-regulation of IRF4 may block the side-effects of NF- κ B on IFN activation.

In addition to immune receptors discussed above, several potentially critical chemokine receptors were highly expressed in translocation positive MALT lymphoma and they included CCR2, CXCR4, CCR5 and CCR7 as shown by GSEA of gene expression microarray study in this thesis.

Several homeostatic chemokines have been shown to play an important role in mucosal immunology including germinal centre formation, homing and trafficking of activated mucosal B cells. Germinal centre formation involves the trafficking and positioning of lymphocytes in the organized lymphoid tissue (Moser & Loetscher, 2001) and homing mechanisms play a role in B-cell recruitment to the secondary lymphoid tissue. CCR7 expression is up-regulated in activated B cells allowing them to acquire the capacity to migrate into the T-cell zone and to follicles in Peyer's patches, where the CCR7 ligands, CCL19 and CCL21 are highly expressed (Okada *et al*, 2002; Reif *et al*, 2002). CCR7 is shown

to play a central role in regulation of normal mucosal lymphocyte re-circulation and homeostasis, particularly in the stomach (Hopken *et al*, 2007). CXCR4 is expressed in B cells at multiple stages of their development. It is required for retention of B-cell precursors in the bone marrow. CXCR4-deficient B-cell precursors that migrated prematurely became localised in splenic follicles despite their unresponsiveness to CXCL13. CXCR4 is also critical for B-cell homing to the Peyer's patches and splenic marginal zone (Nie *et al*, 2004). In both low grade B-cell NHL and classic Hodgkin lymphomas, CCR7 and CXCR4 over-expression were associated with a wide lymph node spread, supporting their role in lymphoma pathogenesis (Lopez-Giral *et al*, 2004; Hopken *et al*, 2002; Trentin *et al*, 2004).

B cells express CCR5 on their cell surfaces, and RANTES, one of four chemokine ligands of CCR5, is mitogenic for B cells (Rabkin *et al*, 1999). Thus, it is tempting to speculate that RANTES and hence CCR5 may play a role in lymphoma expansion by avoiding immune surveillance.

CCR2 (CC chemokine receptor 2) is a receptor for MCP-1 which attracts monocytes and T cells to sites of injury as part of the inflammatory response. Two isoforms of CCR2, namely CCR2A and CCR2B have been cloned (Charo *et al*, 1994; Charo, 1999). It has been suggested that these two isoforms of the receptor might be splice variants of a single gene (Charo *et al*, 1994). CCR2B is the major form of the receptor readily detected in monocytes, whereas CCR2A is less abundant (Charo, 1999). The physiological role of CCR2A is not fully understood (Charo, 1999). Data in this thesis has shown that CCR2A and CCR2B were differentially expressed between translocation positive and negative MALT lymphoma cases with greater variability in CCR2A expression. Flaishon *et al*. described a novel role for CCR2 and its ligand CCL2/JE in inhibiting the chemotactic response of immature B cells to the chemokine CXCL12/stromal cell-derived factor 1 (SDF-1), suggesting that CCR2 and its

ligand act as negative regulators of the homing of immature B cells (Flaishon *et al*, 2004). They also showed that CCR2 is transcribed in immature B cells, while its mRNA is dramatically down regulated at the mature B cells stage. CCR2-deficient mice showed massive accumulation of immature B cells in the lymph nodes in comparison with wild type mice (Flaishon *et al*, 2004). Beside its expression in immature B cells, CCR2 is found to be expressed in mature B-cell neoplasms such as marginal zone B-cell lymphoma (Trentin *et al*, 2004). It has been shown that CCR2 is up-regulated in response to the formation of superoxide free radical molecules and that IL-2 induced the expression of CCR2 in T lymphocytes, which correlated with the response of these cells to MCP-1 in chemotaxis assays (Loetscher *et al*, 1996). Also, IL-10 selectively up-regulated the expression of CCR2 in monocytes by prolonging the mRNA half-life (Sozzani *et al*, 1998). More recently, CCR2 was shown to mediate hematopoietic stem and progenitor cell trafficking to sites of inflammation (Si *et al*, 2010). However, it is still unclear how the up-regulation of CCR2 expression contributes to MALT lymphoma development or whether it is induced by the presence of oxygen free radicals which would occur during *H. pylori* mediated inflammatory responses. It may be that infection with *H. pylori* leads to chronic inflammation which may later cause the B cells to initiate the expression of CCR2 amongst other chemokines leading to their trafficking to inflammation sites. Once the inflammation subsides, CCR2 expression becomes reduced, however some of the cells within the inflammatory site may acquire an oncogenic event such as t(11;18)/API2-MALT1 leading to the constant expression of CCR2 via aberrant NF- κ B and MAPK pathways activation. Over-expression of CCR2A and B, CCR5 and CXCR4 has been shown to activate NF- κ B, Jak/STAT and MAPK pathways (Okada *et al*, 2002). This, together with the TCR, BCR and CD40 signalling may form a

positive feedback autoregulatory loop in API2-MALT1 or BCL10 mediated NF- κ B activation, thus leading to constitutive NF- κ B activation.

7.2.2 Aberrant molecular mechanisms of translocation negative MALT lymphoma

In contrast to translocation-positive MALT lymphoma, translocation-negative cases were characterised by expression of a strong inflammatory gene signature. GSEA and leading edge analysis also revealed common core subset genes involving several related biological processes or molecular pathways, which were enriched in translocation-negative MALT lymphoma. The top examples included proinflammatory cytokines IL8 and IL1 β , molecules involved in B- and T- cell interaction such as CD86, CD28 and ICOS, several chemokine and chemokine receptors, NR4A3 (also known as MINOR) and TLR2 (Figure 3.10).

IL8 and IL1 β are the hallmark of a proinflammatory cytokine profile in response to *H. pylori* infection. IL8 is critical for neutrophil infiltration and activation, while IL1 β induces gastrin release, inhibits acid secretion and promotes apoptosis of epithelial cells (McNamara & El Omar, 2008). The finding of over-expression of these proinflammatory cytokines in translocation-negative gastric MALT lymphomas, indicates the presence of active *H. pylori* infection. In keeping with this, translocation-negative gastric MALT lymphomas show a higher number of blast cells than translocation-positive cases (Okabe *et al*, 2003). In addition, a number of chemokines and chemokine receptors was highly expressed in the translocation-negative cases. This may reflect the trafficking and retention of various immune cells in response to an active *H. pylori* infection.

Most importantly, GSEA showed up-regulated expression of the surface molecules involved in B- and T- cell interaction namely CD86, CD28 and ICOS in translocation-negative gastric

MALT lymphoma. Although residual reactive follicles may be present and contribute to the high CD86, CD28 and ICOS expression in translocation negative cases, the germinal centre markers CD10 and BCL6 were expressed in much lower levels in MALT lymphoma (Figure 3.3). More importantly, over-expression of CD86 in tumour cells was clearly demonstrated by qRT-PCR on microdissected samples and immunohistochemistry. In line with these findings, a previous study showed significantly higher CD86 expression in gastric MALT lymphomas that responded to *H. pylori* eradication than those resistant to the therapy (66% VS 10%) (de Jong *et al*, 2001). Although the chromosome translocation status in these cases is not available, it is most likely that the cases responded to *H. pylori* were translocation-negative (Liu *et al*, 2002b). Taken together, these findings suggest that there is an active immune response to *H. pylori* infection in translocation-negative gastric MALT lymphoma, and this most likely underscores the tumour cell survival and expansion, and thus determines its response to *H. pylori* eradication.

NR4A3 is another molecule significantly enriched and over-expressed in translocation negative MALT lymphoma. NR4A3 is a member of the nerve growth factor-1B (NGF1B, or NR4A1 or Nur77) subfamily of nuclear orphan receptors. In T cells, NGF1B and NR4A3 are involved in TCR mediated cell death and thymocyte negative selection (He, 2002). These nuclear orphan receptors are also involved in the apoptotic process of other cell types in response to external signals (Hashida *et al*, 2007). The function of NR4A3 in B cells is currently unclear. Nonetheless, NR4A3 is one of the top over-expressed genes in cured, as opposed to fatal/refractory, DLBCL (Shipp *et al*, 2002). It is possible that over-expression of NR4A3 in lymphoma cells may predispose them to apoptosis following *H. pylori* eradication and elimination of the microbial mediated immune stimulation.

7.2.3 Molecular mechanisms of BCL10, MALT1 and API2-MALT1 mediated NF- κ B activation

Cytospin and immunohistochemistry data from this thesis showed that over-expression of BCL10 led to its subcellular localisation in the nucleus. Co-immunoprecipitation data showed that over-expression of BCL10 led to its interaction with MALT1 in BJAB B cells. Functional data showed that only BCL10 over-expression with LPS stimulation led to I κ B β degradation. In addition, subcellular localization and co-IP data showed more BCL10 in the presence of MALT1 reflecting the possibility that increased MALT1-BCL10 interaction might lead to increase in BCL10 expression. However, BCL10 was shown to interact with transcription factor IIB which plays an important role in the assembly of transcription activators that make up the RNA polymerase II pre-initiation complex (Liu *et al*, 2004c) suggesting a possible role as a transcriptional activator. Taken together, it can be hypothesised that excess BCL10 interacts with MALT1 either by affecting its stabilisation or its expression. Either way, the cytoplasmic level of BCL10 and MALT1 needs to be maintained to allow the formation of the CBM signalosome upstream of the NF- κ B subunits. Closer to the NF- κ B subunits, BCL10 over-expression together with stimulation by LPS in B cells or CD3/CD28 in T cells stimulation led to constitutive NF- κ B activation via I κ B β degradation. It has been shown that TCR/CD28 co-stimulation induces I κ B α , I κ B β and I κ B ϵ degradation (Li *et al*, 2005). I κ B α and I κ B β use slightly different mechanisms of NF- κ B activation. One hypothesis proposes that I κ B α masks the NLS of p65 in addition to the fact that it contains nuclear export sequencing that enables newly synthesized I κ B α to shuttle nuclear NF- κ B/Rel dimers into the cytoplasm (Phelps *et al*, 2000). In contrast, I κ B β does not contain nuclear export sequence and is able to mask the NLS domains of both p65 and p50. While detailed control of I κ B nuclear import and export has yet to be defined, these unique

properties of I κ B α and I κ B β are thought to provide the fine tuned regulation of NF- κ B/Rel proteins, whereby I κ B α controls transient NF- κ B/Rel activation and I κ B β regulates sustained NF- κ B/Rel activity. Studies using embryonic fibroblasts derived from various I κ B knockout mice (Hoffmann *et al*, 2002), showed that I κ B α resulted in high oscillatory NF- κ B nuclear activity, whereas I κ B β displayed a constant steady increase in nuclear NF- κ B activity that plateaued without subsequent decline, allowing sustainable NF- κ B activation in the case of prolonged stimulation (Hoffmann *et al*, 2002). Also, studies have shown that when I κ B β is degraded, NF- κ B activation becomes persistent; even though newly synthesized I κ B α accumulates to high levels in unstimulated cells. This is partly because the newly synthesised I κ B β is an unphosphorylated protein that binds to a portion of newly made NF- κ B and sequesters it from I κ B α . The unphosphorylated I κ B β , however, fails to mask the NLS and DNA binding domain on NF- κ B, resulting in the nuclear uptake of the unphosphorylated NF- κ B/I κ B β complex (Suyang *et al*, 1996). Thus, data from this thesis showed that over-expression of BCL10 leads to I κ B β degradation causing constitutive NF- κ B activation. This partly explains the biochemical mechanisms behind the NF- κ B reporter assay observations showing that BCL10 expression together with surface receptor stimulation led to increased NF- κ B activation. In addition, phosphorylated BCL10 was shown to form a complex with another NF- κ B inhibitor, BCL3, to enter the nucleus (Yeh *et al*, 2006), thus it might be that BCL10 may move to the nucleus with BCL3. However, details of BCL10 nuclear import and export as well as the function of nuclear BCL10 remain to be determined. Collectively, it can be hypothesised that BCL10 may indirectly (e.g. via interaction with the IKK complex or some unknown molecule) degrades I κ B β , since BCL10 is not part of the transcription factor complex that binds the NF- κ B promoter, nor does it affect the ability of NF- κ B to bind the DNA. This degradation of I κ B β may cause different NF- κ B to transactivate slightly different

set of NF- κ B target genes thus explaining the slightly different gene expression profiles of the NF- κ B target genes between MALT lymphoma with and without chromosome translocation.

A hypothesis on the molecular mechanisms underlying MALT lymphoma with and without chromosomal translocation can be generated from the data described above. In translocation positive MALT lymphoma, over-expression of API2-MALT1, BCL10 or MALT1 activates the canonical NF- κ B pathway. Canonical NF- κ B activation is augmented by B-cell receptor signalling, TLR signalling and potentially CCR2 signalling. The non-canonical NF- κ B pathway may be activated by CD40 and LT β receptor signalling. Activation of the canonical and non-canonical NF- κ B pathways leads to enhanced expression of the NF- κ B target genes, particularly TLR6, CCR2A, CCR2B CD69, IRF4 and BCL2. Over-expression of these immune receptors may provide a further positive feedback to the activation of the NF- κ B pathways. In addition, expression of TLR6 and CCR2 may trigger activation of the MAPK pathway. Over-expression of BCL2 is expected to promote tumour cell survival. In essence, the above chromosome translocations cause constitutive NF- κ B activation with expression of their target genes forming a potential positive feedback loop, and the relentless NF- κ B activation, which in the case of gastric MALT lymphoma confers its resistance to *H. pylori* eradication (Figure 7.1)

In translocation negative MALT lymphoma, the ongoing inflammatory and immune responses maintain active cognate B- and T- cell interaction via co-stimulating molecules CD86/CD28, B7RP1/ICOS, which are the major determinants of tumour cell survival and thus explain, in the cases of gastric MALT lymphoma, their responses to *H. pylori* eradication (Figure 7.1).

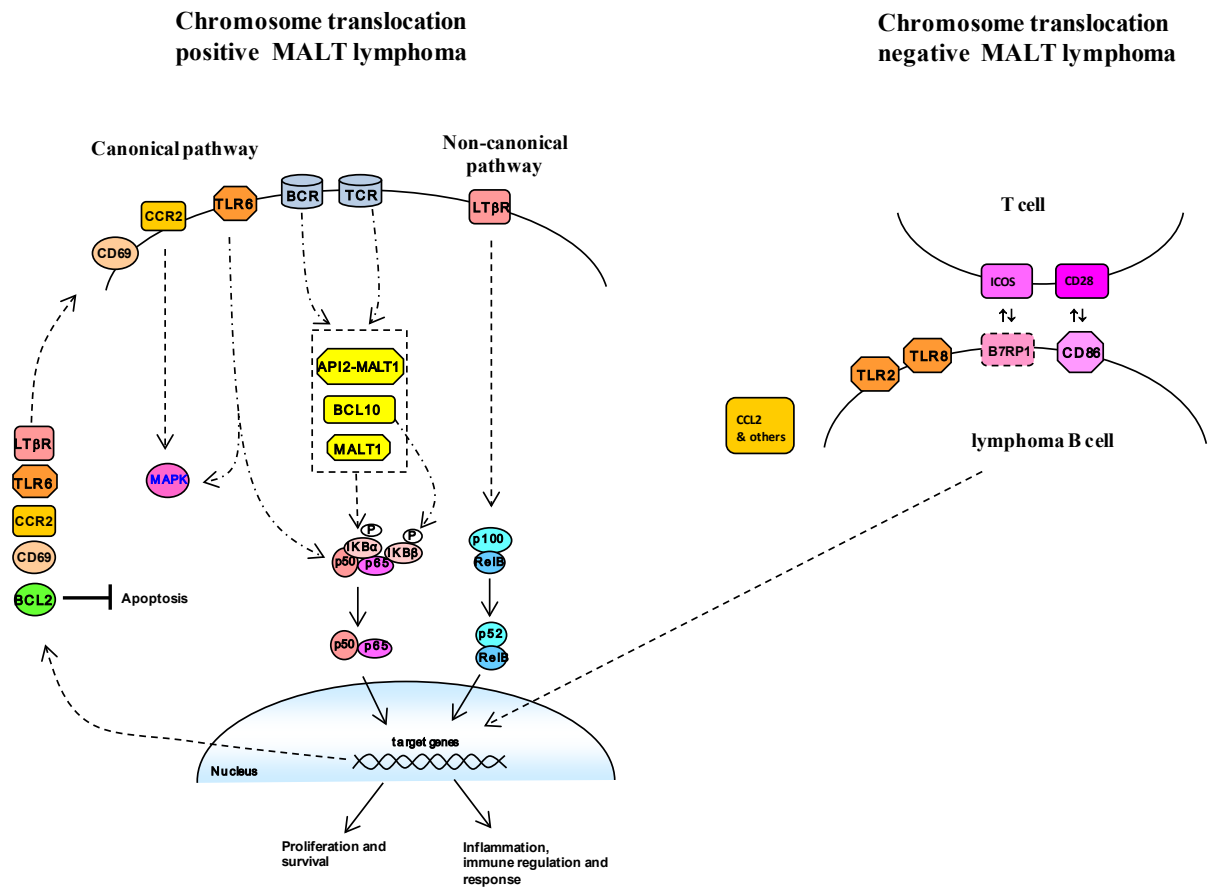


Figure 7.1 - Summary and hypothesis on molecular mechanisms of MALT lymphoma with and without chromosomal translocation.

In translocation positive MALT lymphoma, over-expression of *API2-MALT1*, *BCL10* and *MALT1* activates the canonical NF- κ B pathway (e.g. in the case of *BCL10* via degradation of I κ B β), leading to enhanced expression of the NF- κ B target genes, particularly *TLR6*, *CCR2*, *CD69* and *BCL2*. Over-expression of *TLR6* may provide a further positive feedback to the activation of the NF- κ B pathway. Similar positive feedback may also be expected from the CCR2 signalling, and in addition both TLR6 and CCR2 may trigger activation of the MAPK pathway. The pathogenic implication of enhanced *CD69* expression is currently unknown. Over-expression of *BCL2* is expected to promote the tumor cell survival. In essence, the above chromosome translocations cause constitutive NF- κ B activation with the expression of their target genes forming a potential positive feedback loop, and the relentless NF- κ B activation, which in the case of gastric MALT lymphoma, confers its resistance to *H. pylori* eradication.

In translocation negative MALT lymphoma, the ongoing inflammatory and immune responses maintain active cognate B- and T- cell interaction via the co-stimulating molecules; CD86/CD28, B7RP1/ICOS, which are the major determinants of tumor cell survival and thus explain, in the cases of gastric MALT lymphoma, their responses to *H. pylori* eradication.

7.3 MALT lymphoma specific phenotypic marker identification

Comparison of MALT expression microarray data with other lymphomas demonstrated Lactoferrin to be highly expressed in MALT lymphoma but not in other lymphoma subtypes. This was confirmed by qRT-PCR showing *Lactoferrin* to be significantly over expressed in all MALT lymphoma cases compared to FL or MCL. Currently, the only reported marker for marginal zone lymphomas is myeloid cell nuclear differentiation antigen (MNDA), a nuclear protein expressed by myeloid cells and a subset of B cells (Kanellis *et al*, 2009). It was shown to be expressed in normal tissue by a subset of the marginal zone B cells as well as subgroups of CLL, MCL and DLBCL, but it is highly expressed by MALT, SMZL and nodal marginal zone lymphoma (NMZL) and rarely expressed in FL making it potentially a useful marker for distinguishing between NMZL and FL (Kanellis *et al*, 2009). Both microarray and qRT-PCR results from this thesis showed that *Lactoferrin* mRNA is more highly expressed in MALT compared to other lymphomas. It can be hypothesised that if the Lactoferrin protein expression follows a similar pattern as its mRNA expression, then Lactoferrin may prove to be a better phenotypic marker for MALT lymphoma than MNDA.

Lactoferrin belongs to a family of iron-binding proteins that modulate iron metabolism, haematopoiesis and immunologic reactions. It has been shown that Lactoferrin which is present at mucosal surfaces and neutrophil specific granules (Baggiolini *et al*, 1970) (Raphael *et al*, 1989), readily binds CpG-containing DNA which binds to B cells via interaction with DNA on the cell surface (Bennett *et al*, 1983), mediated through the highly charged N-terminal sequence of Lactoferrin (Kawasaki *et al*, 2000). Lactoferrin inhibited CpG ODN stimulation of CD86 expression in the human Ramos B cell line and decreased cellular uptake of ODN, a process required for CpG bioactivity. Lactoferrin binding of CpG-containing ODN may serve to modulate and terminate host response to immunostimulatory

molecules such as CD86 and CD80 at mucosal surfaces and sites of bacterial infection. (Britigan *et al*, 2001). In addition, various studies show that there is an increase in Lactoferrin expression and *H. pylori* infection and gastric inflammation (Mannick *et al*) (Wen and Wen). Also, clinical studies showed that supplementation with Lactoferrin could be effective in increasing eradication rates of anti-*H. pylori* therapy, which could be helpful for patients with *H. pylori* eradication failure (Zou *et al.*) and that fecal Lactoferrin levels were elevated and this was found to be useful in the detection of colorectal diseases including MALT lymphoma (Hirata *et al.*).

Since the starting point of MALT lymphoma is thought to be infection with a pathogen and most of the samples analysed were *H. pylori* positive gastric MALT lymphoma, this may explain why Lactoferrin seem to be more highly expressed in MALT compared to other lymphomas. Besides its inhibitory effect on CpG-containing ODN in human B cells, Lactoferrin has been shown to affect phenotypic changes in immature B-cell populations and has an effect on the antigen presenting function of these cells (Zimecki *et al*, 1995). Lactoferrin also plays a role in the maturation of cells of the immune system and, together with the demonstration of the involvement of Lactoferrin in the maturation of T cells (Zimecki *et al*, 1991), this provides evidence that Lactoferrin can enhance the induction phase of the immune response.

In conclusion, Lactoferrin is a likely phenotypic marker for MALT lymphoma but further confirmation by immunohistochemistry is needed.

7.4 Conclusions

The results detailed in this study allow the following conclusions to be drawn:

- 1) Unsupervised clustering of MALT lymphoma with FL and MCL shows that MALT lymphoma is a distinct entity. Nonetheless, there is an overlap in the gene expression profiles between translocation positive and negative MALT lymphomas as both activate NF- κ B pathway but leading to the expression of different sets of NF- κ B target genes.
- 2) Translocation positive MALT lymphoma was characterised by an enhanced expression of NF- κ B target genes, particularly CCR2, TLR6, CD69, IRF4 and BCL2.
- 3) Translocation negative MALT lymphoma was featured by active inflammatory and immune responses to *H. pylori* infection. Tumour cell interaction with infiltrating T cells through co-stimulatory molecules (especially CD86/CD28) may have an important role in their survival and clonal expansion.
- 4) *In vitro* assays show cooperation between the expression of MALT lymphoma associated oncogenes and signalling via surface receptors including BCR, TLR and TCR. Such cooperation may be operational *in vivo*.
- 5) BCL10 expression with surface receptor stimulation leads to I κ B β degradation. Over-expression of BCL10 together with LPS stimulation in BJAB B cells may also activate NF- κ B inactivated by I κ B β .
- 6) Comparison of MALT lymphoma expression microarrays with other lymphomas showed Lactoferrin to be a putative MALT lymphoma specific marker.

7.5 Future perspectives

This thesis has identified novel mechanisms involved in MALT lymphoma pathogenesis, however many questions remain to be addressed.

7.5.1 CCR2 involvement in the molecular mechanism of MALT lymphomagenesis

Genes highly expressed in translocation positive MALT lymphoma include CCR2A and B isoforms. It would be useful to determine the role of each of these in MALT lymphomagenesis. This can be done in a similar way to the functional experiments carried out on TLR6 by identifying which pathways (e.g. NF- κ B and MAPK) they affect and whether there is a synergy between them and MALT lymphoma associated oncogenes in the activation of those pathways. Once this is established, it would be helpful to construct inducible stable cellular models with each of the above genes together with MALT lymphoma associated oncogenes to confirm any synergy between each of the above genes and MALT lymphoma associated oncogenes. Migration assays can be carried out on the cellular model to study the effect of CCR2 expression on B-cell migration. Expression microarray experiments can be carried out on the cellular models by expression of CCR2 alone and together with MALT lymphoma associated oncogenes. GSEA and GO analysis will then lead to the identification of the specific pathways affected by the above genes that may be involved in MALT lymphomagenesis. Validation of genes involved in those pathways can be carried out on MALT lymphoma patient samples.

7.5.2 Nuclear BCL10 function

Identification of BCL10 binding partners would help to determine the functions of nuclear BCL10 which may help to explain its role in the regulation of the NF- κ B pathway and its interaction with MALT1. Co-immunoprecipitation of nuclear BCL10 can be carried out by isolating the nuclear BCL10 fraction from BCL10 BJAB cells. BCL10 has been shown to form a complex with BCL3 which is a transcriptional co-activator of NF- κ B (Yeh *et al*, 2006), thus co-IP products of nuclear BCL10 can be investigated for the potential presence of NF- κ B subunits as potential binding partners by Western blotting. Co-IP extracts can also be investigated for the presence of unknown binding partners. Extracts can be separated by PAGE and the proteins visualised by silver staining. The proteins within bands unique to extracts from cells expressing nuclear BCL10 protein can be identified by mass spectrometry. Confirmation of the identity of any putative nuclear BCL10 binding partners can then be achieved by Western blotting of co-IP products for the presence of these targets. Site-specific mutagenesis of BCL10 expression constructs could be carried out to determine the exact region of the BCL10 protein required for binding to these partners.

BCL10 has been shown to bind to transcriptional activator TBII (Liu *et al*, 2004b). The role of BCL10 as a transcriptional activator could be investigated by Chromatin immunoprecipitation (ChIP) assay on cell lines with over-expressed BCL10 and compared to those with normal BCL10 expression. This will answer the question whether BCL10 may play a role as a transcriptional activator and if so whether it affects MALT1 expression amongst other genes which might partly explain the mechanism by which over-expression of BCL10 leads to MALT1 interaction.

7.5.3 Lactoferrin expression in MALT lymphoma by immunohistochemistry

A practically useful specific marker of MALT lymphoma needs to be developed. Lactoferrin seems to be the most promising candidate as confirmed by qRT-PCR. However, the initial Lactoferrin antibody used to validate the microarray and qRT-PCR produced inconclusive immunohistochemical data and the immunohistochemistry need to be repeated with a different Lactoferrin antibody. Two antibodies; the polyclonal rabbit anti-human (product no. A0061, DakoCytomation, Cambridge, UK) and the monoclonal mouse anti-human (Clone 1A1, product no. H86024M, Meridian Life Science, Maine, USA) were successfully used on FFPE tissue of clear cell carcinoma (Giuffre *et al*, 2007). Another antibody is the polyclonal rabbit anti-human anti-Lactoferrin (product no. 07-685, Upstate (Millipore), Massachusetts, USA) which was successfully used on nasopharyngeal carcinoma tissue microarray (Zhou *et al*, 2008). MNDA was shown to be a useful marker for distinguishing between NMZL and FL. Thus comparison between MNDA and the above two Lactoferrin marker on the same series of NHL B-cell lymphomas including CLL/SLL is warranted.

References

- Aamot,H.V., Micci,F., Holte,H., Delabie,J., Heim,S. (2005) G-banding and molecular cytogenetic analyses of marginal zone lymphoma. *Br.J.Haematol.*, *130*, 890-901.
- Adams,J.M. & Cory,S. (1998) The Bcl-2 protein family: arbiters of cell survival. *Science*, *281*, 1322-1326.
- Aggarwal,B.B. (2003) Signalling pathways of the TNF superfamily: a double-edged sword. *Nat.Rev.Immunol.*, *3*, 745-756.
- Akira,S. & Takeda,K. (2004) Toll-like receptor signalling. *Nat.Rev.Immunol.*, *4*, 499-511.
- Al Saleem,T. & Al Mondhiry,H. (2005) Immunoproliferative small intestinal disease (IPSID): a model for mature B-cell neoplasms. *Blood*, *105*, 2274-2280.
- Aldinucci,D., Gloghini,A., Pinto,A., De Filippi,R., Carbone,A. (2010) The classical Hodgkin's lymphoma microenvironment and its role in promoting tumour growth and immune escape. *J.Pathol.*, *221*, 248-263.
- Alizadeh,A.A., Eisen,M.B., Davis,R.E., Ma,C., Lossos,I.S., Rosenwald,A., Boldrick,J.C., Sabet,H., Tran,T., Yu,X., Powell,J.I., Yang,L., Marti,G.E., Moore,T., Hudson,J., Jr., Lu,L., Lewis,D.B., Tibshirani,R., Sherlock,G., Chan,W.C., Greiner,T.C., Weisenburger,D.D., Armitage,J.O., Warnke,R., Levy,R., Wilson,W., Grever,M.R., Byrd,J.C., Botstein,D., Brown,P.O., Staudt,L.M. (2000) Distinct types of diffuse large B-cell lymphoma identified by gene expression profiling. *Nature*, *403*, 503-511.
- An,F.Q., Compitello,N., Horwitz,E., Sramkoski,M., Knudsen,E.S., Renne,R. (2005) The latency-associated nuclear antigen of Kaposi's sarcoma-associated herpesvirus modulates cellular gene expression and protects lymphoid cells from p16 INK4A-induced cell cycle arrest. *J.Biol.Chem.*, *280*, 3862-3874.
- Asaka,M., Takeda,H., Sugiyama,T., Kato,M. (1997) What role does *Helicobacter pylori* play in gastric cancer? *Gastroenterology*, *113*, S56-S60.
- Baens,M., Fevery,S., Sagaert,X., Noels,H., Hagens,S., Broeckx,V., Billiau,A.D., Wolf-Peeters,C., Marynen,P. (2006) Selective expansion of marginal zone B cells in Emicro-API2-MALT1 mice is linked to enhanced IkappaB kinase gamma polyubiquitination. *Cancer Res.*, *66*, 5270-5277.
- Baggiolini,M., De Duve,C., Masson,P.L., Heremans,J.F. (1970) Association of lactoferrin with specific granules in rabbit heterophil leukocytes. *J.Exp.Med.*, *131*, 559-570.
- Baldwin,D.N., Shepherd,B., Kraemer,P., Hall,M.K., Sycuro,L.K., Pinto-Santini,D.M., Salama,N.R. (2007) Identification of *Helicobacter pylori* genes that contribute to stomach colonization. *Infect.Immun.*, *75*, 1005-1016.

- Banks,P.M. (2007) Gastrointestinal lymphoproliferative disorders. *Histopathology*, *50*, 42-54.
- Barrans,S.L., Fenton,J.A., Banham,A., Owen,R.G., Jack,A.S. (2004) Strong expression of FOXP1 identifies a distinct subset of diffuse large B-cell lymphoma (DLBCL) patients with poor outcome. *Blood*, *104*, 2933-2935.
- Barton,G.M. & Medzhitov,R. (2002) Control of adaptive immune responses by Toll-like receptors. *Curr.Opin.Immunol.*, *14*, 380-383.
- Barton,G.M. & Medzhitov,R. (2003) Toll-like receptor signaling pathways. *Science*, *300*, 1524-1525.
- Basak,S., Kim,H., Kearns,J.D., Tergaonkar,V., O'Dea,E., Werner,S.L., Benedict,C.A., Ware,C.F., Ghosh,G., Verma,I.M., Hoffmann,A. (2007) A fourth IkappaB protein within the NF-kappaB signaling module. *Cell*, *128*, 369-381.
- Basak,S., Shih,V.F., Hoffmann,A. (2008) Generation and activation of multiple dimeric transcription factors within the NF-kappaB signaling system. *Mol.Cell Biol.*, *28*, 3139-3150.
- Bayerdorffer,E., Neubauer,A., Rudolph,B., Thiede,C., Lehn,N., Eidt,S., Stolte,M. (1995) Regression of primary gastric lymphoma of mucosa-associated lymphoid tissue type after cure of Helicobacter pylori infection. MALT Lymphoma Study Group. *Lancet*, *345*, 1591-1594.
- Bayley,J.P., Ottenhoff,T.H., Verweij,C.L. (2004) Is there a future for TNF promoter polymorphisms? *Genes Immun.*, *5*, 315-329.
- Begum,S., Sano,T., Endo,H., Kawamata,H., Urakami,Y. (2000) Mucosal change of the stomach with low-grade mucosa-associated lymphoid tissue lymphoma after eradication of Helicobacter pylori: follow-up study of 48 cases. *J.Med.Invest.*, *47*, 36-46.
- Bennett,R.M., Davis,J., Campbell,S., Portnoff,S. (1983) Lactoferrin binds to cell membrane DNA. Association of surface DNA with an enriched population of B cells and monocytes. *J.Clin.Invest.*, *71*, 611-618.
- Bertoni,F., Cazzaniga,G., Bosshard,G., Roggero,E., Barbazza,R., de Boni,M., Capella,C., Pedrinis,E., Cavalli,F., Biondi,A., Zucca,E. (1997) Immunoglobulin heavy chain diversity genes rearrangement pattern indicates that MALT-type gastric lymphoma B cells have undergone an antigen selection process. *Br.J.Haematol.*, *97*, 830-836.
- Blenk,S., Engelmann,J., Weniger,M., Schultz,J., Dittrich,M., Rosenwald,A., Muller-Hermelink,H.K., Muller,T., Dandekar,T. (2007) Germinal Center B Cell-Like (GCB) and Activated B Cell-Like (ABC) Type of Diffuse Large B Cell Lymphoma (DLBCL): Analysis of Molecular Predictors, Signatures, Cell Cycle State and Patient Survival. *Cancer Inform.*, *3:399-420.*, 399-420.
- Bodrug,S.E., Warner,B.J., Bath,M.L., Lindeman,G.J., Harris,A.W., Adams,J.M. (1994) Cyclin D1 transgene impedes lymphocyte maturation and collaborates in lymphomagenesis with the myc gene. *EMBO J.*, *13*, 2124-2130.

- Bolin,T.D., Hunt,R.H., Korman,M.G., Lambert,J.R., Lee,A., Talley,N.J. (1995) Helicobacter pylori and gastric neoplasia: evolving concepts. *Med.J.Aust.*, *163*, 253-255.
- Boxer,L.A., Haak,R.A., Yang,H.H., Wolach,J.B., Whitcomb,J.A., Butterick,C.J., Baehner,R.L. (1982) Membrane-bound lactoferrin alters the surface properties of polymorphonuclear leukocytes. *J.Clin.Invest.*, *70*, 1049-1057.
- Brielmeier,M., Bechet,J.M., Falk,M.H., Pawlita,M., Polack,A., Bornkamm,G.W. (1998) Improving stable transfection efficiency: antioxidants dramatically improve the outgrowth of clones under dominant marker selection. *Nucleic Acids Res.*, *26*, 2082-2085.
- Brigl,M. & Brenner,M.B. (2004) CD1: antigen presentation and T cell function. *Annu.Rev.Immunol.*, *22:817-90.*, 817-890.
- Britigan,B.E., Lewis,T.S., Waldschmidt,M., McCormick,M.L., Krieg,A.M. (2001) Lactoferrin binds CpG-containing oligonucleotides and inhibits their immunostimulatory effects on human B cells. *J.Immunol.*, *167*, 2921-2928.
- Brown,M.P., Grundy,W.N., Lin,D., Cristianini,N., Sugnet,C.W., Furey,T.S., Ares,M., Jr., Haussler,D. (2000) Knowledge-based analysis of microarray gene expression data by using support vector machines. *Proc.Natl.Acad.Sci.*, *97*, 262-267.
- Brune,V., Tiacci,E., Pfeil,I., Doring,C., Eckerle,S., van Noesel,C.J., Klapper,W., Falini,B., von Heydebreck,A., Metzler,D., Brauninger,A., Hansmann,M.L., Kuppers,R. (2008) Origin and pathogenesis of nodular lymphocyte-predominant Hodgkin lymphoma as revealed by global gene expression analysis. *J.Exp.Med.*, *205*, 2251-2268.
- Brynes,R.K., Almaguer,P.D., Leathery,K.E., McCourty,A., Arber,D.A., Medeiros,L.J., Nathwani,B.N. (1996) Numerical cytogenetic abnormalities of chromosomes 3, 7, and 12 in marginal zone B-cell lymphomas. *Mod.Pathol.*, *9*, 995-1000.
- Butler,T.W., Grossi,C.E., Canessa,A., Pistoia,V., Barton,J.C. (1990) Immunoreactive lactoferrin in resting, activated, and neoplastic lymphocytes. *Leuk.Res.*, *14*, 441-447.
- Butte,A.J., Tamayo,P., Slonim,D., Golub,T.R., Kohane,I.S. (2000) Discovering functional relationships between RNA expression and chemotherapeutic susceptibility using relevance networks. *Proc.Natl.Acad.Sci.*, *97*, 12182-12186.
- Calin,G.A., Cimmino,A., Fabbri,M., Ferracin,M., Wojcik,S.E., Shimizu,M., Taccioli,C., Zanesi,N., Garzon,R., Aqeilan,R.I., Alder,H., Volinia,S., Rassenti,L., Liu,X., Liu,C.G., Kipps,T.J., Negrini,M., Croce,C.M. (2008) MiR-15a and miR-16-1 cluster functions in human leukemia. *Proc.Natl.Acad.Sci.*, *105*, 5166-5171.
- Catz,S.D. & Johnson,J.L. (2001) Transcriptional regulation of bcl-2 by nuclear factor kappa B and its significance in prostate cancer. *Oncogene*, *20*, 7342-7351.
- Cerroni,L., Zochling,N., Putz,B., Kerl,H. (1997) Infection by Borrelia burgdorferi and cutaneous B-cell lymphoma. *J.Cutan.Pathol.*, *24*, 457-461.

Cerutti,P.A. & Trump,B.F. (1991) Inflammation and oxidative stress in carcinogenesis. *Cancer Cells.*, 3, 1-7.

Chanudet,E., Huang,Y., Ichimura,K., Dong,G., Hamoudi,R.A., Radford,J., Wotherspoon,A.C., Isaacson,P.G., Ferry,J., Du,M.Q. (2010) A20 is targeted by promoter methylation, deletion and inactivating mutation in MALT lymphoma. *Leukemia*, 24, 483-487.

Chanudet,E., Ye,H., Ferry,J., Bacon,C.M., Adam,P., Muller-Hermelink,H.K., Radford,J., Pileri,S.A., Ichimura,K., Collins,V.P., Hamoudi,R.A., Nicholson,A.G., Wotherspoon,A.C., Isaacson,P.G., Du,M.Q. (2009) A20 deletion is associated with copy number gain at the TNFA/B/C locus and occurs preferentially in translocation-negative MALT lymphoma of the ocular adnexa and salivary glands. *J.Pathol.*, 217, 420-430.

Chanudet,E., Zhou,Y., Bacon,C.M., Wotherspoon,A.C., Muller-Hermelink,H.K., Adam,P., Dong,H.Y., de Jong,D., Li,Y., Wei,R., Gong,X., Wu,Q., Ranaldi,R., Goteri,G., Pileri,S.A., Ye,H., Hamoudi,R.A., Liu,H., Radford,J., Du,M.Q. (2006) Chlamydia psittaci is variably associated with ocular adnexal MALT lymphoma in different geographical regions. *J.Pathol.*, 209, 344-351.

Charo,I.F. (1999) CCR2: from cloning to the creation of knockout mice. *Chem.Immunol.*, 72:30-41., 30-41.

Charo,I.F., Myers,S.J., Herman,A., Franci,C., Connolly,A.J., Coughlin,S.R. (1994) Molecular cloning and functional expression of two monocyte chemoattractant protein 1 receptors reveals alternative splicing of the carboxyl-terminal tails. *Proc.Natl.Acad.Sci.*, 91, 2752-2756.

Che,T., You,Y., Wang,D., Tanner,M.J., Dixit,V.M., Lin,X. (2004) MALT1/paracaspase is a signaling component downstream of CARMA1 and mediates T cell receptor-induced NF-kappaB activation. *J.Biol.Chem.*, 279, 15870-15876.

Chen,F. & Castranova,V. (2007) Nuclear factor-kappaB, an unappreciated tumor suppressor. *Cancer Res.*, 67, 11093-11098.

Chen,L.T., Lin,J.T., Shyu,R.Y., Jan,C.M., Chen,C.L., Chiang,I.P., Liu,S.M., Su,I.J., Cheng,A.L. (2001) Prospective study of Helicobacter pylori eradication therapy in stage I(E) high-grade mucosa-associated lymphoid tissue lymphoma of the stomach. *J.Clin.Oncol.*, 19, 4245-4251.

Cheng,T.Y., Lin,J.T., Chen,L.T., Shun,C.T., Wang,H.P., Lin,M.T., Wang,T.E., Cheng,A.L., Wu,M.S. (2006) Association of T-cell regulatory gene polymorphisms with susceptibility to gastric mucosa-associated lymphoid tissue lymphoma. *J.Clin.Oncol.*, 20, 3483-3489.

Chng,W.J., Remstein,E.D., Fonseca,R., Bergsagel,P.L., Vrana,J.A., Kurtin,P.J., Dogan,A. (2009) Gene expression profiling of pulmonary mucosa-associated lymphoid tissue lymphoma identifies new biologic insights with potential diagnostic and therapeutic applications. *Blood*, 113, 635-645.

Clarke,P.A., te,P.R., Wooster,R., Workman,P. (2001) Gene expression microarray analysis in cancer biology, pharmacology, and drug development: progress and potential. *Biochem.Pharmacol.*, *62*, 1311-1336.

Coornaert,B., Baens,M., Heyninck,K., Bekaert,T., Haegman,M., Staal,J., Sun,L., Chen,Z.J., Marynen,P., Beyaert,R. (2008) T cell antigen receptor stimulation induces MALT1 paracaspase-mediated cleavage of the NF-kappaB inhibitor A20. *Nat.Immunol.*, *9*, 263-271.

Craig,V.J., Cogliatti,S.B., Arnold,I., Gerke,C., Balandat,J.E., Wundisch,T., Muller,A. (2010) B-cell receptor signaling and CD40 ligand-independent T cell help cooperate in Helicobacter-induced MALT lymphomagenesis. *Leukemia*, *24*, 1186-1196.

D'Ellos,M.M., Amedei,A., Del Prete,G. (2003) Helicobacter pylori antigen-specific T-cell responses at gastric level in chronic gastritis, peptic ulcer, gastric cancer and low-grade mucosa-associated lymphoid tissue (MALT) lymphoma. *Microbes.Infect.*, *5*, 723-730.

D'Ellos,M.M., Manghetti,M., Almerigogna,F., Amedei,A., Costa,F., Burrioni,D., Baldari,C.T., Romagnani,S., Telford,J.L., Del Prete,G. (1997) Different cytokine profile and antigen-specificity repertoire in Helicobacter pylori-specific T cell clones from the antrum of chronic gastritis patients with or without peptic ulcer. *Eur.J.Immunol.*, *27*, 1751-1755.

Dagg,M.K. & Levitt,D. (1981) Human B-lymphocyte subpopulations. I. Differentiation of density-separated B lymphocytes. *Clin.Immunol.Immunopathol.*, *21*, 39-49.

Daibata,M., Nemoto,Y., Togitani,K., Fukushima,A., Ueno,H., Ouchi,K., Fukushi,H., Imai,S., Taguchi,H. (2006) Absence of Chlamydia psittaci in ocular adnexal lymphoma from Japanese patients. *Br.J.Haematol.*, *132*, 651-652.

Dave,S.S., Fu,K., Wright,G.W., Lam,L.T., Kluin,P., Boerma,E.J., Greiner,T.C., Weisenburger,D.D., Rosenwald,A., Ott,G., Muller-Hermelink,H.K., Gascoyne,R.D., Delabie,J., Rimsza,L.M., Braziel,R.M., Grogan,T.M., Campo,E., Jaffe,E.S., Dave,B.J., Sanger,W., Bast,M., Vose,J.M., Armitage,J.O., Connors,J.M., Smeland,E.B., Kvaloy,S., Holte,H., Fisher,R.I., Miller,T.P., Montserrat,E., Wilson,W.H., Bahl,M., Zhao,H., Yang,L., Powell,J., Simon,R., Chan,W.C., Staudt,L.M. (2006) Molecular diagnosis of Burkitt's lymphoma. *N.Engl.J.Med.*, *354*, 2431-2442.

Davies,A.J., Rosenwald,A., Wright,G., Lee,A., Last,K.W., Weisenburger,D.D., Chan,W.C., Delabie,J., Braziel,R.M., Campo,E., Gascoyne,R.D., Jaffe,E.S., Muller-Hermelink,K., Ott,G., Calaminici,M., Norton,A.J., Goff,L.K., Fitzgibbon,J., Staudt,L.M., Andrew,L.T. (2007) Transformation of follicular lymphoma to diffuse large B-cell lymphoma proceeds by distinct oncogenic mechanisms. *Br.J.Haematol.*, *136*, 286-293.

Davis,R.E., Ngo,V.N., Lenz,G., Tolar,P., Young,R.M., Romesser,P.B., Kohlhammer,H., Lamy,L., Zhao,H., Yang,Y., Xu,W., Shaffer,A.L., Wright,G., Xiao,W., Powell,J., Jiang,J.K., Thomas,C.J., Rosenwald,A., Ott,G., Muller-Hermelink,H.K., Gascoyne,R.D., Connors,J.M., Johnson,N.A., Rimsza,L.M., Campo,E., Jaffe,E.S., Wilson,W.H., Delabie,J., Smeland,E.B., Fisher,R.I., Braziel,R.M., Tubbs,R.R., Cook,J.R., Weisenburger,D.D., Chan,W.C., Pierce,S.K., Staudt,L.M. (2010) Chronic active B-cell-receptor signalling in diffuse large B-cell lymphoma. *Nature*, *463*, 88-92.

de Jong,D., Koster,A., Hagenbeek,A., Raemaekers,J., Veldhuizen,D., Heisterkamp,S., de Boer,J.P., van Glabbeke,M. (2009) Impact of the tumor microenvironment on prognosis in follicular lymphoma is dependent on specific treatment protocols. *Haematologica*, *94*, 70-77.

de Jong,D., Vyth-Dreese,F., DelleMijn,T., Verra,N., Ruskone-Fourmesttraux,A., Lavergne-Slove,A., Hart,G., Boot,H. (2001) Histological and immunological parameters to predict treatment outcome of Helicobacter pylori eradication in low-grade gastric MALT lymphoma. *J.Pathol.*, *193*, 318-324.

de Sousa,M., Smithyman,A., Tan,C. (1978) Suggested models of ecotaxopathy in lymphoreticular malignancy. A role for iron-binding proteins in the control of lymphoid cell migration. *Am.J.Pathol.*, *90*, 497-520.

Doglioni,C., Wotherspoon,A.C., Moschini,A., de Boni,M., Isaacson,P.G. (1992) High incidence of primary gastric lymphoma in northeastern Italy. *Lancet*, *339*, 834-835.

Du,M., Diss,T.C., Xu,C., Peng,H., Isaacson,P.G., Pan,L. (1996a) Ongoing mutation in MALT lymphoma immunoglobulin gene suggests that antigen stimulation plays a role in the clonal expansion. *Leukemia*, *10*, 1190-1197.

Du,M.Q. (2007) MALT lymphoma : recent advances in aetiology and molecular genetics. *J.Clin.Exp.Hematop.*, *47*, 31-42.

Du,M.Q. & Isaacson,P.G. (2002) Gastric MALT lymphoma: from aetiology to treatment. *Lancet Oncol.*, *3*, 97-104.

Du,M.Q., Xu,C.F., Diss,T.C., Peng,H.Z., Wotherspoon,A.C., Isaacson,P.G., Pan,L.X. (1996b) Intestinal dissemination of gastric mucosa-associated lymphoid tissue lymphoma. *Blood*, *88*, 4445-4451.

Duwel,M., Welteke,V., Oeckinghaus,A., Baens,M., Kloo,B., Ferch,U., Darnay,B.G., Ruland,J., Marynen,P., Krappmann,D. (2009) A20 negatively regulates T cell receptor signaling to NF-kappaB by cleaving Malt1 ubiquitin chains. *J.Immunol.*, *182*, 7718-7728.

Eidt,S., Stolte,M., Fischer,R. (1994) Helicobacter pylori gastritis and primary gastric non-Hodgkin's lymphomas. *J.Clin.Pathol.*, *47*, 436-439.

Eisen,M.B., Spellman,P.T., Brown,P.O., Botstein,D. (1998) Cluster analysis and display of genome-wide expression patterns. *Proc.Natl.Acad.Sci.*, *95*, 14863-14868.

Ek,S., Hogerkorp,C.M., Dictor,M., Ehinger,M., Borrebaeck,C.A. (2002) Mantle cell lymphomas express a distinct genetic signature affecting lymphocyte trafficking and growth regulation as compared with subpopulations of normal human B cells. *Cancer Res.*, *62*, 4398-4405.

Ellison,R.T., III (1994) The effects of lactoferrin on gram-negative bacteria. *Adv.Exp.Med.Biol.*, *357:71-90.*, 71-90.

- Enno,A., O'Rourke,J.L., Howlett,C.R., Jack,A., Dixon,M.F., Lee,A. (1995) MALToma-like lesions in the murine gastric mucosa after long-term infection with *Helicobacter felis*. A mouse model of *Helicobacter pylori*-induced gastric lymphoma. *Am.J.Pathol.*, *147*, 217-222.
- Erlanson,M., Gronlund,E., Lofvenberg,E., Roos,G., Lindh,J. (1998) Expression of activation markers CD23 and CD69 in B-cell non-Hodgkin's lymphoma. *Eur.J.Haematol.*, *60*, 125-132.
- Falcon,S. & Gentleman,R. (2007) Using GOstats to test gene lists for GO term association. *Bioinformatics*, *23*, 257-258.
- Falini,B. & Mason,D.Y. (2002) Proteins encoded by genes involved in chromosomal alterations in lymphoma and leukemia: clinical value of their detection by immunocytochemistry. *Blood*, *99*, 409-426.
- Farinha,P. & Gascoyne,R.D. (2005) Molecular pathogenesis of mucosa-associated lymphoid tissue lymphoma. *J.Clin.Oncol.*, *23*, 6370-6378.
- Fenwick,C., Na,S.Y., Voll,R.E., Zhong,H., Im,S.Y., Lee,J.W., Ghosh,S. (2000) A subclass of Ras proteins that regulate the degradation of I κ B. *Science*, *287*, 869-873.
- Ferreri,A.J., Guidoboni,M., Ponzoni,M., De Conciliis,C., Dell'Oro,S., Fleischhauer,K., Caggiari,L., Lettini,A.A., Dal Cin,E., Ieri,R., Freschi,M., Villa,E., Boiocchi,M., Dolcetti,R. (2004) Evidence for an association between *Chlamydia psittaci* and ocular adnexal lymphomas. *J.Natl.Cancer Inst.*, *96*, 586-594.
- Ferreri,A.J., Ponzoni,M., Guidoboni,M., Resti,A.G., Politi,L.S., Cortelazzo,S., Demeter,J., Zallio,F., Palmas,A., Muti,G., Dognini,G.P., Pasini,E., Lettini,A.A., Sacchetti,F., De Conciliis,C., Doglioni,C., Dolcetti,R. (2006) Bacteria-eradicating therapy with doxycycline in ocular adnexal MALT lymphoma: a multicenter prospective trial. *J.Natl.Cancer Inst.*, *98*, 1375-1382.
- Figueiredo,C., Machado,J.C., Pharoah,P., Seruca,R., Sousa,S., Carvalho,R., Capelinha,A.F., Quint,W., Caldas,C., van Doorn,L.J., Carneiro,F., Sobrinho-Simoes,M. (2002) *Helicobacter pylori* and interleukin 1 genotyping: an opportunity to identify high-risk individuals for gastric carcinoma. *J.Natl.Cancer Inst.*, *94*, 1680-1687.
- Fischbach,W., Goebeler,M.E., Ruskone-Fourmesttraux,A., Wundisch,T., Neubauer,A., Raderer,M., Savio,A. (2007) Most patients with minimal histological residuals of gastric MALT lymphoma after successful eradication of *Helicobacter pylori* can be managed safely by a watch and wait strategy: experience from a large international series. *Gut*, *56*, 1685-1687.
- Fischbach,W., Goebeler-Kolve,M., Starostik,P., Greiner,A., Muller-Hermelink,H.K. (2002) Minimal residual low-grade gastric MALT-type lymphoma after eradication of *Helicobacter pylori*. *Lancet*, *360*, 547-548.

Fischbach,W., Goebeler-Kolve,M.E., Dragosics,B., Greiner,A., Stolte,M. (2004) Long term outcome of patients with gastric marginal zone B cell lymphoma of mucosa associated lymphoid tissue (MALT) following exclusive Helicobacter pylori eradication therapy: experience from a large prospective series. *Gut*, *53*, 34-37.

Flaishon,L., Becker-Herman,S., Hart,G., Levo,Y., Kuziel,W.A., Shachar,I. (2004) Expression of the chemokine receptor CCR2 on immature B cells negatively regulates their cytoskeletal rearrangement and migration. *Blood*, *104*, 933-941.

Fong,T.C., Wu,Y., Kipps,T.J. (1996) Identification of a promoter element that regulates tissue-specific expression of the human CD80 (B7.1) gene. *J.Immunol.*, *157*, 4442-4450.

Franco,R., Camacho,F.I., Caleo,A., Staibano,S., Bifano,D., De Renzo,A., Tranfa,F., De Chiara,A., Botti,G., Merola,R., Diez,A., Bonavolonta,G., De Rosa,G., Piris,M.A. (2006) Nuclear bcl10 expression characterizes a group of ocular adnexa MALT lymphomas with shorter failure-free survival. *Mod.Pathol.*, *19*, 1055-1067.

Fukuhara,N., Nakamura,T., Nakagawa,M., Tagawa,H., Takeuchi,I., Yatabe,Y., Morishima,Y., Nakamura,S., Seto,M. (2007) Chromosomal imbalances are associated with outcome of Helicobacter pylori eradication in t(11;18)(q21;q21) negative gastric mucosa-associated lymphoid tissue lymphomas. *Genes Chromosomes Cancer*, *46*, 784-790.

Gallardo,F., Bellosillo,B., Espinet,B., Pujol,R.M., Estrach,T., Servitje,O., Romagosa,V., Barranco,C., Boluda,S., Garcia,M., Sole,F., Ariza,A., Serrano,S. (2006) Aberrant nuclear BCL10 expression and lack of t(11;18)(q21;q21) in primary cutaneous marginal zone B-cell lymphoma. *Hum.Pathol.*, *37*, 867-873.

Garrison,J.B., Samuel,T., Reed,J.C. (2009) TRAF2-binding BIR1 domain of c-IAP2/MALT1 fusion protein is essential for activation of NF-kappaB. *Oncogene*, *28*, 1584-1593.

Gilmore,T.D. (2006) Introduction to NF-kappaB: players, pathways, perspectives. *Oncogene*, *25*, 6680-6684.

Giuffre,G., Barresi,V., Skliros,C., Barresi,G., Tuccari,G. (2007) Immunoexpression of lactoferrin in human sporadic renal cell carcinomas. *Oncol.Rep.*, *17*, 1021-1026.

Glas,A.M., Knoops,L., Delahaye,L., Kersten,M.J., Kibbelaar,R.E., Wessels,L.A., van Laar,R., van Krieken,J.H., Baars,J.W., Raemaekers,J., Kluin,P.M., van't Veer,L.J., de Jong,D. (2007) Gene-expression and immunohistochemical study of specific T-cell subsets and accessory cell types in the transformation and prognosis of follicular lymphoma. *J.Clin.Oncol.*, *25*, 390-398.

Goatly,A., Bacon,C.M., Nakamura,S., Ye,H., Kim,I., Brown,P.J., Ruskone-Fourmestreaux,A., Cervera,P., Streubel,B., Banham,A.H., Du,M.Q. (2008) FOXP1 abnormalities in lymphoma: translocation breakpoint mapping reveals insights into deregulated transcriptional control. *Mod.Pathol.*, *21*, 902-911.

Golub,T.R., Slonim,D.K., Tamayo,P., Huard,C., Gaasenbeek,M., Mesirov,J.P., Coller,H., Loh,M.L., Downing,J.R., Caligiuri,M.A., Bloomfield,C.D., Lander,E.S. (1999) Molecular classification of cancer: class discovery and class prediction by gene expression monitoring. *Science*, *286*, 531-537.

Gomariz,R.P., Arranz,A., Juarranz,Y., Gutierrez-Canas,I., Garcia-Gomez,M., Leceta,J., Martinez,C. (2007) Regulation of TLR expression, a new perspective for the role of VIP in immunity. *Peptides*, *28*, 1825-1832.

Greiner,A., Knorr,C., Qin,Y., Sebald,W., Schimpl,A., Banchereau,J., Muller-Hermelink,H.K. (1997) Low-grade B cell lymphomas of mucosa-associated lymphoid tissue (MALT-type) require CD40-mediated signaling and Th2-type cytokines for in vitro growth and differentiation. *Am.J.Pathol.*, *150*, 1583-1593.

Grumont,R.J. & Gerondakis,S. (2000) Rel induces interferon regulatory factor 4 (IRF-4) expression in lymphocytes: modulation of interferon-regulated gene expression by rel/nuclear factor kappaB. *J.Exp.Med.*, *191*, 1281-1292.

Gyrd-Hansen,M., Darding,M., Miasari,M., Santoro,M.M., Zender,L., Xue,W., Tenev,T., da Fonseca,P.C., Zvelebil,M., Bujnicki,J.M., Lowe,S., Silke,J., Meier,P. (2008) IAPs contain an evolutionarily conserved ubiquitin-binding domain that regulates NF-kappaB as well as cell survival and oncogenesis. *Nat.Cell Biol.*, *10*, 1309-1317.

Hajeer,A.H. & Hutchinson,I.V. (2000) TNF-alpha gene polymorphism: clinical and biological implications. *Microsc.Res.Tech.*, *50*, 216-228.

Hamoudi,R.A., Johnston,S., Hutchinson,G., D'Errico,J. (2002) High Throughput Methods for Gene Identification, Cloning and Functional Genomics Using the GeneTAC G3 Robotics Workstation. *Journal of the Association for Laboratory Automation*, *7*, 53-59.

Hara,T., Jung,L.K., Bjorndahl,J.M., Fu,S.M. (1986) Human T cell activation. III. Rapid induction of a phosphorylated 28 kD/32 kD disulfide-linked early activation antigen (EA 1) by 12-o-tetradecanoyl phorbol-13-acetate, mitogens, and antigens. *J.Exp.Med.*, *164*, 1988-2005.

Haralambieva,E., Adam,P., Ventura,R., Katzenberger,T., Kalla,J., Holler,S., Hartmann,M., Rosenwald,A., Greiner,A., Muller-Hermelink,H.K., Banham,A.H., Ott,G. (2006b) Genetic rearrangement of FOXP1 is predominantly detected in a subset of diffuse large B-cell lymphomas with extranodal presentation. *Leukemia.*, *20*, 1300-1303.

Haralambieva,E., Adam,P., Ventura,R., Katzenberger,T., Kalla,J., Holler,S., Hartmann,M., Rosenwald,A., Greiner,A., Muller-Hermelink,H.K., Banham,A.H., Ott,G. (2006a) Genetic rearrangement of FOXP1 is predominantly detected in a subset of diffuse large B-cell lymphomas with extranodal presentation. *Leukemia*, *20*, 1300-1303.

Hashida,R., Ohkura,N., Saito,H., Tsujimoto,G. (2007) The NR4A nuclear receptor family in eosinophils. *J.Hum.Genet.*, *52*, 13-20.

- Hayden,M.S. & Ghosh,S. (2004) Signaling to NF-kappaB. *Genes Dev.*, *18*, 2195-2224.
- Hayden,M.S. & Ghosh,S. (2008) Shared principles in NF-kappaB signaling. *Cell*, *132*, 344-362.
- He,Y.W. (2002) Orphan nuclear receptors in T lymphocyte development. *J.Leukoc.Biol.*, *72*, 440-446.
- Hinz,M., Loser,P., Mathas,S., Krappmann,D., Dorken,B., Scheidereit,C. (2001) Constitutive NF-kappaB maintains high expression of a characteristic gene network, including CD40, CD86, and a set of antiapoptotic genes in Hodgkin/Reed-Sternberg cells. *Blood*, *97*, 2798-2807.
- Hirata,I., Hoshimoto,M., Saito,O., Kayazawa,M., Nishikawa,T., Murano,M., Toshina,K., Wang,F.Y., Matsuse,R. (2007) Usefulness of fecal lactoferrin and hemoglobin in diagnosis of colorectal diseases. *World J.Gastroenterol.*, *13*, 1569-1574.
- Ho,L., Davis,R.E., Conne,B., Chappuis,R., Berczy,M., Mhaweck,P., Staudt,L.M., Schwaller,J. (2005) MALT1 and the API2-MALT1 fusion act between CD40 and IKK and confer NF-kappa B-dependent proliferative advantage and resistance against FAS-induced cell death in B cells. *Blood*, *105*, 2891-2899.
- Hoffmann,A. & Baltimore,D. (2006) Circuitry of nuclear factor kappaB signaling. *Immunol.Rev.*, *210:171-86.*, 171-186.
- Hoffmann,A., Levchenko,A., Scott,M.L., Baltimore,D. (2002) The IkappaB-NF-kappaB signaling module: temporal control and selective gene activation. *Science*, *298*, 1241-1245.
- Hofmann,K., Bucher,P., Tschopp,J. (1997) The CARD domain: a new apoptotic signalling motif. *Trends Biochem.Sci.*, *22*, 155-156.
- Hofmann,W.K., de Vos,S., Tsukasaki,K., Wachsman,W., Pinkus,G.S., Said,J.W., Koeffler,H.P. (2001) Altered apoptosis pathways in mantle cell lymphoma detected by oligonucleotide microarray. *Blood*, *98*, 787-794.
- Hopken,U.E., Foss,H.D., Meyer,D., Hinz,M., Leder,K., Stein,H., Lipp,M. (2002) Up-regulation of the chemokine receptor CCR7 in classical but not in lymphocyte-predominant Hodgkin disease correlates with distinct dissemination of neoplastic cells in lymphoid organs. *Blood*, *99*, 1109-1116.
- Hopken,U.E., Wengner,A.M., Loddenkemper,C., Stein,H., Heimesaat,M.M., Rehm,A., Lipp,M. (2007) CCR7 deficiency causes ectopic lymphoid neogenesis and disturbed mucosal tissue integrity. *Blood.*, *109*, 886-895.
- Howbrook,D.N., van der Valk,A.M., O'Shaughnessy,M.C., Sarker,D.K., Baker,S.C., Lloyd,A.W. (2003) Developments in microarray technologies. *Drug Discov.Today.*, *8*, 642-651.

Howden,C.W. & Hunt,R.H. (1998) Guidelines for the management of Helicobacter pylori infection. Ad Hoc Committee on Practice Parameters of the American College of Gastroenterology. *Am.J.Gastroenterol.*, *93*, 2330-2338.

Hrdlickova,R., Nehyba,J., Bose,H.R., Jr. (2001) Interferon regulatory factor 4 contributes to transformation of v-Rel-expressing fibroblasts. *Mol.Cell Biol.*, *21*, 6369-6386.

Hu,H., Wang,B., Borde,M., Nardone,J., Maika,S., Allred,L., Tucker,P.W., Rao,A. (2006a) Foxp1 is an essential transcriptional regulator of B cell development. *Nat.Immunol.*, *7*, 819-826.

Hu,S., Du,M.Q., Park,S.M., Alcivar,A., Qu,L., Gupta,S., Tang,J., Baens,M., Ye,H., Lee,T.H., Marynen,P., Riley,J.L., Yang,X. (2006b) cIAP2 is a ubiquitin protein ligase for BCL10 and is dysregulated in mucosa-associated lymphoid tissue lymphomas. *J.Clin.Invest.*, *116*, 174-181.

Huang,X., Zhang,Z., Liu,H., Ye,H., Chuang,S.S., Wang,J., Lin,S., Gao,Z., Du,M.Q. (2003) T(11;18)(q21;q21) in gastric MALT lymphoma and diffuse large B-cell lymphoma of Chinese patients. *Hematol.J.*, *4*, 342-345.

Hummel,M., Bentink,S., Berger,H., Klapper,W., Wessendorf,S., Barth,T.F., Bernd,H.W., Cogliatti,S.B., Dierlamm,J., Feller,A.C., Hansmann,M.L., Haralambieva,E., Harder,L., Hasenclever,D., Kuhn,M., Lenze,D., Lichter,P., Martin-Subero,J.I., Moller,P., Muller-Hermelink,H.K., Ott,G., Parwaresch,R.M., Pott,C., Rosenwald,A., Rosolowski,M., Schwaenen,C., Sturzenhofecker,B., Szczepanowski,M., Trautmann,H., Wacker,H.H., Spang,R., Loeffler,M., Trumper,L., Stein,H., Siebert,R. (2006) A biologic definition of Burkitt's lymphoma from transcriptional and genomic profiling. *N.Engl.J.Med.*, *354*, 2419-2430.

Hussell,T., Isaacson,P.G., Crabtree,J.E., Dogan,A., Spencer,J. (1993a) Immunoglobulin specificity of low grade B cell gastrointestinal lymphoma of mucosa-associated lymphoid tissue (MALT) type. *Am.J.Pathol.*, *142*, 285-292.

Hussell,T., Isaacson,P.G., Crabtree,J.E., Spencer,J. (1993b) The response of cells from low-grade B-cell gastric lymphomas of mucosa-associated lymphoid tissue to Helicobacter pylori. *Lancet*, *342*, 571-574.

Hussell,T., Isaacson,P.G., Crabtree,J.E., Spencer,J. (1996) Helicobacter pylori-specific tumour-infiltrating T cells provide contact dependent help for the growth of malignant B cells in low-grade gastric lymphoma of mucosa-associated lymphoid tissue. *J.Pathol.*, *178*, 122-127.

Huynh,M.Q., Wacker,H.H., Wundisch,T., Sohlbach,K., Daniel,K.T., Krause,M., Stabla,K., Roth,P., Fischbach,W., Stolte,M., Neubauer,A. (2008) Expression profiling reveals specific gene expression signatures in gastric MALT lymphomas. *Leuk.Lymphoma.*, *49*, 974-983.

Inoue,J., Kerr,L.D., Kakizuka,A., Verma,I.M. (1992) I kappa B gamma, a 70 kd protein identical to the C-terminal half of p110 NF-kappa B: a new member of the I kappa B family. *Cell*, *68*, 1109-1120.

- Irizarry,R.A., Hobbs,B., Collin,F., Beazer-Barclay,Y.D., Antonellis,K.J., Scherf,U., Speed,T.P. (2003) Exploration, normalization, and summaries of high density oligonucleotide array probe level data. *Biostatistics*, *4*, 249-264.
- Isaacson,P. & Wright,D.H. (1983) Malignant lymphoma of mucosa-associated lymphoid tissue. A distinctive type of B-cell lymphoma. *Cancer*, *52*, 1410-1416.
- Isaacson,P.G. & Norton,A.J. (1994) *Extranodal Lymphomas*, 1 edn, pp. 1-330.
- Isaacson,P.G. (1995) The MALT lymphoma concept updated. *Ann.Oncol.*, *6*, 319-320.
- Isaacson,P.G. & Du,M.Q. (2004) MALT lymphoma: from morphology to molecules. *Nat.Rev.Cancer.*, *4*, 644-653.
- Isaacson,P.G. & Spencer,J. (1987) Malignant lymphoma of mucosa-associated lymphoid tissue. *Histopathology*, *11*, 445-462.
- Isaacson,P.G. & Spencer,J. (1995) The biology of low grade MALT lymphoma. *J.Clin.Pathol.*, *48*, 395-397.
- Jacobs,M.D. & Harrison,S.C. (1998) Structure of an IkappaBalpha/NF-kappaB complex. *Cell*, *95*, 749-758.
- Jang,S.K., Krausslich,H.G., Nicklin,M.J., Duke,G.M., Palmenberg,A.C., Wimmer,E. (1988) A segment of the 5' nontranslated region of encephalomyocarditis virus RNA directs internal entry of ribosomes during in vitro translation. *J.Virol.*, *62*, 2636-2643.
- Jost,P.J. & Ruland,J. (2007) Aberrant NF-kappaB signaling in lymphoma: mechanisms, consequences, and therapeutic implications. *Blood*, *109*, 2700-2707.
- Kanellis,G., Roncador,G., Arribas,A., Mollejo,M., Montes-Moreno,S., Maestre,L., Campos-Martin,Y., Rios Gonzalez,J.L., Martinez-Torrecedrada,J.L., Sanchez-Verde,L., Pajares,R., Cigudosa,J.C., Martin,M.C., Piris,M.A. (2009) Identification of MNDA as a new marker for nodal marginal zone lymphoma. *Leukemia.*, *23*, 1847-1857.
- Karin,M. & Lin,A. (2002) NF-kappaB at the crossroads of life and death. *Nat.Immunol.*, *3*, 221-227.
- Kassan,S.S., Thomas,T.L., Moutsopoulos,H.M., Hoover,R., Kimberly,R.P., Budman,D.R., Costa,J., Decker,J.L., Chused,T.M. (1978) Increased risk of lymphoma in sicca syndrome. *Ann.Intern.Med.*, *89*, 888-892.
- Kato,I., Tajima,K., Suchi,T., Aozasa,K., Matsuzuka,F., Kuma,K., Tominaga,S. (1985) Chronic thyroiditis as a risk factor of B-cell lymphoma in the thyroid gland. *Jpn.J.Cancer Res.*, *76*, 1085-1090.

Kato,M., Sanada,M., Kato,I., Sato,Y., Takita,J., Takeuchi,K., Niwa,A., Chen,Y., Nakazaki,K., Nomoto,J., Asakura,Y., Muto,S., Tamura,A., Iio,M., Akatsuka,Y., Hayashi,Y., Mori,H., Igarashi,T., Kurokawa,M., Chiba,S., Mori,S., Ishikawa,Y., Okamoto,K., Tobinai,K., Nakagama,H., Nakahata,T., Yoshino,T., Kobayashi,Y., Ogawa,S. (2009) Frequent inactivation of A20 in B-cell lymphomas. *Nature*, *459*, 712-716.

Kawasaki,Y., Sato,K., Shinmoto,H., Dosako,S. (2000) Role of basic residues of human lactoferrin in the interaction with B lymphocytes. *Biosci.Biotechnol.Biochem.*, *64*, 314-318.

Koch,R. (1884) Die Aetiologie der Tuberkulose. *Mitt Kaiser Gesundh*, 1-88.

Krikos,A., Laherty,C.D., Dixit,V.M. (1992) Transcriptional activation of the tumor necrosis factor alpha-inducible zinc finger protein, A20, is mediated by kappa B elements. *J.Biol.Chem.*, *267*, 17971-17976.

Kuo,S.H., Chen,L.T., Yeh,K.H., Wu,M.S., Hsu,H.C., Yeh,P.Y., Mao,T.L., Chen,C.L., Doong,S.L., Lin,J.T., Cheng,A.L. (2004) Nuclear expression of BCL10 or nuclear factor kappa B predicts Helicobacter pylori-independent status of early-stage, high-grade gastric mucosa-associated lymphoid tissue lymphomas. *J.Clin.Oncol.*, *22*, 3491-3497.

Kuppers,R. (2005) Mechanisms of B-cell lymphoma pathogenesis. *Nat.Rev.Cancer.*, *5*, 251-262.

Kutting,B., Bonsmann,G., Metze,D., Luger,T.A., Cerroni,L. (1997) Borrelia burgdorferi-associated primary cutaneous B cell lymphoma: complete clearing of skin lesions after antibiotic pulse therapy or intralesional injection of interferon alfa-2a. *J.Am.Acad.Dermatol.*, *36*, 311-314.

Ladner,K.J., Caligiuri,M.A., Guttridge,D.C. (2003) Tumor necrosis factor-regulated biphasic activation of NF-kappa B is required for cytokine-induced loss of skeletal muscle gene products. *J.Biol.Chem.*, *278*, 2294-2303.

Lamothe,B., Besse,A., Campos,A.D., Webster,W.K., Wu,H., Darnay,B.G. (2007) Site-specific Lys-63-linked tumor necrosis factor receptor-associated factor 6 auto-ubiquitination is a critical determinant of I kappa B kinase activation. *J.Biol.Chem.*, *282*, 4102-4112.

Lawrie,C.H., Gal,S., Dunlop,H.M., Pushkaran,B., Liggins,A.P., Pulford,K., Banham,A.H., Pezzella,F., Boulwood,J., Wainscoat,J.S., Hatton,C.S., Harris,A.L. (2008a) Detection of elevated levels of tumour-associated microRNAs in serum of patients with diffuse large B-cell lymphoma. *Br.J.Haematol.*, *141*, 672-675.

Lawrie,C.H., Saunders,N.J., Soneji,S., Palazzo,S., Dunlop,H.M., Cooper,C.D., Brown,P.J., Troussard,X., Mossafa,H., Enver,T., Pezzella,F., Boulwood,J., Wainscoat,J.S., Hatton,C.S. (2008b) MicroRNA expression in lymphocyte development and malignancy. *Leukemia.*, *22*, 1440-1446.

Lecuit,M., Abachin,E., Martin,A., Poyart,C., Pochart,P., Suarez,F., Bengoufa,D., Feuillard,J., Lavergne,A., Gordon,J.I., Berche,P., Guillevin,L., Lortholary,O. (2004) Immunoproliferative small intestinal disease associated with *Campylobacter jejuni*. *N.Engl.J.Med.*, *350*, 239-248.

Lee,K.Y., D'Acquisto,F., Hayden,M.S., Shim,J.H., Ghosh,S. (2005) PDK1 nucleates T cell receptor-induced signaling complex for NF-kappaB activation. *Science*, *308*, 114-118.

Lehours,P., Menard,A., Dupouy,S., Bergey,B., Richy,F., Zerbib,F., Ruskone-Fourmestraux,A., Delchier,J.C., Megraud,F. (2004) Evaluation of the association of nine *Helicobacter pylori* virulence factors with strains involved in low-grade gastric mucosa-associated lymphoid tissue lymphoma. *Infect.Immun.*, *72*, 880-888.

Lenz,G., Davis,R.E., Ngo,V.N., Lam,L., George,T.C., Wright,G.W., Dave,S.S., Zhao,H., Xu,W., Rosenwald,A., Ott,G., Muller-Hermelink,H.K., Gascoyne,R.D., Connors,J.M., Rimsza,L.M., Campo,E., Jaffe,E.S., Delabie,J., Smeland,E.B., Fisher,R.I., Chan,W.C., Staudt,L.M. (2008) Oncogenic CARD11 mutations in human diffuse large B cell lymphoma. *Science*, *319*, 1676-1679.

Lette,G. & Rioux,J.D. (2008) Autoimmune diseases: insights from genome-wide association studies. *Hum.Mol.Genet.*, *17*, R116-R121.

Levy,M., Copie-Bergman,C., Gameiro,C., Chaumette,M.T., Delfau-Larue,M.H., Haioun,C., Charachon,A., Hemery,F., Gaulard,P., Leroy,K., Delchier,J.C. (2005) Prognostic value of translocation t(11;18) in tumoral response of low-grade gastric lymphoma of mucosa-associated lymphoid tissue type to oral chemotherapy. *J.Clin.Oncol.*, *23*, 5061-5066.

Li,C., Inagaki,H., Kuo,T.T., Hu,S., Okabe,M., Eimoto,T. (2003) Primary cutaneous marginal zone B-cell lymphoma: a molecular and clinicopathologic study of 24 asian cases. *Am.J.Surg.Pathol.*, *27*, 1061-1069.

Li,Q. & Verma,I.M. (2002) NF-kappaB regulation in the immune system. *Nat.Rev.Immunol.*, *2*, 725-734.

Li,W.Z. & Karin,M. (2006) NF-kB Signal Transduction by IKK Complexes. *NF-kB/Rel Transcription Factor Family* (ed. by Hsiou-Chi Liou), pp. 12-19. Springer science and business media, New York.

Li,Y., Sedwick,C.E., Hu,J., Altman,A. (2005) Role for protein kinase Ctheta (PKCtheta) in TCR/CD28-mediated signaling through the canonical but not the non-canonical pathway for NF-kappaB activation. *J.Biol.Chem.*, *280*, 1217-1223.

Li,Z., Wang,H., Xue,L., Shin,D.M., Roopenian,D., Xu,W., Qi,C.F., Sangster,M.Y., Orihuela,C.J., Tuomanen,E., Rehg,J.E., Cui,X., Zhang,Q., Morse,H.C., III, Morris,S.W. (2009) Emu-BCL10 mice exhibit constitutive activation of both canonical and noncanonical NF-kappaB pathways generating marginal zone (MZ) B-cell expansion as a precursor to splenic MZ lymphoma. *Blood*, *114*, 4158-4168.

Lin,X. & Wang,D. (2004) The roles of CARMA1, Bcl10, and MALT1 in antigen receptor signaling. *Semin.Immunol.*, *16*, 429-435.

Liu,H., Hamoudi,R.A., Ye,H., Ruskone-Fourmesttraux,A., Dogan,A., Isaacson,P.G., Du,M.Q. (2004a) t(11;18)(q21;q21) of mucosa-associated lymphoid tissue lymphoma results from illegitimate non-homologous end joining following double strand breaks. *Br.J.Haematol.*, *125*, 318-329.

Liu,H., Huang,X., Zhang,Y., Ye,H., Hamidi,A.E., Kocjan,G., Dogan,A., Isaacson,P.G., Du,M.Q. (2002a) Archival fixed histologic and cytologic specimens including stained and unstained materials are amenable to RT-PCR. *Diagn.Mol.Pathol.*, *11*, 222-227.

Liu,H., Ruskon-Fourmesttraux,A., Lavergne-Slove,A., Ye,H., Molina,T., Bouhnik,Y., Hamoudi,R.A., Diss,T.C., Dogan,A., Megraud,F., Rambaud,J.C., Du,M.Q., Isaacson,P.G. (2001a) Resistance of t(11;18) positive gastric mucosa-associated lymphoid tissue lymphoma to *Helicobacter pylori* eradication therapy. *Lancet*, *357*, 39-40.

Liu,H., Ye,H., Dogan,A., Ranaldi,R., Hamoudi,R.A., Bearzi,I., Isaacson,P.G., Du,M.Q. (2001b) T(11;18)(q21;q21) is associated with advanced mucosa-associated lymphoid tissue lymphoma that expresses nuclear BCL10. *Blood*, *98*, 1182-1187.

Liu,H., Ye,H., Ruskone-Fourmesttraux,A., de Jong,D., Pileri,S., Thiede,C., Lavergne,A., Boot,H., Caletti,G., Wundisch,T., Molina,T., Taal,B.G., Elena,S., Thomas,T., Zinzani,P.L., Neubauer,A., Stolte,M., Hamoudi,R.A., Dogan,A., Isaacson,P.G., Du,M.Q. (2002b) T(11;18) is a marker for all stage gastric MALT lymphomas that will not respond to *H. pylori* eradication. *Gastroenterology*, *122*, 1286-1294.

Liu,Y., Dong,W., Chen,L., Zhang,P., Qi,Y. (2004b) Characterization of Bcl10 as a potential transcriptional activator that interacts with general transcription factor TFIIB. *Biochem.Biophys.Res.Commun.*, *320*, 1-6.

Liu,Y., Dong,W., Chen,L., Zhang,P., Qi,Y. (2004c) Characterization of Bcl10 as a potential transcriptional activator that interacts with general transcription factor TFIIB. *Biochem.Biophys.Res.Commun.*, *320*, 1-6.

Liu,Y., Dong,W., Chen,L., Zhang,P., Qi,Y. (2004d) Characterization of Bcl10 as a potential transcriptional activator that interacts with general transcription factor TFIIB. *Biochem.Biophys.Res.Commun.*, *320*, 1-6.

Lockhart,D.J., Dong,H., Byrne,M.C., Follettie,M.T., Gallo,M.V., Chee,M.S., Mittmann,M., Wang,C., Kobayashi,M., Horton,H., Brown,E.L. (1996) Expression monitoring by hybridization to high-density oligonucleotide arrays. *Nat.Biotechnol.*, *14*, 1675-1680.

Loetscher,P., Seitz,M., Baggiolini,M., Moser,B. (1996) Interleukin-2 regulates CC chemokine receptor expression and chemotactic responsiveness in T lymphocytes. *J.Exp.Med.*, *184*, 569-577.

Lopez-Cabrera,M., Munoz,E., Blazquez,M.V., Ursa,M.A., Santis,A.G., Sanchez-Madrid,F. (1995) Transcriptional regulation of the gene encoding the human C-type lectin leukocyte receptor AIM/CD69 and functional characterization of its tumor necrosis factor-alpha-responsive elements. *J.Biol.Chem.*, *270*, 21545-21551.

- Lopez-Giral,S., Quintana,N.E., Cabrerizo,M., Alfonso-Perez,M., Sala-Valdes,M., De Soria,V.G., Fernandez-Ranada,J.M., Fernandez-Ruiz,E., Munoz,C. (2004) Chemokine receptors that mediate B cell homing to secondary lymphoid tissues are highly expressed in B cell chronic lymphocytic leukemia and non-Hodgkin lymphomas with widespread nodular dissemination. *J.Leukoc.Biol.*, *76*, 462-471.
- Macintyre,E., Willerford,D., Morris,S.W. (2000) Non-Hodgkin's Lymphoma: Molecular Features of B Cell Lymphoma. *Hematology.Am.Soc.Hematol.Educ.Program.*, 180-204.
- Maeda,S. & Mentis,A.F. (2007) Pathogenesis of *Helicobacter pylori* infection. *Helicobacter*, *12 Suppl 1:10-4.*, 10-14.
- Maes,B., Demunter,A., Peeters,B., Wolf-Peeters,C. (2002) BCL10 mutation does not represent an important pathogenic mechanism in gastric MALT-type lymphoma, and the presence of the API2-MLT fusion is associated with aberrant nuclear BCL10 expression. *Blood*, *99*, 1398-1404.
- Maneva,A.I., Sirakov,L.M., Manev,V.V. (1983) Lactoferrin binding to neutrophilic polymorphonuclear leucocytes. *Int.J.Biochem.*, *15*, 981-984.
- Mannick,E.E., Schurr,J.R., Zapata,A., Lentz,J.J., Gastanaduy,M., Cote,R.L., Delgado,A., Correa,P., Correa,H. (2004) Gene expression in gastric biopsies from patients infected with *Helicobacter pylori*. *Scand.J.Gastroenterol.*, *39*, 1192-1200.
- Marko,N.F., Frank,B., Quackenbush,J., Lee,N.H. (2005) A robust method for the amplification of RNA in the sense orientation. *BMC Genomics*, *6*, 27.
- Marshall,B.J. & Warren,J.R. (1984) Unidentified curved bacilli in the stomach of patients with gastritis and peptic ulceration. *Lancet*, *1*, 1311-1315.
- Mason,D.Y. & Taylor,C.R. (1978) Distribution of transferrin, ferritin, and lactoferrin in human tissues. *J.Clin.Pathol.*, *31*, 316-327.
- Matsumoto,R., Wang,D., Blonska,M., Li,H., Kobayashi,M., Pappu,B., Chen,Y., Wang,D., Lin,X. (2005) Phosphorylation of CARMA1 plays a critical role in T Cell receptor-mediated NF-kappaB activation. *Immunity*, *23*, 575-585.
- McNamara,D. & El Omar,E. (2008) *Helicobacter pylori* infection and the pathogenesis of gastric cancer: a paradigm for host-bacterial interactions. *Dig.Liver Dis.*, *40*, 504-509.
- Mestecky,J., Russell,M.W., Elson,C.O. (1999) Intestinal IgA: novel views on its function in the defence of the largest mucosal surface. *Gut*, *44*, 2-5.
- Montalban,C. & Norman,F. (2006) Treatment of gastric mucosa-associated lymphoid tissue lymphoma: *Helicobacter pylori* eradication and beyond. *Expert.Rev.Anticancer Ther.*, *6*, 361-371.

- Mootha,V.K., Lindgren,C.M., Eriksson,K.F., Subramanian,A., Sihag,S., Lehar,J., Puigserver,P., Carlsson,E., Ridderstrale,M., Laurila,E., Houstis,N., Daly,M.J., Patterson,N., Mesirov,J.P., Golub,T.R., Tamayo,P., Spiegelman,B., Lander,E.S., Hirschhorn,J.N., Altshuler,D., Groop,L.C. (2003) PGC-1alpha-responsive genes involved in oxidative phosphorylation are coordinately downregulated in human diabetes. *Nat.Genet.*, *34*, 267-273.
- Morente,M., Piris,M.A., Orradre,J.L., Rivas,C., Villuendas,R. (1992) Human tonsil intraepithelial B cells: a marginal zone-related subpopulation. *J.Clin.Pathol.*, *45*, 668-672.
- Morgner,A., Miehle,S., Fischbach,W., Schmitt,W., Muller-Hermelink,H., Greiner,A., Thiede,C., Schetelig,J., Neubauer,A., Stolte,M., Ehninger,G., Bayerdorffer,E. (2001) Complete remission of primary high-grade B-cell gastric lymphoma after cure of *Helicobacter pylori* infection. *J.Clin.Oncol.*, *19*, 2041-2048.
- Morgner,A., Schmelz,R., Thiede,C., Stolte,M., Miehle,S. (2007) Therapy of gastric mucosa associated lymphoid tissue lymphoma. *World J.Gastroenterol.*, *13*, 3554-3566.
- Morris,S.W. (2001) American Society of Hematology, Washington. (Abstract).*American Society of Hematology Education Program Book*, 191-204.
- Morton,L.M., Wang,S.S., Cozen,W., Linet,M.S., Chatterjee,N., Davis,S., Severson,R.K., Colt,J.S., Vasef,M.A., Rothman,N., Blair,A., Bernstein,L., Cross,A.J., De Roos,A.J., Engels,E.A., Hein,D.W., Hill,D.A., Kelemen,L.E., Lim,U., Lynch,C.F., Schenk,M., Wacholder,S., Ward,M.H., Hoar,Z.S., Chanock,S.J., Cerhan,J.R., Hartge,P. (2008) Etiologic heterogeneity among non-Hodgkin lymphoma subtypes. *Blood*, *112*, 5150-5160.
- Moser,B. & Loetscher,P. (2001) Lymphocyte traffic control by chemokines. *Nat.Immunol.*, *2*, 123-128.
- Mulder,M.M., Heddema,E.R., Pannekoek,Y., Faridpooya,K., Oud,M.E., Schilder-Tol,E., Saeed,P., Pals,S.T. (2006) No evidence for an association of ocular adnexal lymphoma with *Chlamydia psittaci* in a cohort of patients from the Netherlands. *Leuk.Res.*, *30*, 1305-1307.
- Murdoch,C. & Finn,A. (2000) Chemokine receptors and their role in inflammation and infectious diseases. *Blood*, *95*, 3032-3043.
- Murphy,P.M., Baggiolini,M., Charo,I.F., Hebert,C.A., Horuk,R., Matsushima,K., Miller,L.H., Oppenheim,J.J., Power,C.A. (2000) International union of pharmacology. XXII. Nomenclature for chemokine receptors. *Pharmacol.Rev.*, *52*, 145-176.
- Nakagawa,M., Hosokawa,Y., Yonezumi,M., Izumiyama,K., Suzuki,R., Tsuzuki,S., Asaka,M., Seto,M. (2005) MALT1 contains nuclear export signals and regulates cytoplasmic localization of BCL10. *Blood*, *106*, 4210-4216.
- Negrini,R., Savio,A., Poiesi,C., Appelmelk,B.J., Buffoli,F., Paterlini,A., Cesari,P., Graffeo,M., Vaira,D., Franzin,G. (1996) Antigenic mimicry between *Helicobacter pylori* and gastric mucosa in the pathogenesis of body atrophic gastritis. *Gastroenterology*, *111*, 655-665.

Nelson,D.E., Ihekweba,A.E., Elliott,M., Johnson,J.R., Gibney,C.A., Foreman,B.E., Nelson,G., See,V., Horton,C.A., Spiller,D.G., Edwards,S.W., McDowell,H.P., Unitt,J.F., Sullivan,E., Grimley,R., Benson,N., Broomhead,D., Kell,D.B., White,M.R. (2004) Oscillations in NF-kappaB signaling control the dynamics of gene expression. *Science*, *30*, 704-708.

NHL Lymphoma Classification Project (1997) A clinical evaluation of the International Lymphoma Study Group classification of non-Hodgkin's lymphoma. The Non-Hodgkin's Lymphoma Classification Project. *Blood*, *89*, 3909-3918.

Nie,Y., Waite,J., Brewer,F., Sunshine,M.J., Littman,D.R., Zou,Y.R. (2004) The role of CXCR4 in maintaining peripheral B cell compartments and humoral immunity. *J.Exp.Med.*, *200*, 1145-1156.

Nieters,A., Beckmann,L., Deeg,E., Becker,N. (2006) Gene polymorphisms in Toll-like receptors, interleukin-10, and interleukin-10 receptor alpha and lymphoma risk. *Genes Immun.*, *7*, 615-624.

Novak,A., Akasaka,T., Manske,M., Gupta,M., Witzig,T., Dyer,M., Dogan,A., Remstein,E., & Ansell,S. (2008) Elevated expression of GPR34 and its association with a novel translocation t(X;14)(p11;q32) involving IgHs and GPR34 in MALT Lymphoma. (Abstract).*American Society of Haematology*.

Novak,U., Rinaldi,A., Kwee,I., Nandula,S.V., Rancoita,P.M., Compagno,M., Cerri,M., Rossi,D., Murty,V.V., Zucca,E., Gaidano,G., Dalla-Favera,R., Pasqualucci,L., Bhagat,G., Bertoni,F. (2009) The NF- κ B negative regulator TNFAIP3 (A20) is inactivated by somatic mutations and genomic deletions in marginal zone lymphomas. *Blood*, *113*, 4918-4921.

O'Rourke,J.L. (2008) Gene expression profiling in Helicobacter-induced MALT lymphoma with reference to antigen drive and protective immunization. *J.Gastroenterol.Hepatol.*, *23 Suppl 2:S151-6.*, S151-S156.

Oeckinghaus,A., Wegener,E., Welteke,V., Ferch,U., Arslan,S.C., Ruland,J., Scheidereit,C., Krappmann,D. (2007) Malt1 ubiquitination triggers NF-kappaB signaling upon T-cell activation. *EMBO J.*, *26*, 4634-4645.

Ohmae,T., Hirata,Y., Maeda,S., Shibata,W., Yanai,A., Ogura,K., Yoshida,H., Kawabe,T., Omata,M. (2005) Helicobacter pylori activates NF-kappaB via the alternative pathway in B lymphocytes. *J.Immunol.*, *175*, 7162-7169.

Okabe,M., Inagaki,H., Ohshima,K., Yoshino,T., Li,C., Eimoto,T., Ueda,R., Nakamura,S. (2003) API2-MALT1 fusion defines a distinctive clinicopathologic subtype in pulmonary extranodal marginal zone B-cell lymphoma of mucosa-associated lymphoid tissue. *Am.J.Pathol.*, *162*, 1113-1122.

Okada,T., Ngo,V.N., Ekland,E.H., Forster,R., Lipp,M., Littman,D.R., Cyster,J.G. (2002) Chemokine requirements for B cell entry to lymph nodes and Peyer's patches. *J.Exp.Med.*, *196*, 65-75.

Ortutay,C. & Vihinen,M. (2006) Immunome: a reference set of genes and proteins for systems biology of the human immune system. *Cell Immunol.*, *244*, 87-89.

Ortutay,C. & Vihinen,M. (2009) Immunome knowledge base (IKB): an integrated service for immunome research. *BMC.Immunol.*, *10:3.*, 3.

Otake,Y., Soundararajan,S., Sengupta,T.K., Kio,E.A., Smith,J.C., Pineda-Roman,M., Stuart,R.K., Spicer,E.K., Fernandes,D.J. (2007) Overexpression of nucleolin in chronic lymphocytic leukemia cells induces stabilization of bcl2 mRNA. *Blood*, *109*, 3069-3075.

Pahl,H.L. (1999) Activators and target genes of Rel/NF-kappaB transcription factors. *Oncogene*, *18*, 6853-6866.

Park,S.G., Schulze-Luehrman,J., Hayden,M.S., Hashimoto,N., Ogawa,W., Kasuga,M., Ghosh,S. (2009) The kinase PDK1 integrates T cell antigen receptor and CD28 coreceptor signaling to induce NF-kappaB and activate T cells. *Nat.Immunol.*, *10*, 158-166.

Parveen,T., Navarro-Roman,L., Medeiros,L.J., Raffeld,M., Jaffe,E.S. (1993) Low-grade B-cell lymphoma of mucosa-associated lymphoid tissue arising in the kidney. *Arch.Pathol.Lab Med.*, *117*, 780-783.

Perkins,N.D. (2006) Post-translational modifications regulating the activity and function of the nuclear factor kappa B pathway. *Oncogene*, *25*, 6717-6730.

Perkins,N.D. (2007) Integrating cell-signalling pathways with NF-kappaB and IKK function. *Nat.Rev.Mol.Cell Biol.*, *8*, 49-62.

Pernis,A.B. (2002) The role of IRF-4 in B and T cell activation and differentiation. *J.Interferon Cytokine Res.*, *22*, 111-120.

Phelps,C.B., Sengchanthalangsy,L.L., Huxford,T., Ghosh,G. (2000) Mechanism of I kappa B alpha binding to NF-kappa B dimers. *J.Biol.Chem.*, *275*, 29840-29846.

Pijpe,J., van Imhoff,G.W., Spijkervet,F.K., Roodenburg,J.L., Wolbink,G.J., Mansour,K., Vissink,A., Kallenberg,C.G., Bootsma,H. (2005) Rituximab treatment in patients with primary Sjogren's syndrome: an open-label phase II study. *Arthritis Rheum.*, *52*, 2740-2750.

Pongpruttipan,T., Sitthinamsuwan,P., Rungkaew,P., Ruangchira-urai,R., Vongjirad,A., Sukpanichnant,S. (2007) Pitfalls in classifying lymphomas. *J.Med.Assoc.Thai.*, *90*, 1129-1136.

Prinz,C., Hafsi,N., Volland,P. (2003) Helicobacter pylori virulence factors and the host immune response: implications for therapeutic vaccination. *Trends Microbiol.*, *11*, 134-138.

Rabkin,C.S., Yang,Q., Goedert,J.J., Nguyen,G., Mitsuya,H., Sei,S. (1999) Chemokine and chemokine receptor gene variants and risk of non-Hodgkin's lymphoma in human immunodeficiency virus-1-infected individuals. *Blood*, *93*, 1838-1842.

Rahn,W. Molecular analysis of *Helicobacter pylori*-associated gastric inflammation in chronically infected and immune mice. Dr.med dissertation , 36. 2003.

Raphael,G.D., Jeney,E.V., Baraniuk,J.N., Kim,I., Meredith,S.D., Kaliner,M.A. (1989) Pathophysiology of rhinitis. Lactoferrin and lysozyme in nasal secretions. J.Clin.Invest., 84, 1528-1535.

Raychaudhuri,S., Stuart,J.M., Altman,R.B. (2000) Principal components analysis to summarize microarray experiments: application to sporulation time series. Pac.Symp.Biocomput., 455-466.

Reed,D. (1902) On the pathological changes in Hodgkin's disease, with special reference to its relation to tuberculosis. Johns Hopkins Hospital Report, 10, 133-196.

Reif,K., Ekland,E.H., Ohl,L., Nakano,H., Lipp,M., Forster,R., Cyster,J.G. (2002) Balanced responsiveness to chemoattractants from adjacent zones determines B-cell position. Nature, 416, 94-99.

Remstein,E.D., Dogan,A., Einerson,R.R., Paternoster,S.F., Fink,S.R., Law,M., Dewald,G.W., Kurtin,P.J. (2006) The incidence and anatomic site specificity of chromosomal translocations in primary extranodal marginal zone B-cell lymphoma of mucosa-associated lymphoid tissue (MALT lymphoma) in North America. Am.J.Surg.Pathol., 30, 1546-1553.

Remstein,E.D., Kurtin,P.J., James,C.D., Wang,X.Y., Meyer,R.G., Dewald,G.W. (2002) Mucosa-associated lymphoid tissue lymphomas with t(11;18)(q21;q21) and mucosa-associated lymphoid tissue lymphomas with aneuploidy develop along different pathogenetic pathways. Am.J.Pathol., 161, 63-71.

Rhodes,D.R., Kalyana-Sundaram,S., Mahavisno,V., Varambally,R., Yu,J., Briggs,B.B., Barrette,T.R., Anstet,M.J., Kincead-Beal,C., Kulkarni,P., Varambally,S., Ghosh,D., Chinnaiyan,A.M. (2007) Oncomine 3.0: genes, pathways, and networks in a collection of 18,000 cancer gene expression profiles. Neoplasia., 9, 166-180.

Rosebeck,S., Madden,L., Jin,X., Gu,S., Apel,I.J., Appert,A., Hamoudi,R.A., Noels,H., Sagaert,X., Van Loo,P., Baens,M., Du,M.Q., Lucas,P.C., McAllister-Lucas,L.M. (2011) Cleavage of NIK by the API2-MALT1 fusion oncoprotein leads to noncanonical NF-kappaB activation. Science., 331, 468-472.

Rossmann,J.S., Stoicheva,N.G., Langel,F.D., Patterson,G.H., Lippincott-Schwartz,J., Schaefer,B.C. (2006) POLKADOTS are foci of functional interactions in T-Cell receptor-mediated signaling to NF-kappaB. Mol.Biol.Cell., 17, 2166-2176.

Roy,N., Deveraux,Q.L., Takahashi,R., Salvesen,G.S., Reed,J.C. (1997) The c-IAP-1 and c-IAP-2 proteins are direct inhibitors of specific caspases. EMBO J., 16, 6914-6925.

Rubtsov,A.V., Swanson,C.L., Troy,S., Strauch,P., Pelanda,R., Torres,R.M. (2008) TLR agonists promote marginal zone B cell activation and facilitate T-dependent IgM responses. J.Immunol., 180, 3882-3888.

Ruland,J., Duncan,G.S., Elia,A., del,B.B., I, Nguyen,L., Plyte,S., Millar,D.G., Bouchard,D., Wakeham,A., Ohashi,P.S., Mak,T.W. (2001) Bcl10 is a positive regulator of antigen receptor-induced activation of NF-kappaB and neural tube closure. *Cell*, *104*, 33-42.

Ruskone-Fourmesttraux,A., Lavergne,A., Aegerter,P.H., Megraud,F., Palazzo,L., de Mascarel,A., Molina,T., Rambaud,J.L. (2001) Predictive factors for regression of gastric MALT lymphoma after anti-Helicobacter pylori treatment. *Gut*, *48*, 297-303.

Sackmann,M., Morgner,A., Rudolph,B., Neubauer,A., Thiede,C., Schulz,H., Kraemer,W., Boersch,G., Rohde,P., Seifert,E., Stolte,M., Bayerdoerffer,E. (1997) Regression of gastric MALT lymphoma after eradication of Helicobacter pylori is predicted by endosonographic staging. MALT Lymphoma Study Group. *Gastroenterology*, *113*, 1087-1090.

Sagaert,X., de Paepe,P., Libbrecht,L., Vanhentenrijk,V., Verhoef,G., Thomas,J., Wlodarska,I., Wolf-Peeters,C. (2006a) Forkhead box protein P1 expression in mucosa-associated lymphoid tissue lymphomas predicts poor prognosis and transformation to diffuse large B-cell lymphoma. *J.Clin.Oncol.*, *24*, 2490-2497.

Sagaert,X., Theys,T., Wolf-Peeters,C., Marynen,P., Baens,M. (2006b) Splenic marginal zone lymphoma-like features in API2-MALT1 transgenic mice that are exposed to antigenic stimulation. *Haematologica*, *91*, 1693-1696.

Sagaert,X., Wolf-Peeters,C., Noels,H., Baens,M. (2007) The pathogenesis of MALT lymphomas: where do we stand? *Leukemia*, *21*, 389-396.

Sancho,D., Gomez,M., Sanchez-Madrid,F. (2005) CD69 is an immunoregulatory molecule induced following activation. *Trends Immunol.*, *26*, 136-140.

Saxena,V., Orgill,D., Kohane,I. (2006) Absolute enrichment: gene set enrichment analysis for homeostatic systems. *Nucleic Acids Res.*, *34*, e151.

Schechter,N.R. & Yahalom,J. (2000) Low-grade MALT lymphoma of the stomach: a review of treatment options. *Int.J.Radiat.Oncol.Biol.Phys.*, *46*, 1093-1103.

Schena,M., Shalon,D., Davis,R.W., Brown,P.O. (1995) Quantitative monitoring of gene expression patterns with a complementary DNA microarray. *Science*, *270*, 467-470.

Schneider,U., Schwenk,H.U., Bornkamm,G. (1977) Characterization of EBV-genome negative "null" and "T" cell lines derived from children with acute lymphoblastic leukemia and leukemic transformed non-Hodgkin lymphoma. *Int.J.Cancer.*, *19*, 621-626.

Sen,R. & Baltimore,D. (1986) Multiple nuclear factors interact with the immunoglobulin enhancer sequences. *Cell*, *46*, 705-716.

Shaffer,A.L., Emre,N.C., Lamy,L., Ngo,V.N., Wright,G., Xiao,W., Powell,J., Dave,S., Yu,X., Zhao,H., Zeng,Y., Chen,B., Epstein,J., Staudt,L.M. (2008) IRF4 addiction in multiple myeloma. *Nature.*, *454*, 226-231.

Shambharkar,P.B., Blonska,M., Pappu,B.P., Li,H., You,Y., Sakurai,H., Darnay,B.G., Hara,H., Penninger,J., Lin,X. (2007) Phosphorylation and ubiquitination of the IkappaB kinase complex by two distinct signaling pathways. *EMBO J.*, *26*, 1794-1805.

Shimizu,T., Kida,Y., Kuwano,K. (2007) Triacylated lipoproteins derived from *Mycoplasma pneumoniae* activate nuclear factor-kappaB through toll-like receptors 1 and 2. *Immunology*, *121*, 473-483.

Shinohara,H., Yasuda,T., Aiba,Y., Sanjo,H., Hamadate,M., Watarai,H., Sakurai,H., Kurosaki,T. (2005) PKC beta regulates BCR-mediated IKK activation by facilitating the interaction between TAK1 and CARMA1. *J.Exp.Med.*, *202*, 1423-1431.

Shiow,L.R., Rosen,D.B., Brdickova,N., Xu,Y., An,J., Lanier,L.L., Cyster,J.G., Matloubian,M. (2006) CD69 acts downstream of interferon-alpha/beta to inhibit S1P1 and lymphocyte egress from lymphoid organs. *Nature*, *440*, 540-544.

Shipp,M.A., Ross,K.N., Tamayo,P., Weng,A.P., Kutok,J.L., Aguiar,R.C., Gaasenbeek,M., Angelo,M., Reich,M., Pinkus,G.S., Ray,T.S., Koval,M.A., Last,K.W., Norton,A., Lister,T.A., Mesirov,J., Neuberg,D.S., Lander,E.S., Aster,J.C., Golub,T.R. (2002) Diffuse large B-cell lymphoma outcome prediction by gene-expression profiling and supervised machine learning. *Nat.Med.*, *8*, 68-74.

Si,Y., Tsou,C.L., Croft,K., Charo,I.F. (2010) CCR2 mediates hematopoietic stem and progenitor cell trafficking to sites of inflammation in mice. *J.Clin.Invest.*, *120*, 1192-1203.

Smedby,K.E., Baecklund,E., Askling,J. (2006) Malignant lymphomas in autoimmunity and inflammation: a review of risks, risk factors, and lymphoma characteristics. *Cancer Epidemiol.Biomarkers Prev.*, *15*, 2069-2077.

Smith,W.J., Price,S.K., Isaacson,P.G. (1987) Immunoglobulin gene rearrangement in immunoproliferative small intestinal disease (IPSID). *J.Clin.Pathol.*, *40*, 1291-1297.

Smoot,D.T. (1997) How does *Helicobacter pylori* cause mucosal damage? Direct mechanisms. *Gastroenterology*, *113*, S31-S34.

Sommer,K., Guo,B., Pomerantz,J.L., Bandaranayake,A.D., Moreno-Garcia,M.E., Ovechkina,Y.L., Rawlings,D.J. (2005) Phosphorylation of the CARMA1 linker controls NF-kappaB activation. *Immunity*, *23*, 561-574.

Sozzani,S., Ghezzi,S., Iannolo,G., Luini,W., Borsatti,A., Polentarutti,N., Sica,A., Locati,M., Mackay,C., Wells,T.N., Biswas,P., Vicenzi,E., Poli,G., Mantovani,A. (1998) Interleukin 10 increases CCR5 expression and HIV infection in human monocytes. *J.Exp.Med.*, *187*, 439-444.

Spencer,J., Finn,T., Pulford,K.A., Mason,D.Y., Isaacson,P.G. (1985) The human gut contains a novel population of B lymphocytes which resemble marginal zone cells. *Clin.Exp.Immunol.*, *62*, 607-612.

- Springael,J.Y., Urizar,E., Parmentier,M. (2005) Dimerization of chemokine receptors and its functional consequences. *Cytokine Growth Factor Rev.*, *16*, 611-623.
- Stangegaard,M., Dufva,I.H., Dufva,M. (2006) Reverse transcription using random pentadecamer primers increases yield and quality of resulting cDNA. *Biotechniques*, *40*, 649-657.
- Starostik,P., Patzner,J., Greiner,A., Schwarz,S., Kalla,J., Ott,G., Muller-Hermelink,H.K. (2002) Gastric marginal zone B-cell lymphomas of MALT type develop along 2 distinct pathogenetic pathways. *Blood*, *99*, 3-9.
- Steinitz,M. & Klein,G. (1975) Comparison between growth characteristics of an Epstein--Barr virus (EBV)-genome-negative lymphoma line and its EBV-converted subline in vitro. *Proc.Natl.Acad.Sci.*, *72*, 3518-3520.
- Stilo,R., Liguoro,D., Di Jeso,B., Formisano,S., Consiglio,E., Leonardi,A., Vito,P. (2004) Physical and functional interaction of CARMA1 and CARMA3 with Ikappa kinase gamma-NFkappaB essential modulator. *J.Biol.Chem.*, *279*, 34323-34331.
- Stolte,M., Bayerdorffer,E., Morgner,A., Alpen,B., Wundisch,T., Thiede,C., Neubauer,A. (2002) Helicobacter and gastric MALT lymphoma. *Gut*, *50 Suppl 3:III19-24.*, III19-III24.
- Stolte,M. & Eidt,S. (1989) Lymphoid follicles in antral mucosa: immune response to *Campylobacter pylori*? *J.Clin.Pathol.*, *42*, 1269-1271.
- Streubel,B., Lamprecht,A., Dierlamm,J., Cerroni,L., Stolte,M., Ott,G., Raderer,M., Chott,A. (2003) T(14;18)(q32;q21) involving IGH and MALT1 is a frequent chromosomal aberration in MALT lymphoma. *Blood*, *101*, 2335-2339.
- Streubel,B., Seitz,G., Stolte,M., Birner,P., Chott,A., Raderer,M. (2006) MALT lymphoma associated genetic aberrations occur at different frequencies in primary and secondary intestinal MALT lymphomas. *Gut*, *55*, 1581-1585.
- Streubel,B., Simonitsch-Klupp,I., Mullauer,L., Lamprecht,A., Huber,D., Siebert,R., Stolte,M., Trautinger,F., Lukas,J., Puspok,A., Formanek,M., Assanasen,T., Muller-Hermelink,H.K., Cerroni,L., Raderer,M., Chott,A. (2004) Variable frequencies of MALT lymphoma-associated genetic aberrations in MALT lymphomas of different sites. *Leukemia*, *18*, 1722-1726.
- Streubel,B., Vinatzer,U., Lamprecht,A., Raderer,M., Chott,A. (2005) T(3;14)(p14.1;q32) involving IGH and FOXP1 is a novel recurrent chromosomal aberration in MALT lymphoma. *Leukemia*, *19*, 652-658.
- Su,H., Bidere,N., Zheng,L., Cubre,A., Sakai,K., Dale,J., Salmena,L., Hakem,R., Straus,S., Lenardo,M. (2005) Requirement for caspase-8 in NF-kappaB activation by antigen receptor. *Science*, *307*, 1465-1468.

Subramanian,A., Tamayo,P., Mootha,V.K., Mukherjee,S., Ebert,B.L., Gillette,M.A., Paulovich,A., Pomeroy,S.L., Golub,T.R., Lander,E.S., Mesirov,J.P. (2005) Gene set enrichment analysis: a knowledge-based approach for interpreting genome-wide expression profiles. *Proc.Natl.Acad.Sci.*, *102*, 15545-15550.

Sun,L., Deng,L., Ea,C.K., Xia,Z.P., Chen,Z.J. (2004) The TRAF6 ubiquitin ligase and TAK1 kinase mediate IKK activation by BCL10 and MALT1 in T lymphocytes. *Mol.Cell.*, *14*, 289-301.

Sun,S.C., Ganchi,P.A., Ballard,D.W., Greene,W.C. (1993) NF-kappa B controls expression of inhibitor I kappa B alpha: evidence for an inducible autoregulatory pathway. *Science*, *259*, 1912-1915.

Suyang,H., Phillips,R., Douglas,I., Ghosh,S. (1996) Role of unphosphorylated, newly synthesized I kappa B beta in persistent activation of NF-kappa B. *Mol.Cell Biol.*, *16*, 5444-5449.

Swerdlow,S.H., Campo,E., Harris,N.L., Jaffe,E.S., Pileri,S.A., Stein,H., Thiele,J., & Vardiman,J.W. (2008) *WHO Classification of tumours of haematopoietic and lymphoid tissues*, 4 edn, pp. 1-439.

Takeda,K., Kaisho,T., Akira,S. (2003) Toll-like receptors. *Annu.Rev.Immunol.*, *21*:335-76. *Epub; %2001 Dec; %19.*, 335-376.

Takeuchi,O., Kawai,T., Muhlratt,P.F., Morr,M., Radolf,J.D., Zychlinsky,A., Takeda,K., Akira,S. (2001) Discrimination of bacterial lipoproteins by Toll-like receptor 6. *Int.Immunol.*, *13*, 933-940.

Talal,N., Sokoloff,L., Barth,W.F. (1967) Extrasalivary lymphoid abnormalities in Sjogren's syndrome (reticulum cell sarcoma, "pseudolymphoma," macroglobulinemia). *Am.J.Med.*, *43*, 50-65.

Tamayo,P., Slonim,D., Mesirov,J., Zhu,Q., Kitareewan,S., Dmitrovsky,E., Lander,E.S., Golub,T.R. (1999) Interpreting patterns of gene expression with self-organizing maps: methods and application to hematopoietic differentiation. *Proc.Natl.Acad.Sci.*, *96*, 2907-2912.

The Tumor Analysis Best Practices Working Group (2004) Expression profiling--best practices for data generation and interpretation in clinical trials. *Nat.Rev.Genet.*, *5*, 229-237.

Thieblemont,C., Bastion,Y., Berger,F., Rieux,C., Salles,G., Dumontet,C., Felman,P., Coiffier,B. (1997) Mucosa-associated lymphoid tissue gastrointestinal and nongastrointestinal lymphoma behavior: analysis of 108 patients. *J.Clin.Oncol.*, *15*, 1624-1630.

Thiede,C., Morgner,A., Alpen,B., Wundisch,T., Herrmann,J., Ritter,M., Ehninger,G., Stolte,M., Bayerdorffer,E., Neubauer,A. (1997) What role does *Helicobacter pylori* eradication play in gastric MALT and gastric MALT lymphoma? *Gastroenterology*, *113*, S61-S64.

- Thome,M. (2004) CARMA1, BCL-10 and MALT1 in lymphocyte development and activation. *Nat.Rev.Immunol.*, 4, 348-359.
- Thome,M. (2008) Multifunctional roles for MALT1 in T-cell activation. *Nat.Rev.Immunol.*, 8, 495-500.
- Tian,B., Nowak,D.E., Jamaluddin,M., Wang,S., Brasier,A.R. (2005a) Identification of direct genomic targets downstream of the nuclear factor-kappaB transcription factor mediating tumor necrosis factor signaling. *J.Biol.Chem.*, 280, 17435-17448.
- Tian,M.T., Gonzalez,G., Scheer,B., DeFranco,A.L. (2005b) Bcl10 can promote survival of antigen-stimulated B lymphocytes. *Blood*, 106, 2105-2112.
- Tichopad,A., Dilger,M., Schwarz,G., Pfaffl,M.W. (2003) Standardized determination of real-time PCR efficiency from a single reaction set-up. *Nucleic Acids Res.*, 31, e122.
- Tokunaga,F., Sakata,S., Saeki,Y., Satomi,Y., Kirisako,T., Kamei,K., Nakagawa,T., Kato,M., Murata,S., Yamaoka,S., Yamamoto,M., Akira,S., Takao,T., Tanaka,K., Iwai,K. (2009) Involvement of linear polyubiquitylation of NEMO in NF-kappaB activation. *Nat.Cell Biol.*, 11, 123-132.
- Toualbi-Abed,K., Daniel,F., Guller,M.C., Legrand,A., Mauriz,J.L., Mauviel,A., Bernuau,D. (2008) Jun D cooperates with p65 to activate the proximal kappaB site of the cyclin D1 promoter: role of PI3K/PDK-1. *Carcinogenesis*, 29, 536-543.
- Trentin,L., Cabrelle,A., Facco,M., Carollo,D., Miorin,M., Tosoni,A., Pizzo,P., Binotto,G., Nicolardi,L., Zambello,R., Adami,F., Agostini,C., Semenzato,G. (2004) Homeostatic chemokines drive migration of malignant B cells in patients with non-Hodgkin lymphomas. *Blood*, 104, 502-508.
- Uren,A.G., O'Rourke,K., Aravind,L.A., Pisabarro,M.T., Seshagiri,S., Koonin,E.V., Dixit,V.M. (2000) Identification of paracaspases and metacaspases: two ancient families of caspase-like proteins, one of which plays a key role in MALT lymphoma. *Mol.Cell*, 6, 961-967.
- van Berkel,M.E. & Oosterwegel,M.A. (2006) CD28 and ICOS: similar or separate costimulators of T cells? *Immunol.Lett.*, 105, 115-122.
- Van Gelder,R.N., von Zastrow,M.E., Yool,A., Dement,W.C., Barchas,J.D., Eberwine,J.H. (1990) Amplified RNA synthesized from limited quantities of heterogeneous cDNA. *Proc.Natl.Acad.Sci.*, 87, 1663-1667.
- Van Snick,J.L. & Masson,P.L. (1976) The binding of human lactoferrin to mouse peritoneal cells. *J.Exp.Med.*, 144, 1568-1580.

- Vargas,R.L., Fallone,E., Felgar,R.E., Friedberg,J.W., Arbini,A.A., Andersen,A.A., Rothberg,P.G. (2006) Is there an association between ocular adnexal lymphoma and infection with *Chlamydia psittaci*? The University of Rochester experience. *Leuk.Res.*, *30*, 547-551.
- Vejabhuti,C., Harris,G.J., Erickson,B.A., Nishino,H., Chevez-Barrios,P., Chang,C.C. (2005) BCL10 expression in ocular adnexal lymphomas. *Am.J.Ophthalmol.*, *140*, 836-843.
- Velculescu,V.E., Zhang,L., Vogelstein,B., Kinzler,K.W. (1995) Serial analysis of gene expression. *Science.*, *270*, 484-487.
- Vereecke,L., Beyaert,R., van Loo,G. (2009) The ubiquitin-editing enzyme A20 (TNFAIP3) is a central regulator of immunopathology. *Trends Immunol.*, *30*, 383-391.
- Verstrepen,L., Adib-Conquy,M., Kreike,M., Carpentier,I., Adrie,C., Cavillon,J.M., Beyaert,R. (2008) Expression of the NF-kappaB inhibitor ABIN-3 in response to TNF and toll-like receptor 4 stimulation is itself regulated by NF-kappaB. *J.Cell Mol.Med.*, *12*, 316-329.
- Vinatzer,U., Gollinger,M., Mullauer,L., Raderer,M., Chott,A., Streubel,B. (2008) Mucosa-associated lymphoid tissue lymphoma: novel translocations including rearrangements of ODZ2, JMJD2C, and CNN3. *Clin.Cancer Res.*, *14*, 6426-6431.
- Wagner,S., Carpentier,I., Rogov,V., Kreike,M., Ikeda,F., Lohr,F., Wu,C.J., Ashwell,J.D., Dotsch,V., Dikic,I., Beyaert,R. (2008) Ubiquitin binding mediates the NF-kappaB inhibitory potential of ABIN proteins. *Oncogene*, *27*, 3739-3745.
- Wang,S.S., Cozen,W., Cerhan,J.R., Colt,J.S., Morton,L.M., Engels,E.A., Davis,S., Severson,R.K., Rothman,N., Chanock,S.J., Hartge,P. (2007) Immune mechanisms in non-Hodgkin lymphoma: joint effects of the TNF G308A and IL10 T3575A polymorphisms with non-Hodgkin lymphoma risk factors. *Cancer Res.*, *67*, 5042-5054.
- Wen,S., Felley,C.P., Bouzourene,H., Reimers,M., Michetti,P., Pan-Hammarstrom,Q. (2004) Inflammatory gene profiles in gastric mucosa during *Helicobacter pylori* infection in humans. *J.Immunol.*, *172*, 2595-2606.
- Wen,S., Velin,D., Felley,C.P., Du,L., Michetti,P., Pan-Hammarstrom,Q. (2007) Expression of *Helicobacter pylori* virulence factors and associated expression profiles of inflammatory genes in the human gastric mucosa. *Infect.Immun.*, *75*, 5118-5126.
- Willis,T.G., Jadayel,D.M., Du,M.Q., Peng,H., Perry,A.R., Abdul-Rauf,M., Price,H., Karran,L., Majekodunmi,O., Wlodarska,I., Pan,L., Crook,T., Hamoudi,R., Isaacson,P.G., Dyer,M.J. (1999) Bcl10 is involved in t(1;14)(p22;q32) of MALT B cell lymphoma and mutated in multiple tumor types. *Cell*, *96*, 35-45.
- Wiseman,H. & Halliwell,B. (1996) Damage to DNA by reactive oxygen and nitrogen species: role in inflammatory disease and progression to cancer. *Biochem.J.*, *313*, 17-29.

Wlodarska,I., Veyt,E., de Paepe,P., Vandenberghe,P., Nooijen,P., Theate,I., Michaux,L., Sagaert,X., Marynen,P., Hagemeyer,A., Wolf-Peeters,C. (2005) FOXP1, a gene highly expressed in a subset of diffuse large B-cell lymphoma, is recurrently targeted by genomic aberrations. *Leukemia*, *19*, 1299-1305.

Wlodarska,M., Tousseyn,T., De Leval,L., Finalet Ferreiro,J., Urbankova,H., Michaux,L., Dierickx,D., Wolter,P., Vandenberghe,P., Marynen,P., De Wolf-Peeters,C., & Baens,M. (2009) Novel t(X;14)(p11.4;q32.33) resulting in upregulation of GPR34 and activation of the NF-kB pathway is recurrent in MALT lymphomas. (Abstract).*Haematologica*, **94**, 271-272.

Woo,Y., Affourtit,J., Daigle,S., Viale,A., Johnson,K., Naggert,J., Churchill,G. (2004) A comparison of cDNA, oligonucleotide, and Affymetrix GeneChip gene expression microarray platforms. *J.Biomol.Tech.*, *15*, 276-284.

Wotherspoon,A.C. (1996) Gastric MALT lymphoma and *Helicobacter pylori*. *Yale J.Biol.Med.*, *69*, 61-68.

Wotherspoon,A.C., Doglioni,C., Diss,T.C., Pan,L., Moschini,A., de Boni,M., Isaacson,P.G. (1993) Regression of primary low-grade B-cell gastric lymphoma of mucosa-associated lymphoid tissue type after eradication of *Helicobacter pylori*. *Lancet*, *342*, 575-577.

Wotherspoon,A.C., Ortiz-Hidalgo,C., Falzon,M.R., Isaacson,P.G. (1991) *Helicobacter pylori*-associated gastritis and primary B-cell gastric lymphoma. *Lancet*, *338*, 1175-1176.

Wu,C.J. & Ashwell,J.D. (2008) NEMO recognition of ubiquitinated Bcl10 is required for T cell receptor-mediated NF-kappaB activation. *Proc.Natl.Acad.Sci.*, *105*, 3023-3028.

Wu,C.J., Conze,D.B., Li,T., Srinivasula,S.M., Ashwell,J.D. (2006) Sensing of Lys 63-linked polyubiquitination by NEMO is a key event in NF-kappaB activation [corrected]. *Nat.Cell Biol.*, *8*, 398-406.

Wundisch,T., Neubauer,A., Stolte,M., Ritter,M., Thiede,C. (2003) B-cell monoclonality is associated with lymphoid follicles in gastritis. *Am.J.Surg.Pathol.*, *27*, 882-887.

Wundisch,T., Thiede,C., Morgner,A., Dempfle,A., Gunther,A., Liu,H., Ye,H., Du,M.Q., Kim,T.D., Bayerdorffer,E., Stolte,M., Neubauer,A. (2005) Long-term follow-up of gastric MALT lymphoma after *Helicobacter pylori* eradication. *J.Clin.Oncol.*, *23*, 8018-8024.

Xiang,C.C., Chen,M., Ma,L., Phan,Q.N., Inman,J.M., Kozhich,O.A., Brownstein,M.J. (2003) A new strategy to amplify degraded RNA from small tissue samples for microarray studies. *Nucleic Acids Res.*, *31*, e53.

Xue,L., Morris,S.W., Orihuela,C., Tuomanen,E., Cui,X., Wen,R., Wang,D. (2003) Defective development and function of Bcl10-deficient follicular, marginal zone and B1 B cells. *Nat.Immunol.*, *4*, 857-865.

Yamamoto,K. (2003) Pathogenesis of Sjogren's syndrome. *Autoimmun.Rev.*, *2*, 13-18.

Ye,H., Dogan,A., Karran,L., Willis,T.G., Chen,L., Wlodarska,I., Dyer,M.J., Isaacson,P.G., Du,M.Q. (2000) BCL10 expression in normal and neoplastic lymphoid tissue. Nuclear localization in MALT lymphoma. *Am.J.Pathol.*, 157, 1147-1154.

Ye,H., Gong,L., Liu,H., Hamoudi,R.A., Shirali,S., Ho,L., Chott,A., Streubel,B., Siebert,R., Gesk,S., Martin-Subero,J.I., Radford,J.A., Banerjee,S., Nicholson,A.G., Ranaldi,R., Remstein,E.D., Gao,Z., Zheng,J., Isaacson,P.G., Dogan,A., Du,M.Q. (2005) MALT lymphoma with t(14;18)(q32;q21)/IGH-MALT1 is characterized by strong cytoplasmic MALT1 and BCL10 expression. *J.Pathol.*, 205, 293-301.

Ye,H., Gong,L., Liu,H., Ruskone-Fourmesttraux,A., de Jong,D., Pileri,S., Thiede,C., Lavergne,A., Boot,H., Caletti,G., Wundisch,T., Molina,T., Taal,B.G., Elena,S., Neubauer,A., MacLennan,K.A., Siebert,R., Remstein,E.D., Dogan,A., Du,M.Q. (2006) Strong BCL10 nuclear expression identifies gastric MALT lymphomas that do not respond to H pylori eradication. *Gut*, 55, 137-138.

Ye,H., Liu,H., Attygalle,A., Wotherspoon,A.C., Nicholson,A.G., Charlotte,F., Leblond,V., Speight,P., Goodlad,J., Lavergne-Slove,A., Martin-Subero,J.I., Siebert,R., Dogan,A., Isaacson,P.G., Du,M.Q. (2003) Variable frequencies of t(11;18)(q21;q21) in MALT lymphomas of different sites: significant association with CagA strains of H pylori in gastric MALT lymphoma. *Blood*, 102, 1012-1018.

Yeh,P.Y., Kuo,S.H., Yeh,K.H., Chuang,S.E., Hsu,C.H., Chang,W.C., Lin,H.I., Gao,M., Cheng,A.L. (2006) A pathway for tumor necrosis factor-alpha-induced Bcl10 nuclear translocation. Bcl10 is up-regulated by NF-kappaB and phosphorylated by Akt1 and then complexes with Bcl3 to enter the nucleus. *J.Biol.Chem.*, 281, 167-175.

Yokota,S., Ohnishi,T., Muroi,M., Tanamoto,K., Fujii,N., Amano,K. (2007) Highly-purified Helicobacter pylori LPS preparations induce weak inflammatory reactions and utilize Toll-like receptor 2 complex but not Toll-like receptor 4 complex. *FEMS Immunol.Med.Microbiol.*, 51, 140-148.

Zhang,Q., Siebert,R., Yan,M., Hinzmann,B., Cui,X., Xue,L., Rakestraw,K.M., Naeve,C.W., Beckmann,G., Weisenburger,D.D., Sanger,W.G., Nowotny,H., Vesely,M., Callet-Bauchu,E., Salles,G., Dixit,V.M., Rosenthal,A., Schlegelberger,B., Morris,S.W. (1999) Inactivating mutations and overexpression of BCL10, a caspase recruitment domain-containing gene, in MALT lymphoma with t(1;14)(p22;q32). *Nat.Genet.*, 22, 63-68.

Zhou,H., Du,M.Q., Dixit,V.M. (2005) Constitutive NF-kappaB activation by the t(11;18)(q21;q21) product in MALT lymphoma is linked to deregulated ubiquitin ligase activity. *Cancer Cell*, 7, 425-431.

Zhou,H., Wertz,I., O'Rourke,K., Ultsch,M., Seshagiri,S., Eby,M., Xiao,W., Dixit,V.M. (2004) Bcl10 activates the NF-kappaB pathway through ubiquitination of NEMO. *Nature*, 427, 167-171.

Zhou,Y., Ye,H., Martin-Subero,J.I., Gesk,S., Hamoudi,R., Lu,Y.J., Wang,R., Shipley,J., Siebert,R., Isaacson,P.G., Dogan,A., Du,M.Q. (2007) The pattern of genomic gains in salivary gland MALT lymphomas. *Haematologica*, 92, 921-927.

Zhou,Y., Ye,H., Martin-Subero,J.I., Hamoudi,R., Lu,Y.J., Wang,R., Siebert,R., Shipley,J., Isaacson,P.G., Dogan,A., Du,M.Q. (2006) Distinct comparative genomic hybridisation profiles in gastric mucosa-associated lymphoid tissue lymphomas with and without t(11;18)(q21;q21). *Br.J.Haematol.*, *133*, 35-42.

Zhou,Y., Zeng,Z., Zhang,W., Xiong,W., Wu,M., Tan,Y., Yi,W., Xiao,L., Li,X., Huang,C., Cao,L., Tang,K., Li,X., Shen,S., Li,G. (2008) Lactotransferrin: a candidate tumor suppressor-Deficient expression in human nasopharyngeal carcinoma and inhibition of NPC cell proliferation by modulating the mitogen-activated protein kinase pathway. *Int.J.Cancer.*, *123*, 2065-2072.

Zimecki,M., Mazurier,J., Machnicki,M., Wieczorek,Z., Montreuil,J., Spik,G. (1991) Immunostimulatory activity of lactotransferrin and maturation of CD4- CD8- murine thymocytes. *Immunol.Lett.*, *30*, 119-123.

Zimecki,M., Mazurier,J., Spik,G., Kapp,J.A. (1995) Human lactoferrin induces phenotypic and functional changes in murine splenic B cells. *Immunology*, *86*, 122-127.

Zou,G.M. & Hu,W.Y. (2005) LIGHT regulates CD86 expression on dendritic cells through NF-kappaB, but not JNK/AP-1 signal transduction pathway. *J.Cell Physiol.*, *205*, 437-443.

Zou,J., Dong,J., Yu,X.F. (2009) Meta-analysis: the effect of supplementation with lactoferrin on eradication rates and adverse events during *Helicobacter pylori* eradication therapy. *Helicobacter.*, *14*, 119-127.

Zucca,E., Bertoni,F., Roggero,E., Cavalli,F. (2000) The gastric marginal zone B-cell lymphoma of MALT type. *Blood*, *96*, 410-419.

Appendix I – Details of bioinformatics analysis

I.I Preprocessing algorithm for Affymetrix expression arrays

Preprocessing Affymetrix expression arrays usually involves three steps: background adjustment, normalisation and summarisation. The bioconductor software (<http://www.bioconductor.org>) which use the R programming platform (<http://www.r-project.org/>), implements a wide range of methods for each of these steps. Self-contained routines for background correction and normalisation usually take an AffyBatch as input and return a process AffyBatch. Routines for summarisation produce exprSet objects containing expression summary values.

There are currently 4 main algorithms that can be used for preprocessing the samples; MAS5, RMA, gcRMA and dChip. Literature studies comparing the above algorithms showed that dChip does not perform in a consistent manner, however none of the comparison studies showed the best algorithm to use to preprocess data from Affymetrix expression arrays. Some studies preferred MAS5 while others suggested that either RMA or gcRMA is best. Therefore, for this thesis a novel strategy was used to preprocess the raw CEL files using both gcRMA and MAS5. This was followed by non-specific filtering of the probes to eliminate non-variant probes.

The algorithm for MAS5 non-specific filtering was as follows:

```
FOR (each probe)
{
    IF ((probe raw value > 50) in > x MALT lymphoma samples) THEN
    {
        Label that probe as variant and keep
    }
    ELSE
    {
        Discard that probe and move to the next probe
    }
}
x = is the group containing the least samples
```

So x in this thesis = 2 because the group containing the least samples is the t(14;18) and this has 2 cases

The algorithm for gcRMA non-specific filtering was as follows:

```
FOR (each probe)
{
    Calculate the CV for the probe across all samples
    IF (probe CV > 10% across all MALT lymphoma samples) THEN
    {
        Label that probe as variant and keep
    }
    ELSE
    {
        Discard that probe and move to the next probe
    }
}
```

Once this is done, a new set of probes is constructed from common probes that passed both gcRMA and MAS5 preprocessing.

The advantage of using this strategy is that MAS5 is used to filter the probes on their absolute values, thus it will keep the low copy variant probes as well as the obvious highly variant probes. gcRMA is used to eliminate any non-variant probes across all samples, which is good where some probes might be high due to the tissue specificity and not because their contribution to the tumour part of the sample.

This strategy is totally unsupervised and proved to be the best for normalising and filtering probes from difficult studies such as in this thesis where; firstly, there are no controls as such, thus the comparison is made between groups of the same entity i.e. MALT lymphoma. Secondly, the number of cases in some of the groups is very small to be statistically feasible e.g. only two cases of t(14;18) and 4 cases of t(1;14) (3 t(1;14) and 1 t(1;2)) were available. Systematic testing of individual preprocessing algorithms and combination of (RMA and MAS5) and (RMA and gcRMA) followed by false discovery rate (FDR) multiple testing corrections showed the consistent loss of probes mapping to BCL10, TLR6 and CD69.

However gcRMA and MAS5 gave the best trade-off with MAS5 giving high number of probes with some false positive but gcRMA giving lower number of probes with few false positive. This strategy was used as the initial step for analysis of all the array data in this thesis.

I.II Analysis of differentially expressed genes

Many microarray studies are designed to detect genes associated with different groups (phenotypes), for example in this thesis, the comparison of MALT lymphoma with and without chromosome translocation cases and comparison of MALT lymphoma against other lymphomas. The distribution of gene expression data is generally parametric thus the array data was log transformed in order to make the distribution of the replicated measurements per gene roughly symmetric and close to normal. A variance stabilizing transformation derived from an *error model* for microarray measurements was employed to make the variance of the measured intensities independent of their expected value. This can be advantageous for gene-wise statistical tests that rely on variance homogeneity, because it will diminish differences in variance between experimental conditions that are due to differences in the intensity level, but differences in variance between conditions may also have gene-specific biological reasons, and these will remain untouched.

Generally, for the comparison of MALT lymphoma with and without chromosomal translocation in chapter 3, t-test (ANOVA on two groups) was applied with the *error model* to obtain set of genes that are differentially expressed between the two groups. However, for the phenotypic marker study in chapter 6, multiple group ANOVA and eBayes which is part of the limma package in bioconductor, were applied separately to the same set of probes and the common probes from each analysis were combined to create a new set.

eBayes fits the probe data to a linear model and works best when the variability of the log-ratios is as homogenous as possible across the probes, whereas multiple group ANOVA can cope with slight heterogeneity in the data. eBayes is more stringent because it shrinks the data and results in few genes across the groups whereas multiple group ANOVA is less stringent and give larger set of genes with more false positives even after the stringent Bonferroni multiple testing correction. Thus a combination of both for the phenotypic marker study proved the best strategy. Finally in order to manage the vast amount of testing between the groups, a relational database management software was constructed as described in Appendix II.

I.III Construction and annotation of gene sets for GSEA

Creation and annotation of human immune gene sets

The Gene Set Enrichment Analysis (GSEA) is a powerful technique for elucidating various groups of genes that may be important from gene expression data. However, one drawback of the current implementation of GSEA is that the gene sets are only as good as the annotation and the immunology gene set annotations from GO are poor and do not follow a certain pathway. Thus in addition to running the 4395 pathways as mentioned in section 2.2.5.4, the challenge was to see which of the immune system pathways are significantly enriched in MALT lymphomas with and without chromosome translocations. For this thesis, the genes and proteins of the essential human immunome were identified and collected by literature search, reviewing the existing databases such as Immunome at: <http://bioinf.uta.fi/Immunome/>, ImmTree at: <http://bioinf.uta.fi/ImmTree/>, immune pathways in GeneGo (<http://www.genego.com/>) and immune pathways in Ingenuity (<http://www.ingenuity.com/>). It is difficult to strictly define immunome genes. In this thesis, a pragmatic approach was taken, where the gene products have to be essential for immunity, but not be widely expressed in many cells and tissues. Using this strategy and in house software tools such as relational database management systems, human immune gene sets were created that broadly fall into the following categories:

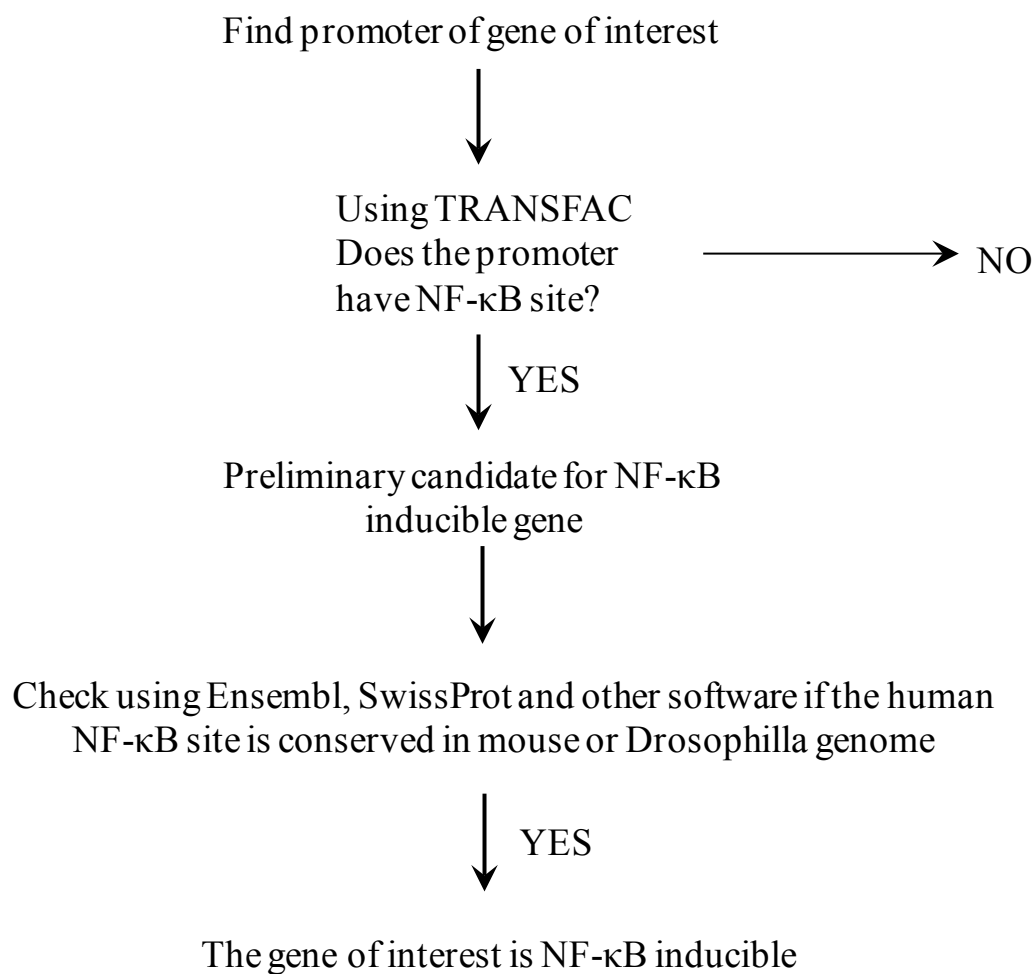
- 1) Antigen Presentation
- 2) CD genes
- 3) Cellular Immunity
- 4) Chemokine
- 5) Complement System
- 6) Humoral Immunity
- 7) Inflammation
- 8) Innate Immunity
- 9) Phagocytosis
- 10) Transcription Factor
- 11) B-cell receptor signalling
- 12) T-cell receptor signalling
- 13) TLR signalling pathway
- 13) Chemotaxis of leukocytes
- 14) Immune response to bacteria

Creation and annotation of NF- κ B target genes set

NF- κ B target gene is defined in broad terms as a gene that has a κ B site in its promoter. To date there is no comprehensive list of NF- κ B target genes, thus a comprehensive list of NF- κ B target genes was collated by bioinformatics, literature search and Internet search of NF- κ B target genes list at: <http://people.bu.edu/gilmore/nf-kb/target/index.html> and <http://bioinfo.lifl.fr/NF-KB/>

Bioinformatics strategy

Bioinformatics search algorithm is summarised as follows:



This strategy identified the following genes:

| Gene symbol | Gene full name |
|-------------|---|
| TRIP10 | thyroid hormone receptor interactor 10 |
| IL32 | interleukin 32 |
| RCP9 | calcitonin gene-related peptide-receptor component pro |
| ANKRD1 | ankyrin repeat domain 1 (cardiac muscle) |
| TNFRSF10B | tumor necrosis factor receptor superfamily, member 10b |
| AKR1C2 | aldo-keto reductase family 1, member C2 (dihydrodiol de |
| LDHB | lactate dehydrogenase B |
| TEAD1 | TEA domain family member 1 (SV40 transcriptional enl |
| PRDM2 | PR domain containing 2, with ZNF domain |
| BACE2 | beta-site APP-cleaving enzyme 2 |
| SUV39H1 | suppressor of variegation 3-9 homolog 1 (Drosophila) |
| IL1F9 | interleukin 1 family, member 9 |
| ALOX12B | arachidonate 12-lipoxygenase, 12R type |
| CARD15 | caspase recruitment domain family, member 15 |
| CD74 | CD74 antigen (invariant polypeptide of major histocom |
| CXCL2 | chemokine (C-X-C motif) ligand 2 |
| DEFB4 | defensin, beta 4 |
| IL15RA | interleukin 15 receptor, alpha |
| TPMT | thiopurine S-methyltransferase |
| TLR6 | toll-like receptor 6 |
| TLR4 | toll-like receptor 4 |
| SH3BGRL3 | SH3 domain binding glutamic acid-rich protein like 3 |
| PLA2G2E | phospholipase A2, group IIE |
| ADAMTS12 | ADAM metallopeptidase with thrombospondin type 1 m |
| CSF2RA | colony stimulating factor 2 receptor, alpha, low-affinity |
| MMP8 | matrix metallopeptidase 8 (neutrophil collagenase) |
| CCL7 | chemokine (C-C motif) ligand 7 |
| TNFRSF21 | tumor necrosis factor receptor superfamily, member 21 |
| PLA2G4A | phospholipase A2, group IVA (cytosolic, calcium-depend |
| LAMC2 | laminin, gamma 2 |
| BCL2L10 | BCL2-like 10 (apoptosis facilitator) |
| TNFSF6 | tumor necrosis factor superfamily, member 6 |
| CD105 | homodimeric transmembrane protein which is a major gl |
| TNFRSF6 | tumor necrosis factor receptor superfamily, member 6, d |
| TNFSF5 | tumor necrosis factor superfamily, member 5 |
| BM2 | influenza B virus BM2 |
| HC3 | proteasome subunit HC3 |
| SIAT8A | ST8 alpha-N-acetyl-neuraminide alpha-2,8-sialyltransfer |
| TBR | tuberin |
| TNFRSF5 | tumor necrosis factor receptor superfamily, member 5, d |
| RBCK1 | RanBP-type and C3HC4-type zinc finger containing 1 |
| CCR2A | chemokine (C-C motif) receptor 2 isoform A |
| CCR2B | chemokine (C-C motif) receptor 2 isoform B |

Those genes are not found on the websites mentioned above or literature search.

Literature search

Literature search identified the following genes:

BIRC2, ICAM1, CX3CL1, NR4A3 and BCL10

Internet search

Internet search of NF- κ B target genes list was carried out at:

<http://people.bu.edu/gilmore/nf-kb/target/index.html> and <http://bioinfo.lifl.fr/NF-KB/>

Summary of the categories and genes found in each is presented in the following table:

| Category | Number of Genes |
|--|------------------------|
| Cytokines/Chemokines and their modulators | 29 |
| Immunoreceptors | 20 |
| Acute phase proteins | 1 |
| Stress response genes | 5 |
| Growth factors, ligands and their modulators | 15 |
| Early response genes | 3 |
| Proteins involved in antigen | 1 |
| Cell adhesion molecules | 6 |
| Cell surface receptors | 10 |
| Regulators of apoptosis | 9 |
| Transcription factors | 20 |
| Viruses | 4 |
| Enzymes | 33 |
| Miscellaneous | 41 |
| Total no. | 200 |

Using all 3 strategies but removing duplication a total of 271 NF- κ B target genes were identified. A full list is provided in the complementary DVD attached to the back cover of this thesis.

Overall, a total of 4395 gene sets were identified including 56 custom sets which was constructed as mentioned in this appendix.

Gene set details are summarised in the following table:

| Name of Gene set | No. of gene sets | No of genes | Source | Description |
|---|------------------|-------------|---|---|
| NF-κB target genes | 1 | 271 | http://www.nf-κb.org http://bioinfo.ill.fr/NF-κB http://people | Genes contain κB binding sites in their promoters and are transactivated by NF-κB |
| Gene Sets from Immunome Database | | | | |
| Innate immunity | 1 | 44 | http://bioinf.uta.fi/immunome | |
| Antigen processing and presentation | 1 | 45 | http://bioinf.uta.fi/immunome | |
| Inflammation | 1 | 131 | http://bioinf.uta.fi/immunome | |
| Phagocytosis | 1 | 18 | http://bioinf.uta.fi/immunome | |
| Cellular Immunity | 1 | 100 | http://bioinf.uta.fi/immunome | |
| Humoral Immunity | 1 | 103 | http://bioinf.uta.fi/immunome | |
| Transcription factor | 1 | 38 | http://bioinf.uta.fi/immunome | |
| Complement System | 1 | 56 | http://bioinf.uta.fi/immunome | |
| Chemokine receptors | 1 | 240 | http://bioinf.uta.fi/immunome | |
| Cluster of differentiation (CD) | 1 | 301 | http://bioinf.uta.fi/immunome | |
| Gene Sets in biological processes annotated from Gene Ontology | | | | |
| Immunological process genes | 1 | 1327 | http://wiki.geneontology.org/index.php/Immunologically_Im | Genes related to immunological process and listed according to their priority score |
| B and T cell receptor signalling pathway | 1 | 113 | http://www.geneontology.org/ | Contains 69 and 44 genes for B and T cell receptor signalling respectively |
| Immune response (GO:0006955) | 1 | 596 | http://www.geneontology.org/ | immune response genes derived from gene ontology root category of the term GO:0006955 |
| Adaptive immune response (GO:0002250) | 1 | 43 | http://www.geneontology.org/ | adaptive immune response genes derived from gene ontology root category of the term GO:0002250 |
| Activation of immune response (GO:0002253) | 1 | 41 | http://www.geneontology.org/ | activation of immune response genes derived from gene ontology root category of the term GO:0002253 |
| Regulation of adaptive immune response (GO:0002819) | 1 | 11 | http://www.geneontology.org/ | genes from regulation of adaptive immune response derived from gene ontology root category of the term GO:0002819 |
| Immunoglobulin mediated immune response (GO:0016064) | 1 | 14 | http://www.geneontology.org/ | genes involved in immunoglobulin mediated immune response derived from gene ontology root category of the term GO:0016064 |
| Innate immune response (GO:0045087) | 1 | 62 | http://www.geneontology.org/ | genes involved with innate immune response derived from gene ontology root category of the term GO:0045087 |
| Regulation of innate immune response (GO:0045088) | 1 | 14 | http://www.geneontology.org/ | genes involved with regulation of innate immune response derived from gene ontology root category of the term GO:0002250 |
| Regulation of immune response (GO:0050776) | 1 | 45 | http://www.geneontology.org/ | genes involved in regulation of immune response derived from gene ontology root category of the term GO:0050776 |
| Negative regulation of immune response (GO:0050777) | 1 | 9 | http://www.geneontology.org/ | genes involved with negative regulation of immune response derived from gene ontology root category of the term GO:0050777 |
| Positive regulation of immune response (GO:0050778) | 1 | 60 | http://www.geneontology.org/ | genes involved with positive regulation of immune response derived from gene ontology root category of the term GO:0050778 |
| Lymphocyte mediated immunity (GO:0002449) | 1 | 38 | http://www.geneontology.org/ | genes involved in lymphocyte mediated immunity derived from gene ontology root category of the term GO:0002449 |
| T cell mediated immunity (GO:0002456) | 1 | 11 | http://www.geneontology.org/ | genes involved in T cell mediated immunity derived from gene ontology root category of the term GO:0002456 |
| Humoral immune response (GO:0006959) | 1 | 45 | http://www.geneontology.org/ | genes involved in humoral immune response derived from gene ontology root category of the term GO:0006959 |
| Adaptive immune response (GO:0002250) | 1 | 97 | http://www.geneontology.org/ | genes involved in adaptive immune response derived from gene ontology root category of the term GO:0002250 |
| Anti apoptosis (GO:0004916) | 1 | 165 | http://www.geneontology.org/ | genes involved in anti-apoptosis derived from gene ontology root category of the term GO:0004916 |
| Caspase activation (GO:0006919) | 1 | 40 | http://www.geneontology.org/ | genes involved in caspase activation derived from gene ontology root category of the term GO:0006919 |
| Inflammatory response (GO:0006954) | 1 | 294 | http://www.geneontology.org/ | genes involved in inflammatory response derived from gene ontology root category of the term GO:0006954 |
| I-kappaB kinase NF kappaB cascade (GO:0007249) | 1 | 41 | http://www.geneontology.org/ | genes involved in I-kappaB kinase NF kappaB cascade derived from gene ontology root category of the term GO:0007249 |
| Activation of NF kappaB inducing kinase (GO:0007250) | 1 | 13 | http://www.geneontology.org/ | genes involved in the activation of NF kappaB inducing kinase derived from gene ontology root category of the term GO:0007250 |
| T cell activation (GO:0042110) | 1 | 59 | http://www.geneontology.org/ | genes involved in T cell activation derived from gene ontology root category of the term GO:0042110 |
| B cell activation (GO:0042113) | 1 | 43 | http://www.geneontology.org/ | genes involved in B cell activation derived from gene ontology root category of the term GO:0042113 |
| Chemokine (GO:0042379) | 1 | 50 | http://www.geneontology.org/ | genes relating to chemokines derived from gene ontology root category of the term GO:0042379 |
| Positive regulation of I kappaB kinase NF kappaB cascade (GO:0043123) | 1 | 101 | http://www.geneontology.org/ | genes involved in the positive regulation of I kappaB kinase NF kappaB cascade derived from gene ontology root category of the term GO:0043123 |
| Innate immune response (GO:0045087) | 1 | 105 | http://www.geneontology.org/ | genes involved in the innate immune response derived from gene ontology root category of the term GO:0045087 |
| Lymphocyte activation (GO:0046649) | 1 | 137 | http://www.geneontology.org/ | genes involved in lymphocyte activation derived from gene ontology root category of the term GO:0046649 |
| Regulation of T cell activation (GO:0050863) | 1 | 70 | http://www.geneontology.org/ | genes involved in the regulation of T cell activation derived from gene ontology root category of the term GO:0050863 |
| Regulation of lymphocyte activation (GO:0051249) | 1 | 120 | http://www.geneontology.org/ | genes involved in the regulation of lymphocyte activation derived from gene ontology root category of the term GO:0051249 |
| Gene sets derived from pathways annotated by GeneGo | | | | |
| B Cell Lymphoma | 1 | 50 | http://www.genego.com/ | Genes involved in B cell lymphoma derived from the GeneGo Metacore software |
| T Cell Receptor Signalling | 1 | 46 | http://www.genego.com/ | Genes involved in T cell receptor signalling derived from the GeneGo Metacore software |
| TLR Signalling Pathway | 1 | 82 | http://www.genego.com/ | Genes involved in TLR signalling pathway derived from the GeneGo Metacore software |
| CD28 | 1 | 71 | http://www.genego.com/ | CD28 pathway related genes derived from the GeneGo Metacore software |
| ICOS | 1 | 93 | http://www.genego.com/ | Genes that are linked to ICOS pathway, derived from the GeneGo Metacore software |
| Chemotaxis Leukocyte | 1 | 110 | http://www.genego.com/ | genes that are involved chemotaxis leukocyte, derived from the GeneGo Metacore software |
| Immune Response Bacteria | 1 | 47 | http://www.genego.com/ | genes that are involved in bacterial immune response pathway derived from the GeneGo Metacore software |
| BCR Pathway | 1 | 75 | http://www.genego.com/ | genes related to B cell receptor signalling pathway, derived from the GeneGo Metacore software |
| TCR CD28 costimulation leading to NFκB | 1 | 70 | http://www.genego.com/ | genes involved in T-cell receptor signalling and CD28 costimulation leading to NFκB activation derived from the GeneGo Metacore software |
| Gene set derived from Pathways annotated by Ingenuity Systems | | | | |
| Antigen Receptor GO | 1 | 17 | http://www.ingenuity.com | genes to do with antigen receptor signalling derived from the gene ontology part of the Ingenuity pathway analysis software |
| B cell activation | 1 | 95 | http://www.ingenuity.com | genes to do with b cell activation derived from the gene ontology part of the Ingenuity pathway analysis software |
| B cell receptor signalling | 1 | 60 | http://www.ingenuity.com | genes to do with b cell receptor signalling derived from the gene ontology part of the Ingenuity pathway analysis software |
| Chemokine signalling | 1 | 36 | http://www.ingenuity.com | genes to do with chemokine signalling derived from the gene ontology part of the Ingenuity pathway analysis software |
| T cell activation GO | 1 | 95 | http://www.ingenuity.com | genes to do with t cell activation derived from the gene ontology part of the Ingenuity pathway analysis software |
| T cell receptor signalling | 1 | 57 | http://www.ingenuity.com | genes to do with t cell receptor signalling derived from the gene ontology part of the Ingenuity pathway analysis software |
| TLR signalling | 1 | 33 | http://www.ingenuity.com | genes to do with TLR signalling derived from the gene ontology part of the Ingenuity pathway analysis software |
| Gene Sets from Molecular Signature Database | | | | |
| C2: Curated gene sets derived from online pathway database and publications | 1892 | | http://www.broad.mit.edu/sea/msigdb/index.jsp | This is derived from the Broad Institute website at: http://www.broad.mit.edu/sea/msigdb/downloads.jsp and enriched using IPA and GeneGo Metacore software. The molecular signature pathways that are derived are from version 2.5. |
| C2: Canonical pathway gene sets from pathway databases | 639 | | http://www.broad.mit.edu/sea/msigdb/index.jsp | Canonical pathway gene sets from pathway databases including the followings |
| C2: BioCarta gene sets | 249 | | http://www.biocarta.com | BioCarta gene sets |
| C2: GenMAPP gene sets | 138 | | http://www.genmapp.org/ | GenMAPP gene sets |
| C2: KEGG gene sets | 200 | | http://www.genome.jp/kegg/ | KEGG gene sets |
| C5: GO biological process gene sets | 825 | | http://www.broad.mit.edu/sea/msigdb/index.jsp | GO biological process gene sets |
| C5: GO molecular function gene sets | 396 | | http://www.broad.mit.edu/sea/msigdb/index.jsp | GO molecular function gene sets |
| Total number of gene sets | 4395 | | | |
| Total number of custom sets | | 56 | | |

Finally, in order to manage and query the vast amount of data gathered from microarrays and gene set enrichment analysis, a relational database management software was constructed and included in the complementary DVD attached to the back cover of this thesis.

Appendix II – In house software for gene expression microarray analysis

Two main programming languages were used to write custom made software for analysis of microarray data generated from this thesis; R programming platform with use of some of the bioconductor libraries and Visual Basic programming platform embedded within Microsoft Access in order to write the relational database management software.

II.I R software

R custom software were used to preprocess and analyse the 24 CEL files from MALT lymphoma and 15 CEL files from FL and MCL microarray data, as well as to help post process some of the GSEA data and carry out unsupervised clustering and statistical analysis e.g. for qRT-PCR and identification of differentially expressed genes using Bayesian analysis such as eBayes.

A list of all the custom software is included in the complementary DVD attached to the back cover of this thesis.

The main software R code for pre-processing and analysing microarray data from both the U133A&B and U133plus2 platforms is as follows:

```

#
# Analysis of U133A&B MALT lymphoma and U133plus2 FL and MCL
# Software written by Rifat Hamoudi, 2010
#

```

```

library(affy)
library(gcrma)
library(genefilter)
library(gplots)
library(annotate)
library(hgu133a.db)
library(hgu133b.db)
library(hgu133aprobe)
library(hgu133bprobe)
library(gsubfn)

```

```

#####
#
# Read the U133plus chips of FL & MCL
#
#####

```

```

setwd("/media/disk/RawArrayData/Cel Files/U133/FL_MCL")

```

```

MCL_FL<-ReadAffy()      # read affy files after changedir. Read into
AffyBatch object

```

```

sampleNames(MCL_FL)

```

```

sampleNames(MCL_FL)[1] <- "FL14"
sampleNames(MCL_FL)[2] <- "FL16"
sampleNames(MCL_FL)[3] <- "FL17"
sampleNames(MCL_FL)[4] <- "FL18"
sampleNames(MCL_FL)[5] <- "FL19"
sampleNames(MCL_FL)[6] <- "FL20"
sampleNames(MCL_FL)[7] <- "FL21"
sampleNames(MCL_FL)[8] <- "MCL22"
sampleNames(MCL_FL)[9] <- "MCL23"
sampleNames(MCL_FL)[10] <- "MCL24"
sampleNames(MCL_FL)[11] <- "MCL25"
sampleNames(MCL_FL)[12] <- "MCL26"
sampleNames(MCL_FL)[13] <- "MCL27"
sampleNames(MCL_FL)[14] <- "MCL28"
sampleNames(MCL_FL)[15] <- "MCL29"

```

```

gcrma_mcl_fl <-gcrma(MCL_FL) # normalization via gcrma
mas_mcl_fl <- mas5(MCL_FL, sc=100) # normalization via MAS5

```

```

# MCL FL groups definition

flnum <- seq(1:7)
mclnum <- c(8,9,10,11,12,13,14,15)
allnum <- c(flnum, mclnum)

# GCRMA groups implementation

flgc <- gcrma_mcl_fl[,flnum]
mclgc <- gcrma_mcl_fl[,mclnum]
allflmclgc <- gcrma_mcl_fl[,allnum]

# MAS5 groups implementation

flmas <- mas_mcl_fl[,flnum]
mclmas <- mas_mcl_fl[,mclnum]
allflmclmas <- mas_mcl_fl[,allnum]

# filter stuff on MAS5 abs values

fl<-kOverA(7, 50) # if a gene is 50 or more raw value in more than 7
samples then pass it
ff <-filterfun(fl)
masselect_flmcl <-genefilter(mas_mcl_fl, ff)
sum(masselect_flmcl)
esetmasflmcl <- mas_mcl_fl[masselect_flmcl,]

# filtering gcrma on CV

cvfun <- cv(0.1, 1.0)
ffun <- filterfun(cvfun)
gcselect_flmcl <- genefilter(gcrma_mcl_fl, ffun)
sum(gcselect_flmcl)
esetgcrmaflmcl <- gcrma_mcl_fl[gcselect_flmcl,]

# Extract the correct set on gcrma and MAS5

selectgenes_flmcl <- intersect(featureNames(esetmasflmcl),
featureNames(esetgcrmaflmcl))
selectgenes_flmcl
length(selectgenes_flmcl)

esetgcgoodflmcl <- gcrma_mcl_fl[selectgenes_flmcl,] # gcrma
esetgcgoodflmcl

esetmasgoodflmcl <- mas_mcl_fl[selectgenes_flmcl,] # MAS5
esetmasgoodflmcl

gn <- featureNames(MCL_FL)
ps <- probeset(MCL_FL, gn[1:2])

```

```

probeNames (MCL_FL) [1:5]

gcrmafmlclexp <- exprs(gcrma_mcl_fl)

# eliminate AFFX and _x_
idsflmcl <- featureNames(esetmasgoodflmcl)
ids.affx <- grep("^AFFX", idsflmcl)
#noX <- grep("_x_", ids)
ids.noaffx_flmcl <- setdiff(c(1:length(idsflmcl)), ids.affx)
#ids.noaffx <- setdiff(c(1:length(idsflmcl)), noX)

esetgcfinalflmcl <- esetgcgoodflmcl[ids.noaffx_flmcl,]
esetgcfinalflmcl

esetmasfinalflmcl <- esetmasgoodflmcl[ids.noaffx_flmcl,]
esetmasfinalflmcl

#####
#
# Read U133A MALT lymphomas
#
#####

setwd("/media/disk/RawArrayData/Cel Files/U133/MALT/HG133_A")

MALT_A<-ReadAffy() # read affy files after changedir. Read into
AffyBatch object

sampleNames (MALT_A)

sampleNames (MALT_A) [1] <- "11_18_G0015_A"
sampleNames (MALT_A) [2] <- "11_18_G5125_A"
sampleNames (MALT_A) [3] <- "11_18_G5661_A"
sampleNames (MALT_A) [4] <- "11_18_G6071_A"
sampleNames (MALT_A) [5] <- "11_18_86_14635_Samp11V_A"
sampleNames (MALT_A) [6] <- "11_18_95_10509_Samp1F_A"
sampleNames (MALT_A) [7] <- "11_18_92_10232_Samp2F_A"
sampleNames (MALT_A) [8] <- "11_18_96_8361_Samp3F_A"
sampleNames (MALT_A) [9] <- "11_18_97_107717_Samp7V_A"
sampleNames (MALT_A) [10] <- "1_14_Bel_A"
sampleNames (MALT_A) [11] <- "1_14_G0186_A"
sampleNames (MALT_A) [12] <- "1_14_G0262_A"
sampleNames (MALT_A) [13] <- "1_2_G6389_A"
sampleNames (MALT_A) [14] <- "14_18_02_101211_Samp8V_A"
sampleNames (MALT_A) [15] <- "14_18_97_21350_Samp16V_A"
sampleNames (MALT_A) [16] <- "3_14_G0046_A"
sampleNames (MALT_A) [17] <- "NEG_G0019_A"
sampleNames (MALT_A) [18] <- "NEG_G0055_Nuc_A"
sampleNames (MALT_A) [19] <- "NEG_G0078_Nuc_A"
sampleNames (MALT_A) [20] <- "NEG_G5018_A"
sampleNames (MALT_A) [21] <- "NEG_G6352_Nuc_A"
sampleNames (MALT_A) [22] <- "NEG_88_20237_Samp12V_A"
sampleNames (MALT_A) [23] <- "NEG_92_8149_Samp4F_A"

```

```

sampleNames(MALT_A)[24] <- "NEG_91_6360_Samp5F_A"
sampleNames(MALT_A)[25] <- "NEG_96_9991_Samp6F_A"
sampleNames(MALT_A)[26] <- "NEG_89_01810_Samp13V_A"

gcrmamalt_a<-gcrma(MALT_A) # normalization via gcrma
masmalt_a <- mas5(MALT_A, sc=100) # normalization via MAS5

# groups definition

neg_A <- c(17,18,19,20,21,22,23,24,25,26)
tr11_18_A <- c(1,2,3,4,5,6,7,8,9)
tr1_14_A <- c(10,11,12,13)
tr14_18_A <- c(14,15)

t11_18set_A <- c(tr11_18_A,neg_A)
t1_14set_A <- c(tr1_14_A, neg_A)
t14_18set_A <- c(tr14_18_A, neg_A)

# GCRMA groups implementation

posneggcrma_A <- c(tr1_14_A, tr11_18_A, tr14_18_A, neg_A)
posneggcrma_A <- gcrmamalt_a[,posneggcrma_A]
pData(posneggcrma_A)$sample <- c(1:25)

t11_18gc_A <- gcrmamalt_a[,t11_18set_A]
t1_14gc_A <- gcrmamalt_a[,t1_14set_A]
t14_18gc_A <- gcrmamalt_a[,t14_18set_A]

# MAS5 groups implementation

posnegv_A <- c(tr1_14_A, tr11_18_A, tr14_18_A, neg_A)
posnegmas_A <- masmalt_a[,posnegv_A]
pData(posnegmas_A)$sample <- c(1:25)

t11_18mas_A <- masmalt_a[,t11_18set_A]
t1_14mas_A <- masmalt_a[,t1_14set_A]
t14_18mas_A <- masmalt_a[,t14_18set_A]

#####
#
# Read U133B MALT lymphomas
#
#####

setwd("/media/disk/RawArrayData/Cel Files/U133/MALT/HG133_B")

MALT_B<-ReadAffy() # read affy files after changedir. Read into
AffyBatch object

```

```

sampleNames(MALT_B)

sampleNames(MALT_B)[1] <- "11_18_G0015_B"
sampleNames(MALT_B)[2] <- "11_18_G5125_B"
sampleNames(MALT_B)[3] <- "11_18_G5661_B"
sampleNames(MALT_B)[4] <- "11_18_G6071_B"
sampleNames(MALT_B)[5] <- "11_18_86_14635_Samp11V_B"
sampleNames(MALT_B)[6] <- "11_18_95_10509_Samp1F_B"
sampleNames(MALT_B)[7] <- "11_18_92_10232_Samp2F_B"
sampleNames(MALT_B)[8] <- "11_18_96_8361_Samp3F_B"
sampleNames(MALT_B)[9] <- "11_18_97_107717_Samp7V_B"
sampleNames(MALT_B)[10] <- "1_14_Bel_B"
sampleNames(MALT_B)[11] <- "1_14_G0186_B"
sampleNames(MALT_B)[12] <- "1_14_G0262_B"
sampleNames(MALT_B)[13] <- "1_2_G6389_B"
sampleNames(MALT_B)[14] <- "14_18_02_101211_Samp16V_B"
sampleNames(MALT_B)[15] <- "14_18_97_21350_Samp8V_B"
sampleNames(MALT_B)[16] <- "3_14_G0046_B"
sampleNames(MALT_B)[17] <- "NEG_G0019_B"
sampleNames(MALT_B)[18] <- "NEG_G0055_Nuc_B"
sampleNames(MALT_B)[19] <- "NEG_G0078_Nuc_B"
sampleNames(MALT_B)[20] <- "NEG_G5018_B"
sampleNames(MALT_B)[21] <- "NEG_G6352_Nuc_B"
sampleNames(MALT_B)[22] <- "NEG_88_20237_Samp12V_B"
sampleNames(MALT_B)[23] <- "NEG_92_8149_Samp4F_B"
sampleNames(MALT_B)[24] <- "NEG_91_6360_Samp5F_B"
sampleNames(MALT_B)[25] <- "NEG_96_9991_Samp6F_B"
sampleNames(MALT_B)[26] <- "NEG_89_01810_Samp13V_B"

gcrmamalt_b <- gcrma(MALT_B) # normalization via gcrma
masmalt_b <- mas5(MALT_B, sc=100) # normalization via MAS5

# groups definition Bchips

neg_B <- c(17,18,19,20,21,22,23,24,25,26)
tr11_18_B <- c(1,2,3,4,5,6,7,8,9)
tr1_14_B <- c(10,11,12,13)
tr14_18_B <- c(14,15)

t11_18set_B <- c(tr11_18_B, neg_B)
t1_14set_B <- c(tr1_14_B, neg_B)
t14_18set_B <- c(tr14_18_B, neg_B)

# GCRMA groups implementation

posneggcrma_b <- c(tr1_14_B, tr11_18_B, tr14_18_B, neg_B)
posneggcrma_B <- gcrmamalt_b[,posneggcrma_b]
pData(posneggcrma_B)$sample <- c(1:25)

t11_18gc_B <- gcrmamalt_b[,t11_18set_B]
t1_14gc_B <- gcrmamalt_b[,t1_14set_B]
t14_18gc_B <- gcrmamalt_b[,t14_18set_B]

```

```

# MAS5 groups implementation

posnegv_B <- c(tr1_14_B, tr11_18_B, tr14_18_B, neg_B)
posnegmas_B <- masmalt_b[,posnegv_B]
pData(posnegmas_B)$sample <- c(1:25)

t11_18mas_B <- masmalt_b[,t11_18set_B]
t1_14mas_B <- masmalt_b[,t1_14set_B]
t14_18mas_B <- masmalt_b[,t14_18set_B]

#####
#
# MALT_A nonspecific filtering
#
#####

# filter stuff on MAS5 abs values A chip

f1<-kOverA(2, 50) # if a gene is 50 or more raw value in more than 2
samples then pass it
ff <-filterfun(f1)
masselect_malt_a <- genefilter(masmalt_a, ff)
sum(masselect_malt_a)
esetmasposneg_a <- posnegmas_A[masselect_malt_a,]

# filtering gcrMA on CV

cvfun <- cv(0.1, 1.0)
ffun <- filterfun(cvfun)
gcselect_malt_a <- genefilter(gcrmamalt_a, ffun)
sum(gcselect_malt_a)
esetgcrmaposneg_a <- posneggcrma_A[gcselect_malt_a,]

# Extract the correct set on gcrMA and MAS5

selectgenes_malt_a <- intersect(featureNames(esetmasposneg_a),
featureNames(esetgcrmaposneg_a))
selectgenes_malt_a
length(selectgenes_malt_a)

esetgcggoodposneg_a <- posneggcrma_A[selectgenes_malt_a,] # gcrMA
esetgcggoodposneg_a

esetmasgoodposneg_a <- posnegmas_A[selectgenes_malt_a,] # MAS5
esetmasgoodposneg_a

gn_a <- featureNames(MALT_A)
ps_a <- probeset(MALT_A, gn_a[1:2])
probeNames(MALT_A)[1:5]

gcrmamaltexp_a <- exprs(gcrmamalt_a)

```

```

# eliminate AFX and _x_
ids_a <- featureNames(esetgcggoodposneg_a)
ids.affx_a <- grep("^AFX", ids_a)
ids.noaffx_malt_a <- setdiff(c(1:length(ids_a)), ids.affx_a)

#noX <- grep("_x_", ids)
#ids.noaffx <- setdiff(c(1:length(ids)), noX)

esetgcfinalposneg_a <- esetgcggoodposneg_a[ids.noaffx_malt_a,]
esetgcfinalposneg_a

esetmasfinalposneg_a <- esetmasgoodposneg_a[ids.noaffx_malt_a,]
esetmasfinalposneg_a

#####
#
# MALT_B nonspecific filtering
#
#####

# filter stuff on MAS5 abs values B chip

f1<-kOverA(2, 50)# if a gene is 50 or more raw value in more than 2
samples then pass it
ff <-filterfun(f1)
masselect_malt_b <- genefilter(masmalt_b, ff)
sum(masselect_malt_b)
esetmasposneg_b <- posnegmas_B[masselect_malt_b,]

# filtering gcrMA on CV

cvfun <- cv(0.1, 1.0)
ffun <- filterfun(cvfun)
gcselect_malt_b <- genefilter(gcrmamalt_b, ffun)
sum(gcselect_malt_b)
esetgcrmaposneg_b <- posneggcrma_B[gcselect_malt_b,]

# Extract the correct set on gcrMA and MAS5

selectgenes_malt_b <- intersect(featureNames(esetmasposneg_b),
featureNames(esetgcrmaposneg_b))
selectgenes_malt_b
length(selectgenes_malt_b)

esetgcggoodposneg_b <- posneggcrma_B[selectgenes_malt_b,] # gcrMA
esetgcggoodposneg_b

esetmasgoodposneg_b <- posnegmas_B[selectgenes_malt_b,] # MAS5
esetmasgoodposneg_b

```

```

gn_b <- featureNames(MALT_B)
ps_b <- probeset(MALT_B, gn_b[1:2])
probeNames(MALT_B)[1:5]

gcrmamaltexp_b <- exprs(gcrmamalt_b)

# eliminate AFX and _x_
ids_b <- featureNames(esetgcgoodposneg_b)
ids.affx_b <- grep("^AFX", ids_b)
ids.noaffx_malt_b <- setdiff(c(1:length(ids_b)), ids.affx_b)

#noX <- grep("_x_", ids)
#ids.noaffx <- setdiff(c(1:length(ids)), noX)

esetgcfinalposneg_b <- esetgcgoodposneg_b[ids.noaffx_malt_b,]
esetgcfinalposneg_b

esetmasfinalposneg_b <- esetmasgoodposneg_b[ids.noaffx_malt_b,]
esetmasfinalposneg_b

#####
#
# Map all the MALT_A probes on the FLMCL
#
#####

maltprobes_a <- featureNames(esetmasfinalposneg_a)

esetfinalflmclgc_a <- gcrma_mcl_fl[maltprobes_a,]
esetfinalflmclmas_a <- mas_mcl_fl[maltprobes_a,]

#####
#
# Map all the MALT_B probes on the FLMCL
#
#####

maltprobes_b <- featureNames(esetmasfinalposneg_b)

esetfinalflmclgc_b <- gcrma_mcl_fl[maltprobes_b,]
esetfinalflmclmas_b <- mas_mcl_fl[maltprobes_b,]

```

```

#####
#
# Find common probes between MALT_A and MALT_B and FLMCL
#
#####

# MALT_A

flmclmaltprobes_a <- intersect(featureNames(esetmasfinalflmcl),
featureNames(esetmasfinalposneg_a))
instersectflmclmaltgc_a <- esetgcgoodflmcl[flmclmaltprobes_a,]
instersectflmclmaltmas_a <- esetmasgoodflmcl[flmclmaltprobes_a,]

instersectmaltgc_a <- esetgcgoodposneg_a[flmclmaltprobes_a,]
instersectmaltmas_a <- esetmasgoodposneg_a[flmclmaltprobes_a,]

# MALT_B

flmclmaltprobes_b <- intersect(featureNames(esetmasfinalflmcl),
featureNames(esetmasfinalposneg_b))
instersectflmclmaltgc_b <- esetgcgoodflmcl[flmclmaltprobes_b,]
instersectflmclmaltmas_b <- esetmasgoodflmcl[flmclmaltprobes_b,]

instersectmaltgc_b <- esetgcgoodposneg_b[flmclmaltprobes_b,]
instersectmaltmas_b <- esetmasgoodposneg_b[flmclmaltprobes_b,]

##### write out #####

setwd("/media/Linux/malt_flmcl_res")

# MALT_A writeout

write.table(exprs(posnegmas_A), file="MALT MAS5 Achip 22283.xls",
append = FALSE, sep="\t", eol="\n", row.names=TRUE, col.names=TRUE,
qmethod=c("escape", "double"))

write.table(exprs(posneggcrma_A), file="MALT GCRMA Achip 22283.xls",
append = FALSE, sep="\t", eol="\n", row.names=TRUE, col.names=TRUE,
qmethod=c("escape", "double"))

write.table(exprs(esetgcfinalposneg_a), file="MALT GCRMA Filtered Achip
norm 8181.xls", append = FALSE, sep="\t", eol="\n", row.names=TRUE,
col.names=TRUE, qmethod=c("escape", "double"))

write.table(exprs(esetmasfinalposneg_a), file="MALT MAS5 Filtered Achip
raw 8181.xls", append = FALSE, sep="\t", eol="\n", row.names=TRUE,
col.names=TRUE, qmethod=c("escape", "double"))

```

```

# MALT_B writeout

write.table(exprs(posnegmas_B), file="MALT MAS5 Bchip 22645.xls",
append = FALSE, sep="\t", eol="\n", row.names=TRUE, col.names=TRUE,
qmethod=c("escape", "double"))

write.table(exprs(posneggcrma_B), file="MALT GCRMA Bchip 22645.xls",
append = FALSE, sep="\t", eol="\n", row.names=TRUE, col.names=TRUE,
qmethod=c("escape", "double"))

write.table(exprs(esetgcfinalposneg_b), file="MALT GCRMA Filtered Bchip
norm 8622.xls", append = FALSE, sep="\t", eol="\n", row.names=TRUE,
col.names=TRUE, qmethod=c("escape", "double"))

write.table(exprs(esetmasfinalposneg_b), file="MALT MAS5 Filtered Bchip
raw 8622.xls", append = FALSE, sep="\t", eol="\n", row.names=TRUE,
col.names=TRUE, qmethod=c("escape", "double"))

# FLMCL writeout

write.table(exprs(mas_mcl_fl), file="FLMCL MAS5 U133plus2 54675.xls",
append = FALSE, sep="\t", eol="\n", row.names=TRUE, col.names=TRUE,
qmethod=c("escape", "double"))

write.table(exprs(gcrma_mcl_fl), file="FLMCL GCRMA U133plus2
54675.xls", append = FALSE, sep="\t", eol="\n", row.names=TRUE,
col.names=TRUE, qmethod=c("escape", "double"))

write.table(exprs(esetgcfinalflmcl), file="FLMCL GCRMA Filtered
U133plus2 norm 10652.xls", append = FALSE, sep="\t", eol="\n",
row.names=TRUE, col.names=TRUE, qmethod=c("escape", "double"))

write.table(exprs(esetmasfinalflmcl), file="FLMCL MAS5 Filtered
U133plus2 raw 10652.xls", append = FALSE, sep="\t", eol="\n",
row.names=TRUE, col.names=TRUE, qmethod=c("escape", "double"))

# FLMCL on MALT writeout

write.table(exprs(esetfinalflmclgc_a), file="FLMCL_MALT_GC Achip
8181.xls", append = FALSE, sep="\t", eol="\n", row.names=TRUE,
col.names=TRUE, qmethod=c("escape", "double"))

write.table(exprs(esetfinalflmclmas_a), file="FLMCL_MALT_MAS Achip
8181.xls", append = FALSE, sep="\t", eol="\n", row.names=TRUE,
col.names=TRUE, qmethod=c("escape", "double"))

write.table(exprs(esetfinalflmclgc_b), file="FLMCL_MALT_GC Bchip
8622.xls", append = FALSE, sep="\t", eol="\n", row.names=TRUE,
col.names=TRUE, qmethod=c("escape", "double"))

write.table(exprs(esetfinalflmclmas_b), file="FLMCL_MALT_MAS Bchip
8622.xls", append = FALSE, sep="\t", eol="\n", row.names=TRUE,
col.names=TRUE, qmethod=c("escape", "double"))

```

```

# FLMCL on MALT intersect writeout

write.table(exprs(instersectflmclmaltgc_a), file="FLMCL_MALT_A_GC FLMCL
intersect 3871.xls", append = FALSE, sep="\t", eol="\n",
row.names=TRUE, col.names=TRUE, qmethod=c("escape", "double"))

write.table(exprs(instersectflmclmaltmas_a), file="FLMCL_MALT_A_MAS
FLMCL intersect 3871.xls", append = FALSE, sep="\t", eol="\n",
row.names=TRUE, col.names=TRUE, qmethod=c("escape", "double"))

write.table(exprs(instersectmaltgc_a), file="FLMCL_MALT_GC MALT_A
intersect 3871.xls", append = FALSE, sep="\t", eol="\n",
row.names=TRUE, col.names=TRUE, qmethod=c("escape", "double"))

write.table(exprs(instersectmaltmas_a), file="FLMCL_MALT_MAS MALT_A
intersect 3871.xls", append = FALSE, sep="\t", eol="\n",
row.names=TRUE, col.names=TRUE, qmethod=c("escape", "double"))

write.table(exprs(instersectflmclmaltgc_b), file="FLMCL_MALT_B_GC FLMCL
intersect 3034.xls", append = FALSE, sep="\t", eol="\n",
row.names=TRUE, col.names=TRUE, qmethod=c("escape", "double"))

write.table(exprs(instersectflmclmaltmas_b), file="FLMCL_MALT_B_MAS
FLMCL intersect 3034.xls", append = FALSE, sep="\t", eol="\n",
row.names=TRUE, col.names=TRUE, qmethod=c("escape", "double"))

write.table(exprs(instersectmaltgc_b), file="FLMCL_MALT_GC MALT_B
intersect 3034.xls", append = FALSE, sep="\t", eol="\n",
row.names=TRUE, col.names=TRUE, qmethod=c("escape", "double"))

write.table(exprs(instersectmaltmas_b), file="FLMCL_MALT_MAS MALT_B
intersect 3034.xls", append = FALSE, sep="\t", eol="\n",
row.names=TRUE, col.names=TRUE, qmethod=c("escape", "double"))

```

```

#
# Software to annotate GSEA results and define leading edge
# genes that drive the set
#
# Software written by Rifat Hamoudi, 2010
#

library(hgu133a.db)
library(hgu133b.db)
library(hgu133plus2.db)

ls(2)

flist <- list.files(".", pattern="report.*.txt$")

for (f in 1:length(flist))
{
    filename = flist[f]

    print(filename)

    # input BACs file
    genes <- readLines(filename)

    maxGenes <- length(genes)
    genset <- vector(length = maxGenes, mode = "numeric")

    for (i in 1:maxGenes)
    {
        genset[i] <- length(unlist(strsplit(genes[[i]], "\t"))) - 2
    }

    max.size.G <- max(maxGenes)
    gs <- matrix(rep("null", maxGenes*max.size.G), nrow=maxGenes,
ncol= max.size.G)

    temp.names <- vector(length = maxGenes, mode = "character")
    temp.desc <- vector(length = maxGenes, mode = "character")
    gs.count <- 1

    genesmatrix <- matrix(nrow=1000, ncol=8)
    genesmatrix <- as.table(genesmatrix)

    i = 2

    gene.set.size <- length(unlist(strsplit(genes[[i]], "\t")))
    gs.line <- noquote(unlist(strsplit(genes[[i]], "\t")))

    gene.set.num <- gs.line[1]
    gene.set.gene <- gs.line[2]

```

```

gene.set.sym <- gs.line[3]
gene.set.desc <- gs.line[4]
gene.set.list <- gs.line[5]
gene.set.s2n <- gs.line[6]
gene.set.res <- gs.line[7]
gene.set.core <- gs.line[8]

for (i in 1:maxGenes)
{
  gene.set.size <- length(unlist(strsplit(genes[[i]], "\t")))
  gs.line <- noquote(unlist(strsplit(genes[[i]], "\t")))

  for (j in 1:gene.set.size)
  {
    genesmatrix[i,j] <- gs.line[j]
  }
}

affymatrix <- matrix(nrow=1000, ncol=10)
affymatrix <- as.table(affymatrix)

i = 1

gene.set.size <- length(unlist(strsplit(genes[[i]], "\t")))
gs.line <- noquote(unlist(strsplit(genes[[i]], "\t")))

for (j in 1:gene.set.size)
{
  affymatrix[i,j] <- gs.line[j]
}

affymatrix[1,1] <- "Num"
affymatrix[1,2] <- "Gene"
affymatrix[1,3] <- "Description"
affymatrix[1,4] <- "ChromBand"
affymatrix[1,5] <- "EntrezID"
affymatrix[1,6] <- "ListLoc"
affymatrix[1,7] <- "S2N"
affymatrix[1,8] <- "ES_pval"
affymatrix[1,9] <- "Core_Enrichment"

options(show.error.messages = FALSE)

for (i in 2:maxGenes)
{
  affysym = FALSE

  affymatrix[i,1] <- genesmatrix[i,1]
  affymatrix[i,2] <- genesmatrix[i,2]
}

```

```

    curgene <- affymatrix[i,2]

#       feat = getFeature(symbol = curgene, type =
"affy_hg_u133_plus_2", mart = mart)

#       affysymarr <- get(curgene, revmap(hgu133plus2SYMBOL))

#       feat <-
getBM(attributes=c("affy_hg_u133_plus_2","hgnc_symbol"),
filters="hgnc_symbol", values=curgene, mart=mart)

#       affysymarr <- feat$affy_hg_u133_plus_2[1]

#       affysym <- affysymarr[1]

    probeids <- NULL
    probeids <-
try(unlist(mget(curgene, revmap(hgu133plus2SYMBOL))))
    affysym <- probeids[[1]]

    temp <- unlist(strsplit(affysym,""))

    if ((temp[1] == "E") || is.na(affysym) || (affysym == "") ||
is.null(affysym))
    {
        affymatrix[i,3] <- curgene
        affymatrix[i,4] <- curgene
        affymatrix[i,5] <- curgene
        affymatrix[i,6] <- genesmatrix[i,5]
        affymatrix[i,7] <- genesmatrix[i,6]
        affymatrix[i,8] <- genesmatrix[i,7]
        affymatrix[i,9] <- genesmatrix[i,8]
    }
    else
    {
        get(affysym, hgu133plus2SYMBOL)

        affymatrix[i,3] <- get(affysym,
hgu133plus2GENENAME)[1]
        affymatrix[i,4] <- get(affysym, hgu133plus2MAP)[1]
        affymatrix[i,5] <- get(affysym,
hgu133plus2ENTREZID)[1]

        affymatrix[i,6] <- genesmatrix[i,5]
        affymatrix[i,7] <- genesmatrix[i,6]
        affymatrix[i,8] <- genesmatrix[i,7]
        affymatrix[i,9] <- genesmatrix[i,8]
    }
}

```

```

options(show.error.messages = TRUE)

Flip = 0

x <- as.numeric(affymatrix[,8])
x <- x[!is.na(x)]
plot(x)

endpoint <- length(x)
endpoint <- endpoint + 1

midpoint <- round(endpoint / 2)

enrich <- x[midpoint:(endpoint-1)]

begin <- as.numeric(x[3])
begin1 <- as.numeric(x[4])

last <- as.numeric(x[endpoint-1])
lastbutone <- as.numeric(x[endpoint-2])

if (((begin > 0) && (begin1 > 0)) && ((last > 0) && (lastbutone >
0)) || ((begin < 0) && (begin1 < 0)) && ((last < 0) && (lastbutone <
0)))
{
    Flip = 0
}
else
{
    Flip = 1
}

if (Flip == 1)
{
    if ((last < 0) && (lastbutone < 0))
    {
        enrichpoint <- min(enrich)
    }
    else
    {
        enrichpoint <- max(enrich)
    }

    x <- as.numeric(affymatrix[,8])

    enrichpoint <- as.numeric(enrichpoint)

    endpoint <- endpoint - 1
}

```

```

for (i in endpoint:midpoint)
{
  if (!is.na(enrichpoint))
  {
    if (x[i] == enrichpoint)
    {
      point_inflection <- i
    }
  }
}

try(affymatrix[point_inflection:endpoint,9] <- "YES")
}

affymatrix[is.na(affymatrix)] <- ""

filename <- paste(c(filename), c(".xls"), sep="")

write.table(affymatrix, file=filename, append = FALSE, sep="\t",
eol="\n", col.names = FALSE, row.names=FALSE, qmethod=c("escape",
"double"))
}

```

```

#
# Software to annotate NFkB inducible genes
#
# Software written by Rifat Hamoudi, 2010
#

setwd("D:\\CGP2005\\GSEA\\GSEA-P-R\\MALT\\Results\\RMA Sets for the
MALTarray paper Reviewer 17\\Norm\\Final sig C sets")

dir.create("nfkb annot")

# input Genes file

# filename = "MALT Pos v
Neg.CELL_CELL_SIGNALING.report.MALTNeg.2.txt.xls"

# input NFkB location

nfkb <- readLines("NFkB list.txt")

maxkb <- length(nfkb)
kbset <- vector(length = maxkb, mode = "numeric")

for (i in 1:maxkb)
{
    kbset[i] <- unlist(strsplit(nfkb[[i]], "\t"))
}

flist <- list.files(".", pattern="report.*.xls$")

for (f in 1:length(flist))
{

    filename = flist[f]

    print(filename)

    genes <- readLines(filename)

    maxGenes <- length(genes)
    genset <- vector(length = maxGenes, mode = "numeric")

    for (i in 1:maxGenes)
    {
        genset[i] <- length(unlist(strsplit(genes[[i]], "\t"))) - 2
    }

    max.size.G <- max(maxGenes)
    gs <- matrix(rep("null", maxGenes*max.size.G), nrow=maxGenes,
ncol= max.size.G)

    temp.names <- vector(length = maxGenes, mode = "character")

```

```

temp.desc <- vector(length = maxGenes, mode = "character")
gs.count <- 1

genesmatrix <- matrix(nrow=1000, ncol=9)
genesmatrix <- as.table(genesmatrix)

i = 2

gene.set.size <- length(unlist(strsplit(genes[[i]], "\t")))
gs.line <- noquote(unlist(strsplit(genes[[i]], "\t")))

gene.set.num <- gs.line[1]
gene.set.gene <- gs.line[2]
gene.set.desc <- gs.line[3]
gene.set.list <- gs.line[4]
gene.set.s2n <- gs.line[5]
gene.set.res <- gs.line[6]
gene.set.core <- gs.line[7]

for (i in 1:maxGenes)
{
  gene.set.size <- length(unlist(strsplit(genes[[i]], "\t")))
  gs.line <- noquote(unlist(strsplit(genes[[i]], "\t")))

  for (j in 1:gene.set.size)
  {
    genesmatrix[i,j] <- gs.line[j]
  }
}

outputmatrix <- matrix(nrow=1000, ncol=10)
outputmatrix <- as.table(outputmatrix)

i = 1

gene.set.size <- length(unlist(strsplit(genes[[i]], "\t")))
gs.line <- noquote(unlist(strsplit(genes[[i]], "\t")))

for (j in 1:gene.set.size)
{
  outputmatrix[i,j] <- gs.line[j]
}

outputmatrix[1,1] <- "Num"
outputmatrix[1,2] <- "Gene"
outputmatrix[1,3] <- "Description"
outputmatrix[1,4] <- "ChromBand"
outputmatrix[1,5] <- "EntrezID"
outputmatrix[1,6] <- "ListLoc"
outputmatrix[1,7] <- "S2N"
outputmatrix[1,8] <- "ES_pval"

```

```

outputmatrix[1,9] <- "Core_Enrichment"
outputmatrix[1,10] <- "NFkB inducible"

for (i in 2:maxGenes)
{
  outputmatrix[i,3] <- genesmatrix[i,3]
  outputmatrix[i,4] <- genesmatrix[i,4]
  outputmatrix[i,5] <- genesmatrix[i,5]
  outputmatrix[i,6] <- genesmatrix[i,6]
  outputmatrix[i,7] <- genesmatrix[i,7]
  outputmatrix[i,8] <- genesmatrix[i,8]
  outputmatrix[i,9] <- genesmatrix[i,9]
  outputmatrix[i,10] <- ""
}

for (i in 2:maxGenes)
{
  outputmatrix[i,1] <- genesmatrix[i,1]
  outputmatrix[i,2] <- genesmatrix[i,2]

  curgene <- outputmatrix[i,2]

  for (j in 1:maxkb)
  {
    if (curgene == kbset[j])
    {
      # cat("YES", i)
      outputmatrix[i,3] <- genesmatrix[i,3]
      outputmatrix[i,4] <- genesmatrix[i,4]
      outputmatrix[i,5] <- genesmatrix[i,5]
      outputmatrix[i,6] <- genesmatrix[i,6]
      outputmatrix[i,7] <- genesmatrix[i,7]
      outputmatrix[i,8] <- genesmatrix[i,8]
      outputmatrix[i,9] <- genesmatrix[i,9]
      outputmatrix[i,10] <- "YES"
    }
  }
}

outputmatrix[is.na(outputmatrix)] <- ""

filename <- paste(c(filename), c(" nfkb_annot.xls"), sep="")

setwd("nfkb annot")

write.table(outputmatrix, file=filename, append = FALSE,
sep="\t", eol="\n", col.names = FALSE, row.names=FALSE,
qmethod=c("escape", "double"))

setwd("../")
}

```

```

#
# Software to identify MALT phenotypic marker by comparing it
# to SMZL, CLL, FL and MCL
#
# Software written by Rifat Hamoudi, 2010
#

library(affy)
library(gcrma)
library(genefilter)
library(annotate)
library(hgu133a.db)
library(hgu133b.db)
library(hgu133aprobe)
library(hgu133bprobe)
library(gsubfn)
library(limma)
library(matchprobes)
library(hgu133acdf)
library(hgu133plus2cdf)

# Load the U133A arrays

setwd("/media/disk/RawArrayData/Cel Files/U133/MALT/HG133_A")
malt <- dir(".", "CEL", recursive=TRUE)

MALT <- ReadAffy(filenamees=malt)

# Load the U133plus2 arrays

setwd("/media/disk/RawArrayData/Cel Files/U133/FL_MCL_CLL")
plus2chip <- dir(".", ".", recursive=FALSE)

FLM_CLL_SMZL <- ReadAffy(filenamees=plus2chip)

# Now combine the 2 platform and normalise them using RMA

phenocomb <- combineAffyBatch(list(MALT,FLM_CLL_SMZL),
c("hgu133aprobe","hgu133plus2probe"), newcdf="newcdfenv", verbose=T)
newcdfenv <- phenocomb$cdf
pheno <- rma(phenocomb$dat)

sampleNames(pheno)

# groups definition

MALT <-
c(1,2,3,4,5,6,7,8,9,10,11,12,13,14,15,16,37,38,39,40,41,42,43,44,45,46)
# group 1

```



```

#
# Unsupervised clustering tree and heatmap software used
# for unsupervised clustering of arrays and qRT-PCR data
# in chapter 4
#
# Software written by Rifat Hamoudi, 2010
#

library(gplots)
library(RColorBrewer)

setwd("D:/PhD related stuff/PhD Thesis Final/Chapters/Figures/Chapter
4/Final Stuff for PhD thesis/clustering")

log2.ratio<-read.table("qPCR genes for clustering transpose proper
thesis.txt", header= TRUE, sep="\t", quote="", comment.char="",
na.strings="#N/A")

log2end <- length(log2.ratio)
log2.ratios <- log2.ratio[2:log2end]

mat=data.matrix(log2.ratios)
xclust<-mat

rownames(xclust) <- as.character(log2.ratio[,1])

#
# heatmap function written by Rifat Hamoudi
#

heatmapcam <- function (x, Rowv = TRUE, Colv = if (symm) "Rowv" else
TRUE, distfun = dist, hclustfun = hclust, dendrogram = c("both", "row",
"column", "none"), symm = FALSE, scale = c("none", "row", "column"),
na.rm = TRUE, revC = identical(Colv, "Rowv"), add.expr, breaks, col =
"heat.colors", colsep, rowsep, sepcolor = "white", sepwidth = c(0.05,
0.05), cellnote, notecex = 1, notecol = "cyan", na.color = par("bg"),
trace = c("column", "row", "both", "none"), tracecol = "cyan", hline =
median(breaks), vline = median(breaks), linecol = tracecol, margins =
c(5,5), ColSideColors, RowSideColors, cexRow = 0.2 + 1/log10(nr),
cexCol = 0.2 + 1/log10(nc), labRow = NULL, labCol = NULL, key = TRUE,
keysize = 1.5, density.info = c("histogram", "density", "none"),
denscol = tracecol, symkey = min(x < 0, na.rm = TRUE), densadj = 0.25,
main = NULL, xlab = NULL, ylab = NULL, ...)
{
  scale01 <- function(x, low = min(x), high = max(x))
  {
    x <- (x - low)/(high - low)
    x
  }
  scale <- if (symm && missing(scale))
    "none"

```

```

else match.arg(scale)
dendrogram <- match.arg(dendrogram)
trace <- match.arg(trace)
density.info <- match.arg(density.info)

if (!missing(breaks) && (scale != "none"))
  warning("Using scale=\"row\" or scale=\"column\" when breaks
are",
         "specified can produce unpredictable results.", "Please
consider using only one or the other.")
if ((Colv == "Rowv") && (!isTRUE(Rowv) || is.null(Rowv)))
  Colv <- FALSE
if (length(di <- dim(x)) != 2 || !is.numeric(x))
  stop("`x' must be a numeric matrix")
nr <- di[1]
nc <- di[2]
if (nr <= 1 || nc <= 1)
  stop("`x' must have at least 2 rows and 2 columns")
if (!is.numeric(margins) || length(margins) != 2)
  stop("`margins' must be a numeric vector of length 2")
if (missing(cellnote))
  cellnote <- matrix("", ncol = ncol(x), nrow = nrow(x))
if (!inherits(Rowv, "dendrogram")) {
  if (((!isTRUE(Rowv)) || (is.null(Rowv))) && (dendrogram %in%
c("both", "row"))) {
    if (is.logical(Colv) && (Colv))
      dendrogram <- "column"
    else dendrogram <- "none"
    warning("Discrepancy: Rowv is FALSE, while dendrogram is
",
           dendrogram, "'. Omitting row dendrogram.")
  }
}
if (!inherits(Colv, "dendrogram")) {
  if (((!isTRUE(Colv)) || (is.null(Colv))) && (dendrogram %in%
c("both", "column"))) {
    if (is.logical(Rowv) && (Rowv))
      dendrogram <- "row"
    else dendrogram <- "none"
    warning("Discrepancy: Colv is FALSE, while dendrogram is
",
           dendrogram, "'. Omitting column dendrogram.")
  }
}
if (inherits(Rowv, "dendrogram")) {
  ddr <- Rowv
  rowInd <- order.dendrogram(ddr)
}
else if (is.integer(Rowv)) {
  hcr <- hclustfun(distfun(x))
  ddr <- as.dendrogram(hcr)
  ddr <- reorder(ddr, Rowv)
  rowInd <- order.dendrogram(ddr)
  if (nr != length(rowInd))
    stop("row dendrogram ordering gave index of wrong length")
}

```

```

}
else if (isTRUE(Rowv)) {
  Rowv <- rowMeans(x, na.rm = na.rm)
  hcr <- hclustfun(distfun(x))
  ddr <- as.dendrogram(hcr)
  ddr <- reorder(ddr, Rowv)
  rowInd <- order.dendrogram(ddr)
  if (nr != length(rowInd))
    stop("row dendrogram ordering gave index of wrong length")
}
else {
  rowInd <- nr:1
}
if (inherits(Colv, "dendrogram")) {
  ddc <- Colv
  colInd <- order.dendrogram(ddc)
}
else if (identical(Colv, "Rowv")) {
  if (nr != nc)
    stop("Colv = \"Rowv\" but nrow(x) != ncol(x)")
  if (exists("ddr")) {
    ddc <- ddr
    colInd <- order.dendrogram(ddc)
  }
  else colInd <- rowInd
}
else if (is.integer(Colv)) {
  hcc <- hclustfun(distfun(if (symm)
    x
  else t(x)))
  ddc <- as.dendrogram(hcc)
  ddc <- reorder(ddc, Colv)
  colInd <- order.dendrogram(ddc)
  if (nc != length(colInd))
    stop("column dendrogram ordering gave index of wrong
length")
}
else if (isTRUE(Colv)) {
  Colv <- colMeans(x, na.rm = na.rm)
  hcc <- hclustfun(distfun(if (symm)
    x
  else t(x)))
  ddc <- as.dendrogram(hcc)
  ddc <- reorder(ddc, Colv)
  colInd <- order.dendrogram(ddc)
  if (nc != length(colInd))
    stop("column dendrogram ordering gave index of wrong
length")
}
else {
  colInd <- 1:nc
}
x <- x[rowInd, colInd]
x.unscaled <- x
cellnote <- cellnote[rowInd, colInd]

```

```

if (is.null(labRow))
  labRow <- if (is.null(rownames(x)))
    (1:nr)[rowInd]
  else rownames(x)
else labRow <- labRow[rowInd]
if (is.null(labCol))
  labCol <- if (is.null(colnames(x)))
    (1:nc)[colInd]
  else colnames(x)
else labCol <- labCol[colInd]
if (scale == "row") {
  x <- sweep(x, 1, rowMeans(x, na.rm = na.rm))
  sx <- apply(x, 1, sd, na.rm = na.rm)
  x <- sweep(x, 1, sx, "/")
}
else if (scale == "column") {
  x <- sweep(x, 2, colMeans(x, na.rm = na.rm))
  sx <- apply(x, 2, sd, na.rm = na.rm)
  x <- sweep(x, 2, sx, "/")
}
if (missing(breaks) || is.null(breaks) || length(breaks) < 1)
  if (missing(col))
    breaks <- 16
  else breaks <- length(col) + 1
if (length(breaks) == 1) {
  breaks <- seq(min(x, na.rm = na.rm), max(x, na.rm = na.rm),
    length = breaks)
}

print(breaks)
cat("length breaks = \n", length(breaks))
cat("\n")

nbr <- length(breaks)
ncol <- length(breaks) - 1
if (class(col) == "function")
  col <- col(ncol)
else if (is.character(col) && length(col) == 1)
  col <- do.call(col, list(ncol))
min.breaks <- min(breaks)
max.breaks <- max(breaks)
x[] <- ifelse(x < min.breaks, min.breaks, x)
x[] <- ifelse(x > max.breaks, max.breaks, x)
lmat <- rbind(4:3, 2:1)
lhei <- lwid <- c(keysize, 4)
if (!missing(ColSideColors)) {
  if (!is.character(ColSideColors) || length(ColSideColors) !=
    nc)
    stop("'ColSideColors' must be a character vector of length
ncol(x)")
  lmat <- rbind(lmat[1, ] + 1, c(NA, 1), lmat[2, ] + 1)
  lhei <- c(lhei[1], 0.2, lhei[2])
}
if (!missing(RowSideColors)) {

```

```

        if (!is.character(RowSideColors) || length(RowSideColors) !=
            nr)
            stop("'RowSideColors' must be a character vector of length
nrow(x)")
        lmat <- cbind(lmat[, 1] + 1, c(rep(NA, nrow(lmat) - 1),
            1), lmat[, 2] + 1)
        lwid <- c(lwid[1], 0.2, lwid[2])
    }
    lmat[is.na(lmat)] <- 0
    op <- par(no.readonly = TRUE)
    on.exit(par(op))
    layout(lmat, widths = lwid, heights = lhei, respect = FALSE)
    if (!missing(RowSideColors)) {
        par(mar = c(margins[1], 0, 0, 0.5))
        image(rbind(1:nr), col = RowSideColors[rowInd], axes = FALSE)
    }
    if (!missing(ColSideColors)) {
        par(mar = c(0.5, 0, 0, margins[2]))
        image(cbind(1:nc), col = ColSideColors[colInd], axes = FALSE)
    }
    par(mar = c(margins[1], 0, 0, margins[2]))
    if (!symm || scale != "none") {
        x <- t(x)
        cellnote <- t(cellnote)
    }
    if (revC) {
        iy <- nr:1
        ddr <- rev(DDR)
        x <- x[, iy]
        cellnote <- cellnote[, iy]
    }
    else iy <- 1:nr
    image(1:nc, 1:nr, x, xlim = 0.5 + c(0, nc), ylim = 0.5 +
        c(0, nr), axes = FALSE, xlab = "", ylab = "", col = col,
        breaks = breaks, ...)
    if (!invalid(na.color) & any(is.na(x))) {
        mmat <- ifelse(is.na(x), 1, NA)
        image(1:nc, 1:nr, mmat, axes = FALSE, xlab = "", ylab = "",
            col = na.color, add = TRUE)
    }
    axis(1, 1:nc, labels = labCol, las = 2, line = -0.5, tick = 0,
        cex.axis = cexCol)
    if (!is.null(xlab))
        mtext(xlab, side = 1, line = margins[1] - 1.25)
    axis(4, iy, labels = labRow, las = 2, line = -0.5, tick = 0,
        cex.axis = cexRow)
    if (!is.null(ylab))
        mtext(ylab, side = 4, line = margins[2] - 1.25)
    if (!missing(add.expr))
        eval(substitute(add.expr))
    if (!missing(colsep))
        for (csep in colsep) rect(xleft = csep + 0.5, ybottom = rep(0,
            length(csep)), xright = csep + 0.5 + sepwidth[1],
            ytop = rep(ncol(x) + 1, csep), lty = 1, lwd = 1,
            col = sepcolor, border = sepcolor)

```

```

if (!missing(rowsep))
  for (rsep in rowsep) rect(xleft = 0, ybottom = (ncol(x) +
    1 - rsep) - 0.5, xright = ncol(x) + 1, ytop = (ncol(x) +
    1 - rsep) - 0.5 - sepwidth[2], lty = 1, lwd = 1,
    col = sepcolor, border = sepcolor)
min.scale <- min(breaks)
max.scale <- max(breaks)
x.scaled <- scale01(t(x), min.scale, max.scale)
if (trace %in% c("both", "column")) {
  for (i in colInd) {
    if (!is.null(vline)) {
      vline.vals <- scale01(vline, min.scale, max.scale)
      abline(v = i - 0.5 + vline.vals, col = linecol,
        lty = 2)
    }
    xv <- rep(i, nrow(x.scaled)) + x.scaled[, i] - 0.5
    xv <- c(xv[1], xv)
    yv <- 1:length(xv) - 0.5
    lines(x = xv, y = yv, lwd = 1, col = tracecol, type = "s")
  }
}
if (trace %in% c("both", "row")) {
  for (i in rowInd) {
    if (!is.null(hline)) {
      hline.vals <- scale01(hline, min.scale, max.scale)
      abline(h = i + hline, col = linecol, lty = 2)
    }
    yv <- rep(i, ncol(x.scaled)) + x.scaled[i, ] - 0.5
    yv <- rev(c(yv[1], yv))
    xv <- length(yv):1 - 0.5
    lines(x = xv, y = yv, lwd = 1, col = tracecol, type = "s")
  }
}
if (!missing(cellnote))
  text(x = c(row(cellnote)), y = c(col(cellnote)), labels =
c(cellnote),
  col = notecol, cex = notecex)
par(mar = c(margins[1], 0, 0, 0))
if (dendrogram %in% c("both", "row")) {
  plot(DDR, horiz = TRUE, axes = FALSE, yaxs = "i", leaflab =
"none")
}
else plot.new()
par(mar = c(0, 0, if (!is.null(main)) 5 else 0, margins[2]))
if (dendrogram %in% c("both", "column")) {
  plot(ddc, axes = FALSE, xaxs = "i", leaflab = "none")
}
else plot.new()
if (!is.null(main))
  title(main, cex.main = 1.5 * op[["cex.main"]])
if (key) {
  par(mar = c(5, 4, 2, 1), cex = 0.75)
  if (symkey) {
    max.raw <- max(abs(x), na.rm = TRUE)
    min.raw <- -max.raw
  }
}

```

```

}
else {
  min.raw <- min(x, na.rm = TRUE)
  max.raw <- max(x, na.rm = TRUE)
}
z <- seq(min.raw, max.raw, length = length(col))
image(z = matrix(z, ncol = 1), col = col, breaks = breaks,
      xaxt = "n", yaxt = "n")
par(usr = c(0, 1, 0, 1))
lv <- pretty(breaks)
xv <- scale01(as.numeric(lv), min.raw, max.raw)
axis(1, at = xv, labels = lv)
if (scale == "row")
  mtext(side = 1, "Row Z-Score", line = 2)
else if (scale == "column")
  mtext(side = 1, "Column Z-Score", line = 2)
else mtext(side = 1, "Value", line = 2)
if (density.info == "density") {
  dens <- density(x, adjust = densadj, na.rm = TRUE)
  omit <- dens$x < min(breaks) | dens$x > max(breaks)
  dens$x <- dens$x[-omit]
  dens$y <- dens$y[-omit]
  dens$x <- scale01(dens$x, min.raw, max.raw)
  lines(dens$x, dens$y/max(dens$y) * 0.95, col = denscol,
        lwd = 1)
  axis(2, at = pretty(dens$y)/max(dens$y) * 0.95,
pretty(dens$y))
  title("Color Key\nand Density Plot")
  par(cex = 0.5)
  mtext(side = 2, "Density", line = 2)
}
else if (density.info == "histogram") {
  h <- hist(x, plot = FALSE, breaks = breaks)
  hx <- scale01(breaks, min.raw, max.raw)
  hy <- c(h$counts, h$counts[length(h$counts)])
  lines(hx, hy/max(hy) * 0.95, lwd = 1, type = "s",
        col = denscol)
  axis(2, at = pretty(hy)/max(hy) * 0.95, pretty(hy))
  title("Color Key\nand Histogram")
  par(cex = 0.5)
  mtext(side = 2, "Count", line = 2)
}
else title("Color Key")
}
else plot.new()
invisible(list(rowInd = rowInd, colInd = colInd))
}

```

```

# What some programs do (like Eisen's cluster) is "threshold" the NA
# values to some arbitrary "large" distance.
# I wrote the following dist function computes distances and then
# replaces any NA values with an arbitrarily
# large distance (10% greater than the largest actual distance).

```

```

# This function may be helpful for input into hclust because NA values
# are replaced

na.dist <- function(x,...)
{
  t.dist <- dist(x,...)
  t.dist <- as.matrix(t.dist)
  t.limit <- 1.1*max(t.dist,na.rm=T)
  t.dist[is.na(t.dist)] <- t.limit
  t.dist <- as.dist(t.dist)
  return(t.dist)
}

# Displaying the cluster tree

ndist<-na.dist(t(log2.ratios), method="euclidean") # t = transpose
ntree<-hclust(ndist, method="ward")
plot(ntree)

#Uses 256 shades of Red and Blue

heatcol<-colorRampPalette(brewer.pal(11, "RdBu"))(256)

csc <- heatcol[seq(from=1,to=256,length=109)]

mat = data.matrix(log2.ratios)

x <- mat
# Displaying the cluster heatmap

dist.x <- dist(x,method="euclidean",diag=TRUE)
clust.x <- hclust(dist.x, method="ward")
dist.y <- dist(t(x), method="euclidean",diag=TRUE)
clust.y <- hclust(dist.y,method="ward")

heatmapcam(x, Rowv=as.dendrogram(clust.x), Colv=as.dendrogram(clust.y),
symkey=FALSE, density.info="none", trace="none", cexRow=0.5,
cexCol=0.5, col = colorpanel(n=99,low="green",mid="black",high="red"),
breaks=c(seq(2,5,length.out=50),seq(4,13,length.out=50)))

```

```

#
# Software to display qRT-PCR data in bar charts with standard
# error bars
#
# Software written by Rifat Hamoudi, 2010
#

setwd("D:/Cambridge Work/Array Projects/Microarray
Documents/Results/qPCR/qPCR on patients/Final Stuff for PhD thesis/qPCR
graphs split on translocation")

# N-MALT

NMALT<-read.table("qPCR NMALT.txt",sep="\t", header=TRUE)

      boxplot(Exp~Translocation,
              data=NMALT,
              border="black",
              col="white",
              boxwex=0.5,
              xlab = "Translocation",
              ylab = "Expression",
              outline = FALSE,
              frame = FALSE,
              main="NMALT")

points(NMALT$Translocation, NMALT$Exp)

# BCL10

bcl10<-read.table("qPCR BCL10.txt",sep="\t", header=TRUE)

      boxplot(Exp~Translocation,
              data=bcl10,
              border="black",
              col="white",
              xlab = "Translocation",
              ylab = "Expression",
              boxwex=0.5,
              outline = FALSE,
              frame = FALSE,
              main="BCL10")

points(bcl10$Translocation, bcl10$Exp)

```

```

# CCR2

ccr2<-read.table("qPCR CCR2.txt",sep="\t", header=TRUE)

      boxplot(Exp~Translocation,
              data=ccr2,
              border="black",
              col="white",
              xlab = "Translocation",
              ylab = "Expression",
              boxwex=0.5,
              outline = FALSE,
              frame = FALSE,
              main="CCR2")

points(ccr2$Translocation, ccr2$Exp)

# CCR5

ccr5<-read.table("qPCR CCR5.txt",sep="\t", header=TRUE)

      boxplot(Exp~Translocation,
              data=ccr5,
              border="black",
              col="white",
              xlab = "Translocation",
              ylab = "Expression",
              boxwex=0.5,
              outline = FALSE,
              frame = FALSE,
              main="CCR5")

points(ccr5$Translocation, ccr5$Exp)

# CD69

cd69<-read.table("qPCR CD69.txt",sep="\t", header=TRUE)

      boxplot(Exp~Translocation,
              data=cd69,
              border="black",
              col="white",
              xlab = "Translocation",
              ylab = "Expression",
              boxwex=0.5,
              outline = FALSE,
              frame = FALSE,
              main="CD69")

points(cd69$Translocation, cd69$Exp)

```

```

# CD86

cd86<-read.table("qPCR CD86.txt",sep="\t", header=TRUE)

      boxplot(Exp~Translocation,
              data=cd86,
              border="black",
              col="white",
              xlab = "Translocation",
              ylab = "Expression",
              boxwex=0.5,
              outline = FALSE,
              frame = FALSE,
              main="CD86")

points(cd86$Translocation, cd86$Exp)

# MINOR

minor<-read.table("qPCR MINOR.txt",sep="\t", header=TRUE)

      boxplot(Exp~Translocation,
              data=minor,
              border="black",
              col="white",
              xlab = "Translocation",
              ylab = "Expression",
              boxwex=0.5,
              outline = FALSE,
              frame = FALSE,
              main="MINOR")

points(minor$Translocation, minor$Exp)

# TLR6

tlr6<-read.table("qPCR TLR6.txt",sep="\t", header=TRUE)

      boxplot(Exp~Translocation,
              data=tlr6,
              border="black",
              col="white",
              xlab = "Translocation",
              ylab = "Expression",
              boxwex=0.5,
              outline = FALSE,
              frame = FALSE,
              main="TLR6")

points(tlr6$Translocation, tlr6$Exp)

```

```
# BCL2

bcl2<-read.table("qPCR BCL2.txt",sep="\t", header=TRUE)

      boxplot(Exp~Translocation,
              data=bcl2,
              border="black",
              col="white",
              xlab = "Translocation",
              ylab = "Expression",
              boxwex=0.5,
              outline = FALSE,
              main="BCL2")

points(bcl2$Translocation, bcl2$Exp)

# IRF4

irf4<-read.table("qPCR IRF4.txt",sep="\t", header=TRUE)

      boxplot(Exp~Translocation,
              data=irf4,
              border="black",
              col="white",
              xlab = "Translocation",
              ylab = "Expression",
              boxwex=0.5,
              outline = FALSE,
              main="IRF4")

points(irf4$Translocation, irf4$Exp)
```

II.II Visual Basic software for relational database management software

Two relational database management software (RDBMS) were written for this thesis. Firstly, an RDBMS entitled “ArrayExplorer RDBMS” which allowed the query and data management generated from the microarray experiments. Secondly an RDBMS entitled “GSEA RDBMS” which contained query and data management functionalities that helped in collating the information generated from GSEA.

Both of these software are included in the complementary DVD attached to the back cover of this thesis.

The following are examples of the software’s functionalities and design



Main page

ArrayExp

04 May 2011
 Programmer : Rifal Hanoud Supervisor : Ming Du

MALT Translocation

Find Data from Chromosome

Find Data from Gene Description

Find Data from Probe ID

List NFkB inducible genes in MALT only

MALT Neg v MCL + FL

List MALT phenotypic markers

Find Data from Chromosome

List NFkB inducible genes in MALT Neg, FL and MCL

Find Data from Gene Description

Find Data from Probe ID

Main Menu

| ProbeID | Description | Chromosome | Ensembl | RefSeq Tran | 1_14+ve G0 | 1_14+ve G0 | 1_14+ve Bc | 1_2+ve G63 | 11_18+ve G | 11_18+ve G | 11_18 |
|-------------|--|-------------------|--------------|--------------|------------|------------|------------|------------|------------|------------|--------|
| 1405_1_at | M21121 /FEATURE= /DEFINITION=HUMTCSM Human T cell-specific protein [F chr17q11.2-q12 | | ENSG00000161 | NM_002985 | 140.1 | 100.6 | 678 | 145.7 | 543.8 | 900 | |
| 1431_at | J02843 /FEATURE=cds /DEFINITION=HUMCYPIE Human cytochrome P45011E1 | chr10q24.3-qter | ENSG00000130 | NM_000773 | 9.2 | 8.7 | 17.1 | 24.5 | 12.6 | 8.3 | |
| 25150_at | Cluster Incl. X60592:Human CDw40 mRNA for nerve growth factor receptor-1 | chr20q12-q13.2 | ENSG00000101 | NM_001250 | 483.3 | 366.4 | 280.6 | 325.4 | 529.1 | 421 | |
| 39402_at | Cluster Incl. M15330:Human interleukin 1-beta (IL1B) mRNA, complete cds / | chr2q14 | ENSG00000125 | NM_000576 | 11.1 | 41.6 | 20.4 | 92.1 | 31.8 | 8.9 | |
| 200642_at | gb:NM_000454.1 /DEF=Homo sapiens superoxide dismutase 1, soluble [amy chr21q22.1] | 21q22.2 | ENSG00000142 | NM_000454 | 950.5 | 1052.9 | 857.6 | 487.1 | 917.8 | 1129.5 | |
| 200737_at | gb:NM_000291.1 /DEF=Homo sapiens phosphoglycerate kinase 1 (PGK1), mR | chrXq13 | ENSG00000102 | NM_000291 | 230.2 | 211.6 | 108.6 | 83.2 | 179 | 176.1 | |
| 200738_s_at | gb:NM_000291.1 /DEF=Homo sapiens phosphoglycerate kinase 1 (PGK1), mR | chrXq13 | ENSG00000102 | NM_000291 | 971.1 | 1164.7 | 579.2 | 306.8 | 688.6 | 1010.5 | |
| 200770_s_at | gb:J03202.1 /DEF=Human laminin B2 chain mRNA, complete cds. /FEA=mRN | chr1q31 | ENSG00000135 | NM_002293 | 29.9 | 56.2 | 36.1 | 81.1 | 29.9 | 56 | |
| 200838_at | gb:NM_001908.1 /DEF=Homo sapiens cathepsin B (CTSB), mRNA. /FEA=mRN | chr8p22 | ENSG00000164 | NM_001908 | 309.9 | 552.6 | 135.4 | 160.2 | 366.6 | 468.1 | |
| 200839_s_at | gb:NM_001908.1 /DEF=Homo sapiens cathepsin B (CTSB), mRNA. /FEA=mRN | chr8p22 | ENSG00000164 | NM_001908 | 451.3 | 828.1 | 546.4 | 122.3 | 579.5 | 1102.3 | |
| 200943_at | gb:NM_004965.1 /DEF=Homo sapiens high-mobility group (nonhistone chro | chr21q22.3 | 21q22.2 | ENSG00000198 | NM_004965 | 527.7 | 1310.7 | 1519 | 361.3 | 527.8 | 873.6 |
| 200944_s_at | gb:NM_004965.1 /DEF=Homo sapiens high-mobility group (nonhistone chro | chr21q22.3 | 21q22.2 | ENSG00000198 | NM_004965 | 1571.5 | 1753.3 | 1410.2 | 700.6 | 1513.5 | 1460.6 |
| 200951_s_at | Consensus includes gb:AW026491 /FEA=EST /DB_XREF=gi:5880021 /DB_XREF= | chr12p13 | ENSG00000118 | NM_001759 | 102.2 | 89.3 | 109.1 | 66.9 | 31.3 | 37.5 | |
| 200952_s_at | Consensus includes gb:A1635187 /FEA=EST /DB_XREF=gi:4686517 /DB_XREF= | chr12p13 | ENSG00000118 | NM_001759 | 66.8 | 76.9 | 65.7 | 119 | 56.8 | 60 | |
| 200953_s_at | gb:NM_001759.1 /DEF=Homo sapiens cyclin D2 (CCND2), mRNA. /FEA=mRNA | chr12p13 | ENSG00000118 | NM_001759 | 646 | 576.6 | 649.3 | 485.7 | 359.2 | 497.4 | |
| 201261_x_at | gb:BC002416.1 /DEF=Homo sapiens, biglycan, clone MGC:2298, mRNA, comp | chrXq28 | ENSG00000182 | NM_001711 | 112.9 | 273.9 | 240.8 | 186 | 167.1 | 103 | |
| 201262_x_at | gb:NM_001711.1 /DEF=Homo sapiens biglycan (BGN), mRNA. /FEA=mRNA /G | chrXq28 | ENSG00000182 | NM_001711 | 29 | 79.7 | 20.6 | 17.5 | 52.3 | 8.1 | |
| 201313_at | gb:NM_001975.1 /DEF=Homo sapiens enolase 2, (gamma, neuronal) (ENO2), | chr12p13 | ENSG00000111 | NM_001975 | 172.1 | 85.2 | 90.2 | 94.9 | 119.1 | 164.2 | |
| 201426_s_at | Consensus includes gb:A1922599 /FEA=EST /DB_XREF=gi:5658563 /DB_XREF= | chr10p13 | ENSG00000026 | NM_003380 | 3439.7 | 2979.1 | 1958.4 | 1079.3 | 2877.1 | 3046.3 | |
| 201473_at | gb:NM_002229.1 /DEF=Homo sapiens jun B proto-oncogene (JUNB), mRNA. | chr19p13.2 | ENSG00000171 | NM_002229 | 231.2 | 424.2 | 226.2 | 171.1 | 205.3 | 262.5 | |
| 201502_s_at | Consensus includes gb:A1078167 /FEA=EST /DB_XREF=gi:3412575 /DB_XREF= | chr14q13 | ENSG00000100 | NM_002529 | 1123.5 | 1578.4 | 1814.3 | 2043.6 | 2308.9 | 2005.2 | |
| 201510_at | gb:AF017307.1 /DEF=Homo sapiens Ets-related transcription factor (ERT) mR | chr14q32 | ENSG00000163 | NM_004433 | 35.8 | 45.4 | 31.3 | 54.6 | 34.1 | 15.3 | |
| 201694_s_at | gb:NM_001964.1 /DEF=Homo sapiens early growth response 1 (EGR1), mRN | chr5q31.1 | ENSG00000120 | NM_001964 | 94.2 | 755.2 | 110.1 | 231.4 | 196.1 | 124.9 | |
| 201700_at | gb:NM_001760.1 /DEF=Homo sapiens cyclin D3 (CCND3), mRNA. /FEA=mRNA | chr9p21 | ENSG00000112 | NM_001760 | 354.8 | 338.4 | 363.6 | 543 | 189.7 | 387.2 | |
| 201746_at | gb:NM_000546.2 /DEF=Homo sapiens tumor protein p53 (L1-Fraumeni syndr | chr17p13.1 | ENSG00000141 | NM_000546 | 239.6 | 207.8 | 244.4 | 184.1 | 315.7 | 218.7 | |
| 201808_s_at | Consensus includes gb:BE732652 /FEA=EST /DB_XREF=gi:10146644 /DB_XREF= | chr9q33-q34.1 | ENSG00000106 | NM_000118 | 26.6 | 7.2 | 8.8 | 13.4 | 54.7 | 27.4 | |
| 201809_s_at | gb:NM_000118.1 /DEF=Homo sapiens endoglin (Osler-Render-Weber syndro | chr9q33-q34.1 | ENSG00000106 | NM_000118 | 76.7 | 288.7 | 130.2 | 293.3 | 128.8 | 164 | |
| 201848_s_at | gb:U15174.1 /DEF=Homo sapiens BCL2adenovirus E1B 19kD-interacting p | chr10q26.3 | ENSG00000176 | NM_004052 | 68.6 | 57.7 | 33.3 | 67 | 55.1 | 43.5 | |
| 201849_at | gb:NM_004052.2 /DEF=Homo sapiens BCL2adenovirus E1B 19kD-interacti | chr10q26.3 | ENSG00000176 | NM_004052 | 26.7 | 65.3 | 60.3 | 61.8 | 36.9 | 43.7 | |
| 201858_s_at | gb:J03223.1 /DEF=Human secretory granule proteoglycan peptide core mR | chr10q22.1 | ENSG00000122 | NM_002727 | 1561.1 | 1701.6 | 611.9 | 226.4 | 698.5 | 1013.8 | |
| 201859_s_at | gb:NM_002727.1 /DEF=Homo sapiens proteoglycan 1, secretory granule (P | chr10q22.1 | ENSG00000122 | NM_002727 | 1050.6 | 1086.6 | 1681.4 | 582.3 | 307.6 | 1047.3 | |
| 201891_s_at | gb:NM_004048.1 /DEF=Homo sapiens beta-2-microglobulin (B2M), mRNA. / | chr15q21-q22.2 | ENSG00000166 | NM_004048 | 6196.2 | 7260.5 | 8292.5 | 6342 | 11229.7 | 5875.9 | |
| 201983_s_at | Consensus includes gb:AW157070 /FEA=EST /DB_XREF=gi:6228471 /DB_XREF= | chr7p12 | ENSG00000126 | NM_005228 | 66.8 | 108 | 90.8 | 67 | 30.1 | 100.9 | |
| 201984_s_at | gb:NM_005228.1 /DEF=Homo sapiens epidermal growth factor receptor (avii | chr7p12 | ENSG00000146 | NM_005228 | 49.7 | 42.5 | 21.1 | 61.2 | 45.3 | 42.3 | |
| 202023_at | gb:NM_004428.1 /DEF=Homo sapiens ephrin-A1 (EFNA1), mRNA. /FEA=mRN | chr1q21-q22 | ENSG00000169 | NM_004428 | 8.8 | 83.7 | 50 | 14.5 | 6.8 | 31.2 | |
| 202071_at | gb:NM_002999.1 /DEF=Homo sapiens syndecan 4 (amphiglycan, ryudocan) (| chr20q12 | ENSG00000124 | NM_002999 | 99 | 399.8 | 227.1 | 178.2 | 98.5 | 74.6 | |
| 202076_at | gb:NM_001166.2 /DEF=Homo sapiens baculoviral IAP repeat-containing 2 (B | chr11q22 | ENSG00000110 | NM_001166 | 255.5 | 406.4 | 334.3 | 266.6 | 333.4 | 265.7 | |
| 202081_at | gb:NM_004907.1 /DEF=Homo sapiens immediate early protein (ETR101), mR | chr19p13.13 | ENSG00000160 | NM_004907 | 694.9 | 1096 | 888.2 | 564.2 | 827.5 | 1165.4 | |
| 202086_at | gb:NM_002462.1 /DEF=Homo sapiens myxovirus (influenza) resistance 1, h | chr21q22.3 | ENSG00000157 | NM_002462 | 208.6 | 208.4 | 124.4 | 152.7 | 826.1 | 633.5 | |
| 202087_s_at | gb:NM_001912.1 /DEF=Homo sapiens cathepsin L (CTSL), mRNA. /FEA=mRN | chr9q21-q22 | ENSG00000135 | NM_001912 | 243.1 | 213 | 196.3 | 174.2 | 132.7 | 187.2 | |
| 202258_s_at | Consensus includes gb:U50532.1 /DEF=Human BRCA2 region, mRNA sequen | chr13q12-q13 | ENSG00000139 | NM_014887 | 235.4 | 193.1 | 481.8 | 174.4 | 292.2 | 254.2 | |
| 202270_at | gb:NM_002053.1 /DEF=Homo sapiens guanylate binding protein 1, interfer | chr12p22.2 | ENSG00000117 | NM_002053 | 29.3 | 47.6 | 119.6 | 39 | 52.1 | 108.3 | |
| 202393_s_at | gb:NM_005655.1 /DEF=Homo sapiens TGFb Inducible early growth response | chr8q22.2 | ENSG00000155 | NM_005655 | 101.5 | 88.3 | 102.4 | 283 | 84.6 | 143.1 | |
| 202431_s_at | gb:NM_002467.1 /DEF=Homo sapiens v-myc avian myelocytomatosis viral or | chr8q24.12-q24.13 | ENSG00000136 | NM_002467 | 182.5 | 252.8 | 39.3 | 52.5 | 431.8 | 323 | |
| 202531_at | gb:NM_002198.1 /DEF=Homo sapiens intercon regulatory factor 1 (IRF1), m | chr5q31.1 | ENSG00000125 | NM_002198 | 294.2 | 248 | 321.2 | 229.4 | 331.9 | 378.9 | |
| 202637_s_at | Consensus includes gb:A608725 /FEA=EST /DB_XREF=gi:4617892 /DB_XREF= | chr19p13.3-p13.2 | ENSG00000090 | NM_000201 | 201 | 453.6 | 158.1 | 286.8 | 197.6 | 155 | |
| 202638_s_at | gb:NM_000201.1 /DEF=Homo sapiens intercellular adhesion molecule 1 (CD | chr19p13.3-p13.2 | ENSG00000090 | NM_000201 | 107.4 | 268.8 | 56.3 | 86.6 | 65.2 | 105.8 | |
| 202644_s_at | gb:NM_006290.1 /DEF=Homo sapiens tumor necrosis factor, alpha-induced | chr6q23 | ENSG00000118 | NM_006290 | 778.2 | 1035.7 | 1067.7 | 873 | 884.5 | 1039.6 | |

List of NF-κB genes across arrays of various lymphomas

Appendix III – GSEA results

III.I NF- κ B target gene set

A list of 271 NF- κ B target genes was compiled as described in appendix I.III. 223 genes were obtained from the website:

However the remaining 48 genes were obtained through bioinformatics and literature search as described in appendix I.III. The 48 genes are listed below:

| Gene symbol | Gene full name | Source |
|-------------|---|---|
| TRIP10 | thyroid hormone receptor interactor 10 | bioinformatics |
| IL32 | interleukin 32 | bioinformatics |
| RCP9 | calcitonin gene-related peptide-receptor component pro | bioinformatics |
| ANKRD1 | ankyrin repeat domain 1 (cardiac muscle) | bioinformatics |
| TNFRSF10B | tumor necrosis factor receptor superfamily, member 10b | bioinformatics |
| AKR1C2 | aldo-keto reductase family 1, member C2 (dihydrodiol de | bioinformatics |
| LDHB | lactate dehydrogenase B | bioinformatics |
| TEAD1 | TEA domain family member 1 (SV40 transcriptional en | bioinformatics |
| PRDM2 | PR domain containing 2, with ZNF domain | bioinformatics |
| BACE2 | beta-site APP-cleaving enzyme 2 | bioinformatics |
| SUV39H1 | suppressor of variegation 3-9 homolog 1 (Drosophila) | bioinformatics |
| IL1F9 | interleukin 1 family, member 9 | bioinformatics |
| ALOX12B | arachidonate 12-lipoxygenase, 12R type | bioinformatics |
| CARD15 | caspase recruitment domain family, member 15 | bioinformatics |
| CD74 | CD74 antigen (invariant polypeptide of major histocom | bioinformatics |
| CXCL2 | chemokine (C-X-C motif) ligand 2 | bioinformatics |
| DEFB4 | defensin, beta 4 | bioinformatics |
| IL15RA | interleukin 15 receptor, alpha | bioinformatics |
| TPMT | thiopurine S-methyltransferase | bioinformatics |
| TLR6 | toll-like receptor 6 | bioinformatics |
| TLR4 | toll-like receptor 4 | bioinformatics |
| SH3BGRL3 | SH3 domain binding glutamic acid-rich protein like 3 | bioinformatics |
| PLA2G2E | phospholipase A2, group IIE | bioinformatics |
| ADAMTS12 | ADAM metalloproteinase with thrombospondin type 1 m | bioinformatics |
| CSF2RA | colony stimulating factor 2 receptor, alpha, low-affinity | bioinformatics |
| MMP8 | matrix metalloproteinase 8 (neutrophil collagenase) | bioinformatics |
| CCL7 | chemokine (C-C motif) ligand 7 | bioinformatics |
| TNFRSF21 | tumor necrosis factor receptor superfamily, member 21 | bioinformatics |
| PLA2G4A | phospholipase A2, group IVA (cytosolic, calcium-depend | bioinformatics |
| LAMC2 | laminin, gamma 2 | bioinformatics |
| BCL2L10 | BCL2-like 10 (apoptosis facilitator) | bioinformatics |
| TNFSF6 | tumor necrosis factor superfamily, member 6 | bioinformatics |
| CD105 | homodimeric transmembrane protein which is a major gl | bioinformatics |
| TNFRSF6 | tumor necrosis factor receptor superfamily, member 6, d | bioinformatics |
| TNFSF5 | tumor necrosis factor superfamily, member 5 | bioinformatics |
| BM2 | influenza B virus BM2 | bioinformatics |
| HC3 | proteasome subunit HC3 | bioinformatics |
| SIAT8A | ST 8 alpha-N-acetyl-neuraminide alpha-2,8-sialyltransfer | bioinformatics |
| TBR | tuberin | bioinformatics |
| TNFRSF5 | tumor necrosis factor receptor superfamily, member 5, d | bioinformatics |
| RBCK1 | RanBP-type and C3HC4-type zinc finger containing 1 | bioinformatics |
| CCR2A | chemokine (C-C motif) receptor 2 isoform A | bioinformatics |
| CCR2B | chemokine (C-C motif) receptor 2 isoform B | bioinformatics |
| BIRC2 | baculoviral IAP repeat-containing 2 | Blood, 15th of August, 2005 ; 106(4) : 1392 - 1399 |
| ICAM1 | intercellular adhesion molecule 1 (CD54), human rhinov | Blood, 15th of August, 2005 ; 106(4) : 1392 - 1399 |
| CX3CL1 | chemokine (C-X3-C motif) ligand 1 | Blood, 15th of August, 2005 ; 106(4) : 1392 - 1399 |
| NR4A3 | nuclear receptor subfamily 4, group A, member 3 | Journal of Biological Chemistry, 12th of August, 2005 ; 280(32) : 29256-29262 |
| BCL10 | B-cell CLL/lymphoma 10 | Journal of Biological Chemistry, 6th of January, 2006 ; 281(1) : 167 - 175 |

III.II Leading edge core set of NF- κ B target genes enriched in MALT lymphoma with and without chromosome translocation

| Rank | Gene | Description | Chromosome Band | Entre z ID | Signal to noise | Enrichment Score |
|---|----------|---|-----------------|------------|-----------------|------------------|
| Expression of genes enriched in translocation negative MALT lymphoma | | | | | | |
| 1 | CXCL5 | chemokine (C-X-C motif) ligand 5 | 4q12-q13 | 6374 | 0.530 | 0.020 |
| 2 | PTGS2 | prostaglandin-endoperoxide synthase 2 (prostaglandin G/H synthase and cyclooxygenase) | 1q25.2-q25.3 | 5743 | 0.519 | 0.039 |
| 3 | NR4A3 | nuclear receptor subfamily 4, group A, member 3 | 9q22 | 8013 | 0.485 | 0.057 |
| 4 | CCL11 | chemokine (C-C motif) ligand 11 | 17q21.1-q21.2 | 6356 | 0.455 | 0.073 |
| 5 | PTGIS | prostaglandin I2 (prostacyclin) synthase | 20q13.13 | 5740 | 0.416 | 0.087 |
| 6 | IL8 | interleukin 8 | 4q13-q21 | 3576 | 0.395 | 0.100 |
| 7 | MMP3 | matrix metalloproteinase 3 (stromelysin 1, progelatinase) | 11q22.3 | 4314 | 0.388 | 0.114 |
| 8 | CXCL2 | chemokine (C-X-C motif) ligand 2 | 4q21 | 2920 | 0.372 | 0.126 |
| 9 | CXCL1 | chemokine (C-X-C motif) ligand 1 (melanoma growth stimulating activity, alpha) | 4q21 | 2919 | 0.370 | 0.140 |
| 10 | CD86 | CD86 molecule | 3q21 | 942 | 0.359 | 0.152 |
| 11 | CCL2 | chemokine (C-C motif) ligand 2 | 17q11.2-q12 | 6347 | 0.346 | 0.161 |
| 12 | IGFBP2 | insulin-like growth factor binding protein 2, 36kDa | 2q33-q34 | 3485 | 0.323 | 0.169 |
| 13 | GZMB | granzyme B (granzyme 2, cytotoxic T-lymphocyte-associated serine esterase 1) | 14q11.2 | 3002 | 0.322 | 0.181 |
| 14 | VEGF | vascular endothelial growth factor | 6p12 | 7422 | 0.313 | 0.190 |
| 15 | SOD2 | superoxide dismutase 2, mitochondrial | 6q25.3 | 6648 | 0.313 | 0.202 |
| 16 | IL11 | interleukin 11 | 19q13.3-q13.4 | 3589 | 0.313 | 0.214 |
| 17 | PLAU | plasminogen activator, urokinase | 10q24 | 5328 | 0.311 | 0.225 |
| 18 | GBP1 | guanylate binding protein 1, interferon-inducible, 67kDa | 1p22.2 | 2633 | 0.310 | 0.237 |
| 19 | SDC4 | syndecan 4 | 20q12 | 6385 | 0.292 | 0.242 |
| 20 | AKR1C2 | aldo-keto reductase family 1, member C2 (dihydrodiol dehydrogenase 2: bile acid) | 10p15-p14 | 1646 | 0.288 | 0.251 |
| 21 | IER3 | immediate early response 3 | 6p21.3 | 8870 | 0.277 | 0.256 |
| 22 | EGR1 | early growth response 1 | 5q31.1 | 1958 | 0.268 | 0.262 |
| 23 | TNC | tenascin C | 9q33 | 3371 | 0.268 | 0.272 |
| 24 | PENK | proenkephalin | 8q23-q24 | 5179 | 0.258 | 0.278 |
| 25 | KITLG | KIT ligand | 12q22 | 4254 | 0.252 | 0.283 |
| 26 | PRF1 | perforin 1 (pore forming protein) | 10q22 | 5551 | 0.245 | 0.289 |
| 27 | GADD45B | growth arrest and DNA-damage-inducible, beta | 19p13.3 | 4616 | 0.237 | 0.292 |
| 28 | FN1 | fibronectin 1 | 2q34 | 2335 | 0.236 | 0.301 |
| 29 | THBS2 | thrombospondin 2 | 6q27 | 7058 | 0.232 | 0.308 |
| 30 | NOO1 | NAD(P)H dehydrogenase, quinone 1 | 16q22.1 | 1728 | 0.232 | 0.317 |
| 31 | TEAD1 | TEA domain family member 1 (SV40 transcriptional enhancer factor) | 11p15.2 | 7003 | 0.229 | 0.323 |
| 32 | AGT | angiotensinogen (serpin peptidase inhibitor, clade A, member 8) | 1q42-q43 | 183 | 0.219 | 0.323 |
| 33 | IL1B | interleukin 1, beta | 2q14 | 3553 | 0.196 | 0.311 |
| 34 | GIF | gastric intrinsic factor (vitamin B synthesis) | 11q13 | 2694 | 0.195 | 0.317 |
| 35 | RBCK1 | RanBP-type and C3HC4-type zinc finger containing 1 | 20p13 | 10616 | 0.195 | 0.324 |
| 36 | CYP7B1 | cytochrome P450, family 7, subfamily B, polypeptide 1 | 8q21.3 | 9420 | 0.188 | 0.324 |
| 37 | IL10 | interleukin 10 | 1q31-q32 | 3586 | 0.186 | 0.329 |
| 38 | ELF3 | E74-like factor 3 (ets domain transcription factor, epithelial-specific) | 1q32.2 | 1999 | 0.183 | 0.332 |
| 39 | TLR2 | toll-like receptor 2 | 4q32 | 7097 | 0.181 | 0.337 |
| 40 | PTX3 | pentraxin-related gene, rapidly induced by IL-1 beta | 3q25 | 5806 | 0.180 | 0.343 |
| 41 | BMP2 | bone morphogenetic protein 2 | 20p12 | 650 | 0.177 | 0.346 |
| 42 | IL1RN | interleukin 1 receptor antagonist | 2q14.2 | 3557 | 0.173 | 0.348 |
| 43 | FCER2 | Fc fragment of IgE, low affinity II, receptor for (CD23) | 19p13.3 | 2208 | 0.167 | 0.346 |
| 44 | UGCG | UDP-glucose ceramide glucosyltransferase | 9q31 | 7357 | 0.167 | 0.352 |
| 45 | BDKRB1 | bradykinin receptor B1 | 14q32.1-q32.2 | 623 | 0.165 | 0.354 |
| 46 | HPSE | heparanase | 4q21.3 | 10855 | 0.162 | 0.356 |
| 47 | EGFR | epidermal growth factor receptor (erythroblastic leukemia viral (v-erb-b) oncogene) | 7p12 | 1956 | 0.158 | 0.357 |
| 48 | BAX | BCL2-associated X protein | 19q13.3-q13.4 | 581 | 0.150 | 0.353 |
| 49 | CCL4 | chemokine (C-C motif) ligand 4 | 17q12 | 6351 | 0.150 | 0.358 |
| 50 | DIO2 | deiodinase, iodothyronine, type II | 14q24.2-q24.3 | 1734 | 0.146 | 0.357 |
| 51 | ORM1 | orosomucoid 1 | 9q31-q32 | 5004 | 0.146 | 0.363 |
| 52 | XDH | xanthine dehydrogenase | 2p23.1 | 7498 | 0.146 | 0.368 |
| 53 | CXCL9 | chemokine (C-X-C motif) ligand 9 | 4q21 | 4283 | 0.145 | 0.372 |
| 54 | TFF3 | trefoil factor 3 (intestinal) | 21q22.3 | 7033 | 0.144 | 0.377 |
| 55 | PTAFR | platelet-activating factor receptor | 1p35-p34.3 | 5724 | 0.144 | 0.382 |
| 56 | TNFRSF21 | tumor necrosis factor receptor superfamily, member 21 | 6p21.1-p12.2 | 27242 | 0.141 | 0.383 |
| 57 | KCNK5 | potassium channel, subfamily K, member 5 | 6p21 | 8645 | 0.139 | 0.383 |
| 58 | JUNB | jun B proto-oncogene | 19p13.2 | 3726 | 0.136 | 0.384 |
| 59 | ICOS | inducible T-cell co-stimulator | 2q33 | 29851 | 0.130 | 0.378 |
| 60 | TLR4 | toll-like receptor 4 | 9q32-q33 | 7099 | 0.127 | 0.378 |
| 61 | DEFB4 | defensin, beta 4 | 8p23.1-p22 | 1673 | 0.125 | 0.378 |
| 62 | UBE2M | ubiquitin-conjugating enzyme E2M (UBC12 homolog, yeast) | 19q13.43 | 9040 | 0.124 | 0.382 |
| 63 | ADH1A | alcohol dehydrogenase 1A (class I), alpha polypeptide | 4q21-q23 | 124 | 0.123 | 0.384 |
| 64 | ICAM1 | intercellular adhesion molecule 1 | 19p13.3-p13.2 | 3383 | 0.118 | 0.378 |
| 65 | BCL2L1 | BCL2-like 1 | 20q11.21 | 598 | 0.117 | 0.381 |
| 66 | FAS | Fas (TNF receptor superfamily, member 6) | 10q24.1 | 355 | 0.114 | 0.378 |
| 67 | BGN | biglycan | Xq28 | 633 | 0.113 | 0.382 |
| 68 | PAX8 | paired box 8 | 2q12-q14 | 7849 | 0.113 | 0.386 |
| 69 | CTSB | cathepsin B | 8p22 | 1508 | 0.112 | 0.387 |
| 70 | ABCA1 | ATP-binding cassette, sub-family A (ABC1), member 1 | 9q31.1 | 19 | 0.111 | 0.390 |

| Expression of genes enriched in translocation positive MALT lymphoma | | | | | | |
|--|---------|--|---------------|-------|--------|--------|
| 146 | KLK3 | kallikrein-related peptidase 3 | 19q13.41 | 354 | -0.165 | -0.161 |
| 147 | UCP2 | uncoupling protein 2 (mitochondrial, proton carrier) | 11q13 | 7351 | -0.171 | -0.160 |
| 148 | MAP4K1 | mitogen-activated protein kinase kinase kinase kinase 1 | 19q13.1-q13.4 | 11184 | -0.183 | -0.161 |
| 149 | IFI44L | interferon-induced protein 44-like | 1p31.1 | 10964 | -0.188 | -0.157 |
| 150 | CCR5 | chemokine (C-C motif) receptor 5 | 3p21 | 1234 | -0.199 | -0.157 |
| 151 | IRF7 | interferon regulatory factor 7 | 11p15.5 | 3665 | -0.202 | -0.150 |
| 152 | PRDM2 | PR domain containing 2, with ZNF domain | 1p36.21 | 7799 | -0.208 | -0.145 |
| 153 | BCL2L10 | BCL2-like 10 (apoptosis facilitator) | 15q21 | 10017 | -0.218 | -0.142 |
| 154 | CCR7 | chemokine (C-C motif) receptor 7 | 17q12-q21.2 | 1236 | -0.231 | -0.137 |
| 155 | IRF4 | interferon regulatory factor 4 | 6p25-p23 | 3662 | -0.262 | -0.134 |
| 156 | LTB | lymphotoxin beta (TNF superfamily, member 3) | 6p21.3 | 4050 | -0.263 | -0.124 |
| 157 | REL | v-rel reticuloendotheliosis viral oncogene homolog (avian) | 2p13-p12 | 5966 | -0.272 | -0.116 |
| 158 | C4BPA | complement component 4 binding protein, alpha | 1q32 | 722 | -0.273 | -0.105 |
| 159 | TLR6 | toll-like receptor 6 | 4p14 | 10333 | -0.287 | -0.097 |
| 160 | BCL10 | B-cell CLL/lymphoma 10 | 1p22 | 8915 | -0.290 | -0.086 |
| 161 | CD69 | CD69 molecule | 12p13-p12 | 969 | -0.352 | -0.078 |
| 162 | TFEC | transcription factor EC | 7q31.2 | 22797 | -0.364 | -0.065 |
| 163 | BCL2 | B-cell CLL/lymphoma 2 | 18q21.33 | 596 | -0.396 | -0.051 |
| 164 | CCR2B | chemokine (C-C motif) receptor 2 isoform B | 3p21.31 | 7E+05 | -0.500 | -0.034 |
| 165 | CCR2A | chemokine (C-C motif) receptor 2 isoform A | 3p21.31 | 7E+05 | -0.927 | 0.000 |

Appendix IV – qRT-PCR results

Normalised qRT-PCR results for various MALT lymphoma translocations

| case no. | site | translocation | RNA con. | 260/280 ratio | BCL10 staining | CD69 | BCL10 | CD86 | CCR5 | TLR6 | CCR2 | MINOR | NMALT | BCL2 | IRF4 |
|--------------------------------------|---------------------|---------------------|---------------------------|---------------|----------------|---|-------|------|------|------|------|-------|-------|------|------|
| Strong BCL10 nuc staining | | | | | | | | | | | | | | | |
| 1 | 601022 | GA | t(1;14)+ve | 419.2 | 1.409 | strong nuc | 2.1 | 2.1 | 7.7 | 5.4 | 8.3 | 4.4 | 8.9 | 7.2 | NA |
| 2 | 95-14772 | GA | t(1;2)+ve | 1302 | 1.43 | strong nuc | 3.0 | 2.0 | 7.5 | 6.1 | 8.5 | 5.7 | 8.1 | 7.2 | 2.7 |
| 3 | 0506-1606 | Lung | t(1;14)+ve | 136 | 1.52 | strong nuc | 6.8 | 4.1 | 7.3 | 7.2 | 10.7 | 4.5 | 11.1 | 7.6 | NA |
| 4 | U05-2633 | GA | t(1;14)+ve | 973 | 1.4 | strong nuc | 2.6 | 0.3 | 8.8 | 5.3 | 10.3 | 4.7 | 10.8 | 8.9 | 2.3 |
| 5 | U02-0909 | Lung | t(1;14)+ve | 1009.6 | 1.441 | strong nuc | 1.7 | -1.3 | 6.2 | 2.2 | 8.0 | 0.0 | 9.2 | 6.7 | 1.5 |
| 6 | U88-1907 | Lung | t(1;14)+ve | 517 | 1.42 | strong nuc | 4.3 | 2.1 | 9.8 | 4.5 | 7.7 | 3.6 | 10.8 | 8.0 | 4.0 |
| 7 | U81-4158 | GA | t(1;14)+ve | 1347.2 | 1.528 | strong nuc | 3.8 | -0.1 | 8.7 | 3.0 | 7.3 | 1.1 | 13.1 | 7.4 | NA |
| t(11;18) +ve | | | | | | | | | | | | | | | |
| 1 | 03602 U88-7646 | SI | t(11;18) +ve | 224 | 1.573 | (-) | 8.0 | 6.6 | 8.1 | 9.9 | 11.3 | 6.0 | 11.1 | 12.4 | NA |
| 2 | 88-1835 | | t(11;18)+ve | 1857.6 | 1.449 | nuc | 6.9 | 5.6 | 8.5 | 6.9 | 9.4 | 3.6 | 13.1 | 8.5 | 5.3 |
| 3 | 92-10232 | GA | t(11;18)+ve | 277 | 1.5 | (-/+) nuc | 6.4 | 5.6 | 2.7 | 7.7 | 9.1 | 4.5 | 9.0 | 14.0 | -2.0 |
| 4 | 95-10509 | | t(11;18)+ve | 777 | 1.36 | nuc | 5.1 | 6.0 | 9.5 | 8.6 | 9.2 | 5.1 | 16.2 | 10.1 | 5.5 |
| 5 | 96-08316 | | t(11;18)+ve | 798.4 | 1.459 | nuc | 4.7 | 4.9 | 9.9 | 7.9 | 9.0 | 4.7 | 10.3 | 8.9 | 4.5 |
| 6 | 96-19533 | GA | t(11;18) +ve | 267 | 1.59 | nuc | 6.6 | 5.9 | 9.8 | 7.8 | 7.2 | 4.8 | 11.2 | 6.7 | 4.0 |
| 7 | B96-11272 | | t(11;18)+ve | 590 | 1.39 | nuc | 5.7 | 6.7 | 11.7 | 9.2 | 9.9 | 7.0 | 15.6 | 8.7 | NA |
| 8 | G404 | | t(11;18)+ve | 1939 | 1.48 | nuc | 4.1 | 5.6 | 8.8 | 7.4 | 8.4 | 2.7 | 8.7 | 6.2 | NA |
| 9 | H97-2048 | | t(11;18)+ve | 898 | 1.38 | nuc | 4.5 | 4.1 | 7.8 | 5.9 | 7.8 | 2.3 | 9.9 | 7.8 | 2.3 |
| 10 | U01-15571 | | t(11;18)+ve | 1404.8 | 1.522 | nuc | 4.9 | 6.3 | 10.0 | 8.1 | 10.0 | 6.2 | 11.5 | 8.3 | NA |
| 11 | U84-2865 (G1924) | SI | t(11;18)+ve | 161 | 1.565 | (+++ +++) nuc | 6.7 | 3.2 | 5.4 | 7.1 | 7.5 | 2.4 | 9.7 | 11.6 | NA |
| 12 | U88-1836 | SI | t(11;18)+ve | 472 | 1.54 | nuc | 7.5 | 6.1 | 11.7 | 7.9 | 10.0 | 4.4 | 11.9 | 9.1 | 4.4 |
| 13 | U89-4172 | GA | t(11;18)+ve | 196 | 1.52 | nuc | 6.7 | 4.7 | 7.0 | 7.0 | 8.7 | 3.8 | 7.3 | 12.1 | 3.4 |
| 14 | U81-4305 | | t(11;18)+ve | 4800 | 1.294 | nuc After Dnase 4120 at 260/280 of 1.668 | 6.4 | 6.6 | 9.5 | 9.4 | 9.3 | 8.9 | 11.8 | 8.6 | 5.1 |
| 15 | U93-1575(G5125) | | t(11;18)+ve | 1563.2 | 1.443 | nuc | 4.5 | 3.3 | 5.8 | 4.6 | 7.0 | 2.5 | 15.4 | 7.9 | NA |
| 16 | U86-2261 | | t(11;18)+ve | 1184 | 1.39 | nuc | 7.3 | 6.7 | 10.1 | 7.3 | 9.6 | 5.1 | 13.3 | 11.4 | 5.1 |
| 17 | U88-14794 | | t(11;18)+ve | 3064.4 | 1.548 | nuc | 6.4 | 6.8 | 9.6 | 9.8 | 9.9 | 7.0 | 12.4 | 9.7 | NA |
| t(14;18) +ve | | | | | | | | | | | | | | | |
| 1 | 99-6609 | Orbital MALT | t(14;18) | | | cyt | NA | NA | NA | NA | NA | NA | 7.1 | NA | NA |
| 2 | 95-2209 | Orbital MALT | t(14;18) | | | cyt | NA | NA | NA | NA | NA | NA | 8 | NA | NA |
| 3 | 99-5369 | Orbital MALT | t(14;18) | | | cyt | NA | NA | NA | NA | NA | NA | 6.85 | NA | NA |
| 4 | 02-01211 | Hepatic MALT | t(14;18) | | | cyt | NA | NA | NA | NA | NA | NA | 5.74 | NA | NA |
| 5 | 519 | Lung MALT | t(14;18) | | | cyt | NA | NA | NA | NA | NA | NA | 6.3 | NA | NA |
| 6 | 453 | Lung MALT | t(14;18) | | | cyt | NA | NA | NA | NA | NA | NA | 6.5 | NA | NA |
| 7 | 55 | Lung MALT | t(14;18) | | | cyt | NA | NA | NA | NA | NA | NA | 7.35 | NA | NA |
| 8 | U057-21250 | nodal adenoid MALT | t(14;18) | | | cyt | NA | NA | NA | NA | NA | NA | 6.8 | NA | NA |
| 9 | NMALT Chinese 14_18 | NMALT Chinese 14_18 | t(14;18) | | | cyt | NA | NA | NA | NA | NA | NA | 3.3 | NA | NA |
| Translocations -ve BCL10 nuc | | | | | | | | | | | | | | | |
| 1 | 00H1993 | Lung | (-) | 187 | 1.6 | nuc | 5.7 | 2.6 | 4.3 | 3.2 | 10.9 | 1.2 | 6.8 | 7.7 | NA |
| 2 | 01H1968 | Lung | (-) | 193 | 1.65 | Nuc | 8.4 | 6.6 | 9.9 | 9.1 | 11.1 | 10.4 | 17.7 | 8.7 | 5.0 |
| 3 | 01H273 | Lung | (-) | 44.8 | 1.647 | nuc, staining not even | 5.2 | 5.6 | 8.4 | 4.5 | 11.3 | 5.3 | 11.6 | 7.5 | NA |
| 4 | 85-11417 | | t(11;18)+ve | 1888 | 1.45 | nuc, staining not even | 5.9 | 5.9 | 8.0 | 10.0 | 9.6 | 12.2 | 9.4 | 15.4 | 4.5 |
| 5 | 06352 | | t(11;18)+ve | 890 | 1.43 | nuc | 6.3 | 6.3 | 8.6 | 7.7 | 10.4 | 5.9 | 13.4 | 10.5 | 7.2 |
| 6 | U90-03700 | | t(11;18)+ve | 4800 | 1.332 | nuc | 6.2 | 5.0 | 6.1 | 7.3 | 9.2 | 9.1 | 9.9 | 8.0 | NA |
| 7 | U91-00078 | GA | (-) | 108 | 1.28 | nuc | 6.3 | 2.4 | 4.8 | 15.1 | 9.2 | 4.9 | 5.2 | 5.1 | NA |
| 8 | U86-6946 | | t(11;18)+ve | 446 | 1.39 | nuc | 7.5 | 6.0 | 9.8 | 7.0 | 11.5 | 9.0 | 8.0 | 9.2 | NA |
| 9 | U86-8768 | Lung | (-) | 500 | 1.653 | weak nuc | 8.1 | 6.1 | 7.2 | 6.3 | 10.2 | 5.7 | 13.6 | 7.8 | NA |
| 10 | U99-4597 (G3604) | | t(11;18)+ve | 3369.6 | 1.558 | (-/+) nuc | 7.4 | 6.8 | 9.3 | 6.5 | 10.0 | 5.5 | 10.2 | 7.4 | 5.0 |
| Translocations -ve BCL10 cyto | | | | | | | | | | | | | | | |
| 1 | 89-1810 | GA | (-) | 86 | 1.59 | Cyt, based on previous reviewed | 8.4 | 2.9 | 4.1 | 7.9 | 10.1 | 6.8 | 9.7 | 6.1 | 14.2 |
| 2 | 02H1701 | Lung | (-) | 278 | 1.723 | cyt | 7.1 | 6.4 | 8.9 | 6.8 | 10.1 | 9.2 | 12.7 | 6.9 | 7.7 |
| 3 | 99-9689 | Lung (Vienna) | (-) | 277 | 1.63 | Cyt, based on previous reviewed | 7.5 | 1.3 | 3.8 | 5.0 | 7.7 | 3.9 | 7.4 | 5.9 | NA |
| 4 | G1033 | SI | (-) | 268 | 1.56 | cyt | 12.1 | 6.7 | 6.3 | 10.0 | 8.9 | 10.1 | 13.6 | 9.9 | NA |
| 5 | G411 | | t(11;18)+ve | 974 | 1.38 | (-/+) cyt | 5.8 | 6.2 | 8.1 | 5.6 | 9.9 | 7.0 | 7.4 | 7.7 | 3.7 |
| 6 | G414 | | t(11;18)+ve | 208 | 1.31 | cyt, small area with nuc | 6.1 | 4.1 | 7.0 | 6.9 | 9.6 | 7.7 | 4.6 | 6.7 | NA |
| 7 | G462 | | t(11;18)+ve | 1222 | 1.43 | (-) no staining | 4.7 | 6.6 | 8.5 | 9.4 | 10.9 | 7.8 | 5.1 | 6.1 | 3.5 |
| 8 | U01-11477 | GA | (-) | 241 | 1.589 | Cyt | 4.4 | 2.5 | 1.4 | 8.8 | 12.1 | 5.6 | 7.0 | 13.3 | NA |
| 9 | U84-6330 | Lung | (-) | 68 | 1.64 | Cyt | 8.1 | 3.9 | 3.5 | 8.1 | 12.2 | 5.0 | 6.5 | 6.6 | NA |
| 10 | U84-9013 | GA | (-) IGH (+) | 598 | 1.63 | Cyt, stain again. | 7.1 | 6.4 | 4.5 | 9.8 | 11.1 | 5.8 | 10.6 | 7.3 | 2.0 |
| 11 | U89-3531(G0055) | | t(11;18)+ve | 174 | 1.31 | cyt | 7.0 | 4.4 | 10.3 | 5.6 | 10.8 | 13.0 | 10.5 | 9.5 | NA |
| 12 | U81-2675 | | t(11;18)+ve | 278 | 1.31 | cyto | -0.5 | -0.5 | 1.1 | 0.7 | 7.9 | -1.1 | 0.0 | 7.6 | NA |
| 13 | U92-4427 (G0422) | Liver | (-) | 296 | 1.48 | cyt (+++), (-/+) cyt | 7.2 | 5.7 | 4.7 | 8.5 | 15.0 | 6.1 | 12.8 | 2.4 | NA |
| 14 | U93-00540 | | t(11;18)+ve | 1184 | 1.45 | cyto, cyt | 8.2 | 7.5 | 9.8 | 9.5 | 11.2 | 10.4 | 7.9 | 9.0 | 7.7 |
| 15 | U84-2115 (G1656) | | t(11;18)+ve | 1680 | 1.452 | (+++ +) cyt, mucosa (++++ +) cyt | 10.4 | 7.7 | 8.5 | 10.0 | 11.1 | 9.8 | 5.9 | 8.6 | 6 |
| BCL6 +ve | | | | | | | | | | | | | | | |
| 18 | U93-4991 | | t(11;18)+ve IGH/BCL6+ve | 1206.4 | 1.407 | nuc, nuc | 7.6 | 6.5 | 8.5 | 7.7 | 10.4 | 9.0 | 6.2 | 18.2 | NA |
| IGH/FOXP1 + ve | | | | | | | | | | | | | | | |
| 14 | U90-00638 | | t(11;18)+ve, IGH/FOXP1+ve | 634 | 1.41 | cyto | 6.6 | 4.8 | 9.2 | 6.6 | 10.4 | 7.2 | 7.3 | 8.1 | NA |
| t(14;18) IGH/BCL2 + ve | | | | | | | | | | | | | | | |
| 56 | U89-3770 | GA | t(14;18)+ve/BCL2 | 203 | 1.46 | cyt | 8.0 | 2.6 | 2.3 | NA | 5.4 | 5.0 | 7.7 | 12.6 | NA |
| (-) DLBCL | | | | | | | | | | | | | | | |
| 42 | 92-588417 | GA? | (-) | 243 | 1.45 | (-) DLBCL | 8.8 | 3.9 | 5.5 | 7.3 | 11.2 | 6.9 | 7.4 | 6.1 | NA |
| 11 | G5601 | | t(11;18)+ve | 667.2 | 1.376 | have large cell component, may need exclusive | 8.6 | 7.0 | 7.9 | 7.7 | 11.9 | 9.9 | 9.1 | 7.6 | NA |
| 49 | S96-3527 | JMC PATH | | 288 | 1.53 | | 8.5 | 6.4 | 10.9 | 7.8 | 11.1 | 4.7 | 14.9 | 5.2 | NA |
| 45 | B179629 | Lung (Italy) | | 59 | 1.32 | (-) | 10.5 | 2.6 | 0.8 | NA | 3.2 | 6.4 | 2.3 | 18.0 | NA |
| 39 | 7638B1 | GA | | 80 | 1.25 | (-) | 9.0 | 1.7 | 2.4 | NA | 8.6 | 3.0 | 4.7 | 8.6 | NA |
| Strong BCL10 nuc staining | | | | | | | | | | | | | | | |
| 1 | G426 | GA | (-) IGH (+) few | 315 | 1.55 | strong nuc | 5.5 | 3.2 | 8.5 | 5.4 | 10.3 | 3.0 | 10.5 | 4.1 | NA |
| 2 | U88-3908 | Lung | (-) | 1753 | 1.712 | strong nuc | 8.0 | 3.4 | 7.8 | 8.3 | 9.7 | 4.7 | 10.5 | 6.7 | NA |

PUBLICATIONS

factors CARMA1 and Bcl10 (3, 4). It is thought that because the API2 moiety mediates autooligomerization, API2-MALT1 can stimulate NF- κ B independent of upstream signals (5, 6). This may explain why t(11;18)-positive MALT lymphomas are not dependent on antigenic stimulation for progression, whereas t(11;18)-negative tumors require ongoing chronic inflammation for survival. The phenomenon is best exemplified by gastric MALT lymphomas, the majority of which arise in the setting of chronic *Helicobacter pylori* gastritis and are cured by eradication of *H. pylori* with antibiotics. In contrast, t(11;18)-positive gastric tumors are resistant to this treatment and are associated with advanced-stage disease (1).

We discovered that besides activating canonical NF- κ B, expression of API2-MALT1 in human embryonic kidney 293T (HEK293T) or the human B lymphoma (SSK41) cells induced proteasome-dependent processing of the NF- κ B precursor, p100, to its mature form, p52, and stimulated nuclear translocation of p52/RelB (Fig. 1, A to D, and fig. S1) (7). These findings indicate that API2-MALT1 activates the “noncanonical” NF- κ B pathway, which requires NF- κ B-inducing kinase (NIK)-dependent phosphorylation and activation of inhibitor of NF- κ B (κ B) kinase- α (IKK α).

This, in turn, triggers proteasome-mediated partial degradation of p100 to p52 and generation of transcriptionally active p52/RelB NF- κ B dimers (8). Consistent with this notion, dominant-negative NIK mutants (9, 10) blocked API2-MALT1-dependent p100 processing and p52 nuclear translocation (Fig. 1, E and F).

cIAP1 and cIAP2 (API2) associate with NIK and promote NIK degradation via RING domain ubiquitin ligase activity (11–13). We hypothesized that API2-MALT1, which lacks the cIAP2 RING domain, stimulates noncanonical signaling through competitive inhibition of cIAP-mediated NIK degradation. In testing this, we discovered that expression of API2-MALT1 instead induced proteolytic cleavage of NIK, generating ~37-kD N-terminal and ~70-kD C-terminal NIK fragments (Fig. 2, A and B, and fig. S2).

API2-MALT1 fusion transcripts invariably contain three intact baculoviral IAP repeat (BIR) domains from API2 and an intact “caspaselike” domain from MALT1, which suggests that these domains are critical for lymphomagenesis (1). The caspaselike domain of wild-type MALT1 has proteolytic activity, and Bcl10 and the NF- κ B inhibitor, A20, are the only known substrates (14, 15). We therefore investigated whether the cas-

paselike domain within API2-MALT1 is also able to cleave NIK. Deletion mutants of API2-MALT1 lacking portions of the caspaselike domain and API2-MALT1-C678A (16), in which the catalytic cysteine within the MALT1 proteolytic domain is replaced with alanine, were unable to induce NIK cleavage (Fig. 2C and fig. S3, A to C). Furthermore, treatment with z-Val-Arg-Pro-Arg-fluoromethylketone (z-VRPR-fmk), a MALT1 protease inhibitor (15), blocked API2-MALT1-induced NIK cleavage, whereas z-IETD-fmk, a caspase-8 inhibitor, had no effect (fig. S3, D and E). Finally, an in vitro cleavage reaction using purified recombinant proteins showed that NIK is a direct substrate of the MALT1 protease domain (Fig. 2D and fig. S4).

Cellular expression of the MALT1 moiety alone was unable to induce NIK cleavage, which suggests that the API2 moiety also contributes in some way (Fig. 2E). Indeed, analyses revealed that NIK physically associates with API2-MALT1 via the API2 moiety (Fig. 2F) and that the region within the API2 moiety that mediates auto-oligomerization of API2-MALT1 (amino acids 49 to 98) (5) is required for efficient API2-MALT1-dependent NIK cleavage and p100 processing (fig. S5). The collaborative relationship of the

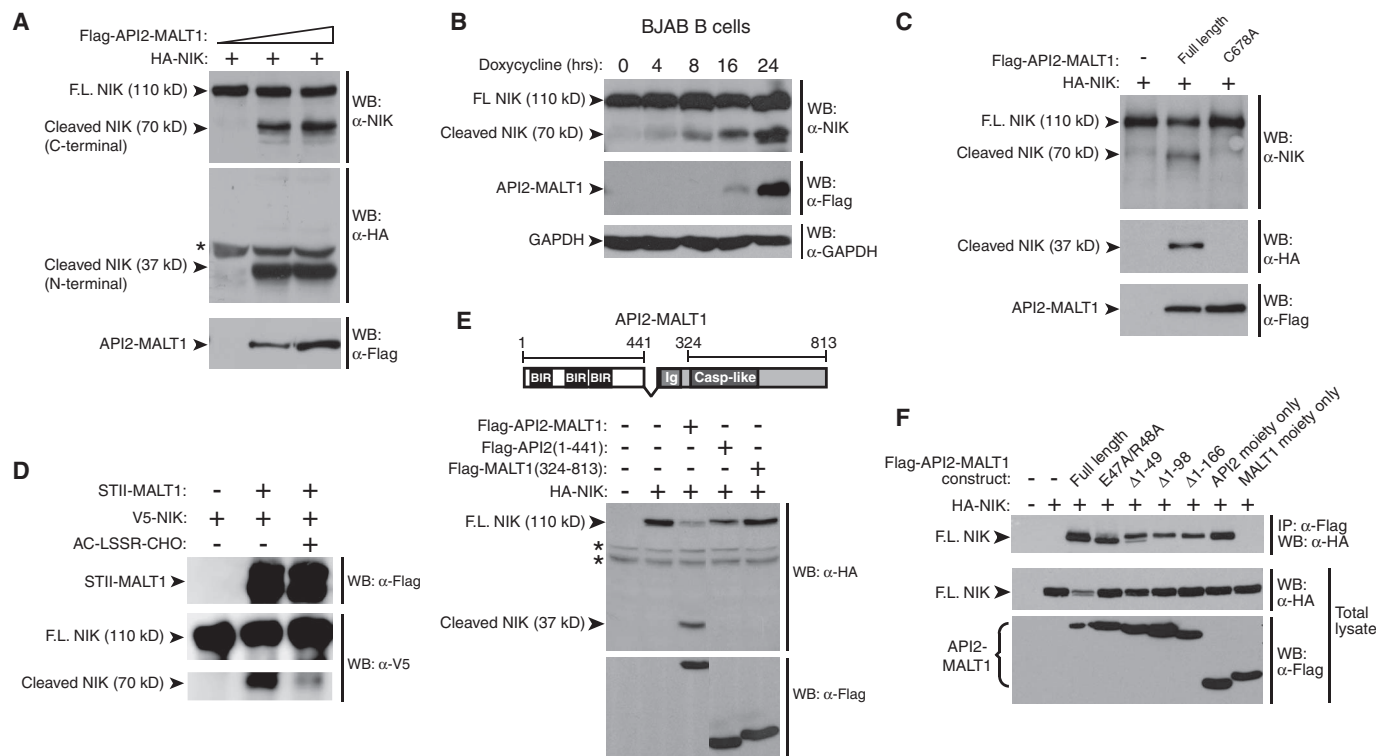


Fig. 2. API2-MALT1 induces NIK cleavage, a phenomenon requiring both the API2 moiety and MALT1 protease activity. (A) HEK293T cells were transfected as indicated, and NIK cleavage fragments were detected by WB. (B) BJAB cells expressing API2-MALT1 from a tetracycline-inducible promoter were treated with doxycycline. WB with an antibody raised against a C-terminal NIK sequence revealed time-dependent generation of an endogenous 70-kD NIK cleavage fragment. To enhance detection of full-length (FL) NIK, cells were incubated with 25 μ M MG132. (C) HEK293T cells were transfected as indicated, and the presence of the N-terminal 37-kD and the C-terminal 70-kD

NIK cleavage fragments was analyzed by WB. (D) Recombinant purified NIK-V5-bioC and StrepII-Flag-tagged MALT1 were incubated in kosmotropic salt buffer for 6 hours at 37°C, with or without 100 μ M MALT1 protease inhibitor Ac-LSSR-CHO, and analyzed by WB. (E) HEK293T cells were transfected as indicated, and the 37-kD NIK cleavage fragment was detected by WB. (F) HEK293T cells were transfected, and immunoprecipitations were carried out using α -Flag-agarose. For a detailed description of API2-MALT1 mutants, see the legend to fig. S5. *Nonspecific band. Data are representative of at least three separate experiments.

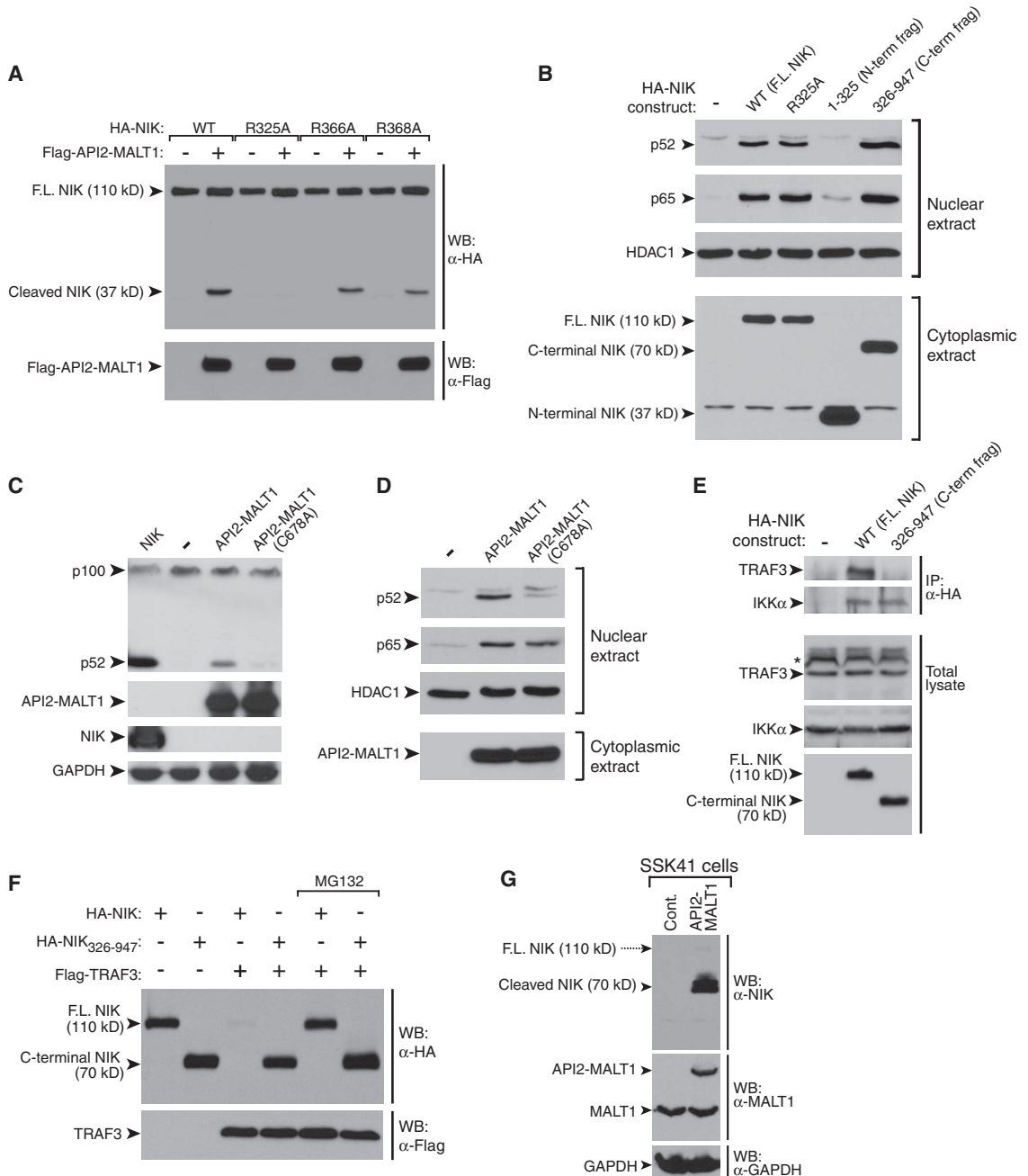
API2 and MALT1 moieties in achieving NIK cleavage was further underscored in several different contexts. First, unlike API2-MALT1, induced expression of wild-type MALT1 in BJAB B cells did not result in NIK cleavage (fig. S6A). Second, NIK cleavage was not observed in SSK41 B cells, which are characterized by *MALT1* gene amplification, overexpression of MALT1, and constitutive MALT1 protease activity (14, 17, 18). In contrast to A20, NIK was cleaved only if SSK41 cells were engineered to express API2-MALT1 (fig. S6B). Third, coexpression of wild-type MALT1 with Bcl10, which triggers MALT1 oligomerization and activation (3), did lead to cleavage of A20 but not of NIK (fig. S6, C and D). Fourth, ligand-induced B cell receptor stimulation, which sim-

ilarly activates the MALT1 protease (14), did not trigger NIK cleavage (fig. S6E). Furthermore, although MALT1 oligomerization and activation require Bcl10 (3), API2-MALT1-mediated NIK cleavage occurred in the absence of Bcl10 (fig. S6F). Together, these findings suggest that NIK is a substrate for the MALT1 protease domain, but only when this domain is present within the context of API2-MALT1.

Structural analyses predict that the MALT1 protease should show specificity for substrates with a basic or uncharged residue at P1 (N-terminal to the cleavage site) (19). Furthermore, the MALT1 cleavage sites of Bcl10 and A20 both contain a P2-serine preceding a P1-arginine (14, 15, 20). Thus, we identified candidate P2-Ser/P1-Arg MALT1

cleavage sites within NIK that would generate fragments of ~37 and 70 kD (fig. S7A), and we individually changed each candidate P1-Arg to Ala. The R366A and R368A NIK mutants were readily cleaved by API2-MALT1; however, the R325A mutant was resistant (Fig. 3A), which suggests that API2-MALT1-dependent cleavage of NIK occurs at R325 (fig. S7B). Expression of the resulting C-terminal NIK cleavage fragment, NIK(326–947), which retains the kinase domain, induced robust p100 processing (fig. S7C), p52 nuclear translocation (Fig. 3B), and noncanonical NF- κ B target gene expression (fig. S7D). NIK(326–947) also induced nuclear translocation of the p65 NF- κ B subunit, which indicated activation of the canonical NF- κ B pathway

Fig. 3. API2-MALT1-dependent cleavage of NIK at R325 generates an active C-terminal fragment. **(A)** HEK293T cells were transfected as indicated, and the 37-kD N-terminal NIK cleavage fragment was detected by WB. **(B)** HEK293T cells were transfected as indicated, and nuclear translocation of p52 and p65 NF- κ B subunits was assessed. **(C and D)** HEK293T cells were transfected as indicated, and endogenous p100 processing (C) and nuclear translocation of NF- κ B subunits (D) were assessed. **(E)** HEK293T cells were transfected as indicated, and the ability of endogenous TRAF3 or IKK α to immunoprecipitate with each NIK protein was assessed. **(F)** HEK293T cells were transfected as indicated and then incubated in the absence or presence of 25 μ M MG132. The presence of NIK was detected by WB. **(G)** Cell lysates were prepared in the absence of MG132 and analyzed by WB to detect full-length (F.L.) NIK and the 70-kD C-terminal NIK cleavage fragment. Data are representative of at least three separate experiments.



as well (Fig. 3B). Conversely, API2-MALT1-C678A, the catalytically inactive mutant that cannot induce NIK cleavage to produce NIK(326–947), failed to stimulate p100 processing (Fig. 3C) and p52 nuclear translocation (Fig. 3D and fig. S8). NIK associates with the adaptor protein, TRAF3, via an N-terminal NIK domain (amino acids 78 to 84), and this interaction targets NIK for proteasomal degradation (21–23). Because cleavage of NIK at R325 separates this TRAF3-binding site from the NIK kinase domain, we hypothesized that the active C-terminal NIK cleavage product would be resistant to TRAF3-directed

degradation. Indeed, NIK(326–947) retained binding to IKK α but not to TRAF3 (Fig. 3E) and, unlike full-length NIK, was resistant to TRAF3-dependent proteasomal degradation (Fig. 3F). We also demonstrated the unique stability of the API2-MALT1-generated C-terminal NIK cleavage fragment in SSK41 B lymphoma cells. In the absence of MG132 (a proteasome inhibitor), expression of full-length NIK was very low, regardless of whether API2-MALT1 was present, consistent with the fact that NIK is subject to constitutive proteasomal degradation (21, 24) (Fig. 3G). In contrast, high levels of

endogenous C-terminal NIK cleavage fragment were detected in SSK41 cells expressing API2-MALT1 (Fig. 3G).
API2-MALT1-dependent generation of the C-terminal NIK cleavage fragment in SSK41 cells was associated with enhanced transcription of noncanonical NF- κ B target genes, including *Pim-2*, an oncogenic kinase that blocks apoptosis by phosphorylating the proapoptotic Bcl-2 family member BAD (fig. S9, A and B) (25–29). RNA interference-mediated knockdown of NIK in API2-MALT1-expressing SSK41 cells led to loss of the 70-kD NIK fragment, loss of p100

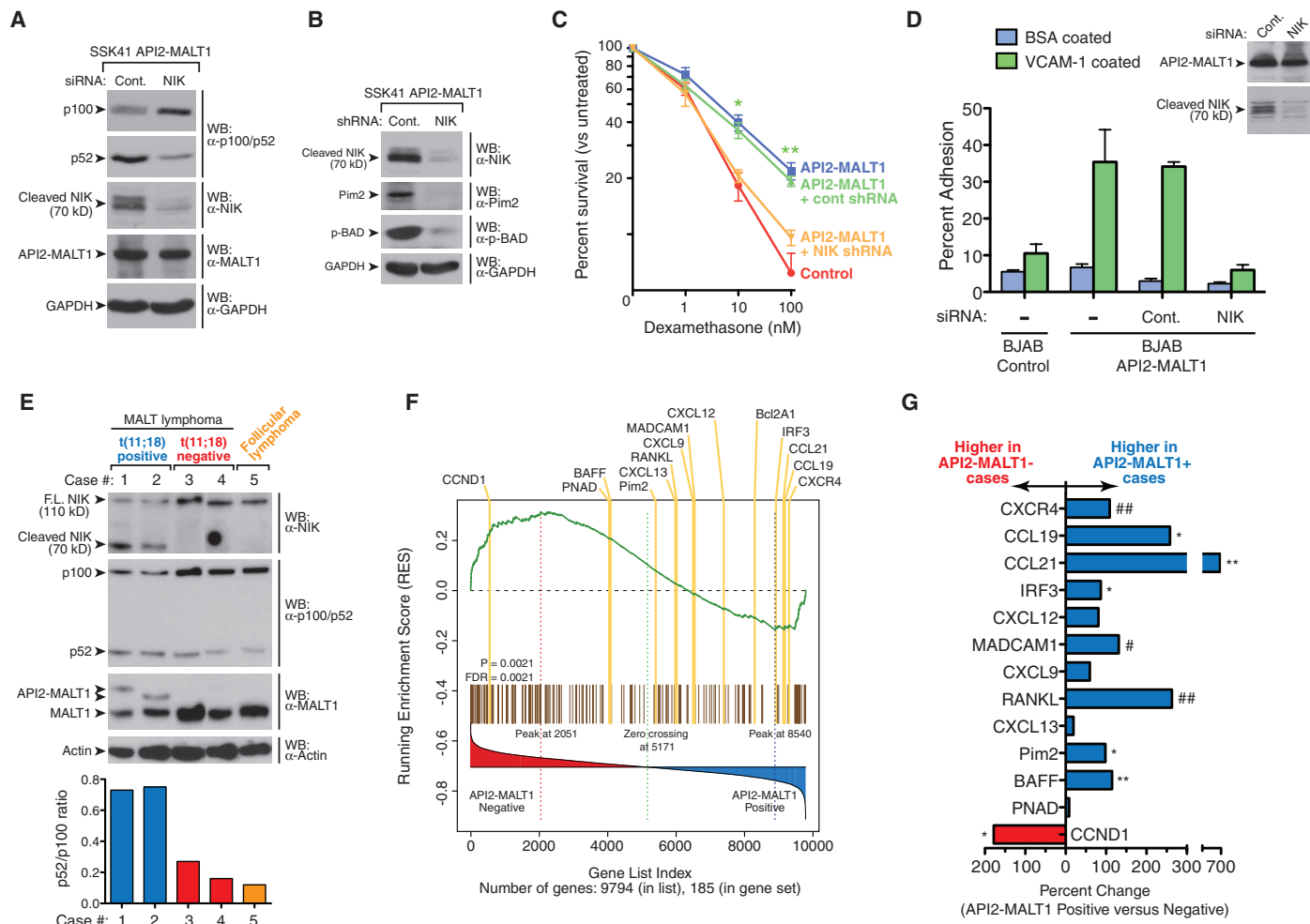


Fig. 4. API2-MALT1-dependent NIK cleavage is associated with up-regulation of noncanonical NF- κ B target genes, results in an altered B cell phenotype, and occurs in t(11;18)-positive MALT lymphoma. (A) API2-MALT1-expressing SSK41 cells were transiently transfected with control or NIK small interfering RNA (siRNA), and p100 processing was assessed by WB. (B and C) API2-MALT1-expressing SSK41 cells were stably infected with control or NIK small hairpin RNA (shRNA) lentiviral particles. The 70-kD NIK cleavage fragment, Pim-2, and phospho-Ser¹¹²-BAD levels were compared by WB (B). Cells were treated for 48 hours with dexamethasone, and percent viability was compared (C). Data are expressed as average \pm SEM for four separate experiments. * P < 0.005, ** P < 0.0001. (D) API2-MALT1-expressing BJAB cells were transfected with control or NIK siRNA, and adhesion to VCAM-1-coated plates was assessed. Error bars represent SEM of duplicate determinations. Data are representative of three separate experiments. (E) Expression of API2-MALT1 in two t(11;18)-positive

MALT lymphoma samples was confirmed by WB. p52/p100 ratios were quantified using densitometry. Both t(11;18)-positive cases had the same breakpoint in the *API2* gene (between exons 7 and 8) but different breakpoints in the *MALT1* gene [between exons 4 and 5 (case 1) and exons 6 and 7 (case 2)]. A follicular lymphoma and two t(11;18)-negative MALT lymphoma tumor specimens were used as controls. (F) GSEA of NF- κ B target genes was performed in a set of MALT lymphomas with t(11;18) versus those without translocation from tumor collection no. 1 (34). The distribution of the genes is listed according to rank position, and known noncanonical NF- κ B gene targets are highlighted in yellow. Absolute enrichment gave P = 0.0021 and false discovery rate (FDR) = 0.0021. (G) Comparison of noncanonical target gene expression in t(11;18)-positive versus negative cases from tumor collection no. 2 (34). Statistical testing for genes differentially expressed between the two types of MALT lymphomas was done by *t* test. # P < 0.05, ## P < 0.01, * P < 0.005, ** P < 0.001.

processing, and loss of API2-MALT1-dependent induction of Pim-2 kinase and BAD phosphorylation (Fig. 4, A and B). In accordance with its effect on antiapoptotic signal transduction, API2-MALT1 expression protected SSK41 cells from dexamethasone-induced cell death, which was reversed by NIK knockdown (Fig. 4, B and C, and fig. S10). Knockdown of IKK α impaired API2-MALT1-dependent protection, which supports a role for the noncanonical NF- κ B pathway in mediating this effect of API2-MALT1-induced NIK cleavage (fig. S11). IKK β knockdown impaired API2-MALT1-dependent protection as well, which implies that the canonical pathway may also contribute (fig. S11).

We next investigated the impact of API2-MALT1-dependent NIK cleavage on B cell adhesion because we had observed that API2-MALT1 induced the expression of B cell integrins (fig. S9A), known noncanonical NF- κ B gene targets (27, 28). API2-MALT1 expression was associated with increased B cell adhesion to plates coated with the endothelial protein vascular cell adhesion molecule VCAM-1, and this proadhesive phenotype was fully dependent on NIK (Fig. 4D). Lymphocyte adhesion is thought to play a role in lymphoma dissemination, thus NIK-cleavage-dependent API2-MALT1-induced adhesion may contribute to the higher rate of tumor spread among t(11;18)-positive MALT lymphomas (1). Again, knockdown of IKK α or IKK β impaired API2-MALT1-dependent adhesion, which suggests that both noncanonical and canonical pathways contribute to the proadhesive phenotype after API2-MALT1-dependent NIK cleavage (fig. S12).

The striking pattern of NIK cleavage and stability observed in API2-MALT1-expressing B lymphoma cell lines was recapitulated in MALT lymphoma patient specimens. Full-length NIK levels were relatively low in all lymphomas, whereas an endogenous 70-kD C-terminal NIK fragment was detected only in t(11;18)-positive MALT lymphomas expressing API2-MALT1 (Fig. 4E). The presence of the NIK cleavage product was associated with an elevated p52/p100 ratio in the t(11;18)-positive tumors, which indicated enhanced noncanonical NF- κ B activation (Fig. 4E). We performed absolute gene set enrichment analysis (GSEA) comparing the expression of NF- κ B target genes between t(11;18)-positive MALT lymphomas ($n = 9$) and those with no translocation ($n = 8$). Analysis revealed a significant difference in the pattern of expression, with most known noncanonical NF- κ B target genes over-represented in the t(11;18)-positive cases (Fig. 4F, fig. S13, and tables S1 and S2). One exception is *cyclin D1*, although its categorization as a noncanonical NF- κ B target gene is controversial (30). We then compared the expression of these noncanonical target genes in a completely separate group of six t(11;18)-positive and eight t(11;18)-negative MALT lymphomas that were collected at a different institution and, again, found that many noncanonical NF- κ B target genes were

more highly expressed in the t(11;18)-positive tumors (Fig. 4G). *CXCR4*, which encodes a chemokine receptor whose expression is associated with widespread lymph node involvement in B lymphomas (31–33), is one intriguing example of a noncanonical gene target that is up-regulated in t(11;18)-positive tumors in both tumor collections (Fig. 4, F and G) (34).

Deregulated NIK activity has been increasingly implicated in the pathogenesis of B cell neoplasms. For example, an EFTUD2-NIK fusion oncoprotein that retains the NIK kinase domain—but lacks the TRAF3-binding site and is resistant to proteasomal degradation—was recently identified in a case of multiple myeloma (24). Another recent report described a murine model of B lymphoproliferative disease in which a NIK mutant lacking the TRAF3-binding domain (NIK Δ T3) was expressed in B cells (35). Compared with control transgenic mice expressing full-length NIK, the NIK Δ T3 mice demonstrated increased NIK levels with enhanced p100 processing in B cells. They also showed expanded MALT and profound splenic marginal zone B cell hyperplasia, a phenotype that bears similarity to the E μ -API2-MALT1 transgenic mouse (36). Together with our results, these findings suggest that separating the TRAF3-binding site on NIK from the kinase domain, either through aberrations of the NIK gene or through proteolytic cleavage of NIK protein, may represent a common mechanism for deregulating NIK activity in B cell neoplasms. Our findings suggest that in API2-MALT1-expressing MALT lymphomas, the API2 moiety mediates auto-oligomerization of API2-MALT1 and recruitment of NIK, and the MALT1 protease domain cleaves NIK, which leads to degradation-resistant NIK kinase and deregulated noncanonical NF- κ B signaling (see model, fig. S14). Data suggest that NIK cleavage protects API2-MALT1-expressing B cells from apoptosis and promotes B cell adhesion, both of which could contribute to the more aggressive phenotype of t(11;18)-positive MALT lymphomas (1). Disrupting the API2-NIK interaction and/or blocking MALT1 protease or NIK kinase activity could represent new treatment approaches for refractory t(11;18)-positive MALT lymphoma.

References and Notes

1. P. G. Isaacson, M. Q. Du, *Nat. Rev. Cancer* **4**, 644 (2004).
2. M. Thome, *Nat. Rev. Immunol.* **8**, 495 (2008).
3. P. C. Lucas *et al.*, *J. Biol. Chem.* **276**, 19012 (2001).
4. L. Sun, L. Deng, C. K. Ea, Z. P. Xia, Z. J. Chen, *Mol. Cell* **14**, 289 (2004).
5. P. C. Lucas *et al.*, *Oncogene* **26**, 5643 (2007).
6. H. Zhou, M. Q. Du, V. M. Dixit, *Cancer Cell* **7**, 425 (2005).
7. Materials and methods are available as supporting material on Science Online.
8. T. D. Gilmore, *Oncogene* **25**, 6680 (2006).
9. N. L. Malinin, M. P. Boldin, A. V. Kovalenko, D. Wallach, *Nature* **385**, 540 (1997).
10. H. Y. Song, C. H. Régnier, C. J. Kirschning, D. V. Goeddel, M. Rothe, *Proc. Natl. Acad. Sci. U.S.A.* **94**, 9792 (1997).
11. S. L. Petersen *et al.*, *Cancer Cell* **12**, 445 (2007).
12. E. Varfolomeev *et al.*, *Cell* **131**, 669 (2007).
13. J. E. Vince *et al.*, *Cell* **131**, 682 (2007).
14. B. Coornaert *et al.*, *Nat. Immunol.* **9**, 263 (2008).
15. F. Rebeaud *et al.*, *Nat. Immunol.* **9**, 272 (2008).
16. Single-letter abbreviations for the amino acid residues are as follows: A, Ala; C, Cys; D, Asp; E, Glu; F, Phe; G, Gly; H, His; I, Ile; K, Lys; L, Leu; M, Met; N, Asn; P, Pro; Q, Gln; R, Arg; S, Ser; T, Thr; V, Val; W, Trp; and Y, Tyr.
17. H. Noels *et al.*, *J. Biol. Chem.* **282**, 10180 (2007).
18. D. Sanchez-Izquierdo *et al.*, *Blood* **101**, 4539 (2003).
19. A. G. Uren *et al.*, *Mol. Cell* **6**, 961 (2000).
20. L. M. McAllister-Lucas, P. C. Lucas, *Nat. Immunol.* **9**, 231 (2008).
21. G. Liao, M. Zhang, E. W. Harhaj, S.-C. Sun, *J. Biol. Chem.* **279**, 26243 (2004).
22. S. Vallabhapurapu *et al.*, *Nat. Immunol.* **9**, 1364 (2008).
23. B. J. Zarnegar *et al.*, *Nat. Immunol.* **9**, 1371 (2008).
24. C. M. Annunziata *et al.*, *Cancer Cell* **12**, 115 (2007).
25. G. Bonizzi *et al.*, *EMBO J.* **23**, 4202 (2004).
26. J. L. Chen, A. Limnander, P. B. Rothman, *Blood* **111**, 1677 (2008).
27. T. Enzler *et al.*, *Immunity* **25**, 403 (2006).
28. F. Guo, D. Weih, E. Meier, F. Weih, *Blood* **110**, 2381 (2007).
29. R. T. Woodland *et al.*, *Blood* **111**, 750 (2008).
30. I. I. Witzel, L. F. Koh, N. D. Perkins, *Biochem. Soc. Trans.* **38**, 217 (2010).
31. S. López-Giral *et al.*, *J. Leukoc. Biol.* **76**, 462 (2004).
32. Y. Nie *et al.*, *J. Exp. Med.* **200**, 1145 (2004).
33. M. Luftig *et al.*, *Proc. Natl. Acad. Sci. U.S.A.* **101**, 141 (2004).
34. See Materials and Methods in Supporting Online Materials for a description of the tumor collections nos. 1 and 2.
35. Y. Sasaki *et al.*, *Proc. Natl. Acad. Sci. U.S.A.* **105**, 10883 (2008).
36. M. Baens *et al.*, *Cancer Res.* **66**, 5270 (2006).
37. We thank M. Dyer for the SSK41 cells, R. Renne for the BJAB Tet-On cells, and G. Nunez for several expression plasmids. A Material Transfer Agreement is required for use of the SSK41 cells expressing API2-MALT1. Microarray data from MALT lymphoma tumor collections are Minimum Information About a Microarray Experiment (MIAME) compliant and are available online at the Gene Expression Omnibus (GEO) with accession number GSE25527 for collection no. 1 and accession number GSE25550 for collection no. 2 (www.ncbi.nlm.nih.gov/projects/geo/). L.M. is a recipient of the Nancy Newton Loeb Pediatric Cancer Research and Helen L. Kay Pediatric Cancer Research Awards and received support from National Institute of Child Health and Human Development, NIH, T32-HD07513. L.M. and S.R. were both supported by National Heart, Lung, and Blood Institute, NIH, T32-HL007622-21A2. M.B. is supported by grants from the Research Foundation—Flanders (FWO) and Belgian Foundation against Cancer. H.N. was an aspirant of the FWO-Vlaanderen. X.S. is a Senior Clinical Investigator of FWO-Vlaanderen, and P.V.L. is a postdoctoral researcher of the FWO. This work was supported by the Shirley K. Schlafer Foundation, the Elizabeth Caroline Crosby Fund, and grants from the University of Michigan Comprehensive Cancer Center (G007839), Leukemia and Lymphoma Research UK, and National Cancer Institute NIH (R01CA124540).

Supporting Online Material

www.sciencemag.org/cgi/content/full/331/6016/468/DC1
Materials and Methods
Figs. S1 to S14
Tables S1 and S2
References

12 October 2010; accepted 22 December 2010
10.1126/science.1198946



Supporting Online Material for

Cleavage of NIK by the API2-MALT1 Fusion Oncoprotein Leads to Noncanonical NF- κ B Activation

Shaun Rosebeck, Lisa Madden, Xiaohong Jin, Shufang Gu, Ingrid J. Apel, Alex Appert, Rifat A. Hamoudi, Heidi Noels, Xavier Sagaert, Peter Van Loo, Mathijs Baens, Ming-Qing Du, Peter C. Lucas,* Linda M. McAllister-Lucas*

*To whom correspondence should be addressed. E-mail: plucas@umich.edu (P.C.L.); lindaluc@umich.edu (L.M.M-L.)

Published 28 January 2011, *Science* **331**, 468 (2011)
DOI: 10.1126/science.1198946

This PDF file includes

Materials and Methods
Figs. S1 to S14
Tables S1 and S2
References

Supporting Online Material

MATERIALS AND METHODS

Expression constructs, mutagenesis and cell lines

The pcDNA3-Flag (-HA and-Myc) API2-MALT1 constructs were described previously (1, 2). For the API2-MALT1 fusion present in these constructs, the breakpoint for API2 corresponds to nucleotide 1323 of the cDNA sequence (AA residue 441), whereas the breakpoint for MALT1 corresponds to nucleotide 649 of the cDNA sequence (AA residue 217). These specific breakpoints represent the majority of clinically observed API2-MALT1 fusions (3). The resulting fusion protein contains three API2 BIR domains, one MALT1 Ig-like domain and the MALT1 “caspase-like” domain. The expression plasmids pcDNA3-Flag-API2(1-441), pcDNA3-Flag-MALT1(324-813), pcDNA3-Flag-E46A/R48A-API2-MALT1, pcDNA3-Flag-(D1-49)API2-MALT1, pcDNA3-Flag-(D1-98)API2-MALT1, pcDNA3-Flag-(D1-166)API2-MALT1, pcDNA3-HA-MALT1, pcDNA3-Myc-Bcl10, pcDNA3-Flag-API2-MALT1(1-762) and pcDNA3-Flag-API2-MALT1(1-700) were constructed as described previously (1, 2, 4). pcDNA-Flag-p100 and pcDNA3-HA/Flag-NIK were provided by Dr. Gabriel Nunez. Point mutants of API2-MALT1 (C678A) and NIK (KK429/430AA, R325A, R366A, and R368A) were prepared using the QuickChange XL Site-Directed Mutagenesis Kit (Stratagene, Cedar Creek, TX, USA). Expression constructs encoding NIK fragments (AAs 624-947, 1-325, and 326-947) were generated by polymerase chain reaction and then subcloned into the *Xba*I and *Apa*I sites of the corresponding pcDNA3 vector (Invitrogen, Carlsbad, CA, USA). NIK(624-947) is a dominant negative mutant that retains IKK α binding but lacks the kinase domain, and NIK KK429/430AA is a kinase-dead NIK dominant negative mutant. All DNA sequences were verified using an ABI Model 3730 automated sequencer.

HEK293T cells were obtained from American Type Culture Collection (ATCC, Manassas, VA, USA). The SSK41 lymphoma cell line with stable expression of A7M3, an API2-MALT1 fusion which contains three API2 BIR domains, two MALT1 Ig-like domains and the MALT1 “caspase-like” domain, has been previously described (5). BJAB B-cells that express API2-MALT1 or MALT1 from a tetracycline inducible promoter were generated as follows: First, a BJAB clone stably transfected with pTet-On (Clontech, Mountain View, CA, USA) was obtained from Dr. Rolf Renne (6). Next, these cells were transfected with pTRE2puro-Flag-API2-MALT1 or pTRE2puro-Flag-MALT1, and clones were selected for puromycin resistance and then screened for doxycycline-inducible expression of Flag-API2-MALT1 or Flag-MALT1 by Western blot.

Cell Culture, Transfection, and RNA interference

HEK293T cells were maintained in DMEM supplemented with 10% fetal bovine serum (FBS) according to standard procedures. A total of 5×10^5 or 1×10^6 HEK293T cells were transfected with indicated plasmids using either a calcium phosphate method or Lipofectamine 2000 (Invitrogen). BJAB cells were maintained at a concentration of 0.2 to 0.8 million cells/ml in RPMI 1640 with 10% FBS. Treatment with 1 μ g/mL of doxycycline (Sigma-Aldrich, St. Louis, MO, USA) was used to induce expression of API2-MALT1 or MALT1. For analysis of the effect of B-cell receptor stimulation in BJAB cells, all cells were first stimulated with 1 μ g/ml doxycycline for 24 hr, and then treated with or without 10 μ g/ml Goat anti-human IgM as indicated for 5 hr. All cells were cultured in the presence of 25 μ M MG132 for 5 hr prior to

harvest. SSK41 cells (7, 8) with stable expression of A7M3 were maintained in DMEM-F12 with 10% FBS plus 1 $\mu\text{g}/\text{mL}$ puromycin and 1.5 mg/mL G418 as described (5).

API2-MALT1-expressing SSK41 and BJAB B-cells were electroporated with control, human NIK-specific, IKK α -specific or IKK β -specific siRNAs (ON-TARGET plus SMART pools, L-003580-00, L-003473-00, and L-003503-00, respectively, Dharmacon, Lafayette, CO) using Amaxa Cell Line Nucleofactor Kit T (Lonza Cologne AG, Germany) and program G16. Cells were allowed to recover for 48 hrs prior to further analysis. In order to generate clones with stable knock-down of NIK, API2-MALT1-expressing SSK41 B-cells were infected with control or NIK shRNA lentiviral particles (Santa Cruz Biotechnology, Santa Cruz, CA, sc-3606065 or sc-108080) at an MOI of 1 on two consecutive days. Infected cells were selected by limiting dilution in 96-well plates, and resultant clones were screened by western blot and/or RT-PCR to assess NIK knock-down.

Immunoprecipitation, nuclear fractionation, and Western blot analysis

Cells were harvested 24-48 hrs after transfection and lysed with RIPA buffer (Sigma-Aldrich) containing complete protease inhibitor (Roche Diagnostics, Mannheim, Germany). Immunoprecipitations were carried out using anti-FLAG antibody M2-Agarose (Sigma-Aldrich, #A2220) or anti-HA (Roche Laboratories, Basel, Switzerland, #11 583 816 001). The immunoprecipitated products were resolved by SDS-PAGE and detected by Western blotting using ECL Western Blotting Substrate (Thermo Scientific, Rockford, IL, USA, #32106) or Lumagen TMA-6 (GE Healthcare UK Ltd., Buckinghamshire, England) according to the manufacturer's instructions. Cytoplasmic and nuclear extracts were prepared using the NE-PER Nuclear and Cytoplasmic Extraction Reagents according to the manufacturer's recommendations (Thermo Scientific, Rockford, IL, USA). Purity of the nuclear extracts was confirmed by Western blot for HDAC1. The following antibodies were used for Western Blot: anti-Flag M2-peroxidase conjugate (Sigma-Aldrich, #A-8592), anti-Myc-HRP (Santa Cruz Biotechnology Inc., sc-40), anti-HA-HRP (Roche Laboratories, #11 667 475 5433), anti-HA (Roche Laboratories, #11 583 816 001), anti-p100/p52 (Cell Signaling Technology, Inc., Danvers, MA, USA, #4882), anti-RelB (Cell Signaling #4922), anti-NIK (Cell Signaling #4994, Santa Cruz Biotechnology #N-19, Santa Cruz Biotechnology #C-20), anti-MALT1 (9) or (Santa Cruz Biotechnology, H-300), anti-Bcl10 (Santa Cruz Biotechnology, sc-5611), anti-A20 (59A426, eBioscience, San Diego, CA, USA), anti-TRAF3 (Santa Cruz Biotechnology, sc-949), anti-IKK α (Santa Cruz Biotechnology, sc-949), anti-IKK β (Santa Cruz Biotechnology, sc-7329-R), anti-Pim-2 (Santa Cruz Biotechnology, sc-13514), anti-phospho Serine 112-BAD (Cell Signaling # 9291), anti BAFF (Abcam, Cambridge, MA, ab65360), anti-GAPDH (Santa Cruz Biotechnology, 6C5), anti-HDAC1 monoclonal antibody (Santa Cruz Biotechnology Inc.), goat-anti-rabbit-HRP (Jackson Laboratories, West Grove, PA, USA, #111-035-046), goat-anti-mouse-HRP (Jackson Laboratories, # 115-035-071).

MALT1 protease assay

As a source of recombinant MALT1 protein, HKB11 cells (Bayer Corporation, ATCC Number CRL-12568) were generated with stable expression of MALT1 fused to an N-terminal combined StrepII-Flag tag (IBA BioTagnology, Gottingen, Germany). Cells were grown in suspension in 293 serum free medium (Invitrogen NV, Merelbeke, Belgium). The StrepII-tagged MALT1 fusion protein was purified on Strep-Tactin columns according to the manufacturer's recommendations using the One-STrEP-tag purification kit (IBA BioTagnology). The MALT1

protease assay was performed in 25 μ l buffer (pH 6.8) consisting of 50 mM MES, 150 mM NaCl, 10% (w/v) sucrose, 0.1% (w/v) CHAPS, 10 mM dithiothreitol and 1 M $(\text{NH}_4)_3\text{citrate}$, supplemented with 100 μ M fluorogenic substrate (Ac-LSSR-AMC, Anaspec, Fremont, CA) and purified StrepII-tagged MALT1 fusion protein, with or without 100 μ M Ac-LSSR-CHO inhibitor. Time-dependent release of free amido-4-methylcoumarin (AMC) was measured on a FLUOstar Galaxy reader (BMG Labtechnologies GmbH, Offenburg, Germany), and activity was expressed as the increase of relative light units per minute per well.

NIK *in vitro* cleavage assay

A vector enabling expression of biotinylated NIK (pcD-NIK-V5-bioC) was constructed by introducing oligonucleotides encoding the biotinylation (bio) sequence (GLNDIFEAQKIEWHE) as described (10) downstream of a C-terminal V5 epitope in the plasmid pcDNA3.1. The bio-immunoprecipitation method was performed as described (5) using paramagnetic streptavidin beads (Dynabeads M-280, Invitrogen). *In vitro* cleavage assays were performed in 50 μ l kosmotropic salt buffer [50 mM MES (pH 6.8), 150 mM NaCl, 10% (w/v) sucrose, 0.1% (w/v) CHAPS, 10 mM dithiothreitol and 1 M $(\text{NH}_4)_3\text{citrate}$] in order to stabilize intermolecular interactions. Reactions were supplemented with streptavidin beads containing NIK-V5-bioC, StrepII/Flag-tagged MALT1, with or without 100 μ M Ac-LSSR-CHO inhibitor. After incubation at 37°C for 6 hrs with constant rotation, an aliquot of the reaction mixture was used for Western blotting with a Flag antibody to verify equal StrepII/Flag-MALT1 concentrations. The streptavidin beads were collected, washed with 1X PBS and boiled for 10 min in 1X SDS gel loading buffer (with a final concentration of 4% SDS and 300 mM β -mercaptoethanol) and western blotting was performed with the V5 antibody (sc-58052).

Dexamethasone-induced apoptosis assay

Dexamethasone was serially diluted in complete RPMI growth medium at the indicated concentrations in white Cliniplates (Labsource, Willowbrook, IL). The SSK41 B cells were plated at 40,000 cells per well. After 48 hrs, cell viability was assessed using the Cell Titer-Glo Luminescent Cell Viability Assay (Promega, Madison, WI) according to the manufacturer's recommendations. Values are calculated as a percentage of control cells receiving no treatment. P values were derived using a two-tailed T test.

B-cell adhesion assay

Adhesion assays were performed as described (11, 12). Briefly, BJAB B-cells with stable, doxycycline-inducible expression of Flag-API2-MALT1, or empty vector control BJAB cells were electroporated with control or NIK siRNA, followed by doxycycline treatment. 5×10^5 cells were applied to 12 well plates (Becton-Dickinson) coated with BSA or VCAM-1, and then allowed to adhere for 30 min at 37°C. Plates were prepared by incubating for one hour at 37°C with 3 μ g/ml VCAM-1 (R & D systems). Nonadherent cells were removed by washing with PBS. Three representative fields were then counted under 20X magnification. Adhesion was calculated as a % of input samples counted before washing. Each condition was performed in triplicate wells.

Quantitative RT-PCR Gene Expression Analyses

Control and API2-MALT1-expressing SSK41 cells were harvested and total RNA was then prepared using the RNeasy Mini Kit (Qiagen). Equivalent amounts of RNA (500-1000 ng)

were used for cDNA synthesis with the Superscript First-Strand Synthesis System (Invitrogen) using oligo dT primers. Quantitative PCR was performed using TaqMan gene expression primers (Applied Biosystems) specific for human CXCR4, Pim-2, BAFF and integrin α L on an Applied Biosystems 7900HT apparatus supplied by the University of Michigan Microarray Core Facility. Cycle Thresholds were determined and normalized with those for reactions performed with GAPDH specific TaqMan primers. For each gene, relative expression was determined, setting a value of 1.0 for expression in control SSK41 cells. P values were derived using a two tailed T test.

Analysis of primary MALT lymphoma specimens

Cases of MALT lymphoma with known chromosomal translocation status were investigated by Western blot with anti-NIK, anti-p100/p52, and anti-C-terminal MALT1 antibody. The p52/p100 ratio was quantified by standard densitometric analysis. The use of archival human tissues for research was approved by the local research ethics committees of the authors' institutions.

Gene expression microarray analysis of two completely separate collections of MALT lymphoma tumor specimens was performed in order to determine if noncanonical NF- κ B target genes are upregulated in tumors expressing API2-MALT1. Collection #1 included nine t(11;18)-positive (8 from the stomach and 1 from lung) and eight t(11;18)-negative MALT lymphomas (all from the stomach). A description of these patient materials and the methodology for gene expression microarray analysis with Affymetrix GeneChip HG-U133A was detailed in a previous study (13) (GEO; <http://www.ncbi.nlm.nih.gov/geo/>, GSE16024). Standard normalization and nonspecific filtering were carried out. As described previously, absolute GSEA was carried out to investigate whether NF- κ B target genes were differentially expressed between t(11;18) positive and translocation negative MALT lymphoma. The NF- κ B target genes were collated from online data base (<http://www.nf-kb.org>), published works (<http://bioinfo.lifl.fr/NF-KB>, <http://people.bu.edu/gilmore/nf-kb/target/index.html>) and careful bioinformatic search (Table S1), and those that are transactivated by the non-canonical NF- κ B pathway were identified according to previous investigations (11, 14-21). The significance of the GSEA results was assessed by statistical analyses (the nominal P value and False Discovery Rate). Leading edge analysis was further performed to identify the biologically important gene subset.

Tumor collection #2 includes 6 t(11;18)-positive and 8 t(11;18)-negative MALT lymphomas and the methods used for tissue sample collection, RNA isolation and reverse transcription have been described previously (22). Five micrograms of RNA were biotin-labeled and hybridized onto human oligonucleotide microarrays (Affymetrix HG-U133 Plus 2.0; Affymetrix, High Wycombe, UK). Data were analyzed using R/Bioconductor.

Statistical Analysis

Data are expressed as mean \pm SEM. Differences between groups were compared for significance using paired or unpaired 2-tailed Student's T tests, as appropriate, with the assistance of GraphPad InStat software. P values of less than 0.05 were considered statistically significant. See above sections and figure legends for statistical methods used to analyze gene expression in patient samples.

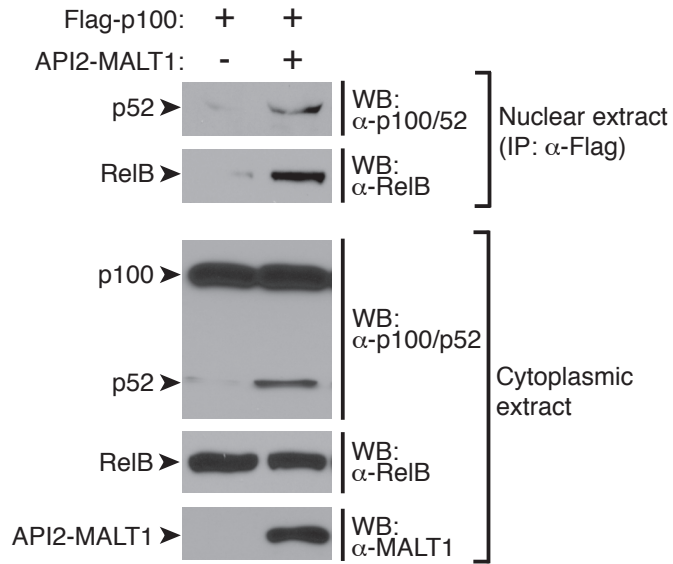


Fig. S1. *API2-MALT1* expression results in the formation of p52/RelB dimers in the nucleus. HEK293T cells were transfected as indicated, and nuclear extracts were prepared. The ability of endogenous RelB to co-immunoprecipitate with nuclear p52 was assessed by Western blot. Data are representative of at least three separate experiments.

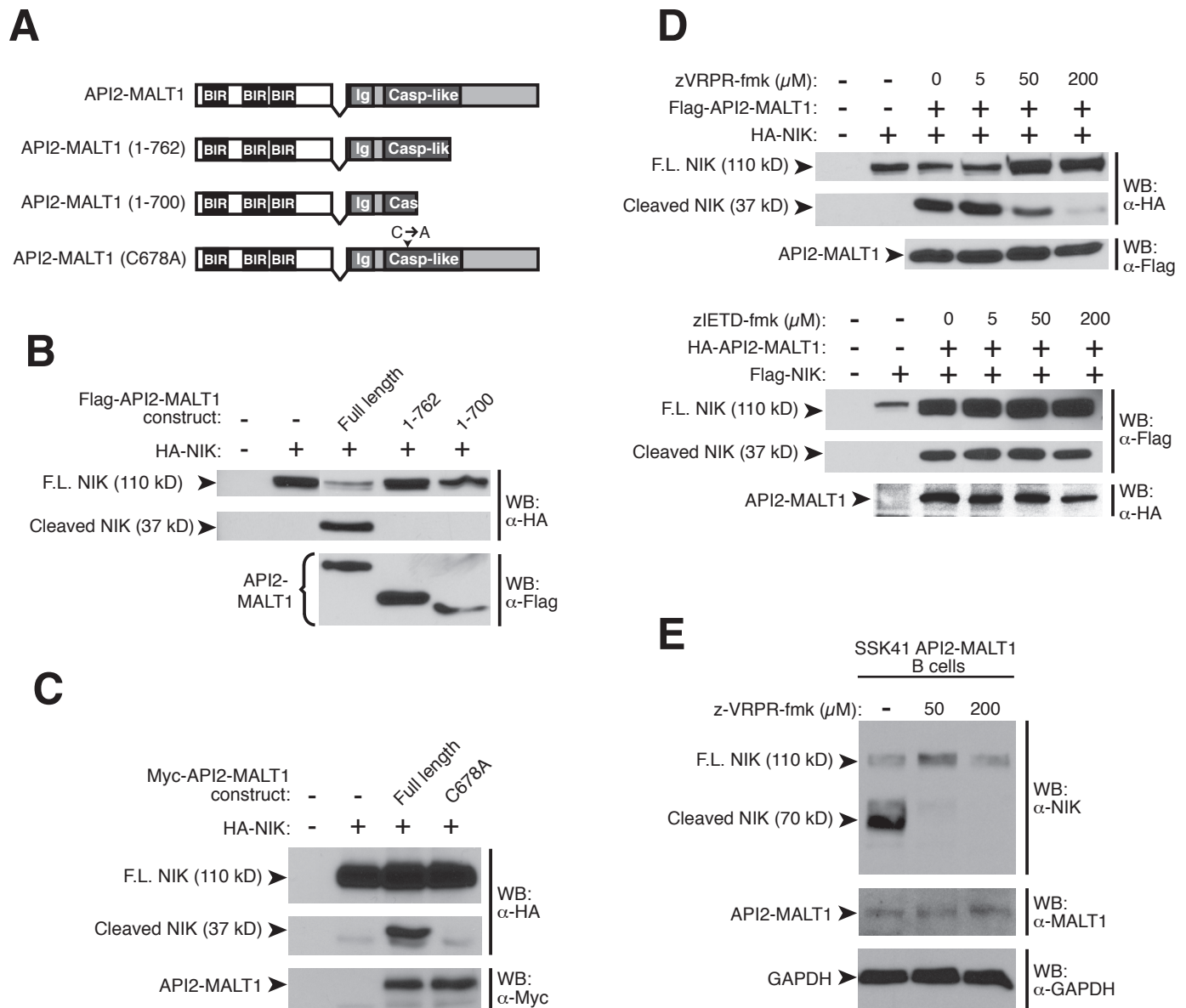


Fig. S3. Deletion, mutation, or inhibition of the MALT1 “caspase-like” domain results in loss of API2-MALT1-dependent NIK cleavage. (A) Schematic of API2-MALT1 mutants. (B) HEK293T cells were transfected with HA-NIK along with various Flag-tagged API2-MALT1 proteins as indicated. The 37 kD N-terminal NIK cleavage fragment was detected by Western blotting with α-HA. (C) HEK293T cells were transfected with either wild-type API2-MALT1 or API2-MALT1(C678A) mutant, along with HA-NIK as indicated. Western blot with α-HA was performed to detect full-length NIK and the 37 kD N-terminal NIK fragment. (D and E) HEK293T cells (D) or SSK41 cells (E) expressing API2-MALT1 were incubated with zVRPR-fmk or zIETD-fmk, and the NIK cleavage fragment was detected by Western blot. Data are representative of at least three separate experiments.

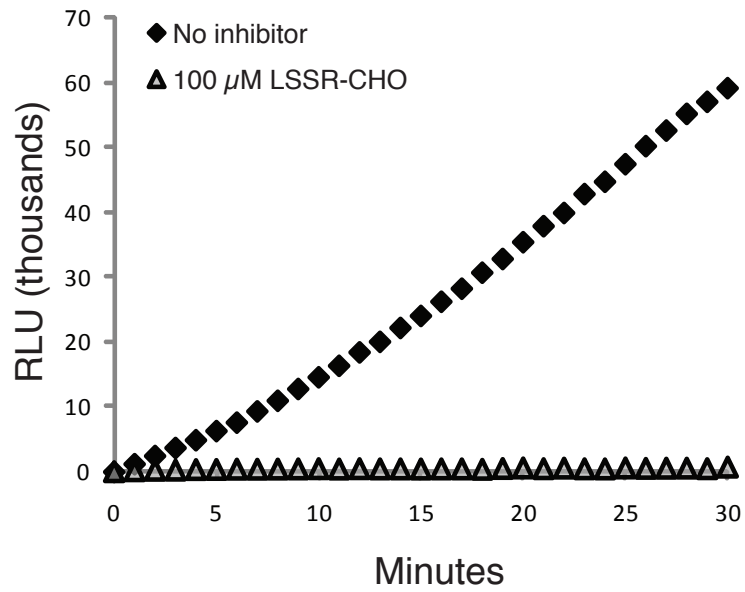


Fig. S4. *MALT1* protease activity assay. Fluorescence release (RLU) due to Ac-LSSR-AMC substrate cleavage (100 μM) in vitro by StrepII-tagged MALT1 (◆). Addition of Ac-LSSR-CHO (100 μM) inhibits MALT1 proteolytic activity (▲).

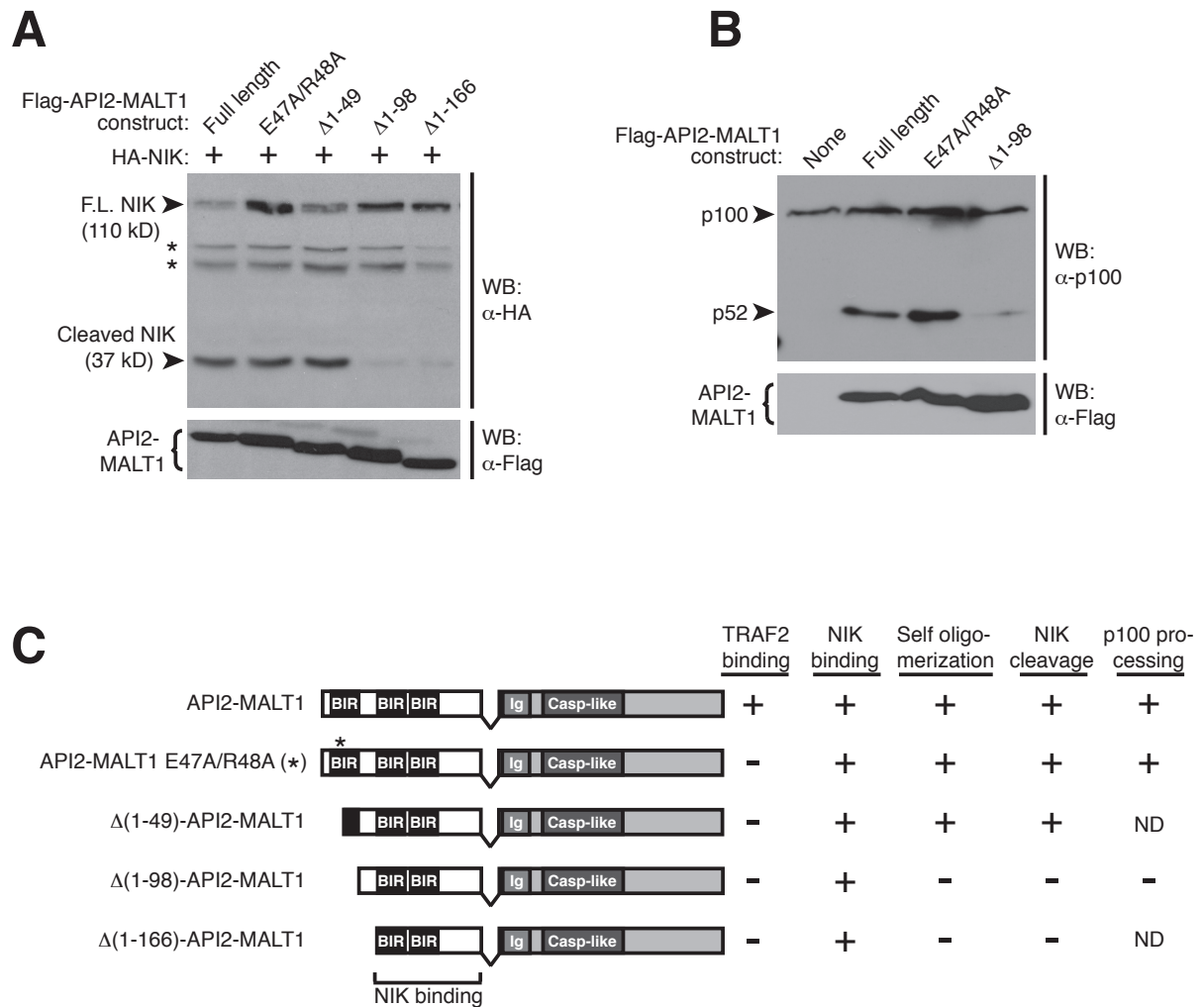


Fig. S5. The API2 moiety is required for association with and cleavage of NIK. (A) The API2-MALT1 auto-oligomerization domain, but not the TRAF2-binding domain, is required for NIK cleavage. HEK293T cells were transfected with HA-NIK, along with the indicated API2-MALT1 deletion mutants, and the generation of the 37 kD N-terminal NIK cleavage product was assessed by Western blotting with α -HA. Mutation or deletion of the previously identified TRAF2 binding site within BIR1 of the API2 moiety (E47A/R48A or Δ 1-49 mutants) does not prevent API2-MALT1-dependent NIK cleavage. In contrast, deletion of the C-terminal half of BIR1 (Δ 1-98), a region that mediates auto-oligomerization of API2-MALT1, does impede API2-MALT1-induced NIK cleavage. (B) API2-MALT1 mutants that lack the ability to bind and cleave NIK are unable to promote p100 processing to p52. HEK293T cells were transfected with the indicated API2-MALT1 mutants and processing of endogenous p100 was analyzed by Western blotting. (C) Schematic summary of the activities of various API2-MALT1 mutants. Results suggest that the API2 moiety of API2-MALT1 interacts with NIK via a site located C-terminal to the BIR1 domain (see Fig. 2F), and that API2 moiety-mediated auto-oligomerization is required to achieve efficient API2-MALT1-dependent NIK cleavage and p100 processing. ND= Not Determined.

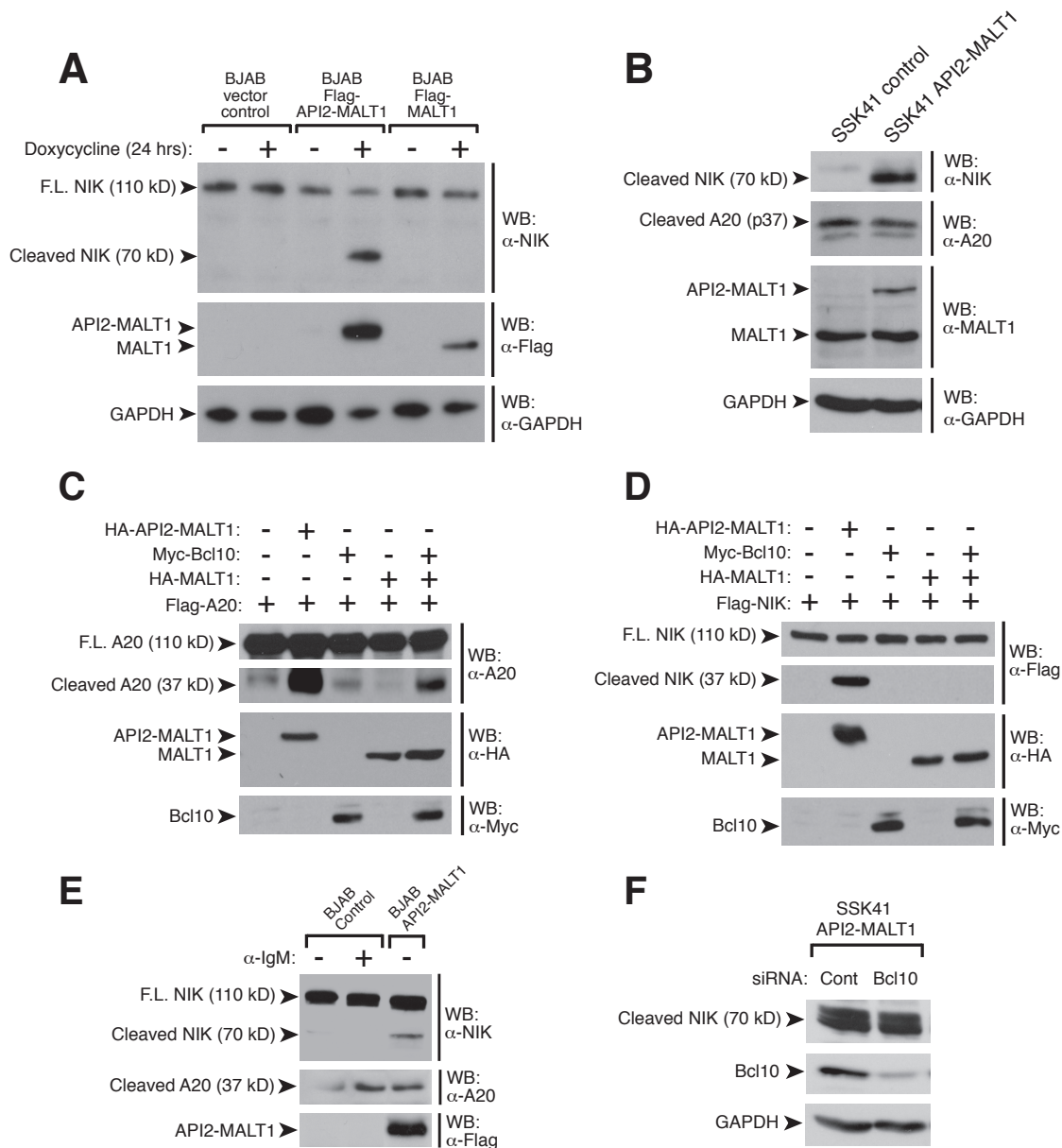


Fig. S6. Activation of wild-type MALT1 within the cell does not induce the cleavage of NIK. (A) BJAB B-cells expressing API2-MALT1 or MALT1 from a tetracycline inducible promoter were treated with or without doxycycline and analyzed for NIK cleavage by Western blot. (B) Unlike A20, NIK is not cleaved in SSK41 cells in the absence of API2-MALT1. Control cells or cells stably expressing API2-MALT1 were analyzed for the presence of the endogenous 70 kD C-terminal NIK cleavage fragment and 37 kD A20 C-terminal cleavage fragment by Western blot. (C and D) Co-expression of Bcl10 and MALT1 activates the MALT1 protease, but does not result in cleavage of NIK. HEK293T cells were transfected with A20 (C) or NIK (D), along with other indicated proteins, and the generation of the A20 (C) or NIK (D) cleavage product was assessed by Western blot. (E) B-cell receptor stimulation activates the MALT1 protease, but does not result in cleavage of NIK. Empty vector control or API2-MALT1-expressing BJAB cells were treated with or without anti-IgM as indicated, and the generation of endogenous cleaved NIK or A20 was detected by Western blot. (F) Bcl10 is not required for API2-MALT1-dependent NIK cleavage. API2-MALT1-expressing SSK41 cells were treated with control or Bcl10-specific siRNA. Bcl10 knock-down and NIK cleavage was then assessed by Western blot. Data are representative of at least three separate experiments.

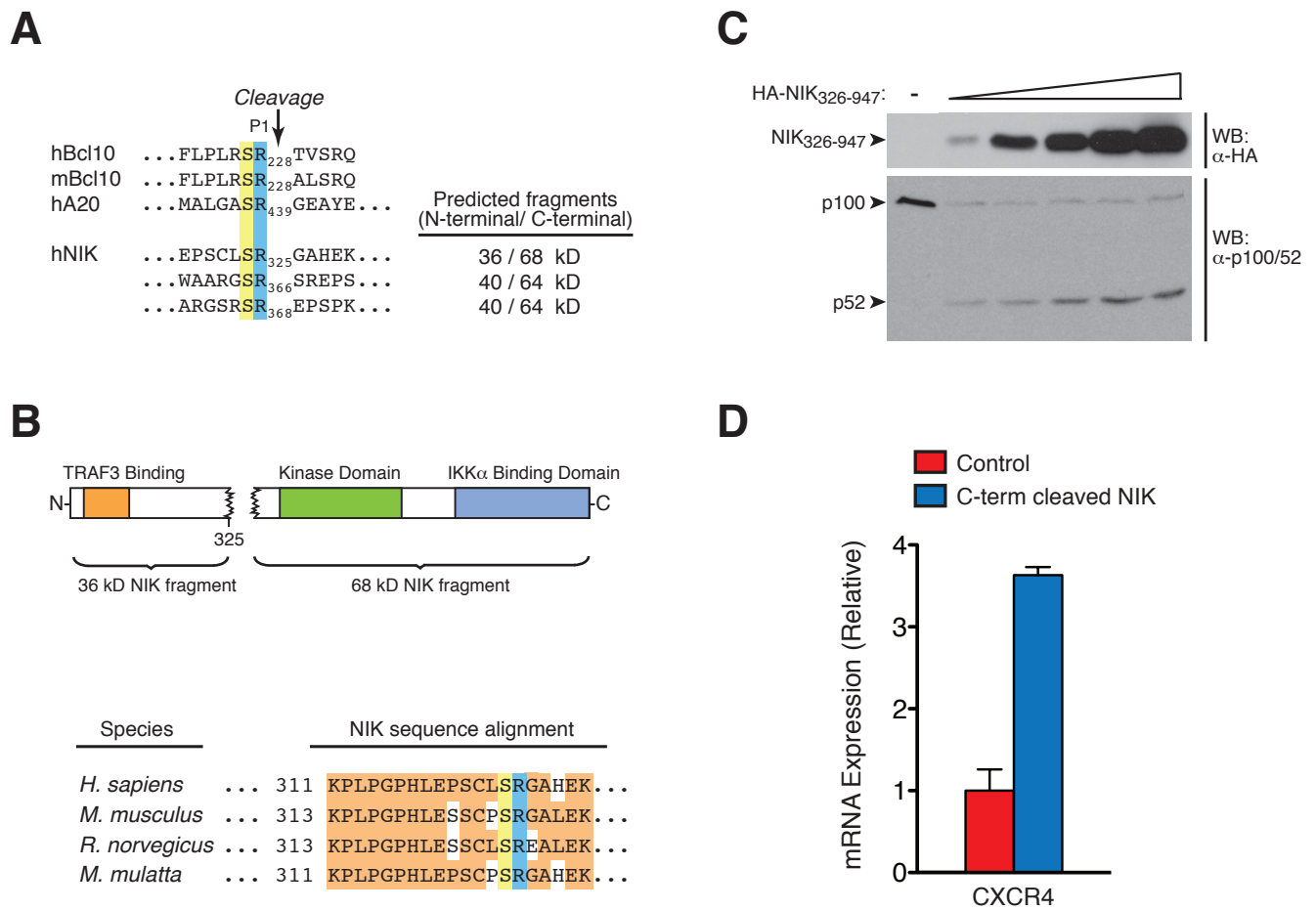


Fig. S7. The 70 kD C-terminal NIK cleavage fragment induces noncanonical NF- κ B signaling. (A) Alignment of the MALT1 cleavage sites in Bcl10 and A20 with candidate sites for NIK cleavage. (B) Top - Schematic of API2-MALT1-dependent NIK cleavage. Bottom - The S324-R325 residues are conserved among species, suggesting that an evolutionarily relevant role for NIK cleavage at this site may exist. (C) The C-terminal NIK cleavage fragment induces concentration-dependent p100 processing. HEK293T cells were transfected with increasing concentrations of HA-NIK(326-947) expression plasmid and the resulting p100 processing was assessed by Western Blot. (D) The C-terminal NIK cleavage fragment induces the expression of CXCR4, a noncanonical NF- κ B gene target (18). CXCR4 is a chemokine receptor that is implicated in B-lymphomagenesis (23, 24). We also found that CXCR4 is significantly upregulated in t(11;18)-positive MALT lymphomas (see Fig. 4F and G).

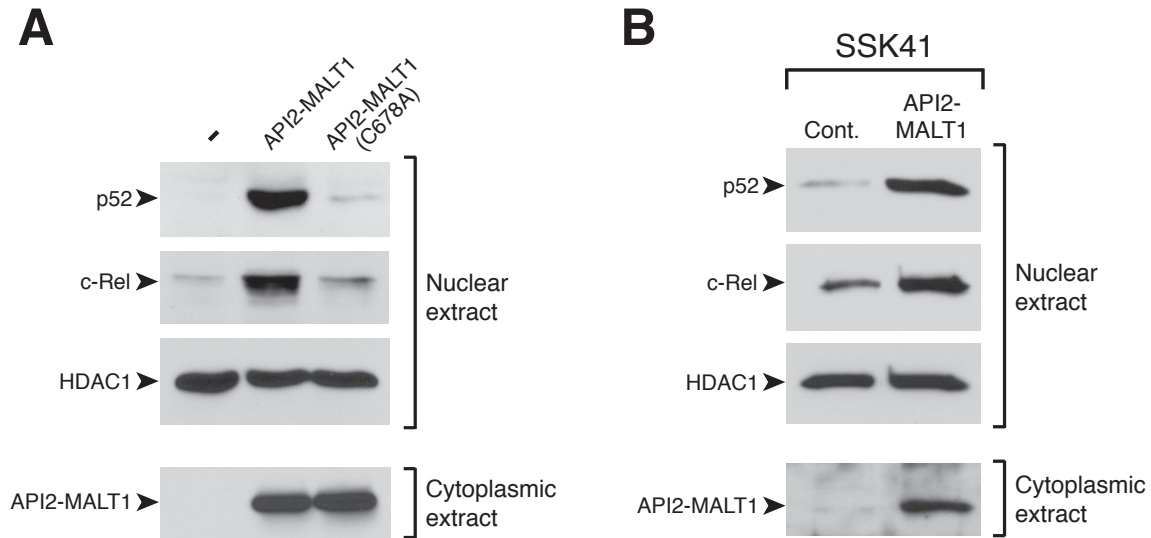


Fig. S8. API2-MALT1 also induces c-Rel nuclear translocation. Because previous work has shown that wild-type MALT1 signals to c-Rel upon BCR ligation (25), we also evaluated the effect of API2-MALT1 on c-Rel. **(A)** API2-MALT1 induces the nuclear translocation of c-Rel, and this requires an intact MALT1 protease domain. HEK293T cells were transfected as indicated, nuclear extracts were prepared, and the resulting nuclear translocation of p52 and c-Rel was assessed by Western blot. **(B)** API2-MALT1 expression in SSK41 cells is associated with enhanced nuclear translocation of p52 and c-Rel. Nuclear extracts were prepared for control and API2-MALT1 expressing SSK41 cells as indicated, and the levels of p52 and c-Rel were assessed by Western Blot.

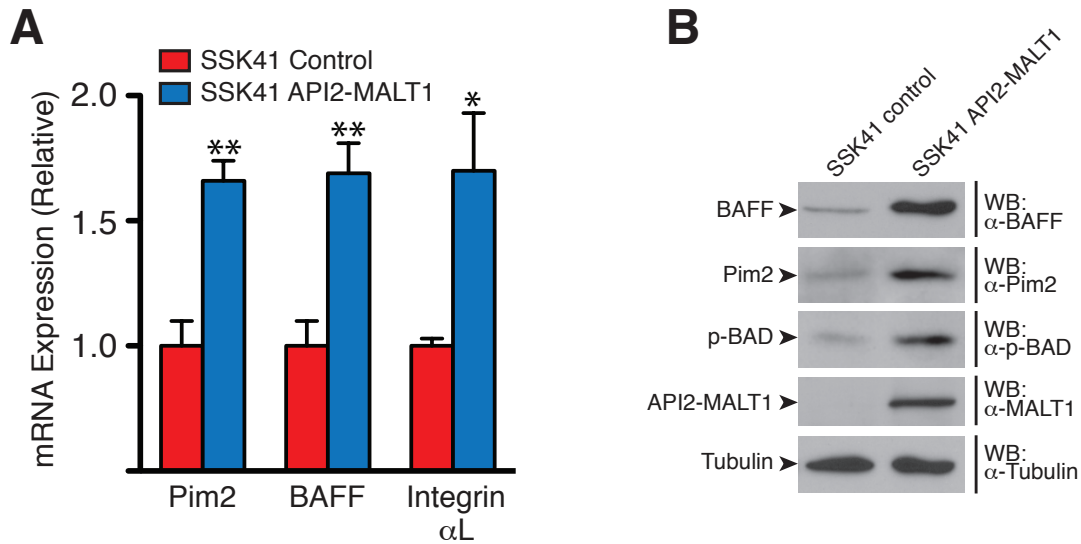


Fig. S9. *API2-MALT1* promotes noncanonical *NF- κ B* target gene expression in *SSK41* B-cells. (A) Levels of mRNA transcript were analyzed by quantitative RT-PCR. Data are expressed as an average \pm SEM for at least three determinations. * = $p < 0.05$, ** = $p < 0.005$. (B) *API2-MALT1* expression results in enhanced levels of BAFF, Pim-2 and phospho-Ser¹¹²-BAD. *SSK41* cell lysates were prepared, and protein levels were compared by Western blotting.

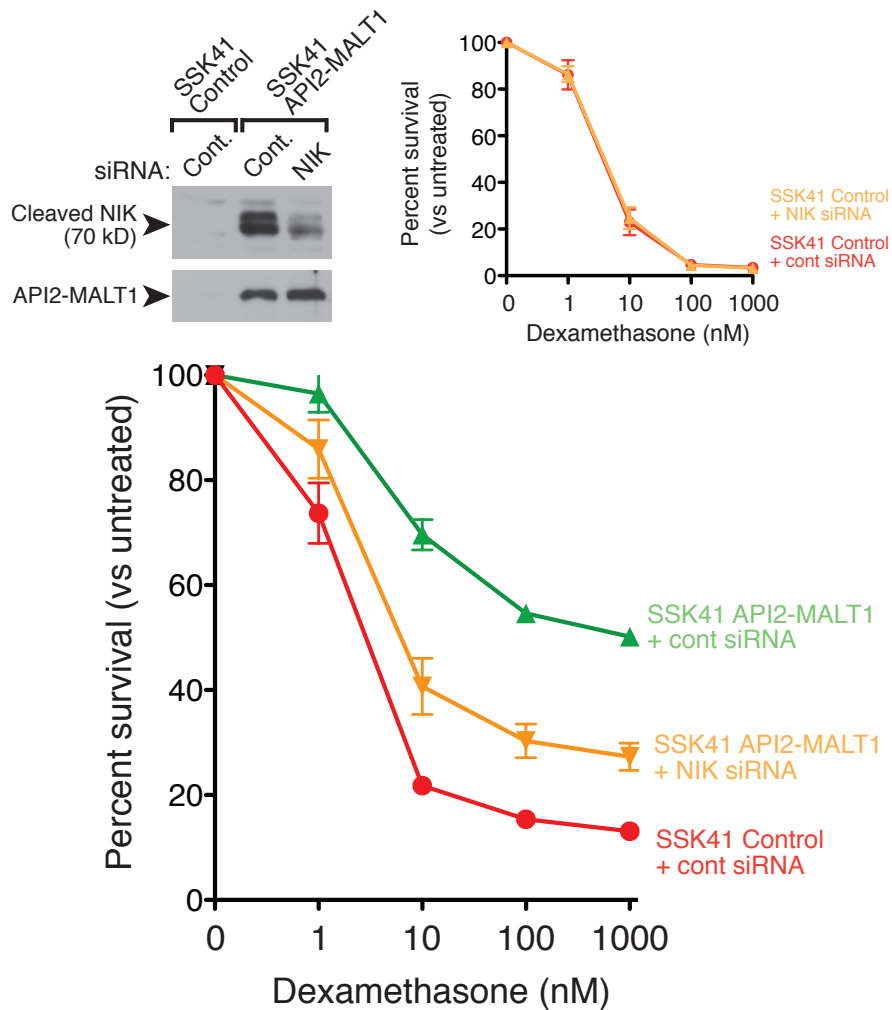


Fig. S10. siRNA-mediated NIK knock-down abrogates API2-MALT1-dependent protection from dexamethasone-induced cell death. Control or API2-MALT1 expressing SSK41 cells were transiently transfected with control or NIK siRNA and then treated with increasing concentrations of dexamethasone. The resulting cell viability was analyzed at 48 hours of dexamethasone treatment. Results are expressed as average \pm SEM of three determinations. **Inserts (top left):** Western blotting demonstrates effective knock-down of the 70kD NIK cleavage fragment, (top right): NIK siRNA had no effect on the control SSK41 cells. Data are representative of at least three separate experiments.

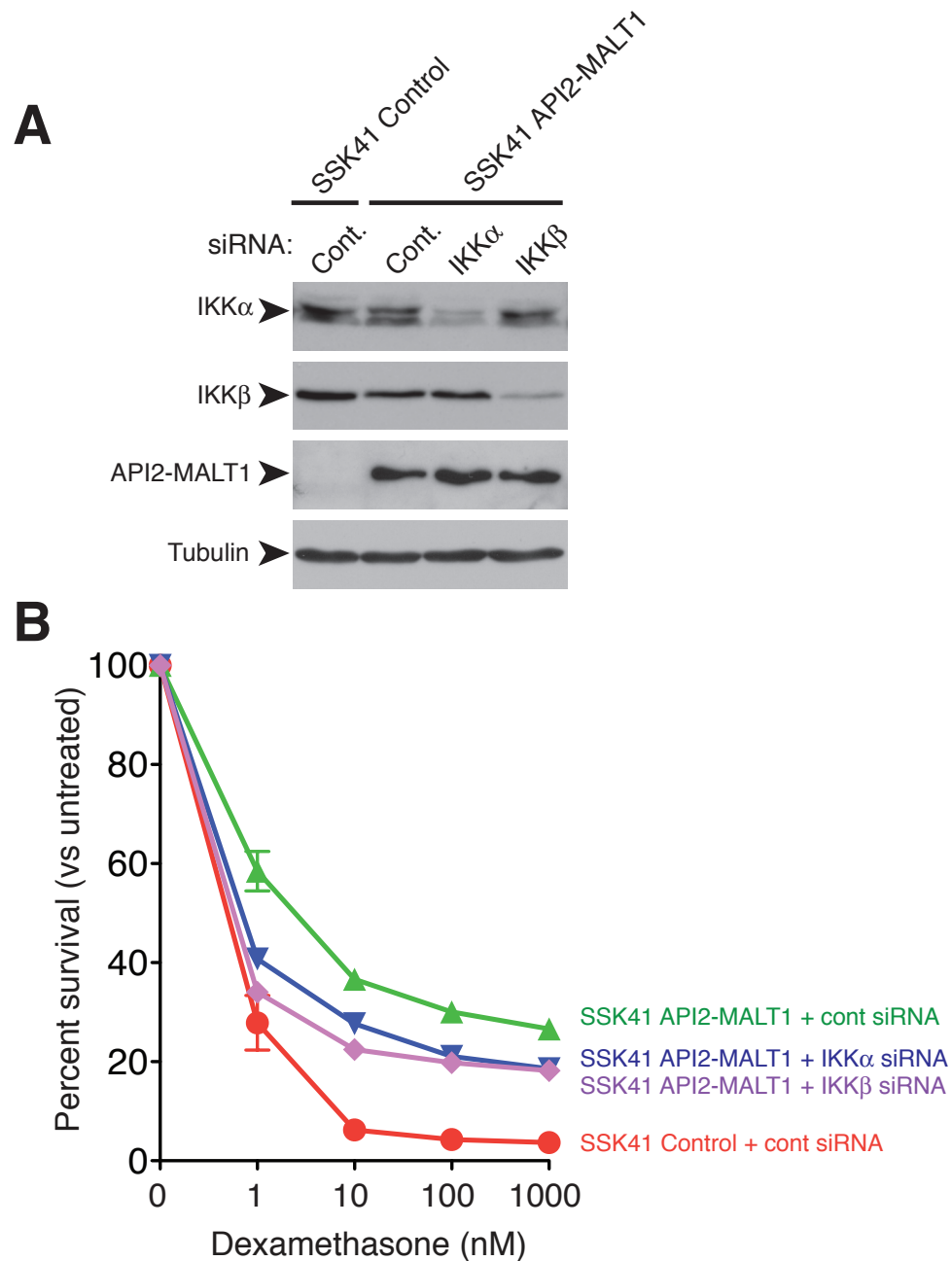


Fig. S11. API2-MALT1-dependent protection from dexamethasone-induced cell death is mediated by a combination of canonical and noncanonical NF- κ B signaling. (A) Control or API2-MALT1 expressing SSK41 cells were transiently transfected with control, IKK α , or IKK β siRNA. Western blotting demonstrates effective and specific knock-down of the IKK subunits and confirms effective expression of API2-MALT1 in cells harboring the transgene. (B) Cells were then treated with increasing concentrations of dexamethasone. The resulting cell viability was analyzed after 48 hours of dexamethasone treatment. Results are expressed as average \pm SEM of three determinations, and are representative of three separate experiments.

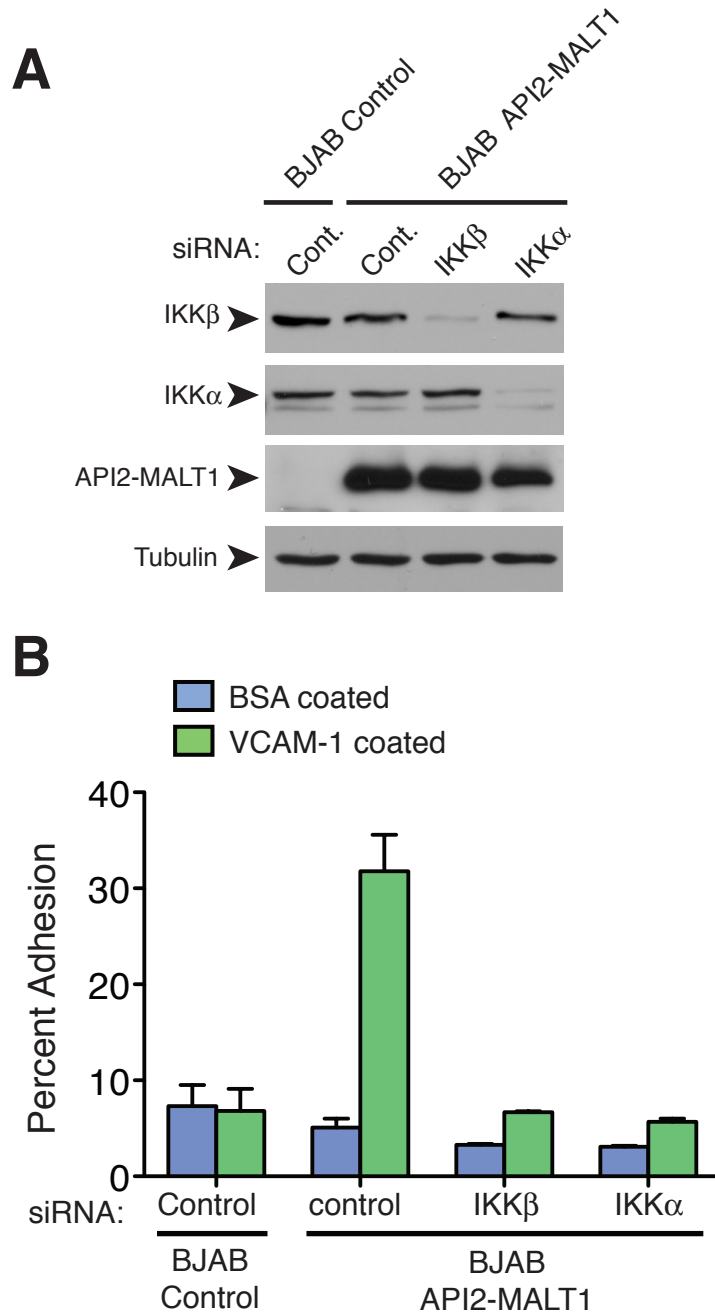


Fig. S12. Both canonical and noncanonical NF- κ B signaling contribute to API2-MALT1-dependent adhesion. Control or API2-MALT1 expressing BJAB cells were transiently transfected with control, IKK β , or IKK α siRNA. After 48 hours, cells were treated for 24 hours with doxycycline to induce API2-MALT1 expression in cells harboring the transgene, and were then plated onto either BSA- or VCAM-1 coated plates. **(A)** Western blotting demonstrates effective and specific knock-down of the IKK subunits as well as effective induction of API2-MALT1. **(B)** Following washing, the percentage of adherent cells was tallied.



Fig. S13. Heat map illustration of gene expression in *t(11;18)*-positive vs. translocation negative MALT lymphomas from Collection #1 (See methods). Genes identified as noncanonical NF- κ B target genes are highlighted in yellow and labeled on the left. The top 20 leading edge core genes are shown.

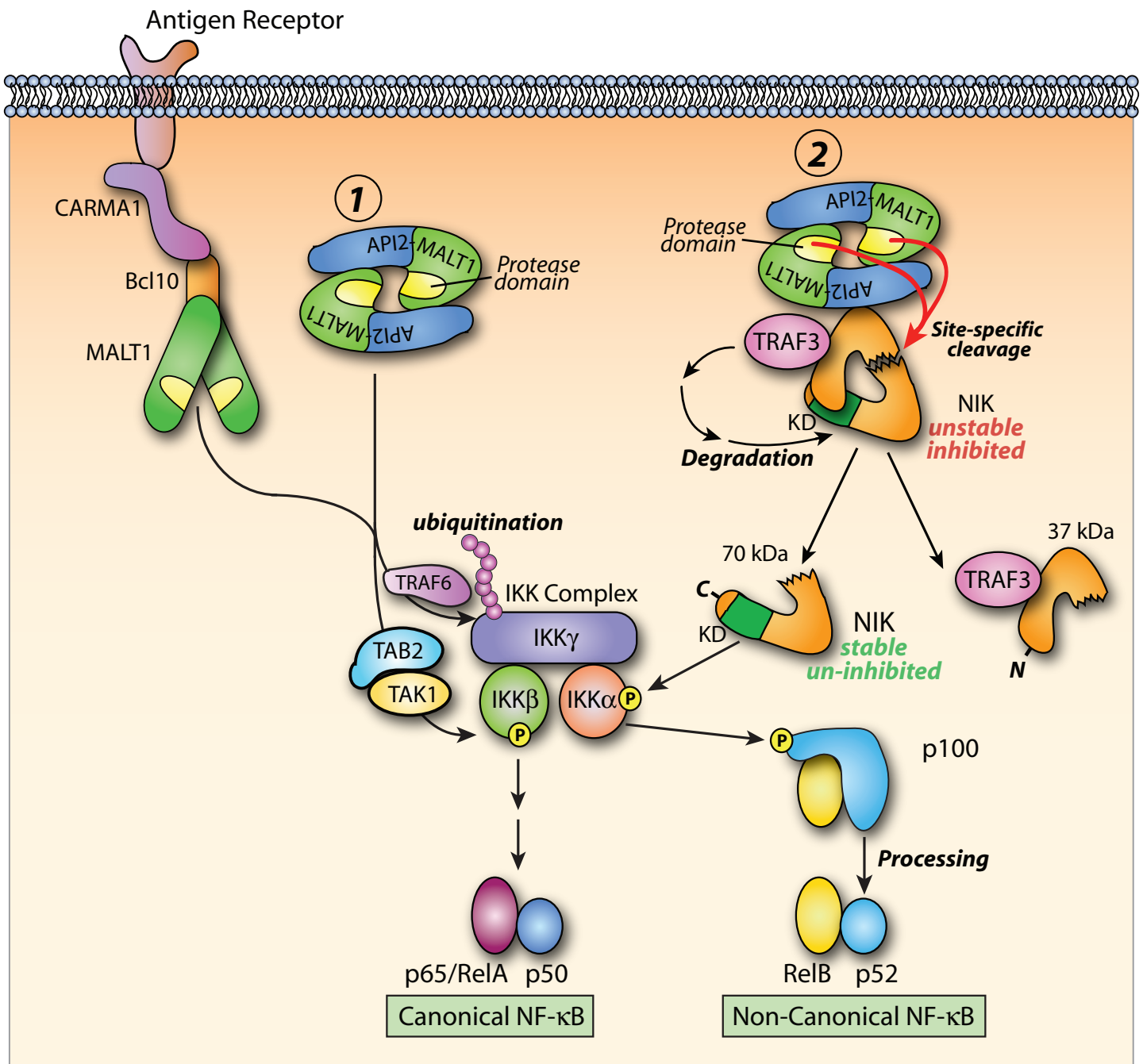


Fig. S14. Schematic illustrating our model for the role of NIK cleavage in API2-MALT1-dependent lymphomagenesis. We propose a model in which: (1) The API2 moiety mediates auto-oligomerization of API2-MALT1 and recruitment of NIK, (2) NIK is then placed in close proximity to the activated MALT1 protease domain and is made available as a substrate, (3) API2-MALT1-dependent NIK cleavage separates the TRAF3 binding site from the active kinase domain, and (4) The stabilized NIK kinase promotes deregulated noncanonical NF- κ B signaling contributing to B-lymphomagenesis. The concept that the N-terminus of NIK contains an autoinhibitory domain that impairs NIK kinase activity (26), in addition to the TRAF3 binding site (27), is incorporated into the model.

Table S1.

| Gene symbol | Gene full name | Source |
|-------------|---|--|
| PIM2 | Pim-2 oncogene | Immunology, 2006; 25: 403-415. Blood, 2008; 111(2): 750-760. |
| CCL21 | chemokine (C-C motif) ligand 21 (Secondary lymphoid tissue chemokine, SLC) | Immunology, 2002; 17: 525-535. EMBO, 2004; 23: 4202-4210. J. Immunol., 2004; 173: 6161-6168. |
| CCL19 | chemokine (C-C motif) ligand 19 (Epstein Barr virus-induced molecule 1 ligand CC chemokine, ELC) | Immunology, 2002; 17: 525-535. EMBO, 2004; 23: 4202-4210. J. Immunol., 2004; 173: 6161-6168. |
| CXCL13 | chemokine (C-X-C motif) ligand 13 (B-lymphocyte chemoattractant, BLC) | Immunology, 2002; 17: 525-535. EMBO, 2004; 23: 4202-4210. J. Immunol., 2004; 173: 6161-6168. |
| TNFSF13B | B-cell activating factor belonging to the TNF family (BAFF) | Immunology, 2002; 17: 525-535. EMBO, 2004; 23: 4202-4210. |
| CXCL12 | chemokine (C-X-C motif) ligand 12 (stromal derived factor-1alpha, SDF-1) | Immunology, 2002; 17: 525-535. EMBO, 2004; 23: 4202-4210. |
| BCL2A1 | BCL2-related protein A1 | Immunology, 2006; 25: 403-415. |
| CXCR4 | chemokine (C-S-C motif) receptor 4 | PNAS, 2004; 101: 141-146. |
| TNFSF11 | tumor necrosis factor (ligand) superfamily, member 11 (RANK-L) | Science, 2001; 293: 1495-1499. |
| CND1 | Cyclin D1 | Endocrinology, 2007; 148(1): 268-278. |
| CXCL9 | chemokine (C-X-C) ligand 9 | PNAS, 2004; 101: 141-146. |
| NTAN1 | N-terminal asparagine amidase (PNAD) | J. Immunol., 2004; 173: 6161-6168. |
| MADCAM1 | mucosal vascular addressin cell adhesion molecule 1 | Blood, 2007; 110: 2381-2389. |
| IRF3 | interferon regulatory factor 3 | EMBO, 2004; 23: 4202-4210. |
| TRIP10 | thyroid hormone receptor interactor 10 | bioinformatics |
| IL32 | interleukin 32 | bioinformatics |
| RCP9 | calcitonin gene-related peptide-receptor component protein | bioinformatics |
| ANKRD1 | ankyrin repeat domain 1 (cardiac muscle) | bioinformatics |
| TNFRSF10B | tumor necrosis factor receptor superfamily, member 10b | bioinformatics |
| AKR1C2 | aldo-keto reductase family 1, member C2 (dihydrodiol dehydrogenase 2) | bioinformatics |
| LDBIB | lactate dehydrogenase B | bioinformatics |
| TEAD1 | TEA domain family member 1 (SV40 transcriptional enhancer factor) | bioinformatics |
| PRDM2 | PR domain containing 2, with ZNF domain | bioinformatics |
| BACE2 | beta-site APP-cleaving enzyme 2 | bioinformatics |
| SUV39H1 | suppressor of variegation 3-9 homolog 1 (Drosophila) | bioinformatics |
| IL1F9 | interleukin 1 family, member 9 | bioinformatics |
| ALOX12B | arachidonate 12-lipoxygenase, 12R type | bioinformatics |
| CARD15 | caspase recruitment domain family, member 15 | bioinformatics |
| CD74 | CD74 antigen (invariant polypeptide of major histocompatibility complex, class II antigen-associated) | bioinformatics |
| CXCL2 | chemokine (C-X-C motif) ligand 2 | bioinformatics |
| DEFB4 | defensin, beta 4 | bioinformatics |
| IL15RA | interleukin 15 receptor, alpha | bioinformatics |
| TPMT | thiopurine S-methyltransferase | bioinformatics |
| TLR6 | toll-like receptor 6 | bioinformatics |
| TLR4 | toll-like receptor 4 | bioinformatics |
| SH3BGRL3 | SH3 domain binding glutamic acid-rich protein like 3 | bioinformatics |
| PLA2G2E | phospholipase A2, group IIE | bioinformatics |
| ADAMTS12 | ADAM metalloproteinase with thrombospondin type 1 motif, 12 | bioinformatics |
| CSF2RA | colony stimulating factor 2 receptor, alpha, low-affinity (granulocyte-macrophage) | bioinformatics |
| MMP8 | matrix metalloproteinase 8 (neutrophil collagenase) | bioinformatics |
| CCL7 | chemokine (C-C motif) ligand 7 | bioinformatics |
| TNFRSF21 | tumor necrosis factor receptor superfamily, member 21 | bioinformatics |
| PLA2G4A | phospholipase A2, group IVA (cytosolic, calcium-dependent) | bioinformatics |
| LAMC2 | laminin, gamma 2 | bioinformatics |
| BCL2L10 | BCL2-like 10 (apoptosis facilitator) | bioinformatics |
| TNFSF6 | tumor necrosis factor superfamily, member 6 | bioinformatics |
| CD105 | homodimeric transmembrane protein which is a major glycoprotein of the vascular endothelium | bioinformatics |
| TNFRSF6 | tumor necrosis factor receptor superfamily, member 6, decoy | bioinformatics |
| TNFSF5 | tumor necrosis factor superfamily, member 5 | bioinformatics |
| BM2 | influenza B virus BM2 | bioinformatics |
| HC3 | proteasome subunit HC3 | bioinformatics |
| SIAT8A | ST8 alpha-N-acetylneuraminidase alpha-2,8-sialyltransferase 1 | bioinformatics |
| TBR | tuberin | bioinformatics |
| TNFRSF5 | tumor necrosis factor receptor superfamily, member 5, decoy | bioinformatics |
| RBCK1 | RanBP-type and C3HC4-type zinc finger containing 1 | bioinformatics |
| CCR2A | chemokine (C-C motif) receptor 2 isoform A | bioinformatics |
| CCR2B | chemokine (C-C motif) receptor 2 isoform B | bioinformatics |
| BIRC2 | baculoviral IAP repeat-containing 2 | Blood, 2005; 106(4): 1392 - 1399 |
| ICAM1 | intercellular adhesion molecule 1 (CD54, human rhinovirus receptor) | Blood, 2005; 106(4): 1392 - 1399 |
| CX3CL1 | chemokine (C-X3-C motif) ligand 1 | Blood, 2005; 106(4): 1392 - 1399 |
| NR4A3 | nuclear receptor subfamily 4, group A, member 3 | Journal of Biological Chemistry, 2005; 280(32): 29256-29262 |
| BCL10 | B-cell CLL/lymphoma 10 | Journal of Biological Chemistry, 2006; 281(1): 167 - 175 |
| LAMP2 | low molecular weight protein 2 | http://people.bu.edu/gilmore/nf-kb/target/index.html |
| CITSL1 | cathepsin L1 | http://people.bu.edu/gilmore/nf-kb/target/index.html |
| KLK3 | kallikrein-related peptidase 3 | http://people.bu.edu/gilmore/nf-kb/target/index.html |
| BMP2 | bone morphogenetic protein 2 | http://people.bu.edu/gilmore/nf-kb/target/index.html |
| AMH | anti-Mullerian hormone | http://people.bu.edu/gilmore/nf-kb/target/index.html |
| NOD2 | nucleotide-binding oligomerization domain containing 2 | http://people.bu.edu/gilmore/nf-kb/target/index.html |
| CYP2C11 | Cytochrome P450 2C11 | http://people.bu.edu/gilmore/nf-kb/target/index.html |
| NK4 | N-terminal hairpin and subsequent four-kringle domains of hepatocyte growth factor | http://people.bu.edu/gilmore/nf-kb/target/index.html |
| CCL15 | chemokine (C-C motif) ligand 15 | http://people.bu.edu/gilmore/nf-kb/target/index.html |
| MYC | v-myc myelocytomatosis viral oncogene homolog (avian) | http://people.bu.edu/gilmore/nf-kb/target/index.html |
| IL1B | interleukin 1, beta | http://people.bu.edu/gilmore/nf-kb/target/index.html |
| TERT | telomerase reverse transcriptase | http://people.bu.edu/gilmore/nf-kb/target/index.html |
| SELP | selectin P (granule membrane protein 140kDa, antigen CD62) | http://people.bu.edu/gilmore/nf-kb/target/index.html |
| TNFAIP3 | tumor necrosis factor, alpha-induced protein 3 | http://people.bu.edu/gilmore/nf-kb/target/index.html |
| CD44 | CD44 antigen (homing function and Indian blood group system) | http://people.bu.edu/gilmore/nf-kb/target/index.html |
| NOS2A | nitric oxide synthase 2A (inducible, hepatocytes) | http://people.bu.edu/gilmore/nf-kb/target/index.html |
| SOD2 | superoxide dismutase 2, mitochondrial | http://people.bu.edu/gilmore/nf-kb/target/index.html |
| CSF3 | colony stimulating factor 3 (granulocyte) | http://people.bu.edu/gilmore/nf-kb/target/index.html |
| BCL3 | B-cell CLL/lymphoma 3 | http://people.bu.edu/gilmore/nf-kb/target/index.html |
| RAGE | renal tumor antigen | http://people.bu.edu/gilmore/nf-kb/target/index.html |
| GRIN1 | glutamate receptor, ionotropic, N-methyl D-aspartate 1 | http://people.bu.edu/gilmore/nf-kb/target/index.html |
| IGHG4 | immunoglobulin heavy constant gamma 4 (G4m marker) | http://people.bu.edu/gilmore/nf-kb/target/index.html |
| IGHG3 | immunoglobulin heavy constant gamma 3 (G3m marker) | http://people.bu.edu/gilmore/nf-kb/target/index.html |
| SERPINA1 | serpin peptidase inhibitor, clade A (alpha-1 antitrypsin, antitrypsin), member 1 | http://people.bu.edu/gilmore/nf-kb/target/index.html |
| NR4A2 | nuclear receptor subfamily 4, group A, member 2 | http://people.bu.edu/gilmore/nf-kb/target/index.html |
| NFKB1 | nuclear factor of kappa light polypeptide gene enhancer in B-cells 1 (p105) | http://people.bu.edu/gilmore/nf-kb/target/index.html |
| NFKBIA | nuclear factor of kappa light polypeptide gene enhancer in B-cells inhibitor, alpha | http://people.bu.edu/gilmore/nf-kb/target/index.html |
| BCL2A1 | BCL2-related protein A1 | http://people.bu.edu/gilmore/nf-kb/target/index.html |
| ADH1A | alcohol dehydrogenase 1A (class I), alpha polypeptide | http://people.bu.edu/gilmore/nf-kb/target/index.html |
| AGER | advanced glycosylation end product-specific receptor | http://people.bu.edu/gilmore/nf-kb/target/index.html |
| AMH | anti-Mullerian hormone | http://people.bu.edu/gilmore/nf-kb/target/index.html |
| ARFRP1 | ADP-ribosylation factor related protein 1 | http://people.bu.edu/gilmore/nf-kb/target/index.html |
| BCL2L1 | BCL2-like 1 | http://people.bu.edu/gilmore/nf-kb/target/index.html |
| BDKRB1 | bradykinin receptor B1 | http://people.bu.edu/gilmore/nf-kb/target/index.html |
| BLR1 | Barkitt lymphoma receptor 1, GTP binding protein (chemokine (C-X-C motif) receptor 5) | http://people.bu.edu/gilmore/nf-kb/target/index.html |
| BMP2 | bone morphogenetic protein 2 | http://people.bu.edu/gilmore/nf-kb/target/index.html |
| CASP4 | caspase 4, apoptosis-related cysteine peptidase | http://people.bu.edu/gilmore/nf-kb/target/index.html |
| CD209 | CD209 antigen | http://people.bu.edu/gilmore/nf-kb/target/index.html |
| CRP | C-reactive protein, pentraxin-related | http://people.bu.edu/gilmore/nf-kb/target/index.html |
| CXCL10 | chemokine (C-X-C motif) ligand 10 | http://people.bu.edu/gilmore/nf-kb/target/index.html |
| CXCL9 | chemokine (C-X-C motif) ligand 9 | http://people.bu.edu/gilmore/nf-kb/target/index.html |
| FTH1 | ferritin, heavy polypeptide 1 | http://people.bu.edu/gilmore/nf-kb/target/index.html |
| GSTP1 | glutathione S-transferase pi | http://people.bu.edu/gilmore/nf-kb/target/index.html |
| HMOX1 | heme oxygenase (decyclinase) 1 | http://people.bu.edu/gilmore/nf-kb/target/index.html |
| IER3 | immediate early response 3 | http://people.bu.edu/gilmore/nf-kb/target/index.html |
| IFNB1 | interferon, beta 1, fibroblast | http://people.bu.edu/gilmore/nf-kb/target/index.html |
| IL1RN | interleukin 1 receptor antagonist | http://people.bu.edu/gilmore/nf-kb/target/index.html |
| KLK3 | kallikrein 3, (prostate specific antigen) | http://people.bu.edu/gilmore/nf-kb/target/index.html |
| NPY1R | neuropeptide Y receptor Y1 | http://people.bu.edu/gilmore/nf-kb/target/index.html |
| NOO1 | NAD(P)H dehydrogenase, quinone 1 | http://people.bu.edu/gilmore/nf-kb/target/index.html |
| OPRM1 | opioid receptor, mu 1 | http://people.bu.edu/gilmore/nf-kb/target/index.html |
| PLAU | plasminogen activator, urokinase | http://people.bu.edu/gilmore/nf-kb/target/index.html |
| PLCD1 | phospholipase C, delta 1 | http://people.bu.edu/gilmore/nf-kb/target/index.html |
| PTAFR | platelet-activating factor receptor | http://people.bu.edu/gilmore/nf-kb/target/index.html |
| PTGDS | prostaglandin D2 synthase 21kDa (brain) | http://people.bu.edu/gilmore/nf-kb/target/index.html |
| PTGS2 | prostaglandin-endoperoxide synthase 2 (prostaglandin G/H synthase and cyclooxygenase) | http://people.bu.edu/gilmore/nf-kb/target/index.html |
| SCNN1A | sodium channel, nonvoltage-gated 1 alpha | http://people.bu.edu/gilmore/nf-kb/target/index.html |
| SELE | selectin E (endothelial adhesion molecule 1) | http://people.bu.edu/gilmore/nf-kb/target/index.html |
| TACR1 | tachykinin receptor 1 | http://people.bu.edu/gilmore/nf-kb/target/index.html |
| TAP1 | transporter 1, ATP-binding cassette, sub-family B (MDR/TAP) | http://people.bu.edu/gilmore/nf-kb/target/index.html |
| TFPI2 | Tissue factor pathway inhibitor 2 | http://people.bu.edu/gilmore/nf-kb/target/index.html |
| TNC | tenascin C (hexabrachion) | http://people.bu.edu/gilmore/nf-kb/target/index.html |
| TNF | tumor necrosis factor (TNF superfamily, member 2) | http://people.bu.edu/gilmore/nf-kb/target/index.html |

| | | |
|----------|---|---|
| TNFRSF9 | tumor necrosis factor receptor superfamily, member 9 | http://people.bu.edu/gilmore/nf-kb/target/index.html |
| VEGF | vascular endothelial growth factor | http://people.bu.edu/gilmore/nf-kb/target/index.html |
| CCL5 | chemokine (C-C motif) ligand 5 | http://people.bu.edu/gilmore/nf-kb/target/index.html |
| CYP2E1 | cytochrome P450, family 2, subfamily E, polypeptide 1 | http://people.bu.edu/gilmore/nf-kb/target/index.html |
| PGK1 | phosphoglycerate kinase 1 | http://people.bu.edu/gilmore/nf-kb/target/index.html |
| CTSB | cathepsin B | http://people.bu.edu/gilmore/nf-kb/target/index.html |
| HMG1 | high-mobility group nucleosome binding domain 1 | http://people.bu.edu/gilmore/nf-kb/target/index.html |
| CND2 | cyclin D2 | http://people.bu.edu/gilmore/nf-kb/target/index.html |
| BGN | biglycan | http://people.bu.edu/gilmore/nf-kb/target/index.html |
| ENO2 | enolase 2 (gamma, neuronal) | http://people.bu.edu/gilmore/nf-kb/target/index.html |
| VIM | vimentin | http://people.bu.edu/gilmore/nf-kb/target/index.html |
| JUNB | jun B proto-oncogene | http://people.bu.edu/gilmore/nf-kb/target/index.html |
| ELF3 | E74-like factor 3 (ets domain transcription factor, epithelial-specific) | http://people.bu.edu/gilmore/nf-kb/target/index.html |
| EGR1 | early growth response 1 | http://people.bu.edu/gilmore/nf-kb/target/index.html |
| CND3 | cyclin D3 | http://people.bu.edu/gilmore/nf-kb/target/index.html |
| TP53 | tumor protein p53 (Li-Fraumeni syndrome) | http://people.bu.edu/gilmore/nf-kb/target/index.html |
| ENG | endoglin (Osler-Rendu-Weber syndrome 1) | http://people.bu.edu/gilmore/nf-kb/target/index.html |
| BNIP3 | BC1.2/adenovirus E1B 19kDa interacting protein 3 | http://people.bu.edu/gilmore/nf-kb/target/index.html |
| EGFR | epidermal growth factor receptor (erythroblastic leukemia viral (v-erb-b) oncogene homolog, avian) | http://people.bu.edu/gilmore/nf-kb/target/index.html |
| SDC4 | syndecan 4 (amphiglycan, ryadocan) | http://people.bu.edu/gilmore/nf-kb/target/index.html |
| IRF2 | interferon inducible protein 2 | http://people.bu.edu/gilmore/nf-kb/target/index.html |
| MX1 | myxovirus (influenza virus) resistance 1, interferon-inducible protein p78 (mouse) | http://people.bu.edu/gilmore/nf-kb/target/index.html |
| GBP1 | guanylate binding protein 1, interferon-inducible, 67kDa | http://people.bu.edu/gilmore/nf-kb/target/index.html |
| KLF10 | Kruppel-like factor 10 | http://people.bu.edu/gilmore/nf-kb/target/index.html |
| IRF1 | interferon regulatory factor 1 | http://people.bu.edu/gilmore/nf-kb/target/index.html |
| IGFBP2 | insulin-like growth factor binding protein 2, 36kDa | http://people.bu.edu/gilmore/nf-kb/target/index.html |
| IL8 | interleukin 8 | http://people.bu.edu/gilmore/nf-kb/target/index.html |
| GCLC | glutamate-cysteine ligase, catalytic subunit | http://people.bu.edu/gilmore/nf-kb/target/index.html |
| SOX9 | SOX (sex determining region Y)-box 9 (campomelic dysplasia, autosomal sex-reversal) | http://people.bu.edu/gilmore/nf-kb/target/index.html |
| STAT5A | signal transducer and activator of transcription 5A | http://people.bu.edu/gilmore/nf-kb/target/index.html |
| THBS2 | thrombospondin 2 | http://people.bu.edu/gilmore/nf-kb/target/index.html |
| UBE2M | ubiquitin-conjugating enzyme E2M (UBC12 homolog, yeast) | http://people.bu.edu/gilmore/nf-kb/target/index.html |
| UPP1 | uridine phosphorylase 1 | http://people.bu.edu/gilmore/nf-kb/target/index.html |
| IRF2 | interferon regulatory factor 2 | http://people.bu.edu/gilmore/nf-kb/target/index.html |
| APOE | apolipoprotein E | http://people.bu.edu/gilmore/nf-kb/target/index.html |
| ABCA1 | ATP-binding cassette, sub-family A (ABCI), member 1 | http://people.bu.edu/gilmore/nf-kb/target/index.html |
| BCL2 | B-cell CLL lymphoma 2 | http://people.bu.edu/gilmore/nf-kb/target/index.html |
| DIO2 | deiodinase, iodothyronine, type II | http://people.bu.edu/gilmore/nf-kb/target/index.html |
| VCAM1 | vascular cell adhesion molecule 1 | http://people.bu.edu/gilmore/nf-kb/target/index.html |
| GCLM | glutamate-cysteine ligase, modifier subunit | http://people.bu.edu/gilmore/nf-kb/target/index.html |
| MMP9 | matrix metalloproteinase 9 (gelatinase B, 92kDa gelatinase, 92kDa type IV collagenase) | http://people.bu.edu/gilmore/nf-kb/target/index.html |
| CD48 | CD48 antigen (B-cell membrane protein) | http://people.bu.edu/gilmore/nf-kb/target/index.html |
| PDGFB | platelet-derived growth factor beta polypeptide (simian sarcoma viral (v-sis) oncogene homolog) | http://people.bu.edu/gilmore/nf-kb/target/index.html |
| TRAF2 | TNF receptor-associated factor 2 | http://people.bu.edu/gilmore/nf-kb/target/index.html |
| IFI44L | interferon-induced protein 44-like | http://people.bu.edu/gilmore/nf-kb/target/index.html |
| CD83 | CD83 antigen (activated B lymphocytes, immunoglobulin superfamily) | http://people.bu.edu/gilmore/nf-kb/target/index.html |
| CXCL1 | chemokine (C-X-C motif) ligand 1 (melanoma growth stimulating activity, alpha) | http://people.bu.edu/gilmore/nf-kb/target/index.html |
| IRF4 | interferon regulatory factor 4 | http://people.bu.edu/gilmore/nf-kb/target/index.html |
| TFE3 | trefoil factor 3 (intestinal) | http://people.bu.edu/gilmore/nf-kb/target/index.html |
| MUC2 | mucin 2, intestinal/tracheal | http://people.bu.edu/gilmore/nf-kb/target/index.html |
| AFP | alpha-fetoprotein | http://people.bu.edu/gilmore/nf-kb/target/index.html |
| FAS | Fas (TNF receptor superfamily, member 6) | http://people.bu.edu/gilmore/nf-kb/target/index.html |
| UGCG | UDP-glucose ceramide glucosyltransferase | http://people.bu.edu/gilmore/nf-kb/target/index.html |
| TLR2 | tolllike receptor 2 | http://people.bu.edu/gilmore/nf-kb/target/index.html |
| PLK3 | polo-like kinase 3 (Drosophila) | http://people.bu.edu/gilmore/nf-kb/target/index.html |
| CD40 | CD40 antigen (TNF receptor superfamily member 5) | http://people.bu.edu/gilmore/nf-kb/target/index.html |
| RELB | v-rel reticulendotheliosis viral oncogene homolog B, nuclear factor of kappa light polypeptide gene enhancer in B-cells 3 (avian) | http://people.bu.edu/gilmore/nf-kb/target/index.html |
| IL6 | interleukin 6 (interferon, beta 2) | http://people.bu.edu/gilmore/nf-kb/target/index.html |
| GAD1 | glutamate decarboxylase 1 (brain, 67kDa) | http://people.bu.edu/gilmore/nf-kb/target/index.html |
| IGFBP1 | insulin-like growth factor binding protein 1 | http://people.bu.edu/gilmore/nf-kb/target/index.html |
| PRL | prolactin | http://people.bu.edu/gilmore/nf-kb/target/index.html |
| TRAF1 | TNF receptor-associated factor 1 | http://people.bu.edu/gilmore/nf-kb/target/index.html |
| CD86 | CD86 antigen (CD28 antigen ligand 2, B7-2 antigen) | http://people.bu.edu/gilmore/nf-kb/target/index.html |
| CD38 | CD38 antigen (p45) | http://people.bu.edu/gilmore/nf-kb/target/index.html |
| POMC | proopiomelanocortin (adrenocorticotropin/ beta-lipotropin/ alpha-melanocyte stimulating hormone/ beta-melanocyte stimulating hormone/ beta-endorphin) | http://people.bu.edu/gilmore/nf-kb/target/index.html |
| APOC3 | apolipoprotein C-III | http://people.bu.edu/gilmore/nf-kb/target/index.html |
| MMP3 | matrix metalloproteinase 3 (stromelysin 1, progelatinase) | http://people.bu.edu/gilmore/nf-kb/target/index.html |
| IL15 | interleukin 15 | http://people.bu.edu/gilmore/nf-kb/target/index.html |
| WT1 | Wilms tumor 1 | http://people.bu.edu/gilmore/nf-kb/target/index.html |
| PTX3 | pentraxin-related gene, rapidly induced by IL-1 beta | http://people.bu.edu/gilmore/nf-kb/target/index.html |
| APOBEC2 | apolipoprotein B mRNA editing enzyme, catalytic polypeptide-like 2 | http://people.bu.edu/gilmore/nf-kb/target/index.html |
| MAP4K1 | mitogen-activated protein kinase kinase kinase kinase 1 | http://people.bu.edu/gilmore/nf-kb/target/index.html |
| CCR7 | chemokine (C-C motif) receptor 7 | http://people.bu.edu/gilmore/nf-kb/target/index.html |
| IL2RA | interleukin 2 receptor, alpha | http://people.bu.edu/gilmore/nf-kb/target/index.html |
| CDX1 | caudal type homeo box transcription factor 1 | http://people.bu.edu/gilmore/nf-kb/target/index.html |
| RAG1 | recombination activating gene 1 | http://people.bu.edu/gilmore/nf-kb/target/index.html |
| P11 | 26 serine protease | http://people.bu.edu/gilmore/nf-kb/target/index.html |
| TFEC | transcription factor EC | http://people.bu.edu/gilmore/nf-kb/target/index.html |
| FCER2 | Fc fragment of IgE, low affinity II, receptor for (CD23A) | http://people.bu.edu/gilmore/nf-kb/target/index.html |
| MTHFR | 5,10-methylenetetrahydrofolate reductase (NADPH) | http://people.bu.edu/gilmore/nf-kb/target/index.html |
| PDYN | prodynorphin | http://people.bu.edu/gilmore/nf-kb/target/index.html |
| CD3G | CD3G antigen, gamma polypeptide (T13 complex) | http://people.bu.edu/gilmore/nf-kb/target/index.html |
| OXTR | oxytocin receptor | http://people.bu.edu/gilmore/nf-kb/target/index.html |
| IL11 | interleukin 11 | http://people.bu.edu/gilmore/nf-kb/target/index.html |
| LTA | lymphotoxin alpha (TNF superfamily, member 1) | http://people.bu.edu/gilmore/nf-kb/target/index.html |
| CCR5 | chemokine (C-C motif) receptor 5 | http://people.bu.edu/gilmore/nf-kb/target/index.html |
| GIF | gastric intrinsic factor (vitamin B synthesis) | http://people.bu.edu/gilmore/nf-kb/target/index.html |
| CSF1 | colony stimulating factor 1 (macrophage) | http://people.bu.edu/gilmore/nf-kb/target/index.html |
| IL12A | interleukin 12A (natural killer cell stimulatory factor 1, cytotoxic lymphocyte maturation factor 1, p35) | http://people.bu.edu/gilmore/nf-kb/target/index.html |
| CD80 | CD80 antigen (CD28 antigen ligand 1, B7-1 antigen) | http://people.bu.edu/gilmore/nf-kb/target/index.html |
| TNIP1 | TNFAIP3 interacting protein 1 | http://people.bu.edu/gilmore/nf-kb/target/index.html |
| EPO | erythropoietin | http://people.bu.edu/gilmore/nf-kb/target/index.html |
| LTB | lymphotoxin beta (TNF superfamily, member 3) | http://people.bu.edu/gilmore/nf-kb/target/index.html |
| CYP7B1 | cytochrome P450, family 7, subfamily B, polypeptide 1 | http://people.bu.edu/gilmore/nf-kb/target/index.html |
| IL10 | interleukin 10 | http://people.bu.edu/gilmore/nf-kb/target/index.html |
| NFKB2 | nuclear factor of kappa light polypeptide gene enhancer in B-cells 2 (p49/p100) | http://people.bu.edu/gilmore/nf-kb/target/index.html |
| IL13 | interleukin 13 | http://people.bu.edu/gilmore/nf-kb/target/index.html |
| IL2 | interleukin 2 | http://people.bu.edu/gilmore/nf-kb/target/index.html |
| CXCL5 | chemokine (C-X-C motif) ligand 5 | http://people.bu.edu/gilmore/nf-kb/target/index.html |
| CCL22 | chemokine (C-C motif) ligand 22 | http://people.bu.edu/gilmore/nf-kb/target/index.html |
| MADCAM1 | mucosal vascular addressin cell adhesion molecule 1 | http://people.bu.edu/gilmore/nf-kb/target/index.html |
| REV3L | REV3-like, catalytic subunit of DNA polymerase zeta (yeast) | http://people.bu.edu/gilmore/nf-kb/target/index.html |
| PTGS1 | prostaglandin I2 (prostaglyclin) synthase | http://people.bu.edu/gilmore/nf-kb/target/index.html |
| IL9 | interleukin 9 | http://people.bu.edu/gilmore/nf-kb/target/index.html |
| IL1A | interleukin 1, alpha | http://people.bu.edu/gilmore/nf-kb/target/index.html |
| KGR | progesterone receptor | http://people.bu.edu/gilmore/nf-kb/target/index.html |
| IRF7 | interferon regulatory factor 7 | http://people.bu.edu/gilmore/nf-kb/target/index.html |
| FGF8 | fibroblast growth factor 8 (androgen-induced) | http://people.bu.edu/gilmore/nf-kb/target/index.html |
| BAX | BCL2-associated X protein | http://people.bu.edu/gilmore/nf-kb/target/index.html |
| ABCC6 | ATP-binding cassette, sub-family C (CFTR/MRP), member 6 | http://people.bu.edu/gilmore/nf-kb/target/index.html |
| SERPINA2 | serpin peptidase inhibitor, clade A (alpha-1 antitrypsinase, antitrypsin), member 2 | http://people.bu.edu/gilmore/nf-kb/target/index.html |
| CND1 | cyclin D1 | http://people.bu.edu/gilmore/nf-kb/target/index.html |
| TAPP3 | TAP binding protein (tapasin) | http://people.bu.edu/gilmore/nf-kb/target/index.html |
| LGALS3 | lectin, galactoside-binding, soluble 3 (galectin 3) | http://people.bu.edu/gilmore/nf-kb/target/index.html |
| UCP2 | uncoupling protein 2 (mitochondrial, proton carrier) | http://people.bu.edu/gilmore/nf-kb/target/index.html |
| PIM1 | pim-1 oncogene | http://people.bu.edu/gilmore/nf-kb/target/index.html |
| GADD45B | growth arrest and DNA-damage-inducible, beta | http://people.bu.edu/gilmore/nf-kb/target/index.html |
| RIPK2 | receptor-interacting serine-threonine kinase 2 | http://people.bu.edu/gilmore/nf-kb/target/index.html |
| ADAM19 | ADAM metalloproteinase domain 19 (meltrin beta) | http://people.bu.edu/gilmore/nf-kb/target/index.html |
| CD69 | CD69 antigen (p60, early T-cell activation antigen) | http://people.bu.edu/gilmore/nf-kb/target/index.html |
| HGF | hepatocyte growth factor (heparin-binding, scatter factor) | http://people.bu.edu/gilmore/nf-kb/target/index.html |
| ABCB1 | ATP-binding cassette, sub-family B (MDR/TAP), member 1 | http://people.bu.edu/gilmore/nf-kb/target/index.html |
| UPK1B | uroplakin 1B | http://people.bu.edu/gilmore/nf-kb/target/index.html |
| CCL11 | chemokine (C-C motif) ligand 11 | http://people.bu.edu/gilmore/nf-kb/target/index.html |
| CXCL11 | chemokine (C-X-C motif) ligand 11 | http://people.bu.edu/gilmore/nf-kb/target/index.html |
| GZMB | granzyme B (granzyme 2, cytotoxic T-lymphocyte-associated serine esterase 1) | http://people.bu.edu/gilmore/nf-kb/target/index.html |
| XDH | xanthine dehydrogenase | http://people.bu.edu/gilmore/nf-kb/target/index.html |
| IFNG | interferon, gamma | http://people.bu.edu/gilmore/nf-kb/target/index.html |
| ICOS | inducible T-cell co-stimulator | http://people.bu.edu/gilmore/nf-kb/target/index.html |

| | | |
|--------|--|---|
| FN1 | fibronectin 1 | http://people.bu.edu/gilmore/nf-kb/target/index.html |
| ERBB2 | v-erb-b2 erythroblastic leukemia viral oncogene homolog 2, neuro/glioblastoma derived oncogene homolog (avian) | http://people.bu.edu/gilmore/nf-kb/target/index.html |
| KITLG | KIT ligand | http://people.bu.edu/gilmore/nf-kb/target/index.html |
| FASLG | Fas ligand (TNF superfamily, member 6) | http://people.bu.edu/gilmore/nf-kb/target/index.html |
| HLA-G | HLA-G histocompatibility antigen, class I, G | http://people.bu.edu/gilmore/nf-kb/target/index.html |
| TGM2 | transglutaminase 2 (C polypeptide, protein-glutamine-gamma-glutamyltransferase) | http://people.bu.edu/gilmore/nf-kb/target/index.html |
| NR3C1 | nuclear receptor subfamily 3, group C, member 1 (glucocorticoid receptor) | http://people.bu.edu/gilmore/nf-kb/target/index.html |
| PENK | proenkephalin | http://people.bu.edu/gilmore/nf-kb/target/index.html |
| PAX8 | paired box gene 8 | http://people.bu.edu/gilmore/nf-kb/target/index.html |
| CCL2 | chemokine (C-C motif) ligand 2 | http://people.bu.edu/gilmore/nf-kb/target/index.html |
| S100A6 | S100 calcium binding protein A6 (calyculin) | http://people.bu.edu/gilmore/nf-kb/target/index.html |
| EDN1 | endothelin 1 | http://people.bu.edu/gilmore/nf-kb/target/index.html |
| HPS2 | heparanase | http://people.bu.edu/gilmore/nf-kb/target/index.html |
| SNAI1 | snail homolog 1 (Drosophila) | http://people.bu.edu/gilmore/nf-kb/target/index.html |
| KCNK5 | potassium channel, subfamily K, member 5 | http://people.bu.edu/gilmore/nf-kb/target/index.html |
| ABCG5 | ATP-binding cassette, sub-family G (WHITE), member 5 (sterolin 1) | http://people.bu.edu/gilmore/nf-kb/target/index.html |
| F11R | F11 receptor | http://people.bu.edu/gilmore/nf-kb/target/index.html |
| G6PD | glucose-6-phosphate dehydrogenase | http://people.bu.edu/gilmore/nf-kb/target/index.html |
| ORM1 | orosomucoid 1 | http://people.bu.edu/gilmore/nf-kb/target/index.html |
| ADORA1 | adenosine A1 receptor | http://people.bu.edu/gilmore/nf-kb/target/index.html |
| C4BPA | complement component 4 binding protein, alpha | http://people.bu.edu/gilmore/nf-kb/target/index.html |
| HAS1 | hyaluronan synthase 1 | http://people.bu.edu/gilmore/nf-kb/target/index.html |
| REL | v-rel reticuloendotheliosis viral oncogene homolog (avian) | http://people.bu.edu/gilmore/nf-kb/target/index.html |
| CCL3 | chemokine (C-C motif) ligand 3 | http://people.bu.edu/gilmore/nf-kb/target/index.html |
| CCL4 | chemokine (C-C motif) ligand 4 | http://people.bu.edu/gilmore/nf-kb/target/index.html |
| CLAR | CASP8 and FADD-like apoptosis regulator | http://people.bu.edu/gilmore/nf-kb/target/index.html |
| PRF1 | perforin 1 (pore forming protein) | http://people.bu.edu/gilmore/nf-kb/target/index.html |
| HBE1 | hemoglobin, epsilon 1 | http://people.bu.edu/gilmore/nf-kb/target/index.html |
| C4A | complement component 4A | http://people.bu.edu/gilmore/nf-kb/target/index.html |
| OLR1 | oxidised low density lipoprotein (lectin-like) receptor 1 | http://people.bu.edu/gilmore/nf-kb/target/index.html |
| AGT | angiotensinogen (serpin peptidase inhibitor, clade A, member 8) | http://people.bu.edu/gilmore/nf-kb/target/index.html |

Table S2.

Leading edge core set of NF- κ B target genes, which are differentially enriched in MALT lymphoma with t(11;18) vs. no translocation

| Rank | Gene | Description | Chromosome Band | Entrez ID | Signal to noise ratio | Enrichment Score |
|---|--------------|---|-----------------|-----------|-----------------------|------------------|
| Expression of genes enriched in translocation negative MALT lymphoma | | | | | | |
| 1 | PLAU | plasminogen activator, urokinase | 10q24 | 5328 | 0.759 | 0.018 |
| 2 | PTGS2 | prostaglandin-endoperoxide synthase 2 (prostaglandin G/H synthase) | 1q25.2-q25.3 | 5743 | 0.714 | 0.034 |
| 3 | NR4A3 | nuclear receptor subfamily 4, group A, member 3 | 9q22 | 8013 | 0.687 | 0.050 |
| 4 | IL8 | interleukin 8 | 4q13-q21 | 3576 | 0.670 | 0.065 |
| 5 | CXCL2 | chemokine (C-X-C motif) ligand 2 | 4q21 | 2920 | 0.658 | 0.080 |
| 6 | CXCL1 | chemokine (C-X-C motif) ligand 1 (melanoma growth stimulating a | 4q21 | 2919 | 0.597 | 0.092 |
| 7 | DEFB4 | defensin, beta 4 | 8p23.1-p22 | 1673 | 0.562 | 0.104 |
| 8 | CXCL5 | chemokine (C-X-C motif) ligand 5 | 4q12-q13 | 6374 | 0.527 | 0.113 |
| 9 | CD86 | CD86 molecule | 3q21 | 942 | 0.497 | 0.120 |
| 10 | BDKRB1 | bradykinin receptor B1 | 14q32.1-q32.2 | 623 | 0.475 | 0.127 |
| 11 | CCL2 | chemokine (C-C motif) ligand 2 | 17q11.2-q12 | 6347 | 0.469 | 0.137 |
| 12 | ICOS | inducible T-cell co-stimulator | 2q33 | 29851 | 0.455 | 0.145 |
| 13 | IL1RN | interleukin 1 receptor antagonist | 2q14.2 | 3557 | 0.451 | 0.155 |
| 14 | SDC4 | syndecan 4 | 20q12 | 6385 | 0.448 | 0.165 |
| 15 | IL1B | interleukin 1, beta | 2q14 | 3553 | 0.433 | 0.172 |
| 16 | MMP3 | matrix metalloproteinase 3 (stromelysin 1, progelatinase) | 11q22.3 | 4314 | 0.416 | 0.176 |
| 17 | NR4A2 | nuclear receptor subfamily 4, group A, member 2 | 2q22-q23 | 4929 | 0.401 | 0.180 |
| 18 | PTAFR | platelet-activating factor receptor | 1p35-p34.3 | 5724 | 0.393 | 0.185 |
| 19 | CYP7B1 | cytochrome P450, family 7, subfamily B, polypeptide 1 | 8q21.3 | 9420 | 0.393 | 0.194 |
| 20 | TLR2 | toll-like receptor 2 | 4q32 | 7097 | 0.384 | 0.198 |
| 21 | IGFBP2 | insulin-like growth factor binding protein 2, 36kDa | 2q33-q34 | 3485 | 0.379 | 0.206 |
| 22 | SOD2 | superoxide dismutase 2, mitochondrial | 6q25.3 | 6648 | 0.376 | 0.213 |
| 23 | TFF3 | trefoil factor 3 (intestinal) | 21q22.3 | 7033 | 0.376 | 0.222 |
| 24 | DIO2 | deiodinase, iodothyronine, type II | 14q24.2-q24.3 | 1734 | 0.366 | 0.226 |
| 25 | CCND1 | cyclin D1 | 11q13 | 595 | 0.364 | 0.233 |
| 26 | FCER2 | Fc fragment of IgE, low affinity II, receptor for (CD23) | 19p13.3 | 2208 | 0.362 | 0.240 |
| 27 | GADD45B | growth arrest and DNA-damage-inducible, beta | 19p13.3 | 4616 | 0.354 | 0.244 |
| 28 | TNC | tenascin C | 9q33 | 3371 | 0.351 | 0.251 |
| 29 | GZMB | granzyme B (granzyme 2, cytotoxic T-lymphocyte-associated serine | 14q11.2 | 3002 | 0.351 | 0.259 |
| 30 | PTGIS | prostaglandin I2 (prostacyclin) synthase | 20q13.13 | 5740 | 0.344 | 0.264 |
| 31 | PAX8 | paired box 8 | 2q12-q14 | 7849 | 0.324 | 0.258 |
| 32 | SERPINA1 | serpin peptidase inhibitor, clade A (alpha-1 antiproteinase, antitryps | 14q32.1 | 5265 | 0.322 | 0.264 |
| 33 | PTX3 | pentraxin-related gene, rapidly induced by IL-1 beta | 3q25 | 5806 | 0.321 | 0.271 |
| 34 | BMP2 | bone morphogenetic protein 2 | 20p12 | 650 | 0.306 | 0.268 |
| 35 | PENK | proenkephalin | 8q23-q24 | 5179 | 0.305 | 0.274 |
| 36 | CCL11 | chemokine (C-C motif) ligand 11 | 17q21.1-q21.2 | 6356 | 0.291 | 0.269 |
| 37 | KITLG | KIT ligand | 12q22 | 4254 | 0.29 | 0.274 |
| 38 | BGN | biglycan | Xq28 | 633 | 0.288 | 0.278 |
| 39 | ADH1A | alcohol dehydrogenase 1A (class I), alpha polypeptide | 4q21-q23 | 124 | 0.275 | 0.273 |
| 40 | IL11 | interleukin 11 | 19q13.3-q13.4 | 3589 | 0.272 | 0.276 |
| 41 | EGFR | epidermal growth factor receptor (erythroblastic leukemia viral (v-e | 7p12 | 1956 | 0.272 | 0.282 |
| 42 | TEAD1 | TEA domain family member 1 (SV40 transcriptional enhancer fact | 11p15.2 | 7003 | 0.272 | 0.288 |
| 43 | THBS2 | thrombospondin 2 | 6q27 | 7058 | 0.266 | 0.289 |
| 44 | FAS | Fas (TNF receptor superfamily, member 6) | 10q24.1 | 355 | 0.264 | 0.294 |
| 45 | APOC3 | apolipoprotein C-III | 11q23.1-q23.2 | 345 | 0.247 | 0.279 |
| 46 | CCL22 | chemokine (C-C motif) ligand 22 | 16q13 | 6367 | 0.245 | 0.284 |
| 47 | IL13 | interleukin 13 | 5q31 | 3596 | 0.239 | 0.282 |
| 48 | KCNK5 | potassium channel, subfamily K, member 5 | 6p21 | 8645 | 0.237 | 0.286 |
| 49 | ELF3 | E74-like factor 3 (ets domain transcription factor, epithelial-specific | 1q32.2 | 1999 | 0.23 | 0.282 |
| 50 | TNFRSF9 | tumor necrosis factor receptor superfamily, member 9 | 1p36 | 3604 | 0.229 | 0.286 |
| 51 | HPSE | heparanase | 4q21.3 | 10855 | 0.228 | 0.29 |
| 52 | IER3 | immediate early response 3 | 6p21.3 | 8870 | 0.224 | 0.292 |
| 53 | AKR1C2 | aldo-keto reductase family 1, member C2 (dihydrodiol dehydrogena | 10p15-p14 | 1646 | 0.224 | 0.298 |
| 54 | PLK3 | polo-like kinase 3 (Drosophila) | 1p34.1 | 1263 | 0.22 | 0.298 |
| 55 | BCL2L1 | BCL2-like 1 | 20q11.21 | 598 | 0.214 | 0.295 |
| 56 | FN1 | fibronectin 1 | 2q34 | 2335 | 0.212 | 0.298 |
| 57 | UPP1 | uridine phosphorylase 1 | 7p12.3 | 7378 | 0.21 | 0.299 |
| 58 | GBP1 | guanylate binding protein 1, interferon-inducible, 67kDa | 1p22.2 | 2633 | 0.208 | 0.302 |
| 59 | UBE2M | ubiquitin-conjugating enzyme E2M (UBC12 homolog, yeast) | 19q13.43 | 9040 | 0.205 | 0.302 |
| 60 | JUNB | jun B proto-oncogene | 19p13.2 | 3726 | 0.203 | 0.304 |
| 61 | PIM1 | pim-1 oncogene | 6p21.2 | 5292 | 0.203 | 0.309 |
| 62 | BNIP3 | BCL2/adenovirus E1B 19kDa interacting protein 3 | 10q26.3 | 664 | 0.201 | 0.312 |

Expression of genes enriched in translocation positive MALT lymphoma

| | | | | | | |
|-----|-----------|--|---------------|-------|---------|-----------|
| 94 | TNFSF13B | tumor necrosis factor (ligand) superfamily, member 13b | 13q32-q34 | 10673 | 0.066 | 0.208 |
| 95 | BCL3 | B-cell CLL/lymphoma 3 | 19q13.1-q13.2 | 602 | 0.064 | 0.205 |
| 96 | SUV39H1 | suppressor of variegation 3-9 homolog 1 (Drosophila) | Xp11.23 | 6839 | 0.062 | 0.204 |
| 97 | TP53 | tumor protein p53 | 17p13.1 | 7157 | 0.045 | 0.175 |
| 98 | UPK1B | uroplakin 1B | 3q13.3-q21 | 7348 | 0.040 | 0.169 |
| 99 | BACE2 | beta-site APP-cleaving enzyme 2 | 21q22.3 | 25825 | 0.030 | 0.150 |
| 100 | CYP2E1 | cytochrome P450, family 2, subfamily E, polypeptide 1 | 10q24.3-qter | 1571 | 0.027 | 0.147 |
| 101 | IL15RA | interleukin 15 receptor, alpha | 10p15-p14 | 3601 | 0.027 | 0.147 |
| 102 | KLF10 | Kruppel-like factor 10 | 8q22.2 | 7071 | 0.026 | 0.146 |
| 103 | ATCB1 | ATP-binding cassette, sub-family B (MDR/TAP), member 1 | 7q21.12 | 5243 | 0.021 | 0.139 |
| 104 | IL2RA | interleukin 2 receptor, alpha | 10p15-p14 | 3559 | 0.013 | 0.125 |
| 105 | CD83 | CD83 molecule | 6p23 | 9308 | 0.006 | 0.112 |
| 106 | MMP9 | matrix metalloproteinase 9 (gelatinase B, 92kDa gelatinase, 92kDa t | 20q11.2-q13.1 | 4318 | -0.011 | 0.082 |
| 107 | PGK1 | phosphoglycerate kinase 1 | Xq13 | 5230 | -0.013 | 0.079 |
| 108 | PIM2 | pim-2 oncogene | Xp11.23 | 11040 | -0.015 | 0.077 |
| 109 | CD80 | CD80 molecule | 3q13.3-q21 | 941 | -0.016 | 0.076 |
| 110 | BAX | BCL2-associated X protein | 19q13.3-q13.4 | 581 | -0.019 | 0.071 |
| 111 | C4BPA | complement component 4 binding protein, alpha | 1q32 | 722 | -0.020 | 0.069 |
| 112 | ENG | endoglin | 9q33-q34.1 | 2022 | -0.023 | 0.066 |
| 113 | AGER | advanced glycosylation end product-specific receptor | 6p21.3 | 177 | -0.027 | 0.0593 |
| 114 | OLR1 | oxidized low density lipoprotein (lectin-like) receptor 1 | 12p13.2-p12.3 | 4973 | -0.0325 | 0.0499 |
| 115 | HMOX1 | heme oxygenase (decycling) 1 | 22q12 | 3162 | -0.0349 | 0.0477 |
| 116 | ENO2 | enolase 2 (gamma, neuronal) | 12p13 | 2026 | -0.0369 | 0.0447 |
| 117 | IL15 | interleukin 15 | 4q31 | 3600 | -0.0438 | 0.0351 |
| 118 | SELP | selectin P (granule membrane protein 140kDa, antigen CD62) | 1q22-q25 | 6403 | -0.0479 | 0.0293 |
| 119 | CXCL13 | chemokine (C-X-C motif) ligand 13 | 4q21 | 10563 | -0.0497 | 0.0271 |
| 120 | TNFSF11 | tumor necrosis factor (ligand) superfamily, member 11 | 13q14 | 8600 | -0.0521 | 0.0243 |
| 121 | TNFAIP3 | tumor necrosis factor, alpha-induced protein 3 | 6q23 | 7128 | -0.0572 | 0.0185 |
| 122 | CFLAR | CASP8 and FADD-like apoptosis regulator | 2q33-q34 | 8837 | -0.0588 | 0.018 |
| 123 | APOE | apolipoprotein E | 19q13.2 | 348 | -0.0591 | 0.0187 |
| 124 | CCL5 | chemokine (C-C motif) ligand 5 | 17q11.2-q12 | 6352 | -0.0606 | 0.0175 |
| 125 | IL32 | interleukin 32 | 16p13.3 | 9235 | -0.0716 | 0.000704 |
| 126 | IL6 | interleukin 6 (interferon, beta 2) | 7p21 | 3569 | -0.0733 | -0.000587 |
| 127 | CXCL9 | chemokine (C-X-C motif) ligand 9 | 4q21 | 4283 | -0.0835 | -0.0169 |
| 128 | MADCAM1 | mucosal vascular addressin cell adhesion molecule 1 | 19p13.3 | 8174 | -0.0837 | -0.0151 |
| 129 | NFKB1 | nuclear factor of kappa light polypeptide gene enhancer in B-cells 1 | 4q24 | 4790 | -0.0842 | -0.0138 |
| 130 | CCND3 | cyclin D3 | 6p21 | 896 | -0.086 | -0.0144 |
| 131 | GCLC | glutamate-cysteine ligase, catalytic subunit | 6p12 | 2729 | -0.0932 | -0.0226 |
| 132 | BLR1 | CXCR5 (Chemotactic cytokine) 5 | 11q23.3 | 643 | -0.102 | -0.0357 |
| 133 | CTSB | cathepsin B | 8p22 | 1508 | -0.107 | -0.0403 |
| 134 | CD3G | CD3g molecule, gamma (CD3-TCR complex) | 11q23 | 917 | -0.114 | -0.0476 |
| 135 | MYC | v-myc myelocytomatosis viral oncogene homolog (avian) | 8q24.21 | 4609 | -0.117 | -0.0509 |
| 136 | CCR5 | chemokine (C-C motif) receptor 5 | 3p21.31 | 1234 | -0.122 | -0.0555 |
| 137 | RELB | v-rel reticuloendotheliosis viral oncogene homolog B | 19q13.32 | 5971 | -0.124 | -0.0565 |
| 138 | GCLM | glutamate-cysteine ligase, modifier subunit | 1p22.1 | 2730 | -0.132 | -0.0646 |
| 139 | STAT5A | signal transducer and activator of transcription 5A | 17q11.2 | 6776 | -0.141 | -0.0746 |
| 140 | CXCL12 | chemokine (C-X-C motif) ligand 12 (stromal cell-derived factor 1) | 10q11.1 | 6387 | -0.142 | -0.0718 |
| 141 | TNFRSF10B | tumor necrosis factor receptor superfamily, member 10b | 8p22-p21 | 8795 | -0.145 | -0.0732 |
| 142 | PTGDS | prostaglandin D2 synthase 21kDa (brain) | 9q34.2-q34.3 | 5730 | -0.15 | -0.0784 |
| 143 | KLK3 | kallikrein-related peptidase 3 | 19q13.41 | 354 | -0.167 | -0.0961 |
| 144 | TPMT | thiopurine S-methyltransferase | 6p22.3 | 7172 | -0.172 | -0.0992 |
| 145 | VCAM1 | vascular cell adhesion molecule 1 | 1p32-p31 | 7412 | -0.175 | -0.0986 |
| 146 | TNF | tumor necrosis factor (TNF superfamily, member 2) | 6p21.3 | 7124 | -0.182 | -0.105 |
| 147 | CCL14 | chemokine (C-C motif) ligand 14 | 17q12 | 6358 | -0.186 | -0.103 |
| 148 | CD74 | CD74 molecule, major histocompatibility complex, class II invariant | 5q32 | 972 | -0.188 | -0.101 |
| 149 | ADAM19 | ADAM metalloproteinase domain 19 (meltrin beta) | 5q32-q33 | 8728 | -0.19 | -0.0977 |
| 150 | CXCL10 | chemokine (C-X-C motif) ligand 10 | 4q21 | 3627 | -0.203 | -0.106 |
| 151 | UCP2 | uncoupling protein 2 (mitochondrial, proton carrier) | 11q13 | 7351 | -0.205 | -0.103 |
| 152 | CD44 | CD44 molecule (Indian blood group) | 11p13 | 960 | -0.209 | -0.101 |
| 153 | BCL2A1 | BCL2-related protein A1 | 15q24.3 | 597 | -0.22 | -0.108 |
| 154 | CD48 | CD48 molecule | 1q21.3-q22 | 962 | -0.239 | -0.124 |
| 155 | NR3C1 | nuclear receptor subfamily 3, group C, member 1 (glucocorticoid re | 5q31.3 | 2908 | -0.243 | -0.121 |
| 156 | BCL10 | B-cell CLL/lymphoma 10 | 1p22 | 8915 | -0.292 | -0.153 |
| 157 | IRF3 | interferon regulatory factor 3 | 19q13.3-q13.4 | 3661 | -0.294 | -0.147 |
| 158 | MAP4K1 | mitogen-activated protein kinase kinase kinase 1 | 19q13.1-q13.4 | 11184 | -0.302 | -0.145 |
| 159 | CD40 | CD40 molecule, TNF receptor superfamily member 5 | 20q12-q13.2 | 958 | -0.307 | -0.141 |

| | | | | | | |
|-----|---------|---|--------------|--------|--------|-----------|
| 160 | CCL21 | chemokine (C-C motif) ligand 21 | 9p13 | 6366 | -0.335 | -0.15 |
| 161 | CCL19 | chemokine (C-C motif) ligand 19 | 9p13 | 6363 | -0.336 | -0.143 |
| 162 | IFI44L | interferon-induced protein 44-like | 1p31.1 | 10964 | -0.354 | -0.144 |
| 163 | CXCR4 | chemokine (C-X-C motif) receptor 4 | 2q21 | 7852 | -0.362 | -0.14 |
| 164 | PRDM2 | PR domain containing 2, with ZNF domain | 1p36.21 | 7799 | -0.414 | -0.147 |
| 165 | REL | v-rel reticuloendotheliosis viral oncogene homolog (avian) | 2p13-p12 | 5966 | -0.422 | -0.139 |
| 166 | IRF2 | interferon regulatory factor 2 | 4q34.1-q35.1 | 3660 | -0.425 | -0.13 |
| 167 | MX1 | myxovirus (influenza virus) resistance 1, interferon-inducible protei | 21q22.3 | 4599 | -0.428 | -0.121 |
| 168 | LTB | lymphotoxin beta (TNF superfamily, member 3) | 6p21.3 | 4050 | -0.438 | -0.114 |
| 169 | IRF7 | interferon regulatory factor 7 | 11p15.5 | 3665 | -0.452 | -0.106 |
| 170 | TLR6 | toll-like receptor 6 | 4p14 | 10333 | -0.453 | -0.0952 |
| 171 | BCL2 | B-cell CLL/lymphoma 2 | 18q21.3 | 596 | -0.462 | -0.0858 |
| 172 | BCL2L10 | BCL2-like 10 (apoptosis facilitator) | 15q21 | 10017 | -0.463 | -0.0751 |
| 173 | CCR7 | chemokine (C-C motif) receptor 7 | 17q12-q21.2 | 1236 | -0.483 | -0.0667 |
| 174 | IRF4 | interferon regulatory factor 4 | 6p25-p23 | 3662 | -0.491 | -0.0557 |
| 175 | CCR2B | chemokine (C-C motif) receptor 2 isoform B | 3p21.31 | 729230 | -0.526 | -0.0479 |
| 176 | TFEC | transcription factor EC | 7q31.2 | 22797 | -0.67 | -0.0404 |
| 177 | CD69 | CD69 molecule | 12p13-p12 | 969 | -0.717 | -0.0252 |
| 178 | CCR2A | chemokine (C-C motif) receptor 2 isoform A | 3p21.31 | 729230 | -1.13 | -0.000728 |

SUPPLEMENTARY TABLE LEGENDS

Table S1. NF- κ B target genes. Genes were collated from an online data base (<http://www.NF-kB.org>) published works (<http://bioinfo.lifl.fr/NF-KB>, <http://people.bu.edu/gilmore/nf-kb/target/index.html>), and careful bioinformatic search. Noncanonical NF- κ B target genes (highlighted in yellow) were identified according to previous investigations (11, 14-21).

Table S2. Leading edge core set of NF- κ B target genes that are differentially enriched in MALT lymphomas with t(11;18) vs. no translocation. Noncanonical NF- κ B target genes (11, 14-21) are highlighted in yellow.

SUPPLEMENTARY REFERENCES

1. P. C. Lucas *et al.*, *Oncogene* **26**, 5643 (2007).
2. P. C. Lucas *et al.*, *J Biol Chem* **276**, 19012 (2001).
3. P. G. Isaacson, M. Q. Du, *Nat Rev Cancer* **4**, 644 (2004).
4. L. M. McAllister-Lucas *et al.*, *J Biol Chem* **276**, 30589 (2001).
5. H. Noels *et al.*, *J Biol Chem* **282**, 10180 (2007).
6. F. Q. An *et al.*, *J Biol Chem* **280**, 3862 (2005).
7. D. Sanchez-Izquierdo *et al.*, *Blood* **101**, 4539 (2003).
8. P. Sideras *et al.*, *Int Immunol* **1**, 631 (1989).
9. H. Ye *et al.*, *J Pathol* **205**, 293 (2005).
10. D. Beckett, E. Kovaleva, P. J. Schatz, *Protein Sci* **8**, 921 (1999).
11. T. Enzler *et al.*, *Immunity* **25**, 403 (2006).
12. T. T. Lu, J. G. Cyster, *Science* **297**, 409 (2002).
13. R. A. Hamoudi *et al.*, *Leukemia* **24**, 1487.
14. G. Bonizzi *et al.*, *Embo J* **23**, 4202 (2004).
15. J. L. Chen, A. Limnander, P. B. Rothman, *Blood* **111**, 1677 (2008).
16. D. L. Drayton *et al.*, *J Immunol* **173**, 6161 (2004).
17. F. Guo, D. Weih, E. Meier, F. Weih, *Blood* **110**, 2381 (2007).
18. M. Luftig *et al.*, *Proc Natl Acad Sci U S A* **101**, 141 (2004).
19. U. Senftleben *et al.*, *Science* **293**, 1495 (2001).
20. R. T. Woodland *et al.*, *Blood* **111**, 750 (2008).
21. J. Zhang, M. A. Warren, S. F. Shoemaker, M. M. Ip, *Endocrinology* **148**, 268 (2007).
22. X. Sagaert *et al.*, *Mod Pathol* **23**, 458.
23. S. Lopez-Giral *et al.*, *J Leukoc Biol* **76**, 462 (2004).
24. Y. Nie *et al.*, *J Exp Med* **200**, 1145 (2004).
25. U. Ferch *et al.*, *Nat Immunol* **8**, 984 (2007).
26. G. Xiao, S. C. Sun, *J Biol Chem* **275**, 21081 (2000).
27. G. Liao, M. Zhang, E. W. Harhaj, S.-C. Sun, *J Biol Chem* **279**, 26243 (2004).

ORIGINAL ARTICLE

Differential expression of NF- κ B target genes in MALT lymphoma with and without chromosome translocation: insights into molecular mechanism

RA Hamoudi¹, A Appert¹, H Ye¹, A Ruskone-Fourmesttraux^{2,3}, B Streubel⁴, A Chott⁴, M Raderer⁵, L Gong¹, I Wlodarska⁶, C De Wolf-Peeters⁷, KA MacLennan⁸, L de Leval⁹, PG Isaacson¹⁰ and M-Q Du¹

¹Department of Pathology, University of Cambridge, Cambridge, UK; ²Service de Gastro-entérologie, Hôpital St Antoine, APHP, Paris, France; ³GELD (Groupe d'Etude des Lymphomes Digestifs), Paris, France; ⁴Department of Pathology, Medical University of Vienna, Vienna, Austria; ⁵Department of Medicine I, University Hospital Vienna, Vienna, Austria; ⁶Center for Human Genetics, Katholieke Universiteit Leuven, Leuven, Belgium; ⁷Department of Morphology and Molecular Pathology, University of Leuven, Leuven, Belgium; ⁸Molecular Medicine Unit, St James's University Hospital, University of Leeds, Leeds, UK; ⁹Department of Pathology, CHU Sart Tilman, Liège, Belgium and ¹⁰Department of Histopathology, University College London, London, UK

Mucosa-associated lymphoid tissue (MALT) lymphoma is characterized by t(11;18)(q21;q21)/API2-MALT1, t(1;14)(p22;q32)/BCL10-IGH and t(14;18)(q32;q21)/IGH-MALT1, which commonly activate the nuclear factor (NF)- κ B pathway. Gastric MALT lymphomas harboring such translocations usually do not respond to *Helicobacter pylori* eradication, while most of those without translocation can be cured by antibiotics. To understand the molecular mechanism of these different MALT lymphoma subgroups, we performed gene expression profiling analysis of 21 MALT lymphomas (13 translocation-positive, 8 translocation-negative). Gene set enrichment analysis (GSEA) of the NF- κ B target genes and 4394 additional gene sets covering various cellular pathways, biological processes and molecular functions have shown that translocation-positive MALT lymphomas are characterized by an enhanced expression of NF- κ B target genes, particularly toll like receptor (TLR)6, chemokine, CC motif, receptor (CCR)2, cluster of differentiation (CD)69 and B-cell CLL/lymphoma (BCL)2, while translocation-negative cases were featured by active inflammatory and immune responses, such as interleukin-8, CD86, CD28 and inducible T-cell costimulator (ICOS). Separate analyses of the genes differentially expressed between translocation-positive and -negative cases and measurement of gene ontology term in these differentially expressed genes by hypergeometric test reinforced the above findings by GSEA. Finally, expression of TLR6, in the presence of TLR2, enhanced both API2-MALT1 and BCL10-mediated NF- κ B activation *in vitro*. Our findings provide novel insights into the molecular mechanism of MALT lymphomas with and without translocation, potentially explaining their different clinical behaviors.

Leukemia (2010) 24, 1487–1497; doi:10.1038/leu.2010.118;
published online 3 June 2010

Keywords: MALT lymphoma; gene expression profiling; NF- κ B activation; chromosome translocation

Introduction

Extranodal marginal zone B-cell lymphoma of mucosa-associated lymphoid tissue (MALT) originates from the MALT acquired as a result of chronic inflammatory or autoimmune disorders.¹ The etiological factors underlying these chronic inflammatory disorders have a pivotal role in MALT lymphomagenesis. This is best exemplified by the causative role of

Helicobacter pylori infection in gastric MALT lymphoma as shown by the compelling evidence from the epidemiological, laboratory and particularly clinical studies, which show long-term complete remission of the lymphoma following *H. pylori* eradication in ~70% of cases.¹ In spite of this, the molecular mechanisms underlying the lymphoma development are not fully understood. Stimulations of antigen receptor by autoantigen, and co-stimulatory molecule CD40 by *H. pylori*-specific T cells are believed to have an important role. Recent studies on MALT lymphoma-associated chromosome translocations provide further insights into its molecular pathogenesis.

t(11;18)(q21;q21)/API2-MALT1, t(1;14)(p22;q32)/BCL10-IGH and t(14;18)(q32;q21)/IGH-MALT1 are specifically associated with MALT lymphoma albeit occurring at considerably variable frequencies in different anatomic sites.^{2–5} Although these translocations involve different oncogenes, molecularly their encoded products commonly activate the canonical nuclear factor (NF)- κ B pathway,^{6–8} accounting for their critical role in lymphomagenesis. Nonetheless, overexpression of these oncogenes alone is insufficient for malignant transformation as both *E μ -API2-MALT1* and *E μ -BCL10* transgenic mice developed splenic marginal zone hyperplasia, but not lymphoma.^{9,10} Thus, other molecular events are required to cooperate with these chromosome translocations in MALT lymphoma development.

The above chromosomal translocations are always mutually exclusive and t(11;18), the most frequent translocation in MALT lymphoma, occurs often as the sole cytogenetic abnormality.¹¹ Several studies suggest that there is a potential cooperation between MALT lymphoma-associated oncogenic products and immunological stimuli in lymphomagenesis. In the *E μ -API2-MALT1* transgenic mice, immunization with the Freund's complete adjuvant led to development of a splenic marginal zone lymphoma-like hyperplasia.¹² *In vitro* assay showed that CD40 stimulation enhanced both API2-MALT1 and MALT1-induced NF- κ B activation.¹³ However, the extent of potential cooperation between MALT lymphoma-associated oncogenic products and immune surface receptor signaling is unknown.

In spite of the presence of a potential overlap in the molecular mechanism of MALT lymphoma with and without translocation as discussed above, there are important differences in the clinical and histological presentations between these different subgroups. Clinically, gastric MALT lymphomas with t(11;18) or t(1;14) are significantly associated with advanced stages and resistance to *H. pylori* eradication.^{14,15} Histologically, t(11;18)-positive MALT lymphomas seem to be more monotonous, lacking apparent transformed blasts.¹⁶ These distinct

Correspondence: Professor M-Q Du, Division of Molecular Histopathology, Department of Pathology, University of Cambridge, Level 3 Lab Block, Box 231, Addenbrooke's Hospital, Hills Road, Cambridge, CB2 2QQ, UK.

E-mail: mqd20@cam.ac.uk

Received 4 November 2009; revised 2 March 2010; accepted 1 April 2010; published online 3 June 2010

clinico-pathological characteristics may indicate important differences in molecular mechanisms between MALT lymphomas with and without translocation. To analyze this and understand further the molecular mechanism of MALT lymphoma, we studied the transcriptional profiles of a well-characterized series of cases with different translocation status and further validated the genes identified and the hypothesis generated.

Materials and methods

Patient materials

Fresh frozen tissues from 24 well-characterized MALT lymphomas (Supplementary Table S1), 7 follicular lymphoma (FL) and 7 mantle cell lymphoma (MCL) were used for gene expression microarray analysis. The MALT lymphomas were nine positive for t(11;18)/API2-MALT1 (eight gastric and one pulmonary), four positive for t(1;14)/BCL10-IGH or t(1;2)/BCL10-IG κ (three gastric and one pulmonary), two positive for t(14;18)/IGH-MALT1 (one hepatic and one ocular adnexal) and nine gastric cases negative for all known MALT lymphoma-associated translocations. The percentage of tumor cells was estimated on hematoxylin and eosin stained slides and crude microdissection was performed to ensure that at least 70% tumor cells was used for expression microarray analysis.

In addition, 73 cases of MALT lymphoma, including 18 positive for t(11;18), 8 positive for t(1;14), 9 positive for t(14;18) and 38 negative for these translocations, were used for validation of the expression microarray findings. The use of archival tissues for research was approved by the local research ethics committees of the authors' institutions.

Gene expression microarray

RNA extraction, synthesis of labeled complementary RNA by *in vitro* transcription and hybridization to Affymetrix (Affymetrix UK Ltd., High Wycombe, UK) GeneChip HG-U133A (MALT lymphoma) or Affymetrix H133 plus 2 (FL and MCL), quality control analysis, microarray data normalization and nonspecific filtering are detailed in Supplementary Methods. All microarray data have been deposited with Gene Expression Omnibus (<http://www.ncbi.nlm.nih.gov/geo/>, GSE18736).

Unsupervised clustering

This was performed using Pearson's correlation coefficient and average linkage as the similarity measure and clustering algorithm respectively within Genespring GX 7.3.1. Separate clustering was performed among all MALT lymphoma, FL and MCL cases and also within the MALT lymphoma group.

Gene set enrichment analysis (GSEA)

GSEA was used to identify gene sets differentially regulated between MALT lymphoma with (13 cases) and without (8 cases) chromosome translocation.¹⁷ As the original GSEA only identifies the gene set showing either uniformly up- or down-regulation, for the gene sets showing both up- and down-regulated genes, absolute GSEA was additionally performed.¹⁸ A total of 4395 gene sets were analyzed (Supplementary Table S2) and they included (1) NF- κ B target genes, collated from online database, published works and careful bioinformatic search (Supplementary Table S3); (2) biological pathways involved in inflammatory and immune responses from human immunome database,¹⁹ gene ontology (GO) and ingenuity and (3) gene sets from Molecular Signature database. The GSEA results were

ranked according to the nominal *P*-value (<0.05) and false discovery rate (≤ 0.25) as described previously.¹⁷

For the gene sets differentially regulated between MALT lymphoma with and without translocation, leading edge analysis was performed to identify the biologically important gene subset.¹⁷ When generating gene sets, for each sample, only the maximum expression value of the multi-probes for a given gene was used for GSEA as described previously.¹⁷

Analysis of differential gene expression in MALT lymphomas with and without translocation

For identification of differentially expressed genes between MALT lymphoma with and without translocation, the MAS5 normalized and filtered data set was used as suggested previously.²⁰ The genes differentially expressed (one-way analysis of variance test, $P < 0.05$) between translocation-positive and -negative MALT lymphomas were identified, and those showing >2.5 -fold differences were selected for functional annotation using GO.

Functional annotation using GO

To assess the biological implication of differential gene expression in MALT lymphomas with and without translocation, we measured the representation of GO terms (association of gene products with their related biological processes and molecular functions) in the above differentially expressed genes using Genespring and hypergeometric tests provided in the R package (GStats, version 2.8.0, <http://www.bioconductor.org>). This allowed us to examine whether any GO term was over- or under-represented as compared with what can occur by chance. Independent analyses of GO categories were performed for overexpressed genes in both translocation-positive and -negative MALT lymphoma.

Quantitative reverse-transcription PCR (qRT-PCR), immunohistochemistry and western blot analysis

Please see description in the Supplementary Methods (Supplementary Table S4–S5).

NF- κ B reporter assay

The potential cooperation between BCL10 (or API2-MALT1) and TLR6 expression in NF- κ B activation was analyzed *in vitro* using a Luciferase Reporter Assay and the experimental details are given in the Supplementary Methods.

Results

Transcriptional profiling defines MALT lymphoma as a distinct entity

The microarray data from 21 MALT lymphomas (13 translocation-positive and 8 translocation-negative), 5 FL and 7 MCL passed the microarray hybridization quality control and were further analyzed and presented below (Supplementary Table S6). The standard normalization and filtering across all these cases yielded a set of 2629 probes. As expected, *CD10* and *BCL6* were found most highly expressed in FL, *CCND1* most highly expressed in MCL, and *MALT1* most highly expressed in MALT lymphoma with t(14;18) or t(11;18) (Supplementary Figure S1). Unsupervised hierarchical clustering showed that MALT lymphomas were clustered as a single branch, irrespective of their origin from different anatomic sites. Within the MALT

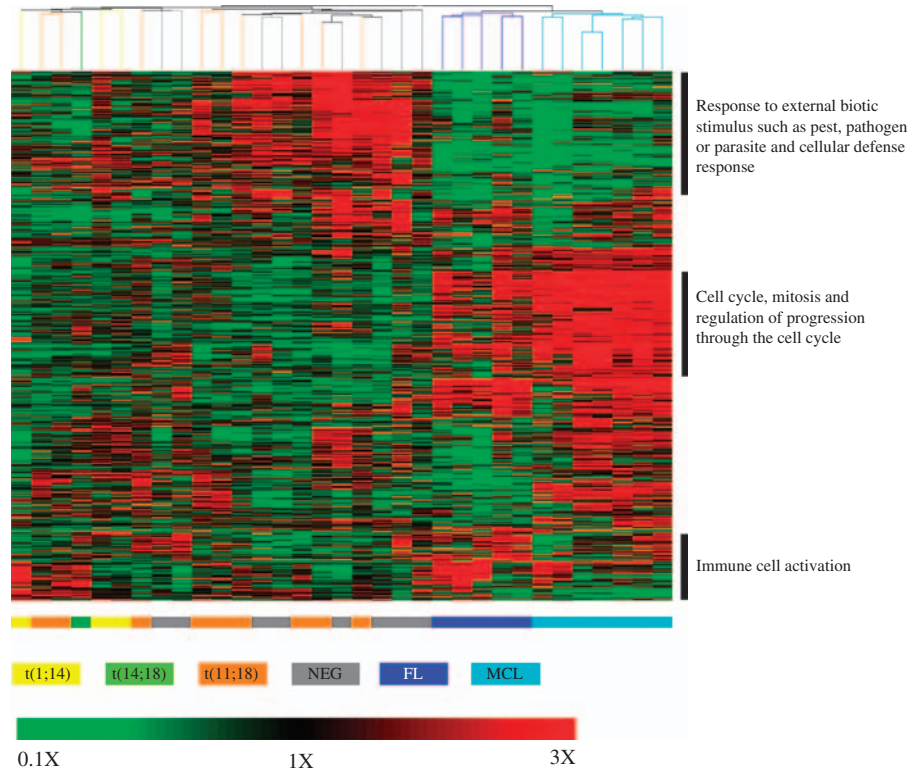


Figure 1 MALT lymphoma shows distinct gene expression profiles from FL and MCL. After standard normalization and filtering, a set of 2629 probes were obtained and used for unsupervised hierarchical clustering analysis. All MALT lymphomas are clustered as single branch, clearly separated from both FL and MCL. Nonetheless, within MALT lymphoma group, cases with and without chromosome translocation are intermingled together. The gene tree was ordered according to biological processes defined by GO, and the gene clusters enriched for a particular biological process in a lymphoma subtype as shown by hypergeometric testing are indicated. The gene sets for cell cycle (GO:7049) and regulation of progression through cell cycle (GO:74) are highly enriched in MCL, whereas those for immune cell activation (GO:45321, GO:46649) are enriched in FL. The gene sets for immune response to biotic stimulus (GO:9607), external biotic stimulus such as pest, pathogen or parasite (GO:9613) and cellular defense response (GO:6952) are highly enriched in MALT lymphoma. The chromosome translocation status of MALT lymphoma, FL and MCL are indicated by different color scheme. On the heatmap, red represents upregulated genes and green downregulated genes, with the scale showed at the bottom of the figure. FL, follicular lymphoma; MCL, mantle cell lymphoma; NEG, translocation-negative MALT lymphoma.

lymphoma group, translocation-positive cases were intermingled with translocation-negative cases (Figure 1), indicating that the translocation status did not have major effect on the hierarchical clustering. We also repeated the unsupervised hierarchical clustering analysis exclusively on MALT lymphoma cases using a set of 6893 variant probes derived from U133A and very similar results were found (Supplementary Figure S2).

Differential expression of NF-κB target genes in MALT lymphoma with and without chromosome translocation

As expected, the absolute GSEA revealed that a subset of the NF-κB target genes was over-represented in the translocation-positive MALT lymphomas, whereas another subset was enriched in translocation-negative cases ($P=0.011$, false discovery rate=0.005, Figure 2a, Supplementary Table S7). Leading edge analysis showed that 19 core genes accounted for the significant enrichment in translocation-positive cases and the top 10 genes included *CCR2A*, *BCL2*, *CD69*, *TLR6*, *TFEC*, *IRF4*, *PRDM2*, *REL*, *CCR7* and *CCR5*. Whereas, 34 core genes underscored the significant enrichment in translocation-negative cases and the top 10 genes were *PTGS2*, *PLAU*, *NR4A3*, *PTGIS*, *IL8*, *CD86*, *CCL2*, *CCL11*, *CXCL5* and *CXCL1*.

NF-κB target genes potentially underpins the differential representation of significant gene sets between MALT lymphomas with and without chromosome translocation

To gain further insights into the potential difference in molecular mechanisms between translocation-positive and -negative MALT lymphomas, we performed GSEA, in which indicated absolute GSEA, on 4394 gene sets covering various cellular pathways, biological processes and molecular functions. A total of 33 gene sets (not including those with very general term or those containing <20 genes) were differentially over-represented between MALT lymphomas with and without translocation ($P<0.05$, false discovery rate<0.20, Table 1).¹⁷ As there was a considerable overlap among the gene sets associated with the related cellular pathways or biological processes, they were grouped according to their involvement in the NF-κB activation pathway, inflammation/immune responses, chemokine and cell migration, G protein-coupled receptor (GPR) signaling and cell proliferation/apoptosis (Table 1). Leading edge analysis was performed to identify the core subset genes that underscored the significant enrichment and were thus most likely biologically important. Interestingly, the NF-κB target genes were frequently presented in each of these core subset genes, often on top of the list (Supplementary

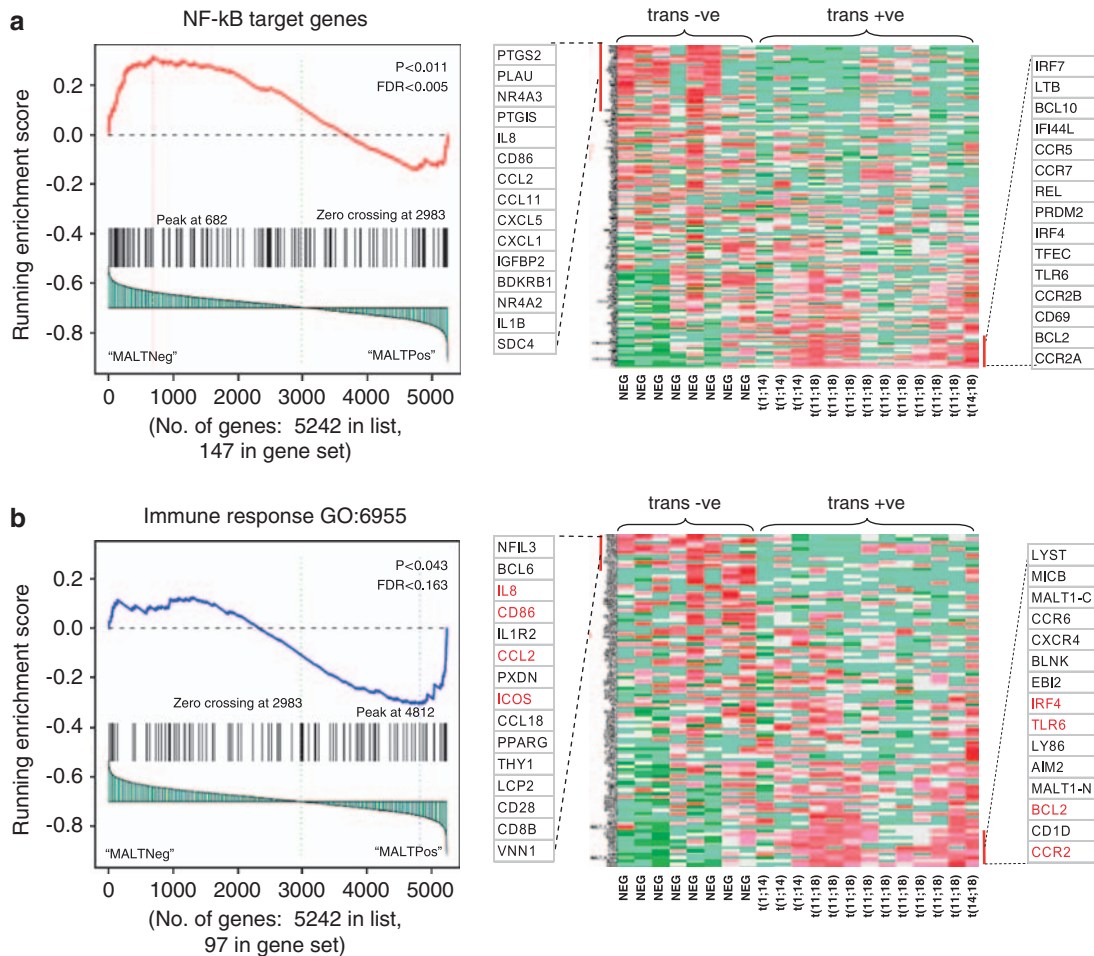


Figure 2 GSEA of NF- κ B target genes (a) and immune response genes (GO:6955) (b) in MALT lymphomas with and without chromosome translocation. Left panel shows the distribution of NF- κ B target genes or immune response genes according to their rank position. Right panel shows heatmap illustration of their expression between MALT lymphoma with and without chromosome translocation. The top 15 leading edge core genes are shown. Trans -ve: translocation-negative MALT lymphoma; trans +ve: translocation-positive MALT lymphoma.

Tables S8–S16, Supplementary Figure S3). Figure 2b shows the results of GSEA of immune response genes (GO:6955) with the top 15 leading edge genes indicated in the heatmap illustration. Several NF- κ B targets such as *CCR2*, *BCL2*, *TLR6* and *IRF4* were enriched in translocation-positive MALT lymphoma, whereas *IL8*, *CD86*, *CCL2* and *ICOS* were over-represented in translocation-negative cases (Supplementary Table S12).

Differential gene expression between MALT lymphomas with and without chromosome translocation

Using one-way analysis of variance test ($P < 0.05$) and a 2.5-folds change as the threshold, we identified 26 and 62 genes significantly overexpressed in translocation-positive and translocation-negative MALT lymphoma respectively (Supplementary Table S17). To assess the biological implication of this differential gene expression in MALT lymphoma with and without chromosome translocation, we measured the representation of GO terms in the above gene sets using hypergeometric tests. Among the genes overexpressed in translocation-positive MALT lymphoma, the GO terms associated with NF- κ B pathway activation, chemokine/GPR signaling, and antigen presentation were significantly over-represented (Supplementary

Table S18). Although among the genes overexpressed in translocation-negative MALT lymphoma, the GO terms related to immune/defense response were significantly over-represented (Supplementary Table S18). These findings from analysis of differentially expressed genes between MALT lymphomas with and without translocation reinforce the above observations by GSEA.

Validation of gene expression by qRT-PCR and immunohistochemistry

To confirm the differential expression of the key candidate genes between MALT lymphoma with and without translocation identified by the above microarray analyses, we analyzed the expression of *MALT1*, *BCL10*, *TLR6*, *CD69*, *CCR2A*, *CCR5*, *CD86* and *NR4A3* by qRT-PCR of the microdissected tumor cells from formalin-fixed paraffin-embedded tissue and wherein possible by immunohistochemistry in a total of 58 cases including 16 used in gene expression profiling. As expected, *MALT1* was most highly expressed in cases with *t(14;18)/IGH-MALT1* and *BCL10* was highest expressed in those with *t(1;14)* (Supplementary Figure S4). In keeping with the expression microarray data, *TLR6*, *CD69* and *CCR2A* were highly expressed in *t(1;14)* or *t(11;18)*-positive MALT lymphomas and

Table 1 Gene sets differentially over-represented between MALT lymphoma with and without chromosome translocation

| Gene sets | Source | SIZE | ES | NES | NOM P-val | FDR q-val | Tag % | Gene % | Leading edge core set genes |
|---|-----------------------------------|------|------|------|-----------|-----------|-------|--------|-----------------------------|
| <i>NF-κB related</i> | | | | | | | | | |
| NF-κB target genes | Supplementary Table S3for details | 147 | 0.44 | 1.64 | 0.0109 | 0.0050 | 0.361 | 0.250 | Supplementary Table S7 |
| Positive regulation of IKK NF-κB cascade | GO:43123 | 43 | 0.49 | 1.80 | 0.0041 | 0.0754 | 0.395 | 0.209 | Supplementary Table S8 |
| Regulation of IKK NF-κB cascade | GO:43122 | 40 | 0.50 | 1.68 | 0.0148 | 0.1235 | 0.400 | 0.206 | |
| <i>Inflammation and immune response</i> | | | | | | | | | |
| Response to chemical stimulus | GO:42221 | 118 | 0.42 | 1.64 | 0.0000 | 0.1388 | 0.475 | 0.356 | Supplementary Table S9 |
| Defense response | GO:6952 | 110 | 0.43 | 1.62 | 0.0079 | 0.1449 | 0.382 | 0.223 | Supplementary Table S10 |
| B-cell activation | GO:42113 | 21 | 0.58 | 1.57 | 0.0183 | 0.1661 | 0.381 | 0.080 | |
| Innate immune response | GO:45087 | 42 | 0.45 | 1.55 | 0.0371 | 0.1503 | 0.548 | 0.359 | Supplementary Table S11 |
| Immune response | GO:6955 | 97 | 0.44 | 1.50 | 0.0431 | 0.1633 | 0.433 | 0.299 | Supplementary Table S12 |
| <i>Chemokine and cell migration</i> | | | | | | | | | |
| Cation homeostasis | GO:55080 | 47 | 0.47 | 1.66 | 0.0022 | 0.1280 | 0.362 | 0.193 | Supplementary Table S13 |
| Cellular cation homeostasis | GO:30003 | 46 | 0.46 | 1.63 | 0.0044 | 0.1376 | 0.348 | 0.193 | |
| Locomotory behavior | GO:7626 | 46 | 0.52 | 1.64 | 0.0166 | 0.1432 | 0.370 | 0.125 | Supplementary Table S14 |
| <i>GPR signaling and MAPK pathway</i> | | | | | | | | | |
| Peptide GPCRs | MSD-C2 (Supplementary Table S2) | 20 | 0.71 | 2.07 | 0.0000 | 0.0096 | 0.550 | 0.153 | Supplementary Table S15 |
| GPCRdb class A rhodopsin like | MSD-C2 (Supplementary Table S2) | 38 | 0.57 | 2.08 | 0.0000 | 0.0100 | 0.421 | 0.163 | |
| Cyclic nucleotide mediated signaling | GO:19935 | 26 | 0.55 | 1.83 | 0.0000 | 0.0379 | 0.308 | 0.134 | |
| G protein signaling coupled to cyclic nucleotide second messenger | GO:7187 | 26 | 0.55 | 1.83 | 0.0000 | 0.0379 | 0.308 | 0.134 | |
| Regulation of kinase activity | GO:43549 | 72 | 0.43 | 1.85 | 0.0000 | 0.0744 | 0.333 | 0.186 | |
| Regulation of protein kinase activity | GO:45859 | 71 | 0.43 | 1.86 | 0.0000 | 0.0838 | 0.338 | 0.186 | |
| Negative regulation of catalytic activity | GO:43086 | 29 | 0.49 | 1.86 | 0.0000 | 0.1257 | 0.483 | 0.275 | |
| Positive regulation of catalytic activity | GO:43085 | 66 | 0.40 | 1.74 | 0.0021 | 0.0876 | 0.273 | 0.178 | |
| Regulation of MAPK activity | GO:43405 | 34 | 0.48 | 1.84 | 0.0024 | 0.0623 | 0.500 | 0.303 | Supplementary Table S16 |
| G protein coupled receptor protein signaling pathway | GO:7186 | 96 | 0.42 | 1.63 | 0.0041 | 0.1337 | 0.302 | 0.185 | |
| G protein signaling coupled to camp nucleotide second messenger | GO:7188 | 19 | 0.55 | 1.70 | 0.0043 | 0.1108 | 0.316 | 0.134 | |
| Positive regulation of signal transduction | GO:9967 | 51 | 0.43 | 1.63 | 0.0143 | 0.1399 | 0.471 | 0.348 | |
| <i>Proliferation and apoptosis</i> | | | | | | | | | |
| Growth | GO:40007 | 24 | 0.52 | 1.74 | 0.0022 | 0.0930 | 0.458 | 0.255 | |
| Regulation of growth | GO:40008 | 22 | 0.51 | 1.64 | 0.0044 | 0.1409 | 0.455 | 0.255 | |
| Regulation of cell growth | GO:0001558 | 21 | 0.50 | 1.62 | 0.0065 | 0.1415 | 0.429 | 0.255 | |
| Anti-apoptosis | GO:6916 | 70 | 0.38 | 1.50 | 0.0397 | 0.1514 | 0.300 | 0.218 | |
| <i>Others</i> | | | | | | | | | |
| B-cell lymphoma | GeneGo | 71 | 0.43 | 1.53 | 0.0489 | 0.1516 | 0.507 | 0.340 | |
| Regulation of transferase activity | GO:51338 | 74 | 0.42 | 1.84 | 0.0000 | 0.0519 | 0.432 | 0.303 | |
| Regulation of translation | GO:6417 | 26 | 0.52 | 1.77 | 0.0000 | 0.0699 | 0.615 | 0.364 | |
| Lian myeloid diff receptors | MSD-C2 (Supplementary Table S2) | 17 | 0.71 | 1.87 | 0.0000 | 0.1504 | 0.647 | 0.156 | |
| Zhan MM CD138 CD2 BS rest | MSD-C2 (Supplementary Table S2) | 24 | 0.57 | 1.83 | 0.0000 | 0.1947 | 0.625 | 0.267 | |
| Behavior | GO:7610 | 57 | 0.51 | 1.69 | 0.0043 | 0.1138 | 0.333 | 0.125 | |
| Ion homeostasis | GO:50801 | 50 | 0.45 | 1.59 | 0.0174 | 0.1728 | 0.340 | 0.193 | |

Abbreviations: ES, enrichment score; FDR, false discovery rate; Gene %, the percentage of genes in the gene list before (for positive ES) or after (for negative ES) the peak in the running enrichment score; GO, gene ontology; GPCRs, G protein-coupled receptors; GPR, G protein-coupled receptor; MAPK, mitogen-activated protein kinase; MSD, molecular signature database (<http://www.broadinstitute.org/gsea/msigdb/index.jsp>); NES, normalised ES; NF, nuclear factor; NOM, nominal; Tag %, the percentage of gene tags before (for positive ES) or after (for negative ES) the peak in the running enrichment score.

CCR5 was highly expressed in t(1;14)-positive cases in comparison with translocation-negative cases (Supplementary Figure S4). Conversely, *CD86* and *NR4A3* were significantly highly expressed in translocation-negative MALT lymphomas (Supplementary Figure S4).

In keeping with the above qRT-PCR data, immunohistochemistry showed that most translocation-positive MALT

lymphomas showed strong to moderate homogeneous BCL2 and CD69 staining in >70% tumor cells, often in most tumor cells, whereas majority of translocation-negative cases showed heterogeneous staining in 30–70% cells or a negative result (Figure 3). Similarly, western blot analyses showed that TLR6 was highly expressed in translocation-positive MALT lymphoma in comparison with the translocation-negative

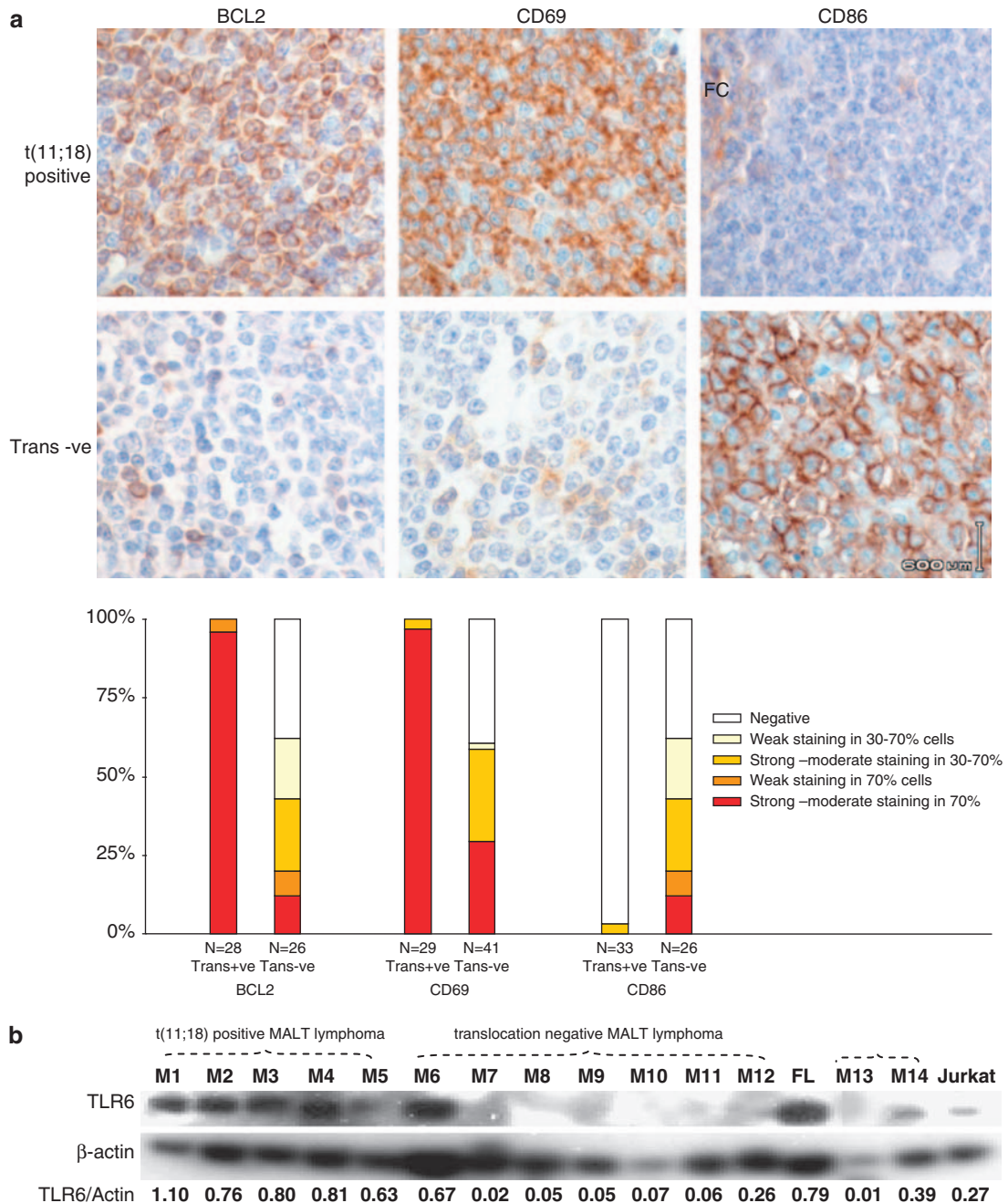


Figure 3 BCL2, CD69, CD86 and TLR6 protein expression in MALT lymphomas with and without chromosomal translocation. **(a)** Top panel: examples of BCL2, CD69 and CD86 immunohistochemistry in MALT lymphomas with and without chromosome translocation. Original magnification $\times 400$ for all panels. Lower panel summaries BCL2, CD69 and CD86 immunohistochemical results in MALT lymphoma with and without chromosome translocation. BCL2 and CD69 are more strongly and homogeneously expressed in translocation-positive than translocation-negative MALT lymphoma ($P=6.9 \times 10^{-5}$, $P=2.2 \times 10^{-4}$ respectively by Fisher's exact test), whereas CD86 is more strongly expressed in translocation-negative than translocation-positive MALT lymphoma ($P=6.4 \times 10^{-7}$ by Fisher's exact test). FC, follicle center; Trans +ve, translocation-positive; Trans -ve, translocation-negative. **(b)** Western blot analysis shows that TLR6 is highly expressed in translocation-positive MALT lymphoma, but at low levels in translocation-negative cases. M, MALT lymphoma; FL, follicular lymphoma.

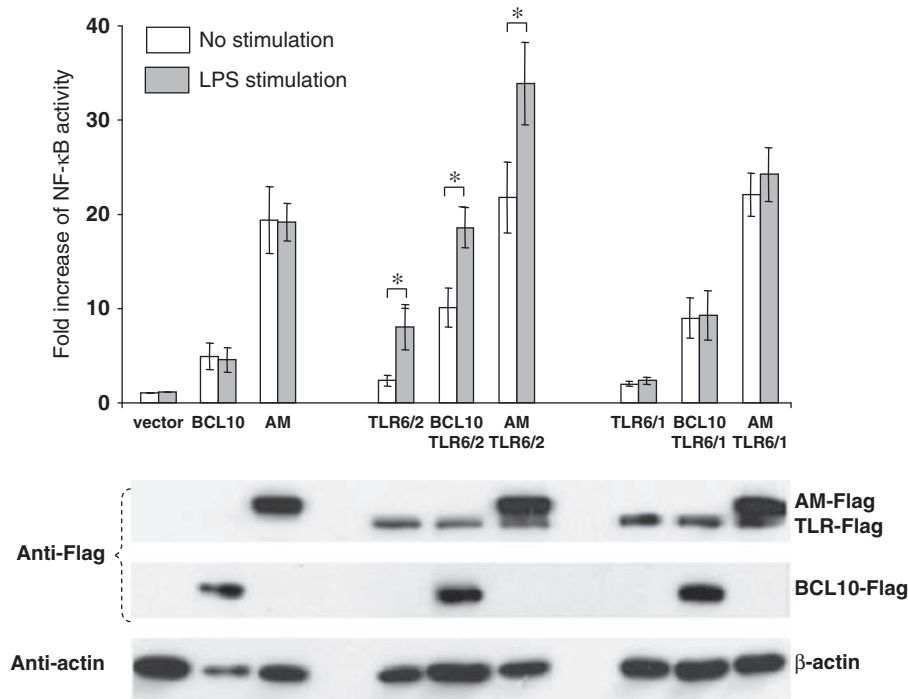


Figure 4 TLR6 enhances BCL10 and API2-MALT1-mediated NF- κ B activation, in presence of TLR2 but not TLR1, in Jurkat T cells. Jurkat T cells were co-transfected with vector (pRESpuro2) or plasmids containing *BCL10*, *API2-MALT1* (AM), *TLR6*, *TLR2* and *TLR1* as indicated, together with NF- κ B luciferase reporter gene. The transfected cells were seeded in multiple cell plates, cultured for 20 h and then treated with LPS or vehicle alone for 6 h. NF- κ B activities were measured in quadruplet experiments and recorded as fold increase in the vector control. Western blot in the lower panel shows appropriate expression of various expression constructs. * $P < 0.01$ by Student's *t*-test.

cases (Figure 3). In contrast, most translocation-positive MALT lymphomas showed no CD86 staining, whereas the majority of translocation-negative cases showed heterogeneous CD86 staining albeit variable in both positivity and intensity (Figure 3).

TLR6 expression enhances NF- κ B activation by BCL10 and API2-MALT1 in vitro

Among the genes highly expressed in translocation-positive MALT lymphoma, *TLR6*, *CCR2A*, *CD69* and *BCL2* were particularly interesting and we selected *TLR6* for further functional investigation because overexpression of this pattern recognition receptor may sensitize the response of tumor cells, particularly those with translocation, to stimulation by microbial antigens. To attest this, we performed a series of NF- κ B reporter assays in Jurkat T cells, which are known not responding to lipopolysaccharides (LPS) stimulation, thus ideal for analyzing TLR signaling. Expression of *TLR6* alone did not enhance BCL10 or API2-MALT1-induced NF- κ B activation in Jurkat cells even in the presence of LPS stimulation (Supplementary Figure S5). *TLR6* functions through the formation of heterodimer with its family member and typically forms heterodimer with TLR2 in responding to stimulation by bacterial antigen.²¹ We next analyzed whether co-expression of *TLR6* and *TLR2* could enhance BCL10 or API2-MALT1-mediated NF- κ B activation in the presence of LPS stimulation. As expected, *TLR6/2* co-expression, in the presence of LPS stimulation, were synergistic with BCL10 and API2-MALT1 in activating the NF- κ B pathway (Figure 4). In contrast, there was no cooperation between co-expression of *TLR6/1* and BCL10 or API2-MALT1 in NF- κ B activation (Figure 4).

Discussion

This study showed that MALT lymphoma was characterized by distinct expression profile in comparison with FL and MCL, in line with the recent finding by Chng *et al.*²² Although unsupervised clustering analyses showed considerable overlap in the gene expression profiles between MALT lymphomas with and without chromosome translocation, there was important difference in the expression of NF- κ B target genes between the two subgroups. By exhaustive GSEA of various molecular pathways and biological processes, we also showed that the gene sets related to inflammation, immune responses, chemokine and GPR signaling are differentially over-represented between these different subgroups. Importantly, several of these molecular pathways or biological processes also lead to NF- κ B activation. These findings were reinforced by independent analyses of differentially expressed genes between MALT lymphomas with and without translocation using hypergeometric tests. Our observations provide several novel insights into the molecular mechanisms of both translocation-positive and -negative MALT lymphomas and potentially explain their different clinical and histological presentations.

Molecular mechanism of translocation-positive MALT lymphoma

In comparison with translocation-negative MALT lymphoma, GSEA and leading edge analyses revealed a common core subset of genes that were overexpressed in translocation-positive cases and a high proportion of them are NF- κ B target genes involving multiple related biological processes or molecular pathways. The top examples included immune

receptors such as TLR6, TLR7, CD69 and CD1D, and chemokine receptor such as CCR2, CXCR4, CCR6 and CCR7, the apoptosis inhibitor BCL2, and positive regulators of the NF- κ B pathway such as REL and molecules involved in GPR signaling (Figure 2, Supplementary Tables S7–S16). The overexpression of CCR2, BCL2, CD69 and TLR6 in translocation-positive cases was further confirmed in a large cohort of MALT lymphomas by qRT-PCR and/or immunohistochemistry/western blot analysis. All these molecules are expected to promote tumor cell survival and proliferation either directly or indirectly. Among these, the overexpression of the above immune surface receptors and chemokine receptors is particularly interesting.

TLR are critical in surveillance of microbial infection by recognizing pathogen-associated molecular patterns such as LPS and bacterial lipopeptides. In mouse model, it has been shown that TLR signaling promotes marginal zone B-cell activation and migration.²³ TLR6 typically forms heterodimers with TLR2 on the cell surface to recognize bacterial antigens.²¹ TLR2/TLR6 signaling activates not only I κ B kinase (IKK) complex that leads to activation of the NF- κ B transcriptional factor, but also the mitogen-activated protein kinase (MAPK) p38 and Jun amino-terminal kinase that lead to activation of the activator protein 1 (AP-1) transcriptional factor.²⁴ Hence, overexpression of TLR6 in translocation-positive MALT lymphoma could potentially augment the NF- κ B activity mediated by MALT lymphoma-associated oncogenic products and also activate the MAPK pathways. In this study, we tested the former hypothesis and showed indeed that expression of TLR6, in presence of TLR2, could enhance both BCL10 and API2-MALT1-mediated NF- κ B activation *in vitro* and this effect was particularly significant on LPS stimulation. A role of TLR signaling in the pathogenesis of translocation-positive MALT lymphoma is also suggested by the followings: (1) *H. pylori* infection is invariably associated with translocation-positive gastric MALT lymphoma; (2) *H. pylori* activates NF- κ B through both the classical and alternative pathway in B lymphocytes and this effect is dependent on LPS but not cag pathogenicity island;²⁵ (3) *H. pylori*-associated LPS-induced NF- κ B activation requires TLR2/TLR6 or TLR2/TLR1 complex.²⁶ Taken together, these findings suggest that there is a potential biological cooperation between MALT lymphoma translocation and TLR signaling in the lymphomagenesis.

CD69, a type II transmembrane glycoprotein, is a potential co-stimulatory receptor and may also have an immunoregulatory role.²⁷ Although the precise function of CD69 in B cells is largely unknown, it is a well-described activation marker in several cell types, and its expression is upregulated in marginal zone B cells on TLR stimulation.²³ CD69 is frequently expressed in low-grade B-cell lymphomas, and in FL, its expression is associated with poor treatment outcome.^{28,29} Our finding of enriched expression of CD69 in translocation-positive MALT lymphoma further implicates its role in lymphoma pathogenesis.

CCR are GPRs and mediate immune cells migration and their retention in the inflammatory site. As B-cell homeostatic chemokine receptor, CCR7, CCR6 and CXCR4 are crucial for this homing process. For example, CCR7 has a central role in the regulation of normal mucosal lymphocyte re-circulation and homeostasis, particularly in the stomach,³⁰ and CXCR4 is critical for B-cell homing to the Peyer's patches and splenic marginal zone.³¹ Although the specific role of CCR2 in B-cell trafficking and homing is unclear, it forms heterodimer with CXCR4,³² thus potentially having a role in mature B-cell homing process. In both low-grade B-cell lymphomas and classic Hodgkin lymphomas, CCR7 and CXCR4 overexpression were associated with a wide lymph node spread, supporting their role

in lymphoma pathogenesis.^{33–35} In addition to homing process, CCR signaling may also promote cell survival and proliferation through its activation of MAPK pathways. In this context, it is noteworthy that GPR is also targeted by chromosomal translocation in MALT lymphoma. A recent study reported deregulation of GPR34 expression by t(X;14)(p11;q32) in a salivary gland MALT lymphoma.³⁶ Importantly, expression of GPR34-induced activation of both the NF- κ B and MAPK pathways *in vitro*.³⁶ In keeping with these findings, our GSEA also showed that several gene sets related to GPR signaling and MAPK pathways were enriched in translocation-positive MALT lymphoma.

As discussed above, several molecular pathways including signaling through TLR, and chemokine receptor may be operational in translocation-positive MALT lymphomas and contribute to the activation of the NF- κ B pathway (Figure 5). Together with MALT lymphoma-associated oncogenic products, they cause relentless NF- κ B activation, leading to the prolonged survival of tumor cells even in the case of obliteration of microbe-mediated immune responses, such as *H. pylori* eradication in gastric MALT lymphoma. In this regard, it is to be noted that the apoptosis inhibitor BCL2 was remarkably uniformly overexpressed virtually in all tumor cells in nearly all translocation-positive cases. In contrast, the protein was heterogeneously expressed, at a much lower level, in tumor cells of translocation-negative cases.

In spite of the above overwhelming evidence of NF- κ B activation in translocation-positive MALT lymphoma, there was considerable heterogeneity in the expression of NF- κ B target genes among these lymphomas. Not all translocation-positive MALT lymphomas showed uniform overexpression of the leading edge core set of the NF- κ B target genes described above, nor each of the translocation-negative cases showed a complete lack of expression of these NF- κ B target genes (Figure 2, Supplementary Figure S4). This is also consistent with the clinical response of gastric MALT lymphoma to *H. pylori* eradication therapy. Although most of t(11;18)-positive gastric MALT lymphomas do not respond to *H. pylori* eradication, there are occasional cases responsive to the antibiotic treatment,³⁷ suggesting that not all translocations have the same biological effect. Equally, the majority of translocation-negative gastric MALT lymphomas can be cured by *H. pylori* eradication, but there are 10–20% cases that are negative for *MALT1*, *BCL10* and *FOXP1* involved translocations, and do not respond to *H. pylori* eradication,³⁷ suggesting presence of other unknown genetic abnormalities that may also target the NF- κ B pathway.

Molecular mechanism of translocation-negative MALT lymphoma

In contrast to translocation-positive MALT lymphoma, translocation-negative cases were characterized by expression of a strong inflammatory gene signature. GSEA and leading edge analysis also revealed common core subset genes involving several related biological processes or molecular pathways, which were enriched in translocation-negative MALT lymphoma. The top examples included proinflammatory cytokines IL8 and IL1 β , molecules involved in B- and T-cell interaction such as CD86, CD28 and ICOS, several chemokine and chemokine receptors and NR4A3 (also known as MINOR) (Figure 2, Supplementary Tables S7, S9, S10, S12, S14).

IL8 and IL1 β are the hallmark of proinflammatory cytokine profile in response to *H. pylori* infection. IL8 is critical for neutrophil infiltration and activation, whereas IL1 β induces gastrin release, inhibits acid secretion and promote apoptosis of epithelial cells.³⁸ The finding of overexpression of these

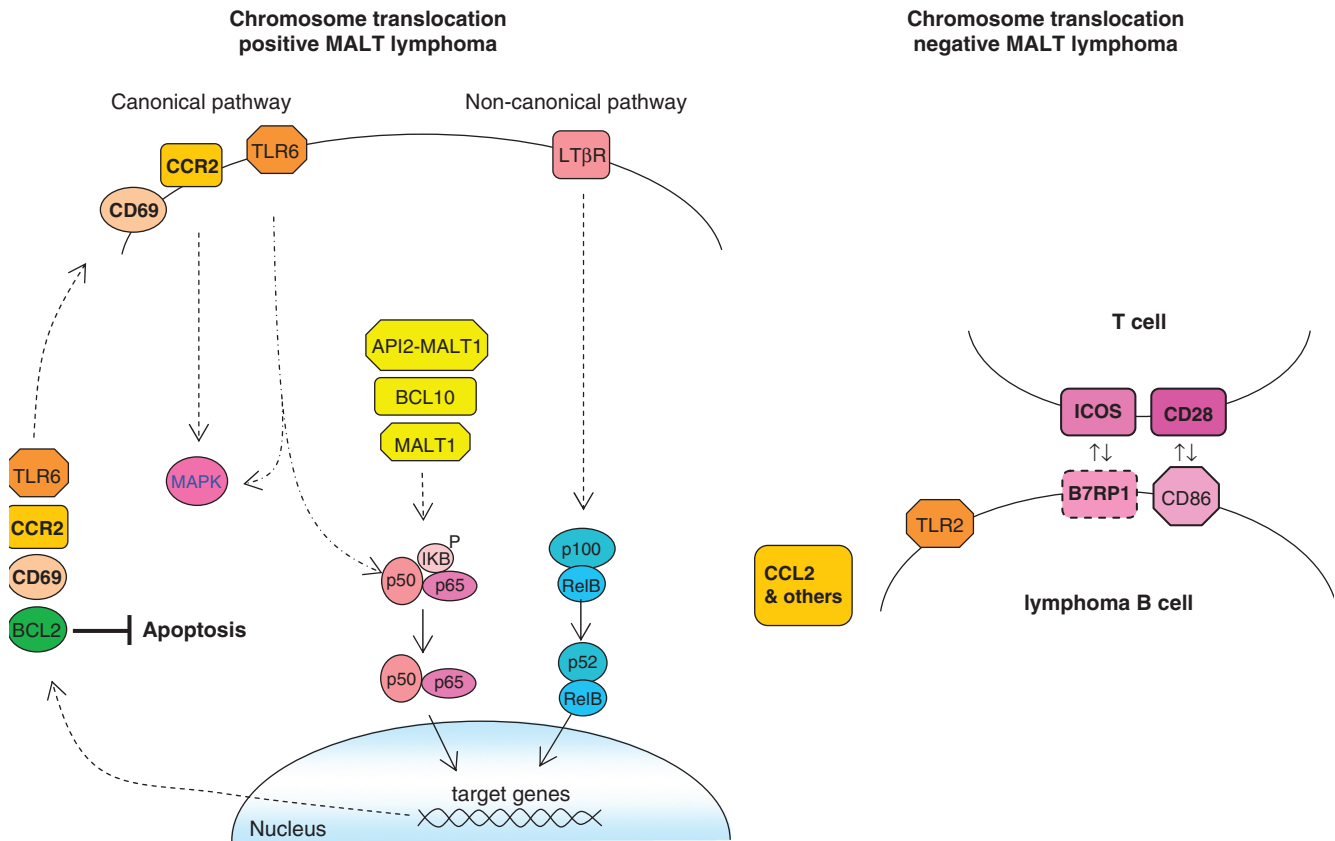


Figure 5 Summary and hypothesis on molecular mechanism of MALT lymphoma with and without chromosomal translocation. In translocation-positive MALT lymphoma, overexpression of API2-MALT1, BCL10 and MALT1 activates the canonical NF-κB pathway, leading to enhanced expression of the NF-κB target genes, particularly *TLR6*, *CCR2*, *CD69* and *BCL2*. Overexpression of *TLR6* may provide a further positive feedback to the activation of the NF-κB pathway. Similar positive feedback may also be expected from the CCR2 signaling, and in addition both *TLR6* and *CCR2* may trigger activation of the MAPK pathway. The pathogenic implication of enhanced *CD69* expression is currently unknown. Overexpression of *BCL2* is expected to promote the tumor cell survival. In essence, the above chromosome translocations cause constitutive NF-κB activation with expression of its target genes forming a potential positive feedback loop, and the relentless NF-κB activation, in the case of gastric MALT lymphoma, confers its resistance to *H. pylori* eradication. In translocation-negative MALT lymphoma, the ongoing inflammatory and immune responses maintain active cognate B and T cell interaction through co-stimulating molecules CD86/CD28, B7RP1/ICOS, which are the major determinants of tumor cell survival and thus explain, in the cases of gastric MALT lymphoma, their responses to *H. pylori* eradication.

proinflammatory cytokines in translocation-negative gastric MALT lymphomas, indicates the presence of active *H. pylori* infection. In keeping with this, translocation-negative gastric MALT lymphomas show a higher number of blast cells than translocation-positive cases.¹⁶ In addition, a number of chemokines and chemokine receptors were highly expressed in the translocation-negative cases. This may reflect the trafficking and retention of various immune cells in response to an active *H. pylori* infection.

Most importantly, GSEA showed enriched expression of the surface molecules involved in B- and T-cell interaction namely CD86, CD28 and ICOS in translocation-negative gastric MALT lymphoma. Although residual reactive follicles may be present and contribute to the high CD86, CD28 and ICOS expression in translocation-negative cases, the germinal center markers CD10 and BCL6 were expressed in much low levels in MALT lymphoma (Supplementary Figure S1), and more importantly overexpression of CD86 in tumor cells was clearly shown by qRT-PCR and immunohistochemistry. In line with our finding, a previous study showed significantly higher CD86 expression in gastric MALT lymphomas that responded to *H. pylori* eradication than those resisted to the therapy (66% vs 10%).³⁹ Although the chromosome translocation status in these cases is not available, it is most likely that the cases

responded to *H. pylori* were translocation-negative.¹⁴ Taken together, these findings suggest that there is an active immune response to *H. pylori* infection in translocation-negative gastric MALT lymphoma, and this most likely underscores the tumor cell survival and expansion, and thus determines their response to *H. pylori* eradication (Figure 5).

In summary, this study shows that (1) translocation-positive MALT lymphoma is in general characterized by an enhanced expression of NF-κB target genes, particularly *CCR2*, *TLR6* and *BCL2*; (2) the oncogenic products of MALT lymphoma-associated translocation may cooperate with signaling from several surface receptors including *TLR6* and chemokine receptors in activation of the NF-κB pathways; and (3) translocation-negative MALT lymphoma is featured by active inflammatory and immune responses to *H. pylori* infection, and tumor cell interaction with infiltrating T cells through co-stimulating molecules (especially CD86/CD28) may have an important role in their survival and clonal expansion.

Conflict of interest

The authors declare no conflict of interest.

Acknowledgements

We would like to thank Professor Ahmet Dogan and Dr Ellen Remstein, Department of Pathology, Mayo Clinic for sharing their pulmonary MALT lymphoma gene expression microarray data; Dr Ian McFarlane, the Microarray CoreLab, National Institute of Health Research, Cambridge Comprehensive Biomedical Research Centre for his technical assistance, Dr Koichi Kuwano, Department of Infectious Medicine, Kurume University School of Medicine, Japan for providing TLR1, TLR2 and TLR6 expression constructs and both previous and present members of Du lab for helpful discussion and assistance. The research in Du lab was supported by research grants from Leukemia Research, UK and the National Institute for Health Research Cambridge Biomedical Research Center. BS was supported by Grant FWF (P19346-B12). LdL is a senior research associate of the FRS-FNRS.

Authors contribution

RAH designed the experiment, collected and analyzed the data. AA, HY and LG contributed to the design and experimental data collection and analysis; ARF, BS, AC, MR, IW, CDWP, KAM, LdL and PGI provided lymphoma cases; MQD designed, analyzed the data and wrote the paper.

References

- Isaacson PG, Du MQ. MALT lymphoma: from morphology to molecules. *Nat Rev Cancer* 2004; **4**: 644–653.
- Ye H, Liu H, Attygalle A, Wotherspoon AC, Nicholson AG, Charlotte F *et al*. Variable frequencies of t(11;18)(q21;q21) in MALT lymphomas of different sites: significant association with CagA strains of *H pylori* in gastric MALT lymphoma. *Blood* 2003; **102**: 1012–1018.
- Ye H, Gong L, Liu H, Hamoudi RA, Shirali S, Ho L *et al*. MALT lymphoma with t(14;18)(q32;q21)/*IGH-MALT1* is characterized by strong cytoplasmic MALT1 and BCL10 expression. *J Pathol* 2005; **205**: 293–301.
- Streubel B, Simonitsch-Klupp I, Mullauer L, Lamprecht A, Huber D, Siebert R *et al*. Variable frequencies of MALT lymphoma-associated genetic aberrations in MALT lymphomas of different sites. *Leukemia* 2004; **18**: 1722–1726.
- Goatly A, Bacon CM, Nakamura S, Ye H, Kim I, Brown PJ *et al*. *FOXP1* abnormalities in lymphoma: translocation breakpoint mapping reveals insights into deregulated transcriptional control. *Mod Pathol* 2008; **21**: 902–911.
- Lucas PC, Yonezumi M, Inohara N, McAllister-Lucas LM, Abazeed ME, Chen FF *et al*. Bcl10 and MALT1, independent targets of chromosomal translocation in MALT lymphoma, cooperate in a novel NF-kappa B signaling pathway. *J Biol Chem* 2001; **276**: 19012–19019.
- Zhou H, Wertz I, O'Rourke K, Ultsch M, Seshagiri S, Eby M *et al*. Bcl10 activates the NF-kappaB pathway through ubiquitination of NEMO. *Nature* 2004; **427**: 167–171.
- Lucas PC, Kuffa P, Gu S, Kohrt D, Kim DS, Siu K *et al*. A dual role for the API2 moiety in API2-MALT1-dependent NF-kappaB activation: heterotypic oligomerization and TRAF2 recruitment. *Oncogene* 2007; **26**: 5643–5654.
- Baens M, Fevery S, Sagaert X, Noels H, Hagens S, Broeckx V *et al*. Selective expansion of marginal zone B cells in Emicro-API2-MALT1 mice is linked to enhanced I kappa B kinase gamma polyubiquitination. *Cancer Res* 2006; **66**: 5270–5277.
- Li Z, Wang H, Xue L, Shin DM, Roopenian D, Xu W *et al*. Emu-BCL10 mice exhibit constitutive activation of both canonical and noncanonical NF-kappaB pathways generating marginal zone (MZ) B-cell expansion as a precursor to splenic MZ lymphoma. *Blood* 2009; **114**: 4158–4168.
- Zhou Y, Ye H, Martin-Subero JI, Hamoudi R, Lu YJ, Wang R *et al*. Distinct comparative genomic hybridisation profiles in gastric mucosa-associated lymphoid tissue lymphomas with and without t(11;18)(q21;q21). *Br J Haematol* 2006; **133**: 35–42.
- Sagaert X, Theys T, Wolf-Peeters C, Marynen P, Baens M. Splenic marginal zone lymphoma-like features in API2-MALT1 transgenic mice that are exposed to antigenic stimulation. *Haematologica* 2006; **91**: 1693–1696.
- Ho L, Davis RE, Conne B, Chappuis R, Berczy M, Mhawech P *et al*. MALT1 and the API2-MALT1 fusion act between CD40 and IKK and confer NF-kappa B-dependent proliferative advantage and resistance against FAS-induced cell death in B cells. *Blood* 2005; **105**: 2891–2899.
- Liu H, Ye H, Ruskone-Fourmestreaux A, de Jong D, Pileri S, Thiede C *et al*. T(11;18) is a marker for all stage gastric MALT lymphomas that will not respond to *H pylori* eradication. *Gastroenterology* 2002; **122**: 1286–1294.
- Ye H, Gong L, Liu H, Ruskone-Fourmestreaux A, de Jong D, Pileri S *et al*. Strong BCL10 nuclear expression identifies gastric MALT lymphomas that do not respond to *H pylori* eradication. *Gut* 2006; **55**: 137–138.
- Okabe M, Inagaki H, Ohshima K, Yoshino T, Li C, Eimoto T *et al*. API2-MALT1 fusion defines a distinctive clinicopathologic subtype in pulmonary extranodal marginal zone B-cell lymphoma of mucosa-associated lymphoid tissue. *Am J Pathol* 2003; **162**: 1113–1122.
- Subramanian A, Tamayo P, Mootha VK, Mukherjee S, Ebert BL, Gillette MA *et al*. Gene set enrichment analysis: a knowledge-based approach for interpreting genome-wide expression profiles. *Proc Natl Acad Sci USA* 2005; **102**: 15545–15550.
- Saxena V, Orgill D, Kohane I. Absolute enrichment: gene set enrichment analysis for homeostatic systems. *Nucleic Acids Res* 2006; **34**: e151.
- Ortutay C, Vihinen M. Immunome: a reference set of genes and proteins for systems biology of the human immune system. *Cell Immunol* 2006; **244**: 87–89.
- Pepper SD, Saunders EK, Edwards LE, Wilson CL, Miller CJ. The utility of MAS5 expression summary and detection call algorithms. *BMC Bioinformatics* 2007; **8**: 273.
- Gomariz RP, Arranz A, Juarranz Y, Gutierrez-Canas I, Garcia-Gomez M, Leceta J *et al*. Regulation of TLR expression, a new perspective for the role of VIP in immunity. *Peptides* 2007; **28**: 1825–1832.
- Chng WJ, Remstein ED, Fonseca R, Bergsagel PL, Vrana JA, Kurtin PJ *et al*. Gene expression profiling of pulmonary mucosa-associated lymphoid tissue lymphoma identifies new biologic insights with potential diagnostic and therapeutic applications. *Blood* 2009; **113**: 635–645.
- Rubtsov AV, Swanson CL, Troy S, Strauch P, Pelanda R, Torres RM. TLR agonists promote marginal zone B cell activation and facilitate T-dependent IgM responses. *J Immunol* 2008; **180**: 3882–3888.
- Akira S, Takeda K. Toll-like receptor signalling. *Nat Rev Immunol* 2004; **4**: 499–511.
- Ohmae T, Hirata Y, Maeda S, Shibata W, Yanai A, Ogura K *et al*. *Helicobacter pylori* activates NF-kappaB via the alternative pathway in B lymphocytes. *J Immunol* 2005; **175**: 7162–7169.
- Yokota S, Ohnishi T, Muroi M, Tanamoto K, Fujii N, Amano K. Highly-purified *Helicobacter pylori* LPS preparations induce weak inflammatory reactions and utilize Toll-like receptor 2 complex but not Toll-like receptor 4 complex. *FEMS Immunol Med Microbiol* 2007; **51**: 140–148.
- Sancho D, Gomez M, Sanchez-Madrid F. CD69 is an immunoregulatory molecule induced following activation. *Trends Immunol* 2005; **26**: 136–140.
- Erlanson M, Gronlund E, Lofvenberg E, Roos G, Lindh J. Expression of activation markers CD23 and CD69 in B-cell non-Hodgkin's lymphoma. *Eur J Haematol* 1998; **60**: 125–132.
- de Jong D, Koster A, Hagenbeek A, Raemaekers J, Veldhuizen D, Heisterkamp S *et al*. Impact of the tumor microenvironment on prognosis in follicular lymphoma is dependent on specific treatment protocols. *Haematologica* 2009; **94**: 70–77.
- Hopken UE, Wengner AM, Lodenkemper C, Stein H, Heimesaat MM, Rehm A *et al*. CCR7 deficiency causes ectopic lymphoid neogenesis and disturbed mucosal tissue integrity. *Blood* 2007; **109**: 886–895.

- 31 Nie Y, Waite J, Brewer F, Sunshine MJ, Littman DR, Zou YR. The role of CXCR4 in maintaining peripheral B cell compartments and humoral immunity. *J Exp Med* 2004; **200**: 1145–1156.
- 32 Springael JY, Urizar E, Parmentier M. Dimerization of chemokine receptors and its functional consequences. *Cytokine Growth Factor Rev* 2005; **16**: 611–623.
- 33 Lopez-Giral S, Quintana NE, Cabrerizo M, Alfonso-Perez M, Sala-Valdes M, De Soria VG *et al*. Chemokine receptors that mediate B cell homing to secondary lymphoid tissues are highly expressed in B cell chronic lymphocytic leukemia and non-Hodgkin lymphomas with widespread nodular dissemination. *J Leukoc Biol* 2004; **76**: 462–471.
- 34 Hopken UE, Foss HD, Meyer D, Hinz M, Leder K, Stein H *et al*. Up-regulation of the chemokine receptor CCR7 in classical but not in lymphocyte-predominant Hodgkin disease correlates with distinct dissemination of neoplastic cells in lymphoid organs. *Blood* 2002; **99**: 1109–1116.
- 35 Trentin L, Cabrelle A, Facco M, Carollo D, Miorin M, Tosoni A *et al*. Homeostatic chemokines drive migration of malignant B cells in patients with non-Hodgkin lymphomas. *Blood* 2004; **104**: 502–508.
- 36 Novak A, Akasaka T, Manske M, Gupta M, Witzig T, Dyer MJS *et al*. Elevated expression of GPR34 and its association with a novel translocation t(X;14)(p11;q32) involving IGHS and GPR34 in MALT lymphoma. *Blood* 2008; **112**: 785, Abstract 2251.
- 37 Du MQ, Atherton JC. Molecular subtyping of gastric MALT lymphomas: implications for prognosis and management. *Gut* 2006; **55**: 886–893.
- 38 McNamara D, El Omar E. *Helicobacter pylori* infection and the pathogenesis of gastric cancer: a paradigm for host-bacterial interactions. *Dig Liver Dis* 2008; **40**: 504–509.
- 39 de Jong D, Vyth-Dreese F, Dellemijn T, Verra N, Ruskone-Fourmestraux A, Lavergne-Slove A *et al*. Histological and immunological parameters to predict treatment outcome of *Helicobacter pylori* eradication in low-grade gastric MALT lymphoma. *J Pathol* 2001; **193**: 318–324.

Supplementary Information accompanies the paper on the Leukemia website (<http://www.nature.com/leu>)

SUPPLEMENTARY METHODS

Rifat A. Hamoudi,¹ Alex Appert,¹ Hongtao Ye,¹ Liping Gong,¹ Ming-Qing Du¹

¹Department of Pathology, University of Cambridge, Cambridge, CB2 0QQ, U.K.;

Gene expression microarray: Total RNA was isolated using the RNeasy kit (Qiagen, Valencia, CA) and the RNA integrity was assessed using an Agilent 2100 Bioanalyzer. Double stranded cDNA was generated from 2-5 μ g of total RNA, followed by *in vitro* transcription with biotin-labeled nucleotides using the Affymetrix RNA transcript labeling kit (Affymetrix Inc, Santa Clara, CA). Biotinylated cRNA was purified and hybridized to Affymetrix GeneChip HG-U133A (MALT lymphoma) or Affymetrix H133 plus 2 (FL and MCL). Except where indicated, transcriptome analyses were performed using R system software packages (version 2.8.0) including Bioconductor (version 2.0) and in house software written using R code. Quality control analysis of the microarray hybridization was performed using Affymetrix GCOS software. A scale factor within mean plus 2 standard deviation and percentage present calls >20% were used as threshold values and only those passed these criteria were used for subsequent analyses according to the criteria recommended by the Tumor Analysis Best Practices Working Group.¹ All microarray data have been deposited with Gene Expression Omnibus (GEO; <http://www.ncbi.nlm.nih.gov/geo/>, GSE18736).

Normalization: Raw gene expression data from Affymetrix CEL files were uploaded to bioconductor where MAS5 and gcRMA normalization were performed separately for each Affymetrix platform. MAS5 data were scaled to a target intensity of 100. The gcRMA normalized data were imported into Genespring 7.3.1, log-transformed and median centered. For comparison between microarray data obtained from HG-U133A and HG-U133 plus2, an additional median polishing normalization step was applied. gcRMA normalized data were used for unsupervised clustering analysis and gene set enrichment analysis (GSEA), while MAS5 normalized data were used for identification of

differentially expressed genes between MATL lymphoma with and without translocation as suggested previously.² Both MAS5 and gcRMA normalized data were used in non-specific filtering.

Non-specific filtering: To filter out non-variant genes, a combination of noise and variance filtering was applied. To filter out non-expressed genes, only probes with a value of 50 or higher in the MAS5 dataset in 2 or more samples were selected. To eliminate non-variant genes, only those with a coefficient of variation (CV) value of 10% or higher in the gcRMA dataset across all cases were considered to be variant and thus selected. Finally, the genes that passed the above two filtering methods were intersected to obtain a common set of variant genes.

For comparison of microarray data between HG-U133A and HG-U133 plus2 platform where indicated, the non-specific filtering was similarly performed separately for each platform as above, then intersected to generate a final common set of variant genes. All the above analyses were performed using scripts written in R. The above procedure for analysis of expression microarray data from HG-U133A and HG-U133 plus2 platform was validated by a serial empirical testing using the published pulmonary MALT lymphoma expression microarray data from the HG-U133 plus2 platform as a reference.³

Quantitative reverse-transcription polymerase chain reaction (qRT-PCR)

The expression of selected genes identified from the expression microarray analysis was validated by qRT-PCR with 18SrRNA as an internal control.⁴ Briefly, total RNA was isolated from tumor cells microdissected from paraffin-embedded tissue sections,⁵ and treated with Turbo DNase. cDNA was synthesized using gene specific primer (Supplementary Table S4) and qPCR was performed in triplicate using an iCycler iQ system (Bio-Rad, Hertfordshire, UK) with SYBR Green-I.⁴

Immunohistochemistry: BCL10, MALT1, BCL2, CD69 and CD86 protein expression were investigated by immunohistochemistry under the conditions detailed in Supplementary Table S5. The

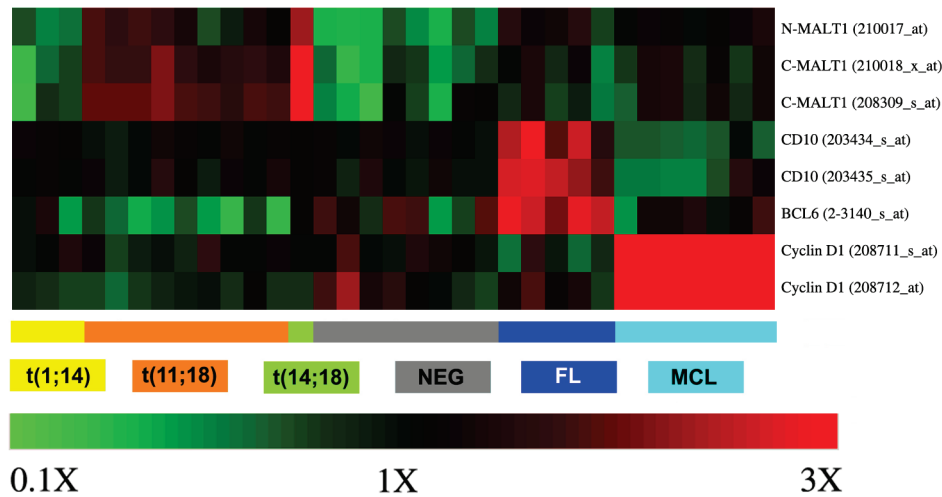
immunostaining was evaluated independently by two assessors (HY, MQD) and scored according to the percentage of positivity (<30%, 30-70%, >70% cells) and staining intensity (strong, moderate, weak, negative). Cases were considered positive when $\geq 30\%$ tumor cells were stained.

Western blot analysis: Protein extracts from frozen tissues or cultured cells were mixed with SDS gel loading buffer, denatured, separated on 4-12% Bis-Tris precast gradient gels using the NuPAGE electrophoresis system (Invitrogen, Paisley, UK). The proteins were electrotransferred onto an Immobilon PVDF membrane, then incubated with a primary antibody, followed by appropriate HRP-conjugated secondary antibody and detected using an Immobilon chemiluminescent HRP substrate (Millipore, Watford, UK). The filter was stripped and similarly re-probed with antibody to β -actin or others. Where indicated, Western blots were quantified using an Advanced Image Data Analyzer (Version 4.18, Raytest, Straubenhardt, Germany).

NF- κ B reporter assay: The full length coding sequence of *BCL10* and *API2-MALT1* was cloned into a modified pIRESpuro2 (Clontech, Saint-Germain-en-Laye, France) expression vector. The expression constructs of *TLR1*, *TLR2* and *TLR6* in pFLAG-CMV1 vector were kindly provided by Dr. Kuwano.⁶ The capacity of these expression constructs to induce NF- κ B activation was measured using the Dual Luciferase Reporter Assay System (Promega, Southampton, UK) in Jurkat T-cells. Briefly, a total of 9 μ g DNA containing 2 μ g of each expression vector, appropriate amount of vector control, 1.5 μ g pNF κ B-luc (a Firefly luciferase reporter for NF- κ B activity), 1.5 μ g pRL-TK (a Renilla luciferase reporter as a control) was transfected into a total of 8×10^6 Jurkat T-cells using Amaxa with solution T and program T16 (Amaxa, Cologne, Germany). The transfected cells were dispatched into 6 to 8 wells of 24-well plates, left for 20 hours to recover and then treated with 10 μ g/ml LPS or vehicle for 6 hours. The cells were harvested, washed with PBS, lysed and assayed for luciferase activities using a VICTOR3 luminometer (PerkinElmer, Beaconsfield, UK) following the manufacture's instructions.

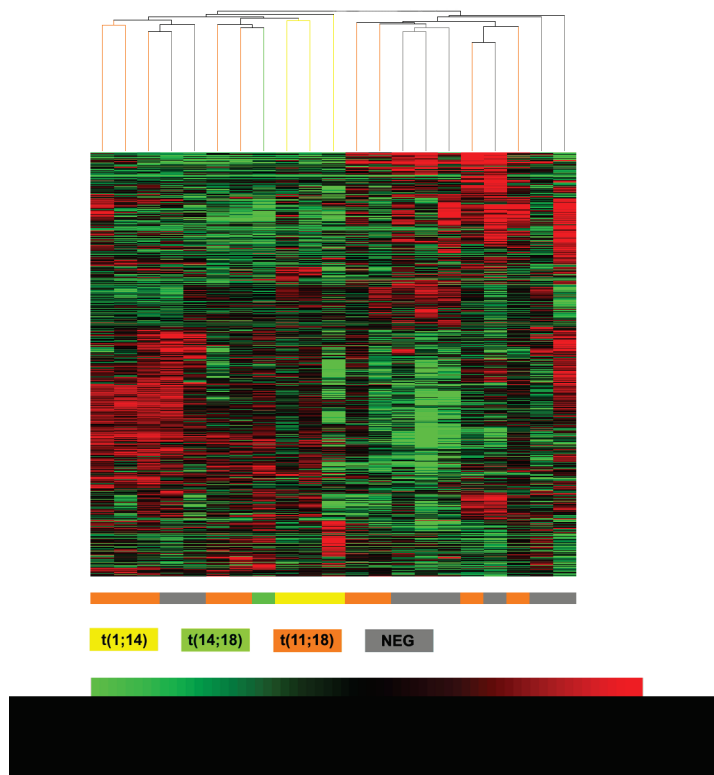
References

- 1 The Tumor Analysis Best Practices Working Group. Expression profiling--best practices for data generation and interpretation in clinical trials. *Nat Rev Genet* 2004; 5:229-237.
- 2 Pepper SD, Saunders EK, Edwards LE, Wilson CL, Miller CJ. The utility of MAS5 expression summary and detection call algorithms. *BMC Bioinformatics* 2007; 8:273.
- 3 Chng WJ, Remstein ED, Fonseca R, Bergsagel PL, Vrana JA, Kurtin PJ et al. Gene expression profiling of pulmonary mucosa-associated lymphoid tissue lymphoma identifies new biologic insights with potential diagnostic and therapeutic applications. *Blood* 2009; 113:635-645.
- 4 Ye H, Gong L, Liu H, Hamoudi RA, Shirali S, Ho L et al. MALT lymphoma with t(14;18)(q32;q21)/IGH-MALT1 is characterized by strong cytoplasmic MALT1 and BCL10 expression. *J Pathol* 2005; 205:293-301.
- 5 Pan LX, Diss TC, Peng HZ, Isaacson PG. Clonality analysis of defined B-cell populations in archival tissue sections using microdissection and the polymerase chain reaction. *Histopathology* 1994; 24:323-327.
- 6 Shimizu T, Kida Y, Kuwano K. A triacylated lipoprotein from *Mycoplasma genitalium* activates NF-kappaB through Toll-like receptor 1 (TLR1) and TLR2. *Infect Immun* 2008; 76:3672-3678.



Supplementary Figure S1: Expression of hallmark genes in MALT lymphoma, FL and MCL.

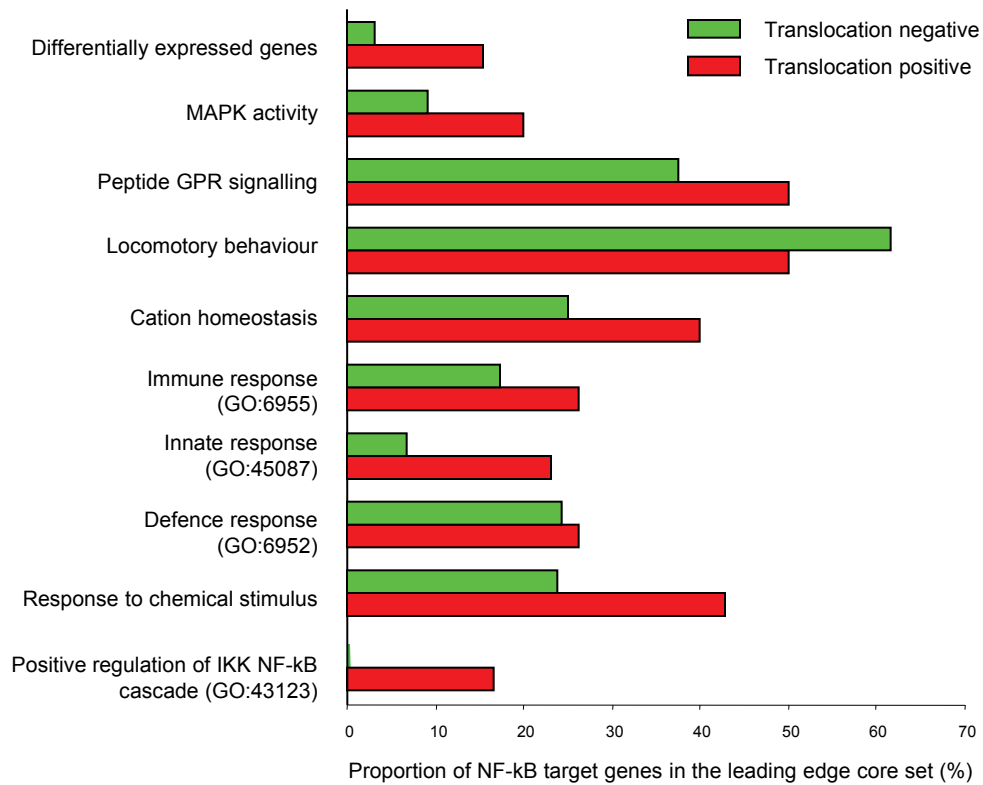
N-MALT1 probe (210017_at) detects only wild type MALT1 transcripts, while C-MALT (210018_x_at & 208309_s_at) probes detect both MALT1 and API2-MALT1 transcripts. The chromosome translocation status of MALT lymphoma is indicated by different colour scheme. On the heatmap, red represents up-regulated genes and green down-regulated genes, with the scale showed at the bottom of the figure.



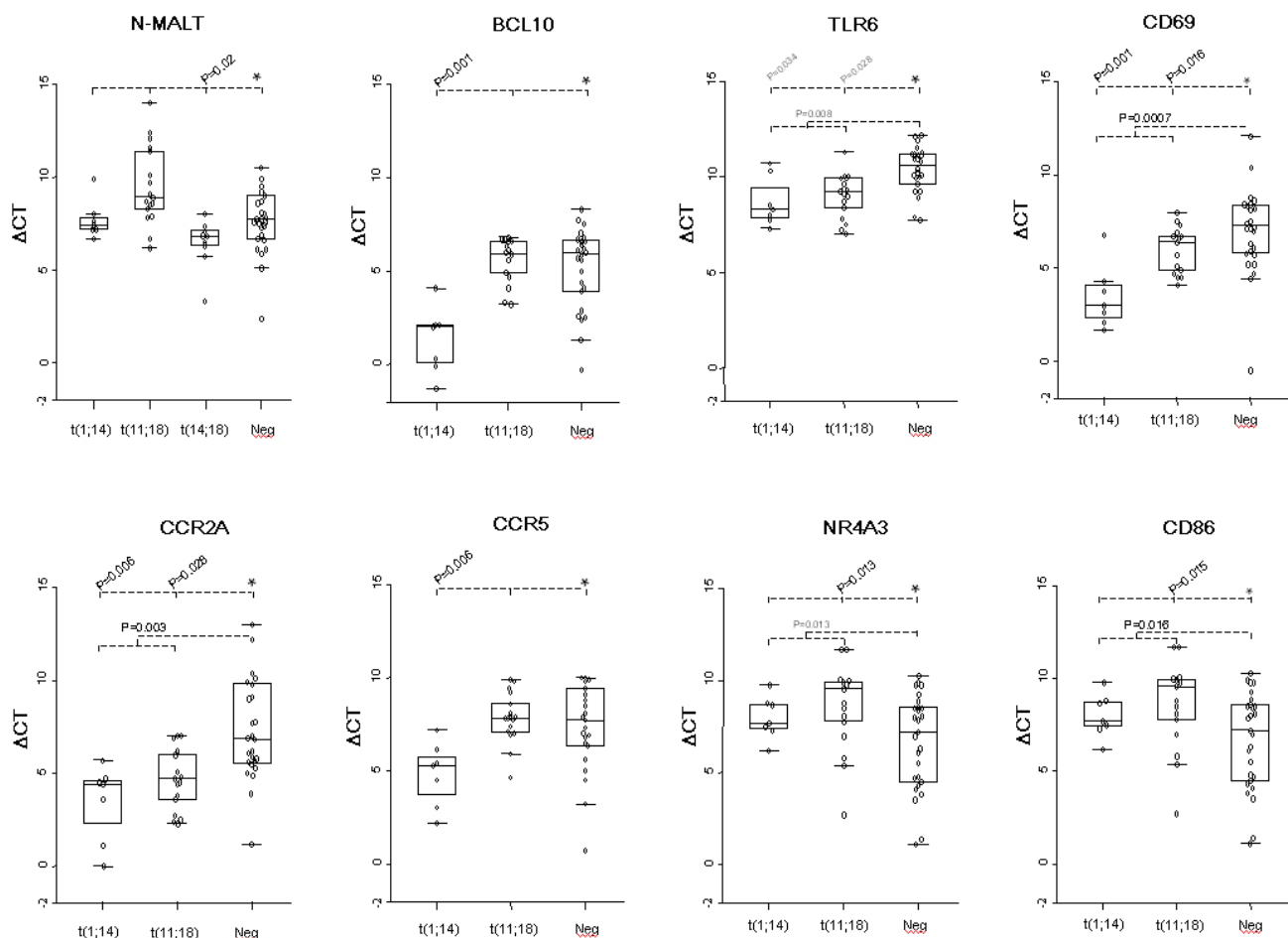
Supplementary Figure S2: Unsupervised hierarchical clustering of MALT lymphoma with different translocation status.

After standard normalisation and filtering, a set of 6893 probes were obtained and used for unsupervised hierarchical clustering analysis. MALT lymphoma cases with and without chromosome translocation are intermingled together.

The chromosome translocation status of MALT lymphoma is indicated by different colour scheme. On the heatmap, red represents up-regulated genes and green down-regulated genes, with the scale showed at the bottom of the figure.

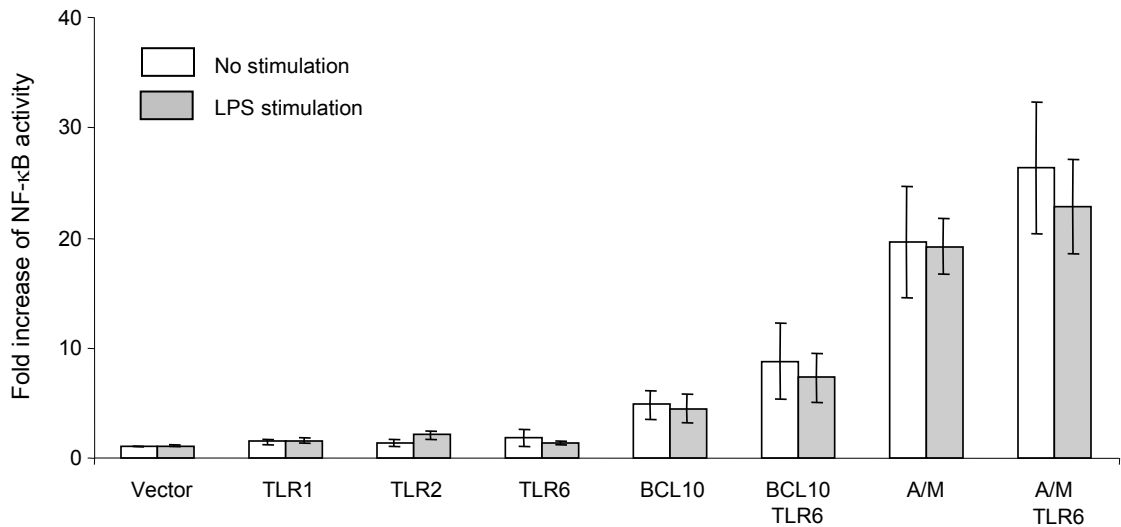


Supplemental Figure S3: Presence of high proportion of NF-κB target genes in the leading edge core set of various gene sets related to inflammation, immune responses, cell migration and GPR signaling.



Supplementary Figure S4: Validation of gene expression in MALT lymphoma with and without chromosome translocation by real-time quantitative RT-PCR.

This was performed in triplicate using RNA samples extracted from tumor cells microdissected from paraffin-embedded tissue sections in a total of 58 cases of MALT lymphoma (7 t(1;14)/*BCL10-IGH* positive, 17 t(11;18)/*API2-MALT1* positive, 9 t(14;18)/*IGH-MALT1* positive and 25 translocation negative) including 16 successfully investigated by gene expression profiling analysis. There are excellent correlations between gene expression profiling and qRT-PCR results. Asterisk indicates statistical significant differences between various translocation positive groups and translocation negative group by Mann-Whitney non-parametric statistical test. The medians are indicated by horizontal bars in the rectangular boxes. Neg: translocation negative MALT lymphoma; NR4A3: nuclear receptor subfamily 4, group A, member 3, also known as mitogen-induced nuclear orphan receptor (MINOR).



Supplementary Figure S5. TLR6 alone fails to enhance BCL10 and API2-MALT1 mediated NF- κ B activation in Jurkat T cells.

Jurkat T cells were co-transfected with vector (pIRESpuro2) or plasmids containing BCL10, API2-MALT1 (AM), TLR1, TLR2, TLR6 as indicated, together with NF- κ B luciferase reporter gene. The transfected cells were seeded in multiple cell plates, cultured for 20 hours and then treated with LPS or vehicle alone for 6 hours. NF- κ B activities were measured and recorded as fold increase of the vector control.

Supplementary Table S1: Summary of clinico-pathological, molecular and immunohistochemical data of MALT lymphoma cases used in gene expression microarray.

| Case No. | Sex | Age | Site | Diagnosis MALT | Translocation status | Stage* | Treatment | Follow-up | BCL10 immunohistochemistry | MALT1 immunohistochemistry |
|----------|-----|-----|---------------|----------------|----------------------|--------|--|-----------------------------|-----------------------------|-------------------------------|
| 1 | M | 67 | Stomach | lymphoma | t(1;2)(p22;q12) | IIIE | Total gastrectomy | N/A | Strong nuclear staining | Negative |
| 2 | F | 55 | Stomach | lymphoma | t(1;14)(p22;q32) | N/A | N/A | N/A | Strong nuclear staining | Weak cytoplasmic staining |
| 3 | NA | NA | Lung | lymphoma | t(1;14)(p22;q32) | N/A | N/A | N/A | Strong nuclear staining | Moderate cytoplasmic staining |
| 4 | M | 71 | Stomach | lymphoma | t(1;14)(p22;q32) | IVE | Gastrectomy | N/A | Strong nuclear staining | Weak cytoplasmic staining |
| 5 | F | 62 | Stomach | MALT lymphoma | t(11;18)(q21;q21) | IE | Gastrectomy, no evidence of lymphoma during 3 years follow-up | N/A | N/A | Weak cytoplasmic staining |
| 6 | M | 48 | Stomach | MALT lymphoma | t(11;18)(q21;q21) | IIIE | total gastrectomy | CR during 10 year follow up | N/A | Negative |
| 7 | M | 54 | Stomach | MALT lymphoma | t(11;18)(q21;q21) | IE | total gastrectomy | CR during 4 year follow up | N/A | Negative |
| 8 | M | 51 | Stomach | MALT lymphoma | t(11;18)(q21;q21) | IE | total gastrectomy | CR during 6 year follow up | N/A | Weak cytoplasmic staining |
| 9 | F | 75 | Lung | MALT lymphoma | t(11;18)(q21;q21) | IE | Surgical resection, 20 years later lymphoma relapsed and | N/A | Moderate nuclear staining | Weak cytoplasmic staining |
| 10 | F | 52 | Stomach | MALT lymphoma | t(11;18)(q21;q21) | IIE | N/A | N/A | Moderate nuclear staining | Weak cytoplasmic staining |
| 11 | M | NA | Stomach | MALT lymphoma | t(11;18)(q21;q21) | | N/A | N/A | Moderate nuclear staining | Weak cytoplasmic staining |
| 12 | F | 72 | Stomach | MALT lymphoma | t(11;18)(q21;q21) | IVE | N/A | N/A | Moderate nuclear staining | Weak cytoplasmic staining |
| 13 | M | 41 | Stomach | MALT lymphoma | t(11;18)(q21;q21) | IIIE | N/A | N/A | Moderate nuclear staining | Weak cytoplasmic staining |
| 14 | F | 56 | Ocular adnexa | MALT lymphoma | t(14;18)(q32;q21) | IE | Treated by radiotherapy, no evidence of lymphoma during 10 years follow-up | N/A | N/A | N/A |
| 15 | F | 62 | Liver | MALT lymphoma | t(14;18)(q32;q21) | IE | Surgical resection, no evidence of lymphoma during 6 years follow-up | N/A | Strong cytoplasmic staining | Strong cytoplasmic staining |
| 16 | M | 55 | Stomach | MALT lymphoma | Negative | N/A | N/A | N/A | Cytoplasmic staining | N/A |
| 17 | M | 50 | Stomach | MALT lymphoma | Negative | IE | Total gastrectomy | CR during 2 year follow up | Cytoplasmic staining | Negative |
| 18 | F | 64 | Stomach | MALT lymphoma | Negative | IE | Total gastrectomy | CR during 6 year follow up | Cytoplasmic staining | Negative |
| 19 | M | 18 | Stomach | MALT lymphoma | Negative | N/A | N/A | N/A | Cytoplasmic staining | Moderate cytoplasmic staining |
| 20 | M | 57 | Stomach | MALT lymphoma | Negative | IIIE | Total gastrectomy | CR during 13 year follow up | Cytoplasmic staining | Weak cytoplasmic staining |
| 21 | M | NA | Stomach | MALT lymphoma | Negative | N/A | N/A | N/A | Weak cytoplasmic staining | Weak cytoplasmic staining |
| 22 | M | 59 | Stomach | MALT lymphoma | Negative | IE | N/A | N/A | Cytoplasmic staining | Negative |
| 23 | NA | NA | Stomach | MALT lymphoma | Negative | N/A | N/A | N/A | Moderate nuclear staining | Weak cytoplasmic staining |
| 24 | M | 62 | Stomach | MALT lymphoma | Negative | IIE | N/A | N/A | Moderate nuclear staining | Weak cytoplasmic staining |

*Clinical staging according to the Ann Arbor system modified by Musshoff. (Musshoff K. Klinische Stadieneinteilung der Nicht-Hodgkin-Lymphoma. Strahlentherapie 1977; 153:218-221).

N/A not available; CR: complete remission; The cases in green were subsequently excluded from analysis as the microarray hybridisation failed to meet the quality control criteria.

Supplementary Table S2: Gene sets used for gene set enrichment analysis

| Name of Gene set | No. of gene sets | No of genes | Source | Description |
|---|------------------|-------------|---|---|
| NF- κ B target genes | 1 | 271 | http://www.nf-kb.org , http://bioinfo.lifl.fr/NF-KB , http://people.bu | Genes contain κ B binding sites in their promoters and are transactivated by NF- κ B |
| Gene Sets from Immune Database | | | | |
| Innate immunity | 1 | 44 | http://bioinf.uta.fi/Immuneome | |
| Antigen processing and presentation | 1 | 45 | http://bioinf.uta.fi/Immuneome | |
| Inflammation | 1 | 131 | http://bioinf.uta.fi/Immuneome | |
| Phagocytosis | 1 | 18 | http://bioinf.uta.fi/Immuneome | |
| Cellular Immunity | 1 | 100 | http://bioinf.uta.fi/Immuneome | |
| Humoural Immunity | 1 | 103 | http://bioinf.uta.fi/Immuneome | |
| Transcription factor | 1 | 38 | http://bioinf.uta.fi/Immuneome | |
| Complement System | 1 | 56 | http://bioinf.uta.fi/Immuneome | |
| Chemokine receptors | 1 | 240 | http://bioinf.uta.fi/Immuneome | |
| Cluster of differentiation (CD) | 1 | 301 | http://bioinf.uta.fi/Immuneome | |
| Gene Sets in biological processes annotated from Gene Ontology | | | | |
| Immunologically important genes | 1 | 1327 | http://wiki.geneontology.org/index.php/Immunologically_important_genes | Genes related to immunological process and listed according to their priority score |
| B and T cell receptor signalling pathway | 1 | 113 | http://www.geneontology.org/ | Contains 69 and 44 genes for B and T cell receptor signalling respectively |
| Immune response (GO:0006955) | 1 | 596 | http://www.geneontology.org/ | immune response genes derived from gene ontology root category of the term GO:0006955 |
| Adaptive immune response (GO:0002250) | 1 | 43 | http://www.geneontology.org/ | adaptive immune response genes derived from gene ontology root category of the term GO:0002250 |
| Activation of immune response (GO:0002253) | 1 | 41 | http://www.geneontology.org/ | activation of immune response genes derived from gene ontology root category of the term GO:0002253 |
| Regulation of adaptive immune response (GO:0002819) | 1 | 11 | http://www.geneontology.org/ | genes from regulation of adaptive immune response derived from gene ontology root category of the term GO:0002819 |
| Immunoglobulin mediated immune response (GO:0016064) | 1 | 14 | http://www.geneontology.org/ | genes involved in immunoglobulin mediated immune response derived from gene ontology root category of the term GO:0016064 |
| Innate immune response (GO:0045087) | 1 | 62 | http://www.geneontology.org/ | genes involved with innate immune response derived from gene ontology root category of the term GO:0045087 |
| Regulation of innate immune response (GO:0045088) | 1 | 14 | http://www.geneontology.org/ | genes involved with regulation of innate immune response derived from gene ontology root category of the term GO:0002250 |
| Regulation of immune response (GO:0050776) | 1 | 77 | http://www.geneontology.org/ | genes involved in regulation of immune response derived from gene ontology root category of the term GO:0050776 |
| Negative regulation of immune response (GO:0050777) | 1 | 9 | http://www.geneontology.org/ | genes involved with negative regulation of immune response derived from gene ontology root category of the term GO:0050777 |
| Positive regulation of immune response (GO:0050778) | 1 | 60 | http://www.geneontology.org/ | genes involved with positive regulation of immune response derived from gene ontology root category of the term GO:0050778 |
| Lymphocyte mediated immunity (GO:0002449) | 1 | 38 | http://www.geneontology.org/ | genes involved in lymphocyte mediated immunity derived from gene ontology root category of the term GO:0002449 |
| T cell mediated immunity (GO:0002456) | 1 | 11 | http://www.geneontology.org/ | genes involved in T cell mediated immunity derived from gene ontology root category of the term GO:0002456 |
| Humoral immune response (GO:0006959) | 1 | 45 | http://www.geneontology.org/ | genes involved in humoral immune response derived from gene ontology root category of the term GO:0006959 |
| Adaptive immune response (GO:0002250) | 1 | 97 | http://www.geneontology.org/ | genes involved in adaptive immune response derived from gene ontology root category of the term GO:0002250 |
| Anti apoptosis (GO:0006916) | 1 | 165 | http://www.geneontology.org/ | genes involved in anti-apoptosis derived from gene ontology root category of the term GO:0006916 |
| Caspase activation (GO:0006919) | 1 | 40 | http://www.geneontology.org/ | genes involved in caspase activation derived from gene ontology root category of the term GO:0006919 |
| Inflammatory response (GO:0006954) | 1 | 294 | http://www.geneontology.org/ | genes involved in inflammatory response derived from gene ontology root category of the term GO:0006954 |
| I κ B kinase NF κ B kinase cascade (GO:0007249) | 1 | 41 | http://www.geneontology.org/ | genes involved in I κ B kinase NF κ B kinase cascade derived from gene ontology root category of the term GO:0007249 |
| Activation of NF κ B kinase cascade (GO:0007250) | 1 | 13 | http://www.geneontology.org/ | genes involved in the activation of NF κ B kinase cascade derived from gene ontology root category of the term GO:0007250 |
| T cell activation (GO:0042110) | 1 | 59 | http://www.geneontology.org/ | genes involved in T cell activation derived from gene ontology root category of the term GO:0042110 |
| B cell activation (GO:0042113) | 1 | 43 | http://www.geneontology.org/ | genes involved in B cell activation derived from gene ontology root category of the term GO:0042113 |
| Chemokine (GO:0042379) | 1 | 50 | http://www.geneontology.org/ | genes relating to chemokines derived from gene ontology root category of the term GO:0042379 |
| Positive regulation of I κ B kinase NF κ B kinase cascade (GO:0043123) | 1 | 101 | http://www.geneontology.org/ | genes involved in the positive regulation of I κ B kinase NF κ B kinase cascade derived from gene ontology root category of the term GO:0043123 |
| Innate immune response (GO:0045087) | 1 | 105 | http://www.geneontology.org/ | genes involved in the innate immune response derived from gene ontology root category of the term GO:0045087 |
| Lymphocyte activation (GO:0046469) | 1 | 137 | http://www.geneontology.org/ | genes involved in lymphocyte activation derived from gene ontology root category of the term GO:0046469 |
| Regulation of T cell activation (GO:0050863) | 1 | 70 | http://www.geneontology.org/ | genes involved in the regulation of T cell activation derived from gene ontology root category of the term GO:0050863 |
| Regulation of lymphocyte activation (GO:0051249) | 1 | 120 | http://www.geneontology.org/ | genes involved in the regulation of lymphocyte activation derived from gene ontology root category of the term GO:0051249 |
| Gene sets derived from pathways annotated by GeneGo | | | | |
| B Cell Lymphoma | 1 | 50 | http://www.genego.com/ | Genes involved in B cell lymphoma derived from the GeneGo Metacore software |
| T Cell Receptor Signalling | 1 | 46 | http://www.genego.com/ | Genes involved in T cell receptor signalling derived from the GeneGo Metacore software |
| TLR Signalling Pathway | 1 | 82 | http://www.genego.com/ | Genes involved in TLR signalling pathway derived from the GeneGo Metacore software |
| CD28 | 1 | 71 | http://www.genego.com/ | CD28 pathway related genes derived from the GeneGo Metacore software |
| ICOS | 1 | 93 | http://www.genego.com/ | Genes that are linked to ICOS pathway, derived from the GeneGo Metacore software |
| Chemotaxis Leukocyte | 1 | 110 | http://www.genego.com/ | genes that are involved chemotaxis leukocyte, derived from the GeneGo Metacore software |
| Immune Response Bacteria | 1 | 47 | http://www.genego.com/ | genes that are involved in bacterial immune response pathway derived from the GeneGo Metacore software |
| BCR Pathway | 1 | 75 | http://www.genego.com/ | genes related to B cell receptor signalling pathway, derived from the GeneGo Metacore software |
| TCR CD28 costimulation leading to NF κ B | 1 | 70 | http://www.genego.com/ | genes involved in T-cell receptor signalling and CD28 costimulation leading to NF κ B activation derived from the GeneGo Metacore software |
| Gene set derived from Pathways annotated by Ingenuity Systems | | | | |
| Antigen Receptor GO | 1 | 17 | http://www.ingenuity.com | genes to do with antigen receptor signalling derived from the gene ontology part of the Ingenuity pathway analysis software |
| B cell activation | 1 | 95 | http://www.ingenuity.com | genes to do with b cell activation derived from the gene ontology part of the Ingenuity pathway analysis software |
| B cell receptor signalling | 1 | 60 | http://www.ingenuity.com | genes to do with b cell receptor signalling derived from the gene ontology part of the Ingenuity pathway analysis software |
| Chemokine signalling | 1 | 36 | http://www.ingenuity.com | genes to do with chemokine signalling derived from the gene ontology part of the Ingenuity pathway analysis software |
| T cell activation GO | 1 | 95 | http://www.ingenuity.com | genes to do with t cell activation derived from the gene ontology part of the Ingenuity pathway analysis software |
| T cell receptor signalling | 1 | 57 | http://www.ingenuity.com | genes to do with t cell receptor signalling derived from the gene ontology part of the Ingenuity pathway analysis software |
| TLR signalling | 1 | 33 | http://www.ingenuity.com | genes to do with TLR signalling derived from the gene ontology part of the Ingenuity pathway analysis software |
| This is derived from the Broad Institute website at: http://www.broad.mit.edu/genome_msiqdb/downloads.jsp and enriched using IPA and GeneGo Metacore software. The molecular signature pathways that are derived are from version 2.5. | | | | |
| Gene Sets from Molecular Signature Database | | | | |
| C2 Curated gene sets derived from online pathway database and publications | 1892 | | http://www.broad.mit.edu/genome_msiqdb/index.jsp | C2 curated gene sets derived from online pathway database and publications |
| C2 Canonical pathway gene sets from pathway databases | 639 | | http://www.broad.mit.edu/genome_msiqdb/index.jsp | Canonical pathway gene sets from pathway databases including the followings |
| C2 BioCarta gene sets | 249 | | http://www.biocarta.com | BioCarta gene sets |
| C2 GenMAPP gene sets | 138 | | http://www.genmapp.org/ | GenMAPP gene sets |
| C2 KEGG gene sets | 200 | | http://www.genome.jp/kegg/ | KEGG gene sets |
| C5 GO biological process gene sets | 825 | | http://www.broad.mit.edu/genome_msiqdb/index.jsp | GO biological process gene sets |
| C5 GO molecular function gene sets | 396 | | http://www.broad.mit.edu/genome_msiqdb/index.jsp | GO molecular function gene sets |
| Total number of gene sets | 4395 | | | |
| Total number of custom sets | 56 | | | |

Download from Table 10 of 101 total items

| Gene Symbol | Gene Name | Accession |
|-------------|----------------------------------|-----------|
| ABR1 | Abundant smooth muscle actin 1 | U05812 |
| ABR2 | Abundant smooth muscle actin 2 | U05813 |
| ABR3 | Abundant smooth muscle actin 3 | U05814 |
| ABR4 | Abundant smooth muscle actin 4 | U05815 |
| ABR5 | Abundant smooth muscle actin 5 | U05816 |
| ABR6 | Abundant smooth muscle actin 6 | U05817 |
| ABR7 | Abundant smooth muscle actin 7 | U05818 |
| ABR8 | Abundant smooth muscle actin 8 | U05819 |
| ABR9 | Abundant smooth muscle actin 9 | U05820 |
| ABR10 | Abundant smooth muscle actin 10 | U05821 |
| ABR11 | Abundant smooth muscle actin 11 | U05822 |
| ABR12 | Abundant smooth muscle actin 12 | U05823 |
| ABR13 | Abundant smooth muscle actin 13 | U05824 |
| ABR14 | Abundant smooth muscle actin 14 | U05825 |
| ABR15 | Abundant smooth muscle actin 15 | U05826 |
| ABR16 | Abundant smooth muscle actin 16 | U05827 |
| ABR17 | Abundant smooth muscle actin 17 | U05828 |
| ABR18 | Abundant smooth muscle actin 18 | U05829 |
| ABR19 | Abundant smooth muscle actin 19 | U05830 |
| ABR20 | Abundant smooth muscle actin 20 | U05831 |
| ABR21 | Abundant smooth muscle actin 21 | U05832 |
| ABR22 | Abundant smooth muscle actin 22 | U05833 |
| ABR23 | Abundant smooth muscle actin 23 | U05834 |
| ABR24 | Abundant smooth muscle actin 24 | U05835 |
| ABR25 | Abundant smooth muscle actin 25 | U05836 |
| ABR26 | Abundant smooth muscle actin 26 | U05837 |
| ABR27 | Abundant smooth muscle actin 27 | U05838 |
| ABR28 | Abundant smooth muscle actin 28 | U05839 |
| ABR29 | Abundant smooth muscle actin 29 | U05840 |
| ABR30 | Abundant smooth muscle actin 30 | U05841 |
| ABR31 | Abundant smooth muscle actin 31 | U05842 |
| ABR32 | Abundant smooth muscle actin 32 | U05843 |
| ABR33 | Abundant smooth muscle actin 33 | U05844 |
| ABR34 | Abundant smooth muscle actin 34 | U05845 |
| ABR35 | Abundant smooth muscle actin 35 | U05846 |
| ABR36 | Abundant smooth muscle actin 36 | U05847 |
| ABR37 | Abundant smooth muscle actin 37 | U05848 |
| ABR38 | Abundant smooth muscle actin 38 | U05849 |
| ABR39 | Abundant smooth muscle actin 39 | U05850 |
| ABR40 | Abundant smooth muscle actin 40 | U05851 |
| ABR41 | Abundant smooth muscle actin 41 | U05852 |
| ABR42 | Abundant smooth muscle actin 42 | U05853 |
| ABR43 | Abundant smooth muscle actin 43 | U05854 |
| ABR44 | Abundant smooth muscle actin 44 | U05855 |
| ABR45 | Abundant smooth muscle actin 45 | U05856 |
| ABR46 | Abundant smooth muscle actin 46 | U05857 |
| ABR47 | Abundant smooth muscle actin 47 | U05858 |
| ABR48 | Abundant smooth muscle actin 48 | U05859 |
| ABR49 | Abundant smooth muscle actin 49 | U05860 |
| ABR50 | Abundant smooth muscle actin 50 | U05861 |
| ABR51 | Abundant smooth muscle actin 51 | U05862 |
| ABR52 | Abundant smooth muscle actin 52 | U05863 |
| ABR53 | Abundant smooth muscle actin 53 | U05864 |
| ABR54 | Abundant smooth muscle actin 54 | U05865 |
| ABR55 | Abundant smooth muscle actin 55 | U05866 |
| ABR56 | Abundant smooth muscle actin 56 | U05867 |
| ABR57 | Abundant smooth muscle actin 57 | U05868 |
| ABR58 | Abundant smooth muscle actin 58 | U05869 |
| ABR59 | Abundant smooth muscle actin 59 | U05870 |
| ABR60 | Abundant smooth muscle actin 60 | U05871 |
| ABR61 | Abundant smooth muscle actin 61 | U05872 |
| ABR62 | Abundant smooth muscle actin 62 | U05873 |
| ABR63 | Abundant smooth muscle actin 63 | U05874 |
| ABR64 | Abundant smooth muscle actin 64 | U05875 |
| ABR65 | Abundant smooth muscle actin 65 | U05876 |
| ABR66 | Abundant smooth muscle actin 66 | U05877 |
| ABR67 | Abundant smooth muscle actin 67 | U05878 |
| ABR68 | Abundant smooth muscle actin 68 | U05879 |
| ABR69 | Abundant smooth muscle actin 69 | U05880 |
| ABR70 | Abundant smooth muscle actin 70 | U05881 |
| ABR71 | Abundant smooth muscle actin 71 | U05882 |
| ABR72 | Abundant smooth muscle actin 72 | U05883 |
| ABR73 | Abundant smooth muscle actin 73 | U05884 |
| ABR74 | Abundant smooth muscle actin 74 | U05885 |
| ABR75 | Abundant smooth muscle actin 75 | U05886 |
| ABR76 | Abundant smooth muscle actin 76 | U05887 |
| ABR77 | Abundant smooth muscle actin 77 | U05888 |
| ABR78 | Abundant smooth muscle actin 78 | U05889 |
| ABR79 | Abundant smooth muscle actin 79 | U05890 |
| ABR80 | Abundant smooth muscle actin 80 | U05891 |
| ABR81 | Abundant smooth muscle actin 81 | U05892 |
| ABR82 | Abundant smooth muscle actin 82 | U05893 |
| ABR83 | Abundant smooth muscle actin 83 | U05894 |
| ABR84 | Abundant smooth muscle actin 84 | U05895 |
| ABR85 | Abundant smooth muscle actin 85 | U05896 |
| ABR86 | Abundant smooth muscle actin 86 | U05897 |
| ABR87 | Abundant smooth muscle actin 87 | U05898 |
| ABR88 | Abundant smooth muscle actin 88 | U05899 |
| ABR89 | Abundant smooth muscle actin 89 | U05900 |
| ABR90 | Abundant smooth muscle actin 90 | U05901 |
| ABR91 | Abundant smooth muscle actin 91 | U05902 |
| ABR92 | Abundant smooth muscle actin 92 | U05903 |
| ABR93 | Abundant smooth muscle actin 93 | U05904 |
| ABR94 | Abundant smooth muscle actin 94 | U05905 |
| ABR95 | Abundant smooth muscle actin 95 | U05906 |
| ABR96 | Abundant smooth muscle actin 96 | U05907 |
| ABR97 | Abundant smooth muscle actin 97 | U05908 |
| ABR98 | Abundant smooth muscle actin 98 | U05909 |
| ABR99 | Abundant smooth muscle actin 99 | U05910 |
| ABR100 | Abundant smooth muscle actin 100 | U05911 |

Supplemental Table S4: PCR primers used for qRT-PCR

| Gene name | Size of amplicon | Primers spanning different exons* | Size of amplicon | Accession Number |
|-----------|--|-----------------------------------|------------------|------------------|
| 18S rRNA | F 5' TGACTCAACACGGGAAACC R 5' TCGCTCCACCAACTAAGAAC | N/A | 114bp | NR_003286 |
| N-MALT1 | F 5' CTCCGCCTCAGTTGCCTAGA R 5' CAACCTTTTTACCCATTAACTTCA | E1 – E2 | 104bp | NM_006785 |
| BCL10 | F 5' GAAGTGAAGAAGGACGCCTTAG R 5' AGATGATCAAAATGTCTCTCAGC | E1 – E2 | 80bp | NM_003921 |
| NR4A3 | F 5' TTCCATCAGGTCAAACACTGC R 5' AATCCACGAAGGCACTGAAG | E6 – E7 | 84bp | NM_173198 |
| CD86 | F 5' GGAATGCTGCTGTGCTTATGC R 5' AGCACCAGAGAGCAGGAAGG | E1 – E2/3 | 121bp | NM_006889 |
| CD69 | F 5' CCACCAGTCCCCATTTCTCAA R 5' TTGGCCCACTGATAAGGCAAT | E2 – E3 | 125bp | NM_001781 |
| TLR6 | F 5' AACAAGTACCACAAGCTGAAG R 5' CTCTAATGTTAGCCCAAAAGAG | No, only one exon | 100bp | NM_006068 |
| CCR5 | F 5' ATCCGTTCCCCTACAAGAACTC R 5' GCAGGGCTCCGATGTATAATAA | E2 – E3 | 100bp | NM_000579 |
| CCR2A | F 5' GCGTTTAATCACATTCGAGTGTTT R 5' CCACTGGCAAATTAGGGAACAA | No | 77bp | NM_000647 |

*Where possible, one of each primer pair was designed to span an exon-exon junction to prevent amplification from any contaminated DNA. The primers for the MALT1 gene targeted its N-terminus, thus will only amplify the wild-type MALT1 but not the API2-MALT1 transcripts.

Supplemental Table S5: Summary of antibody and conditions used for immunohistochemistry or Western blot

| Protein | Primary antibody | Source | Antigen retrieval method | Conditions for immunohistochemistry or Western blot |
|---------------------------------|--|-----------------------------|--|---|
| BCL10 | Mouse monoclonal antibody to human BCL10 (clone 151) | In house | Microwave in DAKO target retrieval solution pH 6.0 for 25-35 mins. | For immunohistochemistry: primary antibody (1/50), 1 hour at RT; biotinylated rabbit antimouse antibody, 30 mins at RT; peroxidase-conjugated extroAvidin, 30 mins at RT. |
| MALT1 | Mouse monoclonal antibody to human C ⁺ -MALT1 | In house | Microwave in DAKO target retrieval solution pH 9.9 for 25 mins. | For immunohistochemistry: primary antibody (1/50), 1 hour at RT; biotinylated rabbit antimouse antibody, 30 mins at RT; peroxidase-conjugated extroAvidin, 30 mins at RT. |
| BCL2 | Mouse monoclonal antibody | Novocastra | Pressure cooking with citrate buffer pH 6.0 for 3 mins. | For immunohistochemistry: primary antibody (1/120), 1 hr at RT; biotinylated rabbit antimouse antibody, 30 mins at RT; peroxidase-conjugated extroAvidin, 30 mins at RT. |
| CD69 | Mouse monoclonal antibody | NeoMarkers | Pressure cooking with 1mM EDTA for 3 mins. | For immunohistochemistry: primary antibody (1/20), 1hr at RT; followed by polymer amplification system. |
| CD86 | Sheep CD86 polyclonal antibody | R & D | Pressure cooking with citrate buffer pH 6.0 for 3 mins. | For immunohistochemistry: primary antibody (1/60), 1 hr at RT; biotinylated donkey antisheep antibody, 30 mins at RT; peroxidase-conjugated extroAvidin, 30 mins at RT. |
| TLR6 | Rabbit polyclonal antibody | Abcam (ab62569) | N/A | For Western blot analysis: used in 1/6,000 dilution, overnight at 4°C in TBST with 5% milk and 1% BSA |
| Flag M2 | Mouse monoclonal antibody | Sigma (F3165) | N/A | For Western blot analysis: used in 1/10,000 dilution at 4°C in TBST with 5% milk and 1% BSA |
| β-actin | Mouse monoclonal antibody | Sigma (A5441) | N/A | For Western blot analysis: used in 1/1million dilution, overnight at 4°C in TBST with 5% milk and 1% BSA |
| Anti-rabbit IgG, HRP conjugated | Whole antibody from donkey | Amersham Bioscience (NA934) | N/A | For Western blot analysis, used as a secondary antibody in 1/20,000 dilution, 1h at RT in TBST with 5% milk and 1% BSA |
| Anti-mouse IgG, HRP conjugated | Whole antibody from sheep | Amersham Bioscience (NA931) | N/A | For Western blot analysis, used as a secondary antibody in 1/20,000 dilution, 1h at RT in TBST with 5% milk and 1% BSA |

RT: room temperature; TBST: Tris-Buffered Saline Tween-20; N/A: not applicable.

Table S6: Quality control metrics and criteria used regarding a microarray hybridisation acceptable for data analyses.*

| Sample | Title | Platform | Chip type | Average | | % Present | GAPDH 3'/5' ratio | GAPDH 3' / M | BioB | BioC | BioD | CreX |
|-----------|---|----------|--------------|----------------------|---------------|-----------|-------------------|--------------|---------|---------|---------|---------|
| | | | | Background | Scale Factors | | | | | | | |
| GSM346784 | MALT_Lymphoma_t(1;2)BCL10-IGK_1 | GPL96 | HG-U133A | 58 | 3.11 | 28 | 2.8 | 1.10 | Present | Present | Present | Present |
| GSM346786 | MALT_Lymphoma_t(1;14)BCL10-IGH_2 | GPL96 | HG-U133A | 58 | 2.28 | 41 | 8.4 | 1.03 | Present | Present | Present | Present |
| GSM346929 | MALT_Lymphoma_t(1;14)BCL10-IGH_3 | GPL96 | HG-U133A | 51 | 2.73 | 40 | 1.6 | 1.03 | Present | Present | Present | Present |
| GSM346938 | MALT_Lymphoma_t(1;14)BCL10-IGH_4 | GPL96 | HG-U133A | 56 | 2.21 | 41 | 1.3 | 1.15 | Present | Present | Present | Present |
| GSM346939 | MALT_Lymphoma_t(1;18)API2-MALT1_5 | GPL96 | HG-U133A | 61 | 3.37 | 36 | 5.2 | 1.05 | Present | Present | Present | Present |
| GSM346967 | MALT_Lymphoma_t(1;18)API2-MALT1_6 | GPL96 | HG-U133A | 66 | 1.94 | 45 | 1.3 | 1.05 | Present | Present | Present | Present |
| GSM347029 | MALT_Lymphoma_t(1;18)API2-MALT1_7 | GPL96 | HG-U133A | 57 | 4.54 | 31 | 5.3 | 1.09 | Present | Present | Present | Present |
| GSM347030 | MALT_Lymphoma_t(1;18)API2-MALT1_8 | GPL96 | HG-U133A | 56 | 2.58 | 42 | 1.7 | 1.06 | Present | Present | Present | Present |
| GSM347031 | MALT_Lymphoma_t(1;18)API2-MALT1_9 | GPL96 | HG-U133A | 57 | 2.15 | 36 | 1.6 | 1.05 | Present | Present | Present | Present |
| GSM347036 | MALT_Lymphoma_t(1;18)API2-MALT1_10 | GPL96 | HG-U133A | 50 | 2.54 | 44 | 2.3 | 1.10 | Present | Present | Present | Present |
| GSM347040 | MALT_Lymphoma_t(1;18)API2-MALT1_11 | GPL96 | HG-U133A | 64 | 1.32 | 48 | 1.4 | 1.15 | Present | Present | Present | Present |
| GSM347046 | MALT_Lymphoma_t(1;18)API2-MALT1_12 | GPL96 | HG-U133A | 57 | 1.46 | 42 | 3.1 | 1.02 | Present | Present | Present | Present |
| GSM347047 | MALT_Lymphoma_t(1;18)API2-MALT1_13 | GPL96 | HG-U133A | 43 | 4.84 | 34 | 2.0 | 1.02 | Present | Present | Present | Present |
| GSM347048 | MALT_Lymphoma_t(14;18)IGH-MALT1_14 | GPL96 | HG-U133A | 40 | 9.33 | 30 | 2.1 | 1.06 | Present | Present | Present | Present |
| GSM347049 | MALT_Lymphoma_t(14;18)IGH-MALT1_15 | GPL96 | HG-U133A | 72 | 1.57 | 38 | 1.4 | 1.02 | Present | Present | Present | Present |
| GSM347050 | MALT_Lymphoma_Translocation Negative_16 | GPL96 | HG-U133A | 69 | 1.54 | 40 | 2.2 | 1.03 | Present | Present | Present | Present |
| GSM347051 | MALT_Lymphoma_Translocation Negative_17 | GPL96 | HG-U133A | 60 | 1.26 | 52 | 1.1 | 1.03 | Present | Present | Present | Present |
| GSM347052 | MALT_Lymphoma_Translocation Negative_18 | GPL96 | HG-U133A | 53 | 6.28 | 23 | 4.0 | 1.04 | Present | Present | Present | Present |
| GSM347053 | MALT_Lymphoma_Translocation Negative_19 | GPL96 | HG-U133A | 52 | 3.16 | 40 | 2.3 | 1.08 | Present | Present | Present | Present |
| GSM347054 | MALT_Lymphoma_Translocation Negative_20 | GPL96 | HG-U133A | 47 | 12.99 | 17 | 7.7 | 1.04 | Present | Present | Present | Present |
| GSM347055 | MALT_Lymphoma_Translocation Negative_21 | GPL96 | HG-U133A | 44 | 1.60 | 54 | 2.5 | 1.18 | Present | Present | Present | Present |
| GSM347056 | MALT_Lymphoma_Translocation Negative_22 | GPL96 | HG-U133A | 49 | 4.03 | 36 | 1.7 | 1.10 | Present | Present | Present | Present |
| GSM347057 | MALT_Lymphoma_Translocation Negative_23 | GPL96 | HG-U133A | 45 | 4.25 | 39 | 4.1 | 1.04 | Present | Present | Present | Present |
| GSM347058 | MALT_Lymphoma_Translocation Negative_24 | GPL96 | HG-U133A | 62 | 1.21 | 45 | 1.2 | 1.05 | Present | Present | Present | Present |
| | | | | Mean of Scale factor | 3.43 | | | | | | | |
| | | | | Standard Deviation | 2.76 | | | | | | | |
| | | | | Mean +1SD | 6.19 | | | | | | | |
| | | | | Mean +2SD | 8.95 | | | | | | | |
| GSM347846 | Follicular_Lymphoma_1 | GPL570 | HG-U133plus2 | 57 | 3.35 | 36 | 1.9 | 1.03 | Present | Present | Present | Present |
| GSM347847 | Follicular_Lymphoma_2 | GPL570 | HG-U133plus2 | 29 | 7.84 | 35 | 1.7 | 1.03 | Present | Present | Present | Present |
| GSM347848 | Follicular_Lymphoma_3 | GPL570 | HG-U133plus2 | 39 | 8.93 | 29 | 2.2 | 1.05 | Present | Present | Present | Present |
| GSM347849 | Follicular_Lymphoma_4 | GPL570 | HG-U133plus2 | 29 | 10.50 | 32 | 2.0 | 1.03 | Present | Present | Present | Present |
| GSM347891 | Follicular_Lymphoma_5 | GPL570 | HG-U133plus2 | 37 | 4.03 | 39 | 9.2 | 1.17 | Present | Present | Present | Present |
| GSM347898 | Follicular_Lymphoma_6 | GPL570 | HG-U133plus2 | 40 | 5.37 | 31 | 2.4 | 1.06 | Present | Present | Present | Present |
| GSM347903 | Follicular_Lymphoma_7 | GPL570 | HG-U133plus2 | 35 | 4.60 | 37 | 2.0 | 1.06 | Present | Present | Present | Present |
| GSM347986 | Mantle_cell_lymphoma_1 | GPL570 | HG-U133plus2 | 52 | 1.77 | 40 | 2.1 | 1.06 | Present | Present | Present | Present |
| GSM347991 | Mantle_cell_lymphoma_2 | GPL570 | HG-U133plus2 | 49 | 1.21 | 40 | 1.7 | 1.02 | Present | Present | Present | Present |
| GSM347994 | Mantle_cell_lymphoma_3 | GPL570 | HG-U133plus2 | 51 | 1.77 | 39 | 1.4 | 1.01 | Present | Present | Present | Present |
| GSM347996 | Mantle_cell_lymphoma_4 | GPL570 | HG-U133plus2 | 47 | 1.27 | 45 | 1.6 | 1.02 | Present | Present | Present | Present |
| GSM347997 | Mantle_cell_lymphoma_5 | GPL570 | HG-U133plus2 | 45 | 1.43 | 43 | 1.5 | 1.02 | Present | Present | Present | Present |
| GSM347998 | Mantle_cell_lymphoma_6 | GPL570 | HG-U133plus2 | 45 | 1.84 | 40 | 1.4 | 1.03 | Present | Present | Present | Present |
| GSM347999 | Mantle_cell_lymphoma_7 | GPL570 | HG-U133plus2 | 43 | 1.59 | 41 | 1.7 | 1.02 | Present | Present | Present | Present |
| GSM348000 | Mantle_cell_lymphoma_8 | GPL570 | HG-U133plus2 | 51 | 1.61 | 39 | 1.4 | 1.03 | Present | Present | Present | Present |
| | | | | Mean of Scale factor | 3.81 | | | | | | | |
| | | | | Standard Deviation | 3.06 | | | | | | | |
| | | | | Mean +1SD | 6.87 | | | | | | | |
| | | | | Mean +2SD | 9.93 | | | | | | | |

1) RNA/cRNA quality: All RNA isolated and labelled were run on either MOPS gel or Agilent nano chip to ensure that RNA is intact and 18S and 28S bands are visible.

2) Chip hybridisation:

a) All the ".DAT" files were visually examined for possible artefacts;

b) average background was checked to be between 20 and 100;

c) a scaling factor < mean plus 2 SD within dataset derived from the same platform;

d) MASS.0 present call > 20%;

e) GAPDH 3'/5' ratio: The commonly accepted GAPDH 3'/5' ratio is <3.0. However, this threshold has been hugely debated, because 1) there is only one single 3' and one single 5' probe set for GAPDH. The lack of replicate probe sets makes it impossible to estimate the variance of these probe signals, thus the variance of 3'/5' ratio; 2) the probes are usually designed to be within the most 3' 600bp of a transcript, and the distance between 3' and 5' probe set of GAPDH is 9101, 869bp; 3) there is a lack of consistent results in calculation of GAPDH 3'/5' ratio using the MAS5.0, RMA and gcRMA algorithms; and 4) experimental data showed that GAPDH 3'/5' ratio was not an efficient approach for assessment of RNA quality (Li et al 2008; Archer et al 2006). Among our cases investigated, there are 4 cases (GSM346939, GSM347029, GSM347052 and GSM3407057) showing slightly higher GAPDH 3'/5' ratios, but all other quality control parameters including scale factor, present call, GAPDH3'/M and presence of other control probe signals are good. We performed a parallel full set of unsupervised clustering, gene set enrichment analyses and functional annotation using gene ontology with and without these 4 cases and found very similar results. Because of these reasons, we did not exclude the 4 cases

Li M, Reilly C. Assessing the quality of hybridized RNA in Affymetrix GeneChips using linear regression. J Biomol Tech. 2008; 19: 122-8.

Archer KJ, Dumur CI, Joel SE, Ramakrishnan V. Assessing quality of hybridized RNA in Affymetrix GeneChip experiments using mixed-effects models. Biostatistics. 2006; 7: 198-212.

Only the array hybridisation met the above criteria was used for subsequent data analyses. Those highlighted in green were excluded from subsequent data analysis.

Supplementary Table S7: Leading edge core set of NF- κ B target genes, which are differentially enriched in MALT lymphoma with and without chromosome translocation.

| Rank | Gene | Description | Chromosome Band | Entrez ID | to noise | Enrichment Score |
|---|---------|---|-----------------|-----------|----------|------------------|
| Expression of genes enriched in translocation negative MALT lymphoma | | | | | | |
| 1 | PTGS2 | prostaglandin-endoperoxide synthase 2 | 1q25.2-q25.3 | 5743 | 0.703 | 0.020 |
| 2 | PLAU | plasminogen activator, urokinase | 10q24 | 5328 | 0.681 | 0.040 |
| 3 | NR4A3 | nuclear receptor subfamily 4, group A, member 3 | 9q22 | 8013 | 0.676 | 0.060 |
| 4 | PTGIS | prostaglandin I2 (prostacyclin) synthase | 20q13.13 | 5740 | 0.647 | 0.079 |
| 5 | IL8 | interleukin 8 | 4q13-q21 | 3576 | 0.570 | 0.090 |
| 6 | CD86 | CD86 molecule | 3q21 | 942 | 0.557 | 0.105 |
| 7 | CCL2 | chemokine (C-C motif) ligand 2 | 17q11.2-q12 | 6347 | 0.508 | 0.112 |
| 8 | CCL11 | chemokine (C-C motif) ligand 11 | 17q21.1-q21.1 | 6356 | 0.503 | 0.126 |
| 9 | CXCL5 | chemokine (C-X-C motif) ligand 5 | 4q12-q13 | 6374 | 0.490 | 0.137 |
| 10 | CXCL1 | chemokine (C-X-C motif) ligand 1 | 4q21 | 2919 | 0.483 | 0.149 |
| 11 | IGFBP2 | insulin-like growth factor binding protein 2 | 2q33-q34 | 3485 | 0.482 | 0.163 |
| 12 | BDKRB1 | bradykinin receptor B1 | 14q32.1-q32.1 | 623 | 0.471 | 0.173 |
| 13 | NR4A2 | nuclear receptor subfamily 4, group A, member 2 | 2q22-q23 | 4929 | 0.469 | 0.186 |
| 14 | IL1B | interleukin 1, beta | 2q14 | 3553 | 0.454 | 0.195 |
| 15 | SDC4 | syndecan 4 | 20q12 | 6385 | 0.442 | 0.203 |
| 16 | FN1 | fibronectin 1 | 2q34 | 2335 | 0.435 | 0.213 |
| 17 | DEFB4 | defensin, beta 4 | 8p23.1-p22 | 1673 | 0.427 | 0.222 |
| 18 | IL1RN | interleukin 1 receptor antagonist | 2q14.2 | 3557 | 0.425 | 0.235 |
| 19 | MMP3 | matrix metalloproteinase 3 | 11q22.3 | 4314 | 0.425 | 0.246 |
| 20 | IER3 | immediate early response 3 | 6p21.3 | 8870 | 0.423 | 0.258 |
| 21 | SOD2 | superoxide dismutase 2, mitochondrial | 6q25.3 | 6648 | 0.405 | 0.263 |
| 22 | EGFR | epidermal growth factor receptor (erythroblastic leukemia viral (7p12 | 7p12 | 1956 | 0.404 | 0.274 |
| 23 | THBS2 | thrombospondin 2 | 6q27 | 7058 | 0.389 | 0.276 |
| 24 | ICOS | inducible T-cell co-stimulator | 2q33 | 29851 | 0.380 | 0.282 |
| 25 | CXCL2 | chemokine (C-X-C motif) ligand 2 | 4q21 | 2920 | 0.372 | 0.288 |
| 26 | GZMB | granzyme B (granzyme 2, cytotoxic T-lymphocyte-associated se | 14q11.2 | 3002 | 0.357 | 0.287 |
| 27 | TNC | tenascin C | 9q33 | 3371 | 0.354 | 0.295 |
| 28 | AGT | angiotensinogen (serpin peptidase inhibitor, clade A, member 8) | 14q42-q43 | 183 | 0.328 | 0.285 |
| 29 | TLR2 | toll-like receptor 2 | 4q32 | 7097 | 0.327 | 0.292 |
| 30 | GADD45B | growth arrest and DNA-damage-inducible, beta | 19p13.3 | 4616 | 0.320 | 0.297 |
| 31 | TFF3 | trefoil factor 3 (intestinal) | 21q22.3 | 7033 | 0.313 | 0.299 |
| 32 | PRF1 | perforin 1 (pore forming protein) | 10q22 | 5551 | 0.312 | 0.307 |
| 33 | EGR1 | early growth response 1 | 5q31.1 | 1958 | 0.306 | 0.310 |
| 34 | BMP2 | bone morphogenetic protein 2 | 20p12 | 650 | 0.305 | 0.319 |
| Expression of genes enriched in translocation positive MALT lymphoma | | | | | | |
| 127 | KLK3 | kallikrein-related peptidase 3 | 19q13.41 | 354 | -0.257 | -0.133 |
| 128 | CD44 | CD44 molecule | 11p13 | 960 | -0.266 | -0.133 |
| 129 | TERT | telomerase reverse transcriptase | 5p15.33 | 7015 | -0.276 | -0.133 |
| 130 | C4BPA | complement component 4 binding protein, alpha | 1q32 | 722 | -0.278 | -0.126 |
| 131 | IRF7 | interferon regulatory factor 7 | 11p15.5 | 3665 | -0.282 | -0.120 |
| 132 | LTB | lymphotoxin beta (TNF superfamily, member 3) | 6p21.3 | 4050 | -0.300 | -0.121 |
| 133 | BCL10 | B-cell CLL/lymphoma 10 | 1p22 | 8915 | -0.302 | -0.113 |
| 134 | IFI44L | interferon-induced protein 44-like | 1p31.1 | 10964 | -0.306 | -0.106 |
| 135 | CCR5 | chemokine (C-C motif) receptor 5 | 3p21 | 1234 | -0.309 | -0.099 |
| 136 | CCR7 | chemokine (C-C motif) receptor 7 | 17q12-q21.2 | 1236 | -0.362 | -0.114 |
| 137 | REL | v-rel reticuloendotheliosis viral oncogene homolog | 2p13-p12 | 5966 | -0.411 | -0.117 |
| 138 | PRDM2 | PR domain containing 2, with ZNF domain | 1p36.21 | 7799 | -0.414 | -0.105 |
| 139 | IRF4 | interferon regulatory factor 4 | 6p25-p23 | 3662 | -0.493 | -0.106 |
| 140 | TFEC | transcription factor EC | 7q31.2 | 22797 | -0.518 | -0.093 |
| 141 | TLR6 | toll-like receptor 6 | 4p14 | 10333 | -0.542 | -0.079 |
| 142 | CCR2B | chemokine (C-C motif) receptor 2 isoform B | 3p21.31 | 1231 | -0.560 | -0.063 |
| 143 | CD69 | CD69 molecule | 12p13-p12 | 969 | -0.573 | -0.047 |
| 144 | BCL2 | B-cell CLL/lymphoma 2 | 18q21.33 | 596 | -0.690 | -0.030 |
| 145 | CCR2A | chemokine (C-C motif) receptor 2 isoform A | 3p21.31 | 1231 | -1.080 | 0.000 |

Supplementary Table S8: Leading edge core set of genes positively regulating NF-kB cascade (GO:43123), which are differentially enriched in MALT lymphoma with and without chromosome translocation.

| Rank | Gene | Description | Chromosome Band | EntrezID | Signal to noise ratio | Enrichment Score | NF-kB target gene |
|---|---------|--|-----------------|----------|-----------------------|------------------|-------------------|
| Expression of genes enriched in translocation positive MALT lymphoma | | | | | | | |
| 1 | MALT1 | N- MALT1 N-terminal | 18q21 | 10892 | -0.681 | 0.0025 | |
| 2 | TRAF5 | TNF receptor-associated factor 5 | 1q32 | 7188 | -0.556 | -0.0586 | |
| 3 | TLR6 | toll-like receptor 6 | 4p14 | 10333 | -0.542 | -0.111 | YES |
| 4 | CASP8 | caspase 8, apoptosis-related cysteine peptidase | 2q33-q34 | 841 | -0.5 | -0.16 | |
| 5 | EEF1D | eukaryotic translation elongation factor 1 delta (guanine nucleotide | 8q24.3 | 1936 | -0.499 | -0.208 | |
| 6 | REL | v-rel reticuloendotheliosis viral oncogene homolog (avian) | 2p13-p12 | 5966 | -0.411 | -0.239 | YES |
| 7 | TRIM13 | tripartite motif-containing 13 | 13q14 | 10206 | -0.404 | -0.277 | |
| 8 | ZDHHC17 | zinc finger, DHHC-type containing 17 | 12q21.2 | 23390 | -0.383 | -0.311 | |
| 9 | MALT1_C | MALT1 C-terminal | 18q21 | 10892 | -0.375 | -0.345 | |
| 10 | BCL10 | B-cell CLL/lymphoma 10 | 1p22 | 8915 | -0.302 | -0.347 | YES |
| 11 | LTB | lymphotoxin beta (TNF superfamily, member 3) | 6p21.3 | 4050 | -0.3 | -0.375 | YES |
| 12 | TRIM38 | tripartite motif-containing 38 | 6p21.3 | 10475 | -0.272 | -0.387 | |
| Expression of genes enriched in translocation negative MALT lymphoma | | | | | | | |
| 38 | GJA1 | gap junction protein, alpha 1, 43kDa | 6q21-q23.2 | 2697 | 0.31 | 0.0986 | |
| 39 | SECTM1 | secreted and transmembrane 1 | 17q25 | 6398 | 0.334 | 0.0892 | |
| 40 | ECM1 | extracellular matrix protein 1 | 1q21 | 1893 | 0.361 | 0.0793 | |
| 41 | PLK2 | polo-like kinase 2 (Drosophila) | 5q12.1-q13.2 | 10769 | 0.411 | 0.0756 | |
| 42 | IL1B | interleukin 1, beta | 2q14 | 3553 | 0.454 | 0.055 | YES |
| 43 | GPR177 | G protein-coupled receptor 177 | 1p31.3 | 79971 | 0.464 | 0.0147 | |

Supplementary Table S9: Leading edge core set of the genes related to responses to chemical stimulus, which are differentially enriched in MALT lymphoma with and without chromosome translocation.

| Rank | Gene | Description | Chromosome Band | Entrez ID | Signal to noise ratio | Enrichment Score | NF-kB target gene |
|---|----------|--|-----------------|-----------|-----------------------|------------------|-------------------|
| Expression of genes enriched in translocation negative MALT lymphoma | | | | | | | |
| 1 | PLAU | plasminogen activator, urokinase | 10q24 | 5328 | 0.681 | 0.0237 | YES |
| 2 | IL8 | interleukin 8 | 4q13-q21 | 3576 | 0.57 | 0.0388 | YES |
| 3 | FPR1 | formyl peptide receptor 1 | 19q13.4 | 2357 | 0.553 | 0.0571 | |
| 4 | CCL2 | chemokine (C-C motif) ligand 2 | 17q11.2-q12 | 6347 | 0.508 | 0.068 | YES |
| 5 | CCL11 | chemokine (C-C motif) ligand 11 | 17q21.1-q21.2 | 6356 | 0.503 | 0.0859 | YES |
| 6 | CXCL5 | chemokine (C-X-C motif) ligand 5 | 4q12-q13 | 6374 | 0.49 | 0.101 | YES |
| 7 | PLAUR | plasminogen activator, urokinase receptor | 19q13 | 5329 | 0.485 | 0.116 | |
| 8 | CXCL1 | chemokine (C-X-C motif) ligand 1 | 4q21 | 2919 | 0.483 | 0.134 | YES |
| 9 | FOSL1 | FOS-like antigen 1 | 11q13 | 8061 | 0.472 | 0.148 | |
| 10 | SEMA3C | sema domain, immunoglobulin domain (Ig) | 7q21-q31 | 10512 | 0.457 | 0.159 | |
| 11 | CLEC7A | C-type lectin domain family 7, member A | 12p13.2 | 64581 | 0.436 | 0.168 | |
| 12 | DEFB4 | defensin, beta 4 | 8p23.1-p22 | 1673 | 0.427 | 0.179 | YES |
| 13 | GSTM3 | glutathione S-transferase M3 (brain) | 1p13.3 | 2947 | 0.421 | 0.191 | |
| 14 | SERPINH1 | serpin peptidase inhibitor, clade H | 11q13.5 | 871 | 0.416 | 0.204 | |
| 15 | SOD2 | superoxide dismutase 2, mitochondrial | 6q25.3 | 6648 | 0.405 | 0.215 | YES |
| 16 | DNAJB5 | DnaJ (Hsp40) homolog, subfamily B, member 5 | 9p13.3 | 25822 | 0.405 | 0.23 | |
| 17 | DHCR24 | 24-dehydrocholesterol reductase | 1p33-p31.1 | 1718 | 0.39 | 0.235 | |
| 18 | MTIX | metallothionein 1X | 16q13 | 4501 | 0.386 | 0.246 | |
| 19 | CCL8 | chemokine (C-C motif) ligand 8 | 17q11.2 | 6355 | 0.384 | 0.26 | |
| 20 | HSPB7 | heat shock 27kDa protein family, member 7 | 1p36.23-p34.3 | 27129 | 0.375 | 0.268 | |
| 21 | CXCL2 | chemokine (C-X-C motif) ligand 2 | 4q21 | 2920 | 0.372 | 0.28 | YES |
| 22 | CCL18 | chemokine (C-C motif) ligand 18 | 17q11.2 | 6362 | 0.368 | 0.291 | |
| 23 | DUOX2 | dual oxidase 2 | 15q15.3 | 50506 | 0.357 | 0.295 | |
| 24 | HSPA2 | heat shock 70kDa protein 2 | 14q24.1 | 3306 | 0.341 | 0.295 | |
| 25 | SCARA3 | scavenger receptor class A, member 3 | 8p21 | 51435 | 0.331 | 0.299 | |
| 26 | NDUFS8 | NADH dehydrogenase (ubiquinone) | 11q13 | 4728 | 0.328 | 0.309 | |
| 27 | PPARG | peroxisome proliferator-activated receptor gamma | 3p25 | 5468 | 0.326 | 0.319 | |
| 28 | RALA | v-ral simian leukemia viral oncogene homolog A | 7p15-p13 | 5898 | 0.313 | 0.319 | |
| 29 | CCL13 | chemokine (C-C motif) ligand 13 | 17q11.2 | 6357 | 0.31 | 0.327 | |
| 30 | KRT19 | keratin 19 | 17q21.2 | 3880 | 0.309 | 0.337 | |
| 31 | NDUFA6 | NADH dehydrogenase (ubiquinone) 1 alpha subcomplex | 22q13.2-q13.31 | 4700 | 0.261 | 0.295 | |
| 32 | ME1 | malic enzyme 1, NADP(+)-dependent, cytosolic | 6q12 | 4199 | 0.258 | 0.302 | |
| 33 | ENSA | endosulfine alpha | 1q21.2 | 2029 | 0.257 | 0.31 | |
| 34 | C5AR1 | complement component 5a receptor 1 | 19q13.3-q13.4 | 728 | 0.246 | 0.307 | |
| 35 | SLC22A18 | solute carrier family 22, member 18 | 11p15.5 | 5002 | 0.246 | 0.315 | |
| 36 | ABAT | 4-aminobutyrate aminotransferase | 16p13.2 | 18 | 0.241 | 0.319 | |
| 37 | STC1 | stanniocalcin 1 | 8p21-p11.2 | 6781 | 0.24 | 0.326 | |
| 38 | DNAJB4 | DnaJ (Hsp40) homolog, subfamily B, member 4 | 1p31.1 | 11080 | 0.239 | 0.333 | |
| 39 | LTB4R2 | leukotriene B4 receptor 2 | 14q11.2-q12 | 56413 | 0.236 | 0.34 | |
| 40 | CXCL9 | chemokine (C-X-C motif) ligand 9 | 4q21 | 4283 | 0.232 | 0.342 | YES |
| 41 | CHIA | chitinase, acidic | 1p13.1-p21.3 | 27159 | 0.226 | 0.341 | |
| 42 | HSPB1 | heat shock 27kDa protein 1 | 7q11.23 | 3315 | 0.224 | 0.347 | |
| Expression of genes enriched in translocation positive MALT lymphoma | | | | | | | |
| 112 | CCR7 | chemokine (C-C motif) receptor 7 | 17q12-q21.2 | 1236 | -0.362 | -0.0912 | YES |
| 113 | CCR6 | chemokine (C-C motif) receptor 6 | 6q27 | 1235 | -0.376 | -0.0815 | |
| 114 | CXCR4 | chemokine (C-X-C motif) receptor 4 | 2q21 | 7852 | -0.378 | -0.0683 | |
| 115 | HSPA6 | heat shock 70kDa protein 6 (HSP70B') | 1q23 | 3310 | -0.449 | -0.07 | |
| 116 | PMAIP1 | phorbol-12-myristate-13-acetate-induced protein 1 | 18q21.32 | 5366 | -0.663 | -0.0621 | |
| 117 | BCL2 | B-cell CLL/lymphoma 2 | 18q21.33 | 596 | -0.69 | -0.0375 | YES |
| 118 | CCR2 | chemokine (C-C motif) receptor 2 | 3p21.31 | 1231 | -1.08 | -9.65E-16 | YES |

Supplementary Table S10: Leading edge core set of defense response related genes, which are differentially enriched in MALT lymphoma with and without chromosome translocation.

| Rank | Gene | Description | Chromosome Band | Entrez ID | Signal to noise ratio | Enrichment Score | NF-kB target gene |
|---|----------|---|-----------------|-----------|-----------------------|------------------|-------------------|
| Expression of genes enriched in translocation positive MALT lymphoma | | | | | | | |
| 1 | CCR2 | chemokine (C-C motif) receptor 2 | 3p21.31 | 1231 | -1.08 | 2.14E-14 | YES |
| 2 | CD1D | CD1d molecule | 1q22-q23 | 912 | -0.794 | -0.0379 | |
| 3 | RNASE6 | ribonuclease, RNase A family, k6 | 14q11.2 | 6039 | -0.706 | -0.0659 | |
| 4 | BCL2 | B-cell CLL/lymphoma 2 | 18q21.33 | 596 | -0.69 | -0.0911 | YES |
| 5 | TLR6 | toll-like receptor 6 | 4p14 | 10333 | -0.542 | -0.11 | YES |
| 6 | HDAC9 | histone deacetylase 9 | 7p21.1 | 9734 | -0.536 | -0.129 | |
| 7 | BLNK | B-cell linker | 10q23.2-q23.33 | 29760 | -0.447 | -0.138 | |
| 8 | MNDA | myeloid cell nuclear differentiation antigen | 1q22 | 4332 | -0.432 | -0.151 | |
| 9 | CXCR4 | chemokine (C-X-C motif) receptor 4 | 2q21 | 7852 | -0.378 | -0.152 | |
| 10 | CCR6 | chemokine (C-C motif) receptor 6 | 6q27 | 1235 | -0.376 | -0.164 | |
| 11 | MICB | MHC class I polypeptide-related sequence B | 6p21.3 | 4277 | -0.372 | -0.177 | |
| 12 | CCR7 | chemokine (C-C motif) receptor 7 | 17q12-q21.2 | 1236 | -0.362 | -0.187 | YES |
| 13 | SP140 | SP140 nuclear body protein | 2q37.1 | 11262 | -0.352 | -0.197 | |
| 14 | LYST | lysosomal trafficking regulator | 1q42.1-q42.2 | 1130 | -0.324 | -0.196 | |
| 15 | TLR7 | toll-like receptor 7 | Xp22.3 | 51284 | -0.323 | -0.207 | |
| 16 | HP | haptoglobin | 16q22.1 | 3240 | -0.32 | -0.218 | |
| 17 | BCL10 | B-cell CLL/lymphoma 10 | 1p22 | 8915 | -0.302 | -0.219 | YES |
| 18 | FAIM3 | Fas apoptotic inhibitory molecule 3 | 1q32.1 | 9214 | -0.297 | -0.227 | |
| 19 | CYBB | Cytochrome b-245, beta polypeptide | Xp21.1 | 1536 | -0.29 | -0.235 | |
| Expression of genes enriched in translocation negative MALT lymphoma | | | | | | | |
| 78 | FOS | v-fos FBJ murine osteosarcoma viral oncogene homolog | 14q24.3 | 2353 | 0.222 | 0.197 | |
| 79 | INHBA | Inhibin, beta A | 7p15-p13 | 3624 | 0.228 | 0.197 | |
| 80 | ELF3 | E74-like factor 3 | 1q32.2 | 1999 | 0.23 | 0.19 | YES |
| 81 | CXCL9 | chemokine (C-X-C motif) ligand 9 | 4q21 | 4283 | 0.232 | 0.185 | YES |
| 82 | CEBPG | CCAAT/enhancer binding protein (C/EBP), gamma | 19q13.11 | 1054 | 0.24 | 0.188 | |
| 83 | C5AR1 | complement component 5a receptor 1 | 19q13.3-q13.4 | 728 | 0.246 | 0.187 | |
| 84 | COLEC1 | collectin sub-family member 12 | 18pter-p11.3 | 81035 | 0.25 | 0.18 | |
| 85 | TNFRSF1A | Tumor necrosis factor receptor superfamily, member 1A | 12p13.2 | 7132 | 0.259 | 0.184 | |
| 86 | CFP | complement factor properdin | Xp11.3-p11.23 | 5199 | 0.262 | 0.178 | |
| 87 | MST1R | macrophage stimulating 1 receptor | 3p21.3 | 4486 | 0.27 | 0.175 | |
| 88 | AOC3 | Amine oxidase, copper containing 3 | 17q21 | 8639 | 0.295 | 0.194 | |
| 89 | GNLY | granulysin | 2p11.2 | 10578 | 0.304 | 0.192 | |
| 90 | CCL13 | chemokine (C-C motif) ligand 13 | 17q11.2 | 6357 | 0.31 | 0.187 | |
| 91 | PRF1 | perforin 1 (pore forming protein) | 10q22 | 5551 | 0.312 | 0.178 | YES |
| 92 | TFF3 | trefoil factor 3 (intestinal) | 21q22.3 | 7033 | 0.313 | 0.167 | YES |
| 93 | KIR3DL2 | Killer cell immunoglobulin-like receptor | 19q13.4 | 3812 | 0.321 | 0.164 | |
| 94 | TYROBP | TYRO protein tyrosine kinase binding protein | 19q13.1 | 7305 | 0.326 | 0.156 | |
| 95 | LSP1 | lymphocyte-specific protein 1 | 11p15.5 | 4046 | 0.34 | 0.157 | |
| 96 | TPST1 | tyrosylprotein sulfotransferase 1 | 7q11.21 | 8460 | 0.36 | 0.16 | |
| 97 | ADORA2A | adenosine A2a receptor | 22q11.23 | 135 | 0.365 | 0.149 | |
| 98 | CXCL2 | chemokine (C-X-C motif) ligand 2 | 4q21 | 2920 | 0.372 | 0.142 | YES |
| 99 | NCF2 | neutrophil cytosolic factor 2 | 1q25 | 4688 | 0.373 | 0.129 | |
| 100 | S100A8 | S100 calcium binding protein A8 | 1q21 | 6279 | 0.389 | 0.126 | |
| 101 | C2 | complement component 2 | 6p21.3 | 717 | 0.397 | 0.117 | |
| 102 | ANXA1 | annexin A1 | 9q12-q21.2 | 301 | 0.418 | 0.113 | |
| 103 | LGALS3 | Lectin, galactoside-binding, soluble, 3 binding protein | 17q25 | 3959 | 0.467 | 0.118 | |
| 104 | FOSL1 | FOS-like antigen 1 | 11q13 | 8061 | 0.472 | 0.103 | |
| 105 | CXCL1 | Chemokine (C-X-C motif) ligand 1 | 4q21 | 2919 | 0.483 | 0.0891 | YES |
| 106 | S100A9 | S100 calcium binding protein A9 | 1q21 | 6280 | 0.487 | 0.0731 | |
| 107 | CCL11 | chemokine (C-C motif) ligand 11 | 17q21.1-q21.2 | 6356 | 0.503 | 0.0601 | YES |
| 108 | TNFAIP6 | Tumor necrosis factor, alpha-induced protein 6 | 2q23.3 | 7130 | 0.52 | 0.0459 | |
| 109 | MGLL | monoglyceride lipase | 3q21.3 | 11343 | 0.561 | 0.0325 | |
| 110 | IL8 | interleukin 8 | 4q13-q21 | 3576 | 0.57 | 0.0133 | YES |

Supplementary Table S11: Leading edge core set of genes related to innate immune response regulation (GO:45087), which are differentially enriched in MALT lymphoma with and without chromosome translocation.

| Rank | Gene | Description | Chromosome Band | EntrezID | Signal to noise ratio | Enrichment Score | NF- κ B target gene |
|---|----------|---|-----------------|----------|-----------------------|------------------|----------------------------|
| Expression of genes enriched in translocation negative MALT lymphoma | | | | | | | |
| 1 | CFB | complement factor B | 6p21.3 | 629 | 0.644 | 0.0653 | |
| 2 | CFD | complement factor D (adipsin) | 19p13.3 | 1675 | 0.573 | 0.121 | |
| 3 | CLEC7A | C-type lectin domain family 7, member A | 12p13.2 | 64581 | 0.436 | 0.133 | |
| 4 | IL1R1 | interleukin 1 receptor, type I | 2q12 | 3554 | 0.428 | 0.174 | |
| 5 | C2 | complement component 2 | 6p21.3 | 717 | 0.397 | 0.2 | |
| 6 | CFH | H factor 1 (complement) | 1q31.3 | 3075 | 0.36 | 0.213 | |
| 7 | TLR2 | toll-like receptor 2 | 4q32 | 7097 | 0.327 | 0.221 | YES |
| 8 | C1QA | complement component 1, A chain | 1p36.12 | 712 | 0.303 | 0.231 | |
| 9 | TUBB2C | tubulin, beta 2C | 9q34 | 10383 | 0.279 | 0.233 | |
| 10 | C1QB | complement component 1, B chain | 1p36.12 | 713 | 0.277 | 0.26 | |
| 11 | CFP | complement factor properdin | Xp11.3-p11.23 | 5199 | 0.262 | 0.273 | |
| 12 | CFI | complement factor I | 4q25 | 3426 | 0.253 | 0.29 | |
| 13 | COLEC12 | collectin sub-family member 12 | 18pter-p11.3 | 81035 | 0.25 | 0.31 | |
| 14 | CEBPG | CCAAT/enhancer binding protein | 19q13.11 | 1054 | 0.24 | 0.325 | |
| 15 | CFH | complement factor H | 1q32 | 3075 | 0.23 | 0.335 | |
| Expression of genes enriched in translocation positive MALT lymphoma | | | | | | | |
| 30 | CR1 | complement component (3b/4b) receptor 1 | 1q32 | 1378 | -0.105 | -0.0348 | |
| 31 | HSPC111 | hypothetical protein HSPC111 | 5q35.2 | 51491 | -0.116 | -0.0365 | |
| 32 | KRT1 | keratin 1 | 12q12-q13 | 3848 | -0.128 | -0.0372 | |
| 33 | APOBEC3G | apolipoprotein B mRNA editing enzyme | 22q13.1-q13.2 | 60489 | -0.132 | -0.029 | |
| 34 | CD180 | CD180 molecule | 5q12 | 4064 | -0.169 | -0.0623 | |
| 35 | IFIH1 | interferon induced with helicase C domain 1 | 2q24 | 64135 | -0.222 | -0.105 | |
| 36 | DDX58 | DEAD (Asp-Glu-Ala-Asp) box polypeptide 58 | 9p12 | 23586 | -0.229 | -0.0896 | |
| 37 | TLR1 | toll-like receptor 1 | 4p14 | 7096 | -0.27 | -0.095 | |
| 38 | C4BPA | complement component 4 binding protein, alpha | 1q32 | 722 | -0.278 | -0.0723 | YES |
| 39 | BCL10 | B-cell CLL/lymphoma 10 | 1p22 | 8915 | -0.302 | -0.0542 | YES |
| 40 | TLR7 | toll-like receptor 7 | Xp22.3 | 51284 | -0.323 | -0.0322 | |
| 41 | CR2 | complement component receptor 2 | 1q32 | 1380 | -0.337 | -0.00162 | |
| 42 | TLR6 | toll-like receptor 6 | 4p14 | 10333 | -0.542 | 0.00788 | YES |

Supplementary Table S12: Leading edge core set of genes related to immune response regulation (GO:6955), which are differentially enriched in MALT lymphoma with and without chromosome translocation.

| Rank | Gene | Description | Chromosome Band | Entrez ID | Signal to noise ratio | Enrichment Score | NF-kB target gene |
|---|------------|---|-----------------|-----------|-----------------------|------------------|-------------------|
| Expression of genes enriched in translocation positive MALT lymphoma | | | | | | | |
| 1 | CCR2 | chemokine (C-C motif) receptor 2 | 3p21.31 | 1231 | -1.08 | 2.24E-14 | YES |
| 2 | CD1D | CD1d molecule | 1q22-q23 | 912 | -0.794 | -0.0431 | |
| 3 | BCL2 | B-cell CLL/lymphoma 2 | 18q21.33 | 596 | -0.69 | -0.0745 | YES |
| 4 | MALT1_N_te | MALT1 N-terminal | 18q21.33 | 10892 | -0.681 | -0.102 | |
| 5 | AIM2 | absent in melanoma 2 | 1q22 | 9447 | -0.612 | -0.129 | |
| 6 | LY86 | lymphocyte antigen 86 | 6p25.1 | 9450 | -0.585 | -0.153 | |
| 7 | TLR6 | toll-like receptor 6 | 4p14 | 10333 | -0.542 | -0.174 | YES |
| 8 | IRF4 | interferon regulatory factor 4 | 6p25-p23 | 3662 | -0.493 | -0.192 | YES |
| 9 | EBI2 | EBV-induced G protein-coupled receptor 2 | 13q32.3 | 1880 | -0.486 | -0.211 | |
| 10 | BLNK | B-cell linker | 10q23.2-q23.33 | 29760 | -0.447 | -0.225 | |
| 11 | CXCR4 | chemokine (C-X-C motif) receptor 4 | 2q21 | 7852 | -0.378 | -0.225 | |
| 12 | CCR6 | chemokine (C-C motif) receptor 6 | 6q27 | 1235 | -0.376 | -0.24 | |
| 13 | MALT1_C_te | MALT1 C-terminal | 18q21.33 | 10892 | -0.375 | -0.256 | |
| 14 | MICB | MHC class I polypeptide-related sequence B | 6p21.3 | 4277 | -0.372 | -0.27 | |
| 15 | LYST | lysosomal trafficking regulator | 1q42.1-q42.2 | 1130 | -0.324 | -0.265 | |
| 16 | TLR7 | toll-like receptor 7 | Xp22.3 | 51284 | -0.323 | -0.278 | |
| 17 | LY9 | lymphocyte antigen 9 | 1q21.3-q22 | 4063 | -0.314 | -0.287 | |
| 18 | BCL10 | B-cell CLL/lymphoma 10 | 1p22 | 8915 | -0.302 | -0.292 | YES |
| 19 | IGHG1 | immunoglobulin heavy constant gamma 1 | 14q32.33 | 3500 | -0.283 | -0.294 | |
| Expression of genes enriched in translocation negative MALT lymphoma | | | | | | | |
| 75 | GBP2 | guanylate binding protein 2, interferon-inducible | 1p22.2 | 2634 | 0.236 | 0.142 | |
| 76 | CEBPG | CCAAT/enhancer binding protein (C/EBP), gamma | 19q13.11 | 1054 | 0.24 | 0.138 | |
| 77 | SBNO2 | strawberry notch homolog 2 (Drosophila) | 19p13.3 | 22904 | 0.248 | 0.137 | |
| 78 | CD8A | CD8a molecule | 2p12 | 925 | 0.258 | 0.138 | |
| 79 | AP2B1 | adaptor-related protein complex 2, beta 1 subunit | 17q11.2-q12 | 163 | 0.259 | 0.129 | |
| 80 | CD1E | CD1e molecule | 1q22-q23 | 913 | 0.26 | 0.12 | |
| 81 | FCN1 | ficolin (collagen/fibrinogen domain containing) 1 | 9q34 | 2219 | 0.262 | 0.111 | |
| 82 | IGSF6 | immunoglobulin superfamily, member 6 | 16p12-p13 | 10261 | 0.271 | 0.108 | |
| 83 | VNN1 | vanin 1 | 6q23-q24 | 8876 | 0.282 | 0.11 | |
| 84 | CD8B | CD8b molecule | 2p12 | 926 | 0.291 | 0.109 | |
| 85 | CD28 | CD28 molecule | 2q33 | 940 | 0.298 | 0.103 | |
| 86 | LCP2 | lymphocyte cytosolic protein 2 | 5q33.1-qter | 3937 | 0.316 | 0.11 | |
| 87 | THY1 | Thy-1 cell surface antigen | 11q22.3-q23 | 7070 | 0.322 | 0.103 | |
| 88 | PPARG | peroxisome proliferator-activated receptor gamma | 3p25 | 5468 | 0.326 | 0.0929 | |
| 89 | CCL18 | chemokine (C-C motif) ligand 18 | 17q11.2 | 6362 | 0.368 | 0.114 | |
| 90 | ICOS | inducible T-cell co-stimulator | 2q33 | 29851 | 0.38 | 0.107 | YES |
| 91 | PXDN | peroxidasin homolog (Drosophila) | 2p25 | 7837 | 0.477 | 0.136 | |
| 92 | CCL2 | chemokine (C-C motif) ligand 2 | 17q11.2-q12 | 6347 | 0.508 | 0.125 | YES |
| 93 | IL1R2 | interleukin 1 receptor, type II | 2q12-q22 | 7850 | 0.533 | 0.109 | |
| 94 | CD86 | CD86 molecule | 3q21 | 942 | 0.557 | 0.0899 | YES |
| 95 | IL8 | interleukin 8 | 4q13-q21 | 3576 | 0.57 | 0.0687 | YES |
| 96 | BCL6 | B-cell CLL/lymphoma 6 | 3q27 | 604 | 0.584 | 0.0466 | |
| 97 | NFIL3 | nuclear factor, interleukin 3 regulated | 9q22 | 4783 | 0.698 | 0.0277 | |

Supplementary table S13: Leading edge core set of genes related to cation homeostasis, which are differentially enriched in MALT lymphoma with and without chromosome translocation.

| Rank | Gene | Description | Chromosome Band | Entrez ID | Signal to noise ratio | Enrichment Score | NF-kB target gene |
|---|--------|---|-----------------|-----------|-----------------------|------------------|-------------------|
| Expression of genes enriched in translocation negative MALT lymphoma | | | | | | | |
| 1 | CCL2 | chemokine (C-C motif) ligand 2 | 17q11.2-q12 | 6347 | 0.508 | 0.0276 | YES |
| 2 | CCL11 | chemokine (C-C motif) ligand 11 | 17q21.1-q21.2 | 6356 | 0.503 | 0.0711 | YES |
| 3 | BDKRB1 | bradykinin receptor B1 | 14q32.1-q32.2 | 623 | 0.471 | 0.103 | YES |
| 4 | EDNRA | endothelin receptor type A | 4q31.23 | 1909 | 0.426 | 0.123 | |
| 5 | ATP1A2 | ATPase, Na ⁺ /K ⁺ transporting, alpha 2 (+) polypeptide | 1q21-q23 | 477 | 0.413 | 0.153 | |
| 6 | BDKRB2 | bradykinin receptor B2 | 14q32.1-q32.2 | 624 | 0.365 | 0.155 | |
| 7 | MT2A | metallothionein 2A | 16q13 | 4502 | 0.335 | 0.161 | |
| 8 | F2RL1 | coagulation factor II (thrombin) receptor-like 1 | 5q13 | 2150 | 0.331 | 0.188 | |
| 9 | PLCE1 | phospholipase C, epsilon 1 | 10q23 | 51196 | 0.323 | 0.209 | |
| 10 | THY1 | Thy-1 cell surface antigen | 11q22.3-q23 | 7070 | 0.322 | 0.237 | |
| 11 | SLC9A1 | solute carrier family 9 | 1p36.1-p35 | 6548 | 0.317 | 0.26 | |
| 12 | CCL13 | chemokine (C-C motif) ligand 13 | 17q11.2 | 6357 | 0.31 | 0.281 | |
| Expression of genes enriched in translocation positive MALT lymphoma | | | | | | | |
| 43 | CCR7 | chemokine (C-C motif) receptor 7 | 17q12-q21.2 | 1236 | -0.362 | -0.179 | |
| 44 | CCR6 | chemokine (C-C motif) receptor 6 | 6q27 | 1235 | -0.376 | -0.15 | |
| 45 | CXCR4 | chemokine (C-X-C motif) receptor 4 | 2q21 | 7852 | -0.378 | -0.118 | |
| 46 | BCL2 | B-cell CLL/lymphoma 2 | 18q21.33 | 596 | -0.69 | -0.0925 | YES |
| 47 | CCR2 | chemokine (C-C motif) receptor 2 | 3p21.31 | 1231 | -1.08 | -1.5E-14 | YES |

Supplementary Table S14: Leading edge core set of genes related to locomotory behaviour, which are differentially enriched in MALT lymphoma with and without chromosome translocation.

| Rank | Gene | Description | Chromosome Band | Entrez ID | Signal to noise ratio | Enrichment Score | NF-kB target gene |
|---|-------|--|-----------------|-----------|-----------------------|------------------|-------------------|
| Expression of genes enriched in translocation negative MALT lymphoma | | | | | | | |
| 1 | PLAU | plasminogen activator, urokinase | 10q24 | 5328 | 0.681 | 0.0507 | YES |
| 2 | IL8 | interleukin 8 | 4q13-q21 | 3576 | 0.57 | 0.0883 | YES |
| 3 | FPR1 | formyl peptide receptor 1 | 19q13.4 | 2357 | 0.553 | 0.128 | |
| 4 | CCL2 | chemokine (C-C motif) ligand 2 | 17q11.2-q12 | 6347 | 0.508 | 0.16 | YES |
| 5 | CCL11 | chemokine (C-C motif) ligand 11 | 17q21.1-q21.2 | 6356 | 0.503 | 0.197 | YES |
| 6 | CXCL5 | chemokine (C-X-C motif) ligand 5 | 4q12-q13 | 6374 | 0.49 | 0.232 | YES |
| 7 | PLAUR | plasminogen activator, urokinase receptor | 19q13 | 5329 | 0.485 | 0.267 | |
| 8 | CXCL1 | chemokine (C-X-C motif) ligand 1 | 4q21 | 2919 | 0.483 | 0.303 | YES |
| 9 | FOSL1 | FOS-like antigen 1 | 11q13 | 8061 | 0.472 | 0.336 | |
| 10 | DEFB4 | defensin, beta 4 | 8p23.1-p22 | 1673 | 0.427 | 0.351 | YES |
| 11 | CCL8 | chemokine (C-C motif) ligand 8 | 17q11.2 | 6355 | 0.384 | 0.358 | |
| 12 | CXCL2 | chemokine (C-X-C motif) ligand 2 | 4q21 | 2920 | 0.372 | 0.378 | YES |
| 13 | CCL18 | chemokine (C-C motif) ligand 18 (pulmonary and activation-regulated) | 17q11.2 | 6362 | 0.368 | 0.404 | |
| Expression of genes enriched in translocation positive MALT lymphoma | | | | | | | |
| 43 | CCR7 | chemokine (C-C motif) receptor 7 | 17q12-q21.2 | 1236 | -0.362 | -0.0976 | YES |
| 44 | CCR6 | chemokine (C-C motif) receptor 6 | 6q27 | 1235 | -0.376 | -0.073 | |
| 45 | CXCR4 | chemokine (C-X-C motif) receptor 4 | 2q21 | 7852 | -0.378 | -0.0448 | |
| 46 | CCR2 | chemokine (C-C motif) receptor 2 | 3p21.31 | 1231 | -1.08 | 3.11E-14 | YES |

Supplementary Table S15: Leading edge core set of genes related to peptide GPR signalling, which are differentially enriched in MALT lymphoma with and without chromosome translocation.

| Ran | Gene | Description | Chromosome | Entrez | Signal to | Enrichment | NF-kB |
|---|-------------|------------------------------------|-------------------|---------------|------------------|-------------------|---------------|
| k | | | Band | ID | noise | Score | target |
| | | | | | ratio | | gene |
| Expression of genes enriched in translocation negative MALT lymphoma | | | | | | | |
| 1 | FPR1 | formyl peptide receptor 1 | 19q13.4 | 2357 | 0.553 | 0.0847 | YES |
| 2 | BDKRB1 | bradykinin receptor B1 | 14q32.1-q32.2 | 623 | 0.471 | 0.147 | YES |
| 3 | EDNRA | endothelin receptor type A | 4q31.23 | 1909 | 0.426 | 0.202 | YES |
| 4 | BDKRB2 | bradykinin receptor B2 | 14q32.1-q32.2 | 624 | 0.365 | 0.228 | |
| 5 | TACR2 | tachykinin receptor 2 | 10q11-q21 | 6865 | 0.358 | 0.284 | |
| 6 | CXCR6 | chemokine (C-X-C motif) receptor 6 | 3p21 | 10663 | 0.341 | 0.33 | |
| 7 | CCR10 | chemokine (C-C motif) receptor 10 | 17q21.1-q21.3 | 2826 | 0.339 | 0.385 | |
| 41 | TACR2 | tachykinin receptor 2 | 10q11-q21 | 6865 | 0.0973 | 0.241 | |
| Expression of genes enriched in translocation positive MALT lymphoma | | | | | | | |
| 17 | CCR7 | chemokine (C-C motif) receptor 7 | 17q12-q21.2 | 1236 | -0.362 | -0.269 | YES |
| 18 | CCR6 | chemokine (C-C motif) receptor 6 | 6q27 | 1235 | -0.376 | -0.209 | |
| 19 | CXCR4 | chemokine (C-X-C motif) receptor 4 | 2q21 | 7852 | -0.378 | -0.146 | |
| 20 | CCR2 | chemokine (C-C motif) receptor 2 | 3p21.31 | 1231 | -1.08 | -1.19E-15 | YES |

Supplementary Table S16: Leading edge core set of genes related to MAPK activity, which are differentially enriched in MALT lymphoma with and without chromosome translocation.

| Ran k | Gene | Description | Chromosome Band | Entrez ID | Signal to noise ratio | Enrichment Score | NF- κ B target gene |
|---|--------|---|--------------------|--------------|-----------------------------|---------------------|----------------------------------|
| Expression of genes enriched in translocation negative MALT lymphoma | | | | | | | |
| 1 | TRIB2 | tribbles homolog 2 (Drosophila) | 2p25.1-p24.3 | 28951 | 0.632 | 0.0732 | |
| 2 | FPR1 | formyl peptide receptor 1 | 19q13.4 | 2357 | 0.553 | 0.134 | |
| 3 | EGFR | epidermal growth factor receptor (erythroblastic leukemia virus | 7p12 | 1956 | 0.404 | 0.137 | YES |
| 4 | DUSP8 | dual specificity phosphatase 8 | 11p15.5 | 1850 | 0.396 | 0.18 | |
| 5 | PLCE1 | phospholipase C, epsilon 1 | 10q23 | 51196 | 0.323 | 0.165 | |
| 6 | RGS4 | regulator of G-protein signaling 4 | 1q23.3 | 5999 | 0.315 | 0.195 | |
| 7 | SPRED2 | sprouty-related, EVH1 domain containing 2 | 2p14 | 200734 | 0.28 | 0.193 | |
| 8 | DUSP9 | dual specificity phosphatase 9 | Xq28 | 1852 | 0.277 | 0.222 | |
| 9 | DUSP2 | dual specificity phosphatase 2 | 2q11 | 1844 | 0.261 | 0.238 | |
| 10 | TRIB1 | tribbles homolog 1 (Drosophila) | 8q24.13 | 10221 | 0.254 | 0.261 | |
| 11 | C5AR1 | complement component 5a receptor 1 | 19q13.3-q13.4 | 728 | 0.246 | 0.282 | |
| Expression of genes enriched in translocation positive MALT lymphoma | | | | | | | |
| 25 | DAXX | death-domain associated protein | 6p21.3 | 1616 | -0.196 | -0.226 | |
| 26 | CD24 | CD24 molecule | 6q21 | 1E+08 | -0.208 | -0.215 | |
| 27 | PIK3CB | phosphoinositide-3-kinase, catalytic, beta polypeptide | 3q22.3 | 5291 | -0.209 | -0.191 | |
| 28 | MAP4K1 | mitogen-activated protein kinase kinase kinase kinase 1 | 19q13.1-q13.4 | 11184 | -0.23 | -0.186 | YES |
| 29 | PDCD4 | programmed cell death 4 (neoplastic transformation inhibitor) | 10q24 | 27250 | -0.314 | -0.208 | |
| 30 | DUSP22 | dual specificity phosphatase 22 | 6p25.3 | 56940 | -0.356 | -0.184 | |
| 31 | CXCR4 | chemokine (C-X-C motif) receptor 4 | 2q21 | 7852 | -0.378 | -0.146 | |
| 32 | TRIB3 | tribbles homolog 3 (Drosophila) | 20p13-p12.2 | 57761 | -0.403 | -0.104 | |
| 33 | TLR6 | toll-like receptor 6 | 4p14 | 10333 | -0.542 | -0.0616 | YES |
| 34 | ADRB2 | adrenergic, beta-2-, receptor, surface | 5q31-q32 | 154 | -0.574 | 0.00576 | |

Supplemental Table S18: Representation of gene ontology terms in over-expressed genes in MALT lymphoma with and without chromosome translocation.

| Category | GO category | Genes in Category | % of Genes in Category | Genes in List in Category | % of Genes in List in Category | p-Value |
|--|--------------------|-------------------|------------------------|---------------------------|--------------------------------|----------|
| Gene ontology term over-represented in translocation positive MALT lymphoma | | | | | | |
| GO:7250: activation of NF-kappaB-inducing kinase | Biological process | 17 | 0.105 | 2 | 10.53 | 0.000174 |
| GO:16493: C-C chemokine receptor activity | Molecular function | 22 | 0.128 | 2 | 10.53 | 0.000264 |
| GO:19957: C-C chemokine binding | Molecular function | 22 | 0.128 | 2 | 10.53 | 0.000264 |
| GO:1637: G-protein chemoattractant receptor activity | Molecular function | 37 | 0.215 | 2 | 10.53 | 0.000753 |
| GO:4950: chemokine receptor activity | Molecular function | 37 | 0.215 | 2 | 10.53 | 0.000753 |
| GO:19956: chemokine binding | Molecular function | 39 | 0.227 | 2 | 10.53 | 0.000837 |
| GO:50790: regulation of enzyme activity | Biological process | 380 | 2.336 | 4 | 21.05 | 0.00086 |
| GO:43085: positive regulation of enzyme activity | Biological process | 176 | 1.082 | 3 | 15.79 | 0.00106 |
| GO:8955: peptidoglycan glycosyltransferase activity | Molecular function | 1 | 0.00582 | 1 | 5.263 | 0.00111 |
| GO:30882: lipid antigen binding | Molecular function | 1 | 0.00582 | 1 | 5.263 | 0.00111 |
| GO:30884: exogenous lipid antigen binding | Molecular function | 1 | 0.00582 | 1 | 5.263 | 0.00111 |
| GO:30881: beta-2-microglobulin binding | Molecular function | 1 | 0.00582 | 1 | 5.263 | 0.00111 |
| GO:15014: heparan sulfate proteoglycan biosynthesis, polysaccha | Biological process | 1 | 0.00615 | 1 | 5.263 | 0.00117 |
| GO:48006: antigen presentation, endogenous lipid antigen | Biological process | 1 | 0.00615 | 1 | 5.263 | 0.00117 |
| GO:48003: antigen presentation, lipid antigen | Biological process | 1 | 0.00615 | 1 | 5.263 | 0.00117 |
| GO:30210: heparin biosynthesis | Biological process | 2 | 0.0123 | 1 | 5.263 | 0.00233 |
| GO:30202: heparin metabolism | Biological process | 2 | 0.0123 | 1 | 5.263 | 0.00233 |
| GO:19276: UDP-N-acetylgalactosamine metabolism | Biological process | 2 | 0.0123 | 1 | 5.263 | 0.00233 |
| GO:45084: positive regulation of interleukin-12 biosynthesis | Biological process | 2 | 0.0123 | 1 | 5.263 | 0.00233 |
| GO:6063: uronic acid metabolism | Biological process | 2 | 0.0123 | 1 | 5.263 | 0.00233 |
| Gene ontology term over-represented in translocation negtiave MALT lymphoma | | | | | | |
| GO:46870: cadmium ion binding | Molecular function | 10 | 0.0582 | 4 | 8 | 1.31E-08 |
| GO:5507: copper ion binding | Molecular function | 79 | 0.459 | 5 | 10 | 3.25E-06 |
| GO:50874: organismal physiological process | Biological process | 2656 | 16.33 | 21 | 44.68 | 4.48E-06 |
| GO:6817: phosphate transport | Biological process | 124 | 0.762 | 5 | 10.64 | 2.82E-05 |
| GO:5201: extracellular matrix structural constituent | Molecular function | 162 | 0.942 | 5 | 10 | 0.000105 |
| GO:15698: inorganic anion transport | Biological process | 209 | 1.285 | 5 | 10.64 | 0.00033 |
| GO:6955: immune response | Biological process | 1187 | 7.297 | 11 | 23.4 | 0.000451 |
| GO:6820: anion transport | Biological process | 257 | 1.58 | 5 | 10.64 | 0.000845 |
| GO:6952: defense response | Biological process | 1306 | 8.029 | 11 | 23.4 | 0.001 |
| GO:9611: response to wounding | Biological process | 568 | 3.492 | 7 | 14.89 | 0.00114 |
| GO:9613: response to pest, pathogen or parasite | Biological process | 751 | 4.617 | 8 | 17.02 | 0.00126 |
| GO:43207: response to external biotic stimulus | Biological process | 762 | 4.684 | 8 | 17.02 | 0.00139 |
| GO:9607: response to biotic stimulus | Biological process | 1361 | 8.367 | 11 | 23.4 | 0.00141 |
| GO:6968: cellular defense response | Biological process | 171 | 1.051 | 4 | 8.511 | 0.00148 |
| GO:7155: cell adhesion | Biological process | 978 | 6.012 | 9 | 19.15 | 0.0017 |
| GO:6801: superoxide metabolism | Biological process | 22 | 0.135 | 2 | 4.255 | 0.00182 |
| GO:9605: response to external stimulus | Biological process | 1015 | 6.24 | 9 | 19.15 | 0.0022 |
| GO:3817: complement factor D activity | Molecular function | 1 | 0.00582 | 1 | 2 | 0.00291 |
| GO:48513: organ development | Biological process | 900 | 5.533 | 8 | 17.02 | 0.00391 |
| GO:16066: cellular defense response | Biological process | 37 | 0.227 | 2 | 4.255 | 0.0051 |

Category: the name of the category within the ontology; Genes in Category: the total number of genes in the genome that have been assigned to the category; % of Genes in Category: the percentage of genes in this category assigned to this GO term; Genes in List in Category: the total number of genes that are present both in the selected gene list and in the category; % of Genes in List in Category: the percentage of genes of this category in the selected gene list that are assigned to this Go term; P-value-a hypergeometric p-value. This is a measure of the statistical significance of the overlap. i.e. the likelihood that it is a coincidence that this many genes were in both the gene list and the category. Only top 20 are shown.

- 3 Ghia P, Ferreri AM, Caligaris-Cappio F. Chronic lymphocytic leukemia. *Crit Rev Oncol Hematol* 2007; **64**: 234–246.
- 4 Secchiero P, di Iasio MG, Gonelli A, Zauli G. The MDM2 inhibitors Nutlins as an innovative therapeutic tool for the treatment of hematological malignancies. *Curr Pharm Des* 2008; **14**: 2100–2110.
- 5 Zenz T, Kröber A, Scherer K, Häbe S, Bühler A, Benner A *et al.* Mono-allelic TP53 inactivation is associated with poor prognosis in CLL: results from a detailed genetic characterization with long term follow-up. *Blood* 2008; **112**: 3322–3329.
- 6 Arora V, Cheung HH, Plenchette S, Micali OC, Liston P, Korneluk RG. Degradation of survivin by the X-linked inhibitor of apoptosis (XIAP)-XAF1 complex. *J Biol Chem* 2007; **282**: 26202–26209.
- 7 Steele AJ, Prentice AG, Hoffbrand AV, Yogashangary BC, Hart SM, Lowdell MW *et al.* p53-mediated apoptosis of CLL cells: evidence for a transcription-independent mechanism. *Blood* 2008; **112**: 3827–3834.
- 8 Wang J, He H, Yu L, Xia HH, Lin MC, Gu Q *et al.* HSF1 down-regulates XAF1 through transcriptional regulation. *J Biol Chem* 2006; **281**: 2451–2459.

A20 is targeted by promoter methylation, deletion and inactivating mutation in MALT lymphoma

Leukemia (2010) **24**, 483–487; doi:10.1038/leu.2009.234; published online 12 November 2009

Four recurrent chromosomal translocations, namely t(11;18)(q21;q21)/*API2-MALT1*, t(1;14)(p22;q32)/*BCL10-IGH*, t(14;18)(q32;q21)/*IGH-MALT1* and t(3;14)(p13;q32)/*FOXP1-IGH*, have been described in extranodal marginal zone B-cell lymphoma of mucosa-associated lymphoid tissue (MALT lymphoma). The oncogenic products of the first three translocations are believed to exert their oncogenic activity through activation of the transcription factor NF- κ B, whereas the role of FOXP1 in lymphomagenesis remains to be investigated.¹ These translocations occur at variable incidences in MALT lymphomas of different sites, and are rare or absent in the ocular adnexa, salivary glands and thyroid.¹

To characterize the genetic makeup of MALT lymphoma lacking the above chromosomal translocations, we investigated the genomic profiles of translocation negative MALT lymphomas of the ocular adnexa and lung by array-comparative genomic hybridization (array-CGH) and identified *A20* as the target of 6q23.3 deletion and *TNF* locus as a potential target of 6p21 gain exclusively in ocular adnexal cases.² Subsequent fluorescence *in situ* hybridization screening showed that *A20* deletion occurred preferentially in MALT lymphomas of the ocular adnexa, salivary glands and thyroid. In ocular adnexal cases, in which clinical information was available, *A20* deletion was significantly associated with adverse clinical parameters, and this association was independent of the presence of other genetic abnormalities.² Interestingly, among the 12 cases showing *A20* deletion, 3 displayed a homozygous deletion, indicating complete inactivation of the gene. While preparing our manuscript, four independent studies reported biallelic inactivation of *A20* by mutation and/or deletion in 67/381 (17.5%) B-cell lymphomas, including MALT lymphoma, diffuse large B-cell lymphoma and Hodgkin lymphoma.^{3–6} *A20*, also known as TNF α -induced protein 3 (*TNFAIP3*), is a well-known negative regulator of the NF- κ B activation pathway and can attenuate the NF- κ B activity triggered by signaling from TNF and Toll-like receptors.⁷ In view of these findings, *A20* could potentially act as a tumor suppressor gene. Nonetheless, it remains to be investigated whether *A20*, like other tumor suppressor genes, is also targeted for inactivation by promoter methylation and whether *A20* abnormalities impact on clinical presentation and treatment response. In this study, we investigated *A20* genetic and epigenetic abnormalities, and also examined the clinical impact of *A20* inactivation in MALT lymphoma.

A total of 17 MALT lymphomas with available adequate DNA samples or tissue materials were screened for mutation in the *A20* coding sequence by PCR and sequencing using DNA samples extracted from microdissected tumor cells of formalin-fixed paraffin-embedded tissue biopsies (Supplementary Materials and methods; Supplementary Table S1). They included seven cases showing *A20* hemizygous deletion with or without *TNF* locus gain, four cases with *TNF* locus gain only and a further six cases without these abnormalities.² A total of 4 mutations were detected in 3 (17.6%) of the 17 cases examined. All the mutations were confirmed by sequencing at least two independent PCR products from both orientations and excluded from the known polymorphisms. Cases 9 and 12 showed one nonsense mutation each, whereas case 16 showed one nonsense mutation and a 2 bp deletion (frozen tissue was not available, thus not possible to further investigate whether these mutations occurred in one or both alleles) (Table 1). Case 9 showed both *A20* mutation and hemizygous deletion, whereas cases 12 and 16 showed *A20* gene mutation but not deletion.

A20 promoter methylation was investigated in a total of 27 MALT lymphomas of the ocular adnexa (25), salivary glands (1) and thyroid (1) (Supplementary Materials and methods). Genomic DNA was treated by bisulfite to convert unmethylated cytosine to uracil, while keeping methylated cytosines intact, and then analyzed by pyrosequencing to assess methylation of 18 consecutive CpG positions in the *A20* promoter region. High efficiency of bisulfite treatment was demonstrated by internal conversion controls (Figure 1). The reliability of the assay was further ascertained by reproducible results from independent bisulfite treatments and pyrosequencing experiments. *A20* promoter methylation was seen in 7 (26%) of the 27 MALT lymphomas investigated, and they included 5 ocular adnexal cases and both extra-ocular cases (Table 1; Figure 1). Of these seven cases, six showed a similar methylation pattern, with prominent methylation at the 7th, 8th and 9th CpG sites. Remarkably, *A20* promoter methylation was significantly associated with *A20* hemizygous deletion ($P=0.011$, Fisher's exact test), being found in 5/8 (62%) cases with hemizygous deletion, but only in 2/19 (11%) cases with an intact *A20* (Table 1). None of the four cases with *A20* promoter methylation, which were also investigated for mutation, showed *A20* gene mutation. The single case (no. 9) that harbored both *A20* gene deletion and nonsense mutation showed no evidence of *A20* promoter methylation. Thus, it appeared that *A20* promoter methylation and gene mutation are mutually exclusive. To our knowledge, this is the first comprehensive analysis

Table 1 A20 abnormalities and clinicopathological correlation in MALT lymphoma

| Case ^a | Anatomical site | Stage at diagnosis ^b | Sex | Age | Etiology ^c | | A20 ^d | | TNF ^e locus copy number | Treatment (response) | Follow-up period (m) | Lymphoma relapse |
|-------------------|-----------------|---------------------------------|-----|-----|-----------------------|-------------------------------|------------------|------------------------------|------------------------------------|----------------------|----------------------|--|
| | | | | | Infectious | Autoimmune | Gene copy number | Mutation | | | | |
| 1 | Ocular | — | M | 74 | None | None | 1 | No | 2 | RT (CR) | 10 | Axillary LN (10 m) |
| 2 | Ocular | 1 | F | 60 | None | None | 1 | No | 2 | RT (CR) | 20 | Preauricular and submandibular LN (8 m), soft tissue at neural foramen (16 m) |
| 3 | Ocular, LN | 3 | M | 84 | None | None | 1 | No | 2 | Leukeran (PR) | 28 | Alive with disease |
| 4 | Ocular | — | F | 87 | Ulcerative colitis | None | 0 | — | 3 | — | — | — |
| 5 | Ocular | 1 | M | 51 | None | None | 2 | — | 3-4 | Excision + RT (CR) | 73 | None |
| 6 | Ocular | — | M | 69 | None | None | 2 | — | 2 | — | — | — |
| 7 | Ocular | 1 | F | 84 | CPS | None | 1 | No | 2 | RT (CR) | 12 | None |
| 8 | Ocular, LN | 3 | M | 66 | None | None | 1 | No | 4 | RT (CR) | 96 | Submandibular LN (72 m) |
| 9 | Ocular | — | — | — | CPN | — | 1 | C1777T, Gln593Stop | 3 | — | — | — |
| 10 | Ocular | 1 | M | 62 | None | None | 2 | No | 3-4 | NA (CR) | 242 | Opposite orbit (31 m) |
| 11 | Ocular | 1 | M | 68 | None | None | 2 | No | 4-5 | RT (CR) | 30 | None |
| 12 | Ocular | 1 | M | 64 | None | None | 2 | C811T, Arg171Stop | 4 | RT (CR) | 22 | None |
| 13 | Ocular | 1 | F | 60 | HSV1/2 | None | 2 | No | 3 | RT (CR) | 120 | Submandibular LN (108 m) |
| 14 | Ocular | — | F | 71 | ADV8 | — | 2 | No | 4 | — | — | — |
| 15 | Ocular | 4 | M | 49 | None | None | 2 | G460T, Glu162Stop, ΔCT1877-8 | 2 | RT (PR) | 52 | Lip (10 m), eyelid and LG (28 m) |
| 16 | Ocular | 1 | M | 55 | Hepatitis C | None | 2 | — | 2 | RT (CR) | 11 | None |
| 17 | Ocular | NA | F | 44 | None | None | 2 | — | 2 | RT (CR) | 6 | None |
| 18 | Ocular | 1 | F | 76 | None | None | 2 | No | 2 | RT (CR) | 12 | None |
| 19 | Ocular | 1 | F | 79 | None | None | 2 | — | 2 | RT (CR) | 84 | Opposite orbit (72 m) |
| 20 | Ocular | 1 | F | 65 | None | Sarcoidosis | 2 | No | 2 | RT (CR) | 96 | None |
| 21 | Ocular | 1 | F | 89 | CPN | None | 2 | — | 2 | RT (CR) | 72 | None |
| 22 | Ocular | — | M | 66 | None | None | 2 | No | 2 | — | — | — |
| 23 | Ocular | — | M | 80 | None | None | 2 | No | 2 | — | — | — |
| 24 | Ocular | 1 | F | 58 | None | None | 2 | — | 2 | — | — | — |
| 25 | Ocular | 1 | F | 79 | None | None | 2 | — | 2 | — | — | — |
| 26 | Ocular | — | F | 37 | None | — | 2 | No | 2 | — | — | — |
| 27 | Salivary glands | — | F | 44 | — | Sjögren's syndrome, arthritis | 0 | — | 2 | — | — | Cervical LN (18 m), systemic follicular lymphoma ^e (24 m), bone marrow (36 m) |
| 28 | Salivary glands | — | M | 6 | — | — | 1 | No | 4 | — | — | — |
| 29 | Thyroid | — | F | 62 | — | — | 1 | — | 2 | — | — | — |
| 30 | Liver | — | M | 66 | — | — | 0 | — | 3-4 | — | — | — |

ADV8, adenovirus type 8; CPN, *Chlamydia pneumoniae*; CPS, *Chlamydia psittaci*; CR, complete response; HSV1/2, herpes simplex virus type 1 and 2; LN, lymph node; m, months; MALT, mucosa-associated lymphoid tissue; NS, not specified; PR, partial response; RT, radiotherapy; —, unavailable.

^aAll cases were negative for translocations involving *MALT1*, *BCL10* and *FOXP1*, except case 22 that harbored t(1;14)(p22;q32)/*BCL10-IGH*.²

^bClinical staging was carried out by careful clinical examination and computerized tomography (CT) or magnetic resonance imaging (MRI) scan.

^cInfectious status were available from previous studies and clinical history as detailed in Supplementary Information.

^dThe results on A20 and TNF genes copy number changes were obtained from a previous study.²

^eFollicular lymphoma was clonally linked to MALT lymphoma and both lymphomas harbored t(14;18)(q32;q21)/*IGH-BCL2*.

of *A20* promoter methylation by pyrosequencing in lymphoma. While revising our manuscript, Honma *et al.* reported *A20* methylation in 10 of 24 cases of activated B-cell like diffuse large B-cell lymphoma and 3 of 8 cases of mantle cell lymphoma by methylation-specific PCR analysis of a single CpG site upstream of the κ B-binding sites.⁸

To investigate further the impact of *A20* deletion and promoter methylation on its transcript expression, we measured the *A20* mRNA expression in cases with adequate tissue materials by real-time quantitative RT-PCR. RNA was extracted from microdissected tumor cells of formalin-fixed paraffin-embedded tissues in eight cases (Supplementary Materials and methods; Supplementary Table S2). They included three cases without any *A20* abnormalities, one case with hemizygous deletion, three cases with *A20* hemizygous deletion and promoter methylation and one case with homozygous *A20* deletion. Real-time quantitative RT-PCR was performed with two sets of *A20* primers, along with GAPDH and 18S rRNA as reference control. Results from both sets of *A20* primers were similar and showed a trend of correlation between the extent of *A20* abnormalities and the level of *A20* mRNA expression. The lowest expression was seen in the cases with complete *A20* inactivation either by homozygous deletion or hemizygous deletion plus promoter methylation, whereas the highest expression was found in the cases with intact *A20* (Supplementary Figure S1). Although the number of comparable cases allowing direct analysis of the impact of *A20* promoter

methylation on its transcript expression was small, the cases with both hemizygous deletion and promoter methylation did show a lower *A20* transcript expression than the case with only *A20* hemizygous deletion. These preliminary results are in line with the expected role of promoter methylation in transcriptional silencing of the remaining *A20* allele.

Thus, concurrent *A20* hemizygous deletion and promoter methylation or mutation, as well as homozygous *A20* deletion, could result in complete *A20* gene inactivation, whereas *A20* hemizygous deletion or promoter methylation most likely lead to partial *A20* inactivation. In keeping with this notion, there was a significant correlation between the extent of *A20* abnormalities and clinicopathological presentations in ocular adnexal MALT lymphoma. Clinicopathological data were available in 17 cases (follow-up: 6–242 months, median 30 months, Table 1). Most of these patients were treated by radiotherapy. The case (no.16) that harbored two mutations was excluded from clinical correlation analyses, as it was not possible to determine whether the mutations affect one or both alleles, thus define whether *A20* was completely or partially inactivated. Both *A20* complete and partial inactivation were associated with concurrent involvement of different adnexal tissues or distant spread at diagnosis ($P=0.016$, $P=0.047$, respectively, Fisher's exact test). Importantly, *A20* complete inactivation was significantly associated with a shorter lymphoma-free survival ($P<0.001$, Figure 2), whereas cases with partial inactivation shared a similar

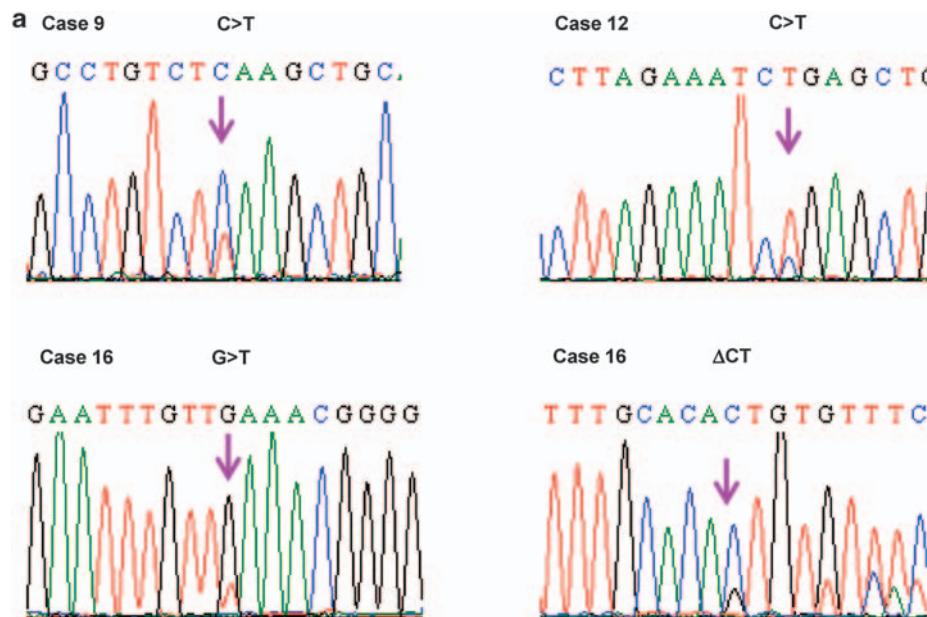


Figure 1 Screening of *A20* gene mutation and promoter methylation by DNA sequencing and pyrosequencing respectively. (a) Examples of *A20* gene mutations. All mutations including nucleotide substitutions in the three cases generate or lead to a stop codon. (b) Upper panel: *A20* promoter sequence. The κ B-binding sites are shown in green boxes and the sequence of the first exon appears in the red text. A 222 bp fragment was examined on a PyroMark MD platform (Biotage). The positions of PCR and pyrosequencing primers for the bisulfite converted sequence are, respectively, indicated by a solid underline (forward primer $5'G G G G T A A A G T A G A T T G 3'$, reverse biotinylated primer $5' C C C A A A T C C T A A T C A A A A C 3'$) and a dotted underline ($5' G T A G T T T G T A G T T T 3'$ and $5' G T T A A G A G A G A T T A T A T T T T A G T 3'$). The CpG sites successfully investigated are shown in bold. Lower panel: examples of pyrosequencing. The top panel shows methylation at the CpG sites 6, 7, 8 and 9 in an ocular adnexal MALT lymphoma (case 3) with a hemizygous *A20* deletion. The bottom panel displays no methylation at these CpG sites in an ocular adnexal MALT lymphoma without *A20* deletion (case 10). All results were confirmed in two independent bisulfite treatments and pyrosequencing experiments. The y axis represents the signal intensity in arbitrary units, whereas x axis shows the dispensation order. The CpG sites are highlighted in gray. The expected intensities are shown as gray histograms. The percentage of methylation at individual CpG positions is shown at the top of the pyrogram. The cut-off values used to define methylation is 20%, based on the mean +3 s.d. of the percentages of CpG methylation from normal lymphoid tissue and MALT lymphoma cases clearly lacking evidence of methylation. The efficiency of the bisulfite conversion was assessed for each sample by dispensing a cytosine (C) after a thymine (T) converted from a non-methylated C and no signal is seen for the C residue (highlighted in yellow), indicating complete conversion.



Figure 1 Continued.

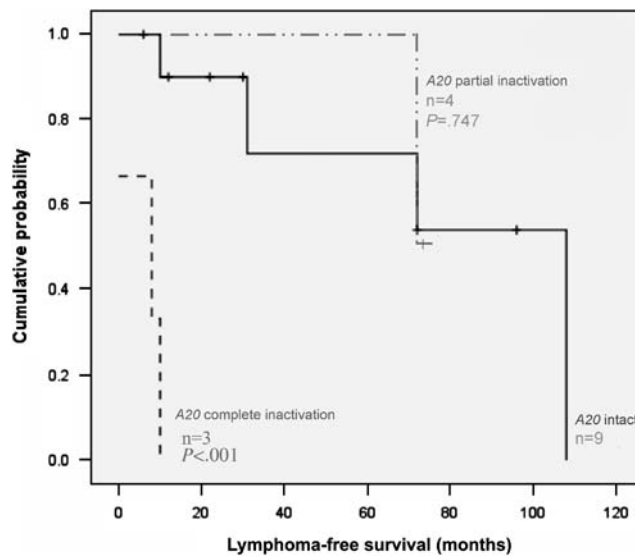


Figure 2 Clinical impact of A20 inactivation on lymphoma-free survival in ocular adnexal MALT lymphoma. Kaplan–Meier estimates of lymphoma-free survival according to A20 gene status, using log-rank test for comparison (event ‘relapse’ right-censored, Statistical Package for Social Sciences SPSS UK version 13). Complete inactivation is defined by the presence of both A20 hemizygous deletion and promoter methylation (three cases), whereas partial inactivation corresponds to the presence of A20 hemizygous deletion (two cases) or promoter methylation (one case) or mutation (one case).

profile to those without *A20* abnormalities. Although these findings await confirmation by study of large cohort of cases, the observation highlights for the first time the importance of complete inactivation of the *A20* gene in lymphoma development.

Our findings showed, for the first time, that promoter methylation was an alternative mechanism for *A20* inactivation in MALT lymphoma, in addition to gene deletion and mutation reported very recently.^{3–6,8} The biallelic inactivation by promoter methylation and deletion, hemizygous deletion and mutation, homozygous deletion is in line with the Knudson's two-hit hypothesis on the inactivation of tumor suppressor genes. As expected, re-expression of wild-type *A20* in cell lines with biallelic inactivation of the *A20* gene induced apoptosis and cell growth arrest and these effects depended on its negative regulation of NF- κ B pathway.^{5,6,8} Together, these findings indicate that *A20* is a new tumor suppressor in lymphoma. In view of the critical role of *A20* as a central negative regulator of NF- κ B activation pathway and the diverse functions of NF- κ B in B- and T-cell development and biology, the extent of *A20* involvement in various lymphoma subtypes remains to be investigated.

Conflict of interest

The authors declare no conflict of interest.

Acknowledgements

We thank Dr Yoko Ito, Cambridge Research Institute, for technical and analytical advice on pyrosequencing, and Dr Ash Ibrahim and Miss Ana Luisa De Silva for helpful discussions. This work was supported by the Elimination of Leukemia Fund (ELF/7/3/8), UK, the Lady Tata Memorial Trust, and Leukemia Research, UK (LRF06061).

E Chanudet¹, Y Huang¹, K Ichimura¹, G Dong¹,
RA Hamoudi¹, J Radford², AC Wotherspoon³, PG Isaacson⁴,
J Ferry⁵ and M-Q Du¹

¹Department of Pathology, University of Cambridge, Cambridge, UK;

²Department of Medical Oncology, Christie NHS Foundation Trust and University of Manchester, Manchester, UK;

³Department of Histopathology, Royal Marsden Hospital, London, UK;

⁴Department of Histopathology, University College London, London, UK and

⁵Department of Pathology, Massachusetts General Hospital, Boston, MA, USA

E-mails: mqd20@cam.ac.uk or ec338@cam.ac.uk

References

- 1 Du MQ. MALT lymphoma: recent advances in aetiology and molecular genetics. *J Clin Exp Hematop* 2007; **47**: 31–42.
- 2 Chanudet E, Ye H, Ferry J, Bacon CM, Adam P, Muller-Hermelink HK *et al*. *A20* deletion is associated with copy number gain at the TNFA/B/C locus and occurs preferentially in translocation-negative MALT lymphoma of the ocular adnexa and salivary glands. *J Pathol* 2009; **217**: 420–430.
- 3 Novak U, Rinaldi A, Kwee I, Nandula SV, Rancoita PM, Compagno M *et al*. The NF- κ B negative regulator TNFAIP3 (*A20*) is inactivated by somatic mutations and genomic deletions in marginal zone lymphomas. *Blood* 2009; **113**: 4918–4921.
- 4 Schmitz R, Hansmann ML, Bohle V, Martin-Subero JI, Hartmann S, Mechtersheimer G *et al*. TNFAIP3 (*A20*) is a tumor suppressor gene in Hodgkin lymphoma and primary mediastinal B cell lymphoma. *J Exp Med* 2009; **206**: 981–989.
- 5 Kato M, Sanada M, Kato I, Sato Y, Takita J, Takeuchi K *et al*. Frequent inactivation of *A20* in B-cell lymphomas. *Nature* 2009; **459**: 712–716.
- 6 Compagno M, Lim WK, Grunn A, Nandula SV, Brahmachary M, Shen Q *et al*. Mutations of multiple genes cause deregulation of NF- κ B in diffuse large B-cell lymphoma. *Nature* 2009; **459**: 717–721.
- 7 Coornaert B, Carpentier I, Beyaert R. *A20*: central gatekeeper in inflammation and immunity. *J Biol Chem* 2009; **284**: 8217–8221.
- 8 Honma K, Tsuzuki S, Nakagawa M, Tagawa H, Nakamura S, Morishima Y *et al*. TNFAIP3/*A20* functions as a novel tumor suppressor gene in several subtypes of non-Hodgkin lymphomas. *Blood* 2009; **114**: 2467–2475.

Supplementary Information accompanies the paper on the *Leukemia* website (<http://www.nature.com/leu>)

Original Paper

A20 deletion is associated with copy number gain at the TNFA/B/C locus and occurs preferentially in translocation-negative MALT lymphoma of the ocular adnexa and salivary glands

E Chanudet,¹ H Ye,¹ J Ferry,² CM Bacon,¹ P Adam,³ HK Müller-Hermelink,³ J Radford,⁴ SA Pileri,⁵ K Ichimura,¹ VP Collins,¹ RA Hamoudi,¹ AG Nicholson,⁶ AC Wotherspoon,⁷ PG Isaacson⁸ and MQ Du^{1*}

¹Division of Molecular Histopathology, Department of Pathology, University of Cambridge, UK

²Department of Pathology, Massachusetts General Hospital, Boston, MA, USA

³Institute of Pathology, University of Würzburg, Germany

⁴Cancer Research UK, Department of Medical Oncology, Christie Hospital, Manchester, UK

⁵Unità Operativa di Emolinfopatia, Università degli Studi di Bologna, Italy

⁶Department of Histopathology, Royal Brompton Hospital, London, UK

⁷Department of Histopathology, Royal Marsden Hospital, London, UK

⁸Department of Histopathology, University College London, UK

*Correspondence to:

MQ Du, Division of Molecular Histopathology, Department of Pathology, University of Cambridge, Box 231, Level 3, Lab Block, Addenbrooke's Hospital, Hills Road, Cambridge CB2 0QQ, UK.
E-mail: mqd20@cam.ac.uk

No conflicts of interest were declared.

Abstract

The genetic basis of MALT lymphoma is largely unknown. Characteristic chromosomal translocations are frequently associated with gastric and pulmonary cases, but are rare at other sites. We compared the genetic profiles of 33 ocular adnexal and 25 pulmonary MALT lymphomas by 1 Mb array-comparative genomic hybridization (CGH) and revealed recurrent 6q23 losses and 6p21.2–6p22.1 gains exclusive to ocular cases. High-resolution chromosome 6 tile-path array-CGH identified NF- κ B inhibitor A20 as the target of 6q23.3 deletion and TNFA/B/C locus as a putative target of 6p21.2–22.1 gain. Interphase fluorescence *in situ* hybridization showed that A20 deletion occurred in MALT lymphoma of the ocular adnexa (8/42 = 19%), salivary gland (2/24 = 8%), thyroid (1/9 = 11%) and liver (1/2), but not in the lung (26), stomach (45) and skin (13). Homozygous deletion was observed in three cases. A20 deletion and TNFA/B/C gain were significantly associated ($p < 0.001$) and exclusively found in cases without characteristic translocation. In ocular cases, A20 deletion was associated with concurrent involvement of different adnexal tissues or extraocular sites at diagnosis ($p = 0.007$), a higher proportion of relapse (67% versus 37%) and a shorter relapse-free survival ($p = 0.033$). A20 deletion and gain at TNFA/B/C locus may thus play an important role in the development of translocation-negative MALT lymphoma.

Copyright © 2008 Pathological Society of Great Britain and Ireland. Published by John Wiley & Sons, Ltd.

Keywords: A20; TNF; MALT lymphoma; array comparative genomic hybridization

Received: 21 July 2008
Revised: 28 August 2008
Accepted: 24 September 2008

Introduction

Extranodal marginal zone B cell lymphoma of mucosa-associated lymphoid tissue (MALT lymphoma) arises in the acquired MALT resulting from chronic inflammatory or autoimmune disorders. MALT lymphomas of the stomach, skin and ocular adnexa are linked, although to variable degrees, to infection with *Helicobacter pylori*, *Borrelia burgdorferi* and *Chlamydia psittaci*, respectively, while those of the salivary gland and thyroid are closely associated with the autoimmune disorders lymphoepithelial sialadenitis and Hashimoto thyroiditis, respectively [1].

The acquisition of genetic abnormalities plays a critical role in the development of MALT lymphoma [1].

Four recurrent chromosomal translocations occur at markedly variable frequencies in MALT lymphoma of different sites. t(11;18)(q21;q21)/API2–MALT1 occurs frequently in the lung (40%), stomach (25%) and ocular adnexa (~10%) [2]. t(1;14)(p22;q32)/BCL10–IGH, t(14;18)(q32;q21)/IGH–MALT1 and t(3;14)(p13;q32)/FOXP1–IGH, are relatively infrequent, t(1;14) and t(14;18) occurring mostly in the lung (6–7%) and t(3;14) in the stomach (4%) [3–6]. While the role of the early B cell development regulator FOXP1 in lymphoma remains unclear [7], chromosomal translocations involving BCL10 or MALT1 exert their oncogenic activities through the constitutive activation of NF- κ B [8], leading to the expression of a

number of genes involved in cell survival and proliferation. Importantly, gastric MALT lymphomas harbouring t(11;18)(q21;q21)/*API2-MALT1* do not respond to *H. pylori* eradication, underlying the importance of detecting these translocations in clinical management [9,10].

The majority of MALT lymphomas are negative for these chromosomal translocations and their molecular genetics is poorly understood. Several trisomies are frequently associated with MALT lymphoma [11,12], particularly those without t(11;18)(q21;q21). Our previous study of translocation-negative MALT lymphomas of the stomach and salivary glands by metaphase comparative genomic hybridization (CGH) showed recurrent trisomies (3/12/18) and discrete gains at 9q34, 11q11–13 and 18q21 [13,14]. Interestingly, these regions contain a number of genes encoding positive regulators of the NF- κ B pathway, such as *CARD9*, *TRAF2*, *RELA* and *MALT1*. To address whether MALT lymphomas of other sites show common or distinct genetic alterations, we investigated the genomic profiles of ocular and pulmonary MALT lymphomas by array-CGH, and characterized novel abnormalities by interphase fluorescence *in situ* hybridization (FISH) in MALT lymphomas of various sites.

Methods

Tissue specimens

Archival formalin-fixed paraffin-embedded tissue (FFPE) biopsies from primary MALT lymphomas were used for genomic profiling (ocular adnexa, 46 cases; lung, 31 cases) and FISH investigation (various anatomical sites, 185 cases). Local ethical guidelines were followed for the use of archival tissues for research with the approval of the ethics committees of the institutions involved.

DNA preparation

Tumour cells were microdissected from haematoxylin-stained slides and digested with proteinase K [15]. DNA was purified using phenol-chloroform or QIAamp DNA Micro Kit (QIAGEN, Crawley, UK) and quantified by Picogreen™ (Molecular Probes, Eugene, OR, USA). DNA quality was assessed by amplification of variously sized gene fragments [16]: only cases with adequate DNA quantity and successful amplification of 200 bp (19% cases) or larger product (81% cases) were used for array-CGH.

Infectious agents and translocation status

Newly retrieved ocular adnexal MALT lymphoma cases from Massachusetts General Hospital, Boston, USA (cases 1–24, Table 2), were screened for *Chlamydia psittaci* (CPS), *C. trachomatis* (CTR) and *C. pneumoniae* (CPN) by PCR and for translocations

t(11;18)(q21;q21), t(1;14)(p22;q32), t(14;18)(q32;q21) and t(3;14)(p13;q32) by interphase FISH, as previously described [16,17], while data for the remaining cases were available from previous studies [2,4,16,17,18].

Array-CGH

Genomic profiles were obtained using in-house 1 Mb resolution genomic arrays containing 3038 BAC clones in duplicate [15,19]. Briefly, 400 ng tumour and reference DNA were labelled with Cy5 and Cy3, respectively, using a Bioprime labelling kit (Invitrogen, Carlsbad, CA, USA). Array hybridization was carried out for 48 h. Slides were scanned using an Axon 4100A scanner (Molecular Devices, Sunnyvale, CA, USA), images quantified using GenePix Pro 5.1 software (Molecular Devices) and primary data analysed using Microsoft Excel [19]. Genomic changes were identified by an integrated approach combining visual inspection and statistical analysis, with the mean ± 3.2 SD (\log_2 value ± 0.20) from normal male/female hybridization used as the threshold value, as previously optimized for FFPE tissues [15]. Genomic changes were ascertained by an adaptive threshold (3–5.5 median absolute deviation) determined from a hidden Markov model to take into account intra- and intersample variations (RH, EC, MQD, manuscript in preparation). Regions showing recurrent copy number changes were searched for potential targeted genes (http://www.ensembl.org/Homo_sapiens).

High-resolution chromosome 6 tile-path array-CGH was performed similarly, using an in-house array containing 1780 BAC/PAC clones in duplicate [20].

Interphase FISH

BAC clones bPG296P20 (*TNFA/B/C* locus, 6p21) and RP11-356i2 (*A20* locus, 6q23), were labelled with spectrum orange and spectrum green, respectively, by nick translation (Abbott Laboratories, Maidenhead, UK). Following confirmation of specificity by FISH on metaphase spreads, the labelled probes were pooled with the chromosome 6 centromere probe CEP6 aqua (Abbott Laboratories) and interphase FISH on FFPE tissue sections was performed as described previously [2]. Image acquisition and processing was performed using a fluorescent microscope (Olympus, BX61, Tokyo, Japan) and Cytovision software (version 2.75; Applied Imaging International, Newcastle, UK). The three-colour FISH assay was validated using cases with and without genetic changes identified by chromosome 6 tile-path array-CGH. The mean + 3SD of false-positive signals in 100 nuclei from three reactive tonsils and three MALT lymphomas without chromosome 6 abnormality by tile-path array-CGH was used as the cut-off value for the diagnosis of aberrations.

Statistical analysis

Correlations between array-CGH/FISH results and clinical parameters were performed using Fisher's

exact test ('stats Package' in R version 2.5.1). The probability of lymphoma relapse-free survival was calculated by the Kaplan–Meier method, with log-rank test for comparison (Statistical Package for Social Sciences version 13, Woking, UK).

Results

1 Mb genomic profile of pulmonary MALT lymphoma

Twenty-five pulmonary MALT lymphomas were successfully analysed by 1 Mb array–CGH. Nine cases had t(11;18)(q21;q21), 2 had t(1;14)(p22;q32) and 14 were negative for the four MALT lymphoma-associated translocations. Overall, chromosomal gains were more frequent than losses (Figure 1a). Trisomies were exclusively found in t(11;18)(q21;q21)-negative cases, including t(1;14)(p22;q32)-positive cases (Table 1). Trisomies 3, 12 and 18 were seen in four, two and three cases, respectively, and concurrent in two cases (Table 1).

Recurrent small discrete gains were found mainly at 8q24 (68%), 9q34 (68%) and 11q12–q13 (36%). They were frequently concurrent, with 16/25 cases showing gain at two of the three loci. Discrete deletions were mainly observed at 9q33 (12%) and 14q32 (12%) (Figure 1a). There was no significant difference in the frequencies of discrete gains and losses between cases with and without t(11;18)(q21;q21) (Table 1).

1 Mb genomic profile of ocular adnexal MALT lymphoma

Thirty-three ocular adnexal MALT lymphomas were successfully investigated by 1 Mb array–CGH. The vast majority (30/33) were negative for the four MALT-lymphoma-associated translocations. Their genomic profiles showed several similarities to pulmonary MALT lymphoma. First, trisomies 3, 12 and 18, often concurrent, were frequent and restricted to t(11;18)-negative cases, including the t(1;14)(p22;q32)-positive case. Second, discrete gains were more frequent than losses, and mainly found at 8q24 (67%), 9q34 (48%) and 11q12–q13 (18%) (Table 2; Figure 1a).

However, unlike pulmonary cases, ocular adnexal MALT lymphoma further showed alterations in chromosome 6 (Figure 1a). Gain of chromosome 6 was found in eight cases (18%), including trisomy 6 (1/8), and gain of whole or a major part of the p arm (6/8) or 6p21–22 (1/8) (Table 2). Interestingly, 6p gain was significantly associated with trisomy 3 (Table 2). Loss of 6q was seen in four cases with a minimum common region (MCR) of deletion involving a single BAC clone (RP11-95M15). Concurrent gain of chromosome 6/6p and loss of 6q23 was observed in two cases (Table 2).

Characterization of chromosome 6 abnormalities by high-resolution chromosome 6 tile-path array–CGH

This manuscript focused on the novel chromosome 6 abnormalities in ocular adnexal MALT lymphoma. Chromosome 6 tile-path array–CGH was performed on eight ocular adnexal cases showing chromosome 6 alterations by 1 Mb array–CGH, and nine cases from the ocular adnexa (7) and lung (2) without evidence of chromosome 6 changes. All chromosome 6 copy number changes identified by 1 Mb array–CGH were confirmed by tile-path array–CGH (Figure 1b).

Of the four cases with 6q deletion, tile-path array–CGH revealed a MCR spanning 1226 kb (137.2–138.4 Mb) at 6q23.3 (Figure 1b). Homozygous deletion was seen in one case that also had trisomy 6, while deletion was hemizygous in three cases. The MCR of deletion harboured six genes, including interleukin 22 receptor $\alpha 2$ (*IL22RA2*), interferon- γ receptor 1 (*IFNGR1*) and TNF-induced protein 3 (TNFAIP3, also known as *A20*) (Figure 1b). Statistical analysis among 6q-deleted cases showed a 603 kb region (137.6–138.2 Mb) consistently within the lowest \log_2 value in each case and this region contained only *A20*, a potent inhibitor of NF- κ B signalling [21,22].

Tile-path array–CGH identified gain at 6p21 in two additional cases without unequivocal 1 Mb array–CGH evidence of a 6p gain, and defined a restricted MCR of gain of 8.2 Mb at 6p21.2–6p22.1. Four cases further showed a recurrent focal peak (3–6 copies) within the MCR, centred at BAC clone bPG296p20 (6p21.33) (Figure 1b). A search of the 15 genes in this BAC clone and its vicinity revealed *NF κ BIL1* (NF- κ B inhibitor-like 1), *TNF* (also known as *TNFA*), lymphotoxin α (*LTA* or *TNFB*) and lymphotoxin β (*LTB* or *TNFC*) as putative targets.

Characterization of chromosome 6 abnormalities by FISH

Our FISH assay, simultaneously detecting *A20*, *TNFA/B/C* and chromosome 6 centromere loci, confirmed all the alterations identified by array–CGH and was successfully applied to 166 MALT lymphomas from various sites (Figure 2a–d).

Interphase FISH confirmed gain of extra copies (1–3) of the *TNFA/B/C* locus with or without gain of extra centromere probe signals (Table 3). Gain was frequent in MALT lymphomas of the ocular adnexa (11/42 = 26%) and salivary glands (5/24 = 21%), but was rare or absent in those of the lung, stomach and skin (Figure 2e).

A20 deletion was found exclusively in MALT lymphoma of the ocular adnexa (8/42 = 19%), salivary glands (2/24 = 8%), thyroid (1/9 = 11%) and liver (1/2) (Figure 2e). *A20* homozygous deletion was seen in 3/12 cases (Figure 2d). Interestingly, there was a significant association between *A20* deletion and *TNFA/B/C* locus gain ($p < 0.001$; Figure 2f).

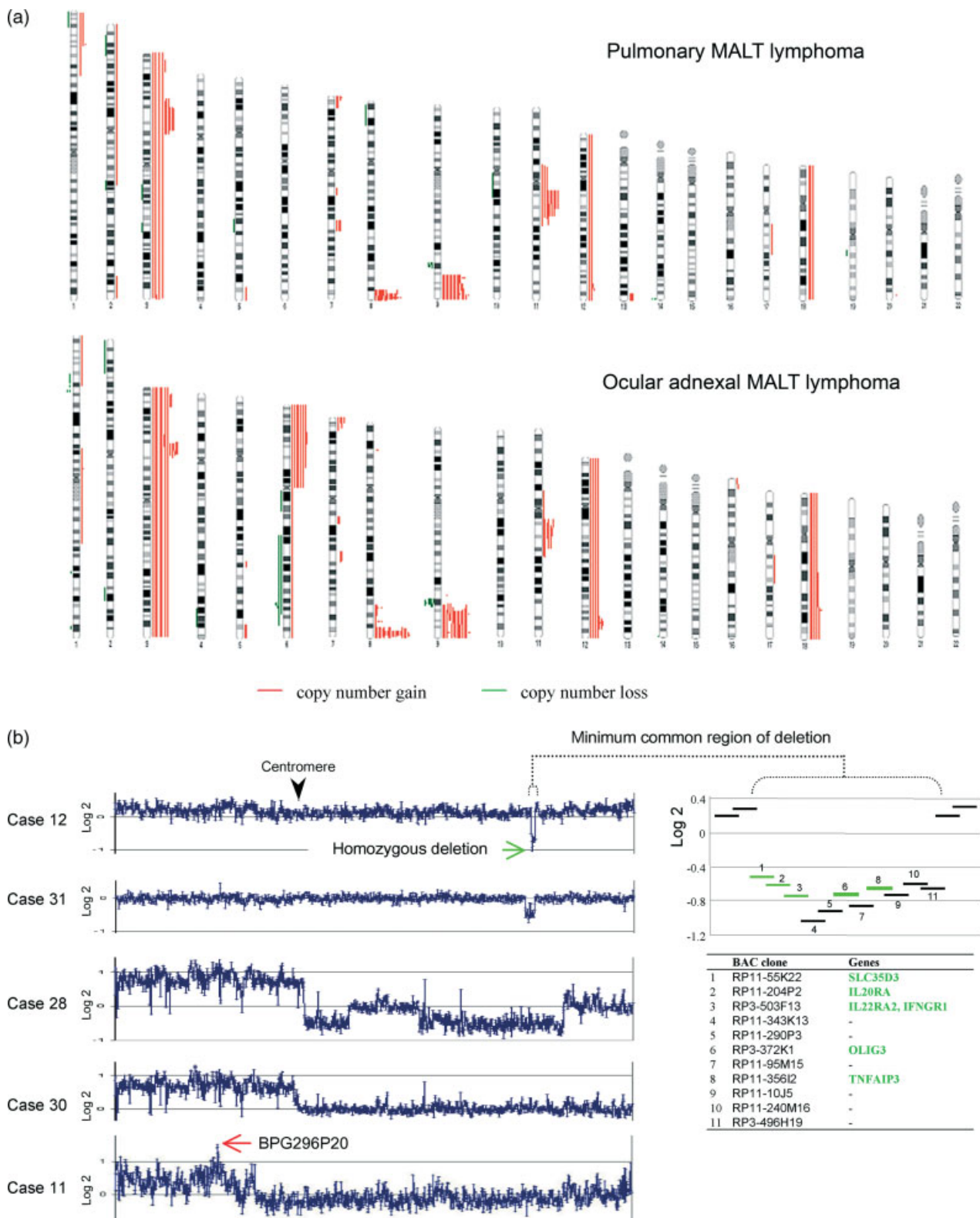


Figure 1. Genomic profiles of MALT lymphoma by array-comparative genomic hybridization. (a) 1 Mb resolution array-CGH profiles of 25 pulmonary and 33 ocular adnexal MALT lymphomas. (b) Characterization of chromosome 6 abnormalities in ocular adnexal MALT lymphoma by high-resolution tile-path chromosome 6 array-CGH. Log₂-transformed normalized Cy5: Cy3 intensity ratios were plotted against clone position (arranged in genomic order from pter on the left to qter on the right). Cases 12, 31 and 28: examples of 6q deletion with a MCR of 1226 kb at 6q23.3 spanning 11 overlapping BAC clones containing six genes (*SLC35D3*, solute carrier family 35 member D3; *IL20RA*, interleukin 20 receptor α ; *IL22RA2*, interleukin 22 receptor α ; *IFNGRI*, interferon- γ receptor 1; *OLIG3*, oligodendrocyte transcription factor 3; *TNFAIP3*, tumour necrosis factor- α -induced protein 3, also known as A20). Cases 28, 30 and 11: examples of partial tetrasomy 6, involving a whole or major part of 6p. Case 11 shows a focal peak centred at BAC clone bPG296p20, which contains the *TNFA/B/C* locus (6p21.33). Case 12 shows trisomy 6 and 6q23 homozygous deletion, while case 28 displays partial tetrasomy 6 and 6q hemizygous deletion

Table 1. Chromosomal gains and losses in pulmonary MALT lymphomas identified by 1 Mb array-CGH analysis

| Case | Translocation | Infectious agents and autoimmune disease | Chromosomal changes ^a | |
|------|---------------|--|--|---|
| | | | Gains | Losses |
| 1 | t(11;18) | CPN, CTR | None | None |
| 2 | t(11;18) | None | 8q24, 9q34, 11p11-q13 | 9q33 |
| 3 | t(11;18) | None | 8q24, 11q12-13 | None |
| 4 | t(11;18) | None | None | 14q32 |
| 5 | t(11;18) | Haemolytic anaemia | 8q24, 9q34 | None |
| 6 | t(11;18) | CTR | 3p14-21, 8q24, 9q34, 11q12-13 | None |
| 7 | t(11;18) | CTR | 1p32-36, 2q35-37, 3p25, 3p14-21, 7p22, 8q24, 9q34, 11q12-13, 13q34 | None |
| 8 | t(11;18) | CTR | 3p21, 8q24 | None |
| 9 | t(11;18) | None | 8q24, 9q34 | None |
| 10 | t(1;14) | CTR | 1p35, 3, 7p22, 7q22, 8q24, 9q34, 11p11-q13, 12, 18 | 9q33 |
| 11 | t(1;14) | None | 3, 8q24, 9q34, 12, 18 | 8p22-23 |
| 12 | None | CPS | 2p25-q22, 3, 8q24, 9q34, 17q12-21 | 2q22 |
| 13 | None | CTR | 1p35-36, 7p22, 8q24, 9q34, 11p11-q13 | 9q33 |
| 14 | None | None | 12q24 | 1p36, 2p24-25, 3q13, 3q22-23, 5q23, 10q11-21, 14q32 |
| 15 | None | CPN | None | None |
| 16 | None | None | 7q11, 9q34 | 14q32 |
| 17 | None | None | 3p21, 5q35, 8q24, 9q34, 20q13 | 19q13 |
| 18 | None | Chronic bronchitis | 3p21, 7q22, 9q34 | None |
| 19 | None | CPS | 3, 8q24, 9q34, 18 | None |
| 20 | None | CTR, chronic bronchitis | 8q24, 9q34, 11q12-13 | None |
| 21 | None | None | 8q24, 9q34, 13q34 | None |
| 22 | None | None | 3p14-21, 7p22, 7q22, 8q24, 9q34, 11q12-13, 13q34 | None |
| 23 | None | None | None | None |
| 24 | None | CPN | 8q24, 9q34, 11q12-13 | None |
| 25 | None | CPN | None | None |

^a Single BAC clone changes were included only if they were confirmed by tile-path array or fluorescence *in situ* hybridization. CPS, *Chlamydia psittaci*; CTR, *C. trachomatis*; CPN, *C. pneumoniae*.

Both *A20* deletion and *TNFA/B/C* gain were significantly associated with translocation-negative MALT lymphomas ($p = 0.002$ and $p < 0.001$, respectively). With the exception of one case, No. 13, FOXP1/unknown partner, and a further case, No. 16, t(14;18)(q32;q21)/*IGH-BCL2* [24], all other cases with chromosome 6 abnormalities were negative for MALT lymphoma-associated translocations (Table 3), while 44% of the cases without chromosome 6 abnormalities had a translocation. There was no significant correlation between *TNFA/B/C* locus gain or *A20* deletion and the pattern of expression of *BCL10* and *MALT1* protein by immunohistochemistry.

Clinicopathological correlations

Unless otherwise stated, clinicopathological correlations were assessed in ocular adnexal MALT lymphoma, for which a sufficient number of cases with adequate clinical data were available (Table 3). Most of the patients were treated by radiotherapy, with a follow-up period of 6–242 months (median 64 months). *A20* deletion was significantly associated with the involvement of the orbital soft tissue by

lymphoma at diagnosis ($p = 0.027$) and with concurrent involvement of different adnexal tissues or distant spread at diagnosis ($p = 0.007$) (see Supporting information, Table S1). *A20* deletion was also significantly associated with a shorter lymphoma relapse-free survival ($p = 0.033$; Figure 3a). Lymphoma relapse was more frequent (4/6, 67%) and occurred much earlier (median 11 months) in the cases with *A20* deletion than in those lacking the deletion (6/16 cases, 37.5%; median 51.5 months).

Trisomy 12 was significantly associated with lymphoma relapse ($p = 0.047$), being found in three of nine relapsed cases, which involved distant lymph nodes in two cases and the lip in the remaining case, but in none of the 14 cases without relapse. Trisomy 12 was also significantly associated with a shorter lymphoma relapse-free survival (median 10 months versus 51.5 months without trisomy 12; $p < 0.001$; Figure 3b). Among the three cases with trisomy 12 showing lymphoma relapse, one had *A20* deletion, one showed concurrent trisomies 3 and 18, and the remaining case did not harbour any of these abnormalities. Interestingly, the case with concurrent *A20* deletion and trisomy 12 showed repeated lymphoma

Table 2. Chromosomal gains and losses in ocular adnexal MALT lymphomas identified by 1 Mb array-CGH analysis

| Case | Anatomical location | Translocation | Infectious agents ^a and autoimmune disease | Chromosomal changes ^{b,c} | |
|------|--|---------------------------|---|---|------------------------------------|
| | | | | Gains | Losses |
| 1 | Conjunctiva | t(11;18) | CPS | 7p22, 8q24, 9q34 | 9q33 |
| 2 | Orbital soft tissue | t(1;14) | None | 3, 8q24, 9q33-34, 12 | 9q33 |
| 3 | Orbital soft tissue | FOXP1 and unknown partner | None | 6p21-22, 8q24, 9q33-34, 11q12-13, 18q21 | None |
| 4 | Orbital soft tissue | None | None | 3, 8q24, 9q34, 12, 18 | 9q33 |
| 5 | Orbital soft tissue | None | None | 3, 6p, 8q24, 9q32-34, 11p11-q13 | None |
| 6 | Conjunctiva | None | None | 7q11, 9q33-34 | 9q33 |
| 7 | Orbital soft tissue | None | None | 12q24 | 1p32-34 |
| 8 | Lachrymal glands, orbital soft tissue | None | None | 3p25, 3p21, 8q24, 9q33-34, 12 | 2q33-34 |
| 9 | Orbital soft tissue | None | None | 7q11, 7q22, 8q24, 16p13 | None |
| 10 | Orbital soft tissue | None | None | 8q24 | None |
| 11 | Orbital soft tissue | None | None | 3, 6p21-25, 8q24 | None |
| 12 | Conjunctiva, lachrymal glands, orbital soft tissue | None | Ulcerative colitis | 3, 6, 8q24, 18 | 6q23 |
| 13 | Conjunctiva, orbital soft tissue | None | None | 3p25, 3p21, 8q24 | 6q16-25, 14q32 |
| 14 | Orbital soft tissue | None | None | 3, 8q24, 9q33-34, 17q12-21 | None |
| 15 | Orbital soft tissue | None | None | 6p, 9q32-34, 18q21 | None |
| 16 | Lachrymal glands, orbital soft tissue | None | None | 3p14-21, 6p, 7p22, 8q24 | None |
| 17 | Lachrymal glands | None | None | 7p22, 8q24 | None |
| 18 | Lachrymal glands | None | None | 5q35, 8q24 | None |
| 19 | Orbital soft tissue | None | Hepatitis C | 8q24, 9q33-34, 11q12-13 | None |
| 20 | Lachrymal glands | None | None | 9q33-34, 11q12-13 | None |
| 21 | Orbital soft tissue | None | CPS | 5q35, 7p22, 7q22, 8q24, 9q34 | None |
| 22 | Orbital soft tissue | None | CPS | 8p21, 8q24, 11q12-13 | None |
| 23 | Orbital soft tissue | None | None | 1p32-36, 1p21-q23, 8q24, 11q12-13 | None |
| 24 | Lachrymal glands | None | Hypothyroidism | 3p21, 12 | None |
| 25 | Conjunctiva | None | None | 5q23, 9q33-34 | None |
| 26 | Ocular adnexa (NS) | None | None | 9q33-34, 18q12-23 | None |
| 27 | Lachrymal glands | None | CPN | None | None |
| 28 | Orbital soft tissue | None | None | 6p, 8p21, 8q24 | 6q12-14, 6q16/24 |
| 29 | Lachrymal glands | None | HSV1/2 | None | 9q33 |
| 30 | Ocular adnexa (NS) | None | ADV8 | 3, 6p, 8q24, 12q24, 18 | None |
| 31 | Orbital soft tissue | None | CPS | None | 1p32, 6q23 |
| 32 | Orbital soft tissue | None | Previous sarcoidosis | 1p12, 9q34, 12q24 | 1p36, 1q41, 1q31, 2p24-25, 4q32-34 |
| 33 | Conjunctiva | None | None | 3p21, 8q24, 9q34, 18 | 9q33 |

^a Herpes simplex virus and adenovirus status were available in cases 25-33 from a previous study [16].

^b Single BAC clone changes were included only if they were confirmed by tile-path array or fluorescence *in situ* hybridization.

^c 6p gain was associated with trisomy 3: 4/8 (50%) cases with 6p gain had a trisomy 3, while only 3/25 (12%) cases without 6p gain had trisomy 3 ($p = 0.042$).

NS, not specified; CPS, *Chlamydia psittaci*; CTR, *C. trachomatis*; CPN, *C. pneumoniae*; HSV, herpes simplex virus; ADV, adenovirus.

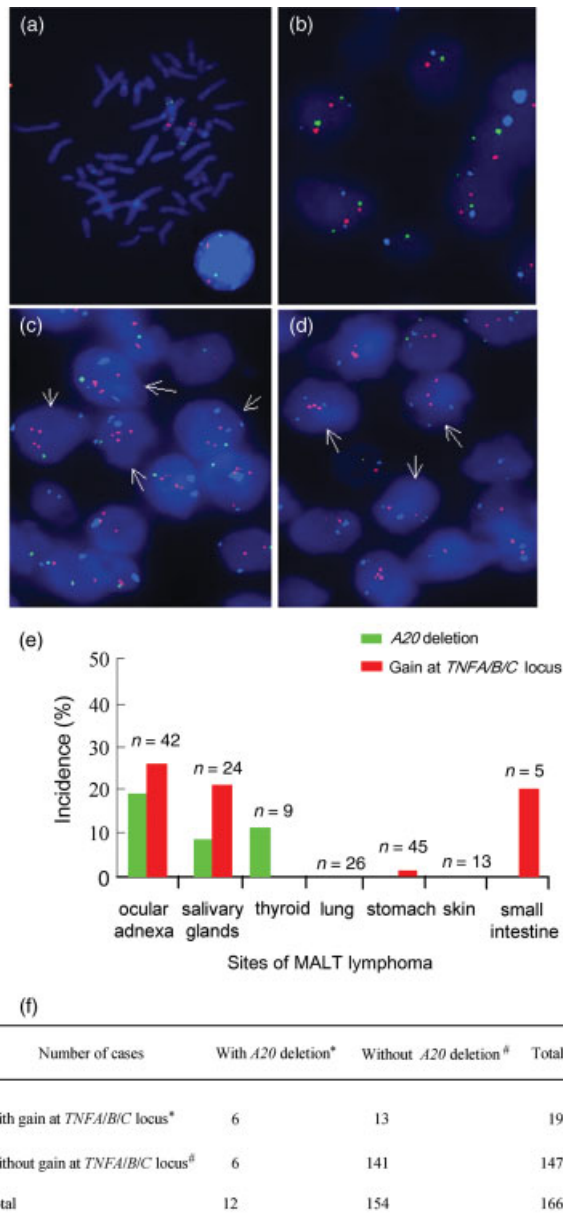


Figure 2. A20 deletion and TNFA/B/C gain in MALT lymphoma of various sites. (a–d) Three-colour FISH assay for investigation of copy number changes at the A20 (RP11-356i2 labelled with spectrum green) and TNFA/B/C (bPG296P20 labelled with spectrum orange) loci, together with centromeric probe CEP 6 (spectrum aqua); cell nuclei showing chromosome 6 abnormalities are indicated by arrows. (a) Validation of FISH probes on metaphase spreads. (b) Ocular adnexal MALT lymphoma case 32 without evidence of chromosome 6 genetic abnormalities by high-resolution tile-path array–CGH. (c) Ocular adnexal MALT lymphoma case 28, showing A20 heterozygous deletion, four copies of the TNFA/B/C and three copies of CEP6 probe signals. (d) Ocular adnexal MALT lymphoma case 12, showing A20 homozygous deletion and gain of an extra copy of the TNFA/B/C and CEP6 probe signals. (e) Incidence of A20 deletion and TNFA/B/C gain in MALT lymphomas of various anatomical sites. Additionally, both A20 deletion and TNFA/B/C gain have been found in one of the two hepatic MALT lymphomas. (f) Association between A20 deletion and TNFA/B/C gain in MALT lymphomas of various anatomical sites ($p < 0.001$). *A20 deletion and gain at the TNFA/B/C locus were exclusively found in cases negative for MALT lymphoma-associated chromosomal translocations. [#]44% of the cases without chromosome 6 abnormalities had a MALT lymphoma-associated chromosomal translocation

relapses and the shortest relapse-free survival (case 2, Table 3).

There was no significant correlation between the presence of clinical features of autoimmunity and genomic abnormalities including A20 deletion and TNFA/B/C locus gain. However, among the three cases with homozygous A20 deletion, clinical data was available in two and both cases had an autoimmune disorder (Table 3).

In both ocular adnexal and pulmonary MALT lymphoma, there was no other apparent correlations among genomic abnormalities, evidence of *Chlamydia* infection, histological features, including plasma cell differentiation and extent of high-grade blast transformation, BCL10 staining pattern, age, sex, geographical origin, treatment and lymphoma relapse.

Discussion

The genomic profiles of 33 ocular adnexal MALT lymphomas and 25 pulmonary MALT lymphomas by 1 Mb array–CGH revealed both common and distinct recurrent chromosomal imbalances. Both MALT lymphomas of the ocular adnexa and lung showed frequent trisomies 3, 12 and 18 in t(11;18)(q21;q21)-negative cases and recurrent discrete gains at 8q24, 9q34 and 11q11–13, similar to the previous findings in gastric and salivary gland MALT lymphomas [13,14]. More importantly, we identified recurrent gains of chromosome 6/6p and deletion of 6q23 in ocular adnexal but not in pulmonary MALT lymphoma.

Deletion of 6q occurs frequently in a range of solid tumours and haematological malignancies [25–27]. Nevertheless, the regions of 6q deletion are relatively large and heterogeneous, and the genes targeted remain elusive [28]. In contrast, our study defined a MCR restricted to 1226 kb at 6q23.3. Bioinformatic search identified A20 as the target of the deletion. While preparing our manuscript, Honma and colleagues demonstrated a similar diminutive deletion at 6q23.3–24.1 in six of 24 ocular adnexal MALT lymphoma cases and proposed A20 as the deletion target [29,30]. A20, a potent inhibitor of NF- κ B signalling, is required for termination of TNF α and TLR-induced NF- κ B activation [21,22]. A20 can specifically remove K63-linked polyubiquitin chains from TRAF6, a key molecule downstream of the CARMA1–BCL10–MALT1 complex in the NF- κ B activation pathway [31]. A recent study shows that MALT1 and API2–MALT1 can proteolytically cleave A20 [32], further implicating it in the molecular pathogenesis of MALT lymphoma.

By interphase FISH screening, we revealed that A20 deletion occurred preferentially in MALT lymphoma of the ocular adnexa, salivary glands, thyroid and liver, but not in those of the lung, stomach, skin and small intestine. Importantly, A20 homozygous deletion, hence complete inactivation of the gene, was seen in three of the 12 cases, suggesting that A20 is likely a tumour suppresser gene. It remains to be investigated

Table 3. Demographic and clinico-pathological characteristics of MALT lymphomas with chromosome 6 abnormalities identified by interphase fluorescence *in situ* hybridization

| Case ^a | Anatomical location | Stage at diagnosis | Sex | Age | Copy number by FISH | | | Autoimmune Disease | Treatment (response) | Follow-up period (months) | Lymphoma relapse | Outcome |
|-------------------|--------------------------------------|--------------------|-----|-----|---------------------|-----------------------------|----------------|-------------------------------|----------------------|---------------------------|--|---------------------|
| | | | | | A20 ^b | TNFA/B/C locus ^c | CEP6 | | | | | |
| 1 | Orbital soft tissue | — | M | 74 | 1 | 2 | 2 | None | — | 10 | Axillary LN (10 m) | Alive with lymphoma |
| 2 | Orbital soft tissue, LG | I | F | 60 | 1 | 2 | 2 | None | RT (CR) | 20 | Preauricular and submandibular LN (8 m), soft tissue at neural foramen (16 m) | Alive with lymphoma |
| 3 | Orbital soft tissue, Conjunctiva | — | F | 85 | 1 | 2 | 2 | None | RT (CR) | 33 | None | Alive, no lymphoma |
| 4 | Orbital soft tissue | I | F | 84 | 1 | 2 | 2 | None | RT (CR) | 12 | None | Alive, no lymphoma |
| 5 | Orbital soft tissue, iliac LN | 3 | M | 66 | 1 | 4 | 3 ^d | None | RT (CR) | 96 | Submandibular LN (72 m) | Alive, no lymphoma |
| 6 | Orbital soft tissue | I | F | 63 | 1 | 3 | 2 | None | RT (CR) | 97 | Scalene LN (12), opposite orbit (95 m), bone marrow (96 m) | Alive with lymphoma |
| 7 | Orbital soft tissue | — | — | — | 1 | 3 | 3 | — | — | — | — | — |
| 8 | Orbital soft tissue, LG, conjunctiva | — | F | 84 | 0 | 3 | 3 | Ulcerative colitis | — | — | — | — |
| 9 | Orbital soft tissue | I | M | 51 | 2 | 3–4 | 2 | None | Excision + RT (CR) | 73 | None | Alive, no lymphoma |
| 10 | Orbital soft tissue | I | M | 78 | 2 | 3–4 | 3–4 | None | RT (CR) | 76 | None | Alive, no lymphoma |
| 11 | Orbital soft tissue | I | M | 68 | 2 | 4–5 | 2 | None | RT (CR) | 30 | None | Alive, no lymphoma |
| 12 | Orbital soft tissue | I | M | 64 | 2 | 4 | 3–4 | None | RT (CR) | 22 | None | Alive, no lymphoma |
| 13 | Orbital soft tissue, LG | I | M | 62 | 2 | 3–4 | 3 ^d | None | NA (CR) | 242 | Opposite orbit (31 m) | Alive, no lymphoma |
| 14 | LG | I | F | 60 | 2 | 3 | 2 | None | RT (CR) | 120 | Submandibular LN (108 m) | Alive, no lymphoma |
| 15 | Ocular adnexa | — | F | 71 | 2 | 4 | 3 ^d | — | — | — | — | — |
| 16 | Salivary glands | — | F | 44 | 0 | 2 | 2 | Sjögren's syndrome, arthritis | — | 36 | Cervical LN (18 m), systemic follicular lymphoma ^e (24 m), bone marrow (36 m) | Alive with lymphoma |
| 17 | Salivary glands | — | M | 6 | 1 | 3–4 | 2 | — | — | — | — | — |
| 18 | Salivary glands | — | F | 76 | 2 | 3 | 2 | — | — | — | — | — |
| 19 | Salivary glands | — | F | 64 | 2 | 3–4 | 3 ^d | — | — | — | — | — |
| 20 | Salivary glands | — | — | — | 2 | 3 | 2 | Sjögren's syndrome | — | — | — | — |
| 21 | Salivary glands | — | M | 40 | 3 | 3 | 3 | — | — | — | — | — |
| 22 | Thyroid | — | F | 62 | 1 | 2 | 2 | — | — | — | — | — |
| 23 | Liver | — | M | 66 | 0 | 3–4 | 3 ^d | — | — | — | — | — |
| 24 | Small intestine, Mesenteric LN | — | F | 46 | 2 | 4 | 2 | — | — | — | — | — |
| 25 | Stomach | I | F | 77 | 2 | 3 | 2 | — | — | — | — | — |

^a With exception of case 9 (FOXP1 with an unknown partner), all other cases are negative for translocations involving MALT1, BCL10 and FOXP1. Cases 2–4 with A20 deletion correspond to array–CGH cases 8, 13 and 31, respectively; cases 9–15 with gain at TNFA/B/C locus correspond to array–CGH cases 3, 5, 11, 15, 16, 29 and 30, respectively; cases 5 and 8 with both chromosome 6 abnormalities correspond to array–CGH cases 28 and 12, respectively, in Table 2.

^b The abnormal A20 probe signal (one copy or less) was found in >50% of nuclei in 9/12 (75%) cases (overall range, 17–94%; median, 52%).

^c The abnormal TNFA/B/C probe signal (three copies or more) was in >50% of nuclei in 13/19 (68%) cases (overall range, 20–94%; median, 61%).

^d Gains of only one extra copy of the centromeric probe 6 associated with two extra copies of the TNFA/B/C locus, suggesting the presence of an isochromosome 6p–6p [23].

^e Follicular lymphoma is clonally linked to MALT lymphoma and both lymphomas harbour t(14;18)(q32;q21)/IGH-BCL2 [24].

CEP, centromeric probe; —, unavailable; RT, radiotherapy; CR, complete response; m, months; LG, lachrymal glands; LN, lymph node.

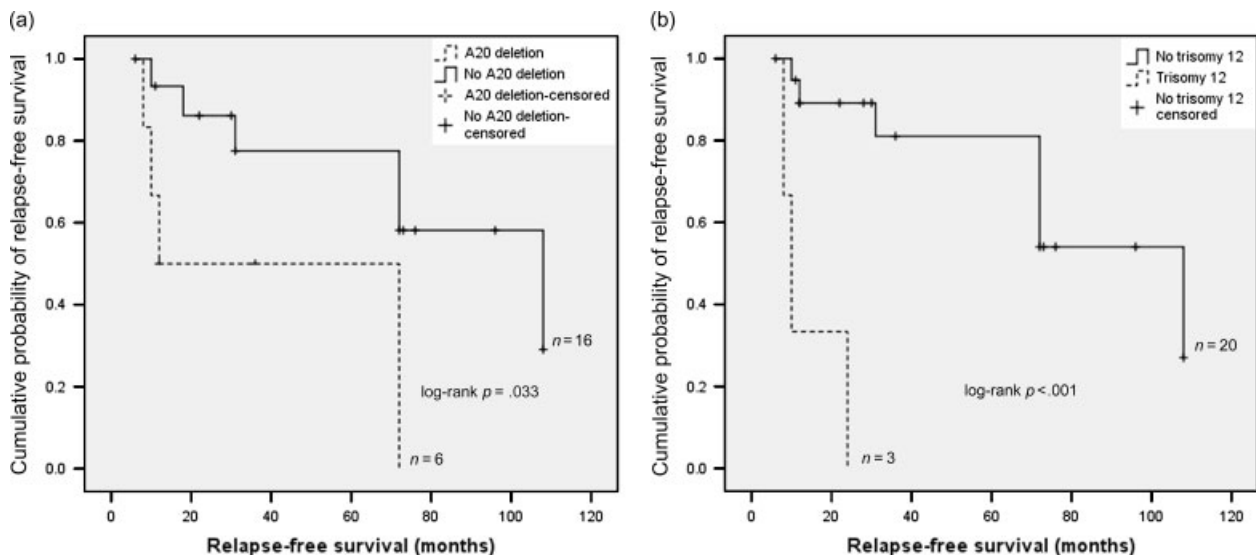


Figure 3. Relapse-free survival in ocular adnexal MALT lymphoma. Kaplan–Meier estimates with and without: (a) *A20* deletion; (b) trisomy 12. The lymphoma relapse-free survival was measured from the time of the diagnosis to the date of the first relapse. The event ‘relapse’ was right-censored

whether *A20* is also inactivated by somatic mutation and/or promoter methylation. Importantly, we also report for the first time evidence of an association between *A20* deletion and gain at the *TNFA/B/C* locus. High-resolution chromosome 6 tile-path array–CGH defined a 8.2 Mb MCR of gain at 6p21.2–22 and identified a novel recurrent focal peak within this MCR in four cases, which was centred at BAC clone bPG296p20 (6p21.33). Interphase FISH confirmed that this locus was further selected for extra copy gain, albeit at a moderate level, and showed that such gain was significantly associated with *A20* deletion. Among 15 genes within this BAC clone and its vicinity, *TNFA*, *TNFB*, *TNFC* and *NFκBIL1* are the most relevant in the context of lymphomagenesis. *NFκBIL1*, despite its name, does not function as an *NF-κB* inhibitor and may be involved in mRNA processing or translational regulation [33]. *TNFA/B/C* are powerful pro-inflammatory cytokines and potent activators of the *NF-κB* pathway [34]. The increased dosage of their genes may enhance their expression and thus *NF-κB*-activation. *A20* restricts TNF-induced *NF-κB* activities by inactivating and targeting the receptor interacting protein RIP, an essential mediator of TNF receptor signalling [35], for degradation through regulation of its ubiquitination [36]. A reduced *A20* gene dosage may impair such negative regulation and thus act synergistically with enhanced TNF receptor signalling.

The *NF-κB* activation pathway is commonly targeted by the oncogenic product of MALT lymphoma-associated translocations *t(11;18)(21;q21)/API2–MALT1*, *t(1;14)(p22;q32)/BCL10–IGH* and *t(14;18)(q32;q21)/IGH–MALT1* [8]. Our study revealed that *A20* deletion and *TNFA/B/C* gain occurred exclusively in MALT lymphomas without these translocations, providing evidence that genetic alterations in translocation negative MALT lymphoma also target

the *NF-κB* pathway. Thus, a common molecular mechanism may be operational in these MALT lymphomas involving different oncogenic events.

A20 deletion was preferentially associated with MALT lymphoma of the ocular adnexa, salivary gland and thyroid. MALT lymphomas of the salivary gland and thyroid are closely associated with lymphoepithelial sialadenitis and Hashimoto thyroiditis, respectively [1]. There is evidence suggesting an association between autoimmunity and ocular adnexal MALT lymphoma, such as the involvement of the ocular adnexa by systemic lupus erythematosus and Sjögren’s syndrome [37–38], frequent detection of serum rheumatoid factor in patients with ocular adnexal MALT lymphoma [39] and recurrent use of the autoimmune prone immunoglobulin heavy chain variable gene VH3–23 by the lymphoma cells [40]. TNF and TNF receptor signalling are critical to many immune responses and their deregulation is linked to several autoimmune disorders, including rheumatoid arthritis and systemic lupus erythematosus [41]. Recently, SNP genotyping shows that the *A20* gene locus is also associated with risk of rheumatoid arthritis [42] and systemic lupus erythematosus [43]. Clinical correlation in our series of ocular adnexal MALT lymphoma did not show significant correlation between *A20* deletion or *TNFA/B/C* locus gain and the presence of autoimmune disease, although two cases with homozygous *A20* deletion had an autoimmune disorder. The retrospective nature of our study may have underestimated the prevalence of autoimmunity in our patient cohort, and study of additional patients with clinical and laboratory evidence of autoimmunity is warranted.

A20 deletion and trisomy 12 were associated with adverse clinical parameters in ocular adnexal MALT lymphoma. *A20* deletion was significantly associated with lymphoma involvement of the orbital soft tissue

and with concurrent involvement of different adnexal tissues or distant spread at diagnosis. *A20* deletion was also more frequent in cases with lymphoma relapse than those without relapse and was significantly associated with a shorter lymphoma relapse-free survival. Similarly, trisomy 12 was significantly associated with both lymphoma relapse and a shorter lymphoma relapse-free survival. In view of the recent reports that a proportion of ocular adnexal MALT lymphoma is associated with *Chlamydia psittaci* infection and could be successfully treated by antibiotics [16,44], it is pertinent to investigate whether these genetic abnormalities impact on such treatment response and to prospectively validate the above clinical correlations in a large cohort of cases.

In summary, we identified NF- κ B inhibitor *A20* as the target of 6q23 deletion in ocular adnexal MALT lymphoma and demonstrated that *A20* deletion was significantly associated with *TNFA/B/C* locus gain and occurred preferentially in translocation negative MALT lymphoma of the ocular adnexa and salivary glands, but not in those of the lung and stomach. *A20* deletion, associated with adverse clinical parameters in ocular adnexal MALT lymphoma, may play a critical role in the development of MALT lymphoma, particularly translocation-negative cases arising from sites involved by autoimmunity. Our study warrants further investigations to assess the potential link between *A20* deletion, *TNFA/B/C* gain, NF- κ B activation, autoimmunity and the development of MALT lymphoma.

Acknowledgements

We thank Dr Paul Duthie, Christie Hospital NHS Foundation Trust, Dr Campidelli, University of Bologna, and Ms Sue Goddard, University College London, for their help in retrieving clinical data, as well as Dr Danita Pearson and Miss Alison Goatly for providing BAC clones and probe-labelling protocol for fluorescence *in situ* hybridization. The Du lab is supported by the Leukaemia and Lymphoma Society, the Elimination of Leukaemia fund, and Leukemia Research Fund. CB is supported by a Senior Clinician Scientist Fellowship from The Health Foundation, The Royal College of Pathologists and The Pathological Society of Great Britain and Ireland. The fluorescence microscope used in this study was funded by Cambridge Fund for the Prevention of Disease (CAMPOD), the Pathological Society of Great Britain and Ireland, and Openwork Foundation, Swindon. Array-CGH row data are available in the supporting information to this article.

Supporting information

Supporting information may be found in the online version of this article.

References

- Du MQ. MALT lymphoma: recent advances in aetiology and molecular genetics. *J Clin Exp Hematop* 2007;**47**:31–42.
- Ye H, Liu H, Attygalle A, Wotherspoon AC, Nicholson AG, Charlotte F, *et al*. Variable frequencies of t(11; 18)(q21; q21) in MALT lymphomas of different sites: significant association with CagA strains of *H. pylori* in gastric MALT lymphoma. *Blood* 2003;**102**:1012–1018.
- Remstein ED, Dogan A, Einerson RR, Paternoster SF, Fink SR, Law M, *et al*. The incidence and anatomic site specificity of chromosomal translocations in primary extranodal marginal zone B-cell lymphoma of mucosa-associated lymphoid tissue (MALT lymphoma) in North America. *Am J Surg Pathol* 2006;**30**:1546–1553.
- Ye H, Gong L, Liu H, Ruskone-Fourmestreaux A, de Jong D, Pileri S, *et al*. Strong BCL10 nuclear expression identifies gastric MALT lymphomas that do not respond to *H. pylori* eradication. *Gut* 2006;**55**:137–138.
- Goatly A, Bacon CM, Nakamura S, Ye H, Kim I, Brown PJ, *et al*. FOXP1 abnormalities in lymphoma: translocation breakpoint mapping reveals insights into deregulated transcriptional control. *Mod Pathol* 2008;**21**:902–911.
- Haralambieva E, Adam P, Ventura R, Katzenberger T, Kalla J, Holler S, *et al*. Genetic rearrangement of FOXP1 is predominantly detected in a subset of diffuse large B-cell lymphomas with extranodal presentation. *Leukemia* 2006;**20**:1300–1303.
- Hu H, Wang B, Borde M, Nardone J, Maika S, Allred L, *et al*. Foxp1 is an essential transcriptional regulator of B cell development. *Nat Immunol* 2006;**7**:819–826.
- Isaacson PG, Du M.Q. MALT lymphoma: from morphology to molecules. *Nat Rev Cancer* 2004;**4**:644–653.
- Liu H, Ruskone Fourmestreaux A, Lavergne-Slove A, Ye H, Molina T, Bouhnik Y, *et al*. Resistance of t(11; 18) positive gastric mucosa-associated lymphoid tissue lymphoma to *Helicobacter pylori* eradication therapy. *Lancet* 2000;**357**:39–40.
- Ye H, Gong L, Liu H, Ruskone-Fourmestreaux A, de Jong D, Pileri S, *et al*. Strong BCL10 nuclear expression identifies gastric MALT lymphomas that do not respond to *H. pylori* eradication. *Gut* 2006;**55**:137–138.
- Brynes RK, Almaguer PD, Leathery KE, McCourty A, Arber DA, Medeiros LJ, *et al*. Numerical cytogenetic abnormalities of chromosomes 3, 7, and 12 in marginal zone B-cell lymphomas. *Mod Pathol* 1996;**9**:995–1000.
- Streubel B, Simonitsch-Klupp I, Mullauer L, Lamprecht A, Huber D, Siebert R, *et al*. Variable frequencies of MALT lymphoma-associated genetic aberrations in MALT lymphomas of different sites. *Leukemia* 2004;**18**:1722–1726.
- Zhou Y, Ye H, Martin-Subero JI, Hamoudi R, Lu YJ, Wang R, *et al*. Distinct comparative genomic hybridization profiles in gastric mucosa-associated lymphoid tissue lymphomas with and without t(11; 18)(q21; q21). *Br J Haematol* 2006;**133**:35–42.
- Zhou Y, Ye H, Martin-Subero JI, Gesk S, Hamoudi RA, Lu YJ, *et al*. The pattern of genomic gains in salivary gland MALT lymphomas. *Haematologica* 2007;**92**:921–927.
- Johnson NA, Hamoudi RA, Ichimura K, Liu L, Pearson DM, Collins VP, *et al*. Application of array CGH on archival formalin-fixed paraffin-embedded tissues including small numbers of microdissected cells. *Lab Invest* 2006;**86**:968–978.
- Chanudet E, Zhou Y, Bacon C, Wotherspoon A, Muller-Hermelink HK, Adam P, *et al*. *Chlamydia psittaci* is variably associated with ocular adnexal MALT lymphoma in different geographical regions. *J Pathol* 2006;**209**:344–351.
- Ye H, Dogan A, Karran L, Willis TG, Chen L, Wlodarska I, *et al*. BCL10 expression in normal and neoplastic lymphoid tissue: nuclear localization in MALT lymphoma. *Am J Pathol* 2000;**157**:1147–1154.
- Chanudet E, Adam P, Nicholson AG, Wotherspoon AC, Ranaldi R, Goteri G, *et al*. *Chlamydia* and *Mycoplasma* infections in pulmonary MALT lymphoma. *Br J Cancer* 2007;**97**:949–951.
- McCabe MG, Ichimura K, Liu L, Plant K, Backlund LM, Pearson DM, *et al*. High-resolution array-based comparative genomic hybridization of medulloblastomas and supratentorial primitive neuroectodermal tumors. *J Neuropathol Exp Neurol* 2006;**65**:549–561.
- Ichimura K, Mungall AJ, Fiegler H, Pearson DM, Dunham I, Carter NP, *et al*. Small regions of overlapping deletions on 6q26

- in human astrocytic tumours identified using chromosome 6 tile path array-CGH. *Oncogene* 2006;**25**:1261–1271.
21. Boone DL, Turer EE, Lee EG, Ahmad RC, Wheeler MT, Tsui C, et al. The ubiquitin-modifying enzyme A20 is required for termination of Toll-like receptor responses. *Nat Immunol* 2004;**5**:1052–1060.
 22. Otipari AW Jr, Boguski MS, Dixit VM. The A20 cDNA induced by tumor necrosis factor alpha encodes a novel type of zinc finger protein. *J Biol Chem* 1990;**265**:14705–14708.
 23. Whang Peng J, Knutsen T, Jaffe E, Raffeld M, Zhao WP, Duffey P, et al. Cytogenetic study of two cases with lymphoma of mucosa-associated lymphoid tissue. *Cancer Genet Cytogenet* 1994;**77**:74–80.
 24. Aiello A, Du MQ, Diss TC, Peng HZ, Pezzella F, Papini D, et al. Simultaneous phenotypically distinct but clonally identical mucosa-associated lymphoid tissue and follicular lymphoma in a patient with Sjogren's syndrome. *Blood* 1999;**94**:2247–2251.
 25. Menasce LP, Orphanos V, Santibanez-Koref M, Boyle JM, Harrison CJ. Common region of deletion on the long arm of chromosome 6 in non-Hodgkin's lymphoma and acute lymphoblastic leukaemia. *Genes Chromosomes Cancer* 1994;**10**:286–288.
 26. Ross CW, Ouillet PD, Saddler CM, Shedden KA, Malek SN. Comprehensive analysis of copy number and allele status identifies multiple chromosome defects underlying follicular lymphoma pathogenesis. *Clin Cancer Res* 2007;**13**:4777–4785.
 27. Tagawa H, Suguro M, Tsuzuki S, Matsuo K, Karnan S, Ohshima K, et al. Comparison of genome profiles for identification of distinct subgroups of diffuse large B-cell lymphoma. *Blood* 2005;**106**:1770–1777.
 28. Taborelli M, Tibiletti MG, Martin V, Pozzi B, Bertoni F, Capella C. Chromosome band 6q deletion pattern in malignant lymphomas. *Cancer Genet Cytogenet* 2006;**165**:106–113.
 29. Kim WS, Honma K, Karnan S, Tagawa H, Kim YD, Oh YL, et al. Genome-wide array-based comparative genomic hybridization of ocular marginal zone B cell lymphoma: comparison with pulmonary and nodal marginal zone B cell lymphoma. *Genes Chromosomes Cancer* 2007;**46**:776–783.
 30. Honma K, Tsuzuki S, Nakagawa M, Karnan S, Aizawa Y, Kim WS, et al. TNFAIP3 is the target gene of chromosome band 6q23.3-q24.1 loss in ocular adnexal marginal zone B cell lymphoma. *Genes Chromosomes Cancer* 2008;**47**:1–7.
 31. Lin SC, Chung JY, Lamothe B, Rajashankar K, Lu M, Lo YC, et al. Molecular basis for the unique deubiquitinating activity of the NF- κ B inhibitor A20. *J Mol Biol* 2008;**376**:526–540.
 32. Coornaert B, Baens M, Heynincx K, Bekaert T, Haegman M, Staal J, et al. T cell antigen receptor stimulation induces MALT1 paracaspase-mediated cleavage of the NFOB inhibitor A20. *Nat Immunol* 2008;**9**:263–271.
 33. Greetham D, Ellis CD, Mewar D, Fearon U, an Ultaigh SN, Veale DJ, et al. Functional characterization of NF- κ B inhibitor-like protein 1 (NF- κ BIL1), a candidate susceptibility gene for rheumatoid arthritis. *Hum Mol Genet* 2007;**16**:3027–3036.
 34. Aggarwal BB. Signalling pathways of the TNF superfamily: a double-edged sword. *Nat Rev Immunol* 2003;**3**:745–756.
 35. Kelliher MA, Grimm S, Ishida Y, Kuo F, Stanger BZ, Leder P. The death domain kinase RIP mediates the TNF-induced NF- κ B signal. *Immunity* 1998;**8**:297–303.
 36. Wertz IE, O'Rourke KM, Zhou H, Eby M, Aravind L, Seshagiri S, et al. De-ubiquitination and ubiquitin ligase domains of A20 downregulate NF- κ B signalling. *Nature* 2004;**430**:694–699.
 37. Arevalo JF, Lowder CY, Muci-Mendoza R. Ocular manifestations of systemic lupus erythematosus. *Curr Opin Ophthalmol* 2002;**13**:404–410.
 38. Bjerrum KB. Primary Sjogren's syndrome and keratoconjunctivitis sicca: diagnostic methods, frequency and social disease aspects. *Acta Ophthalmol Scand Suppl* 2000;**231**:1–37.
 39. Kubota T, Moritani S, Yoshino T, Nagai H, Terasaki H. Ocular adnexal mucosa-associated lymphoid tissue lymphoma with polyclonal hypergammaglobulinemia. *Am J Ophthalmol* 2008;**145**:941–950.
 40. Adam P, Haralambieva E, Hartmann M, Mao Z, Ott G, Rosenwald A. Rare occurrence of IgVH gene translocations and restricted IgVH gene repertoire in ocular MALT-type lymphoma. *Haematologica* 2008;**93**:319–320.
 41. Mackay F, Kalled SL. TNF ligands and receptors in autoimmunity: an update. *Curr Opin Immunol* 2002;**14**:783–790.
 42. Plenge RM, Cotsapas C, Davies L, Price AL, de Bakker PI, Maller J, et al. Two independent alleles at 6q23 associated with risk of rheumatoid arthritis. *Nat Genet* 2007;**39**:1477–1482.
 43. Musone SL, Taylor KE, Lu TT, Nititham J, Ferreira RC, Ortmann W, et al. Multiple polymorphisms in the TNFAIP3 region are independently associated with systemic lupus erythematosus. *Nat Genet* 2007;**39**:1477–1482.
 44. Ferreri AJ, Ponzoni M, Guidoboni M, De Conciliis C, Resti AG, Mazzi B, et al. Regression of ocular adnexal lymphoma after *Chlamydia psittaci*-eradicating antibiotic therapy. *J Clin Oncol* 2005;**23**:5067–5073.

Supplementary Table S1. Clinico-pathological correlations in ocular adnexal MALT lymphoma

| <i>Characteristics</i> | Total cases (%) | <i>Anatomical location of lymphoma</i> | | <i>P</i> ^b |
|-----------------------------|-----------------|--|-------------------------------------|-----------------------|
| | | Orbital soft tissue with or without conjunctiva and/or lachrymal glands ^a (%) | Conjunctiva or lachrymal glands (%) | |
| <i>A20</i> deletion (n=34) | | | | |
| Positive | 8 (20) | 8 (35) | 0 (0) | .027 |
| Negative | 26 (80) | 15 (65) | 11 (100) | |
| <i>TNFA/B/C</i> gain (n=34) | | | | |
| Positive | 10 (29) | 9 (39) | 1 (9) | .077 |
| Negative | 24 (71) | 14 (61) | 10 (91) | |
| Trisomy 12 (n=32) | | | | |
| Positive | 4 (12) | 3 (14) | 1 (9) | NS |
| Negative | 28 (88) | 18 (86) | 10 (91) | |
| Clinical stage (n=21) | | | | |
| I | 16 (76) | 12 (80) | 4 (67) | NS |
| ≥ II | 5 (24) | 3 (20) | 2 (33) | |

| <i>Characteristics</i> | Total cases (%) | <i>Autoimmunity</i> | | <i>P</i> ^b |
|-----------------------------|-----------------|-----------------------|--------------------------|-----------------------|
| | | Clinical evidence (%) | No clinical evidence (%) | |
| <i>A20</i> deletion (n=28) | | | | |
| Positive | 7 (25) | 1 (33) | 6 (24) | NS |
| Negative | 21 (75) | 2 (67) | 19 (76) | |
| <i>TNFA/B/C</i> gain (n=28) | | | | |
| Positive | 9 (32) | 1 (33) | 8 (32) | NS |
| Negative | 19 (68) | 2 (67) | 17 (68) | |
| Trisomy 12 (n=24) | | | | |
| Positive | 3 (12) | 0 (0) | 3 (14) | NS |
| Negative | 21 (88) | 2 (100) | 19 (86) | |
| Clinical stage (n=24) | | | | |
| I | 19 (79) | 2 (100) | 17 (77) | NS |
| ≥ II | 5 (21) | 0 (0) | 5 (33) | |

| <i>Characteristics</i> | Total cases (%) | <i>Lymphoma relapse</i> | | <i>P</i> ^b |
|-----------------------------|-----------------|-------------------------|--------------------|-----------------------|
| | | Relapse (%) | No relapse (%) | |
| <i>A20</i> deletion (n=22) | | | | |
| Positive | 6 (27) | 4 (40) | 2 (17) | .221 |
| Negative | 16 (73) | 6 (60) | 10 (83) | |
| <i>TNFA/B/C</i> gain (n=22) | | | | |
| Positive | 8 (36) | 4 (40) | 4 (33) | NS |
| Negative | 14 (64) | 6 (60) | 8 (67) | |
| Trisomy 12 (n=23) | | | | |
| Positive | 3 (13) | 3 (33) | 0 (0) | .047 |
| Negative | 20 (87) | 6 (67) | 14 (100) | |
| Clinical stage (n=20) | | | | |
| I | 15 (75) | 5 (56) | 10 (91) | .097 |
| ≥ II | 5 (25) | 4 (44) | 1 ^c (9) | |

^a All the 8 cases with *A20* deletion showed involvement of the orbital soft tissue: 3/8 cases had concurrent involvement of the orbital soft tissue and conjunctiva and/or lachrymal glands, 1 additional lymphoma spread to the iliac lymph node, whereas only 1/26 of the cases without *A20* deletion involved more than one adnexal tissue (orbital soft tissue and lachrymal gland, case with 6p gain) and none showed extra-ocular spread at diagnosis.

^bFisher's exact probability test.

^cAlive with disease 28 months (treated by leukeran, partial response).

NS, non significant.

Original Paper

Chlamydia psittaci is variably associated with ocular adnexal MALT lymphoma in different geographical regions

E Chanudet,¹ Y Zhou,² CM Bacon,¹ AC Wotherspoon,³ H-K Müller-Hermelink,⁴ P Adam,⁴ HY Dong,⁵ D de Jong,⁶ Y Li,⁷ R Wei,⁸ X Gong,⁹ Q Wu,¹⁰ R Ranaldi,¹¹ G Goteri,¹¹ SA Pileri,¹² H Ye,¹ RA Hamoudi,¹ H Liu,¹ J Radford¹³ and M-Q Du^{1*}

¹Department of Pathology, University of Cambridge, UK

²Nanfeng Hospital, Southern Medical University, Guangzhou, China

³Department of Histopathology, Royal Marsden Hospital, London, UK

⁴Institute of Pathology, University of Würzburg, Germany

⁵Genzyme Genetics, New York, USA

⁶Department of Pathology, Netherlands Cancer Institute, Amsterdam, The Netherlands

⁷Sun Yat-Sen University Ophthalmologic Hospital, Guangzhou, China

⁸Department of Ophthalmology, Changzheng Hospital, Shanghai, China

⁹Department of Pathology, Hainan Province Hospital, China

¹⁰Sun Yat-Sen University Tumour Hospital, Guangzhou, China

¹¹Anatomia Patologica, Università Politecnica delle Marche, Ancona, Italy

¹²Unità Operativa di Emolinfopatia - Università degli Studi di Bologna, Italy

¹³Cancer Research UK, Department of Medical Oncology, Christie Hospital, Manchester, UK

*Correspondence to:

Professor M-Q Du, University of Cambridge, Division of Molecular Histopathology, Box 231, Level 3, Lab Block, Addenbrooke's Hospital, Hills Road, Cambridge CB2 2QQ, UK.

E-mail: mqd20@cam.ac.uk

Abstract

Infectious agents play a critical role in MALT lymphoma development. Studies from Italy showed *Chlamydia psittaci* infection in 87% of ocular adnexal MALT lymphomas and complete or partial regression of the lymphoma after *C. psittaci* eradication in four of nine cases. However, *C. psittaci* was not demonstrated in ocular adnexal MALT lymphomas from the USA. This study was thus designed to investigate further the role of *C. psittaci*, and other infectious agents commonly associated with chronic eye disease, in the development of ocular adnexal MALT lymphoma. The presence of *C. psittaci*, *C. trachomatis*, *C. pneumoniae*, herpes simplex virus 1 and 2 (HSV1, HSV2), and adenovirus 8 and 19 (ADV8, ADV19) was assessed separately by polymerase chain reaction in 142 ocular adnexal MALT lymphomas, 53 non-marginal zone lymphomas, and 51 ocular adnexal biopsies without a lymphoproliferative disorder (LPD), from six geographical regions. *C. psittaci* was detected at similar low frequencies in non-LPD and non-marginal zone lymphoma groups from different geographical regions (0–14%). Overall, the prevalence of *C. psittaci* was significantly higher in MALT lymphomas (22%) than in non-LPD (10%, $p = 0.042$) and non-marginal zone lymphoma cases (9%, $p = 0.033$). However, the prevalence of *C. psittaci* infection in MALT lymphoma showed marked variation among the six geographical regions examined, being most frequent in Germany (47%), followed by the East Coast of the USA (35%) and the Netherlands (29%), but relatively low in Italy (13%), the UK (12%), and Southern China (11%). No significant differences in the detection of *C. pneumoniae*, *C. trachomatis*, HSV1, HSV2, ADV8, and ADV19 were found between lymphomas and controls from different geographical regions. In conclusion, our results show that *C. psittaci*, but not *C. pneumoniae*, *C. trachomatis*, HSV1, HSV2, ADV8 or ADV19, is associated with ocular adnexal MALT lymphoma and that this association is variable in different geographical areas.

Copyright © 2006 Pathological Society of Great Britain and Ireland. Published by John Wiley & Sons, Ltd.

Keywords: *Chlamydia psittaci*; ocular adnexal MALT lymphoma

Received: 24 January 2006

Revised: 22 February 2006

Accepted: 25 February 2006

Introduction

Extranodal marginal zone B cell lymphoma of mucosa-associated lymphoid tissue (MALT lymphoma) arises at a number of extranodal sites including the gastrointestinal tract, salivary and thyroid glands, lung,

ocular adnexa, and skin. Interestingly, these organs are devoid of native lymphoid tissue: lymphoma at these sites arises from the MALT acquired as a result of a chronic inflammatory or autoimmune disorder [1]. The inflammatory disease associated with MALT lymphoma not only provides a microenvironment that is

crucial for malignant transformation, but the immunological response generated during the inflammatory process also promotes the growth of the lymphoma cells. This is best exemplified in gastric MALT lymphoma, which is driven by *Helicobacter pylori* mediated immune responses and can be effectively treated by eradication of the bacterium in the majority of cases [2–4]. Similarly, *Borrelia burgdorferi* and *Campylobacter jejuni* infections are associated with cutaneous marginal zone B-cell lymphoma and immunoproliferative small intestinal disease respectively, and eradication of these organisms resulted in complete regression of the lymphoma in some cases [5–10]. Together, these findings suggest that the development of MALT lymphomas at other sites may also be associated with infectious agents.

Ocular adnexal MALT lymphoma represents a significant proportion (approximately 12%) of all MALT lymphomas [11] and is the most common lymphoma of the ocular adnexa [12–14], occurring principally in the conjunctiva, orbital soft tissue, and lachrymal apparatus. Analogous to the evolution of gastric MALT lymphoma from *H. pylori* associated chronic gastritis, ocular adnexal MALT lymphoma may be associated with chronic conjunctivitis; interestingly, there is a considerable overlap in both the histological and clinical presentations of chronic conjunctivitis and ocular adnexal MALT lymphoma [15–17]. Ocular adnexal MALT lymphoma thus may arise from the MALT acquired as a result of chronic inflammatory responses. Infectious agents underlying chronic eye infection, particularly those involved in chronic conjunctivitis such as *Chlamydia*, herpes simplex virus (HSV), and adenovirus (ADV) [18–22], may therefore play a role in the development of lymphoma.

The aetiology of ocular adnexal MALT lymphoma is currently unclear. Recent studies from Italy showed evidence of *Chlamydia psittaci* (*C. psittaci*) infection in 87% of ocular adnexal MALT lymphomas [23], and eradication of the organism by antibiotics led to complete or partial regression of the disease in four of nine cases studied [24]. However, such an association was not demonstrated in cases of ocular adnexal MALT lymphoma from South Florida and Rochester (New York) areas in the USA [25,26]. This raises the possibility that *C. psittaci* may be variably associated with ocular adnexal MALT lymphoma in different geographical regions and that other aetiological factors may be involved in the development of this lymphoma. To examine these issues, we screened for infectious agents underlying chronic eye infection, namely *C. psittaci*, *C. trachomatis*, *C. pneumoniae*, HSV types 1 and 2, and ADV types 8 and 19, in ocular adnexal lymphomas of various subtypes as well as ocular adnexal biopsies without a lymphoproliferative disorder (LPD), from six geographical regions.

Materials and methods

Tissue specimens

Archival formalin-fixed paraffin-embedded ocular adnexal biopsies from 263 patients from six geographical areas, obtained between 1981 and 2005, were analysed. Of these cases, 246 had adequate material as judged by quality control polymerase chain reaction (PCR; detailed in a later section), and were thus suitable for PCR screening of infectious agents. These included a total of 195 lymphomas, consisting of 142 MALT lymphomas and 53 non-marginal

Table 1. Demographic and histological characteristics of ocular adnexal lymphomas and controls from different geographical areas

| Characteristics | UK ¹ | Germany | Netherlands | Italy ² | Southern China ³ | East coast USA ⁴ | Total |
|-------------------------|-----------------|-----------|-------------|--------------------|-----------------------------|-----------------------------|-----------|
| No of patients | 80 | 37 | 24 | 21 | 59 | 25 | 246 |
| Median age (range) | 64 (17–93)* | 58 (8–95) | 62 (19–93) | 61 (37–86) | 60 (32–87) [‡] | 69 (28–90) | 62 (8–95) |
| Male/female ratio | 0.9* | 1.3 | 0.6 | 0.5 | 2.6 [‡] | 1.3 | 1.3 |
| Diagnosis | | | | | | | |
| MALT L | 33 | 19 | 21 | 15 | 37 | 17 | 142 |
| Non-MZL ⁵ | 7 | 9 | 3 | 6 | 20 | 8 | 53 |
| Non-LPD ⁶ | 40 | 9 | — | — | 2 | — | 51 |
| Anatomical localization | | | | | | | |
| Conjunctiva | 50 [†] | 22 | 22 | 9 | 1 | 10 | 114 |
| Orbit | 5 [†] | 13 | 2 | 10 | 49 | 9 | 88 |
| Other ⁷ | 6 [†] | 2 | — | 2 | 9 | 6 | 25 |

¹ 51 cases from London, 19 cases from Manchester, and 10 cases from Cambridge.

² 13 cases from Ancona and eight cases from Bologna.

³ 29 cases from Canton, 15 cases from Hainan, and 15 cases from Shanghai.

⁴ 18 cases from northeast, three from mid-east, and four from southeast coast.

⁵ 21 follicular lymphomas, 13 mantle-cell lymphomas, 11 diffuse large B-cell lymphomas, and eight T/NK-cell lymphomas.

⁶ 39 cases were conjunctival biopsies from unselected autopsies with no prior history of conjunctival or ocular disease [27] and the remaining cases were mainly pinguecula and occasionally chalazion.

⁷ Eyelid, lachrymal gland, extraocular muscle, globe, and three ocular adnexal cases without details of biopsy site.

* Excluding 19 cases from Manchester and non-LPD cases, for which data are not available.

[†] Excluding 19 cases from Manchester, for which data are not available.

[‡] Excluding 29 cases from Canton, for which data are not available.

No = number; LPD = lymphoproliferative disorder; MZL = marginal zone lymphoma; MALT L = mucosa-associated lymphoid tissue lymphoma.

zone lymphomas, as well as 51 ocular adnexal biopsies without any histological evidence of a LPD (Table 1). Cases were diagnosed or reviewed by haematopathologists. Table 1 summarises the anatomical location of these biopsies together with the patients' age and sex. Local ethical guidelines were followed for the use of archival paraffin embedded tissues for research, and such use was approved by the local ethics committees of the authors' institutions where required.

DNA extraction

Tissue sections (3–5 µm) were dewaxed in xylene and washed in ethanol. DNA was extracted and purified using QIAamp DNA Mini Kit (QIAGEN) according to the manufacturer's instructions, and quantified using a NanoDrop spectrophotometer (NanoDrop Technologies, Wilmington, USA).

Quality control PCR

The quality of each DNA sample was assessed by PCR amplification of variously sized human gene fragments (100 bp, 200 bp, 300 bp, and 400 bp) (Table 2) [28]. A multiplex PCR was carried out using ABgene Thermo-Start DNA polymerase (Surrey, UK) following the supplier's protocol. PCR products were analysed by electrophoresis on 6% polyacrylamide gels. Only cases with successful amplification of a 200 bp or larger product were used to screen for infectious agents

Detection of infectious agents by PCR

Stringent laboratory procedures for PCR set-up and product analyses were carefully followed to avoid any potential cross contamination. PCRs without template DNA were randomly interspersed among test

samples to monitor potential cross contamination. Procedures for the detection of each *Chlamydia* species were validated by a double blind comparison of two series of DNA samples with known chlamydial status between our laboratory and Dr Dolcetti's laboratory.

Chlamydiae

The detection of *C. trachomatis*, *C. psittaci*, and *C. pneumoniae* was carried out using a previously described Touchdown Enzyme Time-Release (TETR) PCR [23,29], with the following modifications. Instead of multiplex PCR, separate PCRs for each *Chlamydia* species were performed. For *C. trachomatis* and *C. pneumoniae*, new primer sets were designed to target smaller fragments of the 16S rRNA gene (Table 2), thus suitable for screening DNA samples prepared from paraffin-embedded tissues. Additionally, higher touchdown annealing temperatures from 66°C to 56°C were used for *C. trachomatis* detection. For all *Chlamydiae* screening, PCR amplifications were carried out in a 25 µl reaction mixture containing 150 ng of template DNA. PCR products were analysed by electrophoresis on 10% polyacrylamide gels.

In each case, three independent PCR amplifications were carried out for each *Chlamydia* species. To make data comparable, we adopted the approach by Ferreri *et al* [23] and only cases with positive PCR results in at least two of the three independent reactions were regarded as true positives.

Adenovirus and Herpes simplex virus

ADV types 8 and 19 were separately detected by PCR amplification of the viral hexon gene (Table 2). ADV8 PCR was carried out in a 25 µl reaction mixture

Table 2. PCR primers used for DNA quality assessment and the molecular detection of infectious agents

| | Gene | Primer name | Sequence | Product size (bp) |
|--|--|---------------------------|--------------------------------|-------------------|
| Quality control [28] | TBXAS1 exon9 | Q 100s | 5' GCCCGACATTCTGCAAGTCC 3' | 100 |
| | | Q 100as | 5' GGTGTTGCCGGGAAGGGTT 3' | |
| | Recombination activating gene 1 (RAG1) exon2 | Q 200s | 5' TGTTGACTCGATCCACCCCA 3' | 200 |
| | | Q 200as | 5' TGAGCTGCAAGTTTGGCTGAA 3' | |
| | Promyelocytic leukaemia zinc finger (PLZF) exon1 | Q 300s | 5' TGCGATGTGGTCATCATGGTG 3' | 300 |
| | | Q 300as | 5' CGTGTCAATTGTCGTCTGAGGC 3' | |
| ALL1 fused gene from chromosome 4 (AF4) exon11 | Q 400s | 5' CCGCAGCAAGCAACGAACC 3' | 400 | |
| | Q 400as | 5' GCTTCTCTGGCGGCTCC 3' | | |
| <i>C. psittaci</i> [29] | 16S rRNA and 16S–23S spacer rRNA | CPS 100s | 5' CCCAAGGTGAGGCTGATGAC 3' | 111 |
| | | CPS 101as | 5' CAAACCGTCCTAAGACAGTTA 3' | |
| <i>C. pneumoniae</i> [29] | 16S rRNA | CPN 73s | 5' ATTCGATGCAACGCGAAGGACCT 3' | 73 |
| | | CPN 91as | 5' TGCGGAAAGCTGTATTCTACAGTT 3' | |
| <i>C. trachomatis</i> | 16S rRNA | CTR 116s | 5' TATTTGGGCATCCGAGTAACG 3' | 116 |
| | | CTR 116as | 5' AGACGTCATAGCCTTGGTAGGCC 3' | |
| Adenovirus type 19 | Hexon gene for major capsid protein | ADV19 87s | 5' AACCAGCCAAAGAGGATGAAAG 3' | 87 |
| | | ADV19 87as | 5' TGTCTCTGAAGCCAATGTAGTTG 3' | |
| Adenovirus type 8 | Hexon gene for major capsid protein | ADV8 65s | 5' ATGTGGAAGCTCTGCGGTGGACA 3' | 65 |
| | | ADV8 65as | 5' TCCACACCGTGATTCTCAAT 3' | |
| Herpes simplex virus type 1 and 2 [30] | DNA polymerase gene | HSV1/2 92s | 5' CATCACCGACCCGGAGAGGGAC 3' | 92 |
| | | HSV1/2 92as | 5' GGGCCAGGCGCTTGTGGTGTGA 3' | |

using ABgene Thermo-Start DNA polymerase. The touchdown protocol used consisted of 95 °C × 30 s, 63 °C × 45 s (decreased 1 °C every two cycles until 60 °C), and 72 °C × 30 s, followed by 35 cycles with the annealing temperature at 59 °C. The cycle parameters for ADV19 PCR were identical to those used for *C. trachomatis* PCR.

HSV types 1 and 2 (HSV1/2) were simultaneously screened with a common primer set [30] (Table 2). The cycle parameters for HSV1/2 PCR were identical to those used for ADV8 PCR.

PCR products were analysed by electrophoresis on 10% polyacrylamide gels. As with our assays for *Chlamydiae*, a case was considered positive when the virus was detected in at least two of three PCRs.

DNA sequencing

PCR products from selected cases of different geographical origins were purified and sequenced in both orientations using an ABI 377 DNA sequencer (ABI PRISM Perkin Elmer Warrington, UK). Sequences were analysed by BLAST search of the NCBI database (<http://www.ncbi.nlm.nih.gov/blast>, accessed 9 March 2006).

Statistical analysis

Differences in the prevalence of infectious agents among various lymphoma subtypes and controls were analysed using Fisher's exact test ("stats Package" in R version 2.1.1).

Results

C. psittaci is detected at variable frequencies in ocular adnexal MALT lymphomas from different geographical regions

A total of 246 ocular adnexal biopsies were assessed for the presence of *C. trachomatis*, *C. psittaci*, and *C. pneumoniae* by separate PCRs (Figure 1). Quality control did not show any differences in the quality of DNA samples from lymphoma specimens from the various geographical regions. We sequenced 17 *C. psittaci*, 10 *C. trachomatis*, and 10 *C. pneumoniae* PCR products from different geographical regions and all were confirmed to be specific, demonstrating the reliability of the method. With the exception of one *C. psittaci* and two *C. pneumoniae* PCR products, each of which contained a single nucleotide change, the PCR products sequenced did not show any sequence variations.

Overall, 31/142 (22%) cases of MALT lymphoma from all regions were positive for *C. psittaci*, a frequency significantly higher than that observed in both non-LPD samples ($p = 0.042$) and non-marginal zone lymphoma samples ($p = 0.033$) from all areas. *C. psittaci* DNA was detected at broadly similar frequencies in both non-LPD and non-marginal zone lymphoma groups from different geographical regions (0–14%) (Table 3). In contrast, the bacterium was found at variable prevalences in MALT lymphomas from different regions, being more frequent in Germany (47%), followed by the East Coast of the USA (35%) and the Netherlands (29%), but relatively low in

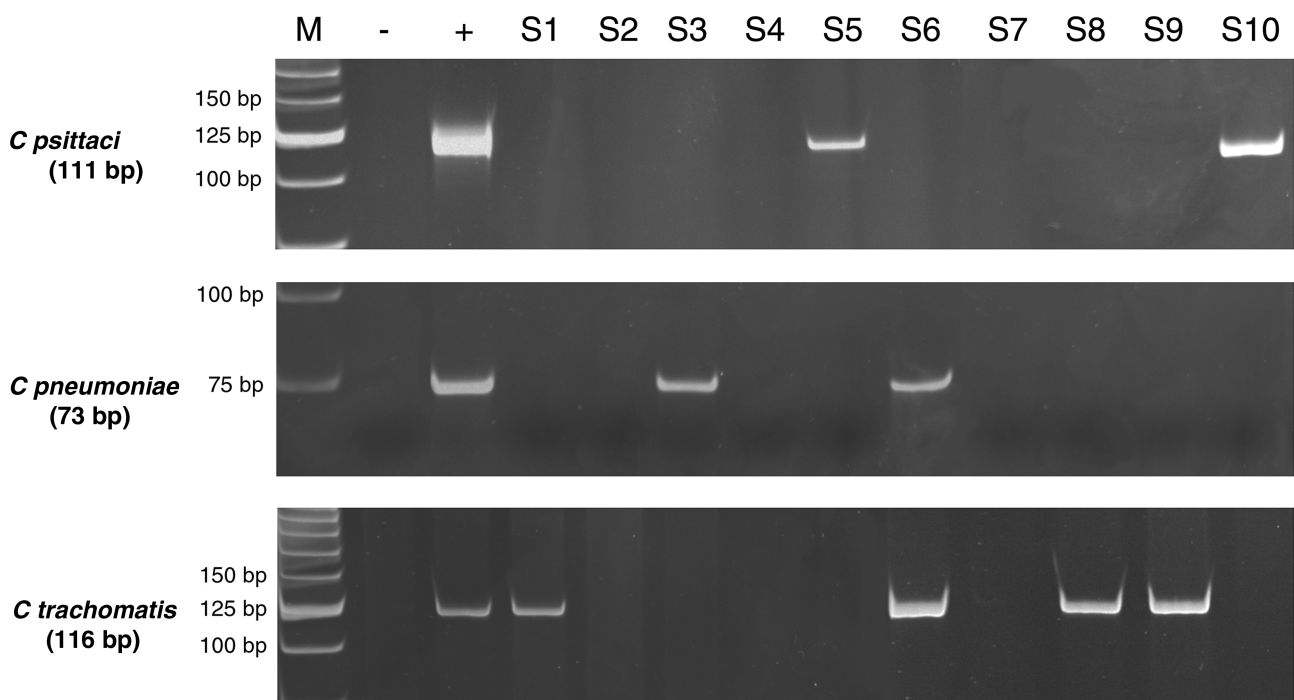


Figure 1. PCR detection of *C. psittaci*, *C. pneumoniae*, and *C. trachomatis* DNA in ocular adnexal MALT lymphoma specimens (10% polyacrylamide gel). M, molecular weight marker; -/+, negative/positive controls. S1–S10: MALT lymphomas (S1–S3 Würzburg, Germany; S4–S5 Manchester, UK; S6–S7, Bologna, Italy; S8, Hainan, China; S9–S10, Canton, China). S6: positive for both *C. pneumoniae* and *C. trachomatis*

Table 3. Frequencies of *Chlamydiae* detected in ocular adnexal lymphomas and controls from different geographical areas*

| <i>Chlamydiae</i> | Diagnosis | UK | | Germany | | Netherlands | | Italy | | Southern China | | East coast USA | | Total | |
|-----------------------|----------------------|-------|----|---------|-----------------|-------------|----|-------|----|----------------|----|----------------|-----------------|--------|-----------------|
| | | No | % | No | % | No | % | No | % | No | % | No | % | No | % |
| <i>C. psittaci</i> | MALT L | 4/33 | 12 | 9/19 | 47 ¹ | 6/21 | 29 | 2/15 | 13 | 4/37 | 11 | 6/17 | 35 ² | 31/142 | 22 ³ |
| | Non-MZL [†] | 1/7 | 14 | 0/9 | 0 | 2/3 | — | 0/6 | 0 | 2/20 | 10 | 0/8 | 0 | 5/53 | 9 |
| | Non-LPD | 4/40 | 10 | 1/9 | 11 | — | — | — | — | 0/2 | — | — | — | 5/51 | 10 |
| <i>C. pneumoniae</i> | MALT L | 5/30 | 17 | 4/19 | 21 | 0/12 | 0 | 0/15 | 0 | 8/37 | 22 | 0/14 | 0 | 17/127 | 13 |
| | Non-MZL [†] | 0/5 | — | 0/9 | 0 | 0/3 | — | 1/6 | 17 | 2/20 | 10 | 0/4 | — | 3/47 | 6 |
| | Non-LPD | 10/40 | 25 | 2/9 | 22 | — | — | — | — | 0/2 | — | — | — | 12/51 | 24 |
| <i>C. trachomatis</i> | MALT L | 6/30 | 20 | 1/19 | 5 | 2/12 | 17 | 1/15 | 7 | 0/37 | 0 | 2/14 | 14 | 12/127 | 9 |
| | Non-MZL [†] | 3/5 | — | 0/9 | 0 | 1/3 | — | 0/6 | 0 | 0/20 | 0 | 1/4 | — | 5/47 | 11 |
| | Non-LPD | 10/40 | 25 | 0/9 | 0 | — | — | — | — | 0/2 | — | — | — | 10/51 | 20 |

* A case was regarded as positive if the screened bacterium was detected in at least two of three independent PCRs [23]. Percentages are only provided for groups with more than five cases.

[†] Follicular lymphoma, mantle-cell lymphoma, diffuse large B-cell lymphoma, and T/NK-cell lymphoma.

¹ Significantly different from non-MZLs from Germany ($p = 0.013$) and also significantly different from MALT lymphomas from the UK ($p = 0.007$), Italy ($p = 0.039$), and Southern China ($p = 0.004$).

² Significantly different from MALT lymphomas from Southern China ($p = 0.041$).

³ Significantly different from all non-LPDs ($p = 0.042$) and from all non-MZLs ($p = 0.033$).

MALT L = mucosa-associated lymphoid tissue lymphoma; MZL = marginal zone lymphoma; LPD = lymphoproliferative disorder.

Italy (13%), the UK (12%), and Southern China (11%) (Table 3). Interestingly, three of the six positive cases detected within our USA group were from Florida and New York, where no association was found between *C. psittaci* infection and ocular adnexal MALT lymphomas in previous studies [25,26]. The prevalence of *C. psittaci* in MALT lymphomas from Germany was significantly higher than those observed in the UK, Italy, and Southern China ($p < 0.04$). There was no correlation between *C. psittaci* positivity and either the age or sex of the patients or the anatomical location of the lymphoma. The prevalence of *C. psittaci* positivity was nearly identical between cases that occurred in the orbit (15%) and those involving the conjunctiva (16%). In addition, there was no apparent difference in the prevalence of *C. psittaci* among various subtypes of non-marginal zone lymphomas.

A total of 225 cases with sufficient DNA quantity were screened for the presence of *C. pneumoniae* and *C. trachomatis*. Both bacteria were found at variable frequencies in non-LPD and non-marginal zone lymphoma groups from different geographical regions (0–25%) (Table 3). Only cases from Southern China showed a trend towards a higher prevalence of *C. pneumoniae* in MALT lymphomas than in non-LPD and non-marginal zone lymphoma cases from the same region (Table 3), but these differences were not statistically significant. There was no difference in the prevalences of *C. trachomatis* between MALT lymphoma and control groups, both non-LPDs, and non-marginal zone lymphomas, from the same geographical regions. In general, the presence of these *Chlamydiae* was mutually exclusive.

To examine whether there was any correlation between the positivity for *Chlamydiae* and the extent of lymphoid infiltration in the non-LPD group, the histology of these cases was reviewed. These specimens

typically showed variable infiltrates of mature lymphocytes and plasma cells within the lamina propria, and some contained a few intraepithelial neutrophils. Occasionally, the infiltrating lymphocytes formed small aggregates but no lymphoid follicles were seen. There was no correlation between the positivity for *Chlamydiae* and the extent of lymphoid infiltration in these control samples.

Adenovirus and herpes simplex virus are not associated with ocular adnexal lymphoma

A total of 152 cases with adequate DNA quality had a sufficient quantity of DNA to screen for the presence of ADV8, ADV19 and HSV1/2. Sequencing confirmed the specificity of the PCR products in all positive cases. Only low levels of positivity (0–14%) for these viruses were found in both control and MALT lymphoma groups. No difference was seen in the prevalences of these viruses between MALT lymphoma and control groups from different geographical regions.

Discussion

By retrospective investigation of archival ocular adnexal MALT lymphomas from six geographical regions, we provide evidence that *C. psittaci* is associated with ocular adnexal MALT lymphoma but that this association is highly variable according to the geographical origin, with a frequency of *C. psittaci* in ocular adnexal MALT lymphoma ranging from 11% to nearly 50% in the different geographical areas examined. Importantly, these findings provide an explanation for the discrepancy between the original study by Ferreri *et al* (Milan, Italy) and subsequent reports: in Italy, *C. psittaci* was detected in 87% of ocular adnexal MALT lymphoma [23], while no evidence of

infection by this bacterium was demonstrated in cases from the South Florida and Rochester (New York) areas of the USA [25,26]. Such geographical variations are further supported by recent meeting abstracts showing a high prevalence of *C. psittaci* in ocular adnexal MALT lymphomas from South Korea (26/33) [31], but an absence or a low prevalence in cases from North America (0/15) [32] and Cuba (1/21) [33]. Interestingly, such a geographically variable association may also exist within the same country as shown by the differences in the prevalence of *C. psittaci* in ocular adnexal MALT lymphomas from Italy and the USA observed between the current study and previous reports [23,25,26,32].

The reasons underlying the marked variations in the prevalences of *C. psittaci* in ocular adnexal MALT lymphoma from different geographical regions are currently unknown. However, such geographical differences in linking infectious organisms with lymphoma, including within the same country, are not unprecedented, as the established associations between lymphoma and respectively hepatitis C virus, *Borrelia burgdorferi* and *H. pylori* are subject to marked geographical variations [34–36]. The prevalences of *C. psittaci* infection among the general populations of the geographical regions studied may vary, but epidemiological data specifically on ocular infection by *C. psittaci* are lacking. Given that the prevalence of *C. psittaci* infection in ocular adnexal MALT lymphoma is relatively low, at least in several geographical regions, and that variable prevalences are also found within the same country, the bacterial infection could be sporadic. Indeed, there is substantial evidence that *C. psittaci* infection in man is significantly associated with the environmental context, especially with exposure to pet birds and pet cats [37]. Interestingly, in the study by Ferreri [23], 13/24 interviewed patients with *C. psittaci*-positive ocular adnexal lymphomas had prolonged contact with household animals.

Overall, *C. psittaci* was found at a significantly higher prevalence in MALT lymphomas than in non-marginal zone lymphomas. The frequency of *C. psittaci* in non-marginal zone lymphoma cases was similar to the frequency observed in the non-LPD cases. These results suggest that the bacterium might be preferentially associated with MALT lymphoma, further implicating its role in the development of MALT lymphoma. In this context, it would be interesting to examine whether different strains of *C. psittaci*, with potentially different pathogenic capacities, could be differentially associated with various types of lymphoma, or with different geographical regions showing variable prevalences of *C. psittaci*-positive MALT lymphoma. Indeed, various strains of *H. pylori* have been shown to be differentially involved in several gastric diseases, with the virulent strains being preferentially associated with gastric cancer or peptic ulcer rather than with gastritis [38–40].

The demonstration of variable association of *C. psittaci* with ocular adnexal MALT lymphoma in

different geographical regions is clinically important. In Italy, eradication of *C. psittaci* by antibiotics led to complete or partial regression of the disease in four of nine cases studied [24]. Patients who responded to antibiotics included some who did not respond to radiotherapy or chemotherapy, or showed repeated relapses of the disease after such treatment. Given that antibiotic treatment has relatively few side effects and ocular adnexal MALT lymphoma is an indolent disease, further clinical trials are warranted to determine the role of antibiotics in the treatment of this lymphoma. In this context, the prevalence of *C. psittaci* in ocular adnexal MALT lymphoma in a given geographical area is likely to be a major determinant of the value of such treatment in each clinical setting.

Among the six geographical regions examined in the current study, the highest prevalence of *C. psittaci* observed was in ocular adnexal MALT lymphomas from Germany (47%). This is much lower than the frequency observed in the original study from Italy (87%) [23]. It could be argued that the concentration of *C. psittaci* DNA in some of the tumour specimens might be low, potentially leading to underestimation of its true prevalence. However, the lower detection rate in the current study is unlikely to be due to a lack of sensitivity of our assays. Firstly, an identical PCR amplification of the same gene fragment specific to *C. psittaci* was used in both the original study and our current study. Secondly, we performed separate PCRs for each *Chlamydia* species and analysed PCR products on high-resolution gels, further ensuring the sensitivity and specificity of the method. The reliability of our data is supported by the finding that, in 80% of the positive cases, *C. psittaci* was detected in all three PCRs independently performed for each case.

Although we provide compelling evidence that ocular adnexal MALT lymphoma may develop from the MALT acquired as a result of chronic inflammation associated with *C. psittaci*, the low prevalence of *C. psittaci* in ocular adnexal MALT lymphoma in several geographical regions raises the possibility that other aetiological factors may be involved in the development of this lymphoma. Several other organisms, including *C. trachomatis*, *C. pneumoniae*, ADV types 8 and 19, and HSV types 1 and 2, are known to cause chronic eye infection [18–20]. We screened our cases for these infectious agents and found that their prevalences in both ocular adnexal MALT lymphoma and control groups were relatively low. Our results thus suggest that these infectious agents are unlikely to be associated with ocular adnexal MALT lymphoma, at least in the geographical regions investigated. Other aetiological factors underlying the development of adnexal MALT lymphoma remain to be investigated. Interestingly, some autoimmune disorders are known to be associated with an increased risk of lymphoma development [41,42], including MALT lymphoma [43–45], and some of them, such as systemic lupus erythematosus and Sjögren's syndrome,

often affect the ocular adnexa [46,47]. In this regard, it would be interesting to examine any possible role for autoimmunity in the development of ocular adnexal MALT lymphoma [48].

In summary, our results demonstrate that *C. psittaci* is variably associated with ocular adnexal MALT lymphoma in different geographical regions. Among different subtypes of ocular adnexal lymphomas, the bacterium appeared to be preferentially associated with MALT lymphomas. These findings have important clinical implications when considering the use of antibiotics to treat ocular adnexal MALT lymphomas.

Acknowledgements

The Du Lab is supported by research grants from the Leukaemia and Lymphoma Society, USA, Association for International Cancer Research, and Leukaemia Research Fund, UK. CB is supported by a Senior Clinician Scientist Fellowship from the Health Foundation, the Royal College of Pathologists, and the Pathological Society of Great Britain and Ireland. We thank Dr Riccardo Dolcetti, IRCCS National Cancer Institute, Aviano Italy, for providing *Chlamydiae* positive control samples and performing the double blind investigation for optimisation of the PCR screening protocols; Dr Hongyi Zhang, Department of Clinical Virology, Addenbrooke NHS Trust, for providing herpes simplex virus positive control samples; and Dr G Gallucci, CDC, Atlanta, for providing adenovirus positive control samples. We would also like to thank Professor Li Qun of Hainan Medical College, Jan Paul de Boer of the Netherlands Cancer, Mr Mark Staveley, and Ms Sue Goddard for retrieving tissue blocks and patient information for the study.

References

- Du MQ, Isaacson PG. Gastric MALT lymphoma: from aetiology to treatment. *Lancet Oncol* 2002;**3**:97–104.
- Hussell T, Isaacson PG, Crabtree JE, Spencer J. The response of cells from low-grade B-cell gastric lymphomas of mucosa-associated lymphoid tissue to *Helicobacter pylori*. *Lancet* 1993;**342**:571–574.
- Hussell T, Isaacson PG, Crabtree JE, Spencer J. *Helicobacter pylori*-specific tumour-infiltrating T cells provide contact dependent help for the growth of malignant B cells in low-grade gastric lymphoma of mucosa-associated lymphoid tissue. *J Pathol* 1996;**178**:122–127.
- Wotherspoon AC, Dogliani C, Diss TC, Pan L, Moschini A, de Boni M, et al. Regression of primary low-grade B-cell gastric lymphoma of mucosa-associated lymphoid tissue type after eradication of *Helicobacter pylori*. *Lancet* 1993;**342**:575–577.
- Kutting B, Bonsmann G, Metz D, Luger TA, Cerroni L. *Borrelia burgdorferi*-associated primary cutaneous B cell lymphoma: complete clearing of skin lesions after antibiotic pulse therapy or intralesional injection of interferon alfa-2a. *J Am Acad Dermatol* 1997;**36**:311–314.
- Cerroni L, Zochling N, Putz B, Kerl H. Infection by *Borrelia burgdorferi* and cutaneous B-cell lymphoma. *J Cutan Pathol* 1997;**24**:457–461.
- Roggero E, Zucca E, Mainetti C, Bertoni F, Valsangiaco C, Pedrinis E, et al. Eradication of *Borrelia burgdorferi* infection in primary marginal zone B-cell lymphoma of the skin. *Hum Pathol* 2000;**31**:263–268.
- Goodlad JR, Davidson MM, Hollowood K, Ling C, MacKenzie C, Christie I, et al. Primary cutaneous B-cell lymphoma and *Borrelia burgdorferi* infection in patients from the Highlands of Scotland. *Am J Surg Pathol* 2000;**24**:1279–1285.
- Lecuit M, Abachin E, Martin A, Poyart C, Pochart P, Suarez F, et al. Immunoproliferative small intestinal disease associated with *Campylobacter jejuni*. *N Engl J Med* 2004;**350**:239–248.
- Al Saleem T, Al Mondhiry H. Immunoproliferative small intestinal disease (IPSID): a model for mature B-cell neoplasms. *Blood* 2005;**105**:2274–2280.
- Isaacson PG, Muller-Hermelink HK, Berger F. Extranodal marginal zone B-cell lymphoma (MALT lymphoma). In *WHO Classification of Tumours, Pathology and Genetics of Tumours of Haematopoietic and Lymphoid Tissue*, Jaffe E, et al (eds). IARC Press: Lyon, 2001; 157–160.
- Jenkins C, Rose GE, Bunce C, Wright JE, Cree IA, Plowman N, et al. Histological features of ocular adnexal lymphoma (REAL classification) and their association with patient morbidity and survival. *Br J Ophthalmol* 2000;**84**:907–913.
- Auw-Haedrich C, Coupland SE, Kapp A, Schmitt-Graff A, Buchen R, Witschel H. Long term outcome of ocular adnexal lymphoma subtyped according to the REAL classification. Revised European and American Lymphoma. *Br J Ophthalmol* 2001;**85**:63–69.
- Fung CY, Tarbell NJ, Lucarelli MJ, Goldberg SI, Linggood RM, Harris NL, et al. Ocular adnexal lymphoma: clinical behavior of distinct World Health Organization classification subtypes. *Int J Radiat Oncol Biol Phys* 2003;**57**:1382–1391.
- Akpek EK, Polcharoen W, Chan R, Foster CS. Ocular surface neoplasia masquerading as chronic blepharconjunctivitis. *Cornea* 1999;**18**:282–288.
- Mannami T, Yoshino T, Oshima K, Takase S, Kondo E, Ohara N, et al. Clinical, histopathological, and immunogenetic analysis of ocular adnexal lymphoproliferative disorders: characterization of MALT lymphoma and reactive lymphoid hyperplasia. *Mod Pathol* 2001;**14**:641–649.
- Lee DH, Sohn HW, Park SH, Kang YK. Bilateral conjunctival mucosa-associated lymphoid tissue lymphoma misdiagnosed as allergic conjunctivitis. *Cornea* 2001;**20**:427–429.
- Darougar S, Monnickendam MA, Woodland RM. Management and prevention of ocular viral and chlamydial infections. *Crit Rev Microbiol* 1989;**16**:369–418.
- Morrow GL, Abbott RL. Conjunctivitis. *Am Fam Physician* 1998;**57**:735–746.
- Lee SY, Laibson PR. Medical management of herpes simplex ocular infections. *Int Ophthalmol Clin* 1996;**36**:85–97.
- Elnifro EM, Cooper RJ, Klapper PE, Bailey AS, Tullo AB. Diagnosis of viral and chlamydial keratoconjunctivitis: which laboratory test? *Br J Ophthalmol* 1999;**83**:622–627.
- Lietman T, Brooks D, Moncada J, Schachter J, Dawson C, Dean D. Chronic follicular conjunctivitis associated with *Chlamydia psittaci* or *Chlamydia pneumoniae*. *Clin Infect Dis* 1998;**26**:1335–1340.
- Ferreri AJ, Guidoboni M, Ponzoni M, De Conciliis C, Dell'Oro S, Fleischhauer K, et al. Evidence for an association between *Chlamydia psittaci* and ocular adnexal lymphomas. *J Natl Cancer Inst* 2004;**96**:586–594.
- Ferreri AJ, Ponzoni M, Guidoboni M, De Conciliis C, Resti AG, Mazzi B, et al. Regression of ocular adnexal lymphoma after *Chlamydia psittaci*-eradicating antibiotic therapy. *J Clin Oncol* 2005;**23**:5067–5073.
- Rosado MF, Byrne GE Jr, Ding F, Fields KA, Ruiz P, Dubovy SR, et al. Ocular adnexal lymphoma: a clinicopathological study of a large cohort of patients with no evidence for an association with *Chlamydia psittaci*. *Blood* 2006;**107**:467–472.
- Vargas RL, Fallone E, Felgar RE, Friedberg JW, Arbin AA, Andersen AA, et al. Is there an association between ocular adnexal lymphoma and infection with *Chlamydia psittaci*? The University of Rochester experience. *Leuk Res* 2005;Oct 21; [Epub ahead of print].
- Wotherspoon AC, Hardman-Lea S, Isaacson PG. Mucosa-associated lymphoid tissue (MALT) in the human conjunctiva. *J Pathol* 1994;**174**:33–37.
- Van Dongen JJ, Langerak AW, Bruggemann M, Evans PA, Hummel M, Lavender FL, et al. Design and standardization of PCR primers and protocols for detection of clonal immunoglobulin and T-cell receptor gene recombinations in

- suspect lymphoproliferations: report of the BIOMED-2 Concerted Action BMH4-CT98–3936. *Leukemia* 2003;**17**:2257–2317.
29. Madico G, Quinn TC, Boman J, Gaydos CA. Touchdown enzyme time release-PCR for detection and identification of *Chlamydia trachomatis*, *C. pneumoniae*, and *C. psittaci* using the 16S and 16S-23S spacer rRNA genes. *J Clin Microbiol* 2000;**38**:1085–1093.
 30. Branco BC, Gaudio PA, Margolis TP. Epidemiology and molecular analysis of herpes simplex keratitis requiring primary penetrating keratoplasty. *Br J Ophthalmol* 2004;**88**:1285–1288.
 31. You C, Ryu M, Huh J, Park J, Ahn H, Lee Y, et al. Ocular adnexal lymphoma is highly associated with *Chlamydia psittaci*. *Proceedings of the European Cancer Conference ECCO 13, Paris France, November 2005* (abstract 982).
 32. Zhang GS, Winter JN, Variakojis D, Reich S, Lissner GS, Bryar P, et al. No association between *Chlamydia psittaci* and ocular adnexal lymphoma in North American samples. *Blood* 2005;**106**:abstr 999.
 33. Gracia E, Mazzucchelli L, Frösch P, Jimerez J, Rodriguez D, Capo V, et al. Low prevalence of *Chlamydia psittaci* infection in ocular adnexal lymphomas (OAL) from Cuban patients. *Ann Oncol* 2005;**16**(suppl):abstr 303.
 34. Negri E, Little D, Boiocchi M, La Vecchia C, Franceschi S. B-cell non-Hodgkin's lymphoma and hepatitis C virus infection: a systematic review. *Int J Cancer* 2004;**111**:1–8.
 35. Wood GS, Kamath NV, Guitart J, Heald P, Kohler S, Smoller BR, et al. Absence of *Borrelia burgdorferi* DNA in cutaneous B-cell lymphomas from the United States. *J Cutan Pathol* 2001;**28**:502–507.
 36. Doglioni C, Wotherspoon AC, Moschini A, de Boni M, Isaacson PG. High incidence of primary gastric lymphoma in north-eastern Italy. *Lancet* 1992;**339**:834–835.
 37. Smith KA, Bradley KK, Stobierski MG, Tengelsen LA. Compendium of measures to control *Chlamydochlamydia psittaci* (formerly *Chlamydia psittaci*) infection among humans (psittacosis) and pet birds, 2005. *J Am Vet Med Assoc* 2005;**226**:532–539.
 38. Van Doorn LJ, Figueiredo C, Sanna R, Plaisier A, Schneeberger P, de Boer W, et al. Clinical relevance of the *cagA*, *vacA* and *iceA* status of *Helicobacter pylori*. *Gastroenterology* 1998;**115**:58–66.
 39. Miehle S, Kirsch C, Agha-Amiri K, Gunther T, Lehn N, Malfertheiner P, et al. The *Helicobacter pylori* *vacA* s1, m1 genotype and *cagA* is associated with gastric carcinoma in Germany. *Int J Cancer* 2000;**87**:322–327.
 40. Correa P, Schneider BG. Etiology of gastric cancer: what is new? *Cancer Epidemiol Biomarkers Prev* 2005;**14**:1865–1868.
 41. Cuttner J, Spiera H, Troy K, Wallenstein S. Autoimmune disease is a risk factor for the development of non-Hodgkin's lymphoma. *J Rheumatol* 2005;**32**:1884–1887.
 42. Engels EA, Cerhan JR, Linet MS, Cozen W, Colt JS, Davis S, et al. Immune-related conditions and immune-modulating medications as risk factors for non-Hodgkin's lymphoma: a case-control study. *Am J Epidemiol* 2005;**162**:1153–1161.
 43. Abbondanzo SL. Extranodal marginal-zone B-cell lymphoma of the salivary gland. *Ann Diagn Pathol* 2001;**5**:246–254.
 44. Hyjek E, Isaacson PG. Primary B cell lymphoma of the thyroid and its relationship to Hashimoto's thyroiditis. *Hum Pathol* 1988;**19**:1315–1326.
 45. Pedersen RK, Pedersen NT. Primary non-Hodgkin's lymphoma of the thyroid gland: a population based study. *Histopathology* 1996;**28**:25–32.
 46. Arevalo JF, Lowder CY, Muci-Mendoza R. Ocular manifestations of systemic lupus erythematosus. *Curr Opin Ophthalmol* 2002;**13**:404–410.
 47. Bjerrum KB. Primary Sjogren's syndrome and keratoconjunctivitis sicca: diagnostic methods, frequency and social disease aspects. *Acta Ophthalmol Scand Suppl* 2000;**231**:1–37.
 48. Nutting CM, Shah-Desai S, Rose GE, Norton AP, Plowman PN. Thyroid orbitopathy possibly predisposes to late-onset of periocular lymphoma. *Eye* 2005;Aug 26; [Epub ahead of print].

Distinct comparative genomic hybridisation profiles in gastric mucosa-associated lymphoid tissue lymphomas with and without t(11;18)(q21;q21)

Yuanping Zhou,^{1,2*} Hongtao Ye,^{1*}
Jose I. Martin-Subero,³ Rifat Hamoudi,¹
Yong-Jie Lu,⁴ Rubin Wang,⁴ Reiner
Siebert,³ Janet Shipley,⁴ Peter G.
Isaacson,⁵ Ahmet Dogan⁵
and Ming-Qing Du¹

¹Division of Molecular Histopathology,
Department of Pathology, University of
Cambridge, UK, ²Nanfang Hospital, Canton,
China, ³Institute of Human Genetics, University
Hospital Schleswig-Holstein, Campus Kiel, Kiel,
Germany, ⁴Molecular Cytogenetics, Institute of
Cancer Research, Sutton, UK, and ⁵Department of
Histopathology, University College London, UK

Received 9 June 2005; accepted for publication 9
December 2005

Correspondence: Ming-Qing Du, Professor of
Oncological Pathology, Division of Molecular
Histopathology, Department of Pathology,
University of Cambridge, Box 231, Level 3 Lab
Block, Addenbrooke's Hospital, Hills Road,
Cambridge, CB2 2QQ, UK.

E-mail: mqd20@cam.ac.uk

*Both these authors contributed equally to the
work.

Three recurrent chromosomal translocations have been identified in mucosa-associated lymphoid tissue (MALT) lymphoma, namely t(11;18)(q21;q21), t(1;14)(p22;q32) and t(14;18)(q32;q21). t(11;18) involves the *API2* and *MALT1* genes and generates a functional API2-MALT1 fusion product (Akagi *et al*, 1999; Dierlamm *et al*, 1999; Morgan *et al*, 1999). t(1;14) and t(14;18) juxtapose the *BCL10* and *MALT1* gene, respectively, to the immunoglobulin gene locus in 14q32 leading to deregulated expression of the oncogene (Willis *et al*, 1999; Zhang *et al*, 1999; Sanchez-Izquierdo *et al*, 2003; Streubel *et al*, 2003). The oncogenic activities of the three chromosome translocations are linked by the physiological role of BCL10 and MALT1 in antigen receptor-mediated nuclear factor (NF) κ B activation (Isaacson & Du, 2004). The

Summary

t(11;18)(q21;q21) occurs specifically in mucosa-associated lymphoid tissue (MALT) lymphoma and the translocation generates a functional API2-MALT1 fusion product that activates nuclear factor (NF) κ B. t(11;18) positive lymphomas usually lack the chromosomal aberrations and microsatellite alterations frequently seen in the translocation-negative MALT lymphomas. To further understand their genetic differences, we investigated gastric MALT lymphomas with and without t(11;18) by comparative genomic hybridisation. In general, both chromosomal gains and losses were far more frequent in t(11;18)-negative (median = 3.4 imbalances) than t(11;18)-positive cases (median = 1.6 imbalances), with gains being more frequent than losses. Recurrent chromosomal gains involving whole or major parts of a chromosome were seen for chromosomes 3, 12, 18 and 22 (23%, 19%, 19% and 27% respectively). Discrete recurrent chromosomal gains were found at 9q34 (11/26 = 42%). Bioinformatic analysis of genes mapping to 9q34 revealed potential targets. Among them, TRAF2 and CARD9 are known interaction partners of BCL10, playing a role in NF κ B activation. Interphase fluorescent *in situ* hybridisation confirmed genomic gain of the TRAF2, CARD9 and MALT1 loci in 5/6 and 2/2 cases showing chromosomal gains at 9q34 and 18q21 respectively. The results further highlight the genetic difference between MALT lymphomas with and without t(11;18). Moreover, our findings suggest that genomic gain of genes that modulate NF κ B activation, such as *MALT1*, *TRAF2* and *CARD9*, may play a role in the pathogenesis of the translocation-negative MALT lymphoma.

Keywords: mucosa-associated lymphoid tissue lymphoma, t(11;18), comparative genomic hybridisation, *TRAF2*, *CARD9*, *MALT1*.

three chromosome translocations occur at markedly variable incidences in MALT lymphoma of different sites but are always mutually exclusive (Isaacson & Du, 2004). Among the three chromosome translocations, t(11;18) is the most frequent, occurring most often in those from the lung (40%) and stomach (30%), moderate in those from the ocular adnexae (15%), but rarely in those from the salivary gland, thyroid and skin (Ye *et al*, 2003; Streubel *et al*, 2004a; Ye *et al*, 2005).

There is growing evidence suggesting that t(11;18) positive cases are distinct from other MALT lymphomas, including those with t(1;14) or t(14;18). t(11;18) positive MALT lymphoma rarely undergoes high grade transformation (Remstein *et al*, 2002; Chuang *et al*, 2003) despite that the translocation is significantly associated with cases at advanced

stages and those not responding to *Helicobacter pylori* eradication (Liu *et al*, 2000; Liu *et al*, 2002). Cytogenetically, t(11;18) positive tumours usually do not show other chromosomal aberrations, such as trisomies 3 and 18, frequently seen in t(11;18) negative tumours including those positive for t(1;14) and t(14;18) (Auer *et al*, 1997; Ott *et al*, 1997; Barth *et al*, 2001; Barth *et al*, 2002; Remstein *et al*, 2002). Furthermore, t(11;18) MALT lymphomas do not show microsatellite alterations, which frequently occur in the translocation-negative tumours (Starostik *et al*, 2002). To further characterise the genetic differences between MALT lymphoma with and without t(11;18), we compared the chromosomal gains and losses between 9 t(11;18) positive, 2 t(1;14) positive and 15 translocation-negative gastric MALT lymphomas using comparative genomic hybridisation (CGH). Interphase fluorescent *in situ* hybridisation (FISH) was applied to confirm the recurrent chromosomal changes.

Materials and methods

Materials

A total of 26 cases of well-characterised gastric MALT lymphoma were included in this study. All these cases were previously studied for the presence of t(11;18), t(1;14) and t(14;18): t(11;18) was investigated by reverse transcription polymerase chain reaction (RT-PCR) of RNA samples extracted from frozen tissues (Ye *et al*, 2003), while t(1;14) and t(14;18) were examined by BCL10 and MALT1 immunohistochemistry followed by interphase FISH (Ye *et al*, 2003; Ye *et al*, 2005). Nine cases were positive for t(11;18), two cases positive for t(1;14) and the remaining 15 cases were negative for all the three translocations. Frozen tumour tissues were available in each case. The use of redundant archival tissues for research was approved by the local ethics committee of each authors' institution.

DNA extraction and labelling

The proportion of tumour cells was estimated on haematoxylin and eosin slides and only tissue specimens containing more than 70% tumour cells were used for DNA extraction. Where necessary, crude dissection was carried out in order to enrich the tumour cells (Pan *et al*, 1994). Tumour DNA was extracted from frozen tissue sections using the Wizard® genomic DNA purification kit (Promega, Southampton, UK). Reference DNA was prepared from normal peripheral blood lymphocytes using a QIAGEN blood and cell culture DNA kit (QIAGEN, West Sussex UK). DNA was quantified using GeneQuant pro (Amersham pharmacia biotech, Cambridge, UK). DNA from the breast cancer cell line MPE 600 containing gain of 1q, small deletion at 1pter and distal 11q, and loss of 9p and 16q (Vysis, Surrey, UK) was used as a positive control.

The tumour and reference DNAs were labelled with SpectrumRed dUTP and SpectrumGreen dUTP (Vysis, Surrey,

UK), respectively, by nick translation as described previously (Lu *et al*, 1997). Briefly, the reaction was carried out in a 50 µl reaction mixture containing 1 µg tumour or reference DNA, 20 µmol/l of each dATP, dCTP and dGTP, 10 µmol/l of dTTP, 10 µmol/l of SpectrumRed dUTP (for tumour DNA) or SpectrumGreen dUTP (for reference DNA), 5 mmol/l of MgCl₂, 10 mmol/l of β-mercaptoethanol, 10 µg/ml of bovine serum albumin and 50 mmol/l of Tris-HCl (pH 7.2), 0.05 U DNase I (Promega, Madison, WI, USA) and 5 U DNA polymerase I (Promega, Madison, WI, USA) at 15°C for 3 h. The reaction was stopped by addition of 3 µl 0.5 mol/l of EDTA. The probe was purified with MicroSpin G-50 column (Amersham Biosciences, Piscataway, NJ, USA) and checked on 1% agarose gels. Under the above conditions, the probes were typically in the range of 0.3–3.0 kb.

Comparative genomic hybridisation and digital image analysis

The labelled tumour and reference DNA (500 ng each) were mixed with 25 µg Cot-1 human DNA (Invitrogen, Paisley, UK), precipitated with sodium acetate and ethanol and dissolved in 10 µl of hybridisation buffer containing 70% formamide, 10% dextran sulphate and 2 × saline sodium citrate (SSC, pH7.0). The DNA samples were denatured at 77°C for 5 min and immediately applied onto normal metaphase spreads that had been just undergone denaturation in 70% formamide/2 × SSC (pH 7.0) and dehydration in series of ethanol. The hybridisation was carried out under a sealed coverslip for 2–3 days at 37°C in a moist chamber. The slides were then sequentially washed in 0.4 × SSC/0.3% (octylphenoxy)polyethoxyethanol (IGEPAL, pH 7.0) (Sigma, St Louis, MO, USA) at 72°C for 2 min, 2 × SSC/0.1% IGEPAL at 42°C for 5 min, and in distilled water at room temperature. Finally, slides were mounted using anti-fade medium with 4',6-diamidino-2-phenylindole (DAPI, Vector Laboratories Inc., Burlingame, CA, USA).

Digital images were captured using a cooled CCD-camera (Photometrics; Tuscon, AZ, USA) with QUIPS software (Version 3-1.2., Vysis, Richmond Surrey, UK) linked to a Zeiss Axioplan epifluorescence microscope (ZEISS, Jena, Germany). Between 6 and 10 images of high quality metaphases in each case were analysed using the same software package. The relative genomic gains and losses were determined by comparing the ratio of red (tumour DNA) and green (reference DNA) fluorescence intensity along all chromosomes and the thresholds used for record of chromosomal gains and losses were 1.20 and 0.80, respectively, according to previous studies (Lu *et al*, 1997; Lu *et al*, 1999). The heterochromatic regions, p-arms of acrocentric chromosomes, and the entire X and Y chromosomes were excluded from analysis.

Interphase fluorescent *in situ* hybridisation

For further analysis of the most frequent chromosomal gains (9q34 and 18q21) detected by CGH analysis, we performed

interphase FISH as detailed below. For chromosomal gains at 18q21, *MALT1* is probably the gene or one of the genes targeted (Sanchez-Izquierdo *et al*, 2003) and interphase FISH was carried out using the commercial LSI *MALT1* dual colour break apart probe (Vysis/Abbott Laboratories Ltd, UK).

Bioinformatic analysis identified several potential target genes in the commonly gained band 9q34. These included the genes encoding tumour necrosis factor (TNF) receptor-associated factor 2 (TRAF2), caspase recruitment domain family member 9 (CARD9), cyclin-dependent kinase 9, G protein-coupled receptor, v-abl Abelson murine leukemia viral oncogene homolog 1 (ABL), Rap guanine nucleotide exchange factor (GEF) 1, growth factor independent 1B (potential regulator of CDKN1A) and Notch homolog 1 (NOTCH1). Among them, TRAF2 and CARD9 seem to be the most relevant in view of their interaction with BCL10 and their role in NF κ B activation (Bertin *et al*, 2000; Yoneda *et al*, 2000). BAC clones RP11-83N9 and RP11-100C15 as well as RP11-251M1 flanking the CARD9 and NOTCH1 loci were selected as interphase FISH probes. The clones were differentially labelled with Spectrum Green (RP11-83N9/RP11-100C15) and Spectrum Red (RP11-251M1) and pooled to obtain a break-apart assay. Similarly, BAC clones RP11-83N9/RP11-100C15 were combined with BAC clone RP11-417A4, which is located telomeric of the TRAF2 locus. In combination, both assays enable the detection of breakpoints affecting the CARD9/NOTCH1 locus or the TRAF2 locus as well as the assessment of copy number changes. Bacterial culture, BAC DNA isolation and labelling, probe preparation were performed as previously described (Martin-Subero *et al*, 2002). These probes were first tested on metaphase spreads to confirm the location and specificity of the probe. Then they were applied to formalin-fixed and paraffin-embedded tissue sections from 8 to 10 reactive tonsils to determine the thresholds (mean of false positives + 3 SD) to diagnose chromosomal alterations in lymphoma cells (Martin-Subero *et al*, 2003).

Locus-specific interphase FISH was performed on paraffin-embedded tissue sections. This was carried out essentially as described previously (Ye *et al*, 2003). Briefly, deparaffinised sections were pre-treated by pressure-cooking for 2 min and 40 s in 1 mmol/l EDTA buffer pH 8.0 and subsequently incubated in pepsin solution (80 μ g/ml) at 37°C for 20 min to increase the probes accessibility. Sections were then fixed in 1% paraformaldehyde for 1 min at room temperature, washed twice in double distilled water, dehydrated through increasing ethanol series, and air-dried. The appropriate probe mixture was applied to tissue sections and sealed with a coverslip. Both probe and target DNA were denatured at 80°C for 25 min and hybridisation was carried out at 37°C for 3 days. After hybridisation, the slides were washed with 0.4 \times SSC/0.3% IGEAL (pH 7.0) (Sigma) at 72°C for 2 min, in 2 \times SSC/0.1% IGEAL at room temperature for 1 min and finally in 2 \times SSC. Slides were mounted using Vectashield anti-fade medium with DAPI (Vector Laboratories Inc.). The image acquisition and processing was performed using a fluorescent microscope with cooled

CCD-camera (Olympus, BX61, Tokyo, Japan) and CYTOVISION software (Version: 2.75, Applied Imaging International Ltd, Newcastle, UK). The FISH slides were viewed and the hybridisation signals for each probe were counted from 100 cells in each case by two investigators independently.

Statistical analysis

The statistical difference in the percentage of cells showing three or more copies of a gene locus by interphase FISH among different groups was investigated by non-parametric Mann-Whitney *U*-test. *P*-values <0.05 were considered significant.

Results

Distinctive CGH profiles in gastric MALT lymphomas with and without t(11;18)

Among the 26 cases studied, one t(1;14) positive case (case 18) was shown to have trisomies 3, 12 and 18 by previous karyotyping analysis (Willis *et al*, 1999). CGH analysis of the same case confirmed gains of chromosome 3, 12 and 18, and also revealed losses at 7p12-q21 (Table I).

In general, both chromosomal gains and losses were far more frequent in t(11;18) negative than positive cases, with chromosomal gains being more frequent than chromosomal losses (Fig 1, Table I). Of the nine t(11;18) positive cases, only five cases showed imbalances. Remarkably, all these imbalances were chromosomal gains. In contrast, all 17 t(11;18) negative cases exhibited chromosomal imbalances (Fig 1, Table I). The median number of imbalances was much higher in t(11;18) negative ($n = 3.4$ imbalances) than t(11;18) positive cases ($n = 1.6$ imbalances). The median number of chromosomal gains and losses in t(11;18) negative cases was 2.64 and 0.76 respectively.

Recurrent gains involving whole or major parts of a chromosome were seen for chromosomes 3, 12, 18 and 22, and these gains were nearly exclusively seen in t(11;18) negative cases. For example, gain of whole or major parts of chromosome 3 and 18 was found in 6/17 (35%) and 5/17 (29%) t(11;18) negative cases, respectively, including those with t(1;14), but not in any of the t(11;18) positive cases. Discrete recurrent chromosomal gains affecting the tip of 9q were detected in 11/26 cases (42%) including 4 t(11;18) positive cases (Fig 1, Table I). The minimum overlapping region was at band 9q34.

Confirmation of chromosomal gains at 9q34 and 18q21 by interphase FISH

To confirm the CGH results, interphase FISH was performed with probes for the *MALT1* locus as well as two assays for 9q34 on 4 μ m paraffin-embedded tissue sections. The cut-off value (mean + 3 SD) for *MALT1*, *TRAF2* and *CARD9* gene probes were 3.4%, 8.4% and 5.1% respectively.

Table I. Chromosomal gains and losses in gastric MALT lymphomas with and without t(11;18) as shown by CGH analysis.

| Case no. | Translocation | Chromosome changes | | Percentage cells showing 3 or more signals by interphase FISH | | |
|----------|---------------|--|-------------------------------------|---|---|--|
| | | Gains | Losses | LSI MALT1 (%) | RP11-83N9/ RP11-100C15 and RP11-417A4 (CARD9/NOTCH1/ TRAF2 BAP) (%) | RP11-83N9/RP11- 100C15 and RP11-251M1 (CARD9/NOTCH1 BAP) (%) |
| Cut off | | | | 3-4 | 8-4 | 5-1 |
| 1 | t(11;18)+ve | | | 0 | 1 | 3 |
| 2 | t(11;18)+ve | | | 0 | 2 | 1 |
| 3 | t(11;18)+ve | | | 0 | 1 | 3 |
| 4 | t(11;18)+ve | | | 0 | 0 | 2 |
| 5 | t(11;18)+ve | 8q22, 16p | | 1 | – | – |
| 6 | t(11;18)+ve | 9q33-34, 22q | | 1 | 18 | 22 |
| 7 | t(11;18)+ve | 9q33-ter | | 0 | 20 | 4 |
| 8 | t(11;18)+ve | 1p33-ter, 9q34, 11p15, 20q, 22q | | 0 | 1 | 2 |
| 9 | t(11;18)+ve | 9q34, 17p12-ter, 17q23-ter, 22q | | – | – | – |
| 10 | trans –ve | 6p | | – | – | – |
| 11 | trans –ve | 3 | | 3 | 0 | 2 |
| 12 | trans –ve | 6q24-ter, 12q24, 16, 17, 20q, 22q | | 2 | 25 | 11 |
| 13 | trans –ve | 3 | | 0 | – | – |
| 14 | t(1;14) +ve | 12 | | 68 | 1 | 2 |
| 15 | trans –ve | 2p13-16, 3 | 2p11-12, 4q, 5p15, 13q, 14q31-32 | 1 | 1 | 2 |
| 16 | trans –ve | 2p13-22, 18q, 21q | 2p11-12, 8p | – | – | – |
| 17 | trans –ve | 18q | | – | – | – |
| 18 | t(1;14)+ve | 3, 12, 18 | 7p12-q21 | 60 | 1 | 2 |
| 19 | trans –ve | 3, 18 | | 53 | – | – |
| 20 | trans –ve | 9q | 6q25-27, 8p21 | – | – | – |
| 21 | trans –ve | 9q34, 12q23-ter | | – | – | – |
| 22 | trans –ve | 3p11-14, 7q11, 9q34, 12q24, 15q25-26, 18q11-21, 22q | | – | – | – |
| 23 | trans –ve | 9q34, 22q | | 2 | – | – |
| 24 | trans –ve | 9q34, 14q32, 22q11-2 | | 0 | 23 | 9 |
| 25 | trans –ve | 1q21-24, 9q, 10q22-24, 15q22-24, 20q | 3p23-ter, 4q | 1 | 32 | 6 |
| 26 | trans –ve | 9q33-34, 11q11-13, 16p11-ter, 17p | 4q11-26 | 0 | 20 | 15 |

–, not done; CGH, comparative genomic hybridisation; MALT, mucosa-associated lymphoid tissue; FISH, fluorescent *in situ* hybridisation.

It has to be stated, that in sections of reactive tonsils used as controls, up to 38% (standard deviation = 6.56) of cells showed only 1 signal with the different FISH probes. This indicates that truncated nuclei, as a result of tissue sectioning, may lead to an significant underestimation of the true percentages of cells harbouring three or four copies of the loci investigated.

Interphase FISH with two dual colour breakapart probes for 9q34, allowing detection of breakpoints affecting the TRAF2 and CARD9 loci as well as chromosomal imbalances was performed separately in 15 cases where adequate tissues were available. These included six cases with chromosomal gain at 9q34 and 9 without evidence of chromosomal gain at this locus by CGH. Of the nine cases without CGH evidence of chromosomal gain at 9q34, one case (no. 12) showed FISH

signals that indicated three or four copies of both the TRAF2 and CARD9 genes in a proportion of cells well above the threshold (mean + 3 SD) respectively (Table I). In contrast, 5/6 cases with chromosomal gain at 9q34 displayed FISH signals indicating three or more copies of the TRAF2 and CARD9 gene (Fig 2, Table I). In support of this, the percentage of cells with three or four copies of the TRAF2 and CARD9 gene was significantly ($P = 0.028$ and $P = 0.028$, respectively) higher in cases with CGH gain at 9q34 than those without CGH gain at this locus. There was no evidence for a chromosomal break in this region in all cases examined.

Similarly, interphase FISH with the MALT1 probe showed extra-copy of the gene in 2/2 cases that had CGH evidence of chromosomal gain at 18q21. In contrast, only 1 of the 17 cases without CGH evidence of chromosomal gain at 18q21 showed

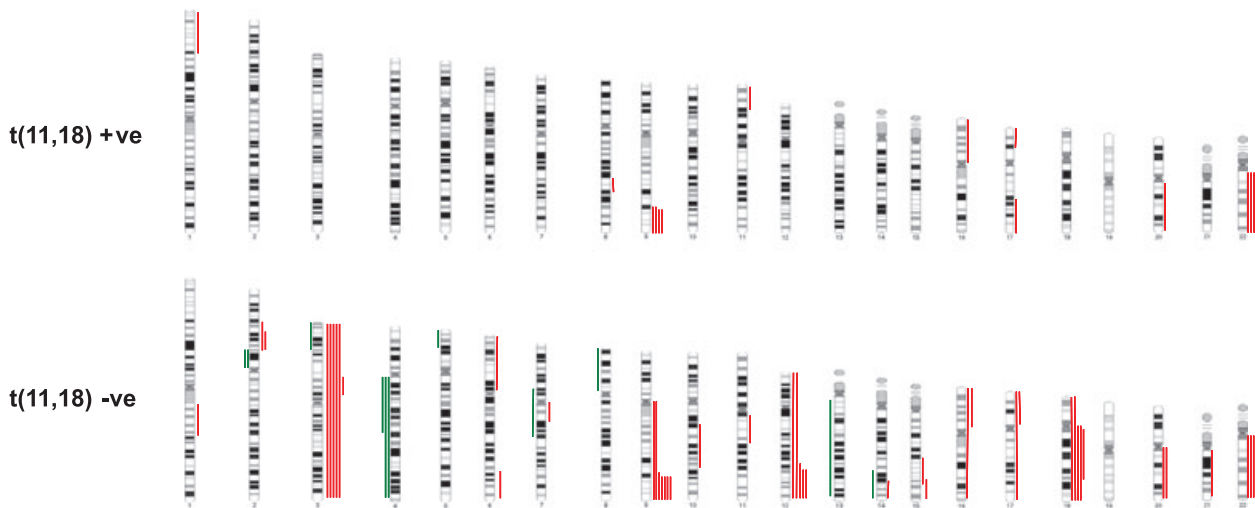


Fig 1. Comparison of chromosomal gains and losses between gastric mucosa-associated lymphoid tissue lymphomas with and without t(11;18) as revealed by comparative genomic hybridisation analysis. Both chromosomal gains (red lines) and losses (green lines) are far more frequent in t(11;18) negative than positive cases.

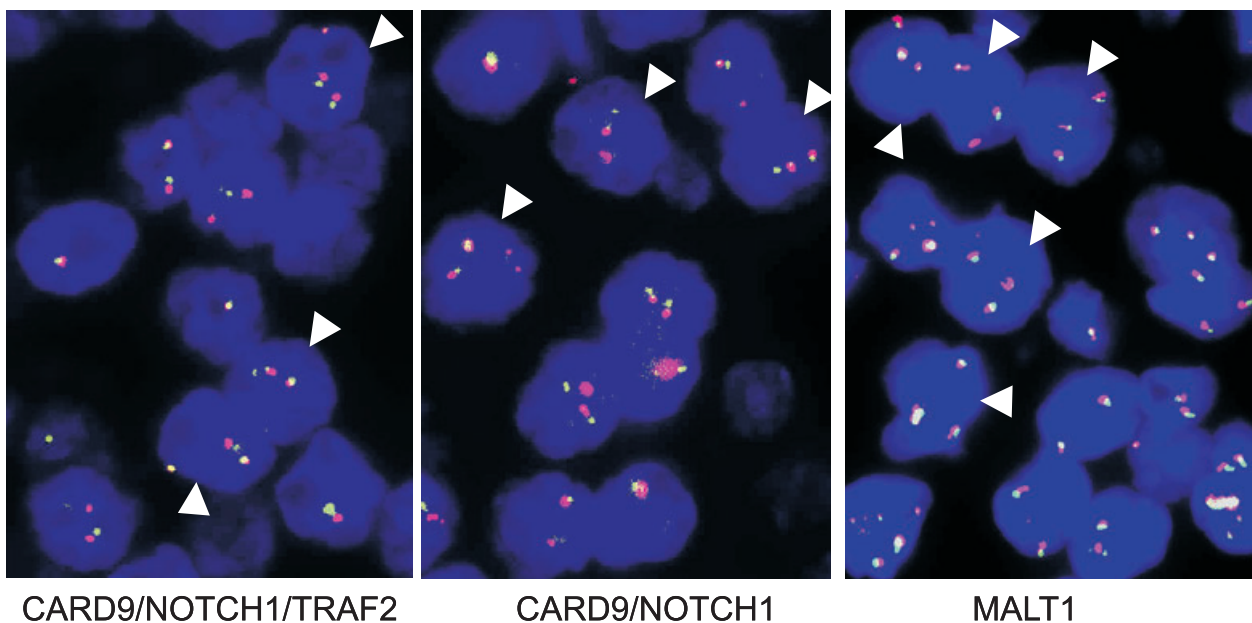


Fig 2. Confirmation of chromosomal gain at 9q34 by interphase fluorescent *in situ* hybridisation (FISH) with probes flanking the TRAF2 and CARD9 loci, and chromosomal gain at 18q21 by interphase FISH with MALT1 probe. A t(11;18) negative case (no. 26) with comparative genomic hybridisation (CGH) gain at 9q34 showing three co-localised green (BAC clones RP11-83N9/RP11-100C15) and red (RP11-417A4) signals (arrowheads), indicating three copies of the 9q34 region including CARD9, NOTCH1 and TRAF2 (left panel). The same case displays three co-localised green (BAC clones RP11-83N9/RP11-100C15) and red (RP11-251M1) signals (arrowheads) for the probe flanking the CARD9 and NOTCH1 genes (centre panel). A t(11;18) negative case (no. 18) with CGH gain at chromosome 18 shows three co-localised green and red signals with MALT1 probe in several cells (indicated by arrowheads), indicating gain of extra-copy of the MALT gene (right panel).

more than two copies of the *MALT1* gene. The percentage of cells with three or four copies of the *MALT1* gene was significantly higher in cases with CGH gain at 18q21 than those without ($P = 0.04$). As expected, all cases with known t(11;18), but not those without the translocation showed signal split with the MALT1 probe.

Discussion

Our present CGH analysis showed further evidence of genetic differences between gastric MALT lymphomas with and without t(11;18). In general, chromosomal gains and losses, particularly the former, are a feature of t(11;18) negative

gastric MALT lymphoma, but not of those with the translocation. Our findings are in line with previous observations that trisomies 3, 12 and 18 are frequently seen in t(11;18) negative MALT lymphoma, but rarely in those positive for this translocation (Auer *et al*, 1997; Ott *et al*, 1997; Remstein *et al*, 2002; Streubel *et al*, 2004a).

Given that t(11;18) is most probably the primary genetic event underlying the malignant transformation, it was intriguing to see no accumulation of further chromosomal abnormalities in t(11;18) positive tumour cells. A possible explanation is that the factors promoting the acquisition of genetic abnormalities, such as oxygen reactive species generated during the inflammatory processes, are no longer evident in the microenvironment where t(11;18) positive tumour cells expand. In support of this hypothesis, t(11;18) positive gastric MALT lymphomas gain "autonomous growth" and are no longer critically dependent on antigenic stimulations as shown by their resistance to *H. pylori* eradication (Liu *et al*, 2000; Liu *et al*, 2002). Histologically, t(11;18) positive MALT lymphomas are characterised by more homogenous tumour cells, lack of transformed blasts, as compared with translocation negative cases, suggesting that chronic antigenic stimulation/inflammatory process is unlikely to be prominent in the translocation positive cases (Okabe *et al*, 2003).

The lack of additional chromosomal abnormalities in t(11;18) positive MALT lymphomas may explain, at least partially, the finding that these tumours rarely undergo high grade transformation (Remstein *et al*, 2002; Chuang *et al*, 2003). The chromosomal aberrations found in t(11;18) negative MALT lymphomas also provide clues for the pathogenesis of these tumours. Among the recurrent changes, gains at chromosome 18q and 9q34 are particularly interesting. For chromosomal gain at 18q21, *MALT1* gene has been proposed as the target gene or one of the target genes (Sanchez-Izquierdo *et al*, 2003). *MALT1* gene amplification has been demonstrated in cell lines from splenic marginal zone B-cell lymphoma and Burkitt's lymphoma (Sanchez-Izquierdo *et al*, 2003). Although *MALT1* gene amplification is rarely seen in primary lymphoma (Sanchez-Izquierdo *et al*, 2003), gain of an extra copy of the gene is a frequent event in MALT lymphoma as shown in the present study and others (Murga Penas *et al*, 2003; Remstein *et al*, 2004; Streubel *et al*, 2004b).

For chromosomal gain at 9q34, our data suggest that *TRAF2* and *CARD9* may be the target genes. Similar to the *MALT1* gene, gain of additional copy of *TRAF2* and *CARD9*, but not its amplification, was seen in 7/17 (41%) of t(11;18) negative gastric MALT lymphomas. In a parallel study, we also found gain of additional copy of chromosome 9q34/*TRAF2*/*CARD9* and 18q21/*MALT1* in the majority of salivary gland MALT lymphomas, which are negative for t(11;18) (Zhou *et al*, 2004). Chromosomal gains at 9q34 and 18q21 have been previously demonstrated in cases of MALT lymphoma (Dierlamm *et al*, 1997). Gains at 9q34 is also a feature of enteropathy type T-cell lymphoma (Zettl *et al*, 2002).

The role of the above chromosomal gains in the pathogenesis of t(11;18) negative MALT lymphoma is unclear. They may

exert their oncogenic activities by enhancing NF κ B activation similar to that implicated in the translocation-positive MALT lymphoma. Mounting evidence indicates that the oncogenic activity of t(11;18), t(1;14) and t(14;18) are linked by the physiological role of BCL10 and MALT1 in antigen receptor-mediated NF κ B activation (Isaacson & Du, 2004). These different chromosomal translocations are believed to exert their oncogenic activities by constitutive activation of NF κ B, a transcriptional factor for a number of growth factors, cytokines and apoptosis inhibitors. In this context, it is worth noting that both TRAF2 and CARD9 have been shown to interact with BCL10 and activate NF κ B (Bertin *et al*, 2000; Yoneda *et al*, 2000). TRAF2 plays a central role in TNF receptor-mediated NF κ B activation during the innate immune responses (Chen, 2005). Recent studies suggest that TRAF2 may also play an important role in antigen receptor-mediated NF κ B activation during adaptive immune responses. It is believed that TRAF2 may, like TRAF6, catalyse the Lys 63-linked polyubiquitination of NEMO (IKK γ) in response to upstream signals from BCL10/MALT1, which is a crucial step leading to NF κ B activation (Sun *et al*, 2004; Chen, 2005). Although TRAF2 expression in MALT lymphoma is unknown, the protein is abundantly expressed in various lymphoma cell lines and in Hodgkin/Reed–Sternberg cells of Hodgkin lymphoma (Zapata *et al*, 2000; Murray *et al*, 2001). The role of CARD9 in NF κ B activation pathway remains to be investigated. Nonetheless, a recent study has shown over-expression of *CARD9* mRNA in gastric MALT lymphoma (Nakamura *et al*, 2005), in keeping with the notion proposed in the current study.

It has been shown that positive regulators, such as BCL10 and MALT1, have synergistic effects in their activation of the NF κ B pathway (McAllister-Lucas *et al*, 2001). Furthermore, these positive regulators are also synergistic with physiological stimulations, such as CD40 in NF κ B activation (Ho *et al*, 2004). It is tentatively speculated that gain of extra copy of *TRAF2*, *CARD9*, *MALT1* and others yet to be identified may bear synergistic effects among themselves as well as with physiological stimulations in NF κ B activation and lead to the same biological consequence as that of the chromosomal translocations discussed above.

Acknowledgements

The Du lab was supported by research grants from Association for International Cancer Research and Leukaemia Research Fund, UK. Reiner Siebert's lab was supported by grants from the Deutsch Krebshilfe.

References

- Akagi, T., Motegi, M., Tamura, A., Suzuki, R., Hosokawa, Y., Suzuki, H., Ota, H., Nakamura, S., Morishima, Y., Taniwaki, M. & Seto, M. (1999) A novel gene, *MALT1* at 18q21, is involved in t(11;18) (q21;q21) found in low-grade B-cell lymphoma of mucosa-associated lymphoid tissue. *Oncogene*, **18**, 5785–5794.

- Auer, I.A., Gascoyne, R.D., Connors, J.M., Cotter, F.E., Greiner, T.C., Sanger, W.G. & Horsman, D.E. (1997) t(11;18)(q21;q21) is the most common translocation in MALT lymphomas. *Annals of Oncology*, **8**, 979–985.
- Barth, T.F., Bentz, M., Leithauser, F., Stilgenbauer, S., Siebert, R., Schlotter, M., Schlenk, R.F., Dohner, H. & Moller, P. (2001) Molecular-cytogenetic comparison of mucosa-associated marginal zone B-cell lymphoma and large B-cell lymphoma arising in the gastro-intestinal tract. *Genes Chromosomes Cancer*, **31**, 316–325.
- Barth, T.F., Bentz, M., Leithauser, F., Stilgenbauer, S., Siebert, R., Schlotter, M., Schlenk, R.F., Dohner, H. & Moller, P. (2002) Pathogenic complexity of gastric B-cell lymphoma. *Blood*, **100**, 1095–1096.
- Bertin, J., Guo, Y., Wang, L., Srinivasula, S.M., Jacobson, M.D., Poyet, J.L., Merriam, S., Du, M.Q., Dyer, M.J., Robison, K.E., DiStefano, P.S. & Alnemri, E.S. (2000) CARD9 is a novel caspase recruitment domain-containing protein that interacts with BCL10/CLAP and activates NF-kappa B. *Journal of Biological Chemistry*, **275**, 41082–41086.
- Chen, Z.J. (2005) Ubiquitin signalling in the NF-kappaB pathway. *Nature Cell Biology*, **7**, 758–765.
- Chuang, S.S., Lee, C., Hamoudi, R.A., Liu, H., Lee, P.S., Ye, H., Diss, T.C., Dogan, A., Isaacson, P.G. & Du, M.Q. (2003) High frequency of t(11;18) in gastric mucosa-associated lymphoid tissue lymphomas in Taiwan, including one patient with high-grade transformation. *British Journal of Haematology*, **120**, 97–100.
- Dierlamm, J., Rosenberg, C., Stul, M., Pittaluga, S., Wlodarska, I., Michaux, L., Dehaen, M., Verhoef, G., Thomas, J., de Kelder, W., Bakker Schut, T., Cassiman, J.J., Raap, A.K., De Wolf Peeters, C., Van den Berghe, H. & Hagemeijer, A. (1997) Characteristic pattern of chromosomal gains and losses in marginal zone B cell lymphoma detected by comparative genomic hybridization. *Leukemia*, **11**, 747–758.
- Dierlamm, J., Baens, M., Wlodarska, I., Stefanova-Ouzounova, M., Hernandez, J.M., Hossfeld, D.K., De Wolf-Peeters, C., Hagemeijer, A., Van den Berghe, H. & Marynen, P. (1999) The apoptosis inhibitor gene *API2* and a novel 18q gene, *MLT*, are recurrently rearranged in the t(11;18)(q21;q21) associated with mucosa-associated lymphoid tissue lymphomas. *Blood*, **93**, 3601–3609.
- Ho, L., Davis, R.E., Conne, B., Chappuis, R., Berczy, M., Mhawech, P., Staudt, L.M. & Schwaller, J. (2004) MALT1 and the API2-MALT1 fusion act between CD40 and IKK and confer NF-kappaB dependent proliferative advantage and resistance against FAS-induced cell death in B cells. *Blood*, **105**, 2891–2899.
- Isaacson, P.G. & Du, M.Q. (2004) MALT lymphoma: from morphology to molecules. *Nature Review Cancer*, **4**, 644–653.
- Liu, H., Ruskone Fourmesttraux, A., Lavergne-Slove, A., Ye, H., Molina, T., Bouhnik, Y., Hamoudi, R.A., Diss, T.C., Dogan, A., Megraud, F., Rambaud, J.C., Du, M.Q. & Isaacson, P.G. (2000) Resistance of t(11;18) positive gastric mucosa-associated lymphoid tissue lymphoma to *Helicobacter pylori* eradication therapy. *Lancet*, **357**, 39–40.
- Liu, H., Ye, H., Ruskone-Fourmesttraux, A., de Jong, D., Pileri, S., Thiede, C., Lavergne, A., Boot, H., Caletti, G., Wundisch, T., Molina, T., Taal, B.G., Elena, S., Thomas, T., Zinzani, P.L., Neubauer, A., Stolte, M., Hamoudi, R.A., Dogan, A., Isaacson, P.G. & Du, M.Q. (2002) T(11;18) is a marker for all stage gastric MALT lymphomas that will not respond to *H. pylori* eradication. *Gastroenterology*, **122**, 1286–1294.
- Lu, Y.J., Birdsall, S., Osin, P., Gusterson, B. & Shipley, J. (1997) Phylloides tumors of the breast analyzed by comparative genomic hybridization and association of increased 1q copy number with stromal overgrowth and recurrence. *Genes Chromosomes Cancer*, **20**, 275–281.
- Lu, Y.J., Dong, X.Y., Shipley, J., Zhang, R.G. & Cheng, S.J. (1999) Chromosome 3 imbalances are the most frequent aberration found in non-small cell lung carcinoma. *Lung Cancer*, **23**, 61–66.
- Martin-Subero, J.I., Chudoba, I., Harder, L., Gesk, S., Grote, W., Novo, F.J., Calasanz, M.J. & Siebert, R. (2002) Multicolor-FICTION: expanding the possibilities of combined morphologic, immunophenotypic, and genetic single cell analyses. *American Journal Pathology*, **161**, 413–420.
- Martin-Subero, J.I., Gesk, S., Harder, L., Grote, W. & Siebert, R. (2003) Interphase cytogenetics of hematological neoplasms under the perspective of the novel WHO classification. *Anticancer Research*, **23**, 1139–1148.
- McAllister-Lucas, L.M., Inohara, N., Lucas, P.C., Ruland, J., Benito, A., Li, Q., Chen, S., Chen, F.F., Yamaoka, S., Verma, I.M., Mak, T.W. & Nunez, G. (2001) Bimp1, a MAGUK family member linking protein kinase C activation to Bcl10-mediated NF-kappaB induction. *Journal of Biological Chemistry*, **276**, 30589–30597.
- Morgan, J.A., Yin, Y., Borowsky, A.D., Kuo, F., Nourmand, N., Koontz, J.I., Reynolds, C., Soreng, L., Griffin, C.A., Graeme-Cook, F., Harris, N.L., Weisenburger, D., Pinkus, G.S., Fletcher, J.A. & Sklar, J. (1999) Breakpoints of the t(11;18)(q21;q21) in mucosa-associated lymphoid tissue (MALT) lymphoma lie within or near the previously undescribed gene *MALT1* in chromosome 18. *Cancer Research*, **59**, 6205–6213.
- Murga Penas, E.M., Hinz, K., Roser, K., Copie-Bergman, C., Wlodarska, I., Marynen, P., Hagemeijer, A., Gaulard, P., Loning, T., Hossfeld, D.K. & Dierlamm, J. (2003) Translocations t(11;18)(q21;q21) and t(14;18)(q32;q21) are the main chromosomal abnormalities involving *MLT/MALT1* in MALT lymphomas. *Leukemia*, **17**, 2225–2229.
- Murray, P.G., Flavell, J.R., Baumforth, K.R., Toomey, S.M., Lowe, D., Crocker, J., Ambinder, R.F. & Young, L.S. (2001) Expression of the tumour necrosis factor receptor-associated factors 1 and 2 in Hodgkin's disease. *Journal of Pathology*, **194**, 158–164.
- Nakamura, S., Nakamura, S., Matsumoto, T., Yada, S., Hirahashi, M., Suekane, H., Yao, T., Goda, K. & Iida, M. (2005) Overexpression of caspase recruitment domain (CARD) membrane-associated guanylate kinase 1 (CARMA1) and CARD9 in primary gastric B-cell lymphoma. *Cancer*, **104**, 1885–1893.
- Okabe, M., Inagaki, H., Ohshima, K., Yoshino, T., Li, C., Eimoto, T., Ueda, R. & Nakamura, S. (2003) API2-MALT1 fusion defines a distinctive clinicopathologic subtype in pulmonary extranodal marginal zone B-cell lymphoma of mucosa-associated lymphoid tissue. *American Journal of Pathology*, **162**, 1113–1122.
- Ott, G., Katzenberger, T., Greiner, A., Kalla, J., Rosenwald, A., Heinrich, U., Ott, M.M. & Muller Hermelink, H.K. (1997) The t(11;18)(q21;q21) chromosome translocation is a frequent and specific aberration in low-grade but not high-grade malignant non-Hodgkin's lymphomas of the mucosa-associated lymphoid tissue (MALT-) type. *Cancer Research*, **57**, 3944–3948.
- Pan, L.X., Diss, T.C., Peng, H.Z. & Isaacson, P.G. (1994) Clonality analysis of defined B-cell populations in archival tissue sections using microdissection and the polymerase chain reaction. *Histopathology*, **24**, 323–327.
- Remstein, E.D., Kurtin, P.J., James, C.D., Wang, X.Y., Meyer, R.G. & Dewald, G.W. (2002) Mucosa-associated lymphoid tissue

- lymphomas with t(11;18)(q21;q21) and mucosa-associated lymphoid tissue lymphomas with aneuploidy develop along different pathogenetic pathways. *American Journal of Pathology*, **161**, 63–71.
- Remstein, E.D., Kurtin, P.J., Einerson, R.R., Paternoster, S.F. & Dewald, G.W. (2004) Primary pulmonary MALT lymphomas show frequent and heterogeneous cytogenetic abnormalities, including aneuploidy and translocations involving *API2* and *MALT1* and *IGH* and *MALT1*. *Leukemia*, **18**, 156–160.
- Sanchez-Izquierdo, D., Buchonnet, G., Siebert, R., Gascoyne, R.D., Climent, J., Karran, L., Marin, M., Blesa, D., Horsman, D., Rosenwald, A., Staudt, L.M., Albertson, D.G., Du, M.Q., Ye, H., Marynen, P., Garcia-Conde, J., Pinkel, D., Dyer, M.J. & Martinez-Climent, J.A. (2003) *MALT1* is deregulated by both chromosomal translocation and amplification in B-cell non-Hodgkin lymphoma. *Blood*, **101**, 4539–4546.
- Starostik, P., Patzner, J., Greiner, A., Schwarz, S., Kalla, J., Ott, G. & Muller-Hermelink, H.K. (2002) Gastric marginal zone B-cell lymphomas of MALT type develop along 2 distinct pathogenetic pathways. *Blood*, **99**, 3–9.
- Streubel, B., Lamprecht, A., Dierlamm, J., Cerroni, L., Stolte, M., Ott, G., Raderer, M. & Chott, A. (2003) T(14;18)(q32;q21) involving *IGH* and *MALT1* is a frequent chromosomal aberration in MALT lymphoma. *Blood*, **101**, 2335–2339.
- Streubel, B., Simonitsch-Klupp, I., Mullauer, L., Lamprecht, A., Huber, D., Siebert, R., Stolte, M., Trautinger, F., Lukas, J., Puspok, A., Formanek, M., Assanasen, T., Muller-Hermelink, H.K., Cerroni, L., Raderer, M. & Chott, A. (2004a) Variable frequencies of MALT lymphoma-associated genetic aberrations in MALT lymphomas of different sites. *Leukemia*, **18**, 1722–1726.
- Streubel, B., Huber, D., Wohrer, S., Chott, A. & Raderer, M. (2004b) Frequency of chromosomal aberrations involving *MALT1* in mucosa-associated lymphoid tissue lymphoma in patients with Sjogren's syndrome. *Clinical Cancer Research*, **10**, 476–480.
- Sun, L., Deng, L., Ea, C.K., Xia, Z.P. & Chen, Z.J. (2004) The TRAF6 ubiquitin ligase and TAK1 kinase mediate IKK activation by *BCL10* and *MALT1* in T lymphocytes. *Molecular Cell*, **14**, 289–301.
- Willis, T.G., Jadayel, D.M., Du, M.Q., Peng, H., Perry, A.R., Abdul-Rauf, M., Price, H., Karran, L., Majekodunmi, O., Wlodarska, I., Pan, L., Crook, T., Hamoudi, R., Isaacson, P.G. & Dyer, M.J. (1999) *Bcl10* is involved in t(1;14)(p22;q32) of MALT B cell lymphoma and mutated in multiple tumor types. *Cell*, **96**, 35–45.
- Ye, H., Liu, H., Attygalle, A., Wotherspoon, A.C., Nicholson, A.G., Charlotte, F., Leblond, V., Speight, P., Goodlad, J., Lavergne-Slove, A., Martin-Subero, J.I., Siebert, R., Dogan, A., Isaacson, P.G. & Du, M.Q. (2003) Variable frequencies of t(11;18)(q21;q21) in MALT lymphomas of different sites: significant association with CagA strains of *H pylori* in gastric MALT lymphoma. *Blood*, **102**, 1012–1018.
- Ye, H., Gong, L., Liu, H., Hamoudi, R.A., Shirali, S., Ho, L., Chott, A., Streubel, B., Siebert, R., Gesk, S., Martin-Subero, J.I., Radford, J.A., Banerjee, S., Nicholson, A.G., Ranaldi, R., Remstein, E.D., Gao, Z., Zheng, J., Isaacson, P.G., Dogan, A. & Du, M.Q. (2005) MALT lymphoma with t(14;18)(q32;q21)/*IGH-MALT1* is characterized by strong cytoplasmic *MALT1* and *BCL10* expression. *Journal of Pathology*, **205**, 293–301.
- Yoneda, T., Imaizumi, K., Maeda, M., Yui, D., Manabe, T., Katayama, T., Sato, N., Gomi, F., Morihara, T., Mori, Y., Miyoshi, K., Hitomi, J., Ugawa, S., Yamada, S., Okabe, M. & Tohyama, M. (2000) Regulatory mechanisms of TRAF2-mediated signal transduction by *Bcl10*, a MALT lymphoma-associated protein. *Journal of Biological Chemistry*, **275**, 11114–11120.
- Zapata, J.M., Krajewska, M., Krajewski, S., Kitada, S., Welsh, K., Monks, A., McCloskey, N., Gordon, J., Kipps, T.J., Gascoyne, R.D., Shabaik, A. & Reed, J.C. (2000) TNFR-associated factor family protein expression in normal tissues and lymphoid malignancies. *Journal of Immunology*, **165**, 5084–5096.
- Zettl, A., Ott, G., Makulik, A., Katzenberger, T., Starostik, P., Eichler, T., Puppe, B., Bentz, M., Muller-Hermelink, H.K. & Chott, A. (2002) Chromosomal gains at 9q characterize enteropathy-type T-cell lymphoma. *American Journal of Pathology*, **161**, 1635–1645.
- Zhang, Q., Siebert, R., Yan, M., Hinzmann, B., Cui, X., Xue, L., Rakestraw, K.M., Naeve, C.W., Beckmann, G., Weisenburger, D.D., Sanger, W.G., Nowotny, H., Vesely, M., Callet-Bauchu, E., Salles, G., Dixit, V.M., Rosenthal, A., Schlegelberger, B. & Morris, S.W. (1999) Inactivating mutations and overexpression of *BCL10*, a caspase recruitment domain-containing gene, in MALT lymphoma with t(1;14)(p22;q32). *Nature Genetics*, **22**, 63–68.
- Zhou, Y., Ye, H., Hamoudi, R., Siebert, R., Gesk, S., Lu, Y.J., Wang, R., Shipley, J., Isaacson, P.G., Dogan, A. & Du, M.Q. (2004) Chromosomal Gains and Losses in MALT lymphomas of the Salivary Gland. (Abstract). *Laboratory Investigation*, **84**, 278A.

Original Paper

MALT lymphoma with t(14;18)(q32;q21)/IGH-MALT1 is characterized by strong cytoplasmic MALT1 and BCL10 expression

Hongtao Ye,^{1†} Liping Gong,^{1,2†} Hongxiang Liu,¹ Rifat A Hamoudi,¹ Sima Shirali,¹ Liza Ho,³ Andreas Chott,⁴ Berthold Streubel,⁴ Reiner Siebert,⁵ Stefan Gesk,⁵ Jose I Martin-Subero,⁵ John A Radford,⁶ Sankar Banerjee,⁷ Andrew G Nicholson,⁸ Renzo Ranaldi,⁹ Ellen D Remstein,¹⁰ Zifen Gao,² Jie Zheng,² Peter G Isaacson,¹¹ Ahmet Dogan¹¹ and Ming-Qing Du^{1*}

¹Department of Pathology, University of Cambridge, Cambridge, UK

²Department of Pathology, Health Science Center, Beijing University, Beijing, PR China

³Department of Clinical Pathology, CMU, Geneva, Switzerland

⁴Department of Clinical Pathology, University of Vienna, Austria

⁵Institute of Human Genetics, University Hospital Schleswig-Holstein, Kiel, Germany

⁶Cancer Research UK, Department of Medical Oncology, Christie Hospital, Manchester, UK

⁷Department of Pathology, Christie Hospital, Manchester, UK

⁸Department of Histopathology, Royal Brompton Hospital, London, UK

⁹Department of Pathology, Institute of Pathological Anatomy and Histopathology, Ancona, Italy

¹⁰Divisions of Anatomic Pathology and Hematopathology, Mayo Clinic, Rochester, Minnesota, USA

¹¹Department of Histopathology, University College London, London, UK

*Correspondence to:

Ming-Qing Du, Division of Molecular Histopathology, Department of Pathology, University of Cambridge, Box 231, Level 3 Lab Block, Addenbrooke's Hospital, Hills Road, Cambridge CB2 2QQ, UK. E-mail: mqd20@cam.ac.uk

†These authors contributed equally to the work.

Abstract

Mucosa-associated lymphoid tissue (MALT) lymphoma is specifically associated with t(11;18)(q21;q21), t(1;14)(p22;q32) and t(14;18)(q32;q21). t(11;18)(q21;q21) fuses the N-terminus of the *API2* gene to the C-terminus of the *MALT1* gene and generates a functional *API2-MALT1* product. t(1;14)(p22;q32) and t(14;18)(q32;q21) bring the *BCL10* and *MALT1* genes respectively to the *IGH* locus and deregulate their expression. The oncogenic activity of the three chromosomal translocations is linked by the physiological role of *BCL10* and *MALT1* in antigen receptor-mediated *NFκB* activation. In this study, *MALT1* and *BCL10* expression was examined in normal lymphoid tissues and 423 cases of MALT lymphoma from eight sites, and their expression was correlated with the above translocations, which were detected by molecular and molecular cytogenetic methods. In normal B-cell follicles, both *MALT1* and *BCL10* were expressed predominantly in the cytoplasm, high in centroblasts, moderate in centrocytes and weak/negative in mantle zone B-cells. In MALT lymphoma, *MALT1* and *BCL10* expression varied among cases with different chromosomal translocations. In 9/9 MALT lymphomas with t(14;18)(q32;q21), tumour cells showed strong homogeneous cytoplasmic expression of both *MALT1* and *BCL10*. In 12/12 cases with evidence of t(1;14)(p22;q32) or variants, tumour cells expressed *MALT1* weakly in the cytoplasm but *BCL10* strongly in the nuclei. In all 67 MALT lymphomas with t(11;18)(q21;q21), tumour cells expressed weak cytoplasmic *MALT1* and moderate nuclear *BCL10*. In MALT lymphomas without the above translocations, both *MALT1* and *BCL10*, in general, were expressed weakly in the cytoplasm. Real-time quantitative RT-PCR showed a good correlation between *MALT1* and *BCL10* mRNA expression and underlying genetic changes, with t(14;18)(q32;q21)- and t(1;14)(p22;q32)-positive cases displaying the highest *MALT1* and *BCL10* mRNA expression respectively. These results show that *MALT1* expression pattern is identical to that of *BCL10* in normal lymphoid tissues but varies in MALT lymphomas, with high cytoplasmic expression of both *MALT1* and *BCL10* characterizing those with t(14;18)(q32;q21).

Copyright © 2005 Pathological Society of Great Britain and Ireland. Published by John Wiley & Sons, Ltd.

Keywords: MALT lymphoma; MALT1; Bcl10; translocation; molecular cytogenetics

Received: 3 August 2004
Revised: 18 October 2004
Accepted: 29 October 2004

Introduction

MALT lymphoma is specifically associated with t(11;18)(q21;q21), t(1;14)(p22;q32), and t(14;18)(q32;

q21) [1]. t(11;18)(q21;q21) fuses the N-terminus of the *API2* gene to the C-terminus of the *MALT1* gene and generates a functional *API2-MALT1* product [2–4]. t(1;14)(p22;q32) and t(14;18)(q32;q21)

bring the *BCL10* and *MALT1* genes respectively to the *IGH* locus and deregulate their expression [5–8]. The oncogenic activity of these translocations is linked by the physiological role of BCL10 and MALT1 in antigen receptor-mediated NF κ B activation [9–12]. In normal B-cells, in response to antigen receptor signalling, BCL10 oligomerizes and interacts with MALT1 and mediates its oligomerization, which leads to NF κ B activation. In t(1;14)(p22;q32)-positive MALT lymphoma, BCL10 is believed to form oligomers via its N-terminal CARD, while in those with t(14;18)(q32;q21)/*IGH-MALT1*, MALT1 oligomerization is thought to depend on BCL10 [13,14]. In MALT lymphoma with t(11;18)(q21;q21), the API2–MALT1 fusion product is believed to self-oligomerize via the N-terminal BIR domain of the API2 molecule [13,14]. Thus, these independent translocations appear to mediate their oncogenic activities through a common pathway.

In general, the above three translocations are differentially involved in MALT lymphomas of various sites. t(11;18)(q21;q21) occurs most frequently in MALT lymphomas from the lung (40%) and stomach (30%), moderately in those from the ocular adnexae (20%), but rarely in those from the salivary gland, thyroid, and skin [15–21]. In gastric MALT lymphoma, the translocation is significantly associated with those not responding to *Helicobacter pylori* eradication [20,22,23]. However, the translocation is rarely seen in transformed MALT lymphoma [24,25].

t(1;14)(p22;q32) occurs in 5% of MALT lymphomas and is described primarily in those from the stomach and lung. Although BCL10 is expressed predominantly in the cytoplasm of normal germinal centre B-cells, the protein is strongly expressed in the nuclei of lymphoma cells with t(1;14)(p22;q32) [26]. Moderate nuclear BCL10 expression is also seen in t(1;14)(p22;q32)-negative MALT lymphomas, including nearly all those with t(11;18)(q21;q21) and up to 20% cases without t(11;18)(q21;q21) [20,21,27]. The remaining t(11;18)(q21;q21)-negative cases express BCL10 in the cytoplasm.

t(14;18)(q32;q21)/*IGH-MALT1* appears to occur more frequently in non-gastrointestinal MALT lymphomas [7,28,29]. However, its true incidence in MALT lymphoma of various sites remains unclear. In a previous study of a single case of t(14;18)(q32;q21)/*IGH-MALT1*-positive MALT lymphoma, we showed that both MALT1 and BCL10 were highly expressed in the cytoplasm of the tumour cells [8]. It is unknown whether this expression pattern characterizes MALT lymphoma with t(14;18)(q32;q21)/*IGH-MALT1*. In the present study, we examined MALT1 expression in both normal and malignant lymphoid tissues and correlated its expression with that of BCL10 and the presence of the three translocations in MALT lymphomas.

Material and methods

Materials

These included 30 normal lymphoid tissues, 490 B-cell lymphomas consisting of 423 MALT lymphomas (Table 1), 22 follicular lymphomas, 18 mantle cell lymphomas, and 27 diffuse large B-cell lymphomas (DLBCL). Of MALT lymphomas, six cases were known to be t(14;18)(q32;q21)/*IGH-MALT1* positive [7,28]. In addition, 86 normal non-lymphoid tissues of 21 types were studied. Local ethical guidelines were followed for the use of archival paraffin-embedded and frozen tissues for research and such use was approved by the local ethics committees of the authors' institutions where required.

Immunohistochemistry

MALT1 was immunostained with a mouse monoclonal antibody to its N-terminus (Genentech, USA) [8]. Where indicated, MALT1 immunohistochemistry was also performed with a mouse monoclonal antibody to its C-terminus, which was generated by immunization of mice with a C-terminal MALT1 recombinant protein (amino acids 701–808), followed by a hybridoma technique in our laboratory. N-terminal MALT1 antibody recognizes full-length MALT1 but not the API2–MALT1 fusion product, while C-terminal MALT1 antibody reacts with both MALT1 and API2–MALT1 fusion product (Figure 1). BCL10 was stained with mouse monoclonal antibody clone 151 [26].

Reverse transcription–polymerase chain reaction (RT-PCR)

t(11;18)(q21;q21) was detected by RT-PCR of the *API2-MALT1* fusion transcripts [23].

Interphase fluorescence *in situ* hybridization (FISH)

Translocations involving MALT1 were detected by interphase FISH with LSI *IGH/MALT1* dual-colour, dual-fusion translocation probes and MALT1 break-apart dual-colour probes (Vysis/Abbott Laboratories Ltd, UK) [8,21].

Real-time RT-PCR

MALT1 and *BCL10* mRNA expression was quantified by real-time RT-PCR using 18S rRNA as an internal control. Total RNA was isolated from tumour cells microdissected from paraffin-embedded tissue sections [23,31]. cDNA was synthesized using random hexamer primers for *MALT1*/18S rRNA and gene-specific primer for *BCL10*/18S rRNA. Real-time PCR was performed using an iCycler iQ system (BIO-RAD, UK) with SYBR Green I. One of each primer pair was designed to span an exon–exon junction to prevent amplification of any contaminated DNA (Table 2)

Table 1. MALT I expression pattern in MALT lymphomas with different chromosomal translocations

| Site of MALT lymphoma | Number of cases | Translocation status* | Number of cases | Intensity of MALT I expression | | |
|-----------------------|-----------------|-----------------------|-----------------|--------------------------------|----------|---------------|
| | | | | Strong | Moderate | Weak/negative |
| Stomach | 185 | t(11;18) +ve | 40 | — | 2 | 38 |
| | | t(1;14) +ve | 8 | — | — | 8 |
| | | t(14;18) +ve | — | — | — | — |
| | | Translocation -ve | 137 | — | 7 | 130 |
| Lung | 47 | t(11;18) +ve | 18 | — | — | 18 |
| | | t(1;14) +ve | 4 | — | — | 4 |
| | | t(14;18) +ve | 3 | 3 | — | — |
| | | Translocation -ve | 22 | — | — | 22 |
| Ocular adnexae | 73 | t(11;18) +ve | 7 | — | 1 | 6 |
| | | t(1;14) +ve | — | — | — | — |
| | | t(14;18) +ve | 5 | 5 | — | — |
| | | Translocation -ve | 61 | — | 7 | 54 |
| Salivary gland | 59 | t(11;18) +ve | 1 | — | — | 1 |
| | | t(1;14) +ve | — | — | — | — |
| | | t(14;18) +ve | — | — | — | — |
| | | Translocation -ve | 58 | — | 8 | 50 |
| Thyroid | 12 | t(11;18) +ve | — | — | — | — |
| | | t(1;14) +ve | — | — | — | — |
| | | t(14;18) +ve | — | — | — | — |
| | | Translocation -ve | 12 | — | 2 | 10 |
| Skin | 37 | t(11;18) +ve | — | — | — | — |
| | | t(1;14) +ve | — | — | — | — |
| | | t(14;18) +ve | — | — | — | — |
| | | Translocation -ve | 37 | — | 9 | 28 |
| Liver | 6 | t(11;18) +ve | — | — | — | — |
| | | t(1;14) +ve | — | — | — | — |
| | | t(14;18) +ve | 1 | 1 | — | — |
| | | Translocation -ve | 5 | — | — | 5 |
| Intestine | 4 | t(11;18) +ve | 1 | — | — | 1 |
| | | t(1;14) +ve | — | — | — | — |
| | | t(14;18) +ve | — | — | — | — |
| | | Translocation -ve | 3 | — | — | 3 |
| Total | 423 | | | 9(2.1%) | 36 | 378 |

* t(14;18)(q32;q21)/IGH-MALT1 and BCL10 break/t(1;14)(p22;q21) were primarily detected by MALT1 and BCL10 immunohistochemistry followed by interphase FISH with appropriate probes. t(11;18)(q21;q21)/API2-MALT1-positive cases were detected by RT-PCR of the API2-MALT1 fusion transcript, with the exception of one pulmonary case that was initially identified by interphase FISH with MALT1 break apart probes.

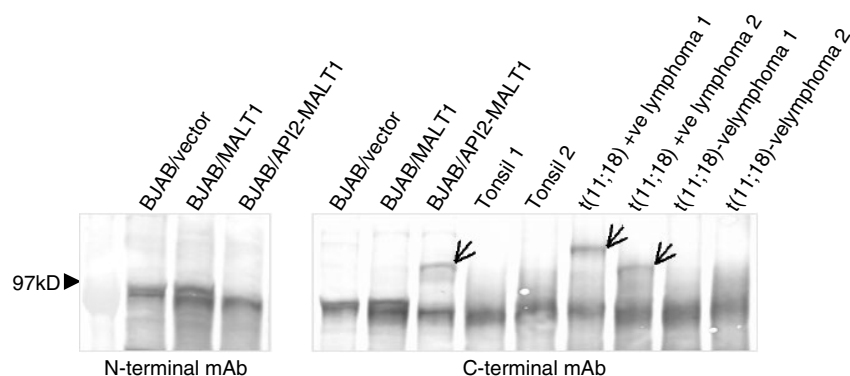


Figure 1. Western blot analysis of human B-cell lymphoma cells (BJAB) transfected with MALT1 or API2-MALT1 expression constructs [30], and MALT lymphoma with and without t(11;18)(q21;q21). The mouse monoclonal antibody (mAb) to the N-terminus of the MALT1 recognizes full-length MALT1, but not the API2-MALT1 fusion product, while the mouse monoclonal antibody to the C-terminus of MALT1 reacts with full-length MALT1 as well as the API2-MALT1 fusion product (indicated by arrows)

[32]. The primers for the *MALT1* gene target its N-terminus and therefore will only amplify wild-type *MALT1* but not *API2-MALT1* transcripts.

The conditions for real-time PCR were optimized prior to data collection. The specificity of the RT-PCR

products for each primer set was confirmed by melt-curve analysis. The standard curves were generated by twofold serial dilutions of 100 ng/ μ l *MALT1* cDNA and 1 ng/ μ l 18S rRNA cDNA prepared from fresh frozen tonsils, and 100 ng/ μ l *BCL10* cDNA and

1 ng/ μ l 18S rRNA cDNA prepared from t(1;14)(p22;q32)-positive frozen tumour tissues. The average coefficient value (R^2) for each standard curve was above 0.99 and the relative efficiency of amplification of *MALT1* and *BCL10* was close to that of 18S rRNA since the absolute value of the slope of log-input amount of cDNA versus ΔC_T was below 0.1.

Once the experimental conditions had been optimized, real-time PCR was performed in a 25 μ l reaction mixture containing 12.5 μ l SYBR Green Super-Mix (BIO-RAD), 200 nM of each sense and anti-sense primer, and 100 ng (*MALT1* and *BCL10*) or 1 ng (18S rRNA) cDNA. All samples were amplified in triplicate using the following parameters: denaturation at 95 °C for 3 min and annealing and extension at 60 °C for 1 min. Real-time PCR of 18S rRNA was run in parallel for each sample. Melt-curve analysis was performed immediately after the amplification protocol for each case and only samples that showed specific amplification were included in the data analysis. The C_T numbers were obtained from each sample and ΔC_T value was calculated by subtracting the C_T value of 18S rRNA from the C_T value of *MALT1* or *BCL10*.

Statistical analysis

Mann–Whitney *U*-test was used to compare *MALT1* and *BCL10* mRNA expression between MALT lymphomas with different translocations. Pearson's correlation test was used for analysis of the relationship between *MALT1* and *BCL10* mRNA expression.

Results

MALT1 expression in normal lymphoid tissues

Immunohistochemistry with both N-terminal and C-terminal MALT1 antibodies showed that the protein expression pattern was identical to that of BCL10 in both B-cell follicles and thymus [26]. In B-cell follicles of tonsil, lymph node and spleen, both MALT1 and BCL10 are differentially expressed in various germinal centre B-cells, strong in centroblasts, moderate in centrocytes, and weak/negative in mantle zone

B-cells (Figure 2). In thymus, MALT1 was weakly positive, while BCL10 was moderately expressed in medullary T-cells. Irrespective of different cell types, both MALT1 and BCL10 are predominantly expressed in the cytoplasm.

MALT1 protein expression appeared to be restricted to lymphoid tissues. It was not found by immunohistochemistry in 21 types of normal tissue, including tongue, oesophagus, duodenum, rectum, liver, gall-bladder, pancreas, bronchus, heart, lung, thyroid, breast, adrenal gland, kidney, bladder, uterus, cervix, ovary, placenta, testis, and skin.

MALT1 expression in malignant lymphoma

MALT1 expression in malignant lymphomas was investigated with the N-terminal MALT1 antibody. As reactive lymphoid follicles are commonly seen in MALT lymphoma, MALT1 and BCL10 expression in B-cells of reactive germinal centres provides an excellent internal control. The level of MALT1 and BCL10 expression in lymphoma cells was therefore recorded with reference to that in centroblasts (strong), centrocytes (moderate), and mantle zone B-cells (weak) of reactive lymphoid follicles.

In a previous study of a single case of t(14;18)(q32;q21)/*IGH-MALT1*-positive MALT lymphoma, we showed that both MALT1 and BCL10 were highly expressed in the cytoplasm of the tumour cells [8]. To examine whether strong cytoplasmic expression of both MALT1 and BCL10 characterizes MALT lymphoma with t(14;18)(q32;q21)/*IGH-MALT1*, we studied the expression of these proteins in 423 cases of MALT lymphoma. Among these cases, 364 had data for BCL10 expression, t(1;14)(p22;q32), and t(11;18)(q21;q21) from previous studies [21]. For the remaining cases, these data were collected during the present study. t(11;18)(q21;q21) was detected by RT-PCR of the *API2-MALT1* fusion transcript, while t(1;14)(p22;q32) or variants were screened by BCL10 immunohistochemistry followed by interphase FISH [21].

In total, 12 cases showed strong BCL10 nuclear staining, and 10 of them showed evidence of t(1;14)(p22;q32) by conventional cytogenetics or interphase FISH. None of these cases showed BCL10 gene amplification. Tumour cells in each of the above cases showed weak/negative MALT1 cytoplasmic staining (Figure 2, Table 1). Sixty-seven cases were t(11;18)(q21;q21) positive and tumour cells in these cases showed moderate or weak BCL10 nuclear staining (Figure 2, Table 1). Of the remaining 344 cases lacking t(1;14)(p22;q32) and t(11;18)(q21;q21), nine cases (ocular adnexae five, lung three, and liver one) showed strong homogeneous cytoplasmic expression of both MALT1 and BCL10 in virtually all tumour cells. The intensity of MALT1 staining was similar to that seen in centroblasts of the reactive germinal centre (Figure 2). Of the remaining cases, 33 showed

Table 2. Primers used for real-time quantitative PCR of *MALT1* and *BCL10* mRNA

| Genes | Primer sequence | Amplicon size (bp) |
|---------|--|--------------------|
| MALT1* | sense 5' ctc cgc ctc agt tgc cta ga anti-sense 5' caa cct ttt tca ccc att aac ttc a | 104 |
| BCL10 | sense 5' gaa gtg aag aag gac gcc tta g anti-sense 5' aga tga tca aaa tgt ctc tca gc | 80 |
| 18SrRNA | sense 5' tga ctc aac acg gga aac c anti-sense 5' tgc ctc cac caa cta aga ac | 114 |

* The primers for the *MALT1* gene were designed to target its N-terminus (nucleotides 363–466 according to its cDNA sequence AF130356), and therefore will only amplify the wild-type *MALT1* but not the *API2-MALT1* transcripts.

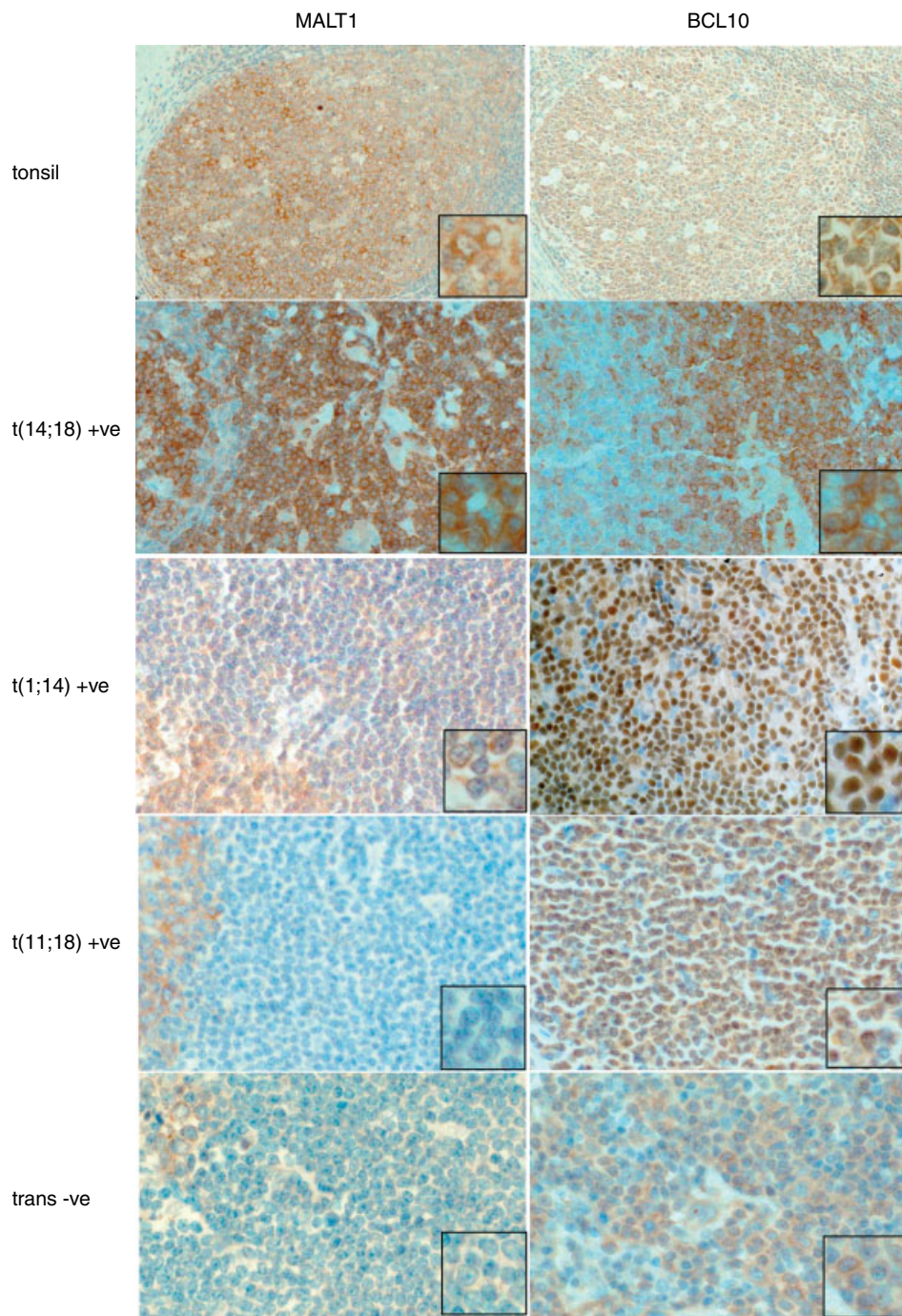


Figure 2. MALT1 and BCL10 expression in reactive tonsil and MALT lymphomas with and without chromosomal translocations. Both MALT1 and BCL10 are similarly expressed in the cytoplasm of various B-cells in reactive tonsil, high in centroblasts, moderate in centrocytes and weak/negative in the mantle zone B-cells. In MALT lymphoma with $t(14;18)(q32;q21)/IGH-MALT1$, all tumour cells show strong MALT1 and BCL10 cytoplasmic expression. In MALT lymphoma with $BCL10$ break/ $t(1;14)(p22;q32)$, tumour cells express weak MALT1 but strong nuclear BCL10. In MALT lymphoma with $t(11;18)(q21;q21)/API2-MALT1$, tumour cells generally show lack of MALT1 expression but moderate nuclear BCL10. In MALT lymphoma without the above chromosomal translocations, tumour cells show weak MALT1 and moderate BCL10 expression in the cytoplasm. FC, follicle centre

moderate and 302 displayed weak/negative MALT1 cytoplasmic staining (Table 1).

Of the nine cases that showed strong homogeneous cytoplasmic expression of both MALT1 and BCL10, six were $t(14;18)(q32;q21)$ positive, as shown in previous studies [7,28]. For the remaining three cases, we performed interphase FISH using $IGH/MALT1$ dual-colour, dual-fusion translocation probes. In each

case, signal patterns indicating the presence of the translocation were detected (Figure 3).

To investigate further that $t(14;18)(q32;q21)/IGH-MALT1$ was truly negative in MALT lymphoma lacking high cytoplasmic expression of MALT1 and BCL10, we performed interphase FISH using $MALT1$ break-apart dual-colour probes. The reliability of the $MALT1$ break-apart assay for the detection of

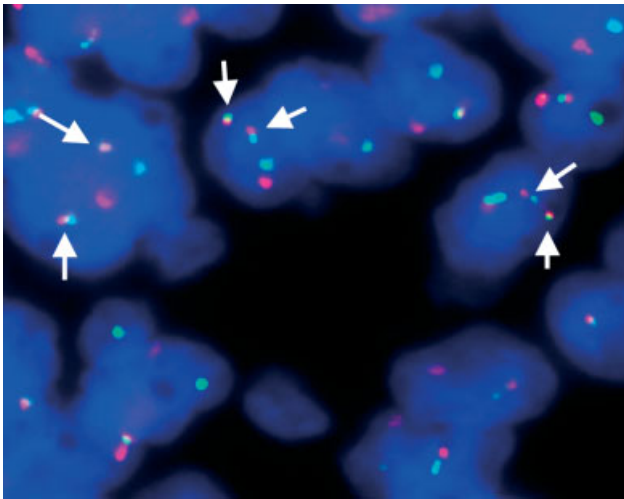


Figure 3. Detection of $t(14;18)/IGH-MALT1$ by interphase FISH with dual-colour, dual-fusion translocation probes. An ocular MALT lymphoma with strong cytoplasmic expression of both MALT1 and BCL10 shows co-localization of green and red signals in interphase nuclei, suggestive of $t(14;18)/IGH-MALT1$

chromosomal translocations involving *MALT1* was first validated in 34 $t(11;18)(q21;q21)$ -positive, 5 $t(14;18)(q32;q21)/IGH-MALT1$ -positive MALT lymphomas and five negative controls. The *MALT1* break-apart assay showed translocations involving *MALT1* in 39/39 positive cases but not in any of the negative controls.

The *MALT1* break-apart assay was performed in 174 cases of MALT lymphoma (salivary gland 48, ocular adnexae 45, lung 23, stomach 31, thyroid 12, skin 12, liver two and small intestine one) lacking evidence of $t(11;18)(q21;q21)$ and $t(1;14)(p22;q32)$ or variants. With the exception of one case, none of the remaining cases displayed evidence of a breakpoint affecting the *MALT1* gene. The only case that showed a breakpoint at the *MALT1* locus was from lung and subsequently

confirmed to be $t(11;18)(q21;q21)$ by interphase FISH with *API2/MALT1* dual-colour, dual-fusion translocation probes. This case was not detected by RT-PCR on RNA samples prepared from paraffin-embedded tissues. It is known that the RT-PCR protocol used misses 7% of rare breakpoints on the *API2* gene [21,23]. Nonetheless, 28 cases showed three copies of the *MALT1* gene in more than 80% of tumour cells, but only three of them displayed moderate MALT1 expression, with the remaining cases exhibiting weak MALT1 expression. There was no evidence of *MALT1* gene amplification in all the cases examined. Figure 4 summarizes the frequencies of $t(14;18)(q32;q21)/IGH-MALT1$, $t(11;18)(q21;q21)$, and $t(1;14)(p22;q32)$ in MALT lymphomas from various sites.

Of the 22 follicular lymphomas examined, 17 showed moderate to strong cytoplasmic MALT1 staining, and the remaining five displayed weak staining. In mantle cell lymphoma, MALT1 expression was weak in 14 and moderate in four cases. Among the 27 DLBCLs studied, 20 showed moderate to strong MALT1 expression and the remaining seven displayed weak staining.

Correlation of MALT1 and BCL10 protein expression with their mRNA expression

In keeping with MALT1 protein expression, *MALT1* mRNA expression was the highest in MALT lymphomas with $t(14;18)(q32;q21)/IGH-MALT1$, significantly higher than those with $t(11;18)(q21;q21)$ or without any of the chromosomal translocations studied (Figure 5). Interestingly, *MALT1* mRNA expression was also significantly higher in MALT lymphomas without any of the chromosomal translocations than in those with $t(11;18)(q21;q21)$ (Figure 5).

Similarly, *BCL10* mRNA expression was the highest in MALT lymphomas with $t(1;14)(p22;q32)$, significantly higher than in those with $t(14;18)(q32;q21)/$

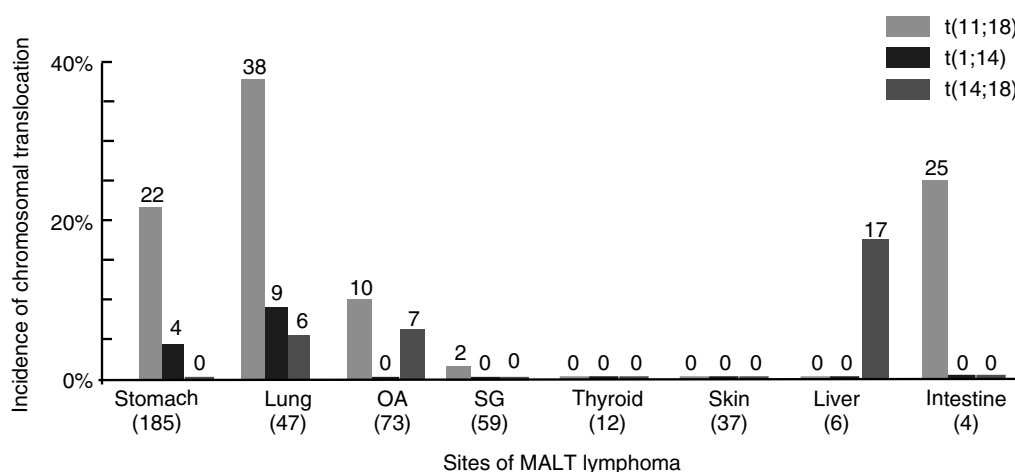


Figure 4. Frequency of $t(14;18)(q32;q21)/IGH-MALT1$, *BCL10* break/ $t(1;14)(p22;q32)$ and $t(11;18)(q21;q21)/API2-MALT1$ in MALT lymphomas from various sites. OA, Ocular adnexae; SG, salivary gland. Numbers in parentheses indicate the number of cases studied. $t(14;18)(q32;q21)/IGH-MALT1$ and *BCL10* break/ $t(1;14)(p22;q32)$ were detected by MALT1 and BCL10 immunohistochemistry followed by interphase FISH. $t(11;18)(q21;q21)/API2-MALT1$ was primarily detected by RT-PCR of the *API2-MALT1* fusion transcript, with the exception of one pulmonary case that was identified by interphase FISH with MALT1 break apart probes

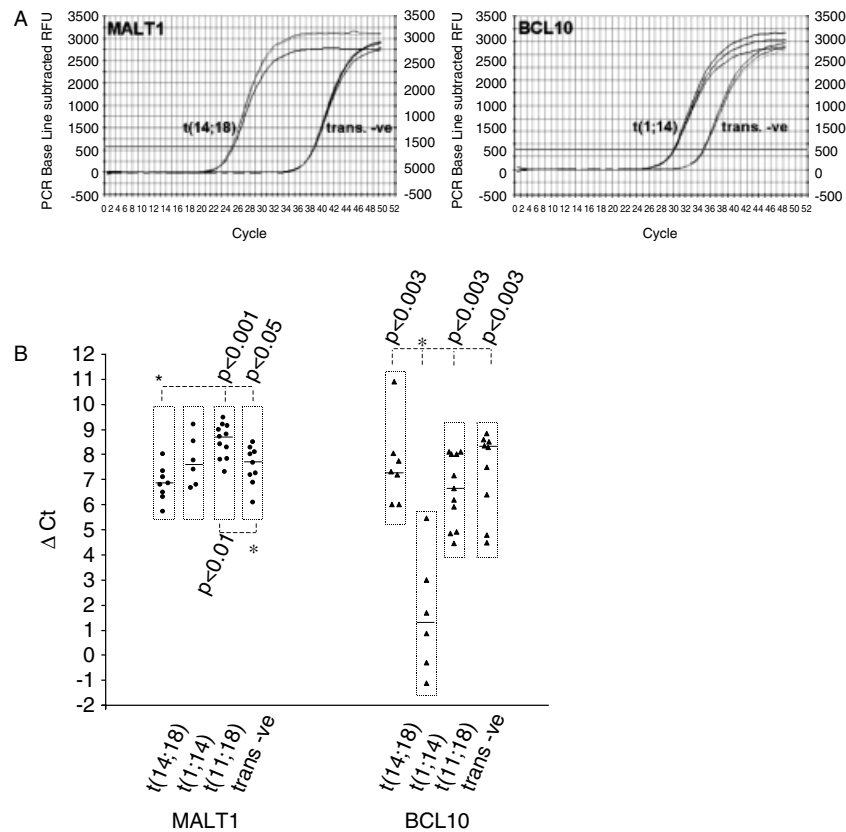


Figure 5. *MALT1* and *BCL10* mRNA expression in MALT lymphoma with different chromosomal translocations. (A) Examples of real-time quantitative RT-PCR with SYBR Green I using an iCycler iQ system. This was carried out in triplicate using RNA samples extracted from tumour cells microdissected from paraffin-embedded tissue sections. For simplicity, reference control 18S rRNA is not shown in the figure. y -axis, relative fluorescent units; x -axis, number of PCR cycles; trans. -ve, translocation-negative case. (B) Comparison of *MALT1* and *BCL10* mRNA expression in MALT lymphomas with different chromosomal translocation status. Asterisk indicates statistically significant difference. The medians are indicated by horizontal bars in the rectangular boxes

IGH-MALT1 or t(11;18)(q21;q21) or without any of these translocations (Figure 5). There was no correlation between *MALT1* and *BCL10* mRNA expression in individual groups with different chromosomal translocation status or in all groups combined together.

Discussion

Mounting evidence indicates that *BCL10* and *MALT1* specifically transduce antigen receptor signalling to activate $\text{NF}\kappa\text{B}$ and play a critical role in the biology of B- and T-cells [33]. This is best demonstrated in *BCL10*-and *MALT1*-deficient mice, which are characterized by impaired B-cell development and function, showing a reduced number of marginal zone B-cells and poor humoral responses to both T-cell-dependent and -independent stimulation [9–12]. It is believed that, in normal B- and T-cells, upon antigen receptor stimulation, *Carma1* is activated to recruit *BCL10* via *CARD*–*CARD* interaction and induces *BCL10* oligomerization. *BCL10* then binds the Ig-like domain of *MALT1* and induces *MALT1* oligomerization, subsequently leading to $\text{NF}\kappa\text{B}$ activation [13,34]. The finding of identical expression pattern of *MALT1* and *BCL10* in B-cell follicles is in line with their roles in B-cell activation and maturation.

One of the remarkable findings of the present study is the characteristic expression pattern of *MALT1* and *BCL10* in MALT lymphoma with different translocations. In those with t(14;18)(q32;q21)/*IGH-MALT1*, the tumour cells are characterized by strong cytoplasmic expression of both *MALT1* and *BCL10*, while MALT lymphoma cells with t(1;14)(p22;q32) or t(11;18)(q21;q21) show strong or moderate *BCL10* nuclear expression respectively, but generally weak *MALT1* cytoplasmic expression. Such differential *MALT1* and *BCL10* expression patterns in MALT lymphoma with various translocations may reflect not only the consequence of these translocations but also the molecular mechanisms involved.

In MALT lymphoma with t(14;18)(q32;q21)/*IGH-MALT1*, strong cytoplasmic *MALT1* expression is expected given the strong transcriptional activity of the *IGH* enhancer. The strong cytoplasmic *BCL10* expression is, to some extent, a surprising finding, but this could well be explained by the molecular mechanism of *MALT1*-mediated $\text{NF}\kappa\text{B}$ activation. *MALT1* lacks structural domains that are capable of mediating its self-oligomerization and over-expression of *MALT1* alone in fibroblasts does not activate $\text{NF}\kappa\text{B}$ [13,14,34]. However, *MALT1* is synergistic with *BCL10* in $\text{NF}\kappa\text{B}$ activation and it is believed

that the oligomerization and activation of MALT1 depend on BCL10 [14]. Thus, it is likely that, in lymphoma cells with t(14;18)(q32;q21)/*IGH-MALT1*, MALT1 interacts with BCL10 and stabilizes it in the cytoplasm, consequently leading to its accumulation. In line with this notion, no alteration in *BCL10* mRNA expression was seen in MALT lymphoma with t(14;18)(q32;q21)/*IGH-MALT1* as compared with other MALT lymphomas lacking a *BCL10*-associated translocation.

Similarly, in view of the direct interaction between BCL10 and MALT1 in their mediated NF κ B activation, one may expect to see MALT1 protein accumulation in lymphoma cells with t(1;14)(p22;q32). Intriguingly, this is not the case: MALT1 is only weakly expressed in the cytoplasm of t(1;14)(p22;q32)-positive cells, in contrast to strong BCL10 expression in the nuclei. Such differential expression of the two proteins in terms of both level and subcellular localization suggests that MALT1 may not be required for BCL10 function. This is supported by knockout mice studies. While BCL10 is essential for antigen receptor mediated NF κ B activation in both B- and T-cells, deficiency of MALT1 expression does not critically affect BCL10-mediated NF κ B activation in B-cells as it does in T-cells [9,12]. It is believed that there is an alternative pathway in BCL10-mediated NF κ B activation in B-cells, which is MALT1 independent. In addition, BCL10 plays an extra role during neurodevelopment, indicating that BCL10 has additional biological activity compared with MALT1 [9].

Similar to t(1;14)(p22;q32)-positive MALT lymphoma, tumour cells with t(11;18)(q21;q21) generally show weak/negative MALT1 cytoplasmic expression but moderate BCL10 nuclear expression. Given that oligomerization of the API2-MALT1 fusion product is most likely mediated by the N-terminal BIR domains of the API2 molecule, API2-MALT1-mediated NF κ B activation is unlikely to require BCL10 or MALT1. In addition, only one allele of the intact *MALT1* gene remains in MALT lymphoma with t(11;18)(q21;q21) and the level of *MALT1* mRNA is much lower in these tumours than in those without this translocation. Hence, weak MALT1 staining in MALT lymphoma with t(11;18)(q21;q21) is expected. However, moderate BCL10 nuclear staining is a surprising finding. The mechanism underlying BCL10 nuclear expression is unclear. Nonetheless, this is unlikely to be related to the level of *BCL10* mRNA expression since there was no significant difference in its transcript expression between cases expressing nuclear BCL10 (excluding those with BCL10-involved chromosomal translocation) or those expressing cytoplasmic BCL10.

As shown previously, strong nuclear BCL10 staining is highly indicative of the presence of t(1;14)(p22;q32) or variants. In the present study, we further showed that high levels of cytoplasmic expression of both MALT1 and BCL10 characterize MALT lymphoma with t(14;18)(q32;q21)/*IGH-MALT1*. This characteristic MALT1 and BCL10 expression pattern

was seen in 9/9 MALT lymphomas with t(14;18)(q32;q21)/*IGH-MALT1*. The absence of t(14;18)(q32;q21)/*IGH-MALT1* in MALT lymphoma lacking strong MALT1 and BCL10 cytoplasmic expression was further confirmed by interphase FISH analyses of 174 t(11;18)(q21;q21)- and t(1;14)(p22;q32)-negative cases. Based on MALT1 and BCL10 immunohistochemistry, followed by interphase FISH analysis, we have demonstrated t(14;18)(q32;q21)/*IGH-MALT1* in MALT lymphoma of the lung (6%), ocular adnexae (7%), and liver (17%) but not in those of the stomach, salivary gland, thyroid, and skin. These findings are in line with previous reports [7,28,29,35]: the translocation is mutually exclusive from t(11;18)(q21;q21) and *BCL10* break/t(1;14)(p22;q32), and occurs more frequently in extra-gastrointestinal sites.

In view of the characteristic BCL10 and MALT1 expression patterns in MALT lymphoma with different translocations, BCL10 and MALT1 immunohistochemistry may be used for screening for these translocations. Since both BCL10 and MALT1 expression patterns in MALT lymphomas with t(1;14)(p22;q32) or t(14;18)(q32;q21)/*IGH-MALT1* are characteristic and the incidence of both translocations is relatively infrequent in MALT lymphoma, it would be rational to screen for these translocations first by BCL10 and MALT1 immunohistochemistry, followed by confirmation with interphase FISH. For MALT lymphoma with t(11;18)(q21;q21), BCL10 and MALT1 immunohistochemistry does not provide a strong indication for the presence of the translocation as up to 20% of t(11;18)(q21;q21)-negative cases also show moderate BCL10 nuclear expression. Detection of this translocation is best carried out by RT-PCR or interphase FISH.

In summary, we have shown that MALT1 expression pattern is identical to that of BCL10 in normal lymphoid tissues but varies in MALT lymphomas, with high levels of cytoplasmic expression of both MALT1 and BCL10 characterizing those with t(14;18)(q32;q21)/*IGH-MALT1*.

Acknowledgements

The study was supported by research grants from the Leukaemia Research Fund, UK, the Leukemia and Lymphoma Society, USA, and the Deutsche Krebshilfe.

References

1. Isaacson PG, Du MQ. MALT lymphoma: from morphology to molecules. *Nat Rev Cancer* 2004; **4**: 644–653.
2. Dierlamm J, Baens M, Wlodarska I, et al. The apoptosis inhibitor gene *API2* and a novel 18q gene, *MLT*, are recurrently rearranged in the t(11;18)(q21;q21) associated with mucosa-associated lymphoid tissue lymphomas. *Blood* 1999; **93**: 3601–3609.
3. Akagi T, Motegi M, Tamura A, et al. A novel gene, *MALT1* at 18q21, is involved in t(11;18)(q21;q21) found in low-grade B-cell lymphoma of mucosa-associated lymphoid tissue. *Oncogene* 1999; **18**: 5785–5794.
4. Morgan JA, Yin Y, Borowsky AD, et al. Breakpoints of the t(11;18)(q21;q21) in mucosa-associated lymphoid tissue (MALT)

- lymphoma lie within or near the previously undescribed gene *MALT1* in chromosome 18. *Cancer Res* 1999; **59**: 6205–6213.
5. Willis TG, Jadayel DM, Du MQ, *et al.* *Bcl10* is involved in t(1;14)(p22;q32) of MALT B-cell lymphoma and mutated in multiple tumor types. *Cell* 1999; **96**: 35–45.
 6. Zhang Q, Siebert R, Yan M, *et al.* Inactivating mutations and over-expression of *BCL10*, a caspase recruitment domain-containing gene, in MALT lymphoma with t(1;14)(p22;q32). *Nat Genet* 1999; **22**: 63–68.
 7. Streubel B, Lamprecht A, Dierlamm J, *et al.* T(14;18)(q32;q21) involving *IGH* and *MALT1* is a frequent chromosomal aberration in MALT lymphoma. *Blood* 2003; **101**: 2335–2339.
 8. Sanchez-Izquierdo D, Buchonnet G, Siebert R, *et al.* *MALT1* is deregulated by both chromosomal translocation and amplification in B-cell non-Hodgkin lymphoma. *Blood* 2003; **101**: 4539–4546.
 9. Ruland J, Duncan GS, Elia A, *et al.* *Bcl10* is a positive regulator of antigen receptor-induced activation of NF-kappaB and neural tube closure. *Cell* 2001; **104**: 33–42.
 10. Xue L, Morris SW, Orihuela C, *et al.* Defective development and function of *Bcl10*-deficient follicular, marginal zone and B1 B cells. *Nat Immunol* 2003; **4**: 857–865.
 11. Ruefli-Brasse AA, French DM, Dixit VM. Regulation of NF-kappaB-dependent lymphocyte activation and development by paracaspase. *Science* 2003; **302**: 1581–1584.
 12. Ruland J, Duncan GS, Wakeham A, Mak TW. Differential requirement for *MALT1* in T and B cell antigen receptor signaling. *Immunity* 2003; **19**: 749–758.
 13. Lucas PC, Yonezumi M, Inohara N, *et al.* *Bcl10* and *MALT1*, independent targets of chromosomal translocation in MALT lymphoma, cooperate in a novel NF-kappa B signaling pathway. *J Biol Chem* 2001; **276**: 19012–19019.
 14. McAllister-Lucas LM, Inohara N, Lucas PC, *et al.* *Bim1*, a MAGUK family member linking protein kinase C activation to *Bcl10*-mediated NF-kappaB induction. *J Biol Chem* 2001; **276**: 30589–30597.
 15. Remstein ED, James CD, Kurtin PJ. Incidence and subtype specificity of *API2-MALT1* fusion translocations in extranodal, nodal, and splenic marginal zone lymphomas. *Am J Pathol* 2000; **156**: 1183–1188.
 16. Baens M, Maes B, Steyls A, *et al.* The product of the t(11;18), an *API2-MLT* fusion, marks nearly half of gastric MALT type lymphomas without large cell proliferation. *Am J Pathol* 2000; **156**: 1433–1439.
 17. Motegi M, Yonezumi M, Suzuki H, *et al.* *API2-MALT1* chimeric transcripts involved in mucosa-associated lymphoid tissue type lymphoma predict heterogeneous products. *Am J Pathol* 2000; **156**: 807–812.
 18. Nakamura T, Nakamura S, Yonezumi M, *et al.* *Helicobacter pylori* and the t(11;18)(q21;q21) translocation in gastric low-grade B-cell lymphoma of mucosa-associated lymphoid tissue type. *Jpn J Cancer Res* 2000; **91**: 301–309.
 19. Kalla J, Stilgenbauer S, Schaffner C, *et al.* Heterogeneity of the *API2-MALT1* gene rearrangement in MALT-type lymphoma. *Leukemia* 2000; **14**: 1967–1974.
 20. Liu H, Ye H, Dogan A, *et al.* T(11;18)(q21;q21) is associated with advanced mucosa-associated lymphoid tissue lymphoma that expresses nuclear *BCL10*. *Blood* 2001; **98**: 1182–1187.
 21. Ye H, Liu H, Attygalle A, *et al.* Variable frequencies of t(11;18)(q21;q21) in MALT lymphomas of different sites: significant association with CagA strains of *H pylori* in gastric MALT lymphoma. *Blood* 2003; **102**: 1012–1018.
 22. Liu H, Ruskone Fourmestraux A, Lavergne-Slove A, *et al.* Resistance of t(11;18) positive gastric mucosa-associated lymphoid tissue lymphoma to *Helicobacter pylori* eradication therapy. *Lancet* 2000; **357**: 39–40.
 23. Liu H, Ye H, Ruskone-Fourmestraux A, *et al.* T(11;18) is a marker for all stage gastric MALT lymphomas that will not respond to *H. pylori* eradication. *Gastroenterology* 2002; **122**: 1286–1294.
 24. Chuang SS, Lee C, Hamoudi RA, *et al.* High frequency of t(11;18) in gastric mucosa-associated lymphoid tissue lymphomas in Taiwan, including one patient with high-grade transformation. *Br J Haematol* 2003; **120**: 97–100.
 25. Remstein ED, Kurtin PJ, James CD, *et al.* Mucosa-associated lymphoid tissue lymphomas with t(11;18)(q21;q21) and mucosa-associated lymphoid tissue lymphomas with aneuploidy develop along different pathogenetic pathways. *Am J Pathol* 2002; **161**: 63–71.
 26. Ye H, Dogan A, Karran L, *et al.* *BCL10* expression in normal and neoplastic lymphoid tissue: nuclear localization in MALT lymphoma. *Am J Pathol* 2000; **157**: 1147–1154.
 27. Maes B, Demunter A, Peeters B, Wolf-Peeters C. *BCL10* mutation does not represent an important pathogenic mechanism in gastric MALT-type lymphoma, and the presence of the *API2-MLT* fusion is associated with aberrant nuclear *BCL10* expression. *Blood* 2002; **99**: 1398–1404.
 28. Remstein ED, Kurtin PJ, Einerson RR, Paternoster SF, Dewald GW. Primary pulmonary MALT lymphomas show frequent and heterogeneous cytogenetic abnormalities, including aneuploidy and translocations involving *API2* and *MALT1* and *IGH* and *MALT1*. *Leukemia* 2004; **18**: 156–160.
 29. Murga Penas EM, Hinz K, Roser K, *et al.* Translocations t(11;18)(q21;q21) and t(14;18)(q32;q21) are the main chromosomal abnormalities involving *MLT/MALT1* in MALT lymphomas. *Leukemia* 2003; **17**: 2225–2229.
 30. Ho L, Davis RE, Conne B, *et al.* *MALT1* and *-MALT1* confer proliferative advantage and resistance against FAS-induced cell death in B cells. *Blood* (in press).
 31. Pan LX, Diss TC, Peng HZ, Isaacson PG. Clonality analysis of defined B-cell populations in archival tissue sections using microdissection and the polymerase chain reaction. *Histopathology* 1994; **24**: 323–327.
 32. Liu H, Huang X, Zhang Y, *et al.* Archival fixed histologic and cytologic specimens including stained and unstained materials are amenable to RT-PCR. *Diagn Mol Pathol* 2002; **11**: 222–227.
 33. Thome M. *CARMA1*, *BCL-10* and *MALT1* in lymphocyte development and activation. *Nat Rev Immunol* 2004; **4**: 348–359.
 34. Uren GA, O'Rourke K, Aravind L, *et al.* Identification of paracaspases and metacaspases: two ancient families of caspase-like proteins, one of which plays a key role in MALT lymphoma. *Mol Cell* 2000; **6**: 961–967.
 35. Streubel B, Huber D, Wohrer S, Chott A, Raderer M. Frequency of chromosomal aberrations involving *MALT1* in mucosa-associated lymphoid tissue lymphoma in patients with Sjogren's syndrome. *Clin Cancer Res* 2004; **10**: 476–480.

t(11;18)(q21;q21) of mucosa-associated lymphoid tissue lymphoma results from illegitimate non-homologous end joining following double strand breaks

Hongxiang Liu,¹ Rifat A. Hamoudi,¹ Hongtao Ye,¹ Agnes Ruskone-Fourmestreaux,² Ahmet Dogan,³ Peter G. Isaacson³ and Ming-Qing Du¹

¹Department of Pathology, University of Cambridge, Cambridge, UK, ²Service de Gastro-entérologie, Hotel-Dieu, AP HP, Paris and Groupe d'Etude des Lymphomes Digestifs, Fondation Francaise de Cancérologie Digestive, France, and ³Department of Histopathology, Royal Free and University College Medical School, London, UK
© 2004 Blackwell Publishing Ltd, *British Journal of Haematology*, 125, 318–329

Summary

t(11;18)(q21;q21) is the most frequent chromosomal aberration specifically associated with mucosa-associated lymphoid tissue (MALT) lymphoma. The translocation fuses the *API2* gene to the *MALT1* gene and generates a functional *API2-MALT1* transcript. The breakpoint of the fusion gene is well characterized at the transcript level but poorly understood at the genomic level and the mechanism underlying the translocation is unknown. We identified the genomic breakpoint in 19 t(11;18)-positive MALT lymphoma cases by polymerase chain reaction and sequencing and analysed the junctional sequences. The breakpoints were scattered in intron 7 and exon 8 of the *API2* gene, and introns 4, 6, 7 and 8 of the *MALT1* gene. Comparative sequence analysis between the *API2-MALT1* fusion on der(11) and the *MALT1-API2* fusion on der(18) showed extensive alterations including deletions, duplications and non-template-based insertions at the fusion junctions in all cases examined. An extensive sequence search failed to reveal any known sequence motifs that might be associated with chromosomal recombination or any novel consensus sequences at or near the breakpoints on both der(11) and der(18) except in one case, in which *Alu* repeats spanned the breakpoint of the *MALT1-API2* fusion. Our results suggest that t(11;18) may result from illegitimate non-homologous end joining following double strand breaks.

Keywords: mucosa-associated lymphoid tissue lymphoma, t(11;18)(q21;q21), double strand break, non-homologous end joining.

Received 11 December 2003; accepted for publication 9 February 2004

Correspondence: Ming-Qing Du, Division of Molecular Histopathology, Department of Pathology, Level 3 Lab Block, Box 231, Addenbrookes Hospital, Hills Road, Cambridge CB2 2QQ, UK. E-mail: mqd20@cam.ac.uk

Mucosa-associated lymphoid tissue (MALT) lymphoma is a distinct subtype of low-grade marginal zone B-cell lymphoma arising from extranodal sites such as the stomach, lung, salivary gland, thyroid, conjunctiva skin, etc. (Isaacson *et al*, 2001; Du & Isaacson, 2002). Interestingly, these organs are normally devoid of any native lymphoid tissue and the lymphoma at these sites arises from the MALT acquired as a consequence of a chronic inflammatory or auto-immune disorder. Notably, gastric MALT lymphoma is invariably preceded by *Helicobacter pylori*-associated chronic gastritis, while salivary gland and thyroid MALT lymphomas are commonly associated with lymphoepithelial sialadenitis and Hashimoto's thyroiditis respectively. Antigenic and immunological stimulation thus plays a critical role in the genesis and expansion of the lymphoma clone. Genetically, MALT

lymphoma is characterized by three specific chromosomal translocations, namely t(11;18)(q21;q21)/*API2-MALT1* (Auer *et al*, 1997; Ott *et al*, 1997), t(1;14)(p22;q32)/*IgH-BCL10* (Wotherspoon *et al*, 1992) and t(14;18)(q32;q21)/*IgH-MALT1* (Sanchez-Izquierdo *et al*, 2003; Streubel *et al*, 2003). Among these, t(11;18) is the most frequent but occurs at dramatically variable frequencies in MALT lymphoma of different sites, from 0–1% in the thyroid and salivary gland to 30–40% in the stomach and lung (Ye *et al*, 2003). These findings suggest that the occurrence of the translocation is heavily influenced by the nature of premalignant diseases associated with MALT lymphoma. In gastric MALT lymphoma, t(11;18) has been shown to be significantly associated with infection by CagA-positive strains of *H. pylori*, further implicating a role of aetiological factors in the occurrence of the translocation (Ye *et al*, 2003).

t(11;18) causes reciprocal fusions of *API2-MALT1* on der(11) and *MALT1-API2* on der(18) (Akagi *et al*, 1999; Dierlamm *et al*, 1999; Morgan *et al*, 1999). As only the *API2-MALT1* fusion transcript is consistently expressed in MALT lymphoma with t(11;18), this fusion product is assumed to be oncogenic (Dierlamm *et al*, 1999; Uren *et al*, 2000; Lucas *et al*, 2001). The fusion junctions at the transcript level have been well characterized. On the *API2* gene, they are always downstream of the third baculovirus inhibitors of apoptosis repeats (BIR) domain but upstream of the C-terminal RING domain, whereas on the *MALT1* gene, they are consistently upstream of the C-terminal caspase-like domain (Fig 1). Thus, the resulting *API2-MALT1* fusion transcript always comprises the N-terminal *API2* with three intact BIR domains and the C-terminal *MALT1* region containing an intact caspase-like domain (Ott *et al*, 1997; Akagi *et al*, 1999; Dierlamm *et al*, 1999, 2000; Baens *et al*, 2000a; Kalla *et al*, 2000; Liu *et al*, 2000, 2001, 2002; Motegi *et al*, 2000; Nakamura *et al*, 2000; Remstein *et al*, 2000; Ye *et al*, 2003). The specific selection of these domains of the *API2* and *MALT1* genes to form a functional fusion product strongly suggests their importance and synergy in oncogenesis.

The mechanisms underlying the occurrence of t(11;18) are unknown. Most lymphoma-associated chromosomal translocations involve the antigen receptor locus and are believed to be the result of illegitimate recombination involving the VDJ recombination machinery (Willis & Dyer, 2000; Kuppers & Dalla-Favera, 2001; Marculescu *et al*, 2002). t(11;18) is one of

the few lymphoma-associated chromosomal translocations that do not involve the antigen receptor locus (Morris *et al*, 1994) and thus it is particularly interesting to investigate the mechanisms underlying the translocation. So far two studies have examined this by sequence analysis of the genomic breakpoints of t(11;18). One study examined five cases and did not reveal any sequence motifs including the VDJ recombination heptamer/nonamer at the breakpoints, which are known to be involved in chromosomal translocations, and concluded that the *API2-MLT* fusion might result from a non-homologous end joining event after multiple double-strand breaks (Baens *et al*, 2000b). In contrast, the other study investigated a single case and identified a VDJ heptamer sequence at the *API2* breakpoint on der(11) and proposed a role of VDJ recombination in t(11;18) (Sato *et al*, 2001). To further understand the mechanism underlying the occurrence of t(11;18), we characterized the junction sequence of both *API2-MALT1* and *MALT1-API2* fusions in 19 t(11;18)-positive MALT lymphomas.

Patients and methods

Patients

Nineteen cases of t(11;18)-positive MALT lymphoma with fresh-frozen tumour tissues were retrieved from Department of Histopathology, University College London, London and the Groupe d'Etude des Lymphomes Digestifs, France. They

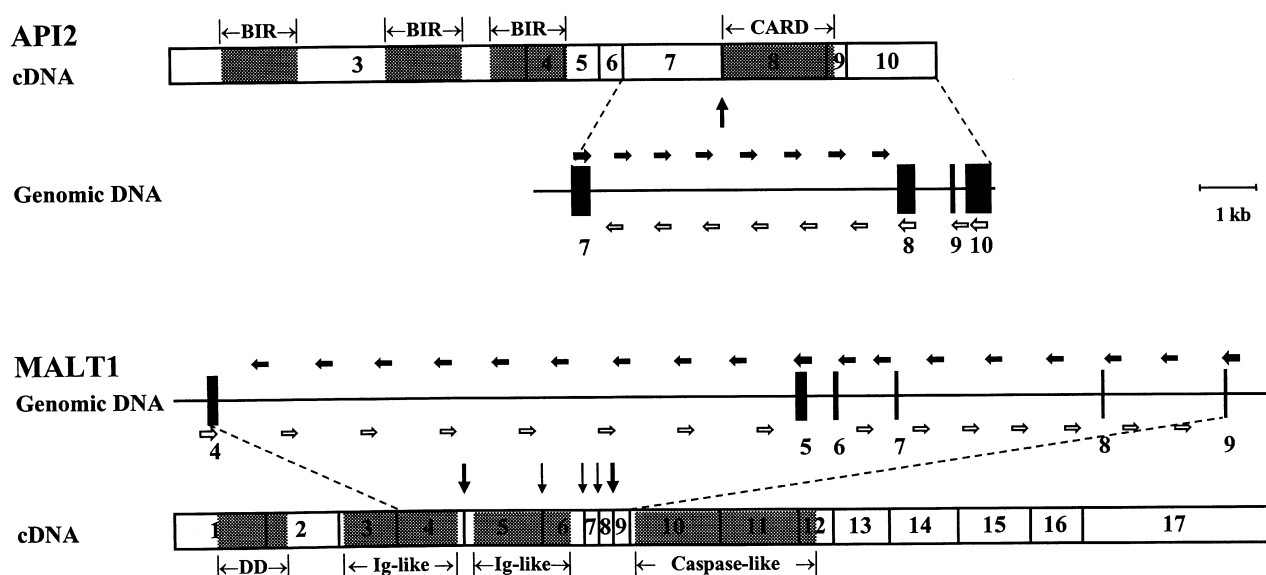


Fig 1. Schematic illustration of the structure of the *API2* and *MALT1* transcripts and genomic regions spanning the breakpoints observed. The *API2* and *MALT1* transcripts were depicted according to GenBank accession numbers NM001165 and AF130356, respectively, with exons numbered, domains shaded and fusion junctions indicated by vertical arrows. The regions of the *API2* (AP001167) and *MALT1* (AC104365) genes spanning the breakpoints are drawn to scale to show the position of the primers used for amplification of the genomic fusion on der(11) (filled horizontal arrows) and der(18) (unfilled horizontal arrows). The primers positioned to exons are used for primary long distance PCR and those positioned to introns are used for nested PCR to narrow down the fragment containing the fusion junction. BIR, baculovirus inhibitors of apoptosis (IAP) repeat; CARD, caspase recruitment domain; DD, death domain.

included 16 from stomach, four from lung and two from small intestine (Table I). t(11;18) and the *API2-MALT1* fusion junction at the transcript level in these cases were identified previously by reverse transcription polymerase chain reaction (RT-PCR) and sequencing (Table I) (Liu *et al*, 2001, 2002).

Amplification and sequencing of t(11;18) genomic fusions

High molecular DNA was extracted from frozen tissues using the Wizard[®] genomic DNA purification kit (Promega, Southampton, UK). To amplify the fusion genes on der(11), a long-distance PCR was performed for each case using TaKaRa LA Taq[™] (TaKaRa Biomedicals, Otsu, Japan) followed by multiple nested PCRs (Fig 1; Table S1). In our previous study, RT-PCR demonstrated that the fusion junctions of the *API2-MALT1* transcript were at the 3'-end of exon 7 on the *API2* gene in all 19 cases but varied at the 5'-end of exons 5 (11 cases), 8 (six cases) and 9 (two cases) on the *MALT1* gene (Fig 1; Table I) (Liu *et al*, 2001, 2002). The genomic breakpoint was assumed to be in the respective introns: i.e. intron 7 of the *API2* gene and introns 4, 7 and 8 of the *MALT1* gene (Fig 1). The primary PCR was therefore performed using a sense primer to the exon 7 of the *API2* gene and an antisense primer to the exon 5 of the *MALT1* gene in cases with putative breakpoints in intron 4 or an antisense primer to the exon 9 in those with putative breakpoints in introns 7 and 8. The PCR was carried out in a 50 µl reaction mixture containing 250 ng template DNA and 2.5 U TaKaRa LA Taq[™] with a two-step cycling protocol comprising an initial denaturation at 94°C for

1 min, 30 cycles of 94°C for 20 s and 65°C for 15 min, and a final extension at 72°C for 10 min. According to genomic sequences of the *API2* (GenBank accession no. AP001167) and *MALT1* (AC104365) genes, the maximum expected size of the genomic fusion flanked by these primers was less than 13.5 kb, a size well within the maximal amplicon (up to 40 kb) allowed by the TaKaRa LA Taq[™]. The amplified products, which varied in sizes depending on the position of the breakpoint, were then used as templates for multiple nested PCRs with a series of sense primers to the intron 7 of the *API2* gene and antisense primers to the corresponding introns of the *MALT1* gene in order to narrow down the region containing the breakpoint (Table S1). The intronic primers were designed with an average interval of 1 kb. Following various combinations of *API2* and *MALT1* primers, the amplified fusion gene fragments of <1 kb were subjected to direct sequencing on both orientations using dRhodamine dye terminators on an ABI Prism 377 sequencer (PE Applied Biosystems, Foster City, CA, USA).

The same strategy was applied to amplification and sequencing of the reciprocal fusion on the der(18) using different sets of primers designed from the same regions (Fig 1; Table S1).

Sequence analysis of the genomic fusion junctions of t(11;18)

A comprehensive analysis of nucleotide sequence at and around the fusion junctions was performed using following

Table I. Characteristics of the fusion junctions of t(11;18) at transcript and genomic level.

| Case no. | Tumour site | Fusion junction on transcript | | Fusion junction on der(11) | | | Fusion junction on der(18) | | | Deletion (-) or duplication (+) | | |
|----------|-----------------|-------------------------------|---------|----------------------------|------|-------|----------------------------|------|-------|---------------------------------|-------|---------|
| | | API2 | MALT1 | PCR size (bp) | API2 | MALT1 | Insertion | API2 | MALT1 | Insertion | API2 | MALT1 |
| 1 | Lung | 3'-Ex 7 | 5'-Ex 5 | 9782 | In 7 | In 4 | | In 7 | In 4 | | -86 | -130 |
| 2 | Stomach | 3'-Ex 7 | 5'-Ex 5 | 9536 | In 7 | In 4 | | In 7 | In 4 | | -1223 | +135 |
| 3 | Stomach | 3'-Ex 7 | 5'-Ex 5 | 10 540 | In 7 | In 4 | | In 7 | In 4 | | -64 | -20 |
| 4 | Stomach | 3'-Ex 7 | 5'-Ex 5 | 11 466 | Ex 8 | In 4 | | | | | | |
| 5 | Stomach | 3'-Ex 7 | 5'-Ex 5 | 6959 | In 7 | In 4 | | In 7 | In 4 | | -1186 | -95 |
| 6 | Stomach | 3'-Ex 7 | 5'-Ex 5 | 7503 | In 7 | In 4 | | In 7 | In 4 | | -645 | -92 |
| 7 | Lung | 3'-Ex 7 | 5'-Ex 5 | 8164 | In 7 | In 4 | | | | | | |
| 8 | Lung | 3'-Ex 7 | 5'-Ex 5 | 3425 | In 7 | In 4 | 'aa' | In 7 | In 4 | | -25 | -90 |
| 9 | Stomach | 3'-Ex 7 | 5'-Ex 5 | 2723 | In 7 | In 4 | | In 7 | In 4 | 't' | -611 | -207 |
| 10 | Stomach | 3'-Ex 7 | 5'-Ex 5 | 5684 | Ex 8 | In 4 | | Ex 8 | In 4 | | +108 | +105 |
| 11 | Stomach | 3'-Ex 7 | 5'-Ex 5 | 2890 | In7 | In 4 | 'agaggaata' | In 7 | In 4 | 'aa' | -15 | -17 |
| 12 | Stomach | 3'-Ex 7 | 5'-Ex 8 | 10 274 | Ex 8 | In 6 | | | | | | |
| 13 | Stomach | 3'-Ex 7 | 5'-Ex 8 | 7156 | In 7 | In 6 | | In 7 | In 8 | | -2166 | +3320 |
| 14 | Lung | 3'-Ex 7 | 5'-Ex 8 | 8496 | In 7 | In 7 | | | | | | |
| 15 | Stomach | 3'-Ex 7 | 5'-Ex 8 | 4382 | In 7 | In 7 | | | | | | |
| 16 | Stomach | 3'-Ex 7 | 5'-Ex 8 | 4031 | In 7 | In 7 | 't' | | | | | |
| 17 | Stomach | 3'-Ex 7 | 5'-Ex 8 | 4031 | In 7 | In 7 | 't' | In 7 | In 4 | | -2012 | -10 585 |
| 18 | Small intestine | 3'-Ex 7 | 5'-Ex 9 | 5655 | In 7 | In 8 | | In 7 | In 8 | | -140 | -160 |
| 19 | Stomach | 3'-Ex 7 | 5'-Ex 9 | 1519 | In 7 | In 8 | | In 7 | In 8 | | -149 | +241 |

MALT, mucosa-associated lymphoid tissue; PCR, polymerase chain reaction; Ex, exon; In, intron.

computer programs. Basic Local Alignment Search Tool (BLAST) 2 sequence was used to identify the intron-exon boundaries of the *API2* and *MALT1* genes and to search for sequence identities between the two genomic regions (<http://www.ncbi.nlm.nih.gov/blast/bl2seq/bl2.html>). Dialign and Bioedit were used to align sequence fragments spanning breakpoints to search for consensus sequence at or near the breakpoints (http://bibiserv.techfak.uni-bielefeld.de/cgi-bin/dialign_submit; <http://www.mbio.ncsu.edu/BioEdit/bioedit.html>). RepeatMasker was used to search for repetitive elements in the *API2* and *MALT1* genes (<http://repeatmasker.org/>). Fuzznuc was used to search for known sequence patterns or motifs at or near the breakpoints (<http://www.hgmp.mrc.ac.uk/Software/EMBOSS/Apps/>). Multiple EM for Motif Elicitation (MEME) was used to search for novel conserved regions at or near the breakpoint (<http://meme.sdsc.edu/meme/website/intro.html>) and Motif Alignment and Search Tool (MAST) was employed to search databases for the identified motifs (<http://meme.sdsc.edu/meme/website/intro.html>).

In order to assess whether the distribution of the breakpoint observed was deterministic or stochastic, comparison was made between the observed breakpoints and 'those' randomly generated by computing. One hundred sets of 19 random 'breakpoints' were generated from the intron 7 and exon 8 of the *API2* gene and from introns 4 to 8 of the *MALT1* gene using the Research Radomizer software (<http://www.randomizer.org/form.htm>) and the data obtained were normalized by ensuring that the ranking order between the observed and experimental points on both the genes was the same. The correlation coefficient was then calculated using the Minitab (<http://www.minitab.com>) as a measure to assess the 'goodness-of-fit' between the observed breakpoints and those generated by the computer program.

Results

Genomic breakpoints on both the API2 and MALT1 gene were scattered

The genomic *API2-MALT1* fusions of up to 11.5 kb on der(11) were amplified by long-distance PCR in all 19 cases analysed (Table I). Subsequent multiple nested PCRs followed by sequencing allowed identification of the genomic breakpoints in all cases and their distribution is shown in Fig 2A. In the majority of cases, the genomic breakpoints on both the *API2* and *MALT1* genes were in the corresponding introns as predicted by the fusion junctions at the transcript level (Table I; Fig 1) (Liu *et al*, 2001, 2002). However, in three cases (cases 4, 10 and 12), the genomic breakpoints on the *API2* gene were in exon 8, although the fusion points at the transcript level were at the 3'-end of exon 7. Similarly, the genomic breakpoints on *MALT1* were in intron 6 in two cases (cases 12 and 13) whereas their fusion points at the transcript level were at the 5'-end of exon 8. These findings strongly indicate that the residual *API2* exon 8 and *MALT1* exon 7 in

the *API2-MALT1* fusion were spliced out during RNA processing in order to generate a functional transcript.

Apart from cases 16 and 17, which shared the same breakpoints on both the *API2* and *MALT1* genes, and cases 5 and 6, which shared the same breakpoint on the *MALT1* gene only, all the remaining cases ($n = 15$) had different breakpoints that appeared to be distributed randomly on both the genes. The breakpoints did not show any tendency of clustering and there was no significant correlation in distribution of the breakpoints between the two genes ($P > 0.05$).

Using the same PCR strategy, the *MALT1-API2* fusion on der(18) was amplified in 13 of 19 cases and their breakpoints were characterized. Comparison of the breakpoints identified from the *MALT1-API2* fusion on der(18) with those observed from the *API2-MALT1* fusion on der(11) revealed deletions, insertions and/or duplications of both the *API2* and *MALT1* gene sequences in all 13 cases (detailed below). Thus, the breakpoints recorded from the *MALT1-API2* fusion on der(18) were different from those obtained on the *API2-MALT1* fusion on der(11) (Fig 2B). Based on the breakpoints from the *MALT1-API2* fusion, three pairs of cases (cases 2 and 3, 5 and 6, 13 and 18) had identical breakpoints on both the *MALT1* and *API2* genes, although the breakpoints for each pair were different. The cases with the same breakpoints had been independently analysed and the possibility of PCR contamination was excluded. The remaining seven cases showed different breakpoints scattered on both genes. Statistical analysis failed to show any significant correlation in distribution of the breakpoints between the two genes ($P > 0.05$).

The breakpoints observed above from both the *API2-MALT1* and *MALT1-API2* fusions were also different from those reported previously (Baens *et al*, 2000b; Sato *et al*, 2001).

Comparison of the breakpoints identified from the *API2-MALT1* and *MALT1-API2* fusions with 100 sets of computer-generated random 'breakpoints' from the same breakage region of both the *API2* and *MALT1* genes showed a significant correlation between the sets of observed data and sets of computer-generated data for both genes ($r > 0.95$ and $P < 0.001$ in each case), suggesting that the observed breakpoints may have occurred in a random fashion.

Extensive sequence alterations occurred at the fusion junction of t(11;18)

Comparative sequence analysis between the *API2-MALT1* fusion on der(11) and the *MALT1-API2* fusion on der(18) revealed extensive alterations at the fusion junctions including deletions, duplications and non-template-based insertions in all 13 cases examined (Table I; Fig 3). Deletions ranged from 15 to 10 585 bp and occurred in 12 cases, affecting both the *API2* and *MALT1* genes in nine cases and only the *API2* gene in the remaining three cases. In one case (case 17), deletion involved a coding exon of the *MALT1* gene, while in the remaining cases, deletions were restricted to the intronic

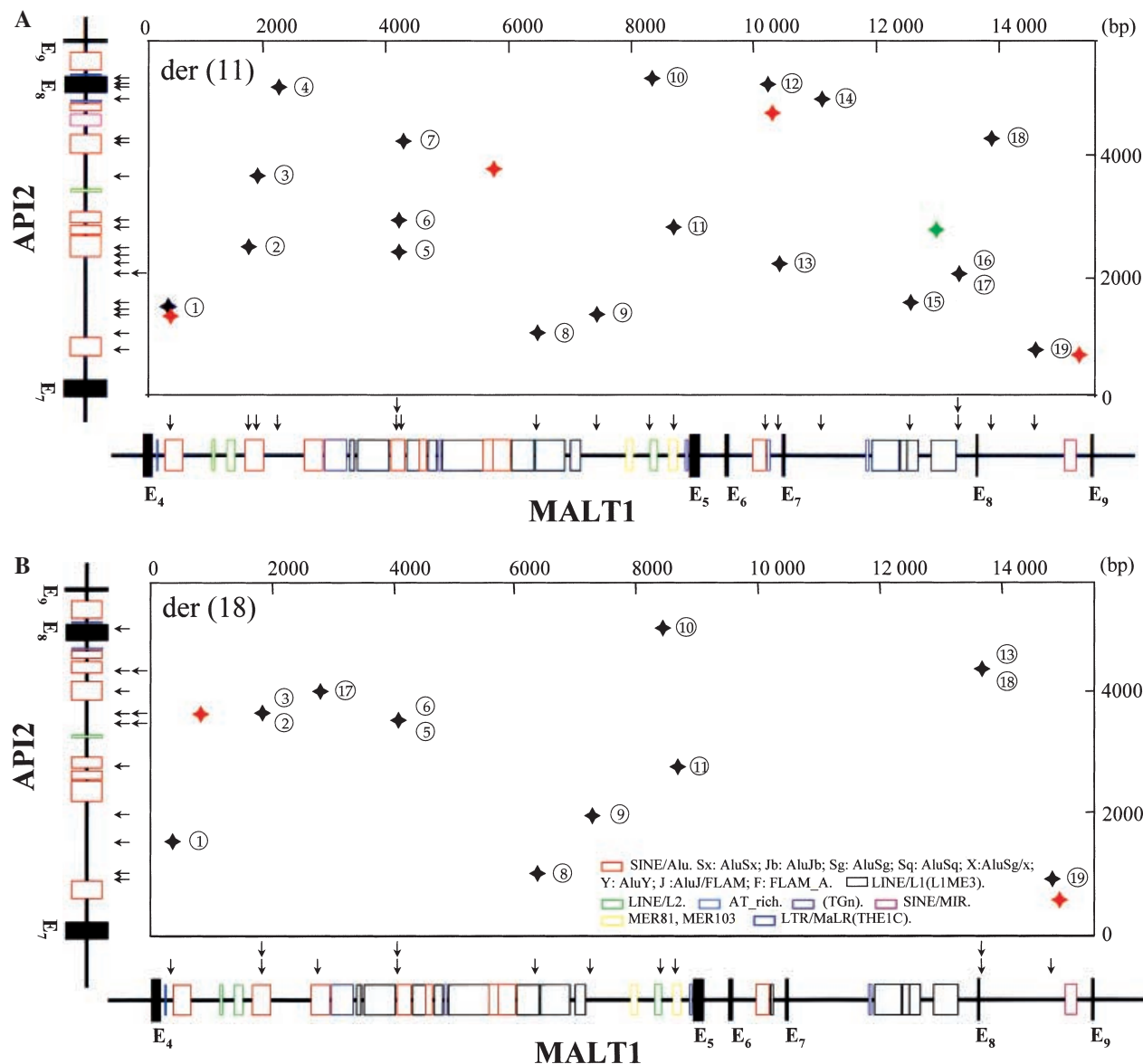


Fig 2. Distribution of the genomic breakpoints of t(11;18) observed on der(11) (A) and der(18) (B). The breakpoint in each case (circled number) is plotted as a co-ordinate against its position (indicated by arrows) on the *API2* (*y*-axis) and *MALT1* (*x*-axis) genes drawn to scale. Solid black boxes represent exons and their numbers are denoted. Open coloured boxes show repetitive elements and an insert illustrates the type of repeat. Breakpoints in red are those identified by Baens *et al* (2000b) and those in green were identified by Sato *et al* (2001).

region. Duplications ranging from 105 to 3320 bp were found in four cases, affecting both the *API2* and *MALT1* genes in one case and only the *MALT1* gene in the remaining three cases. Non-template insertions ranging from 1 to 9 bp were observed in five cases (Tables I and S2). In one case (case 11), insertion occurred at both the junctions of the *API2*-*MALT1* and *MALT1*-*API2* fusions, while in the remaining four cases, insertion took place at the junction of either of the two fusions. Interestingly, non-template insertion was mutually exclusive of duplication in all cases. It was also noted that 19 junctions including 11 on der(11) and eight on der(18) had mono (eight junctions, six of them sharing a 't' nucleotide), di (five

junctions), tri (two junctions), or tetra (two junctions) nucleotides or 16 bp nucleotides (case 17, Figs 3 and 4) common to the sequences of both genes at the breakpoint. The precise fusion points in these cases, therefore, could not be identified (Table S2).

Absence of consensus sequence motifs at or near the breakpoint of t(11;18)

To gain insight into the molecular mechanism of the translocation, sequence motifs known to be associated with chromosomal rearrangement including VDJ recombination

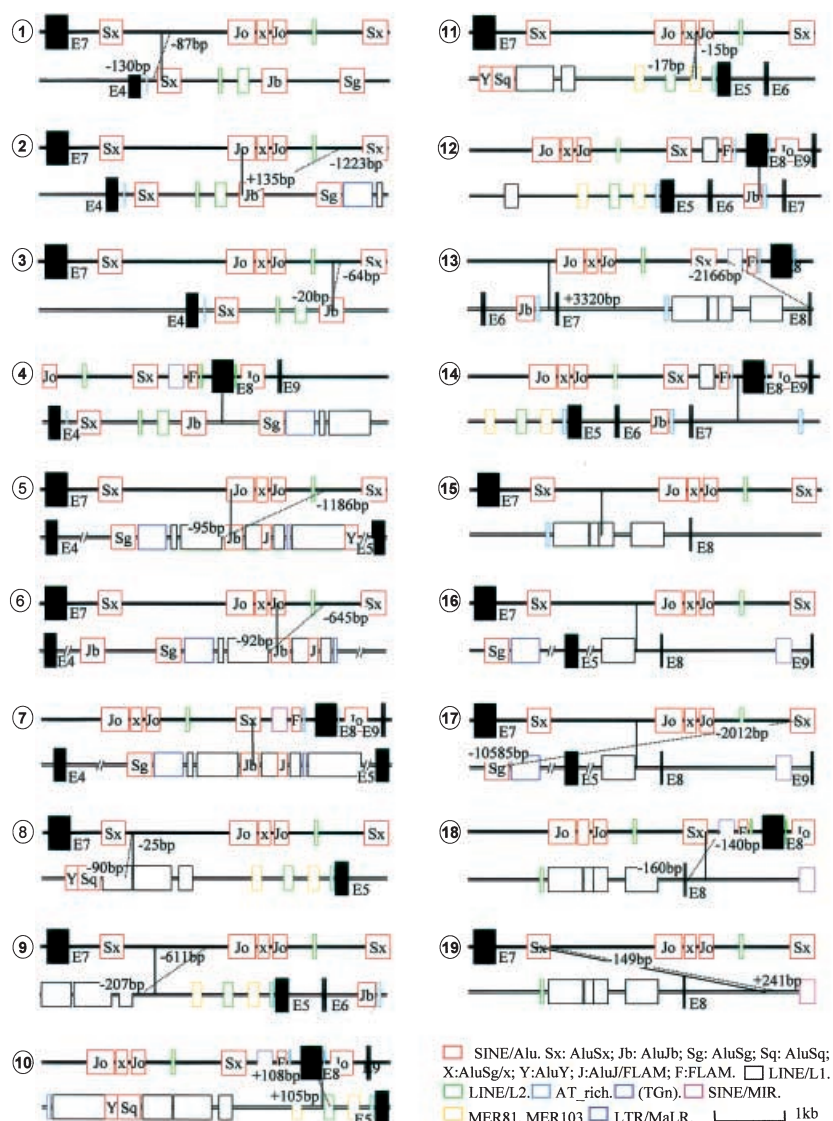


Fig 3. Schematic illustration of breakage and exchange of the *API2* and *MALT1* gene sequences in t(11;18). The regions of the *API2* (top) and *MALT1* (bottom) genes spanning the breakpoints are aligned for each case. The joining sites on der(11) are indicated by a solid vertical line, while those on der(18) are indicated by a dotted line. The size of DNA fragments deleted (–) or duplicated (+) is indicated. No fusion junctions on der(18) were identified in cases 4, 7, 12, 14, 15 and 16. Filled black boxes represent exons and their numbers are denoted. Open coloured boxes represent the position and size of the repetitive elements and an insert indicates the type of repeat. The subfamily of *Alu* repeats is also indicated.

heptamer (5'-CACWGTG) and nonamer (5'-ACAAAAACC) (Tycko & Sklar, 1990; Cayuela *et al*, 1997; Kupperts & Dalla-Favera, 2001; Marculescu *et al*, 2002), immunoglobulin (Ig) class switch pentamer (5'-GRGST) (Dalla Favera *et al*, 1983; Jeffs *et al*, 1998; Kupperts & Dalla-Favera, 2001), eukaryotic topoisomerase II cleavage site (5'-RNYNCCNNGYNGKTN YNY) (Domer *et al*, 1995; Felix *et al*, 1995; Obata *et al*, 1999), chi-like octomer (CCWSYVK) (Wyatt *et al*, 1992), translin binding sequence [5'-ATGCAG-N(0–4 bp)-GCCCWSSW or 5'-GCNCWSSW N(0–2 bp)GCCCWSSW] (Aoki *et al*, 1995; Hosaka *et al*, 2000), DNase I hypersensitive site (5'-CAC-TTAAGCTGTGTACTCCCAT) (Forrester *et al*, 1990), purine–pyrimidine sequences, polypurine and polypyrimidine and

palindromes (Boehm *et al*, 1989) were searched in the 100 bp sequence each side of the fusion junction in all cases using the Fuzznuc program (Table S2). The analysis did not reveal the presence of any of the above sequence motifs at or near the breakpoint in each case, suggesting that these sequence motifs were not involved in t(11;18).

We next examined whether repetitive sequences including short interspersed repetitive elements (SINEs; *Alu* and MIR), long interspersed repetitive elements (LINEs; LINE 1, LINE 2 and L3/CR1), long terminal repeat (LTR) elements (MaLRs, ERVL, ERV_class I and ERV_class II) and DNA elements (MER1_type and MER2_type) were implicated in the occurrence of t(11;18). The frequencies of these repetitive sequences

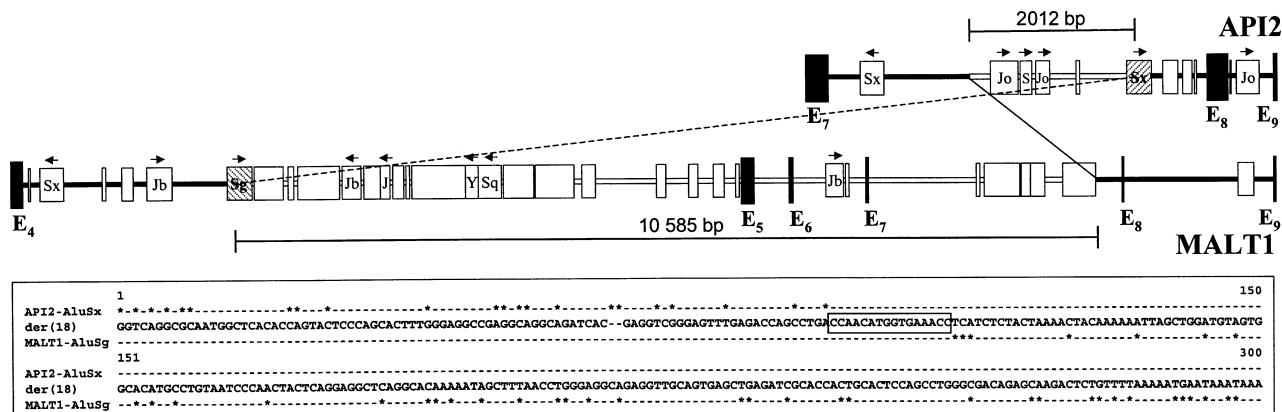


Fig 4. Illustration of an *Alu*-involved recombination of t(11;18) in case 17. Top: partial genomic structure of the *API2* and *MALT1* genes shows breakage and joining on der(11) (solid line) and der(18) (dotted line). The joining on der(18) occurs between the *AluSx* on the *API2* and *AluSg* on the *MALT1*, resulting in deletions of a 2012 bp fragment on the *API2* gene and a 10 585 bp fragment on the *MALT1* gene. Solid black boxes represent exons and open boxes represent repetitive elements with *Alu* repeats indicated. Horizontal arrows indicate the orientation of *Alu* repeats. Bottom: alignment of 300 bp *Alu* repeats from parental genes and the der(18) fusion gene; the resulting *Alu* fusion on der(18) maintains the characteristics of an *Alu* repeat.

between the regions involved in chromosomal breaks and the rest of the *API2* or *MALT1* gene were compared using RepeatMasker. Only the *Alu* and LINE1 repeats were found to be relatively rich in the breakpoint region of the *API2* and *MALT1* gene respectively. *Alu* repeats accounted for 29% of the intron 7 sequence but only 16% of the rest of the intronic sequence of the *API2* gene, while LINE1 repeats contributed to 25% of introns 4–8 but 13% of the rest of the intronic sequence of the *MALT1* gene.

The breakpoints on the *API2* and *MALT1* genes derived from both *API2-MALT1* and *MALT1-API2* fusions were analysed against the location of the above repetitive sequences (Figs 2 and 3). There was no correlation between the position of the breakpoints and the location of SINE/Mer, LINE, LTR and DNA elements in all cases. However, breakpoint was within an *Alu* repeat of both participating genes on der(11) in four cases (cases 2, 5, 6 and 7) and on der(18) in one case (case 17). In four of these five cases, the *Alu* repeats involved were either in opposite orientation (cases 2, 5 and 6) or from different subfamilies (case 7), suggesting that the chromosomal recombination in these cases was unlikely to be mediated by *Alu* repeats. In the remaining case (case 17), the two *Alu* repeats involved, *AluSx* from chromosome 11 and *AluSg* from chromosome 18, were in the same orientation and shared 77% of sequence homology (Fig 4). The recombination occurred within a 16 bp consensus fragment between the two parental *Alu* repeats, resulting in deletions of a 2012 bp fragment from chromosome 11 and a 10 585 bp fragment from chromosome 18.

To further examine whether t(11;18) might be mediated by an unknown novel sequence motif, we compared the 200 bp sequence fragment spanning the junction of both the *API2-MALT1* and *MALT1-API2* fusions in all cases (Table S1) using Dialign and Bioedit programs but failed to identify any

putative consensus sequence. We also separately searched these sequence fragments, the genomic region of *API2* exons 6–7 and *MALT1* exons 4–9 as well as the entire *API2* and *MALT1* genes for palindromic sequences, tandem sequences and novel homologous sequences using MEME. These analyses did not reveal the consistent presence of unknown consensus sequence patterns or motifs at or near the breakpoints, nor was there any significant intra- and inter-chromosomal homology other than the presence of the repetitive sequence as discussed above.

Discussion

Genomic breakpoints on both the API2 and MALT1 gene are scattered

Guided by the known breakpoints of the *API2-MALT1* fusion transcripts, we have amplified the genomic sequence of both the *API2-MALT1* and *MALT1-API2* fusions by long distance PCR and studied the junction sequence in 19 cases of t(11;18) positive MALT lymphoma. The observation of high frequencies of deletions and duplications in both the *API2* and *MALT1* genomic sequences strongly indicates that multiple double strand DNA breaks must have occurred during the translocation process. The observed breakpoints on the *API2* gene were scattered in the intron 7 and exon 8, while those on the *MALT1* gene were distributed in the introns 4, 6, 7 and 8. Despite that recurrent breakpoints were seen in two cases, in general, the breakpoints observed from both fusions appeared to be distributed irregularly and this was also supported by computer modelling. Random distribution of breakpoints was observed in a common reciprocal translocation t(11;22) in Ewing's tumours (Zucman-Rossi *et al*, 1998), albeit the mechanisms underlying such random DNA double strand breaks are unclear. In view of the evidence that the breakpoints

observed were scattered, multiple and were not associated, at least in the majority of cases, with any putative sequence motifs that might play a role in chromosomal recombination, the double strand breaks probably did not result from a regulated cellular event.

Double strand breaks can be induced by exogenous DNA damaging agents such as ionizing radiation or by endogenous metabolic products such as free radicals generated by oxidative respiration. Although the exact cause and nature of the double strand breaks in the present cases are yet unknown, data emerging suggest that the occurrence of t(11;18) is influenced by aetiological factors associated with MALT lymphoma. The translocation occurs at dramatically variable frequencies in MALT lymphoma of different sites, from 0–1% in the thyroid and salivary gland to 30–40% in the stomach and lung (Ye *et al*, 2003). In gastric MALT lymphoma, the translocation has been shown to be significantly associated with infection of CagA positive strains of *H. pylori* (Ye *et al*, 2003), which is more virulent in the induction of inflammatory responses including generation of genotoxic chemicals such as oxygen reactive species. Oxygen reactive species are known to cause a range of DNA damages, particularly double strand breaks (Aman, 1999; Ferguson & Alt, 2001), it is tempting to speculate that the double strand breaks and deletion of the *API2* and *MALT1* gene sequence may be related to genotoxic insults caused by inflammatory responses in premalignant lesions associated with MALT lymphoma.

t(11;18) may result from non-homologous end joining following double strand breaks

To understand the mechanisms underlying the chromosomal recombination following DNA double strand breaks, we systematically searched for known recombination signals and putative sequence motifs that may associate with chromosomal recombination at or near the breakpoints. We examined all the known recombination signals including VDJ recombination heptamer and nonamer (Tycko & Sklar, 1990; Cayuela *et al*, 1997; Kuppers & Dalla-Favera, 2001; Marculescu *et al*, 2002), Ig class switch pentamer (Dalla Favera *et al*, 1983; Jeffs *et al*, 1998; Kuppers & Dalla-Favera, 2001), eukaryotic topoisomerase II cleavage site (Domer *et al*, 1995; Felix *et al*, 1995; Obata *et al*, 1999), chi-like octomer (Wyatt *et al*, 1992), translin binding sequence (Aoki *et al*, 1995; Hosaka *et al*, 2000), DNase I hypersensitive site (Forrester *et al*, 1990), purine-pyrimidine sequences, polypurine and polypyrimidine and palindromes (Boehm *et al*, 1989) and did not find any association between these sequence motifs and the breakpoints observed. Furthermore, our extensive computer-aided sequence search failed to reveal any unknown consensus sequence patterns or motifs that might be implicated in the chromosomal recombination at or near the breakpoints observed. Our results are in line with the findings by Baens *et al* (2000b) who studied five cases of t(11;18)-positive MALT lymphoma but differ from the observation by Sato *et al* (2001) who studied a single case. The latter

study showed the presence of a VDJ recombination heptamer sequence motif at the *API2* breakpoint and a partially matched sequence at the *MALT1* breakpoint on der(11). None of the breakpoints observed in the present study and that by Baens *et al* (2000b) was at or near the VDJ heptamer and, moreover, a sequence search revealed that there is only one VDJ recombination heptamer site in the breakpoint region of the *API2* gene but none in the breakpoint region of the *MALT1* gene. Taken together, the data reported so far do not support a role of the specific sequence-mediated chromosomal recombination in t(11;18).

We next investigated the putative role of repetitive sequences including SINEs, LINEs, LTR elements and DNA elements in t(11;18), as they have been shown to be implicated in gene rearrangement and chromosomal translocation in human tumours (Onno *et al*, 1992; Rudiger *et al*, 1995; Jeffs *et al*, 1998; Hill *et al*, 2000). With the exception of one case (case 17) in which *Alu* repeat might be implicated in the *MALT1-API2* fusion on der(18), there was no evidence of involvement of the above repetitive sequences in both the *API2-MALT1* and *MALT1-API2* fusions in the remaining cases. Thus, homologous recombination is less likely to be involved in t(11;18), at least in the majority of cases.

Although recurrent breakpoints were seen in a few cases, the breakpoints of t(11;18) in general appeared to be scattered and were not commonly associated with any sequence motif that may be potentially associated with chromosomal recombination. The translocation may result from illegitimate non-homologous end joining following double strand breaks. The molecular mechanisms underlying t(11;18) are thus different from those responsible for the antigen receptor-associated chromosomal translocations, in which the VDJ recombination machinery is implicated at least in the double strand break at the antigen receptor locus and the direct recombination between the oncogene and antigen receptor gene (Jaeger *et al*, 1993; Welzel *et al*, 2001).

Non-homologous end joining following double strand breaks is implicated in chromosomal translocations of soft tissue sarcomas and leukaemias (Super *et al*, 1997; Zucman-Rossi *et al*, 1998; Gillert *et al*, 1999; Richardson & Jasin, 2000; Elliott & Jasin, 2002). These translocations are commonly featured by sequence alterations at the fusion junctions including deletions, duplications, non-template-based insertions and inversions, similar to those of t(11;18) observed in the present study. Whereas inversion was not observed in our series, insertion, deletion and/or duplication of various sizes were found in every case at one or both breakpoint junctions. In addition, the sharing of 1–4 bp nucleotides between the *API2* and *MALT1* genes at the breakpoint junctions was frequently seen (19 of 32 junctions, or 60%), which is a key feature of non-homologous end joining known as microhomology (Lieber, 1998). While two DNA ends that do not share sequence homology can still be joined, the frequency of joining between two DNA ends with microhomologous sequence is much higher than random positioning of the join site (Lieber,

1998). These findings suggest that there may be common mechanisms underlying the various translocations of different diseases. Data emerging indicate that defects in molecules participating in non-homologous end joining promote the development of lymphomas and soft tissue sarcomas that harbour chromosomal structural abnormalities including translocations, deletions and duplications. Impairment of various non-homologous end joining components appears to confer different susceptibility to the development of lymphomas or soft tissue sarcomas (Sharpless *et al*, 2001; Zhu *et al*, 2002).

Evidence of selection to express functional API2-MALT1 transcripts

As discussed above, t(11;18) appears to be the result of non-homologous end joining following double strand DNA breaks. A crucial question raised here is why the breakpoints observed are clustered in the regions of intron 7 and exon 8 of the *API2* gene and introns 4, 6, 7 and 8 of the *MALT1* gene. It is possible that the clustering reflects the presence of fragile sites in these regions. It has also been shown recently that the formation of specific translocations in human lymphomas such as t(14;18)(q32;q12) in follicular lymphoma is determined in part by spatial proximity of translocation-prone gene loci (Roix *et al*, 2003). Although the spatial organization of the *API2* and *MALT1* loci is not known yet, the breakpoint pattern observed indicates the involvement of selection of t(11;18) that is capable of generating a functional *API2-MALT1* fusion product and gives a clonal advantage. There are several strands of evidence to support this notion.

First, the *API2-MALT1* fusion transcript is always in frame despite that the genomic fusion occurs between various introns or exons of the two genes leading to a reading frame shift in some cases. This is best illustrated when the *API2-MALT1* genomic fusion involves the exon 8 of the *API2* gene as shown in the present study. In such cases, the residual exon 8 is invariably spliced out during the RNA processing, resulting in the expression of a functional fusion transcript. Secondly, the *API2-MALT1* fusion always comprises the N-terminal *API2* with three intact BIR domains and the C-terminal *MALT1* region containing an intact caspase-like domain. The specific selection of these domains indicates their importance and synergy in oncogenesis. It has been shown that both the *API2* and *MALT1* proteins were unstable, while the *API2-MALT1* product was stable. The domains responsible for protein instability, the C-terminal of *API2* and the N-terminal of *MALT1*, are lost by the translocation (Izumiyama *et al*, 2003). In addition, the *API2-MALT1* fusion product, but not the wild type *API2* or *MALT1*, has been shown to activate nuclear factor κ B (NF κ B), a transcription factor for a number of cell survival and growth related genes (Barkett & Gilmore, 1999). The BIR domain is believed to mediate the self-oligomerization of the fusion product, while the caspase-like domain is required for activating the I κ K complex, consequently triggering a cascade of events leading to NF κ B activation (Lucas *et al*, 2001; McAllister-Lucas

et al, 2001). Furthermore, the deletions observed, although occurring extensively at the breakpoints of both the *API2* and *MALT1* genes, appear to always spare the domains critical for the function of the *API2-MALT1* fusion product. In case 17, deletion involved the *MALT1* exons 5–7 but not its downstream exons that constitute the caspase-like domain. In a further six cases in which the genomic *MALT1-API2* fusion was failed to be amplified despite readily amplification of the *API2-MALT1* fusion, the deletions are anticipated to be beyond the region targeted by the primers used and may involve the entire C-terminal *API2* gene and/or the entire N-terminal *MALT1* gene. A cryptic deletion of a chromosomal 11 fragment including the entire C-terminal *API2* has been found previously in one of the two t(11;18)-positive MALT lymphomas (Dierlamm *et al*, 1999).

In summary, the genomic breakpoints of t(11;18) are generally not associated with any known or putative sequence motif that may associate with chromosomal recombination. Extensive sequence alterations including deletions, duplications and non-template-based insertions occur commonly at the fusion junction. t(11;18) may result from illegitimate non-homologous end joining following double strand breaks.

Supplementary material

The following material is available at <http://www.blackwell-publishing.com/products/journals/suppmat/bjh/bjh4909/bjh4909sm.htm>

Table S1. Primers used for primary and nested PCR and sequencing of t(11;18) breakpoint junctions on der(11) and der(18).

Table S2. Partial genomic junction sequence of *API2-MALT1* on der(11) and *MALT1-API2* on der(18).

Acknowledgments

This study is supported by a research grant from Leukemia Research Fund, UK.

References

- Akagi, T., Motegi, M., Tamura, A., Suzuki, R., Hosokawa, Y., Suzuki, H., Ota, H., Nakamura, S., Morishima, Y., Taniwaki, M. & Seto, M. (1999) A novel gene, *MALT1* at 18q21, is involved in t(11;18)(q21;q21) found in low-grade B-cell lymphoma of mucosa-associated lymphoid tissue. *Oncogene*, **18**, 5785–5794.
- Aman, P. (1999) Fusion genes in solid tumors. *Seminars in Cancer Biology*, **9**, 303–318.
- Aoki, K., Suzuki, K., Sugano, T., Tasaka, T., Nakahara, K., Kuge, O., Omori, A. & Kasai, M. (1995) A novel gene, *Translin*, encodes a recombination hotspot binding protein associated with chromosomal translocations. *Nature Genetics*, **10**, 167–174.
- Auer, I.A., Gascoyne, R.D., Connors, J.M., Cotter, F.E., Greiner, T.C., Sanger, W.G. & Horsman, D.E. (1997) t(11;18)(q21;q21) is the most common translocation in MALT lymphomas. *Annals of Oncology*, **8**, 979–985.

- Baens, M., Maes, B., Steyls, A., Geboes, K., Marynen, P. & De Wolf-Peeters, C. (2000a) The product of the t(11;18), an API2-MLT fusion, marks nearly half of gastric MALT type lymphomas without large cell proliferation. *American Journal of Pathology*, **156**, 1433–1439.
- Baens, M., Steyls, A., Dierlamm, J., De Wolf-Peeters, C. & Marynen, P. (2000b) Structure of the MLT gene and molecular characterization of the genomic breakpoint junctions in the t(11;18)(q21;q21) of marginal zone B-cell lymphomas of MALT type. *Genes, Chromosomes and Cancer*, **29**, 281–291.
- Barkett, M. & Gilmore, T.D. (1999) Control of apoptosis by Rel/NF-kappaB transcription factors. *Oncogene*, **18**, 6910–6924.
- Boehm, T., Mengle-Gaw, L., Kees, U.R., Spurr, N., Lavenir, I., Forster, A. & Rabbitts, T.H. (1989) Alternating purine-pyrimidine tracts may promote chromosomal translocations seen in a variety of human lymphoid tumours. *The EMBO Journal*, **8**, 2621–2631.
- Cayuela, J.M., Gardie, B. & Sigaux, F. (1997) Disruption of the multiple tumor suppressor gene MTS1/p16(INK4a)/CDKN2 by illegitimate V(D)J recombinase activity in T-cell acute lymphoblastic leukemias. *Blood*, **90**, 3720–3726.
- Dalla Favera, R., Martinotti, S., Gallo, R.C., Erikson, J. & Croce, C.M. (1983) Translocation and rearrangements of the c-myc oncogene locus in human undifferentiated B-cell lymphomas. *Science*, **219**, 963–967.
- Dierlamm, J., Baens, M., Wlodarska, I., Stefanova-Ouzounova, M., Hernandez, J.M., Hossfeld, D.K., De Wolf-Peeters, C., Hagemeyer, A., Van den Berghe, H. & Marynen, P. (1999) The apoptosis inhibitor gene API2 and a novel 18q gene, MLT, are recurrently rearranged in the t(11;18)(q21;q21) associated with mucosa-associated lymphoid tissue lymphomas. *Blood*, **93**, 3601–3609.
- Dierlamm, J., Baens, M., Stefanova-Ouzounova, M., Hinz, K., Wlodarska, I., Maes, B., Steyls, A., Driessen, A., Verhoef, G., Gaulard, P., Hagemeyer, A., Hossfeld, D.K., De Wolf-Peeters, C. & Marynen, P. (2000) Detection of t(11;18)(q21;q21) by interphase fluorescence in situ hybridization using API2 and MLT specific probes. *Blood*, **96**, 2215–2218.
- Domer, P.H., Head, D.R., Renganathan, N., Raimondi, S.C., Yang, E. & Atlas, M. (1995) Molecular analysis of 13 cases of MLL/11q23 secondary acute leukemia and identification of topoisomerase II consensus-binding sequences near the chromosomal breakpoint of a secondary leukemia with the t(4;11). *Leukemia*, **9**, 1305–1312.
- Du, M.Q. & Isaacson, P.G. (2002) Gastric MALT lymphoma: from aetiology to treatment. *Lancet Oncology*, **3**, 97–104.
- Elliott, B. & Jasin, M. (2002) Double-strand breaks and translocations in cancer. *Cell and Molecular Life Sciences*, **59**, 373–385.
- Felix, C.A., Lange, B.J., Hosler, M.R., Fertala, J. & Bjornsti, M.A. (1995) Chromosome band 11q23 translocation breakpoints are DNA topoisomerase II cleavage sites. *Cancer Research*, **55**, 4287–4292.
- Ferguson, D.O. & Alt, F.W. (2001) DNA double strand break repair and chromosomal translocation: lessons from animal models. *Oncogene*, **20**, 5572–5579.
- Forrester, W.C., Epner, E., Driscoll, M.C., Enver, T., Brice, M., Pappayannopoulou, T. & Groudine, M. (1990) A deletion of the human beta-globin locus activation region causes a major alteration in chromatin structure and replication across the entire beta-globin locus. *Genes and Development*, **4**, 1637–1649.
- Gillert, E., Leis, T., Repp, R., Reichel, M., Hosch, A., Breitenlohner, I., Angermuller, S., Borkhardt, A., Harbott, J., Lampert, F., Griesinger, F., Greil, J., Fey, G.H. & Marschalek, R. (1999) A DNA damage repair mechanism is involved in the origin of chromosomal translocations t(4;11) in primary leukemic cells. *Oncogene*, **18**, 4663–4671.
- Hill, A.S., Foot, N.J., Chaplin, T.L. & Young, B.D. (2000) The most frequent constitutional translocation in humans, the t(11;22)(q23;q11) is due to a highly specific alu-mediated recombination. *Human Molecular Genetics*, **9**, 1525–1532.
- Hosaka, T., Kanoe, H., Nakayama, T., Murakami, H., Yamamoto, H., Nakamata, T., Tsuboyama, T., Oka, M., Kasai, M., Sasaki, M.S., Nakamura, T. & Toguchida, J. (2000) Translin binds to the sequences adjacent to the breakpoints of the TLS and CHOP genes in liposarcomas with translocation t(12;6). *Oncogene*, **19**, 5821–5825.
- Isaacson, P.G., Muller-Hermelink, H., Piris, M.A., Berger, F., Nathwani, B.N., Swerdlow, S.H. & Harris, N.L. (2001) Extranodal marginal zone B-cell lymphoma of mucosa-associated lymphoid tissue (MALT lymphoma). In: *WHO Classification of Tumours: Pathology and Genetics Tumours of Haematopoietic and Lymphoid Tissues* (ed. by E.S. Jaffe, N.L. Harris, H. Stein & J.W. Vardiman), pp. 157–160. IARC Press, Lyon.
- Izumiyama, K., Nakagawa, M., Yonezumi, M., Kasugai, Y., Suzuki, R., Suzuki, H., Tsubuki, S., Hosokawa, Y., Asaka, M. & Seto, M. (2003) Stability and subcellular localization of API2-MALT1 chimeric protein involved in t(11;18)(q21;q21) MALT lymphoma. *Oncogene*, **22**, 8085–8092.
- Jaeger, U., Purtscher, B., Karth, G.D., Knapp, S., Mannhalter, C. & Lechner, K. (1993) Mechanism of the chromosomal translocation t(14;18) in lymphoma: detection of a 45-Kd breakpoint binding protein. *Blood*, **81**, 1833–1840.
- Jeffs, A.R., Benjes, S.M., Smith, T.L., Sowerby, S.J. & Morris, C.M. (1998) The BCR gene recombines preferentially with Alu elements in complex BCR-ABL translocations of chronic myeloid leukaemia. *Human Molecular Genetics*, **7**, 767–776.
- Kalla, J., Stilgenbauer, S., Schaffner, C., Wolf, S., Ott, G., Greiner, A., Rosenwald, A., Dohner, H., Muller-Hermelink, H.K. & Lichter, P. (2000) Heterogeneity of the API2-MALT1 gene rearrangement in MALT-type lymphoma. *Leukemia*, **14**, 1967–1974.
- Kuppers, R. & Dalla-Favera, R. (2001) Mechanisms of chromosomal translocations in B cell lymphomas. *Oncogene*, **20**, 5580–5594.
- Lieber, M.R. (1998) Warner-Lambert/Parke-Davis Award Lecture. Pathological and physiological double-strand breaks: roles in cancer, aging, and the immune system. *American Journal of Pathology*, **153**, 1323–1332.
- Liu, H., Ruskone Fourmesttraux, A., Lavergne-Slove, A., Ye, H., Molina, T., Bouhnik, Y., Hamoudi, R.A., Diss, T.C., Dogan, A., Megraud, F., Rambaud, J.C., Du, M.Q. & Isaacson, P.G. (2000) Resistance of t(11;18) positive gastric mucosa-associated lymphoid tissue lymphoma to *Helicobacter pylori* eradication therapy. *Lancet*, **357**, 39–40.
- Liu, H., Ye, H., Dogan, A., Ranaldi, R., Hamoudi, R.A., Bearzi, I., Isaacson, P.G. & Du, M.Q. (2001) T(11;18)(q21;q21) is associated with advanced mucosa-associated lymphoid tissue lymphoma that expresses nuclear BCL10. *Blood*, **98**, 1182–1187.
- Liu, H., Ye, H., Ruskone-Fourmesttraux, A., de Jong, D., Pileri, S., Thiede, C., Lavergne, A., Boot, H., Caletti, G., Wundisch, T., Molina, T., Taal, B.G., Elena, S., Thomas, T., Zinzani, P.L., Neubauer, A., Stolte, M., Hamoudi, R.A., Dogan, A., Isaacson, P.G. & Du, M.Q. (2002) T(11;18) is a marker for all stage gastric MALT lymphomas that will not respond to *H. pylori* eradication. *Gastroenterology*, **122**, 1286–1294.

- Lucas, P.C., Yonezumi, M., Inohara, N., McAllister-Lucas, L.M., Abazeed, M.E., Chen, F.F., Yamaoka, S., Seto, M. & Nunez, G. (2001) Bcl10 and MALT1, independent targets of chromosomal translocation in malt lymphoma, cooperate in a novel NF-kappa B signaling pathway. *Journal of Biological Chemistry*, **276**, 19 012–19 019.
- McAllister-Lucas, L.M., Inohara, N., Lucas, P.C., Ruland, J., Benito, A., Li, Q., Chen, S., Chen, F.F., Yamaoka, S., Verma, I.M., Mak, T.W. & Nunez, G. (2001) Bimp1, a MAGUK family member linking PKC activation to Bcl10-mediated NF-kB induction. *Journal of Biological Chemistry*, **276**, 30 589–30 597.
- Marculescu, R., Le, T., Simon, P., Jaeger, U. & Nadel, B. (2002) V(D)J-mediated translocations in lymphoid neoplasms: a functional assessment of genomic instability by cryptic sites. *Journal of Experimental Medicine*, **195**, 85–98.
- Morgan, J.A., Yin, Y., Borowsky, A.D., Kuo, F., Nourmand, N., Koontz, J.I., Reynolds, C., Soreng, L., Griffin, C.A., Graeme-Cook, F., Harris, N.L., Weisenburger, D., Pinkus, G.S., Fletcher, J.A. & Sklar, J. (1999) Breakpoints of the t(11;18)(q21;q21) in mucosa-associated lymphoid tissue (MALT) lymphoma lie within or near the previously undescribed gene MALT1 in chromosome 18. *Cancer Research*, **59**, 6205–6213.
- Morris, S.W., Kirstein, M.N., Valentine, M.B., Dittmer, K.G., Shapiro, D.N., Saltman, D.L. & Look, A.T. (1994) Fusion of a kinase gene, ALK, to a nucleolar protein gene, NPM, in non-Hodgkin's lymphoma. *Science*, **263**, 1281–1284.
- Motegi, M., Yonezumi, M., Suzuki, H., Suzuki, R., Hosokawa, Y., Hosaka, S., Kodera, Y., Morishima, Y., Nakamura, S. & Seto, M. (2000) API2-MALT1 chimeric transcripts involved in mucosa-associated lymphoid tissue type lymphoma predict heterogeneous products. *American Journal of Pathology*, **156**, 807–812.
- Nakamura, T., Nakamura, S., Yonezumi, M., Suzuki, T., Matsuura, A., Yatabe, Y., Yokoi, T., Ohashi, K. & Seto, M. (2000) *Helicobacter pylori* and the t(11;18)(q21;q21) translocation in gastric low-grade B-cell lymphoma of mucosa-associated lymphoid tissue type. *Japanese Journal of Cancer Research*, **91**, 301–309.
- Obata, K., Hiraga, H., Nojima, T., Yoshida, M.C. & Abe, S. (1999) Molecular characterization of the genomic breakpoint junction in a t(11;22) translocation in Ewing's sarcoma. *Genes, Chromosomes and Cancer*, **25**, 6–15.
- Onno, M., Nakamura, T., Hillova, J. & Hill, M. (1992) Rearrangement of the human *trc* oncogene by homologous recombination between Alu repeats of nucleotide sequences from two different chromosomes. *Oncogene*, **7**, 2519–2523.
- Ott, G., Katzenberger, T., Greiner, A., Kalla, J., Rosenwald, A., Heinrich, U., Ott, M.M. & Muller Hermelink, H.K. (1997) The t(11;18)(q21;q21) chromosome translocation is a frequent and specific aberration in low-grade but not high-grade malignant non-Hodgkin's lymphomas of the mucosa-associated lymphoid tissue (MALT-) type. *Cancer Research*, **57**, 3944–3948.
- Remstein, E.D., James, C.D. & Kurtin, P.J. (2000) Incidence and subtype specificity of API2-MALT1 fusion translocations in extranodal, nodal, and splenic marginal zone lymphomas. *American Journal of Pathology*, **156**, 1183–1188.
- Richardson, C. & Jasin, M. (2000) Coupled homologous and non-homologous repair of a double-strand break preserves genomic integrity in mammalian cells. *Molecular and Cellular Biology*, **20**, 9068–9075.
- Roix, J.J., McQueen, P.G., Munson, P.J., Parada, L.A. & Misteli, T. (2003) Spatial proximity of translocation-prone gene loci in human lymphomas. *Nature Genetics*, **34**, 287–291.
- Rudiger, N.S., Gregersen, N. & Kielland-Brandt, M.C. (1995) One short well conserved region of Alu-sequences is involved in human gene rearrangements and has homology with prokaryotic chi. *Nucleic Acids Research*, **23**, 256–260.
- Sanchez-Izquierdo, D., Buchonet, G., Siebert, R., Gascoyne, R.D., Climent, J., Karran, L., Marin, M., Blesa, D., Horsman, D., Rosenwald, A., Staudt, L.M., Albertson, D.G., Du, M.Q., Ye, H., Marynen, P., Garcia-Conde, J., Pinkel, D., Dyer, M.J. & Martinez-Climent, J.A. (2003) MALT1 is deregulated by both chromosomal translocation and amplification in B-cell non-Hodgkin's lymphoma. *Blood*, **101**, 4539–4546.
- Sato, Y., Akiyama, Y., Tanizawa, T., Shibata, T., Saito, K., Mori, S., Kamiyama, R. & Yuasa, Y. (2001) Molecular characterization of the genomic breakpoint junction in the t(11;18) (q21;q21) translocation of a gastric MALT lymphoma. *Biochemical and Biophysical Research Communication*, **280**, 301–306.
- Sharpless, N.E., Ferguson, D.O., O'Hagan, R.C., Castrillon, D.H., Lee, C., Farazi, P.A., Alson, S., Fleming, J., Morton, C.C., Frank, K., Chin, L., Alt, F.W. & DePinho, R.A. (2001) Impaired nonhomologous end-joining provokes soft tissue sarcomas harboring chromosomal translocations, amplifications, and deletions. *Molecular Cell*, **8**, 1187–1196.
- Streubel, B., Lamprecht, A., Dierlamm, J., Cerroni, L., Stolte, M., Ott, G., Raderer, M. & Chott, A. (2003) T(14;18)(q32;q21) involving IGH and MALT1 is a frequent chromosomal aberration in MALT lymphoma. *Blood*, **101**, 2335–2339.
- Super, H.G., Strissel, P.L., Sobulo, O.M., Burian, D., Reshmi, S.C., Roe, B., Zeleznik, L., Diaz, M.O. & Rowley, J.D. (1997) Identification of complex genomic breakpoint junctions in the t(9;11) MLL-AF9 fusion gene in acute leukemia. *Genes, Chromosomes and Cancer*, **20**, 185–195.
- Tycko, B. & Sklar, J. (1990) Chromosomal translocations in lymphoid neoplasia: a reappraisal of the recombinase model. *Cancer Cells*, **2**, 1–8.
- Uren, G.A., O'Rourke, K., Aravind, L., Pisabarro, T.M., Seshagiri, S., Koonin, V.E. & Dixit, M.V. (2000) Identification of paracaspases and metacaspases: two ancient families of caspase-like proteins, one of which plays a key role in MALT lymphoma. *Molecular Cell*, **6**, 961–967.
- Welzel, N., Le, T., Marculescu, R., Mitterbauer, G., Chott, A., Pott, C., Kneba, M., Du, M.Q., Kusec, R., Drach, J., Raderer, M., Mannhalter, C., Lechner, K., Nadel, B. & Jaeger, U. (2001) Templated nucleotide addition. *Cancer Research*, **61**, 1629–1636.
- Willis, T.G. & Dyer, M.J. (2000) The role of immunoglobulin translocations in the pathogenesis of B-cell malignancies. *Blood*, **96**, 808–822.
- Wotherspoon, A.C., Pan, L.X., Diss, T.C. & Isaacson, P.G. (1992) Cytogenetic study of B-cell lymphoma of mucosa-associated lymphoid tissue. *Cancer Genetics and Cytogenetics*, **58**, 35–38.
- Wyatt, R.T., Rudders, R.A., Zelenetz, A., Delellis, R.A. & Krontiris, T.G. (1992) BCL2 oncogene translocation is mediated by a chi-like consensus. *Journal of Experimental Medicine*, **175**, 1575–1588.
- Ye, H., Liu, H., Attygalle, A., Wotherspoon, A.C., Nicholson, A.G., Charlotte, F., Leblond, V., Speight, P.M., Goodlad, J.R., Lavergne-Slove, A., Isaacson, P.G., Dogan, A. & Du, M.Q. (2003) Variable frequencies of t(11;18)(q21;q21) in MALT lymphomas of different sites: significant association with CagA strains of *H. pylori* in gastric MALT lymphoma. *Blood*, **102**, 1012–1018.

Zhu, C., Mills, K.D., Ferguson, D.O., Lee, C., Manis, J., Fleming, J., Gao, Y., Morton, C.C. & Alt, F.W. (2002) Unrepaired DNA breaks in p53-deficient cells lead to oncogenic gene amplification subsequent to translocations. *Cell*, **109**, 811–821.

Zucman-Rossi, J., Legoix, P., Victor, J.M., Lopez, B. & Thomas, G. (1998) Chromosome translocation based on illegitimate recombination in human tumors. *Proceedings of the National Academy of Sciences of the United States of America*, **95**, 11786–11791.

High Throughput Methods for Gene Identification, Cloning and Functional Genomics Using the GeneTAC™ G³ Robotics Workstation

Rifat Hamoudi,¹ Sally Johnston,² George Hutchinson³ and John D'Errico, Ph.D.⁴

Keywords: Automation of cloning and characterization of disease causing genes, GeneTAC™ G³ robotic workstation, Automated high throughput DNA and microarray preparation.

Abstract

Using a single robotic platform, the GeneTAC™ G³, we have automated most of the processes involved in the cloning and characterisation of novel disease causing genes by addressing the following; firstly, identifying the BACs of interest and making shotgun libraries. Secondly, automating the set up of sequencing reactions using methodology that eliminates the need for DNA preparation of 384 clones. Thirdly, generating sub-libraries using selective re-arranging of library clones to enable the determination of the entire genomic sequence of the gene. Fourthly, determining gene function by combination of differential screening and mini Northern's using microarrays printed using the GeneTAC™ G³ system and hybridised using the GeneTAC™ HybStation (Genomics Solutions, Ann Arbor, USA).

Introduction

Although there are many gene identification, cloning and functional genomics techniques, most are cumbersome and slow requiring a team of researchers. Classical physical mapping methods involve isolating YACs mapping to a region where the gene of interest is, using molecular cytogenetics techniques such as fluorescent in situ hybridisation (FISH) and comparative genome hybridization (CGH),^{30, 8} loss of heterozygosity (LOH)² and Linkage.^{21, 31} This is followed by isolating a set of corresponding BACs (Bacterial Artificial Chromosome) then mapping the gene of interest to a minimal set of BACs using techniques such as fingerprinting.⁶ The BACs that are thought to contain the gene of interest are prepared and sequenced using M13 shotgun sequencing strategy.^{9, 10, 16, 24} Gene structure is then identified using cumbersome techniques such as solution hybrid capture²⁷ and exon trapping.¹⁸ Confirmation of the gene is carried out using mutation detection. Once the gene is identified, functional genomics is carried out by gridding cDNA libraries from various tissues and cell lines on slides making microarrays and using the gene as a probe to investigate expression patterns.

As the Human Genome Project (HGP) nears completion, much emphasis is being directed on using the information from the HGP in isolating and characterising novel disease causing genes. We present novel high throughput automated techniques that accelerate gene identification, cloning and the functional genomics process.

Using a single automated platform, the GeneTAC G³, we have successfully automated the following key activities; firstly, identifying the BACs of interest and making shotgun libraries. This is then picked into 384 well plates. Secondly, automating the set up of sequencing reactions using methodology that eliminates the need for DNA preparation of 384 clones. This simplifies and accelerates the whole sequencing process. Thirdly, generating sub-libraries for finishing using selective re-arranging or 'cherry picking' of library clones to enable the definition of the entire genomic sequence of the gene. The structure of the gene can be obtained from the full length cDNA using RACE (Rapid Amplification of cDNA End) or probing the cDNA library with genomic fragments library of the gene and using sequence data from the HGP to fill in any gaps via bioinformatics. Fourthly, determining gene function. Gene function is investigated using expression profiling, differential screening and mini Northern's using microarrays printed using the GeneTAC G³ system and hybridised using the GeneTAC HybStation (Genomics Solutions, Ann Arbor, USA). Whilst there

*Correspondence

¹Department of Histopathology
Rockefeller Building, University
College London, University Street,
London, WC1E 6JJ

² Current Address:

Perkin Elmer Life Sciences
Cambridge Science Park
Milton Road
Cambridge, Cambridgeshire

³ Current Address:

Gilson Internation B.V.,
Laan van's- Gravenmade 80 2495
AJ DEM HAAG, the Netherlands

⁴ Current Address:

Genomic Solutions, Inc.
4355 Varsity Drive
Ann Arbor, Michigan, USA

are many robotic platforms on the market that can perform many of the processes described above, the GeneTAC G³ can perform colony picking, selective re-arranging, gridding on nylon membranes and glass slides and DNA library replication making it ideal for small, medium and industrial genetic laboratories.

Materials and Methods

CONSTRUCTION AND MAINTANANCE OF GENOMIC BAC LIBRARY, DNA SHOTGUN LIBRARIES FOR FINISHING AND CDNA LIBRARIES

A whole genome BAC library was constructed according to De Jung.⁷ A DNA shotgun library, used for BAC sequence finishing purposes, was constructed according to Smedly et al.²³ and a cDNA library was constructed using the ZAP-cDNA synthesis kit (Stratagene). Transformants were plated out on 22x22 Bioassay plates and left at 37°C overnight. White colonies were picked into 384 well plates containing 70µl of LB broth and kanamycin (25µg/ml) with 7.5% glycerol per well using the GeneTAC G³ which has the ability to carry out automated blue/white selection. In order to maintain the library, 3 copies of each library were made using replication facilities of the GeneTAC G³, libraries were then frozen and stored at -80°C. The GeneTAC G³ was also used to expand and contract library plates from 384 to 96 well microtitre plates and vice versa. In order to use the library for gene identification, each library was gridded onto Hybond-N+ nylon membrane filters (Amersham) using the gridding facilities of the GeneTAC G³. Gridding and picking methodologies and strategies were according to Hamoudi et al.¹²

ISOLATING BAC OF INTEREST

BAC library filters were hybridised to genomic markers such as polymorphic markers, sequence tagged sites (STS) or expressed sequence tags (EST) obtained from linkage, molecular cytogenetics or LOH studies. In order to isolate the BACs containing the gene of interest, the re-arranging function was used, whereby the selected samples were picked into 150µl of L-Broth and kanamycin (25 µg/ml) in 96 well microtitre plate using the Librarian tool of the GeneTAC G³. Fluorescent fingerprinting was carried out on the BACs to generate the minimal overlapping set of BACs to narrow down the search for the gene to one or two BACs.¹¹

AUTOMATED DNA TEMPLATE PREPARATION OF BAC FRAGMENTS CONTAINING THE GENE OF INTEREST

A shotgun library of the BAC containing the gene of interest was generated using the GeneTAC G³ as described earlier. 1 to 1.5kb BAC fragments were obtained from five seconds sonication or partial digestion using AluI, Rsa and HaeIII restriction enzymes. These were then subcloned within five minutes into TOPO cloning vector by blunt end ligation using the TOPO sequencing kit (Invitrogen, California, USA). The library clones were picked using the GeneTAC G³, into two 384 well plates containing 70µl LB and ampicillin (50µg/ml) with 7.5% glycerol, and incubated at for 16 hours at 37°C and 200 rpm in a shaking incubator. The grown cultures were replicated into 96 well plates containing a PCR master mix with 2µM of TOPO vector primers such as T7

(5'-GTAATACGACTCACTATAGGGC-3') and T3 (5'-AAT-TAACCTCACTAAAGGG-3') using the GeneTAC G³. 25µl PCR reaction mix was carried out by adding 1.5 mM MgCl₂, 10 mM Tris-HCl (pH 8.3), 50 mM KCl, 0.2 mM dNTP, 0.5 µM T7 and T3 primers and 0.5 U Thermoprime Taq (AB Gene). PCR amplification was carried out using the following cycling conditions; five minutes at 94°C to ensure that bacterial cell wall is destroyed releasing the plasmid containing the BAC fragment, followed by denaturation step at one minute for 94°C, annealing of the vector primers at one minute for 55°C and extension step of two minutes for 72°C for 35 cycles, ensued by an extension step of 10 minutes at 72°C to finish the elongation of most PCR products initiated during last cycle. PCR cycling for 96 and 384 well plates was carried out using Pheonix thermocycler with convertible heating blocks (Helena Biosciences, UK). 5µl of PCR products were checked on 1% agarose gel. PCR products were cleaned up as follows; 30µl of 7.5M Ammonium Acetate and 70µl of 100% isopropanol was added to each PCR product, the plate was left on wet ice for 30 minutes followed by centrifugation at 3000rpm for 1.5 hours. The supernatant was discarded by inverting the plate upside down on dry absorbent paper and spinning at 500rpm for four seconds. The pellet was washed with 150µl of 80% ethanol before centrifuging at 3000rpm for one hour, discarding the supernatant and spinning the plate upright at 3000rpm for 15 minutes. The pellets were resuspended in 10µl of water ready for direct sequencing or 10µl of DMSO ready for spotting on slides onto generate microarray libraries.

AUTOMATED SEQUENCING OF BAC FRAGMENTS CONTAINING THE GENE OF INTEREST

Sequencing was carried out by adding 4µl of the PCR product (50ng/µl) to 4µl of dRhodamine Dye Terminator premix (Applied Biosystems Inc., Foster City, California, USA) and 2µl of vector primer (at 10µM) in 96 well microtitre plate. Cycle sequencing was carried out on the mix using the following cycling protocol; 96°C for 30 seconds, 50°C for 15 seconds and 60°C for one minute, for 25 cycles. The products were then cleaned up to remove excess dye terminator as follows; to each well, 100µl of 80% ethanol and 6µl of 3M sodium acetate at pH 5.2 was added, 1µl of glycogen can optionally be added to visualise the pellet at the bottom of the wells. The microtitre plate was left on wet ice for 30 minutes followed by centrifugation for one hour at 3000rpm. Two layers of dry absorbent paper was placed on top of the plate, the plate was inverted upside down to discard the supernatant onto the paper. This was replaced by a dry set of absorbent paper and placed on the plate holder of the centrifuge and centrifuged for four seconds at 500rpm to ensure that all supernatant is discarded. The plate was turned upright and centrifuged for 15 minutes to ensure that the pellet is at the bottom of the well. The plate was dried for two minutes at 90°C. Samples were run on ABI PRISM[®] 377 DNA Analyzer (Applied Biosystems Inc., Foster City, CA, USA) using 36cm WTR glass plates and Automatrix 4.5% 29:1 acrylamide:bisacrylamide ready made 6M urea gel mix (National Diagnostics, Hull, UK) and ABI PRISM[®] 3100 DNA Analyzer using 36cm capillary and POP-6[™] polymer (Applied Biosystems Inc., Foster City, California, USA).

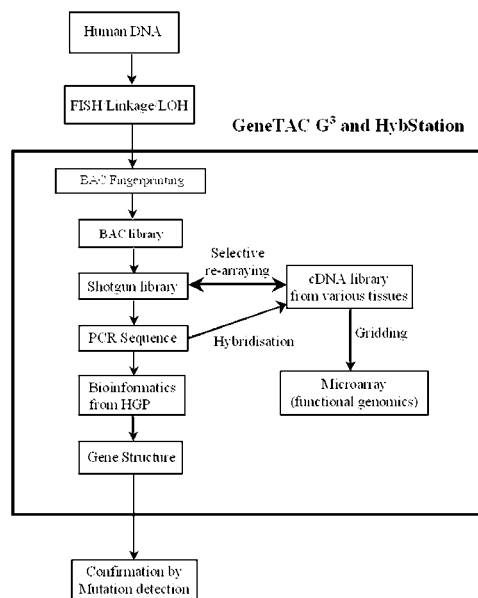


Figure 1. Flow Chart representing the overall strategy for isolating and characterizing genes using the GeneTAC G³.

DETERMINING GENE STRUCTURE

Shotgun sequence data was assembled using Staden software suite.²⁵ The assembled sequence data was extended as much as possible using bioinformatics to fill any holes with finished sequence data from HGP. The bioinformatics strategy is carried out by aligning sequences at the end of the contigs to the HGP data from Ensembl (<http://www.ensembl.org>) (15), and NCBI (http://www.ncbi.nlm.nih.gov/cgi-bin/Entrez/map_search) using in house software to obtain the genomic sequence spanning the gene of interest. cDNA sequence of the gene of interest was obtained by carrying out RACE and probing cDNA libraries made using the GeneTAC G³. The cDNA sequence was used to probe the genomic shotgun library generated using the GeneTAC G³. Any positive colonies were selectively re-arrayed (cherry picked) into LB media with appropriate antibiotic using the Librarian tool of the GeneTAC G³. Cultures were grown overnight, prepared and sequenced using the GeneTAC G³ as described above. Sequences were analysed and intron-exon boundaries were determined producing the overall gene structure by aligning the sequences to genomic sequence using in-house modification of the BLAST software (<http://www.ncbi.nlm.nih.gov/BLAST>). In order to prove that the disease is caused by the gene identified, exon primers were designed and used to screen all affected patients for mutations using FMD technique⁷ followed by sequencing any band with a shift. Mutations were identified by comparing the mutant sequence to a normal using Sequence Navigator software (Applied Biosystems Inc., Foster City, California, USA).

DETERMINING GENE FUNCTION

Once the gene was identified, its expression profile was determined by constructing cDNA libraries from various tissues such as brain, kidney, breast and testis using the ZAP-cDNA synthesis kit (Stratagene, La Jolla, California, USA) and gridding the libraries on glass slides using the GeneTAC G³ to generate microarrays. The

microarrays were hybridised with Cy3-dUTP and Cy5-dUTP labeled RNA from the genes identified and the data clustered to determine the expression profile of the gene of interest. The hybridisation was carried out using the GeneTAC HybStation following a standard pre-programmed protocol. Also subtractive hybridisation experiments were carried out, whereby a tissue library was subjected to a physical or chemical input such as UV radiation or treatment with a reagent or compound and normal library of the same tissue were hybridised with labeled RNA from the gene of interest. The results were compared to determine whether the genes that are up-regulated and down-regulated were as a result of the external input. Mini-Northerns were also carried out using microarrays of various tissues to determine the tissue that the gene of interest was mostly expressed in. Array fabrication and RNA labeling were carried out according to Hegde et al.¹³ Figure 1 shows flow chart of the overall strategy for isolating and characterizing genes using the GeneTAC G³.

Results

CONSTRUCTION OF BAC, cDNA AND SHOTGUN DNA LIBRARIES

Picking was carried out using the 48-pin pneumatic head. It takes around 50 seconds to pick 48 colonies including sterilization. It takes around 30 minutes to pick the 1500 clones generated by the shotgun DNA library, three hours to pick the 10,000 clones generated by the cDNA library and 43 hours to pick the 200,000 clones generated by the entire BAC library without manual intervention. Around four 384-well plates were generated from shotgun DNA library, 28 384-well plates were generated from the cDNA library and 520 384-well plates were generated from the BAC library giving eight-fold coverage. The accuracy of picking is between 99.5% and 100% with usually between 382 and 384 wells growing. Experiments showed that all the clones picked were from isolated colonies and are pure indicating no cross contamination between picking (data not shown).

Using single transfer and double spotting, it takes around 20 minutes to grid the cDNA library and two hours to grid the BAC

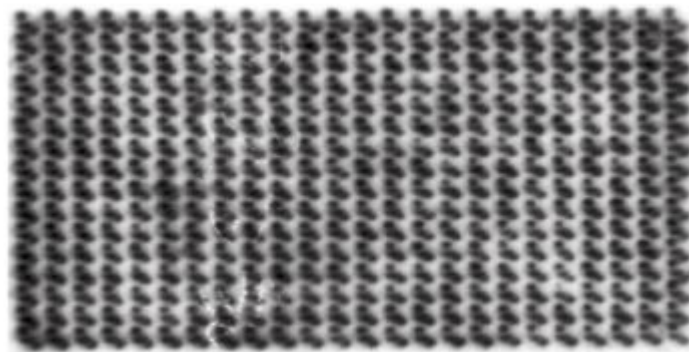


Figure 2. Autoradiograph of 11.9 x 7.8cm Hybond-N+ filter hybridised with BAC clones. Using single transfer and double spotting the BAC library clones were gridded and probed with radioactively labeled polymorphic markers from the area containing the gene of interest. The figure shows that the BACs were gridded consistently and providing good signals to identify the BAC of interest anywhere on a 384 plate.

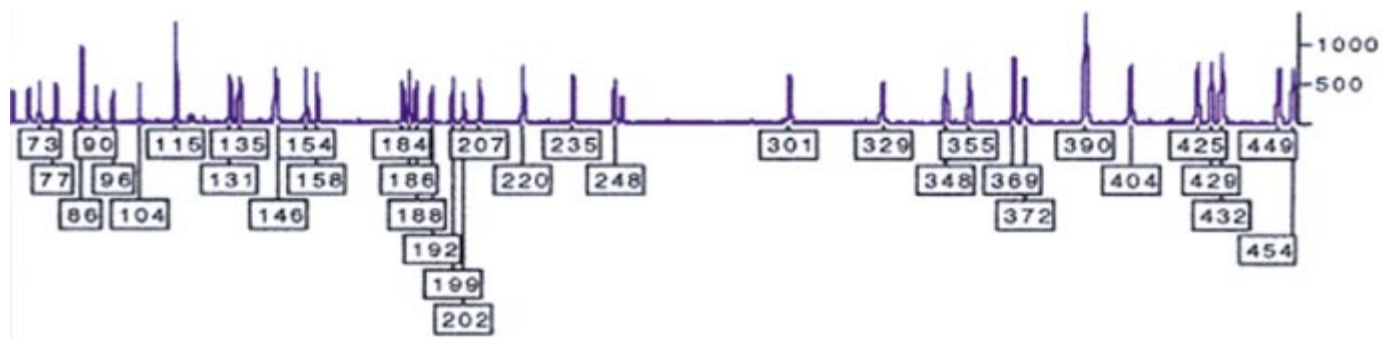
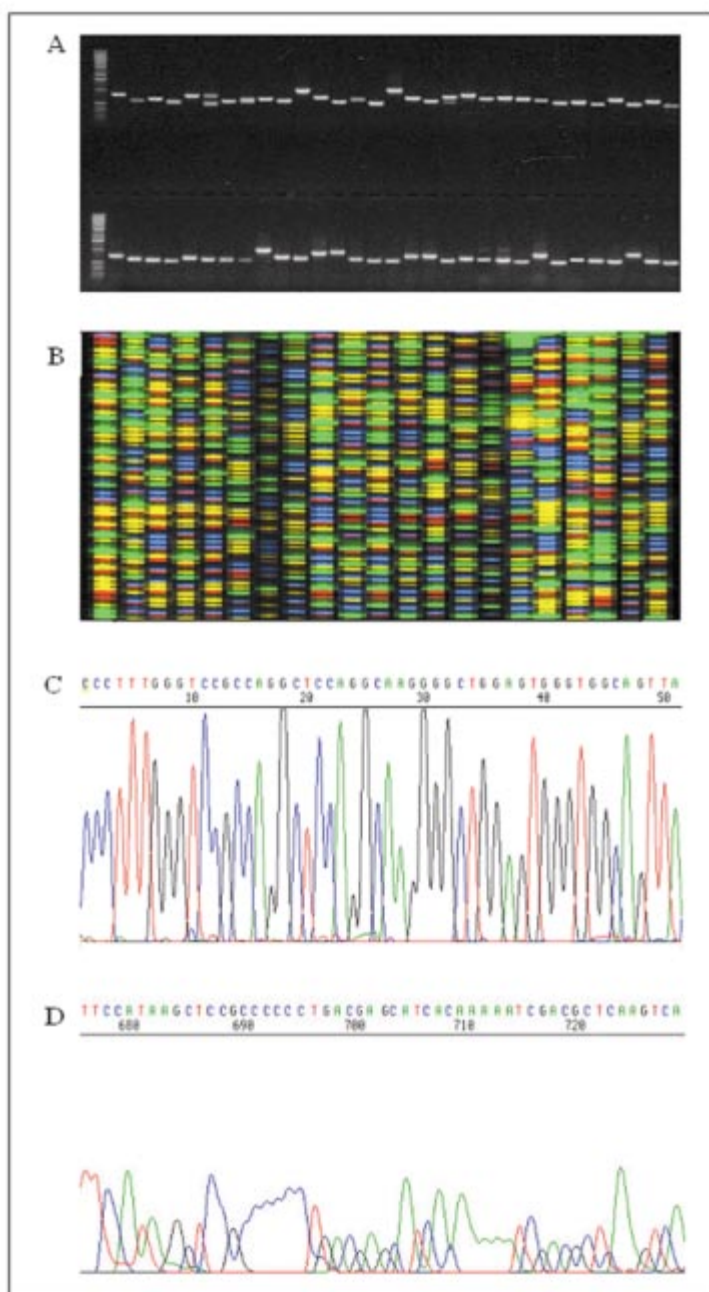


Figure 3. Fluorescent fingerprinting of BAC DNA clone run on ABI PRISM[®] 377 DNA sequencer. Typical BAC clone prepared using GeneTAC G3 and labeled using FAM-dCTP. The BAC in the figure shows good signal to ratio and clean baseline making it easy to call the fingerprinted fragments.



library onto either 11.9x7.8cm or eight 22x22cm Hybond-N+ filters. The maximum resolution on each 11.9x7.8cm filter is 13,824 spots and on 22x22cm filter it is up to 120,000 spots. Figure 2 shows 11.9x7.8cm Hybond-N+ filter gridded with BAC clones using double spotting.

ISOLATING BAC OF INTEREST

Usually around 20 to 40 BACs result from the first round of hybridisation using probes that are thought to be in the region of the gene of interest. Finding minimal overlapping set of BACs is done by fluorescent fingerprinting prepared using the GeneTAC G³. Figure 3 shows typical BAC fingerprinted and ran on ABI PRISM[®] 377 DNA Analyzer.

AUTOMATED SHOTGUN SEQUENCING OF BAC CONTAINING THE GENE OF INTEREST

It takes around 10 seconds to prepare the DNA in the entire 384-well plate and 40 seconds to prepare the DNA for the

Figure 4. Results of direct PCR amplification and sequencing of BAC fragment clones from bacterial L-Broth culture. (A) PCR amplification from BAC fragments from bacterial cultures. The left-most lane in each tier of the gel contains 1-kb ladder. The BAC fragments were cloned in TOPO cloning vector and amplified using T7 and T3 primers. All fragments fall between 1 and 1.5 kb. (B) ABI PRISM[®] 377 DNA Analyzer gel file showing sequences generated using the protocols described here. The sequences were generated from cycle sequencing of DNA fragments amplified directly from bacterial cultures. (C) ABI PRISM[®] 377 DNA Analyzer chromatogram showing the first 50 base pairs of sequence generated using the protocols described here. The sequence gives good signal to noise ratio and can be read clearly from the first base indicating that this method is better and more cost efficient than dye cleanup kits. (D) ABI PRISM[®] 377 DNA Analyzer chromatogram showing the latter parts of a sequence generated using the protocols described here. The sequence around the 700bp gives good quality signal to noise ratio and is readable without any basecalling errors.

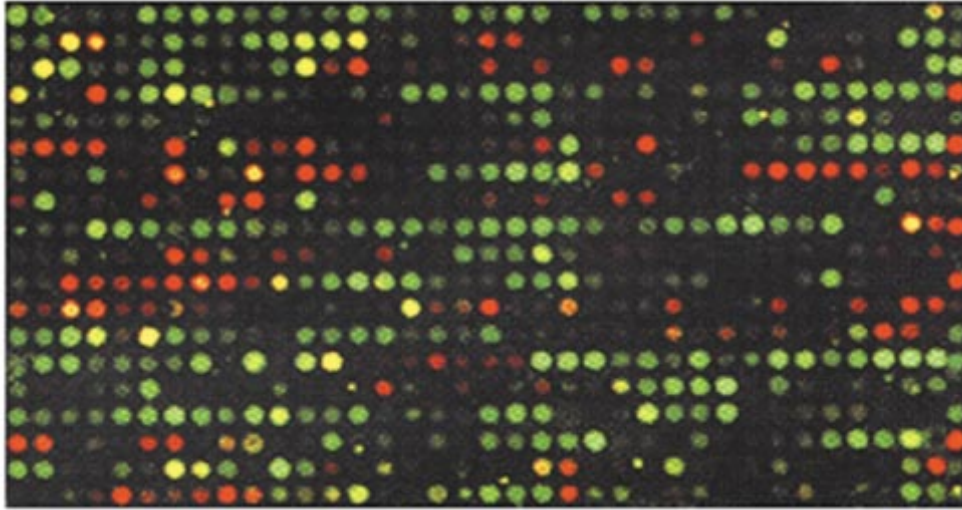


Figure 5. Hybridisation of fluorescently labeled mRNA to a portion of 4800 spot array. RNA extracted from test and reference cell lines were reverse transcribed and labeled with Cy5-dUTP and Cy3-dUTP respectively. These were hybridised to a microarray containing 4800 cDNA clones using GeneTAC HybStation.

entire shotgun library of 1500 DNA clones. Amplification of clones from culture routinely generates very good quality templates with good amplification signals as shown in figure 4a. For more than 20 000 clones, the success rate for single-band amplification is between 96% and 100% which is better than any other DNA preparation method or kit.

The PCR fragments were sequenced directly using T7 and T3 TOPO vector primers, thus eliminating the need for DNA template preparation altogether and giving the advantage of being both more cost efficient and less labour intensive with lower cross contamination rates than amplification from plasmid DNA or DNA template preparation. The method routinely produces excellent quality sequencing data of average read length of 750bp with 98.5% accuracy and average Phred Q20 scores > 700bp. Figure 4b shows a typical gel image file of sequences generated using this method. Figures 4c and 4d show typical chromatograms of the beginning and end of sequence generated using this method run on ABI PRISM[®] 377 DNA Analyzer. Figure 4c shows that the beginning of the sequence has no traces of unincorporated dye terminators obscuring some of the bases indicating that the dye cleanup described is better and more cost efficient than using dye terminator cleanup kits. Figure 4d shows that the latter part of the sequence around 600bp to 750bp is of good, readable quality without any basecalling errors.

Once the full length genomic sequence is determined, intron-exon boundaries were found by probing genomic BAC library of the gene of interest with cDNA probes and sequencing the positive clones, then aligning that to the genomic BAC sequence to obtain the boundaries. This technique successfully isolates small introns which are missed by current gene prediction software such as Genscan and Grail.²⁶ This technique relies on using bioinformatics on HGP data thus it is cheaper, quicker and more accurate than current intron-exon boundary techniques and prediction software.

DETERMINING GENE FUNCTION

different types of experiment are usually carried out on a newly identified gene. Firstly, expression profiling to view the dosage at which the gene is expressed, secondly, subtractive hybridisation to determine how various external physical and biochemical input affect the expression of the gene in various tissues which could lead to delineation of the biochemical pathways the gene is involved in and thirdly, mini-Northerns to determine the level of expression of the gene in various tissues. Although there are other microarray systems such as the Affymetrix GeneChip[®] array (Affymetrix, Santa Clara, California, USA), the GeneTAC G³ provide a cheaper and robust way of generating custom made microarrays mapping to a specific region.

Using the standard pin size of 200 microns, the maximum resolution is 4800 spots per slide, using the 75 micron pins the maximum resolution is 9408 per slide. The GeneTAC G³ grids four slides per hour and can grid up to 24 slides without manual intervention. Thus using the 75 micron pins the GeneTAC G³ can grid up to 225,792 spots in six hours. Figure 5 shows typical image of a microarray printed using the GeneTAC G³ and hybridised using the GeneTAC HybStation.

Discussion

The techniques for isolating and characterizing novel genes using the GeneTAC G³ are essential in confirming any gene prediction using bioinformatics on HGP databases especially where the region involved is not at the finishing stage yet. They also provide cheaper, faster and more accurate way of isolating and determining gene structure. Recently, Brett et al.⁴ have shown that there are many novel genes still unidentified and isolating them is more complex due to the presence of alternative transcripts of those genes, thus the techniques discussed above will help to streamline the process. Almind et al., Nwosu et al. and Pharoah et al.,^{1,19, 20} have shown that almost all currently investigated diseases arise due to the action of more than one set of genes explaining the difficulties in isolating genes involved in diseases such as diabetes, prostate and breast cancer. A combination of microarray together with RACE and gene identification technique will help to pinpoint and characterize the genes involved in those diseases at cost effective rate since all the methods are carried out on a single flexible platform; GeneTAC G³ within a laboratory environment. A combination of the techniques discussed have been used successfully to isolate many genes including the IgG Fc receptor, FcgammaRIIB,⁵ Cylindromatosis,³ PRCC,²² Peutz Jaeger,¹⁴ Bcl9,²⁹ Bcl10²⁸ and RAMP²³ genes. Additionally, the techniques can be easily adapted to isolate and characterize genes from other organisms and species.

Acknowledgements

R. A. Hamoudi was funded by the Institute of Cancer Research which is supported by Cancer Research UK.

REFERENCES

- Almind K., A. Doria and C.R. Kahn. Putting the genes for type II diabetes on the map. *Nature Medicine*, 7, 277-279, 2001.
- Biggs P.J., P. Chapman, S.R. Lakhani, J. Burn and M.R. Stratton. The cylindromatosis gene (cyld1) on chromosome 16q may be the only tumour suppressor gene involved in the development of cylindromas. *Oncogene*, 12,1375-1377, 1996.
- Bignell G.R., W. Warren, S. Seal, M. Takahashi, E. Rapley, R. Barfoot, H. Green, C. Brown, P.J. Biggs, S.R. Lakhani, C. Jones, J. Hansen, E. Blair, B. Hofmann, R. Siebert, G. Turner, D.G. Evans, C. Schrandt-Stumpel, F.A. Beemer, A. van Den Ouweland, D. Halley, B. Delpech, M.G. Cleveland, I. Leigh, J. Leisti and S. Rasmussen. Identification of the familial cylindromatosis tumour-suppressor gene. *Nature Genetics*, 25, 160-165, 2000.
- Brett D., H. Pospisil, J. Valcarcel, J. Reich and P. Bork. Alternative splicing and genome complexity. *Nature Genetics*, 30, 29-30, 2002.
- Callanan M.B., P. Le Baccon, P. Mossuz, S. Duley, C. Bastard, R. Hamoudi, M.J. Dyer, G. Klobeck, R. Rimokh, J.J. Sotot and D. Leroux. The IgG Fc receptor, FcγRIIB, is a target for deregulation by chromosomal translocation in malignant lymphoma. *Proceedings of National Academy of Science, U.S.A.*, 97, 309-314, 2000.
- Carrano A.V., J. Lamerdin, L.K. Ashworth, B. Watkins, E. Branscomb, T. Slezak, M. Raff, P.J. De Jong, D. Keith, McBride L., S. Meister and M. Kronick. A High-Resolution, Fluorescence-Based, Semiautomated Method for DNA Fingerprinting. *Genomics*, 4, 129-136, 1989.
- Edwards S.M., Z. Kote-Jarai, R. Hamoudi and R.A. Eeles. An improved high throughput heteroduplex mutation detection system for screening BRCA2 mutations-fluorescent mutation detection (F-MD). *Human Mutation*, 17, 220-232, 2001.
- Fischer K., S. Frohling, S.W. Scherer, B.J. McAllister, C. Scholl, S. Stilgenbauer, L.C. Tsui, P. Lichter and H. Dohner. Molecular cytogenetic delineation of deletions and translocations involving chromosome band 7q22 in myeloid leukemias. *Blood*, 89, 2036-2041, 1997.
- Giles R.H., F. Petrij, H.G. Dauwerse, A.I. den Hollander, T. Lushnikova, G.J. van Ommen, R.H. Goodman, L.L. Deaven, N.A. Doggett, D.J. Peters and M.H. Breuning. Construction of a 1.2-Mb contig surrounding, and molecular analysis of, the human CREB-binding protein (CBP/CREBBP) gene on chromosome 16p13.3. *Genomics*, 42, 96-114, 1997.
- Glockner G., S. Scherer, R. Schattevoy, A. Boright, J. Weber, L.C. Tsui and A. Rosenthal. Large-scale sequencing of two regions in human chromosome 7q22: analysis of 650 kb of genomic sequence around the EPO and CUTL1 loci reveals 17 genes. *Genome Res.*, 8, 1060-1073, 1998.
- Gregory S.G., G.R. Howell and D.R. Bentley. Genome mapping by fluorescent fingerprinting. *Genome Research*, 7, 1162-1168, 1997.
- Hamoudi R. Automating the construction and maintenance of PAC & cDNA libraries. *International Biotechnology Journal, Volume 18, Issue 2, 12. April 2000.*
- Hegde P., R. Qi, K. Abernathy, C. Gay, S. Dharap, R. Gaspard, J.E. Hughes, E. Snesrud, N. Lee and J. Quackenbush. A concise guide to cDNA microarray analysis. *Biotechniques*, 29, 548-562, 2000.
- Hemminki A., D. Markie, I. Tomlinson, E. Avizienyte, S. Roth, A. Loukola, G. Bignell, W. Warren, M. Aminoff, P. Hoglund, H. Jarvinen, P. Kristo, K. Pelin, M. Ridanpaa, R. Salovaara, T. Toro, W. Bodmer, S. Olschwang, A.S. Olsen, M.R. Stratton, A. de la Chapelle and L.A. Aaltonen. A serine/threonine kinase gene defective in Peutz-Jeghers syndrome. *Nature*, 391, 184-187, 1998.
- Hubbard T., D. Barker, E. Birney, G. Cameron, Y. Chen, L. Clark, T. Cox, J. Cuff, V. Curwen, T. Down, R. Durbin, E. Eyraas, J. Gilbert, M. Hammond, L. Huminiacki, A. Kasprzyk, H. Lehvaslaiho, P. Lijnzaad, C. Melsopp, E. Mongin, R. Pettett, M. Pocock, S. Potter, A. Rust, E. Schmidt, S. Searle, G. Slater, J. Smith, W. Spooner, A. Stabenau, J. Stalker, E. Stupka, A. Ureta-Vidal, I. Vastrik and M. Clamp. The Ensembl genome database project. *Nucleic.Acids.Res.*, 30, 38-41. 2002.
- Hubert R.S., S. Mitchell, X.N. Chen, K. Ekmekji, C. Gadowski, Z. Sun, D. Noya, U.J. Kim, C. Chen, H. Shizuya, M. Simon, P.J. De Jong and J.R. Korenberg. BAC and PAC contigs covering 3.5 Mb of the Down syndrome congenital heart disease region between D21S55 and MX1 on chromosome 21. *Genomics*, 41, 218-226, 1997.
- Ioannou P.A., Amemiya C.T., Garnes J., Kroisel P.M., Shizuya H., Chen C., Batzer M.A. and De Jong P.J. A new bacteriophage P1-derived vector for the propagation of large human DNA fragments. *Nature Genetics*, 6, 84-89, 1994.
- Nehls M., D. Pfeifer and T. Boehm. Exon amplification from complete libraries of genomic DNA using a novel phage vector with automatic plasmid excision facility: application to the mouse neurofibromatosis-1 locus. *Oncogene*, 9, 2169-2175, 1994.
- Nwosu V., J. Carpten, J.M. Trent and R. Sheridan. Heterogeneity of genetic alterations in prostate cancer: evidence of the complex nature of the disease. *Human Molecular Genetics*, 10, 2313-2318, 2001.
- Pharoah P.D., A. Antoniou, M. Bobrow, R.L. Zimmern, D.F. Easton and B.A. Ponder. Polygenic susceptibility to breast cancer and implications for prevention. *Nature Genetics*, 31, 33-36, 2002.
- Rapley E.A., G.P. Crockford, D. Teare, P. Biggs, S. Seal, R. Barfoot, S. Edwards, R. Hamoudi, K. Heimdal, S.D. Fossa, K. Tucker, J. Donald, F. Collins, M. Friedlander, D. Hogg, P. Goss, A. Heidenreich, W. Ormiston, P.A. Daly, D. Forman, T.D. Oliver, M. Leahy, R. Huddart, C.S. Cooper and J.G. Bodmer. Localization to Xq27 of a susceptibility gene for testicular germ-cell tumours. *Nature Genetics*, 24, 197-200, 2000.
- Sidhar S.K., J. Clark, S. Gill, R. Hamoudi, A.J. Crew, R. Gwilliam, M. Ross, W.M. Linehan, S. Birdsall, J. Shipley and C.S. Cooper. The t(X;1)(p11.2;q21.2) translocation in papil

- lary renal cell carcinoma fuses a novel gene PRCC to the TFE3 transcription factor gene. *Human Molecular Genetics*, 5, 1333-1338, 1996.
23. Smedley D., R. Hamoudi, J. Clark, W. Warren, M. Abdul-Rauf, G. Somers, D. Venter, K. Fagan, C. Cooper and J. Shipley. The t(8;13)(p11;q11-12) rearrangement associated with an atypical myeloproliferative disorder fuses the fibroblast growth factor receptor 1 gene to a novel gene RAMP. *Human Molecular Genetics*, 7, 637-642, 1998.
 24. Sood R., T. Blake, I. Aksentijevich, G. Wood, X. Chen, D. Gardner, D.A. Shelton, M. Mangelsdorf, A. Orsborn, E. Pras, J.E.J. Balow, M. Centola, Z. Deng, N. Zaks, N. Richards, N. Fischel-Ghodsian, J.I. Rotter, M. Pras, M. Shohat, L.L. Deaven, D.L. Gumucio, D.F. Callen, R.I. Richards and N.A. Doggett. Construction of a 1-Mb restriction-mapped cosmid contig containing the candidate region for the familial Mediterranean fever locus (MEFV) on chromosome 16p 13.3. *Genomics*, 42, 83-95, 1997.
 25. Staden R., K.F. Beal and J.K. Bonfield. The Staden package, *Methods Mol.Biol.*, 30, 115-130, 1998.
 26. Sze S.H., M.A. Roytberg, M.S. Gelfand, A.A. Mironov, T.V. Astakhova and P.A. Pevzner. Algorithms and software for support of gene identification experiments. *Bioinformatics*, 14, 14-19, 1998.
 27. Tagle D.A., M. Swaroop, M. Lovett and F.S. Collins. Magnetic bead capture of expressed sequences encoded within large genomic segments. *Nature*, 361, 751-753, 1993.
 28. Willis T.G., D.M. Jadayel, M.Q. Du, H. Peng, A.R. Perry, M. Abdul-Rauf, H. Price, L. Karran, O. Majekodunmi, I. Wlodarska, L. Pan, T. Crook, R. Hamoudi, P.G. Isaacson and M.J. Dyer. Bcl10 is involved in t(1;14)(p22;q32) of MALT B cell lymphoma and mutated in multiple tumor types. *Cell*, 96, 35-45, 1999.
 29. Willis T.G., I.R. Zalcborg, L.J. Coignet, I. Wlodarska, M. Stul, D.M. Jadayel, C. Bastard, J.G. Treleaven, D. Catovsky, M.L. Silva and M.J. Dyer. Molecular cloning of translocation t(1;14)(q21;q32) defines a novel gene (BCL9) at chromosome 1q21. *Blood*, 91, 1873-1881, 1998.
 30. Wolman S.R. Applications of fluorescent in situ hybridization (FISH) to genetic analysis of human tumors. *Pathol.Annu*, 30 Pt 2, 227-243, 1995.
 31. Wooster R., S.L. Neuhausen, J. Mangion, Y. Quirk, D. Ford, N. Collins, K. Nguyen, S. Seal, T. Tran and D. Averill. Localization of a breast cancer susceptibility gene, BRCA2, to chromosome 13q12-13. *Science*, 265, 2088-2090, 1994.

If you are interested in seeing more articles like this in JALA, please email jalaneews@virginia.edu, and simply put the code (757) in the subject line.

T(11;18) Is a Marker for All Stage Gastric MALT Lymphomas That Will Not Respond to *H. pylori* Eradication

HONGXIANG LIU,* HONGTAO YE,* AGNES RUSKONE–FOURMESTRAUX,†,§ DAPHNE DE JONG,|| STEFANO PILERI,¶ CHRISTIAN THIEDE,# ANNE LAVERGNE,§,** HENK BOOT,|| GIANCARLO CALETTI,¶ THOMAS WÜNDISCH,†† THIERRY MOLINA,†,§ BABS G. TAAL,|| SABATTINI ELENA,¶ TOGLIANI THOMAS,¶ PIER LUIGI ZINZANI,¶ ANDREAS NEUBAUER,†† MANFRED STOLTE,§§ RIFAT A. HAMOUDI,* AHMET DOGAN,* PETER G. ISAACSON,* and MING–QING DU*

*Department of Histopathology, University College London, London, England; †Service de Gastro-entérologie/Service d'Anatomie Pathologique, Hotel-Dieu, Ap-Hp, Paris, France; §Groupe d'Etude des Lymphomes Digestifs, Fondation Française de Cancérologie Digestive, France; ||Department of Pathology/Gastroenterology, The Netherlands Cancer Institute, Amsterdam, The Netherlands; ¶Servizi di Anatomia Patologica e Gastroenterologia, Università degli Studi di Bologna, Bologna, Italy; #Labor Molekulare Diagnostik, Universitätsklinikum Carl Gustav Carus, Dresden, Germany; **Service d'Anatomie Pathologique, Hopital Lariboisiere, Paris, France; ††Department of Hematology, Oncology and Immunology, Philipps University Marburg, Marburg, Germany; and §§Institut für Pathologie, Klinikum Bayreuth, Bayreuth, Germany

Background & Aims: Eradication of *Helicobacter pylori* leads to cure of gastric mucosa-associated lymphoid tissue (MALT) lymphoma in 75% of localized cases. However, prolonged follow-up is necessary to determine whether a lymphoma responds to therapy. In a small series of cases, we showed that t(11;18)(q21;q21)-positive MALT lymphomas failed to respond to *H. pylori* eradication. The present study aimed to verify this finding in a large cohort and confirm whether the translocation predicts the response of stage I_E tumors, for which clinical staging has little prognostic value. **Methods:** A total of 111 patients with *H. pylori*-positive gastric MALT lymphoma treated with antibiotics were studied. Clinical staging was undertaken before therapy. The response of lymphoma to *H. pylori* eradication was determined by histologic examination of gastric biopsy specimens. Diagnostic biopsy specimens were analyzed for t(11;18)(q21;q21) by reverse-transcription polymerase chain reaction of the API2-MALT1 transcript. **Results:** Forty-seven of the 48 patients who showed complete regression had lymphoma at stage I_E, whereas 43 of the 63 nonresponsive cases were at stage I_E and the remaining cases at stage II_E or above. t(11;18)(q21;q21) was detected in 2 of 48 complete-regression cases, and these positive cases showed relapse of lymphoma in the absence of *H. pylori* reinfection. In contrast, the translocation was present in 42 of the 63 nonresponsive cases, including 26 of 43 (60%) at stage I_E. **Conclusions:** t(11;18)(q21;q21)-positive gastric MALT lymphomas, including those at stage I_E, do not respond to *H. pylori* eradication. Detection of the translocation should help the clinical management of patients with gastric MALT lymphoma.

Gastric mucosa-associated lymphoid tissue (MALT) lymphoma arises from mucosal lymphoid tissue that is acquired usually as a reaction to *Helicobacter pylori* infection.^{1,2} Growth of these lymphoma cells in culture can be stimulated by strain-specific heat-killed *H. pylori*.^{3,4} This response is mediated by intratumoral *H. pylori*-specific T cells and involves CD40 and CD40L costimulatory molecules.^{3,4} Intriguingly, the lymphoma immunoglobulin recognizes a variety of autoantigens without cross-reactivity with *H. pylori*.^{5,6} In the clinical setting, eradication of *H. pylori* leads to complete regression of gastric MALT lymphoma in approximately 75% of cases.^{7–13}

The time for regression to take place after *H. pylori* eradication varies from a few weeks to 18 months.^{7–13} Therefore, prolonged follow-up with repeated endoscopy and gastric biopsies is essential to determine whether a lymphoma responds to *H. pylori* eradication or requires additional therapy. The prognostic value of clinical staging has been extensively examined with the help of endoscopic ultrasonography, which allows assessment of the extent of tumor invasion to the gastric wall and regional lymph nodes.^{11–13} In general, stage II_E or above lymphomas, in which gastric lymph nodes or adjacent or

Abbreviations used in this paper: CR, complete remission; MALT, mucosa-associated lymphoid tissue; NR, nonresponsive; RT-PCR, reverse-transcription polymerase chain reaction.

© 2002 by the American Gastroenterological Association

0016-5085/02/\$35.00

doi:10.1053/gast.2002.33047

remote organs are involved, do not respond to *H. pylori* eradication.^{11–13} In stage I_E cases, in which tumors are confined to the gastric wall, staging has limited value in prediction of the response, although tumors that involve the muscularis propria or serosa (stage I_{E2}) have a higher failure rate than those restricted to the submucosa (stage I_{E1}).^{11–13} However, most gastric MALT lymphomas are at stage I_E at diagnosis, and alternative prognostic markers are therefore needed.

t(11;18)(q21;q21) occurs specifically in MALT lymphomas and is the most frequent genetic abnormality found in this tumor, detected in about 40% of gastric cases.^{14–26} The translocation fuses the amino terminal of the *API2* gene to the carboxyl terminal of the *MALT1* gene and generates a chimeric fusion product.^{16–18} In vitro assays, the *API2-MALT1* fusion product activates nuclear factor κ B,^{27,28} a transcription factor for several survival-related genes, including those encoding cytokines, growth factors, cell adhesion molecules, and several cell apoptosis inhibitors.²⁹ Thus, it is most likely that the fusion product confers a survival advantage to MALT lymphoma cells. In keeping with this, t(11;18)(q21;q21) is significantly associated with more advanced gastric MALT lymphomas.^{26,30,31} In a small series of cases, we showed that t(11;18)(q21;q21)-positive MALT lymphomas failed to respond to *H. pylori* eradication.²⁵ However, this finding remains to be validated in a large cohort. More importantly, it is unknown whether the translocation predicts the response of stage I_E lymphoma to *H. pylori* eradication. We have developed a novel reverse-transcription polymerase chain reaction (RT-PCR) method for detection of t(11;18)(q21;q21) from archival formalin-fixed and paraffin-embedded tissues and addressed these issues in a large cohort of cases collected from 5 European lymphoma centers.

Materials and Methods

Patients and Materials

A series of 111 patients with *H. pylori*-positive gastric MALT lymphoma who were treated with antibiotics alone was retrospectively recruited from the Groupe d'Etude des Lymphomes Digestifs, France (33 cases); Department of Pathology, The Netherlands Cancer Institute, The Netherlands (32 cases); Servizi di Anatomia Patologica e Gastroenterologia, Università degli Studi di Bologna, Italy (24 cases); the German MALT Lymphoma Study Group (18 cases); and Department of Histopathology, University College London (4 cases). The selection of patients was biased toward those who showed no response to *H. pylori* eradication, and the proportion of *H. pylori* eradication nonresponsive (NR) cases in different groups was similar. The diagnosis of gastric MALT lymphoma was made according to histologic criteria described by Isaacson et

al.^{9,32} In all cases, there was dense diffuse infiltrate of centrocyte-like cells in lamina propria with prominent lymphoepithelial lesions. Clinical staging according to the Ann Arbor system modified by Musshoff was performed in each case before therapy.³³ In 64 cases, the extent of lymphoma invasion of the gastric wall and regional lymph nodes was determined by endoscopic ultrasonography, which allows further division of stage I_E tumors into I_{E1} (restricted to the submucosa) and I_{E2} (extended to the muscularis or serosa).¹¹ *H. pylori* eradication was achieved by administration of a 2-week course of amoxicillin (3 × 750 mg daily) and omeprazole (3 × 40 mg daily).^{7,10,12} One month after completing the antibiotic therapy, the first gastric endoscopy and biopsy were performed to detect *H. pylori* infection by histology, culture, and PCR of the *H. pylori*-associated urease gene and tumor regression by histology and molecular analysis. These investigations were repeated every 3–4 months until lymphoma showed complete regression or was judged as NR. After achieving complete regression, patients were examined further every 6 months. Lymphomas showing both complete endoscopic and histologic regression were regarded as complete remission (CR). Those that failed to show histologic regression 12 months after successful eradication of *H. pylori* or progressed during follow-up were judged as NR.

Tissue specimens from diagnostic biopsy specimens, including frozen tissues from 22 patients and formalin-fixed and paraffin-embedded tissues from 89 patients, were retrieved for molecular analysis. Where indicated, follow-up biopsy specimens were also analyzed.

RNA Extraction

For frozen tissues, total RNA was extracted from up to 10 mg tissue using the RNeasy Mini Kit (Qiagen, West Sussex, England).

For formalin-fixed and paraffin-embedded tissues, total RNA was extracted using an Ambion RNA isolation kit (AMS Biotechnology, Oxon, England, United Kingdom). Briefly, 5–10 5- μ m paraffin sections were deparaffinized in xylene. The tissue was digested with proteinase K (1 mg/mL) for 2 hours at 45°C and solubilized in a guanidinium-based buffer. RNA was extracted with acid phenol/chloroform and precipitated in isopropanol. The precipitated RNA was washed in 75% ethanol and redissolved in 20 μ L RNA Storage Solution (AMS Biotechnology).

Detection of t(11;18)(q21;q21) by RT-PCR

The synthesis of complementary DNA (cDNA) and PCR detection of the *API2-MALT1* fusion transcript from frozen tissues was performed as described previously.^{25,26} Briefly, up to 2 μ g total RNA was reverse transcribed into cDNA using the SuperScript Preamplification System (Invitrogen Ltd., Paisley, Scotland, United Kingdom) and oligo(dT) primer. The *API2-MALT1* fusion transcript was amplified by PCR using a pair of primers (f-S and f-AS) that covered all the known breakpoints (Table 1 and Figure 1).²⁶ As control, a 257-base pair fragment of the glucose-6-phosphate dehydro-

Table 1. Primers for RT-PCR of the API2-MALT1 Fusion Transcript and Glucose-6-Phosphate Dehydrogenase

| Tissue type | Gene target | Primer | Primer sequence | Expected major PCR products (base pairs) ^a |
|----------------|-------------------------|--------------|-----------------------------------|---|
| Frozen tissue | API2-MALT1 ^b | Sense | 5'-ACA TTC TTT AAC TGG CCC TC | 669; 730; 1006; 1279 |
| | | Anti-sense | 5'-TAG TCA ATT CGT ACA CAT CC | |
| Paraffin block | G6PD | Sense | 5'-GAG GCC GTG TAC ACC AAG ATG AT | 258 |
| | | Anti-sense | 5'-AAT ATA GGG GAT GGG CTT GG | |
| | API2-MALT1 | Sense | 5'-GGA AGA GGA GAG AGA AAG AGC A | 83 |
| | | Anti-sense 1 | 5'-CCA AGA CTG CCT TTG ACT CT | |
| | | Anti-sense 2 | 5'-GGA TTC AGA GAC GCC ATC AA | |
| | G6PD | Anti-sense 3 | 5'-CAA AGG CTG GTC AGT TGT TT | 73; 100; (133; 197; 230); 409 |
| | | Sense | 5'-ACG-GCA ACA GAT ACA AGA AC | |
| | | Anti-sense | 5'-CGA AGT GCA TCT GGC TCC | |

G6PD, glucose-6-phosphate dehydrogenase.

^aAlternative splice variants are shown in parentheses.

^bGene sequence used for primer design: *API2*, NM_001165; *MALT1*, AF130356; *G6PD*, X55448.1 and M12996.

genase gene spanning 2 exons was amplified in parallel (Table 1). PCR products were analyzed on 0.9% agarose gels by electrophoresis.

For paraffin-embedded samples, cDNA was synthesized using the SuperScript Preamplification System with the following modifications. A mixture of gene-specific primers comprising 1 pmol each of the 3 *MALT1* antisense primers (p-AS1, p-AS2, and p-AS3) and the glucose-6-phosphate dehydrogenase antisense primer (Table 1 and Figure 1) was used. In addition, the temperature for primer annealing and cDNA synthesis was at 50°C, rather than 42°C as used for reverse transcription with oligo(dT) primer. To amplify the API2-MALT1 fusion product, primers were designed to flank a short segment of the fusion junction and hence were suitable for amplification of small fragments of cDNA typically prepared from RNA isolated from paraffin-embedded tissues. Three sets of PCR primers were designed: a common *API2* sense primer (p-S) that covered 93% of the known *API2* breakpoints and 3 antisense primers that targeted all 4 variable breakpoints on the *MALT1* gene (Table 1 and Figure 1).¹⁶⁻²⁶ A separate set of primers was designed for RT-PCR of the glucose-6-phosphate dehydrogenase gene (Table 1 and Figure 1). The size of fragments amplified with these primer pairs is shown in Table 1.

PCR was performed separately with each primer pair using a "hot-start touch-down" program.²⁶ PCR products were analyzed by electrophoresis on 10% polyacrylamide gels. In each case, RT-PCR analysis for API2-MALT1 fusion transcript was performed at least twice in independent experiments.

To validate the efficiency of the RT-PCR system for detection of the API2-MALT1 fusion transcript from paraffin-embedded tissues, we first evaluated the system on 20 t(11;18)(q21;q21)-positive and 10 negative cases that had both frozen and paraffin-embedded tissues and the frozen tissues had been examined for t(11;18) by RT-PCR as described previously.^{25,26} The RT-PCR system developed for paraffin-embedded tissues detected the translocation in each of the 20 positive cases and did not show any nonspecific bands. PCR products representing different API2-MALT1 fusions were confirmed by sequencing. To further determine whether the system can be applied to tissues from small biopsy specimens, we performed RT-PCR on microdissected cells from 3 t(11;18)(q21;q21) cases and the translocation was detected in each occasion. Having established the reliability of the system, we screened unknown cases for t(11;18)(q21;q21). The molecular detection of t(11;18)(q21;q21) was performed blindly without knowledge of the clinical follow-up.

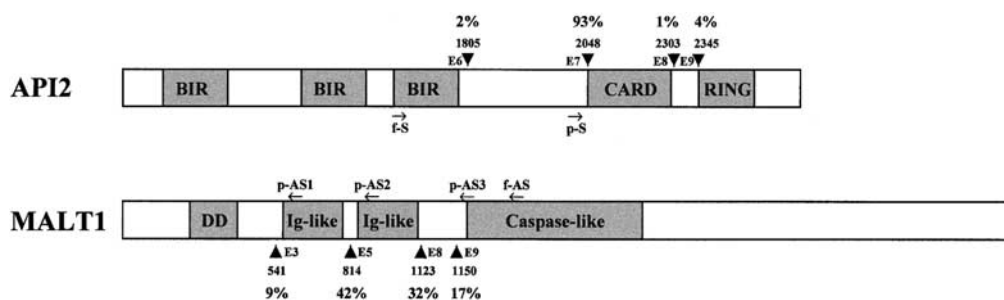


Figure 1. Schematic representation of the *API2* and *MALT1* gene structure and primer positions. Known breakpoints are indicated by arrowheads, and nucleic acids are numbered according to cDNA sequence of the *API2* (GeneBank, NM_001165) and *MALT1* gene (AF130356). The frequency of individual known breakpoints was given.¹⁴⁻²⁶ Arrows indicate the position of primers used. f-S and f-AS, sense and anti-sense primer for PCR from frozen tissue; p-S and p-AS, sense and anti-sense primer for PCR from paraffin-embedded tissues; BIR, baculovirus IAP repeat; CARD, caspase recruitment domain; DD, death domain.^{21,23}

Sequencing of PCR Products

Where indicated, PCR products were gel purified (QIAquick Gel Extraction Kit; Qiagen) and sequenced in both directions using dRhodamine dye terminators on an ABI Prism 377 sequencer (PE Applied Biosystems, Foster City, CA).

Statistical Analysis

χ^2 and Fisher exact tests were used to analyze the correlation between the response of MALT lymphomas to *H. pylori* eradication and clinical staging or t(11;18)(q21;q21) status.

Results

Clinical Staging Predicts Treatment Failure to *H. pylori* Eradication in Stage II_E or Above but Not Stage I_E Gastric MALT Lymphoma

A total of 111 patients with gastric MALT lymphoma were included in the present multicenter study (67 men and 44 women; mean age, 58 years [range, 25–88 years]). *H. pylori* infection was successfully cured in all cases as confirmed by histology and culture of gastric biopsy specimens taken after completion of the antibiotic therapy. After *H. pylori* eradication, patients were followed up by repeated endoscopy and biopsy. The mean period between *H. pylori* eradication and achievement of CR or commencement of other treatment in NR patients was 12 months (range, 1–75 months), and the mean follow-up period to date is 35 months (range, 9–85 months). During follow-up, 48 cases showed CR, whereas 63 cases displayed NR. There is no difference in age and sex between the CR and NR groups. Both groups had similar length of follow-up. Histologically, focal transformed high-grade components were seen in 3 NR but not in any of the CR cases. In the CR group, 2 of 48 cases showed tumor relapse; in both cases, the lymphoma harbored t(11;18) (detailed in the next section).

Among the 48 CR cases, 47 were at stage I_E and 1 at stage II_E. The stage II_E CR case is 1 of 2 that showed lymphoma relapse. Of the 63 NR cases, 20 were at stage II_E or above and the remaining 43 cases were at stage I_E. Despite the fact that most of the lymphomas at stage II_E or above (20 of 21 [95%]) did not respond to *H. pylori* eradication ($P < 0.001$), almost one half of stage I_E tumors also did not respond to *H. pylori* eradication (43 of 90 [48%], $P > 0.05$). Therefore, the staging failed to predict the response of stage I_E gastric MALT lymphoma to *H. pylori* eradication. Among cases with stage I_E lymphoma, there was no difference in age, sex, and

Table 2. Clinical and Histopathologic Features of Stage I_E Gastric MALT Lymphomas and Their Responses to *H. pylori* Eradication Therapy

| | Complete regression | No regression |
|--------------------------------------|---------------------|---------------|
| Number of patients | 47 | 43 |
| Age (yr) | | |
| Mean | 60 | 57 |
| Range | 25–85 | 30–88 |
| Sex | | |
| M | 29 | 21 |
| F | 18 | 22 |
| Histology with high grade component | 0 | 3 |
| Stages by endoscopic ultrasonography | | |
| I _{E1} | 29 | 30 |
| I _{E2} | 3 | 2 |
| Follow-up period (mo) | | |
| Intervals ^a | | |
| Mean | 8.2 | 15 |
| Range | 1–26 | 5–75 |
| Follow-up to date | | |
| Mean | 38 | 30 |
| Range | 10–82 | 9–85 |

^aThe time between *H. pylori* eradication and complete regression or commencement of other treatment in NR cases.

follow-up periods between the CR and NR groups ($P > 0.05$) (Table 2). The extent of lymphoma invasion within the gastric wall was assessed by endoscopic ultrasonography in 64 cases with stage I_E lymphoma. There was no difference in the response of gastric MALT lymphoma to *H. pylori* eradication between cases showing stage I_{E1} and stage I_{E2} disease ($P > 0.05$) (Table 2).

t(11;18)(q21;q21) Is a Marker for Gastric MALT Lymphomas That Do Not Respond to *H. pylori* Eradication, Including Those at Stage I_E

All cases presented in this study showed successful RT-PCR of the reference gene glucose-6-phosphate dehydrogenase. The API2-MALT1 fusion PCR product varied in size depending on the breakpoints and primer sets used, but accurate sizing of the PCR product on polyacrylamide gels and the characteristic PCR patterns allowed detection of t(11;18)(q21;q21) with high confidence (Figure 2). In 13 cases, PCR bands were weak and sequencing confirmation was performed. Overall, t(11;18) was positive in 40% (44 of 111) of cases detected. The positivity of t(11;18) detected from frozen tissues (9 of 22 cases [41%]) was similar to that from paraffin-embedded tissues (35 of 89 cases [39%]) ($P > 0.05$). The combined results from both frozen and paraffin-embedded tissues are summarized as follows.

Of the 48 CR cases, 2 were t(11;18)(q21;q21) positive (Figure 3). One of these 2 cases, a stage I_E tumor,

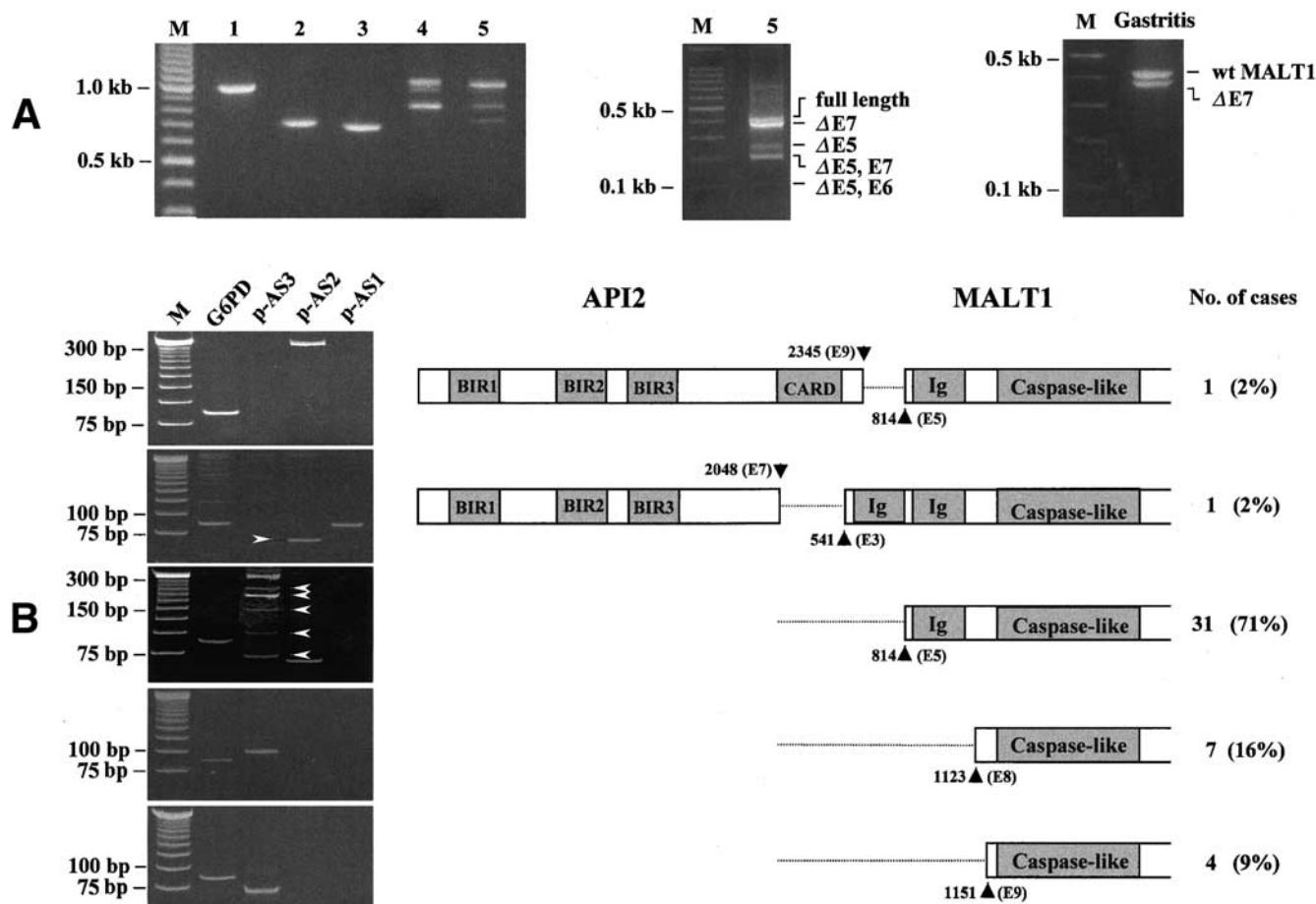


Figure 2. Detection of the API2-MALT1 fusion transcript by RT-PCR. (A) *Left panel:* examples of RT-PCR from frozen tissue samples using primer f-S and f-AS. Cases 4 and 5 harbor an API2-MALT1 fusion with breakpoint immediately upstream of exon 5 of the *MALT1* gene and show alternative splice variants of the fusion transcript. M, molecular-weight marker. *Middle panel:* RT-PCR with primer p-S and f-AS in case 5 shows alternative splice variants of the API2-MALT1 fusion. Deleted exons are indicated. *Right panel:* RT-PCR of the *MALT1* gene from a gastritis tissue shows a major splice variant with deletion of exon 7. wt, wild type. (B) Examples of various API2-MALT1 fusion transcripts detected from paraffin-embedded tissues. PCR products derived from primers p-AS2 or p-AS3 show splice variants, which are indicated by arrowheads. Representative fusion products are illustrated schematically, and their breakpoint and frequency of occurrence are shown.

achieved CR 25 months after *H. pylori* eradication. The remission lasted for 56 months, but tumor reoccurred later in the absence of *H. pylori* reinfection. PCR of the rearranged immunoglobulin gene confirmed the clonal lineage between the original lymphoma and the recurrence. t(11;18)(q21;q21) was detected only in follow-up biopsy specimens showing the tumor relapse but not in those that showed CR. The other t(11;18)(q21;q21)-positive case was a stage II_E tumor, in which CR was achieved 9 months after *H. pylori* eradication, and the remission has been maintained so far for 32 months. However, t(11;18)(q21;q21) was detected in the last follow-up biopsy specimen. A review of histology of the biopsy specimen showed a small crushed fragment of lymphoid tissue suspicious of tumor relapse. *H. pylori* was not seen.

In contrast to the CR group, 42 of the 63 NR cases (67%) were positive for the translocation, including 26

of the 43 stage I_E tumors (60%) (Figure 3). Thus, t(11;18)(q21;q21) could predict the response of most early gastric MALT lymphomas to *H. pylori* eradication ($P < 0.001$). As expected, the frequency of t(11;18)(q21;q21) was much higher in lymphomas at stage II_E or above (16 of 20 [80%]) than those at stage I_E ($P < 0.001$) (Figure 3).

Because the API2-MALT1 fusion products with intact Ig-C2 domains are more potent activators of nuclear factor κB than those without Ig-C2 domains²⁷ and therefore may be more oncogenic,²⁸ we correlated the type of API2-MALT1 fusion with clinical staging. Of the 44 t(11;18)(q21;q21)-positive cases, 33 fusion transcripts had 1 or 2 intact Ig-C2 domains, whereas 11 did not contain Ig-C2 domains (Figure 2). Tumors bearing the fusion product with intact Ig-C2 domains (14 of 33 [42%]) were more often at stage II_E or above than those harboring the fusion product without Ig-C2 domains (3

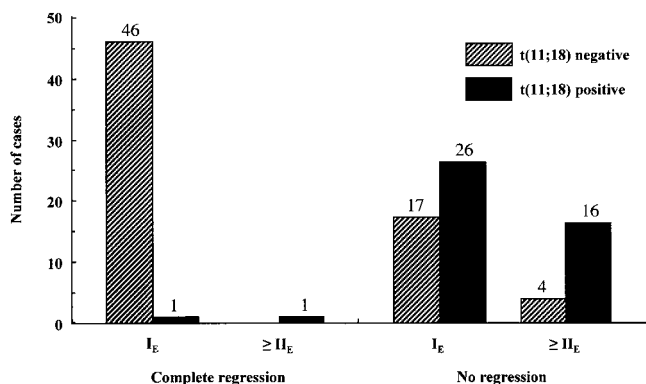


Figure 3. Correlation between response of gastric MALT lymphoma to *H. pylori* eradication therapy and clinical staging and presence of t(11;18)(q21;q21). Clinical staging has little value in predication of the response of stage I_E gastric MALT lymphoma to *H. pylori* eradication therapy. In contrast, the translocation can predict 60% of *H. pylori* therapy NR cases at stage I_E.

of 11 [27%]), although statistical analysis did not show any significant difference ($P > 0.05$).

Alternative Splice Variants of the API2-MALT1 Fusion Transcript

The breakpoint in the *MALT1* gene occurred variably immediately upstream of 4 exons (3, 5, 8, and 9), whereas the breakpoint in the *API2* gene was always immediately downstream of exon 7 with an exception in 1 case that occurred after exon 9. Various API2-MALT1 fusions gave different PCR patterns (Figure 2). When the breakpoint occurred immediately before exons 8 and 9 of the *MALT1* gene, RT-PCR showed only a single band. When the breakpoint occurred before exon 5, 1 expected band together with 4 additional smaller bands were seen. These additional PCR bands were of variable intensity but weaker than the expected fusion product. Sequencing of these bands confirmed that they were API2-MALT1 fusions identical to the corresponding fusion product in each case but with deletion of 1 or more exons of the *MALT1* gene. It is most likely that these additional PCR bands represent alternative splice variants of the fusion transcript.

The splice variants of the API2-MALT1 fusion product are best shown by PCR from frozen tissues with the sense primer positioned just upstream of the *API2* breakpoint (p-S), which yielded smaller fusion products and hence gave better separation on gels. Case 5, which harbored an API2-MALT1 fusion transcript with breakpoint immediately before exon 5 of the *MALT1* gene, showed 4 additional bands (Figure 2). They represented alternative splice variants with deletion of exon 7, exon 5, exons 5 and 7, and exons 5 and 6 of the *MALT1* gene. The variant without exon 7 did not alter the amino acid

reading frame and represented the major splice variant, whereas other splice species were minor and those with deletion of exon 5 or both exons 5 and 7 introduced a stop codon.

To examine whether these alternative splice events occur in wild-type *MALT1*, RT-PCR of the *MALT1* gene was performed. In contrast to the API2-MALT1 fusion, only a splice variant with exon 7 deletion was found in *MALT1* (Figure 2). However, in keeping with the splice variants of the fusion transcript, the *MALT1* transcript with exon 7 deletion was a major type (Figure 2).³⁴

Discussion

H. pylori eradication leads to complete regression of gastric MALT lymphoma in 75% of cases and is widely accepted as the first-line treatment for this tumor.⁷⁻¹³ One of the major dilemmas in clinical management of patients with this disease is the identification of those that will not respond to *H. pylori* eradication and require chemotherapy or radiotherapy. At present, this requires prolonged follow-up with repeated endoscopy and gastric biopsy. Clinical staging is helpful in predicting the response because lymphomas at stage II_E or above rarely respond to *H. pylori* eradication. However, the predictive value of clinical staging for stage I_E tumors is limited¹¹⁻¹³ and better prognostic markers are needed. We have shown that t(11;18)(q21;q21) is a marker for NR gastric MALT lymphomas, including those at stage I_E. In the stage I_E cases, the translocation allows this prediction in 60% of NR cases. None of the CR cases were positive for t(11;18)(q21;q21), with the exception of the 2 equivocal cases described.

Our findings indicate that t(11;18)(q21;q21)-positive gastric MALT lymphomas do not undergo regression after *H. pylori* eradication and require other conventional therapies up front. Nevertheless, *H. pylori* should be eradicated in all cases because this not only eliminates reactive lymphoid infiltrates but most likely has an adjuvant effect because in vitro experiments have shown that *H. pylori* stimulates t(11;18)(q21;q21)-positive lymphoma cells to proliferate via T-cell help.^{3,4} Moreover, eradication of *H. pylori* and reactive lymphoid infiltrates may reduce the risk of developing secondary tumors in the stomach.

Among the NR cases, 33% failed to show t(11;18)(q21;q21) by RT-PCR. Our RT-PCR strategy for frozen tissues would theoretically detect 100% of known breakpoints in both the *API2* and *MALT1* genes. However, the RT-PCR methodology for paraffin-embedded tissues would miss some of the 3 minor *API2* break-

points, which account for 7% of the total API2-MALT1 fusions.^{16–26} Thus, our current results may slightly underestimate the true frequency of t(11;18)(q21;q21). For prospective clinical screening, PCR with primers for these minor breakpoints should be included and multiplex amplification in a single tube may offer a practical approach.³⁵

In about 25% of cases, resistance of gastric MALT lymphoma to *H. pylori* eradication seems to be caused by other factors. MALT lymphomas with chromosomal translocation involving the *BCL10* locus, such as t(1;14)(p22;q32)^{36,37} and t(1;2)(p22;p12),³⁸ are typically those at advanced stages and are unlikely to respond to *H. pylori* eradication.³⁹ Lymphomas bearing these translocations can be detected immunohistochemically by strong BCL10 nuclear expression.⁴⁰ *H. pylori*-associated gastric MALT lymphoma in patients with autoimmune disease has been shown to be resistant to antibiotic treatment.⁴¹ The *fas* gene is frequently mutated in MALT lymphoma in patients with autoimmunity,⁴² and *fas* gene mutations may confer resistance of gastric MALT lymphoma to *H. pylori* eradication.

The breakpoints in the *API2* gene are always downstream of the third BIR domain but upstream of the carboxyl RING, whereas the breakpoints in the *MALT1* gene are consistently upstream of the carboxyl caspase-like domain. Thus, the resulting API2-MALT1 fusion transcripts always comprise the amino terminal *API2* with 3 intact BIR domains and the carboxyl terminal *MALT1* region containing an intact caspase-like domain. The specific selection of these domains of the *API2* and *MALT1* gene to form a fusion product strongly suggests their importance and synergy in oncogenesis. The BIR domain of *API2* has been shown to be antiapoptotic.⁴³ However, the antiapoptotic activity of the *API2* BIR domain was weak and has been shown to be suppressed by its C-terminal RING finger domain.⁴³ As a result, wild-type *API2* did not protect cells from apoptosis on stimulation by death signals.⁴³ The negative effect of the RING finger on BIR function may be associated with its ability to promote autoubiquitination and degradation.^{43,44} Replacement of the C-terminal of *API2* with the C-terminal of *MALT1* by the fusion product would release the intrinsic antiapoptotic activity of the BIR domain and therefore make the new molecule antiapoptotic. Indeed, the API2-MALT1 fusion product, but not *API2* or *MALT1* alone, has been shown to activate nuclear factor κ B, and the caspase-like domain is required for this function.²⁷ Moreover, the fusion products with intact Ig-C2 domains are more potent activators of nuclear factor κ B than those without Ig-C2 domains.^{27,28}

In keeping with this, we found that tumors bearing the fusion product with 1 or 2 intact Ig-C2 domains were more often at stage II_E or above than those harboring the fusion without the Ig-C2 domain. Alternative splice variants of the API2-MALT1 fusion transcript are present, but their functional significance is unclear.

References

1. Wotherspoon AC, Ortiz Hidalgo C, Falzon MR, Isaacson PG. *Helicobacter pylori*-associated gastritis and primary B-cell gastric lymphoma. *Lancet* 1991;338:1175–1176.
2. Parsonnet J, Friedman GD, Vandersteen DP, Chang Y, Vogelstein JH, Orentreich N, Sibley RK. *Helicobacter pylori* infection and the risk of gastric carcinoma. *N Engl J Med* 1991;325:1127–1131.
3. Hussell T, Isaacson PG, Crabtree JE, Spencer J. The response of cells from low-grade B-cell gastric lymphomas of mucosa-associated lymphoid tissue to *Helicobacter pylori*. *Lancet* 1993;342:571–574.
4. Hussell T, Isaacson PG, Crabtree JE, Spencer J. *Helicobacter pylori*-specific tumour-infiltrating T cells provide contact dependent help for the growth of malignant B cells in low-grade gastric lymphoma of mucosa-associated lymphoid tissue. *J Pathol* 1996;178:122–127.
5. Hussell T, Isaacson PG, Crabtree JE, Dogan A, Spencer J. Immunoglobulin specificity of low grade B cell gastrointestinal lymphoma of mucosa-associated lymphoid tissue (MALT) type. *Am J Pathol* 1993;142:285–292.
6. Greiner A, Marx A, Heesemann J, Leebmann J, Schmausser B, Muller-Hermelink HK. Idiotype identity in a MALT-type lymphoma and B cells in *Helicobacter pylori* associated chronic gastritis. *Lab Invest* 1994;70:572–578.
7. Wotherspoon AC, Doglioni C, Diss TC, Pan L, Moschini A, de Boni M, Isaacson PG. Regression of primary low-grade B-cell gastric lymphoma of mucosa-associated lymphoid tissue type after eradication of *Helicobacter pylori*. *Lancet* 1993;342:575–577.
8. Roggero E, Zucca E, Pinotti G, Pascarella A, Capella C, Savio A, Pedrinis E, Paterlini A, Venco A, Cavalli F. Eradication of *Helicobacter pylori* infection in primary low-grade gastric lymphoma of mucosa-associated lymphoid tissue. *Ann Intern Med* 1995;122:767–769.
9. Savio A, Franzin G, Wotherspoon AC, Zamboni G, Negrini R, Buffoli F, Diss TC, Pan L, Isaacson PG. Diagnosis and posttreatment follow-up of *Helicobacter pylori*-positive gastric lymphoma of mucosa-associated lymphoid-tissue — histology, polymerase chain-reaction, or both. *Blood* 1996;87:1255–1260.
10. Thiede C, Morgner A, Alpen B, Wundisch T, Herrmann J, Ritter M, Ehninger G, Stolte M, Bayerdorffer E, Neubauer A. What role does *Helicobacter pylori* eradication play in gastric MALT and gastric MALT lymphoma? *Gastroenterology* 1997;113:S61–S64.
11. Sackmann M, Morgner A, Rudolph B, Neubauer A, Thiede C, Schulz H, Kraemer W, Boersch G, Rohde P, Seifert E, Stolte M, Bayerdoerffer E. Regression of gastric MALT lymphoma after eradication of *Helicobacter pylori* is predicted by endoscopic staging. MALT Lymphoma Study Group. *Gastroenterology* 1997;113:1087–1090.
12. Ruskone-Fourmestreaux A, Lavergne A, Aegerter PH, Megraud F, Palazzo L, de Mascarel A, Molina T, Rambaud JL. Predictive factors for regression of gastric MALT lymphoma after anti-*Helicobacter pylori* treatment. *Gut* 2001;48:297–303.
13. Nakamura S, Matsumoto T, Suekane H, Takeshita M, Hizawa K, Kawasaki M, Yao T, Tsuneyoshi M, Iida M, Fujishima M. Predictive value of endoscopic ultrasonography for regression of gastric low grade and high grade MALT lymphomas after eradication of *Helicobacter pylori*. *Gut* 2001;48:454–460.
14. Auer IA, Gascoyne RD, Connors JM, Cotter FE, Greiner TC, Sanger

- WG, Horsman DE. t(11;18)(q21;q21) is the most common translocation in MALT lymphomas. *Ann Oncol* 1997;8:979-985.
15. Ott G, Katzenberger T, Greiner A, Kalla J, Rosenwald A, Heinrich U, Ott MM, Muller Hermelink HK. The t(11;18)(q21;q21) chromosome translocation is a frequent and specific aberration in low-grade but not high-grade malignant non-Hodgkin's lymphomas of the mucosa-associated lymphoid tissue (MALT-) type. *Cancer Res* 1997;57:3944-3948.
 16. Dierlamm J, Baens M, Wlodarska I, Stefanova-Ouzounova M, Hernandez JM, Hossfeld DK, De Wolf-Peeters C, Hagemeijer A, Van den Berghe H, Marynen P. The apoptosis inhibitor gene API2 and a novel 18q gene, MLT, are recurrently rearranged in the t(11;18)(q21;q21) associated with mucosa-associated lymphoid tissue lymphomas. *Blood* 1999;93:3601-3609.
 17. Akagi T, Motegi M, Tamura A, Suzuki R, Hosokawa Y, Suzuki H, Ota H, Nakamura S, Morishima Y, Taniwaki M, Seto M. A novel gene, MALT1 at 18q21, is involved in t(11;18)(q21;q21) found in low-grade B-cell lymphoma of mucosa-associated lymphoid tissue. *Oncogene* 1999;18:5785-5794.
 18. Morgan JA, Yin Y, Borowsky AD, Kuo F, Nourmand N, Koontz JI, Reynolds C, Soreng L, Griffin CA, Graeme-Cook F, Harris NL, Weisenburger D, Pinkus GS, Fletcher JA, Sklar J. Breakpoints of the t(11;18)(q21;q21) in mucosa-associated lymphoid tissue (MALT) lymphoma lie within or near the previously undescribed gene MALT1 in chromosome 18. *Cancer Res* 1999;59:6205-6213.
 19. Remstein ED, James CD, Kurtin PJ. Incidence and subtype specificity of API2-MALT1 fusion translocations in extranodal, nodal, and splenic marginal zone lymphomas. *Am J Pathol* 2000;156:1183-1188.
 20. Baens M, Maes B, Steyls A, Geboes K, Marynen P, De Wolf-Peeters C. The product of the t(11;18), an API2-MLT fusion, marks nearly half of gastric MALT type lymphomas without large cell proliferation. *Am J Pathol* 2000;156:1433-1439.
 21. Dierlamm J, Baens M, Stefanova-Ouzounova M, Hinz K, Wlodarska I, Maes B, Steyls A, Driessen A, Verhoef G, Gaulard P, Hagemeijer A, Hossfeld DK, De Wolf-Peeters C, Marynen P. Detection of t(11;18)(q21;q21) by interphase fluorescence in situ hybridization using API2 and MLT specific probes. *Blood* 2000;96:2215-2218.
 22. Motegi M, Yonezumi M, Suzuki H, Suzuki R, Hosokawa Y, Hosaka S, Kadera Y, Morishima Y, Nakamura S, Seto M. API2-MALT1 chimeric transcripts involved in mucosa-associated lymphoid tissue type lymphoma predict heterogeneous products. *Am J Pathol* 2000;156:807-812.
 23. Nakamura T, Nakamura S, Yonezumi M, Suzuki T, Matsuura A, Yatabe Y, Yokoi T, Ohashi K, Seto M. *Helicobacter pylori* and the t(11;18)(q21;q21) translocation in gastric low-grade B-cell lymphoma of mucosa-associated lymphoid tissue type. *Jpn J Cancer Res* 2000;91:301-309.
 24. Kalla J, Stilgenbauer S, Schaffner C, Wolf S, Ott G, Greiner A, Rosenwald A, Dohner H, Muller-Hermelink HK, Lichter P. Heterogeneity of the API2-MALT1 gene rearrangement in MALT-type lymphoma. *Leukemia* 2000;14:1967-1974.
 25. Liu H, Ruskone-Fourmesttraux A, Lavergne-Slove A, Ye H, Molina T, Bouhnik Y, Hamoudi RA, Diss TC, Dogan A, Megraud F, Rambaud JC, Du M-Q, Isaacson PG. Resistance of t(11;18) positive gastric mucosa-associated lymphoid tissue lymphoma to *Helicobacter pylori* eradication therapy. *Lancet* 2000;357:39-40.
 26. Liu H, Ye H, Dogan A, Ranaldi R, Hamoudi RA, Bearzi I, Isaacson PG, Du M-Q. T(11;18)(q21;q21) is associated with more advanced MALT lymphoma that expresses nuclear BCL10. *Blood* 2001;98:1182-1187.
 27. Uren GA, O'Rourke K, Aravind L, Pisabarro TM, Seshagiri S, Koonin VE, Dixit MV. Identification of paracaspases and metacaspases: two ancient families of caspase-like proteins, one of which plays a key role in MALT lymphoma. *Mol Cell* 2000;6:961-967.
 28. Lucas PC, Yonezumi M, Inohara N, McAllister-Lucas LM, Abazeed ME, Chen FF, Yamaoka S, Seto M, Nunez G. Bcl10 and MALT1, independent targets of chromosomal translocation in malt lymphoma, cooperate in a novel NF-kappa B signaling pathway. *J Biol Chem* 2001;276:19012-19019.
 29. Bours V, Bentires-Alj M, Hellin AC, Viatour P, Robe P, Delhalle S, Benoit V, Merville MP. Nuclear factor-kappa B, cancer, and apoptosis. *Biochem Pharmacol* 2000;60:1085-1089.
 30. Alpen B, Neubauer A, Dierlamm J, Marynen P, Thiede C, Bayerdorfer E, Stolte M. Translocation t(11;18) absent in early gastric marginal zone B-cell lymphoma of MALT type responding to eradication of *Helicobacter pylori* infection. *Blood* 2000;95:4014-4015.
 31. Sugiyama T, Asaka M, Nakamura S, Yonezumi S, Seto M. API2-MALT1 chimeric transcript is a predictive marker for the responsiveness of *H. pylori* eradication treatment in low-grade gastric MALT lymphoma. *Gastroenterology* 2001;120:1884-1885.
 32. Isaacson PG, Norton AJ. Extranodal lymphomas. Edinburgh: Churchill Livingstone, 1994.
 33. Musshoff K. Klinische stadieneinteilung der nicht-Hodgkin-lymphoma. *Strahlentherapie* 1977;153:218-221.
 34. Baens M, Steyls A, Dierlamm J, De Wolf-Peeters C, Marynen P. Structure of the MLT gene and molecular characterization of the genomic breakpoint junctions in the t(11;18)(q21;q21) of marginal zone B-cell lymphomas of MALT type. *Genes Chromosomes Cancer* 2000;29:281-291.
 35. Inagaki H, Okabe M, Seto M, Nakamura S, Ueda R, Eimoto T. API2-MALT1 fusion transcripts involved in mucosa-associated lymphoid tissue lymphoma: multiplex RT-PCR detection using formalin-fixed paraffin-embedded specimens. *Am J Pathol* 2001;158:699-706.
 36. Willis TG, Jadayel DM, Du MQ, Peng H, Perry AR, Abdul-Rauf M, Price H, Karran L, Majekodunmi O, Wlodarska I, Pan L, Crook T, Hamoudi R, Isaacson PG, Dyer MJ. Bcl10 is involved in t(1;14)(p22;q32) of MALT B cell lymphoma and mutated in multiple tumor types. *Cell* 1999;96:35-45.
 37. Zhang Q, Siebert R, Yan M, Hinzmann B, Cui X, Xue L, Rakestraw KM, Naeve CW, Beckmann G, Weisenburger DD, Sanger WG, Nowotny H, Vesely M, Callet-Bauchu E, Salles G, Dixit VM, Rosenthal A, Schlegelberger B, Morris SW. Inactivating mutations and overexpression of BCL10, a caspase recruitment domain-containing gene, in MALT lymphoma with t(1;14)(p22;q32). *Nat Genet* 1999;22:63-68.
 38. Achuthan R, Bell SM, Leek JP, Roberts P, Horgan K, Markham AF, Selby PJ, MacLennan KA. Novel translocation of the BCL10 gene in a case of mucosa associated lymphoid tissue lymphoma. *Genes Chromosomes Cancer* 2000;29:347-349.
 39. Du M-Q, Peng HZ, Liu H, Hamoudi RA, Diss TC, Willis TG, Ye HT, Dogan A, Wotherspoon AC, Dyer MJS, Isaacson PG. BCL10 mutation in lymphoma. *Blood* 2000;95:3885-3890.
 40. Ye H, Dogan A, Karran L, Willis TG, Chen L, Wlodarska I, Dyer MJ, Isaacson PG, Du MQ. BCL10 expression in normal and neoplastic lymphoid tissue: nuclear localization in MALT lymphoma. *Am J Pathol* 2000;157:1147-1154.
 41. Raderer M, Osterreicher C, Machold K, Formanek M, Fiebigler W, Penz M, Dragosics B, Chott A. Impaired response of gastric MALT-lymphoma to *Helicobacter pylori* eradication in patients with autoimmune disease. *Ann Oncol* 2001;12:937-939.
 42. Gronbaek K, Straten PT, Ralfkiaer E, Ahrenkiel V, Andersen MK, Hansen NE, Zeuthen J, Hou-Jensen K, Guldberg P. Somatic Fas mutations in non-Hodgkin's lymphoma: association with extranodal disease and autoimmunity. *Blood* 1998;92:3018-3024.
 43. Clem RJ, Sheu TT, Richter BW, He W-W, Thornberry NA, Duckett CS, Hardwick JM. C-IAP1 is cleaved by caspases to produce a

pro-apoptotic c-terminal fragment. *J Biol Chem* 2001;276:7602–7608.

44. Yang Y, Fang S, Jensen JP, Weissman AM, Ashwell JD. Ubiquitin protein ligase activity of IAPs and their degradation in proteasomes in response to apoptotic stimuli. *Science* 2000;288:874–877.

Received October 24, 2001. Accepted January 24, 2002.

Address requests for reprints to: Ming-Qing Du, Ph.D., Department of Histopathology, Royal Free and University College Medical School, University College London, Rockefeller Building, University Street, Lon-

don WC1E 6JJ, England. e-mail: m.du@ucl.ac.uk; fax: (44) 20-7387-3674.

Supported by research grants from the Leukemia Research Fund, Cancer Research Campaign, Délégation à la Recherche Clinique, Assistance Publique-Hôpitaux de Paris, Associazione Italiana per la Ricerca sul Cancro, and Deutsche Krebshilfe (grant 70-225I).

H.L. and H.Y. contributed equally to this work.

The authors thank J. Audouin, L. Bedenne, O. Bouche, Y. Bouhnik, J. Fournet, A. De Mascarel, Ph. Moreau, J. Lafon, and A. Pariente of the Groupe d'Etude des Lymphomes Digestifs, France, for contribution of part of the specimens used for this study, Dr. Tim C. Diss for critical reading of the manuscript, and M. Siskaki for technical assistance.

T(11;18)(q21;q21) is associated with advanced mucosa-associated lymphoid tissue lymphoma that expresses nuclear BCL10

Hongxiang Liu, Hongtao Ye, Ahmet Dogan, Renzo Ranaldi, Rifat A. Hamoudi, Italo Bearzi, Peter G. Isaacson, and Ming-Qing Du

The development of gastric mucosa-associated lymphoid tissue (MALT) lymphoma is a multistep process and can be clinico-pathologically divided into *Helicobacter pylori*-associated gastritis, low-grade tumors, and high-grade tumors. The molecular events underlying this progression are largely unknown. However, identification of the genes involved in MALT lymphoma-specific t(11;18)(q21;q21) and t(1;14)(p22;q32) has provided fresh insights into the pathogenesis of this disease. T(11;18)(q21;q21) results in a chimeric transcript between the *API2* and the *MALT1* genes, whereas t(1;14)(p22;q32) causes aberrant nuclear BCL10 expression. Significantly, nuclear BCL10 expression also occurs frequently in

MALT lymphomas without t(1;14)(p22;q32), suggesting an important role for BCL10 in lymphoma development. Thirty-three cases of *H pylori* gastritis, 72 MALT lymphomas, and 11 mucosal diffuse large B-cell lymphomas (DLBCL) were screened for t(11;18)(q21;q21) by reverse transcription-polymerase chain reaction followed by sequencing. BCL10 expression in lymphoma cases was examined by immunohistochemistry. The *API2*-*MALT1* fusion transcript was not detected in *H pylori* gastritis and mucosal DLBCL but was found in 25 of 72 (35%) MALT lymphomas of various sites. Nuclear BCL10 expression was seen in 28 of 53 (53%) of MALT lymphomas. Of the gastric cases, the largest group studied, the frequency of

both t(11;18)(q21;q21) and nuclear BCL10 expression was significantly higher in tumors that showed dissemination to local lymph nodes or distal sites (14 of 18 = 78% and 14 of 15 = 93%, respectively) than those confined to the stomach (3 of 29 = 10% and 10 of 26 = 38%). Furthermore, t(11;18)(q21;q21) closely correlated with BCL10 nuclear expression. These results indicate that both t(11;18)(q21;q21) and BCL10 nuclear expression are associated with advanced MALT lymphoma and that their oncogenic activities may be related to each other. (Blood. 2001;98:1182-1187)

© 2001 by The American Society of Hematology

Introduction

The development of mucosa-associated lymphoid tissue (MALT) lymphoma is a multistage process.¹ This is best understood in gastric MALT lymphoma, the most common form. Typically, low-grade gastric MALT lymphoma arises from mucosal lymphoid tissue that is acquired usually as a reaction to *Helicobacter pylori* infection.^{2,3} Low-grade MALT lymphoma is initially confined to the gastric mucosa, and its growth depends critically on the contact help of *H pylori*-specific intratumoral T cells; therefore, it responds favorably to *H pylori* eradication therapy.⁴⁻⁶ However, when the lymphoma invades the deep layers of the gastric wall and disseminates to local lymph nodes and distal sites, the tumor loses its dependence on *H pylori*-specific T cells and is no longer sensitive to *H pylori* eradication therapy.⁷⁻⁹ Finally, low-grade gastric MALT lymphoma may transform into a more aggressive diffuse large B-cell lymphoma (DLBCL).^{10,11}

Direct¹²⁻¹⁴ and indirect antigen stimulation^{4,5} and several genetic factors, including genetic instability,¹⁵ trisomy 3,¹⁶ p53 mutation/LOH,¹⁷ p16 deletion,¹⁸ t(1;14)(p22;q32),¹⁹ and t(11;18)(q21;q21),^{20,21} are implicated in MALT lymphoma development. However, the molecular events underlying the multistep progression of the tumor remain largely unknown. Identification of the genes involved in MALT lymphoma-specific t(1;14)(p22;

q32)^{22,23} and t(11;18)(q21;q21)²⁴⁻²⁶ has provided fresh insights into the pathogenesis of this disease.

T(1;14)(p22;q32) causes overexpression of BCL10, an apoptosis regulatory molecule.^{22,23} In contrast to its expected oncogenic role, wild-type BCL10 has been shown to be proapoptotic and to behave as a tumor suppressor in cell transformation assays.^{22,23,27-32} Truncated BCL10 mutants have been shown to gain transforming ability²²; however, *BCL10* gene mutation is not a feature of MALT lymphoma with t(1;14)(p22;q32).³³ The mechanism underlying the oncogenic role of t(1;14)(p22;q32) remains unclear; nevertheless, study of BCL10 protein expression pattern provides fresh clues to explain the above paradoxical findings.³⁴ In contrast to normal B cells that express BCL10 in the cytoplasm, MALT lymphoma cells with t(1;14)(p22;q32) express the protein predominantly in the nucleus.³⁴ Interestingly, up to 50% of MALT lymphomas without the translocation also express BCL10 mainly in the nucleus, albeit at a lower level.³⁴ These results suggest that nuclear BCL10 expression is associated with MALT lymphoma development and may confer oncogenic activity.

T(11;18)(q21;q21) results in the expression of a chimeric transcript between the *API2* and *MALT1* genes.²⁴ The *API2* gene contains 3 N-terminal baculovirus IAP repeats (BIR), a middle

From the Department of Histopathology, Royal Free and University College Medical School, London; the Cancer Gene Cloning Center, Institute of Cancer Research, Sutton, United Kingdom; and the Department of Pathology, Institute of Pathological Anatomy and Histopathology, Ancona, Italy.

Submitted November 6, 2000; accepted April 12, 2001.

H.L. and H.Y. contributed equally to this work.

Supported by the Cancer Research Campaign and the Leukaemia Research

Fund, United Kingdom.

Reprints: Ming-Qing Du, Department of Histopathology, Royal Free and University College Medical School, Rockefeller Building, University Street, London WC1E 6JJ, United Kingdom; e-mail: m.du@ucl.ac.uk.

The publication costs of this article were defrayed in part by page charge payment. Therefore, and solely to indicate this fact, this article is hereby marked "advertisement" in accordance with 18 U.S.C. section 1734.

© 2001 by The American Society of Hematology

Table 1. Frequency of t(11;18)(q21;q21) and BCL10 nuclear expression in gastritis, mucosa-associated lymphoid tissue lymphoma, and mucosal diffuse large B-cell lymphomas

| | Total no. cases | No. t(11;18)-positive cases | No. nuclear BCL10-positive cases/no. cases examined |
|-----------------|-----------------|-----------------------------|---|
| Gastritis | 39 | 0 | ND |
| MALT lymphoma | | | |
| Stomach | 56 | 19 (34%) | 22/41 (54%) |
| Small intestine | 1 | 1 | 1/1 |
| Lung | 7 | 4 (57%) | 4/5 (80%) |
| Salivary gland | 6 | 1 (17%) | 1/5 (20%) |
| Conjunctiva | 1 | 0 | ND |
| Thyroid | 1 | 0 | 0/1 |
| Subtotal | 72 | 25 (35%) | 28/53 (53%) |
| Mucosal DLBCL | | | |
| Stomach | 9 | 0 | 0/7 |
| Lung | 1 | 0 | ND |
| Colon | 1 | 0 | 0/1 |
| Subtotal | 11 | 0 | 0/8 |

MALT indicates mucosa-associated lymphoid tissue; DLBCL, diffuse large B-cell lymphomas.

cardiac recruitment domain (CARD), and a C-terminal zinc-binding RING finger domain.³⁵ Full-length API2 has been shown to inhibit the biologic activity of caspases 3, 7, and 9 and is, therefore, believed to be an apoptosis inhibitor.^{35,36} The *MALT1* gene, a paracaspase, comprises an N-terminal death domain (DD), followed by 2 immunoglobulinlike C2-type domains and a caspase-like domain, and its function is unknown.^{24,37} By reverse transcription-polymerase chain reaction (RT-PCR) of the API2-MALT1 fusion transcript, Southern blot analysis, and interphase fluorescence in situ hybridization for t(11;18)(q21;q21), the translocation has been found in 30% to 50% MALT lymphoma of various sites but not in nodal or splenic marginal zone B-cell lymphoma.³⁸⁻⁴² However, it remains to be determined how this translocation contributes to the progression of MALT lymphoma.

Interestingly, there appears to be no difference in histology, immunophenotype, and clinical behavior between MALT lymphomas with t(11;14)(p22;q32) and t(11;18)(q21;q21). It is thus possible that both translocations exert their oncogenic activities through a similar pathway. To understand the role of t(11;18)(q21;q21) and BCL10 nuclear expression during MALT lymphoma development, we screened 33 cases of *H pylori* gastritis, 72 MALT lymphomas, and 11 mucosal DLBCL for t(11;18)(q21;q21) and examined patients with MALT lymphoma for BCL10 expression. T(11;18)(q21;q21) and BCL10 expression pattern were correlated with the clinical staging of lymphoma and with each other.

Materials and methods

Materials

Fresh-frozen gastric biopsies from 39 patients with gastritis were collected from the Hospital of Ancona (Italy). The diagnosis of gastritis was made after histologic examination; lymphoid infiltration was mild in 25 patients and severe with aggregated follicles in 14 patients. Gastric ulcer was seen in 3 patients, including 2 with mild and 1 with severe gastritis. *H pylori* was identified in 33 of 39 gastric biopsy specimens by Warthin Starry staining and histology.

Frozen tissue samples from 72 low-grade MALT lymphomas, including a case with t(11;14)(p22;q32), and 11 mucosal DLBCL were retrieved from the surgical files of the Department of Histopathology, Royal Free and University College Medical School. Three low-grade MALT lymphomas contained a small large-cell component within the B-cell follicles, and no

mucosal DLBCL showed any low-grade MALT lymphoma lesion. Fifty-six MALT lymphomas were from the stomach, and the anatomic origins of the remaining cases are summarized in Table 1. Nine gastric cases with disseminated disease were accompanied by additional tissue from lymph node, spleen, or small intestine. Clinical staging was available in 15 cases, whereas the extent of tumor spread was estimated in 26 gastric cases in which sufficient surgical material was available for histological examination.

RNA extraction and cDNA synthesis

Total RNA was extracted from up to 10 mg frozen tissue using an RNeasy Mini Kit (Qiagen, West Sussex, United Kingdom). Up to 2 μ g total RNA was reverse-transcribed into cDNA in a 20 μ L volume using SuperScript Preamplification System (Life Technologies, Paisley, United Kingdom) and oligo(dT) primer. If the amount of total RNA was below the measurable level, such as from biopsy tissue samples, a maximum volume of RNA preparation was used for cDNA synthesis.

Amplification and sequencing of the API2-MALT1 fusion transcript

One microliter sample cDNA was added to a 25 μ L reaction volume containing 0.2 mM dNTP, 2 mM MgCl₂, 0.2 μ M sense and antisense primers each, and 1 U Platinum *Taq* DNA polymerase (Life Technologies) and amplified on a Phoenix thermal cycler (Helena BioSciences, Sunderland, United Kingdom). The PCR was performed using a so-called touchdown program at 94°C for 4 minutes followed by 1 cycle of denaturing at 94°C for 1 minute, annealing at 65°C (1°C down each cycle until 59°C) for 1 minute and extension at 72°C for 1.5 minutes, and then 35 cycles at 94°C for 1 minute, 58°C for 1 minute, and 72°C for 1.5 minutes. A final extension at 72°C for 10 minutes concluded the reaction. Two sets of primers were used to cover all the known breakpoints in both the *API2* and the *MALT1* genes³⁸⁻⁴¹ (Figure 1) and were used for PCR of all samples unless otherwise indicated. The first set of primers consisted of sense primer (API2-1, 5'-CTG GTG TGA ATG ACA AGG TC-3', nucleic acids 897-916, GenBank accession no. NM_001165) and antisense primer (MALT1-1, 5'-TAG TCA ATT CGT ACA CAT CC-3', nucleic acids 1124-1143, AB026118).³⁹ Primary PCR products were further amplified using nested primers: API2-2 (5'-ACA TTC TTT AAC TGG CCC TC-3', nucleic acids 1505-1524) and MALT1-2 (5'-CAA AGG CTG GTC AGT TGT TT-3', nucleic acids 1030-1049).³⁹ Amplified PCR products were analyzed by electrophoresis on 0.9% agarose gels and ethidium bromide staining. All PCR reactions were performed at least in duplicate.

A 256-bp fragment of the glucose-6-phosphate dehydrogenase (*G6PD*) gene was amplified in parallel as a control to verify RNA quality and RT-PCR efficiency for each sample, using sense primer 5'-GAG GCC GTG TAC ACC AAG ATG AT-3' and antisense primer 5'-AAT ATA GGG GAT GGG CTT GG-3'. Primers were chosen to flank a region containing introns 10 (104 bp) and 11 (105 bp) (GenBank X55448.1, M12996) so that the amplified product of contaminating DNA was distinguishable from that of cDNA.

To assess the sensitivity of RT-PCR for detection of the API2-MALT1 fusion transcript, cell suspensions of 2 gastric MALT lymphomas with different t(11;18)(q21;q21) were serially diluted with tonsillar lymphocytes. Cell mixtures, each containing a total of 2 \times 10⁶ cells but a variable

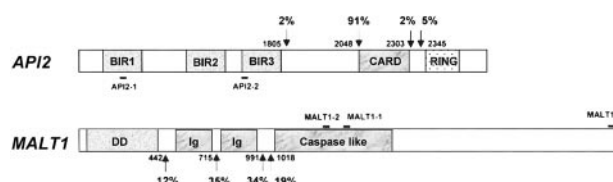


Figure 1. Schematic presentation of API2 and MALT1 gene structure and primer position. Known breakpoints are indicated by arrows, and nucleic acids are numbered according to cDNA sequence of the *API2* (GenBank, NM_001165) and *MALT1* genes (AB026118). The frequency of individual known breakpoints was given.³⁸⁻⁴² Solid bar indicates the position of primers used.

amount of tumor cells, were subjected to RNA isolation and RT-PCR for the *G6PD* and API2-MALT1 fusion transcript.

PCR products were purified using a Concert Rapid PCR Purification System (Life Technologies) and sequenced in both directions with nested primers using dRhodamine dye terminators and AmpliTaq DNA polymerase, FS, on an ABI Prism 377 sequencer (PE Applied Biosystems, Foster City, CA).

BCL10 immunohistochemistry

BCL10 was immunostained using a mouse monoclonal antibody (clone 151) on formalin-fixed and paraffin-embedded tissues as described previously.³⁴ Briefly, 4 μ m tissue sections were heat-retrieved for antigen in target retrieval solution pH 6.0 (Dako, Glostrup, Denmark) in a microwave oven for 25 to 35 minutes, depending on the size of the section. Sections were then incubated with anti-BCL10 antibody at 1:60 dilution for 1 hour followed by biotinylated rabbit antimouse antibody and peroxidase-conjugated ExtroAvidin (Sigma Chemical, St Louis, MO). Finally, the staining was visualized with 3, 3'-diaminobenzidine tetrahydrochloride (Kem-En-Tec A/S, Denmark) in H₂O₂.

Statistical analysis

Fisher exact and χ^2 tests were used to analyze the correlation between the clinical staging of lymphoma with t(11;18)(q21;q21) or BCL10 expression pattern and the association between t(11;18)(q21;q21) and BCL10 expression pattern.

Results

T(11;18)(q21;q21) is absent in *H pylori* gastritis

RT-PCR used for the detection of the API2-MALT1 fusion transcript was highly sensitive. In each of the 2 dilution experiments with MALT lymphomas harboring different t(11;18)(q21;q21), the API2-MALT1 fusion transcript was detectable when the t(11;18)(q21;q21)-positive cells were diluted down to a concentration of 1 in 10⁶ tonsillar cells using a single set of PCR primers (Figure 2A).

RT-PCR of the reference gene *G6PD* was successful in all 39 patients with gastritis, confirming adequate RNA extraction and cDNA synthesis. Despite this and the high sensitivity of RT-PCR for detection of the API2-MALT1 fusion transcript, none of the patients with gastritis were positive for t(11;18)(q21;q21).

T(11;18)(q21;q21) is associated with more advanced MALT lymphomas but is absent in mucosal DLBCL

As with the gastritis samples, RT-PCR of the *G6PD* gene was successful in all lymphoma tissues examined. The API2-MALT1

fusion transcript was detected in 25 of 72 (35%) low-grade MALT lymphomas (Figure 2B, Table 2) but in none of the 11 mucosal diffuse large B-cell lymphomas. All these positive cases were detected by the primary PCR. Secondary nested PCR did not increase the sensitivity for detection of t(11;18)(q21;q21).

The frequency of t(11;18)(q21;q21) in MALT lymphoma of various sites is shown in Table 1. Of those arising in the stomach, the largest group examined, the API2-MALT1 fusion transcript, was found in 19 of 56 (34%) samples. Among t(11;18)(q21;q21)-positive gastric MALT lymphomas, frozen tissues from the lymphoma involving lymph nodes, spleen, or small intestine were available in 6 cases. In each case, RT-PCR of these disseminated lesions showed an API2-MALT1 fusion product identically sized to that of their corresponding gastric lymphoma (Figure 2C, Table 2). Of the 3 cases with a large cell component within the B-cell follicle, 2 were t(11;18)(q21;q21) positive. However, the available frozen tumor tissues in these cases did not contain a prominent large cell component to allow examination of whether t(11;18)(q21;q21) was present in the transformed cells.

Of 56 low-grade gastric MALT lymphomas, the extent of tumor spread was assessed in 47 cases. As shown in Figure 3, t(11;18)(q21;q21) was associated with more advanced gastric MALT lymphomas: 2 of 23 (9%) tumors were confined to the gastric mucosa or submucosa, but 1 of 6 (17%) ($P < .01$; Fisher exact test) tumors invaded the muscular layer or serosa and 14 of 18 (78%) ($P < .0001$; χ^2 test) tumors disseminated beyond the stomach.

Sequencing analysis of the RT-PCR products confirmed the presence of an API2-MALT1 fusion transcript in all positive cases. The breakpoint was invariable at nucleotide 2048 (intron 7) on the *API2* gene (NM_001165) but varied at nucleotide 715 (intron 4, 15 of 25, 60%), 991 (intron 7, 7 of 25, 28%) or 1018 (intron 8, 3 of 25, 12%) on the *MALT1* gene (AB026118),⁴³ fusing the N-terminal of the *API2* gene, which contains 3 intact BIR domains, to variable carboxyl terminal regions of the *MALT1* gene (Table 2).

BCL10 nuclear expression is associated with advanced MALT lymphomas

BCL10 protein expression was investigated in 53 MALT lymphomas. Twenty-eight cases showed BCL10 expression predominantly in the nuclei of most tumor cells, and the remaining cases showed cytoplasmic BCL10 expression. As with t(11;18)(q21;q21), BCL10 nuclear expression was also associated with advanced MALT lymphomas. Of 41 gastric MALT lymphomas in which the lymphoma staging was available, nuclear BCL10 expression was found in 7 of 19 (37%) tumors confined to the mucosa or the submucosa, 3 of 7 (43%) cases in which tumor invaded to muscular

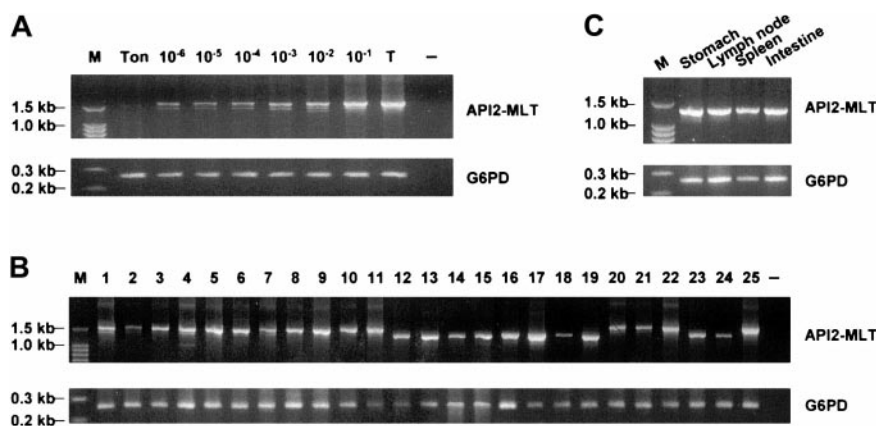


Figure 2. Detection of t(11;18)(q21;q21) by RT-PCR of the API2-MALT1 fusion transcript. (A) Sensitivity of RT-PCR for detection of the API2-MALT1 fusion transcript. Tumor cells harboring t(11;18)(q21;q21) were serially diluted with tonsillar cells and were then subjected to RNA extraction and RT-PCR. Using the first set of PCR primers (API2-1 and MALT1), the API2-MALT1 fusion transcript was detectable when the t(11;18)(q21;q21)-positive cells were diluted down to a concentration of 1 in 10⁶ tonsillar cells. M, molecular weight marker; Ton, tonsillar cell; 10⁻⁶ to 10⁻¹, various tumor cell concentrations; T, undiluted tumor cells; -, negative control. (B) T(11;18)(q21;q21)-positive MALT lymphoma. The number corresponds to the case number in Table 2. -, negative control. (C) Case 16 shows an identically sized API2-MALT1 product between the primary gastric MALT lymphoma and the tumor-involved lymph node, spleen, and small intestine.

Table 2. Summary of clinicopathologic and molecular data of t(11;18)(q21;q21)-positive mucosa-associated lymphoid tissue lymphomas

| Patients | Age | Sex | Origin | Lymphoma staging* | BCL10 nuclear expression | Breaking point‡ | |
|----------|-----|-----|-----------------|--|--------------------------|-----------------|-------|
| | | | | | | API2 | MALT1 |
| 1 | 41 | M | Stomach | III (spleen, lymph node)† | + | 2048 | 715 |
| 2 | 49 | F | Stomach | IIE1 (lymph node) | NA | 2048 | 715 |
| 3 | 42 | F | Stomach | IIE1 (lymph node) | + | 2048 | 715 |
| 4 | 44 | M | Stomach | IIE1 | + | 2048 | 715 |
| 5 | 47 | M | Stomach | IIE | + | 2048 | 715 |
| 6 | 51 | M | Stomach | IE | + | 2048 | 715 |
| 7 | 54 | M | Stomach | IIE | NA | 2048 | 715 |
| 8 | 61 | M | Stomach | IIE2 | + | 2048 | 715 |
| 9 | 62 | M | Stomach | IE | + | 2048 | 715 |
| 10 | 65 | M | Stomach | IIE1 | + | 2048 | 715 |
| 11 | 72 | M | Stomach | III (spleen) | NA | 2048 | 715 |
| 12 | NA | M | Stomach | III | + | 2048 | 991 |
| 13 | 39 | M | Stomach | III (spleen, lymph node) | + | 2048 | 991 |
| 14 | 44 | M | Stomach | IV | + | 2048 | 991 |
| 15 | 49 | M | Stomach | IE | + | 2048 | 991 |
| 16 | 60 | F | Stomach | IV (small intestine, spleen, lymph node) | + | 2048 | 991 |
| 17 | 60 | M | Stomach | IE | + | 2048 | 991 |
| 18 | 44 | F | Stomach | IE | + | 2048 | 1018 |
| 19 | 63 | M | Stomach | III | + | 2048 | 1018 |
| 20 | 49 | M | Lung | NA | NA | 2048 | 715 |
| 21 | 66 | F | Lung | NA | + | 2048 | 715 |
| 22 | 49 | F | Lung | NA | + | 2048 | 715 |
| 23 | 46 | M | Lung | NA | NA | 2048 | 991 |
| 24 | 68 | M | Small intestine | IE | + | 2048 | 1018 |
| 25 | 53 | M | Salivary gland | NA | + | 2048 | 715 |

Other abbreviations are explained in Table 1.

Patients 11 and 18 had a large cell component within the B-cell follicle.

NA, not applicable.

*Ann Arbor-Musshoff staging system for extranodal lymphoma.

†Tissues available for RT-PCR and showing fusion transcripts identical to their corresponding primary tumors are indicated in parentheses.

‡Nucleic acids denote breakpoints according to GenBank NM_001165 for API2 and AB026118 for MALT1.

layer or serosa, and 14 of 15 (93%) cases in which tumor disseminated beyond the stomach ($P < .005$; χ^2 test) (Figure 3). All 8 mucosal DLBCLs examined showed cytoplasmic but not nuclear BCL10 expression.

MALT lymphoma with t(11;18)(q21;q21) expresses nuclear BCL10

In total, 50 cases were examined for both t(11;18)(q21;q21) and BCL10 expression pattern. BCL10 nuclear expression was significantly higher in t(11;18)(q21;q21)-positive (20 of 20, 100%) than in t(11;18)(q21;q21)-negative MALT lymphomas (7 of 30, 23%) (Fisher exact test, $P = .426 \times 10^{-8}$) (Figure 4).

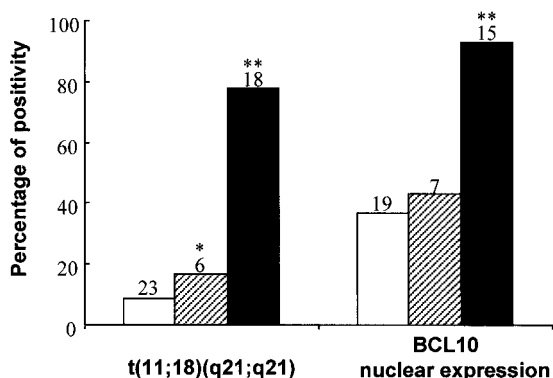


Figure 3. Correlation between clinical staging of gastric MALT lymphoma and t(11;18)(q21;q21) and BCL10 nuclear expression. The number of cases in individual subgroups is indicated at the top of the corresponding histogram. □, submucosa; ▨, muscle and serosa; ■, spread beyond stomach; * $P < .01$; ** $P < .005$.

In view of the significant association between t(11;18)(q21;q21) and nuclear BCL10 expression, we re-examined the 7 cases showing nuclear BCL10 expression but not t(11;18)(q21;q21) to ascertain whether the absence of the translocation in these cases was due to a failure of detection by the primer set used. A new MALT primer (MALT1-3, 5'-TTT TTC AGA AAT TCT GAG CCT G-3), which targets the 3' end of its coding region, and API2-1 primer were used for PCR (Figure 1). All 7 cases consistently showed absence of the API2-MALT1 fusion transcript despite successful amplification of t(11;18)(q21;q21)-positive controls.

Of these 7 cases, 2 showed high BCL10 nuclear expression similar to that seen in t(1;14)(p22;q32)-positive MALT lymphomas.³⁴ However, insufficient frozen tumor tissue was available for Southern blot analysis to test whether these cases harbored t(1;14)(p22;q32).

Discussion

Chromosomal translocations associated with B-cell lymphomas commonly involve the immunoglobulin locus, most likely occur during the VDJ recombination process, and are believed to be the primary events in lymphomagenesis.⁴⁴ At least some of these translocations are known to occur in prelymphomatous lesions. For example, t(14;18)(q32;q21), which is associated with up to 90% of follicular lymphomas, has also been found in approximately 50% of lymphoid hyperplasias and peripheral blood lymphocytes from healthy controls.⁴⁵⁻⁴⁷ To examine whether t(11;18)(q21;q21), a frequent translocation in MALT lymphoma,³⁸⁻⁴¹ is present in

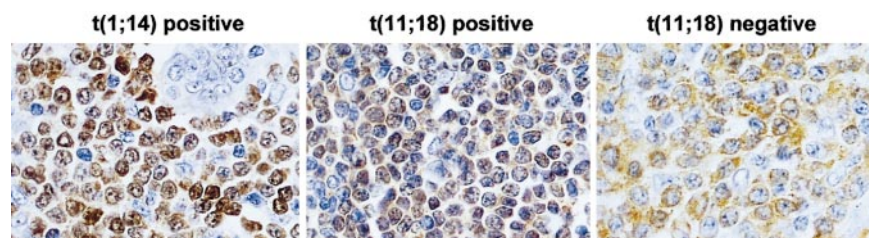


Figure 4. Comparison of BCL10 protein expression between MALT lymphomas with and without t(11;18)(q21;q21). T(11;18)(q21;q21)-positive case shows BCL10 (brown) nuclear expression in most of tumor cells, whereas the negative case displays cytoplasmic BCL10 expression. The level of BCL10 nuclear expression in t(11;18)(q21;q21)-positive cells is much lower than that in t(1;14)(p22;q32)-positive cells. Original magnification, $\times 650$. Sections were counterstained with hematoxylin.

prelymphomatous lesions, we examined *H pylori*-associated gastritis from cases in Italy, where the frequency of *H pylori*-associated gastric MALT lymphoma is high.⁴⁸ Our results indicate that t(11;18)(q21;q21) is absent or at least not a frequent event in *H pylori*-associated gastritis.

The oncogenic role of t(11;18)(q21;q21) in MALT lymphoma development is further underpinned by the finding that the translocation is associated with advanced gastric tumors, particularly those showing tumor spread beyond the stomach. These results are well in agreement with the observation of a high frequency (75%) of t(11;18)(q21;q21) in gastric MALT lymphomas that were resistant to *H pylori* eradication therapy but not in those that responded to the therapy.^{49,50} It has been shown that gastric MALT lymphomas not responsive to *H pylori* therapy are those with invasion of deeper layers of the gastric wall and involvement of regional lymph nodes, whereas responsive tumors are generally those confined to the gastric mucosa.^{8,9} Thus, t(11;18)(q21;q21) is a molecular marker for aggressive gastric MALT lymphomas and those not responsive to *H pylori* therapy.

In view of the significant role of t(11;18)(q21;q21) during MALT lymphoma progression, it is intriguing that the translocation has not been found in transformed MALT lymphoma.³⁸⁻⁴¹ Although mucosal DLBCL may arise de novo, at least a proportion of mucosal DLBCLs are transformed from low-grade MALT lymphomas.^{10,11} It is unlikely that such an important translocation is lost during high-grade transformation. Alternatively, t(11;18)(q21;q21)-positive MALT lymphoma is a distinct subgroup of MALT lymphoma that does not undergo or rarely undergoes high-grade transformation. There are clear differences in gross chromosomal abnormalities between t(11;18)(q21;q21)-positive and -negative MALT lymphomas: the former do not usually show any chromosomal aberrations other than t(11;18)(q21;q21), whereas the latter, including lymphomas with t(1;14)(p22;q32), display various abnormalities including recurrent and rare aberrations.¹⁹⁻²¹ It remains to be determined whether further differences in histology, immunophenotype, and genetic abnormalities such as genetic instability exist between the 2 groups.

The other significant finding of the present study is the strong correlation between t(11;18)(q21;q21) and BCL10 nuclear expression. It is possible that this correlation was simply the result of their independent association with advanced MALT lymphomas. Alternatively, the oncogenic activity of t(11;18)(q21;q21) may be associated with nuclear BCL10 expression. This is indirectly supported by the low frequency of nuclear BCL10 expression in follicular lymphoma and DLBCL,³⁴ in which t(11;18)(q21;q21) is absent.³⁸⁻⁴² More important, both BCL10 and the API2-MALT1 fusion product activate NF κ B, and BCL10 binds MALT1 and some

of the API2-MALT1 products.^{22,37} However, the precise mechanisms underlying the molecular interaction between BCL10 and API2-MALT1 and the functional consequence of such an interaction remain to be investigated.

It is interesting to note that 7 t(11;18)(q21;q21)-negative cases also expressed nuclear BCL10. Nuclear BCL10 expression in 2 cases could be attributed to the presence of t(1;14)(p22;q32) because the BCL10 staining pattern resembled that seen in MALT lymphomas with the translocation.³⁴ The factors underlying nuclear BCL10 expression in the remaining cases are not clear. However, involvement of 11q21 by translocations other than t(11;18)(q21;q21) has been reported in lymphoid malignancies.⁵⁴ Studies are in progress to examine whether these cases harbor API2 rearrangement.

Despite strong evidence of an important role for t(11;18)(q21;q21) in MALT lymphoma progression, the molecular mechanisms underlying its oncogenic activity remain elusive. All the breakpoints in the API2 gene occur between the third BIR domain and the C-terminal RING, with 91% occurring just upstream of the CARD.³⁸⁻⁴¹ In contrast, the breakpoints in the MALT1 gene are more variable.³⁸⁻⁴¹ Thus, the resultant API2-MALT1 fusion transcripts always comprise a truncated API2 with 3 intact BIR domains but without the C-terminal RING or without both the middle CARD and C-terminal RING in most. The characteristic disruption of the API2 gene by the translocation strongly suggests that truncated API2 with retention of the BIR domain, a critical element for antiapoptotic activity, is required for oncogenic activity. This is supported by the finding that the RING domain of cIAP1 and API2 negatively regulates the antiapoptotic activity of their BIR domains.⁵¹ The negative effect of the RING finger on BIR function may be associated with its ability to promote auto-ubiquitination and degradation.⁵¹⁻⁵³ Replacement of the C-terminal of API2 with the C-terminal of MALT1 by the fusion product would release the intrinsic antiapoptotic activity of the BIR domain and, therefore, make the new molecule antiapoptotic. The incoming MALT1 C-terminal may further enhance the antiapoptotic activity of the BIR domain by an unknown mechanism. It has been demonstrated that the API2-MALT1 fusion product, but not API2 or MALT1 alone, was capable of activating NF κ B,³⁷ further suggesting the importance of the C-terminal MALT1 in the oncogenic activity of the fusion product.

Acknowledgment

We thank Dr Tim C. Diss for critical reading of the manuscript.

References

- Du MQ, Isaacson PG. Recent advances in our understanding of the biology and pathogenesis of gastric mucosa-associated lymphoid tissue (MALT) lymphoma. *Forum (Genova)*. 1998;8:162-173.
- Wotherspoon AC, Ortiz Hidalgo C, Falzon MR, Isaacson PG. *Helicobacter pylori*-associated gastritis and primary B-cell gastric lymphoma. *Lancet*. 1991;338:1175-1176.
- Parsonnet J, Hansen S, Rodriguez L, et al. *Helicobacter pylori* infection and gastric lymphoma. *N Engl J Med*. 1994;330:1267-1271.
- Hussell T, Isaacson PG, Crabtree JE, Spencer J.

- The response of cells from low-grade B-cell gastric lymphomas of mucosa-associated lymphoid tissue to *Helicobacter pylori*. *Lancet*. 1993;342:571-574.
5. Hussell T, Isaacson PG, Crabtree JE, Spencer J. *Helicobacter pylori*-specific tumour-infiltrating T cells provide contact dependent help for the growth of malignant B cells in low-grade gastric lymphoma of mucosa-associated lymphoid tissue. *J Pathol*. 1996;178:122-127.
 6. Wotherspoon AC, Dogliani C, Diss TC, et al. Regression of primary low-grade B-cell gastric lymphoma of mucosa-associated lymphoid tissue type after eradication of *Helicobacter pylori*. *Lancet*. 1993;342:575-577.
 7. Neubauer A, Thiede C, Morgner A, et al. Cure of *Helicobacter pylori* infection and duration of remission of low-grade gastric mucosa-associated lymphoid tissue lymphoma. *Natl Cancer Inst*. 1997;89:1350-1355.
 8. Sackmann M, Morgner A, Rudolph B, et al. Regression of gastric MALT lymphoma after eradication of *Helicobacter pylori* is predicted by endosonographic staging. *Gastroenterology*. 1997;113:1087-1090.
 9. Ruskone Fourmestraux A, Lavergne-Slove A. Predictive factors for regression of gastric MALT lymphoma after anti-*Helicobacter pylori* treatment. *Gut*. 2001;48:297-303.
 10. Chan JK, Ng CS, Isaacson PG. Relationship between high-grade lymphoma and low-grade B-cell mucosa-associated lymphoid tissue lymphoma (MALT) of the stomach. *Am J Pathol*. 1990;136:1153-1164.
 11. Peng H, Du M, Diss TC, Isaacson PG, Pan L. Genetic evidence for a clonal link between low- and high-grade components in gastric MALT B-cell lymphoma. *Histopathology*. 1997;30:425-429.
 12. Hussell T, Isaacson PG, Spencer J. Proliferation and differentiation of tumour cells from B-cell lymphoma of mucosa-associated lymphoid tissue in vitro. *J Pathol*. 1993;169:221-227.
 13. Du MQ, Diss TC, Xu CF, Peng HZ, Isaacson PG, Pan LX. Ongoing mutation in MALT lymphoma immunoglobulin VH gene suggests that antigen stimulation plays a role in the clonal expansion. *Leukemia*. 1996;10:1190-1197.
 14. Du MQ, Xu CF, Diss TC, et al. Intestinal dissemination of gastric mucosa-associated lymphoid tissue lymphoma. *Blood*. 1996;88:4445-4451.
 15. Peng H, Chen G, Du M, Singh N, Isaacson PG, Pan L. Replication error phenotype and p53 gene mutation in lymphomas of mucosa-associated lymphoid tissue. *Am J Pathol*. 1996;148:643-648.
 16. Wotherspoon AC, Finn TM, Isaacson PG. Trisomy 3 in low-grade B-cell lymphomas of mucosa-associated lymphoid tissue. *Blood*. 1995;85:2000-2004.
 17. Du M, Peng H, Singh N, Isaacson PG, Pan L. The accumulation of p53 abnormalities is associated with progression of mucosa-associated lymphoid tissue lymphoma. *Blood*. 1995;86:4587-4593.
 18. Neumeister P, Hoefler G, Beham Schmid C, et al. Deletion analysis of the p16 tumor suppressor gene in gastrointestinal mucosa-associated lymphoid tissue lymphomas. *Gastroenterology*. 1997;112:1871-1875.
 19. Wotherspoon AC, Pan LX, Diss TC, Isaacson PG. Cytogenetic study of B-cell lymphoma of mucosa-associated lymphoid tissue. *Cancer Genet Cytogenet*. 1992;58:35-38.
 20. Ott G, Katzenberger T, Greiner A, et al. The t(11;18)(q21;q21) chromosome translocation is a frequent and specific aberration in low-grade but not high-grade malignant non-Hodgkin's lymphomas of the mucosa-associated lymphoid tissue (MALT-) type. *Cancer Res*. 1997;57:3944-3948.
 21. Auer IA, Gascoyne RD, Connors JM, et al. t(11;18)(q21;q21) is the most common translocation in MALT lymphomas. *Ann Oncol*. 1997;8:979-985.
 22. Willis TG, Jadayel DM, Du MQ, et al. Bcl10 is involved in t(11;18)(p22;q32) of MALT B-cell lymphoma and mutated in multiple tumor types. *Cell*. 1999;96:35-45.
 23. Zhang Q, Siebert R, Yan M, et al. Inactivating mutations and overexpression of BCL10, a caspase recruitment domain-containing gene, in MALT lymphoma with t(11;18)(p22;q32). *Nat Genet*. 1999;22:63-68.
 24. Dierlamm J, Baens M, Wlodarska I, et al. The apoptosis inhibitor gene *API2* and a novel 18q gene, *MLT*, are recurrently rearranged in the t(11;18)(q21;q21) associated with mucosa-associated lymphoid tissue lymphomas. *Blood*. 1999;93:3601-3609.
 25. Akagi T, Motegi M, Tamura A, et al. A novel gene, *MALT1* at 18q21, is involved in t(11;18)(q21;q21) found in low-grade B-cell lymphoma of mucosa-associated lymphoid tissue. *Oncogene*. 1999;18:5785-5794.
 26. Morgan JA, Yin Y, Borowsky AD, et al. Breakpoints of the t(11;18)(q21;q21) in mucosa-associated lymphoid tissue (MALT) lymphoma lie within or near the previously undescribed gene MALT1 in chromosome 18. *Cancer Res*. 1999;59:6205-6213.
 27. Costanzo A, Guet C, Vito P. c-E10 is a caspase-recruiting domain-containing protein that interacts with components of death receptors signaling pathway and activates nuclear factor-kappaB. *J Biol Chem*. 1999;274:20127-20132.
 28. Yan M, Lee J, Schilbach S, Goddard A, Dixit V. mE10, a novel caspase recruitment domain-containing proapoptotic molecule. *J Biol Chem*. 1999;274:10287-10292.
 29. Srinivasula SM, Ahmad M, Lin JH, et al. CLAP, a novel caspase recruitment domain-containing protein in the tumor necrosis factor receptor pathway, regulates NF- κ B activation and apoptosis. *J Biol Chem*. 1999;274:17946-17954.
 30. Koseki T, Inohara N, Chen S, et al. CIPER, a novel NF- κ B-activating protein containing a caspase recruitment domain with homology to Herpesvirus-2 protein E10. *J Biol Chem*. 1999;274:9955-9961.
 31. Thome M, Martinon F, Hofmann K, et al. Equine herpesvirus-2 E10 gene product, but not its cellular homologue, activates NF- κ B transcription factor and c-Jun N-terminal kinase. *J Biol Chem*. 1999;274:9962-9968.
 32. Yoneda T, Imaizumi K, Maeda M, et al. Regulatory mechanisms of TRAF2-mediated signal transduction by BCL10, a MALT lymphoma-associated protein. *J Biol Chem*. 2000;275:11114-11120.
 33. Du MQ, Peng HZ, Liu H, et al. BCL10 mutation in lymphoma. *Blood*. 2000;95:3885-3890.
 34. Ye H, Dogan A, Karran L, et al. BCL10 expression in normal and neoplastic lymphoid tissue: nuclear localization in MALT lymphoma. *Am J Pathol*. 2000;157:1147-1154.
 35. Deveraux QL, Reed JC. IAP family proteins—suppressors of apoptosis. *Genes Dev*. 1999;13:239-252.
 36. Roy N, Deveraux QL, Takahashi R, Salvesen GS, Reed JC. The c-IAP-1 and c-IAP-2 proteins are direct inhibitors of specific caspases. *EMBO J*. 1997;16:6914-6925.
 37. Uren GA, O'Rourke K, Aravind L, et al. Identification of paracaspases and metacaspases: two ancient families of caspase-like proteins, one of which plays a key role in MALT lymphoma. *Mol Cell*. 2000;6:961-967.
 38. Baens M, Maes B, Steyls A, Geboes K, Marynen P, De Wolf-Peeters C. The product of the t(11;18), an API2-MLT fusion, marks nearly half of gastric MALT type lymphomas without large cell proliferation. *Am J Pathol*. 2000;156:1433-1439.
 39. Motegi M, Yonezumi M, Suzuki H, et al. API2-MALT1 chimeric transcripts involved in mucosa-associated lymphoid tissue type lymphoma predict heterogeneous products. *Am J Pathol*. 2000;156:807-812.
 40. Nakamura T, Nakamura S, Yonezumi M, et al. *Helicobacter pylori* and the t(11;18)(q21;q21) translocation in gastric low-grade B-cell lymphoma of mucosa-associated lymphoid tissue type. *Jpn J Cancer Res*. 2000;91:301-309.
 41. Dierlamm J, Baens M, Stefanova-Ouzounova M, et al. Detection of t(11;18)(q21;q21) by interphase fluorescence in situ hybridization using API2 and MLT specific probes. *Blood*. 2000;96:2215-2218.
 42. Kalla J, Stilgenbauer S, Schaffner C, et al. Heterogeneity of the API2-MALT1 gene rearrangement in MALT-type lymphoma. *Leukemia*. 2000;14:1967-1974.
 43. Baens M, Steyls A, Dierlamm J, De Wolf-Peeters C, Marynen P. Structure of the MLT gene and molecular characterization of the genomic breakpoint junctions in the t(11;18)(q21;q21) of marginal zone B-cell lymphomas of MALT type. *Genes Chromosomes Cancer*. 2000;29:281-291.
 44. Willis TG, Dyer MJ. The role of immunoglobulin translocations in the pathogenesis of B-cell malignancies. *Blood*. 2000;96:808-822.
 45. Aster JC, Kobayashi Y, Shiota M, Mori S, Sklar J. Detection of the t(14;18) at similar frequencies in hyperplastic lymphoid tissues from American and Japanese patients. *Am J Pathol*. 1992;141:291-299.
 46. Limpens J, de Jong D, van Krieken JH, et al. Bcl-2/JH rearrangements in benign lymphoid tissues with follicular hyperplasia. *Oncogene*. 1991;6:2271-2276.
 47. Liu Y, Hernandez AM, Shibata D, Cortopassi GA. BCL2 translocation frequency rises with age in humans. *Proc Natl Acad Sci U S A*. 1994;91:8910-8914.
 48. Dogliani C, Wotherspoon AC, Moschini A, de Boni M, Isaacson PG. High incidence of primary gastric lymphoma in northeastern Italy. *Lancet*. 1992;339:834-835.
 49. Liu H, Ruskone Fourmestraux A, Lavergne-Slove A, et al. Gastric MALT lymphoma with t(11;18)(q21;q21) fails to respond to *Helicobacter pylori* eradication therapy. *Lancet*. 2001;357:39-40.
 50. Alpen B, Neubauer A, Dierlamm J, et al. Translocation t(11;18) absent in early gastric marginal zone B-cell lymphoma of MALT type responding to eradication of *Helicobacter pylori* infection. *Blood*. 2000;95:4014-4015.
 51. Clem RJ, Sheu TT, Richter BW, et al. c-IAP1 is cleaved by caspases to produce a pro-apoptotic c-terminal fragment. *J Biol Chem*. 2001;276:7602-7608.
 52. Hay BA, Wassarman DA, Rubin GM. *Drosophila* homologs of baculovirus inhibitor of apoptosis proteins function to block cell death. *Cell*. 1995;83:1253-1262.
 53. Yang Y, Fang S, Jensen JP, Weissman AM, Ashwell JD. Ubiquitin protein ligase activity of IAPs and their degradation in proteasomes in response to apoptotic stimuli. *Science*. 2000;288:874-877.
 54. Mitelman Database of Chromosome Aberrations in Cancer. Mitelman F, Johansson B, and Mertens F, eds. <http://cgap.nci.nih.gov/Chromosomes/Mitelman>. Accessed June 6, 2001.

Research letters

Resistance of t(11;18) positive gastric mucosa-associated lymphoid tissue lymphoma to *Helicobacter pylori* eradication therapy

Hongxiang Liu, Agnes Ruskon-Fourmestraux, Anne Lavergne-Slove, Hongtao Ye, Thierry Molina, Yoram Bouhnik, Rifat A Hamoudi, Tim C Diss, Ahmet Dogan, Francis Megraud, Jean Claude Rambaud, Ming-Qing Du, Peter G Isaacson

20–30% of gastric mucosa-associated lymphoid tissue (MALT) lymphoma associated with *Helicobacter pylori* do not regress after antibiotic therapy. Regression can be assessed only by extended follow-up. To assess whether t(11;18, q21;q21), which results in a chimeric transcript between the *API2* and *MLT* genes, predicts lymphoma resistance to antibiotic therapy, we screened for the fusion transcript with RT-PCR in ten responsive and 12 non-responsive gastric MALT lymphomas. The *API2-MLT* transcript was detected in nine (75%) of 12 patients non-responsive to antibiotic therapy but not in responsive patients. Most *H pylori*-associated gastric MALT lymphomas that do not respond to antibiotic therapy are associated with t(11;18, q21;q21).

Gastric B-cell lymphoma of mucosa-associated lymphoid tissue (MALT) arises from mucosal lymphoid tissue that is normally acquired as a reaction to *Helicobacter pylori* infection. The presence of the organism has a profound effect on the lymphoma. Growth of the lymphoma B cells in culture can be stimulated by the addition of heat-killed strain-specific *H pylori*. Surprisingly, lymphoma B-cell immunoglobulin does not recognise *H pylori* antigens but rather various autoantigens. The intratumoral T cells are *H pylori* specific and provide contact-mediated help for the growth of the neoplastic B cells.

Eradication of *H pylori* with antibiotics leads to regression and cure of the lymphoma in 75% of cases.^{1,2} After *H pylori* eradication, regression time varies from a few weeks to 18 months, but histology of the gastric biopsy samples cannot predict which lymphomas will respond and which will be resistant to antibiotic therapy. Thus, repeated endoscopy with gastric biopsies is necessary to assess the reaction of the

lymphoma to the antibiotic therapy before making the decision to give other conventional treatments in resistant cases.

Findings from cytogenetic studies of gastric MALT lymphoma have shown t(11;18, q21;q21) in about 30% of cases. The breakpoint of this translocation involves rearrangement of the *API2* gene on chromosome 11 and a novel gene, *MLT*, on chromosome 18.³ Translocation results in a chimeric transcript with the amino terminal of *API2* fusing with the carboxyl terminal of *MLT*, which can be detected by RT-PCR. The *API2-MLT* fusion is thought to give a survival advantage to MALT lymphoma cells. This theory raises the question of whether t(11;18, q21;q21) would account for *H pylori*-independent survival or growth of gastric MALT lymphoma and could, therefore, predict the resistance of the lymphoma to *H pylori* eradication therapy, thus enabling early identification of patients who require chemotherapy.

As part of the French prospective multicentre study of the Groupe d' Etude des Lymphomes Digestifs, we obtained fresh-frozen gastric biopsy samples taken at the time of diagnosis from 22 patients with clinically staged gastric MALT lymphoma and known *H pylori* status (table) who were subsequently treated with antibiotics. After successful eradication of the organism, we followed up patients by repeated gastric endoscopy and biopsy for 4.5–60.0 months. Histological changes were carefully reviewed by the panel of pathologists' committee without knowledge of molecular data.

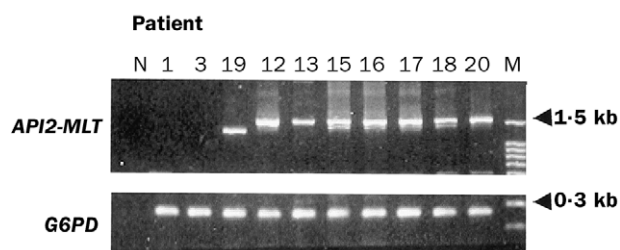
Gastric lymphoma regressed completely after eradication of *H pylori* in nine patients within 3.0–16.0 months, and partly in one patient after 1.5 months, but showed no sign of

| Patient number | Sex | Age (years) | <i>H pylori</i> serology/histology | Stage* | Clonality | Remission after antibiotic therapy | Months between <i>H pylori</i> eradication and remission or other treatment | Other treatment | t(11;18) <i>API2/MLT</i> † |
|----------------|-----|-------------|------------------------------------|------------------|-----------|------------------------------------|---|-----------------|----------------------------|
| 1 | F | 47 | +/+ | I _E | ND | Partial | 1.5 | .. | .. |
| 2 | F | 62 | ND/+ | ND | S | Complete | 3 | .. | .. |
| 3 | F | 71 | +/+ | I _E | S | Complete | 6 | .. | .. |
| 4 | F | 68 | -/+ | I _E | M | Complete | 6 | .. | .. |
| 5 | M | 76 | ND/+ | ND | M | Complete | 9 | .. | .. |
| 6 | M | 70 | +/- | I _E | M | Complete | 11 | .. | .. |
| 7 | F | 55 | +/+ | I _E | ND | Complete | 12 | .. | .. |
| 8 | M | 64 | +/+ | I _E | M | Complete | 12 | .. | .. |
| 9 | F | 25 | +/+ | I _E | S | Complete | 13 | .. | .. |
| 10 | M | 46 | +/+ | I _E | M | Complete | 16 | .. | .. |
| 11 | M | 60 | +/+ | I _E | M | No change | 4.5 | Gastrectomy | .. |
| 12 | M | 54 | -/+ | II _E | M | No change | 5 | Gastrectomy | 2048/715 |
| 13 | F | 62 | +/+ | IV _E | M | No change | 6 | Gastrectomy | 2048/715 |
| 14 | F | 62 | +/+ | I _E | S | No change | 8 | Gastrectomy | .. |
| 15 | M | 65 | +/+ | II _{E1} | M | No change | 10 | Gastrectomy | 2048/715 |
| 16 | M | 61 | -/+ | II _{E2} | M | No change | 10 | Gastrectomy | 2048/715 |
| 17 | M | 47 | +/+ | II _E | S | No change | 12 | Gastrectomy | 2048/715 |
| 18 | M | 44 | +/+ | II _{E1} | M | No change | 12 | Gastrectomy | 2048/715 |
| 19 | M | 49 | -/+ | I _E | M | No change | 12.5 | Gastrectomy | 2048/991 |
| 20 | M | 62 | +/+ | I _E | M | No change | 19 | Gastrectomy | 2048/715 |
| 21 | M | 43 | +/+ | I _E | M | No change | 27 | Gastrectomy | .. |
| 22 | M | 42 | +/+ | II _E | M | No change | 60 | Gastrectomy | 2048/715 |

ND=not done, S=smear, M=monoclonal pattern (monoclonal band can be seen in 80% of MALT lymphoma by PCR-based analysis of rearranged Ig gene heavy-chain genes).

*Ann Arbor staging system; †number denotes the breakpoint in *API2* and *MLT* according to their DNA sequence (GeneBank Accession number: *API2*, NM_0011165; *MLT*, AB026118).

t(11;18, q21;q21) in *H pylori* eradication responsive and non-responsive gastric MALT lymphomas



Detection of t(11;18, q21;q21) by RT-PCR in gastric MALT lymphoma

N=negative control, M=DNA marker.

endoscopic and histological changes in the remaining 12 patients. Of these 12 patients, eight were followed up for 10.0–60.0 months, judged to be resistant to *H pylori* eradication, and subsequently treated by gastrectomy. The remaining four patients were followed up for 4.5–8.0 months before gastrectomy because of tumour growth or complications (haemorrhage), and were tentatively assumed to be non-responsive to *H pylori* eradication.

RNA was extracted from the primary diagnostic biopsy sample from each patient and also from gastrectomy samples from seven patients with RNeasy Mini Kit (QIAGEN, Crawley, UK). cDNA was synthesised with oligo-dT primers using SUPERSRIPT First-Strand Synthesis System (GIBCO-BRL, Paisley, UK). PCR for the *API2-MLT* fusion transcript was done with two sets of primers (*API2* 5'-CTGGTGTGAATGACAAGGTC-3' with either *MLT1* 5'-TAGTCAATTTCGTACACATCC-3' or *MLT2* 5'-CAAAGGCTGGTCAGTTGTTT-3') in separate reactions, which would detect most known t(11;18, q21;q21) breakpoints. PCR products were sequenced further to identify the breakpoint. We did RT-PCR for glucose-6-phosphate dehydrogenase gene (sense strand primer 5'GAGGCCGTGTACACCAAGAT3'; anti-sense strand primer 5AATATAGGGGATGGGCTTGG3') for every patient to control for template quality. Clonality was assessed by PCR analysis of the rearranged immunoglobulin heavy-chain genes for every patient.

None of the samples from patients responding to antibiotic therapy contained t(11;18, q21;q21). This finding is in accordance with the report by Alpen and colleagues,⁴ in which the translocation was not detected in 18 gastric MALT lymphomas responsive to *H pylori* therapy. By contrast, nine (75%) of the 12 antibiotic-resistant patients were positive for the translocation (table, figure), which suggests that the *API2-MLT* fusion protein might confer *H pylori*-independent survival, or growth, of gastric MALT lymphoma. Seven of the nine positive patients were at stage II_e or higher, which also suggests that t(11;18, q21;q21) is associated with more advanced stages of the disease.

Clearly, other genes might lead to a small number of t(11;18, q21;q21) gastric MALT lymphoma patients being non-responsive to *H pylori* eradication. Another cytogenetic abnormality, t(1;14, p22;q32), occurs infrequently in MALT-type lymphoma, and confers *H pylori*-independent growth of tumour cells. The translocation deregulates a novel gene, *BCL10*, which is proapoptotic. Mutations in *BCL10* result in loss of proapoptotic activity but gain of oncogenic potential, and have been found in three (27%) of 11 gastric MALT lymphomas that are resistant to *H pylori* eradication.⁵ Whether t(11;18, q21;q21) and *BCL10* mutations are mutually exclusive in gastric MALT lymphomas non-responsive to *H pylori* therapy is unknown.

If confirmed on a large cohort of patients, detection of t(11;18, q21;q21) in gastric biopsies of MALT-type lymphoma will identify most cases that will not respond to

antibiotic eradication of *H pylori*. This finding should be a great help to clinicians managing patients with non-responsive MALT-type lymphoma, and obviate the need for extended follow-up with repeated gastric endoscopy and biopsy. Detection of the translocation can be done in molecular biology laboratories, provided that fresh tissue has been retained. We are currently investigating methods for detection of t(11;18, q21;q21) in paraffin-embedded material in our laboratory.

We thank F Maitre, F Piard, A de Mascarel, J Audouin, L Bedenne, M Salmeron, J L Legoux, M C Copin, and J M Jouve of the Groupe d'Etude des Lymphomes Digestifs for their contribution of the samples used for this study.

- 1 Wotherspoon AC, Dogliani C, Diss TC, et al. Regression of primary low-grade B-cell gastric lymphoma of mucosa-associated lymphoid tissue type after eradication of *Helicobacter pylori*. *Lancet* 1993; **342**: 575–77.
- 2 Thiede C, Wundisch T, Neubauer B, et al. Eradication of *Helicobacter pylori* and stability of remissions in low-grade gastric B-cell lymphomas of the mucosa-associated lymphoid tissue: results of an ongoing multicenter trial. *Recent Results Cancer Res* 2000; **156**: 125–33.
- 3 Dierlamm J, Baens M, Wlodarska I, et al. The apoptosis inhibitor gene *API2* and a novel 18q gene, *MLT*, are recurrently rearranged in the t(11;18)(q21;q21) associated with mucosa-associated lymphoid tissue lymphomas. *Blood* 1999; **93**: 3601–09.
- 4 Alpen B, Neubauer A, Dierlamm J, et al. Translocation t(11;18) absent in early gastric marginal zone B-cell lymphoma of MALT type responding to eradication of *Helicobacter pylori* infection. *Blood* 2000; **95**: 4014–15.
- 5 Du MQ, Peng HZ, Liu H, et al. *BCL10* mutation in lymphoma. *Blood* 2000; **95**: 3885–90.

Department of Histopathology, Royal Free and University College London Medical School, London WC1 6JJ, UK (H Liu PhD, H Ye MB, T C Diss PhD, A Dogan PhD, M-Q Du PhD, P G Isaacson DSc); Services de Gastro-entérologie et d'Anatomie Pathologique, AP-HP, Paris, France (A Ruskon-Fourmeaux MD, T Molina MD, A Lavergne-Slove MD, Y Bouhnik MD, J-C Rambaud MD); GELD (Groupe d'Etude des Lymphomes Digestifs), Fondation Française de Cancérologie Digestive, Dijon, France (A Ruskon-Fourmeaux, A Lavergne-Slove, T Molina, F Megraud MD, J-C Rambaud); Cancer Gene Cloning Centre, Institute of Cancer Research, Sutton, UK (R A Hamoudi BSc); and Laboratoire de Bactériologie, Bordeaux, France (F Megraud)

Correspondence to: Dr Ming-Qing Du
(e-mail: m.du@ucl.ac.uk)

Effect of vancomycin and rifampicin on meticillin-resistant *Staphylococcus aureus* biofilms

Steven M Jones, Marina Morgan, Tom J Humphrey, Hilary Lappin-Scott

Decolonisation of patients with urinary catheter colonisation by meticillin-resistant *Staphylococcus aureus* (MRSA) is often difficult. Replacement of the catheter after prophylactic vancomycin administration has been one approach that is often unsuccessful in clinical practice. We suspected that formation of MRSA biofilms might account for the persistence of infection, and our study confirms this, also showing that MRSA is able to colonise a silastic rubber surface even in the presence of prophylactic vancomycin or rifampicin.

The increased use of implant devices such as lines, prostheses, and urinary catheters for care of patients brings with it an increased risk of infection. Such infections are frequently initiated by biofilms: surface-associated microorganisms that are difficult to eradicate by chemotherapy.¹ Reports of biofilms and attempts to eradicate these